

Some pages of this thesis may have been removed for copyright restrictions.

If you have discovered material in AURA which is unlawful e.g. breaches copyright, (either yours or that of a third party) or any other law, including but not limited to those relating to patent, trademark, confidentiality, data protection, obscenity, defamation, libel, then please read our [Takedown Policy](#) and [contact the service](#) immediately

thesis of
presented by
Department of Pharmacy

DESIGN AND SYNTHESIS OF POTENTIAL ANTIMICROBIAL AGENTS

NASIM BEGUM KHAN

Doctor of Philosophy

ASTON UNIVERSITY

April 2007

This copy of the thesis has been supplied on condition that anyone who consults it is understood to recognise that its copyright rests with its author and that no quotation from the thesis and no information derived from it may be published without proper acknowledgement

Aston University

Design and Synthesis of Potential Antimicrobial Agents

Thesis submitted by Nasim Begum Khan

for the degree of Doctor of Philosophy

April 2007.

ABSTRACT

Tuberculosis is one of the most devastating diseases in the world primarily due to several decades of neglect and an emergence of multidrug-resistance strains (MDR) of *M. tuberculosis* together with the increased incidence of disseminated infections produced by other mycobacterium in AIDS patients. This has prompted the search for new antimycobacterial drugs. A series of pyridine-2-, pyridine-3-, pyridine-4-, pyrazine and quinoline-2-carboxamidrazone derivatives and new classes of carboxamidrazone were prepared in an automated fashion and by traditional synthesis. Over nine hundred synthesized compounds were screened for their antimycobacterial activity against *M. fortuitum* (NCTC 10394) as a surrogate for *M. tuberculosis*. The new classes of amidrazones were also screened against *tuberculosis* H37 Rv and antimicrobial activities against various bacteria. Fifteen tested compounds were found to provide 90-100% inhibition of *mycobacterium* growth of *M. tuberculosis* H37 Rv in the primary screen at $6.25 \mu\text{g mL}^{-1}$. The most active compound in the carboxamidrazone amide series had an MIC value of $0.1-2 \mu\text{g mL}^{-1}$ against *M. fortuitum*.

The enzyme dihydrofolate reductase (DHFR) has been a drug-design target for decades. Blocking of the enzymatic activity of DHFR is a key element in the treatment of many diseases, including cancer, bacterial and protozoal infection. The x-ray structure of DHFR from *M. tuberculosis* and human DHFR were found to have differences in substrate binding site. The presence of glycerol molecule in the X-ray structure from *M. tuberculosis* DHFR provided opportunity to design new antifolates. The new antifolates described herein were designed to retain the pharmacophore of pyrimethamine (2,4-diamino-5-(4-chlorophenyl)-6-ethylpyrimidine), but encompassing a range of polar groups that might interact with the *M. tuberculosis* DHFR glycerol binding pockets.

Finally, the research described in this thesis contributes to the preparation of molecularly imprinted polymers for the recognition of 2,4-diaminopyrimidine for the binding the target. The formation of hydrogen bonding between the model functional monomer 5-(4-*tert*-butyl-benzylidene)-pyrimidine-2,4,6-trione and 2,4-diaminopyrimidine in the pre-polymerisation stage was verified by $^1\text{H-NMR}$ studies. Having proven that 2,4-diaminopyrimidine interacts strongly with the model 5-(4-*tert*-butyl-benzylidene)-pyrimidine-2,4,6-trione, 2,4-diaminopyrimidine-imprinted polymers were prepared using a novel cyclobarbital derived functional monomer, acrylic acid 4-(2,4,6-trioxo-tetrahydro-pyrimidin-5-ylidenemethyl)phenyl ester, capable of multiple hydrogen bond formation with the 2,4-diaminopyrimidine. The recognition property of the respective polymers toward the template and other test compounds was evaluated by fluorescence. The results demonstrate that the polymers showed dose dependent enhancement of fluorescence emissions. In addition, the results also indicate that synthesized MIPs have higher 2,4-diaminopyrimidine binding ability as compared with corresponding non-imprinting polymers.

Keywords: *Mycobacterial Tuberculosis*, New Classes of Carboxamidrazone, Dihydrofolate Reductase, Molecularly Imprinted Polymers.

ACKNOWLEDGEMENTS

I offer countless thanks to Almighty God who has given me the ability, determination, courage and will to complete this thesis. I offer my respect to the Holy prophet, (May the peace and blessings of God be upon him) who has enabled me to understand my creator better.

I offer sincere thanks and I am truly indebted to my supervisor Dr. Daniel Rathbone for being kind, patient and an inspiring source through often difficult moments in writing my thesis. Without his support, understanding, guidance and help this thesis would have been difficult to complete.

I gratefully acknowledge the support of the School of Life and Health for the provision of a studentship and funding this project.

I would like to thank Professor Peter Lambert for his guidance in the microbiology screens and for allowing me to attend his microbiology lectures.

I would like to thank Dr. Michael Coleman for giving me an opportunity to carry out some work on the cytotoxicity of a 2-pyridylcarboxamidrazone antimycobacterial agent.

I would like thank Dr. C. Schwalbe for the valuable help in the preparation of the X-ray crystal structures.

I would like to express my gratitude for the help and technical assistances given to me by Dr. Mike Davis and Karen Farrow.

Many thanks to final year project students F. Kusar, N. Ellahi, the placement student S. Chuhan and the research student L. Wheeden for carrying out the antimycobacterial tests.

I would like to thank Katy Tim for her assistance in microbiology screens.

Many thanks to Dr Dan Rathbone and my colleagues Nafisa, Ren and Beth for helping me find the way through the complicated world of computers and teaching me some useful tricks associated with the microsoft office package.

Thanks to everybody in the chemistry laboratories who kept me motivated, Nafisa, Aisha, Katy, Ren, Mike, Beth and Simon.

Thanks to Prof. Tisdale, Dr. W. Fraser and Dr. Q. Zheng for their encouragement.

I would like to acknowledge Alison Birch for providing me with enough time to complete this thesis.

I wish to thank my family, my husband my children Jamshed and Aurangzeb, my mum, my brothers and sister for their support, encouragement and patience. Special thanks to my brother Iftekhar for encouragements and just for being there for me.

Finally, unique thoughts of gratitude go to my wonderful Dad Mohammed Ayub Khan. I wish you were still here with us!

CONTENTS

ABSTRACT	2
ACKNOWLEDGEMENTS	3
LIST OF TABLES	13
LIST OF FIGURES	15
LIST OF SCHEMES	21
LIST OF ABBREVIATIONS	23
CHAPTER 1	24
1 Introduction to Tuberculosis	24
1.1 Introduction	24
1.3 Mechanism of Drug Resistance	25
1.3.1 Production of a Drug-Destroying Enzyme	25
1.3.2 Altered Target Enzyme (or Site of Action)	25
1.3.3 Altered Drug Uptake	26
1.3.4 Efflux Pumps	26
1.4 Clinical Resistance	26
1.4.1 Hospital-acquired infections	27
1.4.2 Selection of resistant Bacteria by Overuse and Misuse of Antibiotics	27
1.5 <i>Mycobacterium Tuberculosis</i>	27
1.6 Antimicrobial Drugs: Mechanism of Action	29
1.7 Tuberculosis Treatment	29
1.7.1 Essential Antituberculosis Drugs	29
1.7.2 Isoniazid (INH) (3)	30
1.7.3 Rifamycins (7)	31
1.7.4 Rifapentine (13)	32
1.7.5 Rifabutin (14)	32
1.7.6 Rifamethane (SPA-S-565) (15)	33
1.7.7 Rifalazil (16)	33
1.7.8 Pyrazinamide (PZA) (4)	33
1.7.9 Ethambutol (6)	35
1.7.10 Streptomycin (1)	35
1.8 Second-line Antituberculosis Drugs	36
1.8.1 Kanamycin (23)	37
1.8.2 p-aminosalicylic acid (30)	37
1.8.3 Cycloserine (26)	38
1.8.4 Ethionamide (ETH) (24) / Prothionamide (PTH) (25)	38
1.9 The promising candidate drugs against TB	38
1.9.1 Fluoroquinolones	38
1.9.2 Oxazolidinones	40
1.9.3 Linezolid (43)	40
1.9.4 Nitroimidazole	41
1.9.5 Other Classes of Compounds:	42
1.9.5.1 (a) Azoles	42
1.9.5.2 (b) Amidrazone derivatives	42
1.9.5.2.1 Discovery of Amidrazones	42
1.9.5.2.2 General Structural Relationship/Requirement for Antimycobacterial Activity	43
1.10 Aims and objective	46
1.11 Conclusions	46
CHAPTER 2	47
2 Preparation of carboxamidrazones derivatives	47

2.1	Automated and traditional synthesis of carboxamidrazone derivatives	47
2.2	The heteroarylcarboxamidrazones building blocks.....	47
2.3	Preparation of <i>N</i> ¹ -benzylideneheteroarylcarboxamidrazones	48
2.4	Automated Synthesis of Carboxamidrazone Ketimines.....	49
2.5	Library of Pyridinium Salts of <i>N</i> ¹ -Benzylidenecarboxamidrazones.....	55
2.6	Library Synthesis of Metal Complexes of <i>N</i> ¹ -Benzylidenecarboxamidrazone.....	58
2.7	Synthesis of new classes of carboxamidrazones	61
2.8	Carboxamidrazone Amides.....	61
2.9	Acylation of carboxamidrazones by acyl halides	62
2.10	Synthesis of Carboxamidrazones cyclic imide.....	63
2.11	Acylation of Carboxamidrazones by Carboxylic Acids.	64
2.12	Synthesis of the 4-Isopropyl-benzoic acid (Ca6)	65
2.13	Attempt to reverse the amide group in a previously discovered active amide-substituted <i>N</i> ¹ -benzylidene carboxamidrazone	65
2.13.1	Aminolysis of <i>N</i> ¹ -benzylidene carboxamidrazones containing ester groups.	65
2.14	Reduction of <i>N</i> ¹ -benzylidene carboxamidrazones containing aromatic nitro group.....	67
2.14.1	Attempted Catalytic Hydrogenation Using Palladium-on-Charcoal	67
2.14.2	Attempted Reduction with Tin (II) Chloride.....	68
2.15	Synthesis of Novel Sulphonamides Carboxamidrazone.....	68
2.16	Synthesis of <i>N</i> ¹ -(Benzylidene)pyridine-4-carboxamidrazone-4-N-Oxides	69
2.17	Synthesis of carboxamidrazone Urea	70
2.18	Conclusions.....	71
CHAPTER 3		73
3	Microbiology.....	73
3.1	<i>Mycobacterium fortuitum</i> as a screening model for <i>Mycobacterium tuberculosis</i>	73
3.2	The antimycobacterial testing	73
3.3	Evaluating antimycobacterial activity of compounds prepared by automated synthesis.....	74
3.3.1	Antimycobacterial activity and structure activity relationship of alkylidencarboxamidrazones (ketimine).....	74
3.3.2	Evaluating biological activity and structural activity relationship of quaternary pyridinium salts.....	76
3.3.3	Biological activity of the benzylidene heteroaryl carboxamidrazone metal complexes	79
3.4	Antimycobacterial activity of carboxamidrazone amides compared to their corresponding imines against <i>M. fortuitum</i>	80
3.5	Structural Activity Relationships of Carboxamidrazones Amides	80
3.5.1	Variation of alkyl substituents.....	80
3.5.2	Variation alkoxy substituents.....	82
3.5.3	Replacing the benzene ring	83
3.6	Evaluating miscellaneous carboxamidrazone amides against <i>M. fortuitum</i>	84
3.7	Antimicrobial Activity of Carboxamidrazone Amides	85
3.8	Comparison of the <i>M. fortuitum</i> results with <i>M. tuberculosis</i> results	86
3.9	Comparison of the <i>M. fortuitum</i> results with <i>M. tuberculosis</i> results for carboxamidrazone amides and cyclic imides.....	86
3.10	Evaluating antimycobacterial activities of carboxamidrazone sulphonamides.....	92
3.11	Antimycobacterial testing results versus <i>M. fortuitum</i> and <i>M. tuberculosis</i> for <i>N</i> ¹ - benzenlidene-4-pyridinecarboxamidrazones nitrogen oxides	93
3.12	Antimicrobial activity of pyridine-4-carboxamidrazone-4-N-oxides.....	94
3.13	Comparison of the <i>M. fortuitum</i> results with <i>M. tuberculosis</i> results for carboxamidrazone ureas.....	95
3.14	Crystal Structure of New Classes of Carboxamidrazones.....	96
3.15	Conclusions.....	97
CHAPTER 4		99
4	Introduction to Dihydrofolate Reductase	99
4.1	Agents Acting on the Folate Pathway	100
4.2	Inhibitors of Dihydrofolate Reductase	101
4.3	New Drugs and Drugs in Development (Antibacterials)	103
4.3.1	Novel Inhibitors of bacterial DHFR.....	103

4.4.1.1	Recent diaminopyrimidines.....	103
4.5	DHFR structure and ligand binding site.....	105
4.5.1	Aspects of Drug-Enzyme Interactions.....	105
4.5.2	NADP binding to <i>M. tuberculosis</i> DHFR.....	106
4.5.3	Methorexate binding to to <i>M. tuberculosis</i> -DHFR.....	107
4.5.4	Trimethoprim binding to <i>M. tuberculosis</i> -DHFR.....	109
4.5.5	Br-WR99210 binding to <i>M. tuberculosis</i> -DHFR.....	110
4.5.6	Structural Comparison of <i>M. tuberculosis</i> DHFR and Human DHFR.....	111
4.6.1	The glycerol binding pocket present in <i>M. tuberculosis</i> -DHFR.....	112
4.7	Design and Synthesis of new inhibitors of <i>M. tuberculosis</i> DHFR.....	115
4.7.1	WR99210.....	115
4.7.2	Pyrimethamine (71).....	116
4.7.3	Novel analogues of pyrimethamine that might interact with <i>Mycobacterium tuberculosis</i> DHFR.....	117
4.8	Chemistry.....	117
4.8.1	Preparation of Analogues of Pyrimethamine.....	117
4.8.2	Preparation 2,4-diamino-5-[4'-chloro-3-nitrophenyl]-6-ethyl-pyrimidine 104.....	118
4.8.3	Preparation of 2,4-diamino-5-[4'-chloro-3-nitrophenyl]-6-ethylpyrimidine ethers.....	118
4.8.4	Reaction of 2,4-diamino-5-[4'-chloro-3-nitrophenyl]-6-ethylpyrimidine with sodium alkoxide.....	118
4.8.5	Reaction of 2,4-diamino-5-[4'-chloro-3-nitrophenyl]-6-ethyl-pyrimidine (104) with alcohols.....	119
4.8.6	Reaction of 2,4-diamino-5-[4'-chloro-3-nitrophenyl]-6-ethyl-pyrimidine with an amines.....	119
4.9	Synthesis and Reactions of Amino Pyrimethamine (106).....	120
4.9.1	Preparation of 2,4-diamino-5-[4'-chloro-3'-aminophenyl]-6-ethyl-pyrimidines (106).....	120
4.9.2	Reaction of 2,4-diamino-5-[4'-chloro-3'-aminophenyl]-6-ethyl-pyrimidines with carboxylic acid chlorides.....	120
4.9.3	Preparation of 2-[2-Chloro-5-(2,4-diamino-6-ethylpyrimidin-5-yl)-phenyl]isoindole-1,3-dione (108).....	121
4.10	Evaluating antimycobacterial acitivity of the pyrimethamine derivates.....	122
4.11	Conclusions.....	123
CHAPTER 5	124
5	Introduction to the use of molecular imprinting to guide a chemical synthesis of potential inhibitors of mycobacterial dihydrofolate reductase.....	124
5.1	Introduction.....	124
5.2	Molecular Recognition.....	124
5.3	Synthetic Molecular Recognition.....	124
5.4	Molecular Imprinting.....	125
5.4.1	Principle of molecular imprinting.....	125
5.5	An Anti-idiotypic Approach, a Step toward the Next Generation of Molecular Imptinting.....	126
5.6	Design of a molecularly imprinted polymers (MIPs) with affinity for compounds containing the 2,4-diaminopyrimidine group.....	129
5.6.1	Design of the functional monomer.....	130
5.7	Aim of this work.....	133
5.7.1	Specific Goals.....	134
5.8	A historical development of molecular imprinting.....	134
5.9	Approaches to molecular imprinting.....	134
5.9.1	Covalent methods.....	135
5.9.2	Non-covalent Methods.....	136

5.9.3	Combination of Covalent and Non-covalent Imprinting.....	137
5.10	The functional Monomer.....	138
5.11	The Template.....	139
5.12	Solvent/Porogens.....	139
5.13	Crosslinkers.....	140
5.14	Proportions of Monomer:Template:Porogen.....	141
5.15	Development of Improved Crosslinking Monomers for Molecularly Imprinted Materials..	141
5.16	Applications of MIP technology.....	142
5.16.1	Liquid Chromatography.....	143
5.16.2	Solid Phase Extraction.....	144
5.16.3	Imprinted polymers as enzyme mimics.....	144
5.16.4	Drug Development.....	146
5.16.5	Antibody receptor binding mimics.....	146
5.16.6	Sensors.....	147
5.17	Fluorescent molecularly imprinted polymers.....	149
5.18	Conclusions.....	151
CHAPTER 6	153
6.1	Preparation of polymers capable of recognising 2,4-diaminopyrimidines.....	153
6.2	Preparation of Barbiturates.....	153
6.3	The interaction of Template and a Model Functional Monomer Monitored by ¹ H-NMR	
Titrations	155
6.3.1	NMR titration studies.....	155
6.4	Synthesis of a functional monomer for the recognition of 2,4-diaminopyrimidine.....	161
6.4.1	Synthesis of acrylic acid 4-(2,4,6-trioxotetrahydropyrimidin-5-ylidenemethyl)phenyl ester (85).....	161
6.5	Selectivity studies.....	163
6.5.1	Preparation of Polymers.....	163
6.6	Investigation into the binding selectivities of the imprinted polymers.....	165
6.7	Exposure of imprinted polymers and the control polymers to the templates and the test compounds followed by fluorescence measurements:.....	165
6.8	Fluorescence results for MIP1.....	166
6.8.1.	MIP1 re-exposed to its template (TMP).....	166
6.8.2	A blank polymer 3 (NIP) exposed to (70).....	167
6.8.3	Comparison of MIP1 and polymer 3 (NIP) when exposed to TMP (70).....	167
6.8.4	MIP1 exposed to test compound PMA (71).....	169
6.8.5	A blank polymer 3 (NIP) exposed to test compound PMA (71).....	170
6.8.6	Comparison of MIP1 and polymer 3 (NIP) when exposed to PMA (71).....	170
6.8.7	MIP1 and the blank polymer 3 (NIP) exposed to compound 125.....	171
6.8.8	MIP1 and the blank polymer 3 (NIP) exposed to compound 126.....	174
6.8.10	MIP2 -exposed to its template (71) and the test compounds.....	183
6.8.11	The performance of MIP1 versus MIP2.....	186
6.8.11.1	MIP1 re-exposed to its template and the test compounds.....	186
6.8.11.2	MIP2 re-exposed to is template and the test compounds.....	187
6.8.11.3	Polymer 3 (NIP) exposed to the test compounds.....	188
6.8.11.4	Polymer 4 (TMPTA) re-exposed to the test compound.....	188
8.9	Conclusions.....	189
CHAPTER 7	190
7	Forward To Experimental.....	190
7.1	Instrumentation:.....	190
7.1.2	Synthesis of the Heteroarylcarboxamidrazone.....	190
7.1.3	Pyridine-2-carboxamidrazone (2PY).....	190
7.1.4	Pyridine-3-carboxamidrazone (3PY).....	190
7.1.5	Pyridine-4-carboxamidrazone (4PY).....	191

7.1.6	Pyrazinyl-2-carboxamidrazone (PZ).....	191
7.1.7	Quinoly-2-carboxamidrazone (QN).....	191
7.1.8	Pyridine-4-carboxamidrazone-4-N-oxide (4PY-NO).....	191
7.2.	Synthesis of the <i>N</i> ¹ -arylidene-pyridinecarboxamidrazone.....	192
7.2.1	General method for the preparation of <i>N</i> ¹ -arylidene-pyridinecarboxamidrazone.....	192
7.2.2	Characterisation of of <i>N</i> ¹ -arylidene-pyridine-2-carboxamidrazone.....	192
7.2.3.	<i>N</i> ¹ -(4-Methylbenzylidene)-pyridine-2-carboxamidrazone (2PYaa).....	192
7.2.4	<i>N</i> ¹ -(4-Ethylbenzylidene)-pyridine-2-carboxamidrazone (2PYab).....	192
7.2.5	<i>N</i> ¹ -(2-Ethylbenzylidene)-pyridine-2-carboxamidrazone (2PYac).....	192
7.2.6	<i>N</i> ¹ -(4-Isopropylbenzylidene)-pyridine-2-carboxamidrazone (2PYad).....	193
7.2.7	<i>N</i> ¹ -(4-Acetamidobenzylidene)-pyridine-2-carboxamidrazone (2PYae).....	193
7.2.8	<i>N</i> ¹ -(4- <i>tert</i> -Butylbenzylidene)-pyridine-2-carboxamidrazone (2PYaf).....	193
7.2.9	<i>N</i> ¹ -(1-Naphthylidene)-pyridine-2-carboxamidrazone (2PYag).....	193
7.2.10	<i>N</i> ¹ -(9-Phenanthrene)-pyridine-2-carboxamidrazone (2PYah).....	193
7.2.11	<i>N</i> ¹ -(9-Anthrylidene)-pyridine-2-carboxamidrazone (2PYai).....	194
7.2.12	<i>N</i> ¹ -(2-Benzyloxybenzylidene)-pyridine-2-carboxamidrazone (2PYaj).....	194
7.2.13	<i>N</i> ¹ -(3-Benzyloxy-4-methoxybenzylidene)-pyridine-2-carboxamidrazone (2PYak).....	194
7.2.14	<i>N</i> ¹ -(4-Benzyloxy-3-methoxybenzylidene)-pyridine-2-carboxamidrazone (2PYal).....	194
7.2.15	<i>N</i> ¹ -(4-Formyl-benzoic acid methyl ester)-pyridine-2-carboxamidrazone (2PYan).....	194
7.3	Characterisation of <i>N</i> ¹ -Arylidene-pyridine-3-carboxamidrazone.....	195
7.3.1	<i>N</i> ¹ -(4-Methylbenzylidene)-pyridine-3-carboxamidrazone (3PYaa).....	195
7.3.2	<i>N</i> ¹ -(4-Ethylbenzylidene)-pyridine-3-carboxamidrazone (3PYab).....	195
7.3.3	<i>N</i> ¹ -(4-Isopropylbenzylidene)-pyridine-3-carboxamidrazone (3PYad).....	195
7.3.4	<i>N</i> ¹ -(4-Acetamidobenzylidene)-pyridine-3-carboxamidrazone (3PYae).....	195
7.3.5	<i>N</i> ¹ -(4- <i>tert</i> -Butylbenzylidene)-pyridine-3-carboxamidrazone (3PYaf).....	195
7.3.6	<i>N</i> ¹ -(1-Naphthylidene)-pyridine-3-carboxamidrazone (3PYag).....	195
7.3.7	<i>N</i> ¹ -(9-Phenanthrene)-pyridine-3-carboxamidrazone (3PYah).....	196
7.3.8	<i>N</i> ¹ -(2-Benzyloxybenzylidene)-pyridine-3-carboxamidrazone (3PYaj).....	196
7.3.9	<i>N</i> ¹ -(3-Benzyloxy-4-methoxybenzylidene)-pyridine-3-carboxamidrazone (3PYak).....	196
7.3.10	<i>N</i> ¹ -(4-Benzyloxy-3-methoxybenzylidene)-pyridine-3-carboxamidrazone (3PYal).....	196
7.4	Characterisation of <i>N</i> ¹ -Arylidene-pyridine-4-carboxamidrazone.....	196
7.4.1	<i>N</i> ¹ -(4-Methylbenzylidene)-pyridine-4-carboxamidrazone (4PYaa).....	196
7.4.2	<i>N</i> ¹ -(4-Ethylbenzylidene)-pyridine-4-carboxamidrazone (4PYab).....	196
7.4.3	<i>N</i> ¹ -(2-Ethylbenzylidene)-pyridine-4-carboxamidrazone (4PYac).....	197
7.4.4	<i>N</i> ¹ -(4-Isopropylbenzylidene)-pyridine-4-carboxamidrazone (4PYad).....	197
7.4.5	<i>N</i> ¹ -(4-Acetamidobenzylidene)-pyridine-4-carboxamidrazone (4PYae).....	197
7.4.6	<i>N</i> ¹ -(4- <i>tert</i> -Butylbenzylidene)-pyridine-4-carboxamidrazone (4PYaf).....	197
7.4.7	<i>N</i> ¹ -(1-Naphthylidene)-pyridine-4-carboxamidrazone (4PYag).....	197
7.4.8	4PYah <i>N</i> ¹ -(9-Phenanthrene)-pyridine-4-carboxamidrazone.....	197
7.4.9	<i>N</i> ¹ -(9-Anthrylidene)-pyridine-4-carboxamidrazone (4PYai).....	198
7.4.10	<i>N</i> ¹ -(2-Benzyloxybenzylidene)-pyridine-4-carboxamidrazone (4PYaj).....	198
7.4.11	<i>N</i> ¹ -(3-Benzyloxy-4-methoxybenzylidene)-pyridine-4-carboxamidrazone (4PYak).....	198
7.4.12	<i>N</i> ¹ -(4-Benzyloxy-3-methoxybenzylidene)-pyridine-4-carboxamidrazone (4PYal).....	198
7.4.13	<i>N</i> ¹ -(4-Formyl-benzoic acid methyl ester)-pyridine-4-carboxamidrazone (4PYan).....	198

7.4.14	<i>N</i> ¹ -(4-Nitrobenzylidene)-pyridine-4-carboxamidrazone (4PYar)	198
7.5	Characterisation of <i>N</i> ¹ -Arylidene-pyrazin-2-carboxamidrazone	199
7.5.1	<i>N</i> ¹ -(4-Methylbenzylidene)-pyrazin-2-carboxamidrazone (PZaa).....	199
7.5.2	<i>N</i> ¹ -(4-Ethylbenzylidene)-pyrazin-2-carboxamidrazone (PZab).....	199
7.5.3	<i>N</i> ¹ -(2-Ethylbenzylidene)-pyrazin-2-carboxamidrazone (PZac)	199
7.5.4	<i>N</i> ¹ -(4-Isopropylbenzylidene)-pyrazin-2-carboxamidrazone (PZad).....	199
7.5.5	<i>N</i> ¹ -(4-Acetamidobenzylidene)-pyrazin-2-carboxamidrazone (PZae)	199
7.5.6	<i>N</i> ¹ -(4-tert-Butylbenzylidene)-pyrazin-2-carboxamidrazone (PZaf).....	199
7.5.7	<i>N</i> ¹ -(1-Naphthylidene)-pyrazin-2-carboxamidrazone (PZag)	200
7.5.8	<i>N</i> ¹ -(9-Phenanthrene)-pyrazin-2-carboxamidrazone (PZah).....	200
7.5.9	<i>N</i> ¹ -(9-Anthrylidene)-pyrazin-2-carboxamidrazone (PZai).....	200
7.5.10	<i>N</i> ¹ -(2-Benzyloxybenzylidene)-pyrazin-2-carboxamidrazone (PZaj)	200
7.5.11	<i>N</i> ¹ -(3-Benzyloxy-4-methoxybenzylidene)-pyrazin-2-carboxamidrazone (PZak).....	200
7.5.12	<i>N</i> ¹ -(4-Benzyloxy-3-methoxybenzylidene)-pyrazin-2-carboxamidrazone (PZal).....	200
7.6	Automated Synthesis	201
7.6.1	The <i>N</i> ¹ -Benzylideneheteroarylcarboxamidrazone Library	201
7.6.2	Auomated Synthesis of the <i>N</i> ¹ -Benzylideneheteroarylcarboxamidrazone-Pyridium Salts.....	201
7.6.3	Auomated Synthesis of the <i>N</i> ¹ -Benzylideneheteroarylcarboxamidrazone Metal Complexes	201
7.7	Synthesis of the New Classes of Carboxamidrazones	201
7.7.1	Synthesis of the Carboxamidrazone Amides	201
7.7.2	General method for the preparation of carboxamidrazone Amide	201
7.7.3	Synthesis of the Pyridin-2-carboxamidrazone Amides	202
7.7.4	Characterisation of pyridine-2-carboxamidrazone amides.....	202
7.7.4.1	Pyridine-2-carboxamidrazone <i>N</i> ¹ -(benzoyl)amide (2PYAc1)	202
7.7.4.2	Pyridine-2-carboxamidrazone <i>N</i> ¹ -(4-acetamidobenzoyl)amide (2PYAc2)	202
7.7.4.3	Pyridine-2-carboxamidrazone <i>N</i> ¹ -(4-phenylazo-benzoyl)amide (2PYAc3).....	202
7.7.4.4	Pyridine-2-carboxamidrazone <i>N</i> ¹ -(3-methoxy-benzoyl)amide (2PYAc4)	202
7.7.4.5	Pyridine-2-carboxamidrazone <i>N</i> ¹ -(2-naphthalene)amide (2PYAc5).....	202
7.7.4.6	Pyridine-2-carboxamidrazone <i>N</i> ¹ -(1-naphthalene)amide (2PYAc6).....	203
7.7.4.7	Pyridine-2-carboxamidrazone <i>N</i> ¹ -(4-cyno-benzoyl)amide (2PYAc7)	203
7.7.4.8	Pyridine-2-carboxamidrazone <i>N</i> ¹ -(4-methoxy-benzoyl)amide (2PYAc8)	203
7.7.4.9	Pyridine-2-carboxamidrazone <i>N</i> ¹ -(2-acetoxybenzoyl)amide (2PYAc11).....	203
7.7.4.10	Pyridine-2-carboxamidrazone <i>N</i> ¹ -(5-nitro-2-furoyl)amide (2PYAc13).....	204
7.7.4.11	Pyridine-2-carboxamidrazone <i>N</i> ¹ -(3-nitro-benzoyl)amide (2PYAc14).....	204
7.7.4.12	Pyridine-2-carboxamidrazone <i>N</i> ¹ -(ethyl-benzoyl)amide (2PYAc15)	204
7.7.4.13	Pyridine-2-carboxamidrazone <i>N</i> ¹ -(4-propyl-benzoyl)amide (2PYAc16).....	204
7.7.4.14	Pyridine-2-carboxamidrazone <i>N</i> ¹ -(2,5-dimethoxy-benzoyl)amide (2PYAc17) ..	205
7.7.4.15	Pyridine-2-carboxamidrazone <i>N</i> ¹ -(4-heptyl-benzoyl)amide (2PYAc18).....	205
7.7.4.16	Pyridine-2-carboxamidrazone <i>N</i> ¹ -(2-methoxy-bezoyl)amide (2PYAc19).....	205
7.7.4.17	Pyridine-2-carboxamidrazone <i>N</i> ¹ -(4-tert-butyl-benzoyl)amide (2PYAc20).....	205
7.7.4.18	Pyridine-2-carboxamidrazone <i>N</i> ¹ -(3,4,5-trimethoxy-benzoyl)amide (2PYAc21).....	206
7.7.4.19	Pyridine-2-carboxamidrazone <i>N</i> ¹ -(2-furoyl)amide (2PYAc25)	206
7.8	Synthesis of the Pyridin-4-carboxamidrazone Amides	206
7.8.1	Characterisation of pyridine-4-carboxamidrazone	206
7.8.1.1	Pyridine-4-carboxamidrazone <i>N</i> ¹ -(4-acetamidobenzoyl)amide (4PYAc2)	206
7.8.1.2	Pyridine-4-carboxamidrazone <i>N</i> ¹ -(4-phenylazo-benzoyl)amide (4PYAc3).....	206
7.8.1.3	Pyridine-4-carboxamidrazone <i>N</i> ¹ -(3-methoxy-benzoyl)amide (4PYAc4)	207
7.8.1.4	Pyridine-4-carboxamidrazone <i>N</i> ¹ -(2-naphthalene)amide (4PYAc5).....	207
7.8.1.5	Pyridine-4-carboxamidrazone <i>N</i> ¹ -(1-naphthalene)amide (4PYAc6).....	207
7.8.1.6	Pyridine-4-carboxamidrazone <i>N</i> ¹ -(4-methoxy-benzoyl)amide (4PYAc8)	207
7.8.1.7	Pyridine-4-carboxamidrazone <i>N</i> ¹ -(2,6-dimethoxy-benzoyl)amide (4PYAc9)	207

7.8.1.8	Pyridine-4-carboxamidrazone N^1 -(5-nitro-2-furoyl)amide (4PYAc13)	208
7.8.1.9	Pyridine-4-carboxamidrazone N^1 -(3-nitro-benzoyl)amide (4PYAc14)	208
7.8.1.10	Pyridine-4-carboxamidrazone N^1 -(4-ethyl-benzoyl)amide (4PYAc15)	208
7.8.1.11	Pyridine-4-carboxamidrazone N^1 -(4-propyl-benzoyl)amide (4PYAc16)	208
7.8.1.12	Pyridine-4-carboxamidrazone N^1 -(4-heptyl-benzoyl)amide (4PYAc18)	208
7.8.1.13	Pyridine-4-carboxamidrazone N^1 -(3,4,5-trimethoxy-benzoyl)amide (4PYAc21)	209
7.8.1.14	Pyridine-4-carboxamidrazone N^1 -(2-methyl-benzoyl)amide (4PYAc22)	209
7.8.1.15	Pyridine-4-carboxamidrazone N^1 -(3-methyl-benzoyl)amide (4PYAc23)	209
7.8.1.16	Pyridine-4-carboxamidrazone N^1 -(2,4,6-trimethyl-benzoyl)amide (4PYAc24)	209
7.8.1.17	Pyridine-4-carboxamidrazone N^1 -(2-furoyl)amide (4PYAc25)	209
7.9	Synthesis of Amides from Carboxylic Acid	210
7.9.1	General method for the preparation of carboxamidrazone Amide	210
7.9.2	Synthesis of the pyridine-2-carboxamidrazone amides	210
7.9.3	Characterisation of Pyridine-2-carboxamidrazone Amides	210
7.9.3.2	Pyridine-2-carboxamidrazone N^1 -(4-cyclohexyl-benzoyl) amide (2PYCa2)	210
7.9.3.3	Pyridine-2-carboxamidrazone N^1 -(2-benzyloxy-benzoyl)amide (2PYCa4)	210
7.9.3.4	Characterisation of pyridine-2-carboxamidrazone N^1 -(3,5-di-tert-butyl-2-hydroxy-benzoyl)amide (2PYCa5)	211
7.9.3.5	Characterisation of pyridine-2-carboxamidrazone N^1 -(4-isopropyl-benzoyl)amide (2PYCa6)	211
7.9.4	Synthesis of pyridine-4-carboxamidrazone amides	211
7.9.5	Characterisation of pyridine-4-carboxamidrazones amide	212
7.9.5.2	Pyridine-4-carboxamidrazone N^1 -(2-Benzyloxy-benzoyl)amide (4PYCa4)	212
7.9.5.4	Pyridine-4-carboxamidrazone N^1 -(4-Isopropyl-benzoyl)amide (4PYCa6)	212
7.10	Characterisation of pyridine-3-carboxamidrazone N^1 -(3,5-Di-tert-butyl-2-hydroxy-benzoyl)amide (3PYCa5)	213
7.11	Synthesis of Carboxamidrazones Imide	213
7.11.1	General procedure for preparation of carboxamidrazones Imide	213
7.11.2	Characterisation of Carboxamidrazones Imide	213
7.11.2.1	Pyridine-2-carboxamidrazone N^1 -phthalimide (2PYAnh1)	213
7.11.2.2	Pyridine-2-carboxamidrazone N^1 -1,8-Naphthalimide (2PYAnh2)	213
7.11.3	Synthesis and Characterisation of Pyridine-4-carboxamidrazone N^1 -1,8-Naphthalimide (4PYAnh2)	214
7.11.3.1	Pyridine-4-carboxamidrazone N^1 -1,8-naphthalimide (4PYAnh2)	214
7.12	Synthesis of the 4-Isopropyl-benzoic acid	214
7.13	Preparation of Carboxamidrazones Sulphonamide	214
7.13.1	General method for the preparation of carboxamidrazones sulphonamide	214
7.13.2	Characterisation of Caboxamidrazones Sulphonamide	214
7.13.2.1	Pyridine-2-carboxamidrazone N^1 -(4-tert-butylbenzoyl)sulphonamide (2PYS1)	214
7.13.2.2	Pyridine-2-carboxamidrazone N^1 -(benzoyl)sulphonamide (2PYS2)	214
7.13.2.3	Pyridine-2-carboxamidrazone N^1 -(4-chlorobenzoyl)sulphonamide (2PYS3)	215
7.13.2.4	Pyridine-4-carboxamidrazone N^1 -(4-acetamidobenzoyl)sulphonamide (4PYS4)	215
7.14	N^1 -Arylidene-pyridine-4-carboxamidrazone-4-N-oxides	215
7.14.1	General method for the preparation of N^1 -arylidene-pyridine-4-carboxamidrazone-4-N-oxides	215
7.14.2	Characterisation of N^1 -Arylidene-pyridine-4-carboxamidrazone-4-N-oxides	215
7.14.2.1	N^1 -(3,5-Di-tert-butyl-2-hydroxybenzylidene) pyridinecarbox amidrazone-4-N-oxide (4PYap-N-O)	215
7.14.2.2	N^1 -(1-Naphthylidene)pyridine-4-carboxamidrazone-4-N-oxide (4PYag-N-O)	216
7.14.2.3	N^1 -(4-Acetamidobenzylidene)pyridine-4-carbox-amidrazone-4-N-oxide	216
7.14.2.4	N^1 -(4-tert-Butylbenzylidene)pyridine-4-carboxamidrazone-4-N-oxide (4PYaf-N-O)	216
7.14.2.5	N^1 -(3-Benzyloxy-4-methoxybenzylidene)pyridine-4-carboxamidrazone-4-N-oxide (4PYak-N-O)	216
7.14.2.6	N^1 -(2-(4-Chlorophenyl)thio)benzylidene)pyridine-4-carboxamidrazone-4-N-oxide (4PYaq-N-O)	217

7.14.2.7	<i>N</i> ¹ -(9-Anthrylylidene)pyridine-4-carboxamidrazone-4-N-oxide (4PYai-N-O).....	217
7.14.2.8	<i>N</i> ¹ -(3-Benzyloxybenzylidene)pyridine-4-carboxamidrazone-4-N-oxide (4PYas-N-O).....	217
7.15	Synthesis of the Carboxamidrazone Urea	217
7.15.1	Preparation of pyridid-2-carboxamidrazone-urea	217
7.15.2	General method for the preparation of pyridine-2-carboxamidrazone urea	217
7.15.3	Characterisation of Carboxamidrazone urea	218
7.15.3.2	Pyridine-2-carboxamidrazone <i>N</i> ¹ -(1-phenyl) urea (2PYIs2).....	218
7.15.3.3	Pyridine-2-carboxamidrazone <i>N</i> ¹ -(1-naphthalene)urea (2PYIs3)	218
7.15.3.4	Pyridine-2-carboxamidrazone <i>N</i> ¹ -(4-methyl-benzenesulfonyl)urea (2PYIs4)	218
7.15.3.5	Pyridine-2-carboxamidrazone <i>N</i> ¹ -(4-cyclohexyl)urea (2PYIs5).....	219
7.15.3.6	Pyridine-2-carboxamidrazone <i>N</i> ¹ -(4-bromo-phenyl)urea (2PYIs6)	219
7.15.3.7	Pyridine-2-carboxamidrazone <i>N</i> ¹ -(4-nitro-phenyl)urea (2PYIs7)	219
7.15.3.8	Pyridine-2-carboxamidrazone <i>N</i> ¹ -(4-methyl-phenyl)urea (2PYIs 8).....	219
7.15.3.9	Pyridine-2-carboxamidrazone <i>N</i> ¹ -(3-methyl-phenyl)urea (2PYIs9).....	220
7.15.3.10	Pyridine-2-carboxamidrazone <i>N</i> ¹ -(2-methoxy-phenyl)urea (2PYIs10).....	220
7.15.3.11	Pyridine-2-carboxamidrazone <i>N</i> ¹ -(3-methoxy-phenyl)urea (2PYIs11).....	220
7.15.3.12	Pyridine-2-carboxamidrazone <i>N</i> ¹ -(4-methoxy)urea (2PYIs12).....	220
7.15.3.13	Pyridine-2-carboxamidrazone <i>N</i> ¹ -(4-chloro-phenyl)urea (2PYIs14).....	221
7.15.3.14	Pyridine-2-carboxamidrazone <i>N</i> ¹ -(2-methyl-phenyl)urea (2PYIs15).....	221
7.15.3.16	Pyridine-2-carboxamidrazone <i>N</i> ¹ -(2-nitro-phenyl)urea (2PYIs16)	221
7.16	Preparation of Pyridine-4-carboxamidrazone-Urea	221
7.16.1.	General method for the preparation of pyridine-4-carboxamidrazone-urea.....	221
7.16.2	Characterisation of pyridine-4-carboxamidrazones Urea.....	222
7.16.2.1	Pyridine-4-carboxamidrazone <i>N</i> ¹ -(4-tert-butyl-phenyl)urea (4PYIs1)	222
7.16.2.2	Pyridine-4-carboxamidrazone <i>N</i> ¹ -(1-phenyl)urea (4PYIs2).....	222
7.16.2.3	Pyridine-4-carboxamidrazone <i>N</i> ¹ -(1-naphthalene)urea (4PYIs3)	222
7.16.2.4	Pyridine-4-carboxamidrazone <i>N</i> ¹ -(4-methylbenzenesulfonyl)urea (4PYIs4).....	222
7.16.3.5	Pyridine-4-carboxamidrazone <i>N</i> ¹ -(4-cyclohexyl)urea (4PYIs5).....	222
7.16.3.6	Pyridine-4-carboxamidrazone <i>N</i> ¹ (4-bromo-phenyl)urea (4PYIs6)	223
7.16.3.7	Pyridine-4-carboxamidrazone <i>N</i> ¹ -(4-nitro-phenyl)urea (4PYIs7)	223
7.16.3.8	Pyridine-4-carboxamidrazone <i>N</i> ¹ -(3-methyl-phenyl)urea (4PYIs9).....	223
7.16.3.9	Pyridine-4-carboxamidrazone <i>N</i> ¹ -(2-methoxy-phenyl)urea (4PYIs10).....	223
7.16.3.11	Pyridine-4-carboxamidrazone <i>N</i> ¹ -(4-methoxy phenyl)urea (4PYIs12).....	224
7.16.3.12	Pyridine-4-carboxamidrazone <i>N</i> ¹ -(4-chloro-phenyl)urea (4PYIs14).....	224
7.16.3.13	Pyridine-4-carboxamidrazone <i>N</i> ¹ -(2-methyl-phenyl)urea (4PYIs15).....	224
7.16.3.14	Pyridine-4-carboxamidrazone <i>N</i> ¹ -(2-nitro-phenyl)urea (4PYIs16)	225
7.17	Synthesis of the Derivatives of Pyrimethamine	225
7.17.1	Synthesis of 5-(4-chloro-3-nitro-phenyl)-6-ethyl-pyrimidine-2,4-diamine (104) (Nitro-pyrimethamine).....	225
7.17.2	Synthesis of 2,4-diamino-6-ethyl-5-(4-methoxy-3-nitrophenyl)pyrimidine (105a).....	225
7.17.3	Preparation of 5-(4-ethoxy-3-nitro-phenyl)-6-ethyl-pyrimidine-2,4-diamine (105c).....	226
7.17.4	Preparation of 2-[4-(2,4-diamino-6-ethyl-pyrimidin-5-yl)-2-nitro-phenoxy]ethanol (105e).....	226
7.17.5	6-Ethyl-5-[3-nitro-4-(2-propoxy-ethoxy)-phenyl]-pyrimidine-2,4-diamine (105f).....	226
7.17.6	6-Ethyl-5-[3-nitro-4-[2-(2-propoxy-ethoxy)-ethoxy]-phenyl]-pyrimidine-2,4-diamine (105g).....	226
7.18.	Synthesis of 5-(3-amino-4-chloro-phenyl)-6-ethyl-pyrimidine-2,4-diamine (106) (APMA) ..	227
7.19	General procedure for preparation of derivatives of 106 (i.e. Amides).....	227
7.19.1	Characterisation of 4-tert-butyl-N-[2-chloro-5-(2,4-diamino-6-ethyl-pyrimidin-5-yl)-phenyl]-N-methyl-benzamide (107a).....	227
7.19.2	Preparation of N-[2-Chloro-5-(2,4-diamino-6-ethyl-pyrimidin-5-yl)-phenyl]-4-ethoxy-3-oxo-butamide (107b).....	227

7.19.3	Preparation of 4-[2-Chloro-5-(2,4-diamino-6-ethyl-pyrimidin-5-yl)-phenylcarbamoyl]-butyric acid methyl ester (107c)	228
7.20	Preparation of 2-[2-Chloro-5-(2,4-diamino-6-ethyl-pyrimidin-5-yl)-phenyl]-isoindole-1,3-dione (108)	228
7.21	Microbiology	228
7.21.1	Testing of compounds at 32 $\mu\text{g}\cdot\text{ml}^{-1}$	228
7.21.2	Minimum Inhibitory Concentrations (MICs)	228
7.22	Preparation of Molecularly Imprinted Polymers I	229
7.22.1	Synthesis of the Barbiturates (monomers and the test compounds)	229
7.22.2	General procedure for the preparation of the barbiturates	229
7.22.3	5-(4-Benzoyloxy-2-hydroxy-benzylidene)pyrimidine-2,4,6-trione (122)	229
7.22.4	5-(3,5-Di- <i>tert</i> -butyl-4-hydroxy-benzylidene)-pyrimidine-2,4,6-trione (123)	229
7.22.5	5-(4-Hydroxy-benzylidene)-pyrimidine-2,4,6-trione (124)	229
7.22.6	5-Anthracen-9-ylmethylene-pyrimidine-2,4,6-trione (125)	229
7.22.7	5-Phenanthren-9-ylmethylene-pyrimidine-2,4,6-trione (126)	230
7.22.8	5-Pyren-1-ylmethylene-pyrimidine-2,4,6-trione (127)	230
7.22.9	5-(4-Octyloxy-benzylidene)-pyrimidine-2,4,6-trione (128)	230
7.22.10	5-(4-Benzoyloxy-benzylidene)-pyrimidine-2,4,6-trione (129)	230
7.22.11	5-(4- <i>tert</i> -Butyl-benzylidene)-pyrimidine-2,4,6-trione (130)	230
7.23	$^1\text{H-NMR}$ titration experiments	231
7.24	Synthesis of the Functional Monomer	233
7.24.1	Preparation of Acrylic acid 4-(2,4,6-trioxo-tetrahydro-pyrimidin-5-ylidenemethyl)phenyl ester (85)	233
7.25	General procedure for the preparation of imprinted polymers	234
7.25.1	Preparation of Polymer 1 (MIP1)	234
7.25.2	Preparation of Polymer 2 (MIP2)	234
7.25.3	Preparation of Reference Polymer 3 (NIP)	234
7.25.4	Preparation of Reference Polymer 4 (TMPTA)	235
7.26	Exposure of imprinted polymers to templates and test compounds followed by fluorescence measurements	235
7.26.1	General procedure	235
	REFERENCES	236
	Appendix 1	253
	Appendix 2	254
	Appendix 3	256
	Appendix 4	258
	Appendix 5	259
	Appendix 6	266
	Appendix 7	267
	Appendix 8	268

LIST OF TABLES

Table 2.1a:	Represents the data of methylketimines	50
Table 2.1b:	Represents the data of cycloalkylidenecarboxamidrazones	51
Table 2.1c:	Represents the data of alkylidenecarboxamidrazones	54
Table 2.2:	Represents the data of pyridinium salts.	54
Table 2.3:	Represents the data of metal complexes of <i>N</i> ¹ -benzylidencarboxamidrazones.	60
Table 3.1:	Antimycobacterial activity of various pyridine-2-carboxamidrazone <i>N</i> ¹ -(benzoyl) amide and their corresponding imine	75
Table 3.2:	Antimycobacterial activity of various pyridine-4-carboxamidrazone <i>N</i> ¹ -(benzoyl) amide and the corresponding imine.	77
Table 3.3:	MIC values for alkyl-substituted carboxamidrazone amides against <i>M. fortuitum</i>	82
Table 3.4:	MIC values for methoxy-substituted carboxamidrazone amides against <i>M. fortuitum</i> .	83
Table 3.5:	MIC values for benzoyloxy and alkoxy-substituted carboxamidrazone amides against <i>M. fortuitum</i> .	84
Table 3.6:	MIC values for various ring-substituted carboxamidrazone amides against <i>M. fortuitum</i> .	84
Table 3.7:	MIC values for 5-nitro substituted furanyl carboxamidrazone amide against <i>M. fortuitum</i> .	85
Table 3.8:	MIC values for miscellaneous carboxamidrazone amides against <i>M. fortuitum</i> .	86
Table 3.9:	Comparison of <i>M. fortuitum</i> MIC, with <i>M. tuberculosis</i> H37Rv (<i>M. tuber</i>) MIC and %Inhibition results.	88
Table 3.10:	Comparison of <i>M. fortuitum</i> MIC, with <i>M. tuberculosis</i> H37Rv (<i>M. tuber</i>) MIC and % Inhibition results for <i>tert</i> -butyl substituted carboxamidrazone amides.	89
Table 3.11:	Comparison of <i>M. fortuitum</i> MIC, with <i>M. tuberculosis</i> H37Rv (<i>M. tuber</i>) MIC and %Inhibition results for alkyl-substituted carboxamidrazone amides.	90
Table 3.12:	Comparing MIC values and %Inhibition of 2/4PYAc3 against <i>M. tuberculosis</i> and <i>M. fortuitum</i> .	91
Table 3.13:	Comparing MIC values and %Inhibition of 2/4PYCa4 against <i>M. tuberculosis</i> and <i>M. fortuitum</i> .	91
Table 3.14:	Comparing MIC values and %Inhibition of 2/4PYCa1 against <i>M. tuberculosis</i> and <i>M. fortuitum</i> .	92
Table 3.15:	MIC values and %Inhibition of 2PYCa2 against <i>M. tuberculosis</i> and <i>M. fortuitum</i> .	92
Table 3.16:	MIC values and % Inhibition of carboxamidrazone imides against <i>M. tuberculosis</i> and <i>M. fortuitum</i> .	93
Table 3.17:	Antimycobacterial activity of various carboxamidrazone <i>N</i> ¹ -(benzoyl)sulphonamide against <i>M. fortuitum</i> .	93
Table 3.18:	Antimycobacterial testing results versus <i>M. fortuitum</i> and <i>M. tuberculosis</i> for various <i>N</i> ¹ -benzenlidene-4-pyridinecarboxamidrazones nitrogen oxides and their corresponding imine.	94
Table 3.19:	MIC values for active pyridine-4-carboxamidrazone ureas against <i>M. fortuitum</i> and <i>M. tuberculosis</i> .	96

Table 4.1:	Antimycobacterial activity of pyrimethamine derivatives.	123
Table 6.1:	Substituted aldehydes (Ar) used in scheme 6.1	154
Table 6.2:	Complexation induce shifts from the NMR titration experiments.	161
Table 6.3:	Shows a series of MIPS and the blank polymers 3 and 4 synthesised to investigate the binding performance of MIPS.	165
Table 7.1:	Shows the concentration of TMP (70) was 0.0086 mM and 130 was added from 0.0184 mM to 0.0015 mM, X = component was absent	231
Table 7.2:	Amino induced shifts in the titration of 130 with 70 .	231
Table 7.3:	Complexation induced shifts in the titration of 130 with 70 .	232

LIST OF FIGURES

Figure 1.1:	Complex between vacomycin (9) and the terminal D-alanyl-D-alanine of peptidoglycan. The dotted lines indicate hydrogen bonding.	26
Figure 1.2:	Chemical structures of mycolic acids from <i>M. tuberculosis</i> .	28
Figure 1.3:	Essential antituberculosis drugs, Isoniaz (3), Pyrazinamide (4), Ethambutol (6) and Rifampicin (7).	29
Figure 1.4:	Derivatives of Isonicotinic Acid Hydrazide	31
Figure 1.5:	Structures of rifampicin derivatives.	32
Figure 1.6:	Structure of pyrazinamide (4), nicotinamide (17) and pyrazinoic acid (18)	33
Figure 1.7:	Structure of tert-butyl 5-chloropyrazinamide (19) and 2-(2-methyldecyl)5-chloropyrazinamide (20)	34
Figure 1.8:	Structure of 1-cyclopropyl-6-fluoro-1,4-dihydro-8-methoxy-7-(3-methyl-4(pyrazine-2-carboxamido)methyl)piperazin)-4-oxoquinoline-3-carboxylic acid (21).	35
Figure 1.9:	Structure of Streptomycin (1).	35
Figure 1.10:	Second-line antituberculosis drugs. Amykacin (22), Capreomycin (28), Ciprofloxacin (27), Cycloserine (26), Kanamycin (23), Ofloxacin (29), Ethionamide (24), p-Aminosalicylic acid (30) and Protionamide (25).	36
Figure 1.11:	Structure of D-Cycloserine (26) and D-Alanine.	38
Figure 1.12:	Basic structure of fluoroquinolones nucleus (31) and nalidixic acid (32).	39
Figure 1.13:	Structure of Ofloxacin (33), Sparafloxacin (34), Enofloxacin (35) and Lomefloxacin (36).	39
Figure 1.14:	Structure of gati (37), moxi (38) and Trovafloxacin (39).	39
Figure 1.15:	The structures of some important linezolid	41
Figure 1.16:	Structure of CG-17341 (46) and PA 824 (47).	41
Figure 1.17:	The structures of Miconazole (48), B4157 (49) and Clofazimine (50).	42
Figure 1.18:	The most active compounds discovered by Mamolo <i>et al.</i>	43
Figure 1.19:	The most active compounds discovered by Billington <i>et al.</i>	43
Figure 1.20:	The general structure of the <i>N</i> ¹ -benzylideneheteroarylcarboxamidrazones (59) and amidrazone moiety (60).	44
Figure 1.21:	The structure of 2-nitrobenzenecarboxamidrazone (61) and 2-chlorobenzonitril (62) used in comparison study to see if heteroaryl ring was important for biological activities	44
Figure 1.22:	The structures of the proposed new classes of heteroaryl carboxamidrazones.	45
Figure 1.23:	The structures of the proposed <i>N</i> ¹ -benzylideneheteroaryl-carboxamidrazones derivatives.	45
Figure 2.1:	Heteroarylcarboxamidrazones building blocks.	47
Figure 2.2:	Substituted benzaldehyde derived residues used in preparation of <i>N</i> ¹ -benzylidene carboxamidrazones.	48
Figure 2.3:	Tautomeric forms of pyridine-2-carboxamidrazones.	49
Figure 2.4:	Structures of alkyl halides used in automated synthesis.	55
Figure 2.5:	Acyl chloride derived residues used in amide synthesis.	62

Figure 2.6:	Cyclicacidanhydride derived residues (R) used in carboxamidrazone imide synthesis.	63
Figure 2.7:	Carboxylic acid derived residues (R) used in amide synthesis.	64
Figure 2.8:	Proposed structure for various <i>N</i> ¹ -benzylidene carboxamidrazoneamides.	65
Figure 2.9:	Structure of the TB active compound 113 .	65
Figure 2.10:	The structure of isobutylamine (114) and N-methylphenylamine (115)	66
Figure 2.11:	Sulphonyl chloride derived residues (R) used in sulphonamide synthesis.	68
Figure 2.12:	The structure of most active antibacterial compound.	69
Figure 2.13:	The aldehyde derived residues used in preparation of <i>N</i> ¹ -benzylidene N-Oxides.	70
Figure 2.14:	Isocyanate derived residues (R) used in urea synthesis.	71
Figure 2.15:	The major fragmentation pathway appeared by the cleavage is –CO-NH-R bond of urea moiety.	71
Figure 3.1:	Structure of imine (<i>N</i> ¹ -benzylidene hetroarylcarboxamidrazones the parent compound 124 MIC (8-16 µg/mL), amide 2PYAc20 , MIC (8-16 µg/mL), urea 2PYIs1 MIC (>32 µg/mL) and sulphonylamide 2PYS1 MIC (>32 µg/mL) against <i>M. fortuitum</i> .	96
Figure 3.2:	Superimposed structures of imine, amide, urea and sulphonylamide.	97
Figure 4.1:	The substrate (63), 7,8-dihydrofolate, product (64), 5,6,7,8-tetrahydrofolate and folate (65).	99
Figure 4.2:	The actions of sulphonamides and trimethoprim.	101
Figure 4.3:	Structure of nitrogen-containing heterocyclic ring, where A B is C=C, N-C, or C=N.	101
Figure 4 4:	Structures of Folic Acid Antagonists (DHFR Inhibitors).	102
Figure 4 5:	Structures of novel and in development Inhibitors of DHFR	104
Figure 4.6:	Structure of <i>M. tuberculosis</i> DHFR.	105
Figure 4.7:	Chemical structures of coenzyme NADP (81) and three inhibitors: trimethoprim (70); methotrexate (67) and Br-WR99210 (75c), used in the structure determinations of <i>M. tuberculosis</i> dihydrofolate reductase binary and ternary complexes.	106
Figure 4.8:	Shows Interactions between the <i>M. tuberculosis</i> DHFR and NADP molecule.	107
Figure 4.9:	Shows Interactions between the <i>M. tuberculosis</i> DHFR and inhibitor Methotrexate.	108
Figure 4.10:	Interactions between <i>M. tuberculosis</i> DHFR and inhibitor trimethoprim.	109
Figure 4.11:	Shows Interactions between the <i>M. tuberculosis</i> DHFR and inhibitor Br-WR99210.	110
Figure 4.12:	Comparison of <i>M. tuberculosis</i> DHFR and Human DHFR.	111
Figure 4.13:	Shows the presence of a glycerol molecule in the <i>M. tuberculosis</i> crystal structure IDF7.	112
Figure 4.14:	Shows methotrexate and the adjacent glycerol molecule. View from the <i>M. tuberculosis</i> . DHFR crystal structure IDF7.	113
Figure 4.15:	Ball and stick diagram showing the preferred conformation of the methotrexate and the glycerol molecule viewed from different orientations.	114

Figure 4.16:	Space-filling diagram for the MTX and the glycerol molecule.	114
Figure 4.17:	The electron density map of the ternary Br-WR99210 complex with the <i>M. tuberculosis</i> DHFR.	115
Figure 4.18:	Analogues of WR99210	116
Figure 4.19:	The structure of proguanil (73) and an analogues of pyrimetamine.	116
Figure 4.20:	The structure of 2,4-diamino-5-aryl-6-ethylpyrimidine and its analogues to be synthesised in this study.	117
Figure 5.1:	Templates (inhibitors) and core building block used in anti-idiotypic imprinting.	128
Figure 5.2:	Nucleophilic substituted amines residues used in anti-idiotypic imprinting.	128
Figure 5.3:	The structure of the proposed polymerisable 'receptor' that has the possibility to recognise 2,4-diaminopyrimidine group.	129
Figure 5.4:	Structure of the proposed functional monomer acrylic acid 4-(2,4,6-trioxo-tetrahydro-pyrimidin-5-ylidenemethyl)-phenyl ester (85).	130
Figure 5.5:	The structures of the DHFR inhibitors selected to be used as templates in the current study.	130
Figure 5.6:	Molecular structure of TMP (70) and 5,5-diethyl barbituric acid (86).	131
Figure 5.7:	Packing diagram of the title compound 70 and 86	131
Figure 5.8:	Selection of functional monomers used in non-covalent molecular imprinting.	138
Figure 5.9:	Selection of the cross-linking monomers used in molecular imprinting.	140
Figure 5.10:	The structure of the novel crosslinking monomer that was used in OMNiMIP approach.	142
Figure 5.11:	Biomimetic sensor in which an MIP selective for the fluorescently labelled amino acid dansyl-L-phenylalanine was applied as a layer on the tip of the fibre-optic sensing device.	148
Figure 5.12:	Representation of the functional monomer (93) for D-fuctose-boronic acid complex.	149
Figure 5.13:	The structure of metallophorphyrine monomer (94).	150
Figure 5.14:	The structures of the fluorescence monomers.	150
Figure 5.15:	The structures of the FFM (94), template (95) and the test compounds (96-98).	151
Figure 6.1:	Structure of barbituric acid 121 and several tautomers.	153
Figure 6.2:	A model receptor 130 shown associated with trimethoprim 70 .	155
Figure 6.3:	Watson-Crick binding mode between guanine and cytosine in the double helix of DNA.	155
Figure 6.4:	The ¹ H-NMR spectrum of trimethoprim (TMP) on its own in D ₈ -THF at 300K, along with the structural assignment.	156
Figure 6.5:	The ¹ H-NMR spectrum of 130 on its own in D ₈ -THF at 300K.	157
Figure 6.6:	The ¹ H-NMR spectra of (130) (0.0184 mM) and (70) (0.0086 mM) superimposed in D ₈ -THF at 300K.	157
Figure 6.7:	The ¹ H-NMR spectrum of the complex formation between (70) (0.0086 mM) and (130) (0.0184 mM), superimposed on the ¹ H-NMR spectrum of TMP (70) on its own.	158
Figure 6.8:	The ¹ H-NMR spectrum of the complex formation between 70 (0.0086 mM)	

	and 130 (0.0184 mM), superimposed on the ¹ H-NMR spectrum of 130 on its own.	158
Figure 6.9:	The ¹ H-NMR spectrum of the complex formation between 70 (0.0086 mM) and 130 (0.0015 mM), superimposed on the ¹ H-NMR spectrum of 70 .	159
Figure 6.10:	The ¹ H-NMR spectrum of the complex formation between 70 (0.0086 mM) and 130 (0.0015 mM), superimposed on the ¹ H-NMR spectrum of 130 .	160
Figure 6.11:	Complexation-induced shifts ($\Delta\delta$) of the amino protons of TMP (70), (0.0086 mM) versus total concentration of 130 in THF at 300K.	161
Figure 6.12:	The structures of the templates: TMP (70) and PMA (71).	164
Figure 6.13:	The structures of the test compounds.	165
Figure 6.14:	Fluorescence spectra for MIP1 re-exposed to its template TMP (70) at concentrations of 2 mg/mL and 0.1 mg/mL.	166
Figure 6.15:	Dose-dependent fluorescence spectra for blank polymer 3 (NIP) when exposed to solutions of TMP (70)	167
Figure 6.16:	Fluorescence spectra for MIP1 and NIP re-exposed to TMP (70) at concentrations of 2 mg/mL and 0.1 mg/mL in 200 μ L (PEG) (λ_{ex} = 290 nm).	167
Figure 6.17:	More expanded fluorescence spectra for MIP1 and NIP re-exposed to TMP (70) at concentrations of 2 mg/mL and 0.1 mg/mL (λ_{ex} = 290 nm).	168
Figure 6.18:	Fluorescence spectra for MIP1 re-exposed to PMA (71) at concentrations of 2 mg/mL and 0.1 mg/mL (λ_{ex} = 290 nm).	169
Figure 6.19:	Fluorescence spectra for NIP re-exposed to PMA (71) at concentrations of 2 mg/mL and 0.1 mg/mL in 200 μ L (λ_{ex} = 290).	170
Figure 6.20:	Fluorescence spectra for MIP1 and NIP exposed to PMA at concentrations of 2 mg/mL and 0.1 mg/mL (λ_{ex} = 290).	170
Figure 6.21:	Expanded version of fluorescence spectra for MIP1 and NIP exposed to 71 at concentrations of 2 mg/mL and 0.1 mg/mL (λ_{ex} = 290).	171
Figure 6.22:	Fluorescence spectra for MIP1 exposed to compound 125 at concentrations of 1 mg/mL and 0.1 mg/mL (λ_{ex} = 290).	172
Figure 6.23:	Expanded version of Fluorescence spectra for MIP1 when exposed to 125 at the concentrations of 1 mg/mL and 0.1 mg/mL (λ_{ex} = 290 nm).	172
Figure 6.24:	Fluorescence spectra for NIP exposed to compound 125 at concentrations of 1 mg/mL and 0.1 mg/mL.	173
Figure 6.25:	Fluorescence spectra for MIP1 and NIP exposed to compound 129 at concentrations of 1 mg/mL and 0.1 mg/mL. (λ_{ex} = 290 nm).	173
Figure 6.26:	Expanded version of fluorescence spectra for MIP1 and NIP re-exposed to compound 125 at concentrations of 1 mg/mL and 0.1 mg/mL (λ_{ex} = 290 nm).	174
Figure 6.27:	Fluorescence spectra for MIP1 exposed to compound 126 at concentrations of 2 mg/mL and 0.1 mg/mL (λ_{ex} = 290 nm).	174
Figure 6.28:	Fluorescence spectra for NIP exposed to compound 126 at concentrations of 2 mg/mL and 0.1 mg/mL.	175
Figure 6.29:	Fluorescence spectra for MIP1 and NIP exposed to compound 126 at concentrations of 2 mg/mL and 0.1 mg/mL (λ_{ex} = 290 nm).	175

Figure 6.30:	Expanded version of fluorescence spectra for MIP1 and NIP exposed to compound 126 at concentrations of 2 mg/mL and 0.1 mg/mL ($\lambda_{ex} = 290$ nm).	176
Figure 6.31:	Fluorescence spectra for TMPTA, empty NIP and empty MIP1 ($\lambda_{ex} = 290$ nm).	177
Figure 6.32:	Fluorescence spectra for polymer 4 TMPTA and polymer 3 (NIP) exposed to compound 70 at concentrations of 2 mg/mL and 0.1 mg/mL ($\lambda_{ex} = 290$).	177
Figure 6.33:	Fluorescence spectra for polymer 4 (TMPTA) and polymer 3 (NIP) exposed to compound 71 at concentrations of 2 mg/mL and 0.1 mg/mL. ($\lambda_{ex} = 290$ nm).	178
Figure 6.34:	Fluorescence spectra for polymer 4 (TMPTA) and polymer 3 (NIP) exposed to compound 126 at concentrations of 2 mg/mL and 0.1 mg/mL. ($\lambda_{ex} = 290$ nm).	178
Figure 6.35:	Fluorescence spectra for polymer 4 (TMPTA) exposed to test compounds 70, 71, 125 and 126 at concentrations of 2 mg/mL ($\lambda_{ex} = 290$).	179
Figure 6.36:	Fluorescence spectra for polymer 3 (NIP) exposed to test compounds 70, 71, 125 and 126 at concentrations of 2 mg/mL ($\lambda_{ex} = 290$).	179
Figure 6.37:	Fluorescence spectra for MIP1 exposed to test compounds 70, 71, 125 and 126 at concentrations of 2 mg/mL ($\lambda_{ex} = 290$).	180
Figure 6.38:	Fluorescence spectra for MIP1, NIP and TMPTA when exposed to compound 70 (TMP) at concentrations of 2 mg/mL ($\lambda_{ex} = 290$).	180
Figure 6.39:	Fluorescence spectra for MIP1, NIP and TMPTA when exposed to compound 71 (PMA) at concentrations of 2 mg/mL ($\lambda_{ex} = 290$).	181
Figure 6.40:	Fluorescence spectra for MIP1, NIP and TMPTA when exposed to compound 125 at concentrations of 1 mg/mL ($\lambda_{ex} = 290$).	182
Figure 6.41:	Fluorescence spectra for MIP1, NIP and TMPTA when exposed to compound 126 at concentrations of 2 mg/mL ($\lambda_{ex} = 290$).	182
Figure 6.42:	Fluorescence spectra for MIP2 re-exposed to its template (71) at concentrations of 2 mg/mL and 0.1 mg/mL ($\lambda_{ex} = 290$).	183
Figure 6.43:	Fluorescence spectra for MIP2 exposed to compound 70 at concentrations of 2 mg/mL and 0.1 mg/mL. The quoted errors are the standard deviations of triplicate wells ($\lambda_{ex} = 290$ nm).	184
Figure 6.44:	Fluorescence spectra for MIP2 exposed to 125 at concentrations of 2 mg/mL and 0.1 mg/mL. The quoted errors are the standard deviations of triplicate wells ($\lambda_{ex} = 290$ nm).	184
Figure 6.45:	Fluorescence spectra for MIP2 exposed to compound 126 at concentrations of 2 mg/mL and 0.1 mg/mL. The quoted errors are the standard deviations of triplicate wells ($\lambda_{ex} = 290$ nm).	185
Figure 6.46:	Fluorescence spectra for MIP2 exposed to compounds 70, 71, 126 and 125 at concentrations of 2 mg/mL and 1 mg/mL respectively ($\lambda_{ex} = 290$ nm).	185
Figure 6.47:	Fluorescence output of a MIP1 exposed to solutions of its template 70 and the test compounds 71, 125 and 126 at 2 mg/mL and 0.1 mg/mL respectively ($\lambda_{ex} = 290$ nm, $\lambda_{em} = 340$ nm).	186
Figure 6.48:	Fluorescence output of a MIP2 exposed to solutions of its template 71 and the test compounds 70, 125 and 126 at 2 mg/mL and 0.1 mg/mL respectively ($\lambda_{ex} = 290$ nm, $\lambda_{em} = 340$ nm).	187

Figure 6.49: Fluorescence output of a blank polymer 3 (NIP) exposed to solutions of test compounds **70**, **71**, **125** and **126** at 2 mg/mL and 0.1 mg/mL respectively ($\lambda_{\text{ex}} = 290 \text{ nm}$, $\lambda_{\text{em}} = 340 \text{ nm}$).

188

Figure 6.50: Fluorescence output of a blank polymer 4 (TMPTA) exposed to solutions of test compounds **70**, **71**, **125** and **126** at 2 mg/mL and 0.1 mg/mL respectively ($\lambda_{\text{ex}} = 290 \text{ nm}$, $\lambda_{\text{em}} = 340 \text{ nm}$).

188

LIST OF SCHEMES

Scheme 1.1:	Cleavage of a penicillin (8) by the enzyme β -lactamase, to give the inactive penicillinoic acid.	24
Scheme 1.2:	Reaction products formed from catalase-peroxidase reaction with INH.	29
Scheme 1.3:	Inactivation of rifampicin by different rifampicin-resistant bacteria.	30
Scheme 1.4:	Mannich reaction, preparation of pyrazine derivatives.	33
Scheme 1.5:	Resistance to kanamycin.	36
Scheme 1.6:	Analogue of kanamycin resistant to resistance mechanism.	36
Scheme 2.1:	Preparation of heteroarylcarboxamidrazones, the building blocks.	46
Scheme 2.2:	Synthesis of N^1 -benzylideneheteroarylcarboxamidrazones. R= substituted aldehyde resid.	47
Scheme 2.3:	Preparation of carboxamidrazones ketimines.	48
Scheme 2.4:	The synthetic scheme for alkylating N^1 -benzylidene carboxamidrazones.	54
Scheme 2.5:	Synthesis of N^1 -benzylidene carboxamidrazones metal complex.	58
Scheme 2.6:	The general procedure for preparing amides.	61
Scheme 2.7:	Synthetic scheme for preparation of carboxamidrazones amides.	62
Scheme 2.8:	Synthetic route to carboxamidrazones imides.	62
Scheme 2.9:	Synthetic route for preparation of carboxamidrazones amides using a coupling reagent.	63
Scheme 2.10:	Synthetic route to aminolysis N^1 -benzylidene carboxamidrazones.	65
Scheme 2.11:	Alternative synthetic route to aminolysis N^1 -benzylidene carboxamidrazones.	66
Scheme 2.12:	Schematic synthetic route for hydrogenation of N^1 -benzylidene-carboxamidrazones.	66
Scheme 2.13:	Possible reduction route for N^1 -[4-nitrobenzylidene]-pyridine-4-carboxamidrazones.	67
Scheme 2.14:	Synthetic route for preparation of sulphonamide carboxamidrazones.	68
Scheme 2.15:	Preparation of cyano-heteroaryl N-Oxide.	69
Scheme 2.16:	Synthetic scheme for preparation of N^1 -benzylidene N-Oxides.	69
Scheme 2.17:	Synthetic scheme for preparation of carboxamidrazones ureas.	70
Scheme 4.1:	Synthetic scheme for preparation of various analogues of 2,4-diamino-5-aryl-6-ethylpyrimidine (pyrimethamine) (71).	116
Scheme 4.2:	Synthesis of NPMA ethers where R = Et, Me.	117
Scheme 4.3:	Synthesis of 2,4-diamino-5-[4'-chloro-3-nitrophenyl]-6-ethyl-pyrimidine ethers where R = alcohol or an ethyleneglycol derived residues.	118
Scheme 4.4:	Synthesis of NPMA amine where R = amine derived residues.	118
Scheme 4.5:	The synthesis of amino pyrimethamine (106).	119
Scheme 4.6:	Preparation of pyrimethamine amides R= acyl chloride derived residue.	120
Scheme 4.7:	Synthesis of 2-[2-Chloro-5-(2,4-diamino-6-ethylpyrimidin-5-yl)-phenyl]isoindole-1.3-dione (108).	120
Scheme 5.1:	General scheme for MIP construction.	124
Scheme 5.2:	The process of anti-idiotypic imprinting.	125
Scheme 5.3:	The process of anti-idiotypic imprinting.	126
Scheme 5.4:	Aminotriazine formation.	127

Scheme 5.5:	Schematic representation of an anti-idiotypic imprinting process.	132
Scheme 5.6:	Boronic ester approach to covalent molecular imprinting of PMP using VPMA.	134
Scheme 5.7:	Non-covalent molecular imprinting of theophylline.	135
Scheme 5.8:	Imprinting cholesterol by the sacrificial spacer method.	136
Scheme 5.9:	Use of the imprinted polymer as a chromatographic resin to preferentially achieve the enantiomeric selection of L-phenylalanine from a racemic mixture of L- and D-phenylalanine.	142
Scheme 5.10:	Phosphonic monoesters mimics of the transition state of ester hydrolysis.	144
Scheme 6.1:	General procedure for preparation of pyrimidine-2,4,6-triones.	153
Scheme 6.2:	Attempted synthesis of acrylic acid 4-(2,4,6-trioxotetrahydropyrimidin-5-ylidenemethyl)phenyl ester (85).	161
Scheme 6.3:	Attempted synthesis of acrylic acid 4-formylphenyl ester.	161
Scheme 6.4:	Synthesis of acrylic acid 4-(2,4,6-trioxotetrahydropyrimidin-5-ylidenemethyl)phenyl ester (85).	162
Scheme 6.5:	Schematic representation of molecular imprinting process.	163

CHAPTER 1
LIST OF ABBREVIATIONS

AIBN	Azobisisobutyrylnitrile
APMA	Aminopyrimethamine
CCl ₄	Tetrachloromethane
CHCl ₃	Chloroform
DBU	1,8-Diazabicyclo[5.4.0]undec-7-ene
DCM	Dichloromethane
D ₆ -DMSO	Deuterated dimethylsulphoxide
DHFR	Dihydrofolate reductase
DMAP	Dimethylaminopyridine
DMF	Dimethylformamide
DMSO	Dimethylsulphoxide
DNA	Deoxyribonucleic acid
D ₈ -THF	Deuterated tetrahydrofuran
EGDMA	Ethyleneglycol dimethacrylate
EthOAc	Ethyl acetate
FFM	Fluorescent Functional Monomer
FH ₂	Dihydrofolate
FH ₄	Tetrahydrofolate
GTP	Guanosine triphosphate
¹ H NMR	Proton nuclear magnetic resonance
Hünig's base	<i>N,N</i> -diisopropyl ethylamine
IR	Infra red
MgSO ₄	Magnesium sulphate
MIP	Molecularly imprinted polymers
MTX	Methotrexate
NADP	Nicotinamide adenine dinucleotide phosphate
NIP	Non-imprinted polymer
NMR	Nuclear magnetic resonance
NPMA	Nitropyrimethamine
PMA	Pyrimethamine
RNA	Ribonucleic acid
TEA	Triethylamine
THF	Tetrahydrofuran
TLC	Thin layer chromatography
TMP	Trimethoprim
TMPTA	Trimethylolpropanetriacrylate

CHAPTER 1

1 Introduction to Tuberculosis

1.1 Introduction

Tuberculosis (TB), a disease which man has been fighting for centuries and even had hopes of eradicating in the year 2010, is back in full swing. Considering the risks associated with TB, the World Health Organization (WHO) declared this disease a global health emergency in 1993 [Valadas and Antunes, 2005]. It is estimated that one-third of the world's population is currently infected with the TB bacillus totaling almost three million deaths each year. According to the WHO, each year, 8 million people worldwide develop active TB and almost 3 million die [www.who.int/tb/en/]. The population infected in each of the various regions is as follows: Africa (35%); Americas (18%); Eastern Mediterranean (29%); Europe (15%); South-east Asia (44%) and Western Pacific (35%) [Souza, 2006]. The report goes on to explain that without a coordinated control effort, tuberculosis will infect an estimated 1 billion people by 2020, killing 70 million.

The introduction of the first drugs (see structures in Figure 1.3) for TB treatment some 60 years ago; streptomycin **(1)** (1944), para-aminosalicylic acid **(2)** (1949), isoniazid **(3)** (1952), pyrazinamide **(4)** (1954), cycloserine **(5)** (1955), ethambutol **(6)** (1962) and rifampin **(7)** (1963) along with the widespread use of BCG vaccine led to optimism that the disease could be controlled, if not eradicated. The drugs, coupled with generally increasing standards of health care, caused a rapid decline of tuberculosis in many industrialized countries which produced a climate of indifference to the need for new drugs. During the 1950s, TB rates dropped by 75% and TB hospitals were closing due to lack of patients. In 1987, the Advisory Council for the Elimination of TB put forth a plan to eliminate TB by the year 2010. There was a sigh of relief and it was thought that the three thousand year struggle with TB was over! As a result of this perception by the pharmaceutical industry, that such agents would be unlikely to generate a suitable return on investment, few new drugs have been introduced in the last 35 years. However, from 1985 through 1993, the disease has been undergoing a resurgence driven by a variety of changes in social, medical and economic factors. Thus, a dramatic increase in immunosuppressed individuals due mainly to AIDS (but also to cancer chemotherapy and organ-transplant practices), coupled with increasing urbanization and poverty in developing countries, have compromised primary health care structures and led to large increases in TB incidence [www.who.int/tb/en/, Valadas and Antunes, 2005].

By far, the most threatening influence on the resurgence of TB today is the developing multi-drug resistant strains (MDR-TB) [Neu, 1992, Singh and Chopra 2004]. Drug resistance in TB occurred as a result of tubercle bacillus mutations [Lowe, 1982]. The bacilli subjected to an anti-TB agent to which they are sensitive, will be killed. However, there may be a few drug resistant mutations that will survive and continue to proliferate. There is now recognition that new drugs to treat TB are urgently required, specifically for use in shorter treatment regimes, than are possible with the current agents and which can be employed to treat multidrug-resistant and latent disease.

1.2 Antimicrobial Drugs: Resistance.

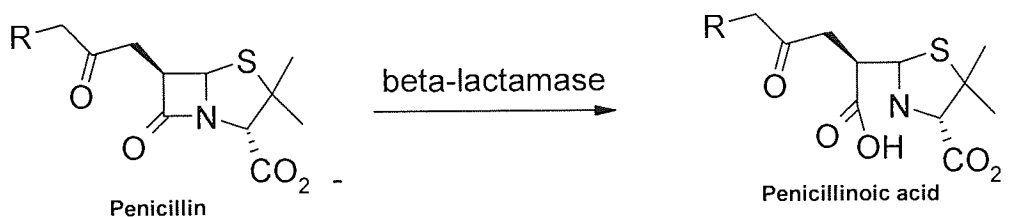
Antibiotic resistance has reached an alarming stage worldwide [Neu, 1992]. Many organisms today have acquired multiple systems to reduce or avoid the action of antibiotics. The most threatening mechanisms of resistance involve changes in the target site for antibiotic interaction, because that confers resistance to all compounds with the same mechanism of action. Therefore, it is vital to be able to identify compounds that target many sites of action or have multiple mechanism of action.

1.3 Mechanism of Drug Resistance

There are four major mechanisms that mediate bacterial resistance to drugs:

1.3.1 Production of a Drug-Destroying Enzyme

Bacteria produce enzymes that inactivate the drug. For example, β -lactamases can inactivate penicillins (**8**) by cleaving the β -lactam ring of the drug.



Scheme 1.1: Cleavage of a penicillin (**8**) by the enzyme β -lactamase, to give the inactive penicillinoic acid.

Resistance can occur by induction of genes that produce new enzymes to degrade the drug (Scheme 1.1) [Silverman, 2004].

1.3.2 Altered Target Enzyme (or Site of Action)

Bacteria synthesize modified targets against which the drug has no effect, for example, a mutant protein in the 30A ribosomal subunit can result in resistance to streptomycin. Another example of this type of mechanism of resistance was presented by Walsh and coworkers for the antibiotic vancomycin (**9**) [Walsh, 1993]. Vancomycin acts by forming a complex with terminal D-alanyl-D-alanine of the peptidoglycan (an essential component of bacterial cell wall) by blocking the reaction that builds up the peptidoglycan. When bacterial cell wall biosynthesis is blocked, the bacteria cannot survive. Interestingly, a resistance to vancomycin arises in bacteria by induction of five new genes namely VanS, VanR, VanA, VanH and VanX; used to construct an altered peptidoglycan in which the terminal D-alanyl-D-alanine is replaced by D-alanyl-D-lactate. The substitution of D-alanine by D-lactate in peptidoglycan leads to the deletion of one hydrogen bond to vancomycin and also produces a nonbonded electron repulsion between the lactate ester oxygen and the amide carbonyl of vancomycin (**Figure 1.1**). This produces a 1000-fold reduction in binding of the drug to the peptidoglycan substrate. In this case, the resistant organism has not mutated an essential enzyme, but has mutated the substrate for the enzyme, which is what forms the complex with the vancomycin.

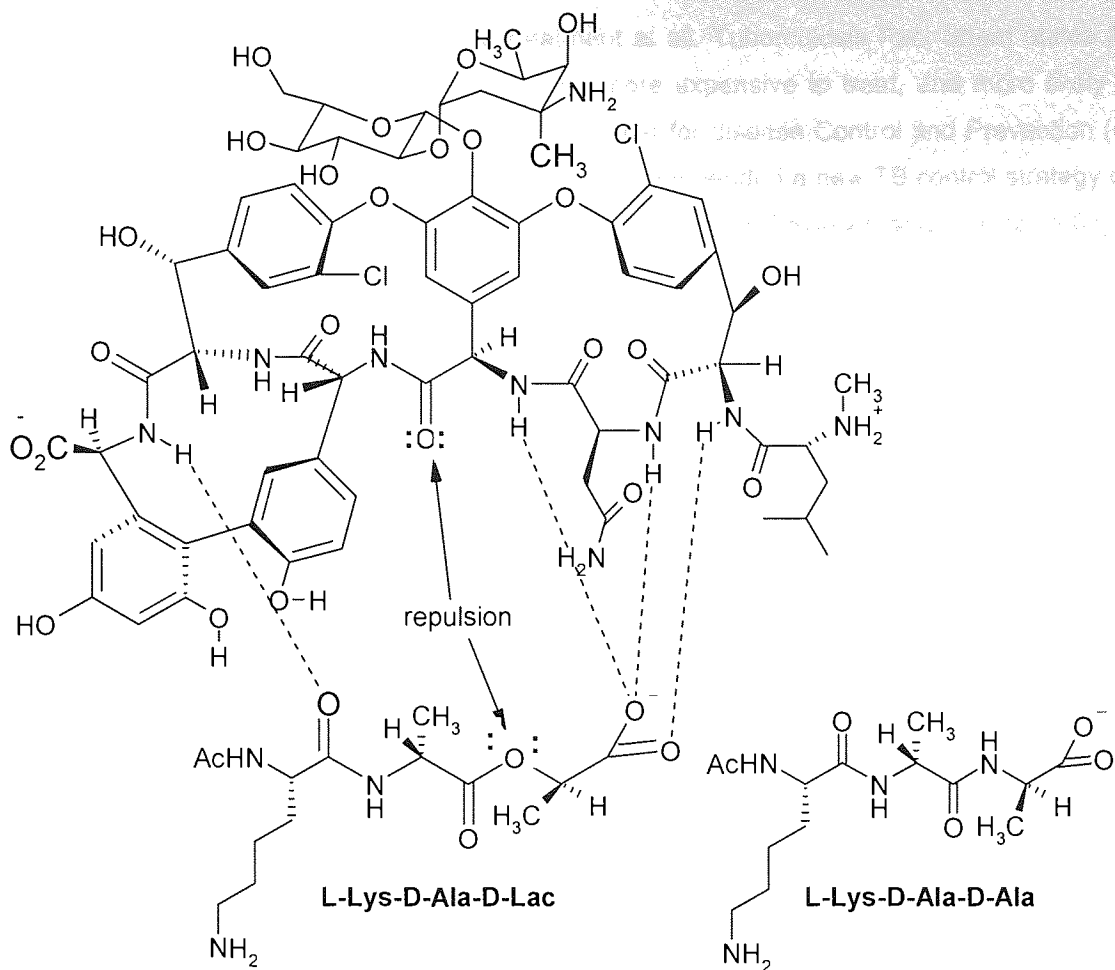


Figure 1.1: Complex between vancomycin (9) and the terminal D-alanyl-D-alanine of peptidoglycan. The dotted lines indicate hydrogen bonding.

1.3.3 Altered Drug Uptake

Bacteria decrease their permeability such that an effective intracellular concentration of drug is not achieved; for example, changes in pores can reduce the amount of drug entering the bacterium.

1.3.4 Efflux Pumps

Bacteria actively export drugs using a "multidrug resistance pump" (MDR pump). The MDR pump imports protons and, in an exchange-type reaction, exports a variety of foreign molecules including certain antibiotics, such as quinolones [Viveiros, *et al*, 2003].

1.4 Clinical Resistance

There are two types of clinical drug resistance, primary and acquired or secondary: Primary occurs when a person who has never been treated for TB in the past becomes infected with resistant organisms. Acquired or secondary resistance develops due to either improper treatment with the wrong antibiotics or combination thereof, or the patient did not follow the prescription regimen correctly. Many patients stop taking their medications when they start to feel better, which leads to the mutation and proliferation of drug resistant strains. When dealing with TB, improper treatment or

incomplete treatment is really worse than no treatment at all. Tuberculosis Fact Sheet states [WHO March, 2006] drug resistant TB is more difficult and more expensive to treat, and more likely to be fatal." In an attempt to circumvent this problem, the Center for disease Control and Prevention (CDC) along with the World Health Organization (WHO) have recommended a new TB control strategy called DOTS (Directly Observed Treatment, Short-course) [Duncan, 2003; Levinson and Jawetz, 2001]]. The DOTS plan requires a health care worker to physically observe and record the patient taking the proper medications on a daily basis.

1.4.1 Hospital-acquired infections

Hospital-acquired infections are significantly more likely to be caused by antibiotic-resistant organisms such as *Staphylococcus aureus* and enteric Gram-negative rods such as *Escherichia coli* and *Pseudomonas aeruginosa* than are community-acquired infections. Antibiotic-resistant organisms are common in the hospital setting because widespread antibiotic use in hospitals selects for these organisms. Furthermore, hospital strains are often resistant to multiple antibiotics. This resistance is usually due to the acquisition of plasmids carrying several genes that encode the enzymes that mediate resistance [Levinson and jawetz, 2001].

1.4.2 Selection of resistant Bacteria by Overuse and Misuse of Antibiotics

Serious outbreaks of diseases caused by Gram-negative rods resistant to multiple antibiotics have occurred in many developing countries. For example, many hospital-acquired infections are caused by multiple resistant organisms. Three main points of overuse and misuse of antibiotics increase the likelihood of these problems by enhancing the selection of resistant mutants:

- (i) Some physicians use multiple antibiotics when one would be sufficient, prescribe unnecessarily long courses of antibiotic therapy, use antibiotic in self-limiting before infections for which they are not needed, and overuse antibiotic for prophylaxis before and after surgery.
- (ii) In many countries, antibiotics are sold over the counter to the general public: this practice encourages the inappropriate and indiscriminate use of the drugs.
- (iii) Antibiotics are used in animal feed to prevent infections and promote growth. This selects for resistant organisms in the animals and may contribute to this pool of resistant organisms in humans [Levinson and jawetz, 2001].

1.5. *Mycobacterium Tuberculosis*

Mycobacterium tuberculosis, along with *M. bovis*, *M. africanum*, and *M. microti* all cause the disease known as tuberculosis (TB) and are pathogenic. *M. tuberculosis* is pathogenic for humans while *M. bovis* is usually pathogenic for animals. *M. tuberculosis*, is classified as acid-fast bacteria due to its cell permeability by certain dyes and stains. An unusual feature of *M. tuberculosis* is its ability to survive for decades within macrophages. Later in life, especially if the immune system becomes weakened by disease or drugs, the infection may be reactivated, spreading in the lungs and even to other organs.



Aston University

Illustration removed for copyright restrictions

COOH

Figure 1.2: Chemical structures of mycolic acids from *M. tuberculosis*. There are five forms of mycolic acids in tuberculosis, illustrated with α -mycolic acid from the H37Ra strain and methoxy- and keto-mycolic acids from *M. tuberculosis* subsp. *hominis* strains DT, PN, and C. Both cyclopropane rings in α -mycolic acid have the *cis* configuration. The methoxy- and ketomycolic acids can have either the *cis* or *trans* configuration on the proximal cyclopropane ring [Takayma and Wang, 2005].

The cell envelope of *M. tuberculosis* is distinctive and is associated with its pathogenicity. Features that are very prominent in the cell envelope are the presence of arabinogalactan-mycolate covalently linked to the cell wall peptidoglycan via a phosphodiester bond located on the inner leaflet of the outer membrane and of a free glycolipid called trehalose dimycolate (TDM), which accumulates in a cord-like fashion on the surface of the cells. This provides a thick layer of lipid on the outer part of the cell and protects the tubercle bacillus from noxious chemicals and the host's immune system. In addition to peptidoglycan, the acid-fast cell wall of mycobacterium contains a large amount of glycolipids, especially, mycolic acids that make up approximately 60% of the acid-fast cell wall. The mycolic acids are α -alkyl, β -hydroxy fatty acids with a species-dependent saturated "short" arm of 20 – 26 carbon atoms and a "long" meromycolic acid arm of 50 – 60 carbon atoms. The latter arm is functionalised at regular intervals by cyclopropyl, α -methyl ketone, or α -methyl methyl ether groups as shown in (Figure 1.2). It is this structure which accounts for the unusual hydrophobicity of mycobacterial cells, mycobacterial cells, the low permeability of the cell wall and their intrinsic resistance to many antibiotics. Hence, bacterial cell-wall biosynthesis is a proven target for new antibacterial drugs.

The most important concept underlying antimicrobial therapy is selective toxicity, i.e. selective inhibition of the growth of the microorganism without damage to the host. Selective toxicity is achieved by exploiting the differences between the metabolism and structure of the microorganism and the corresponding features of human cells. For example, the biochemistry of a bacterial cell differs significantly from that of an animal cell. For example, bacteria may have to synthesize essential vitamins which animal cells can acquire intact from food. The bacterial cells must have the enzymes to catalyse these reactions. Animal cells do not, because the reactions are not required. The five main mechanisms by which antibacterial agents act are: the cell metabolism, the cell wall, the plasma membrane, protein synthesis and nucleic acid function [Patric, 2005].

1.7. Tuberculosis Treatment

1.7.1 Essential Antituberculosis Drugs

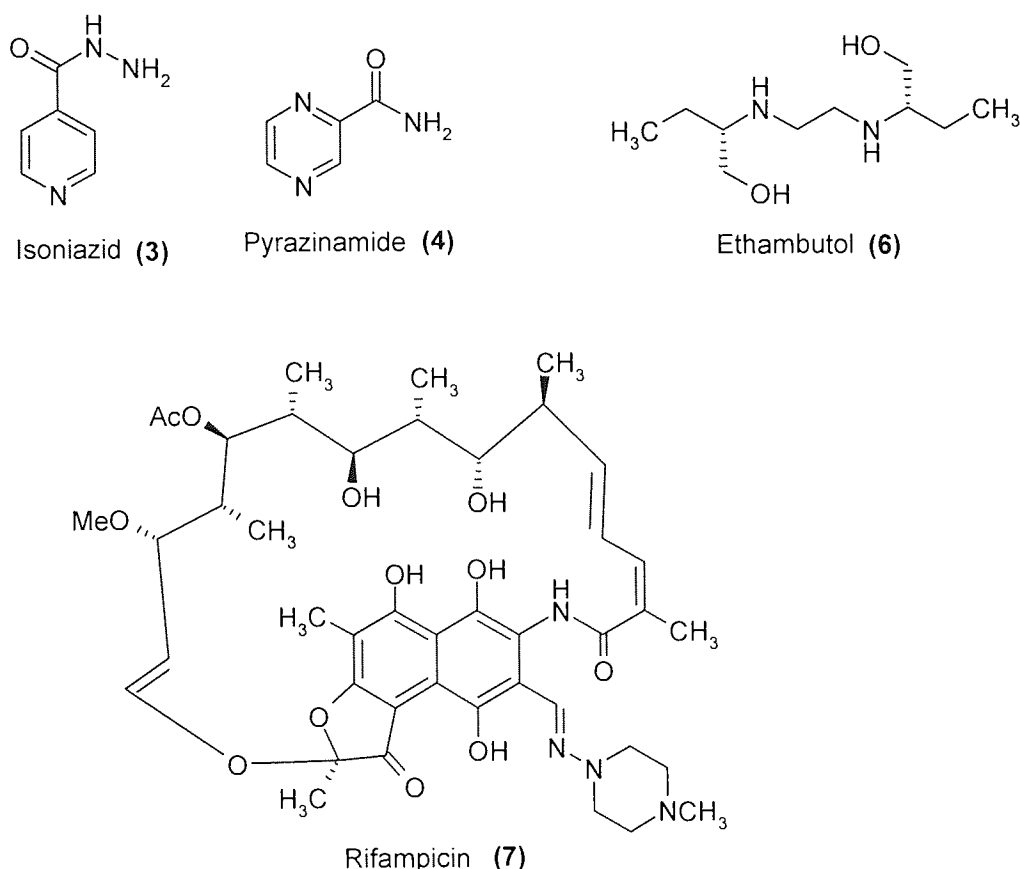


Figure 1.3: Essential antituberculosis drugs, Isoniazid (3), Pyrazinamide (4), Ethambutol (6) and Rifampicin (7).

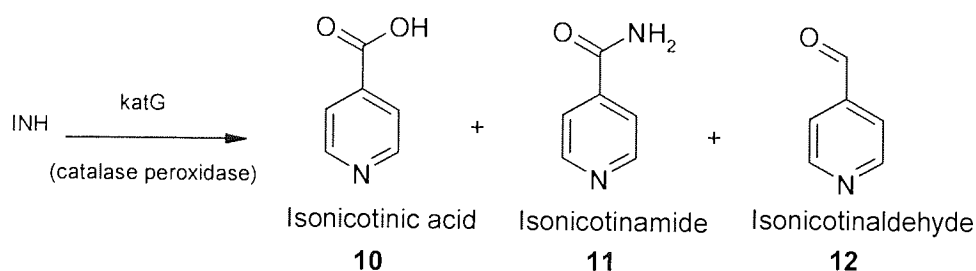
The current treatment against active TB is a combination of first-line drugs isoniazid (3) pyrazinamide (4), ethambutol (6) and rifampicin (7) (Figure 1.3) given in combination over six to nine months. The combinations are important to prevent the emergence of multiple drug resistant organisms, which can lead to an ineffective treatment.

1.7.2. Isoniazid (INH) (3)

Isoniazid was introduced in 1952 and is one of the major drugs worldwide used in the chemotherapy of tuberculosis. INH is water soluble and has an ability to penetrate into phagocytic cells and thus is active against both extracellular and intracellular organisms. It is generally recognized that INH is a prodrug which is activated by mycobacterial catalase-peroxidase (KatG). The INH activation mechanism is not completely understood, but it has been emphasized that KatG plays an important role in mycobacterial metabolism by protecting the bacterium against reactive oxygen intermediates and by increasing the chance of survival in the macrophage. This is achieved by reducing the toxic form of oxygen formed as a consequence of respiratory burst in phagocytic cells and by inhibiting the nitric oxide synthesis related to oxygen independent antimicrobial activity [Jahnsson and Schultz, 1994; Lee *et al*, 2001; Mohamed *et al*, 2004; Johnsson *et al*, 1995].

The KatG from mycobacteria also plays a central role in the mechanism of action of the anti-tuberculosis drug (INH) and therefore the development of one type of isoniazid-resistance is probably due to its role as a component of mycobacterial pathogens. The INH resistance in some strains is due to a loss of KatG activity caused by complete deletion of the *katG* gene or by point mutations as detected in the majority of resistant *M. tuberculosis* strains. The evidence that certain INH-resistant strains of mycobacteria have reduced *katG* activity suggests that this enzyme converts INH into isonicotinic acid and bacteriocidal agent. Johnsson and Schulstse found that although the major product of the reaction of the *katG* of *M. tuberculosis* with isoniazid is isonicotinic acid (10), but other products are also identified. For example, isonicotinamide (11) and pyridine-4-carboxaldehyde (12) were also produced Scheme (1.2).

Most recent work carried out by Kong and Lee [Kong and Lee, 2006] indicates that the major product of the *katG* of *M. biovis* was found to be Isonicotinamide. This could be due to the difference in the protein structure of *katG* of *M. tuberculosis* from *M. biovis*.



Scheme 1.2: Reaction products formed from catalase-peroxidase reaction with INH.

A large number of derivatives of nictotinaldehyde, isonictinaldehyde, and substituted isonicotinic acid hydrazide were made in search for greater potency (Figure 1.4). Isoniazid hydrazones were found to possess activity, but it was discovered that these activities were due to INH. Isoniazid hydrazones were converted to active INH in the gastrointestinal tract. Moreover, the substitution of the hydrazine portion of INH with alkyl substituents (Figure 1.4) resulted in a series of active and inactive derivatives. Substitution on the N2 position resulted in active compounds (R1 and R2 = alkyl; R3 = H), whereas any substitution of the N1 hydrogen with alkyl groups destroyed the activity (R1 and R2 = h;

R3 = alkyl). However, none of these changes produced compounds with the superior activity over INH [Fox and Gibas, 1956].

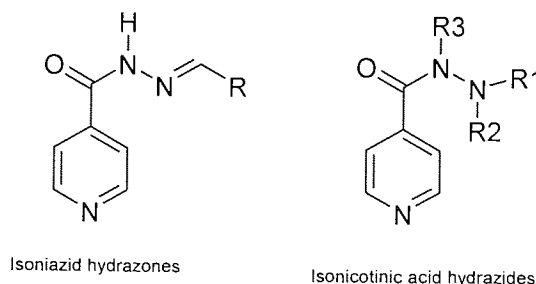
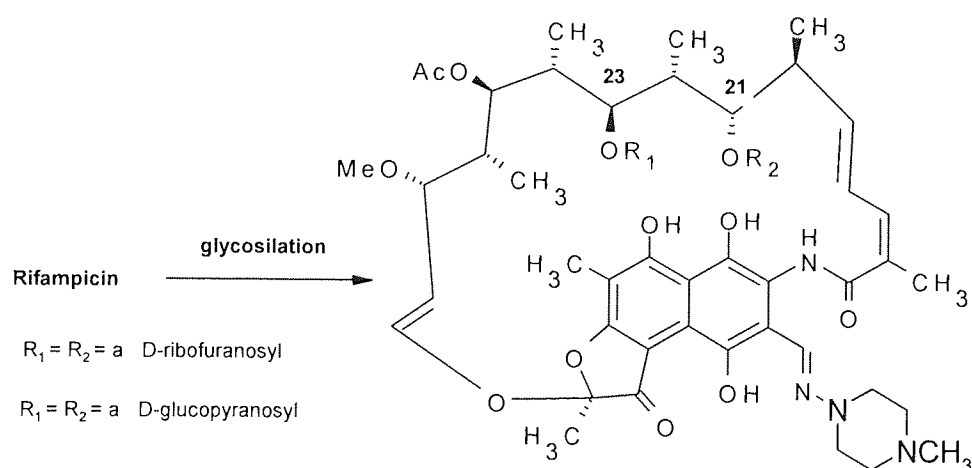


Figure.1.4: Derivatives of Isonicotinic Acid Hydrazide.

1.7.3 Rifamycins (7)

Rifamycins have been used for front-line therapy for over 30 years. Rifamycins are semisynthetic antibiotics which belong to the family of ansamycins. Rifampin (Figure 1.3) became clinically available in 1966 and it is responsible for the reduction of the duration of therapy. Rifampin binds strongly to the β -subunit of bacterial DNA-dependent RNA polymerase and thereby inhibits RNA synthesis. Resistance results from one of several possible point mutations in *rpoB*, the gene for the beta subunit of RNA polymerase. Human RNA polymerase does not bind rifampin and is not inhibited by it. The inactivation of rifampicin by different rifampicin-resistant bacteria is due to the glycosilation or phosphorylation in the C21 and C23 positions (**Scheme 1.3**) [Floss and Yu, 2005].



Scheme 1.3: Inactivation of rifampicin by different rifampicin-resistant bacteria.

Moreover, various rifamycin derivatives have been investigated or are under investigation for use in the prevention and treatment of tuberculosis (see **Figure.1.5**).

1.7.4 Rifapentine (13)

Rifapentine was first developed by Hoechst Marion Roussel under the trade name Priftin. This cyclopentyl-substituted rifampicin was introduced after a thirty year gap, in which no new TB drug was made. In 1998, a longer acting rifapentine received approval by the FDA in the USA as an anti-TB drug. It possesses the same broad spectrum activity as rifampin, but its elimination half-life is almost 4 fold greater than rifampin in humans. This can be explained in terms of higher lipophilicity, which facilitates tissue penetration of this drug, as well as the lack of biotransformation to antimicrobially inactive metabolites. Rifapentine, similar to Rifamycins, Rifampicin and Rifabutin is the inducer of cytochrome P450-3A (CYP3A) system and may affect antiretroviral drugs when used in HIV co-infection [Sharma and Mohan, 2004; Li *et al*, 1997].

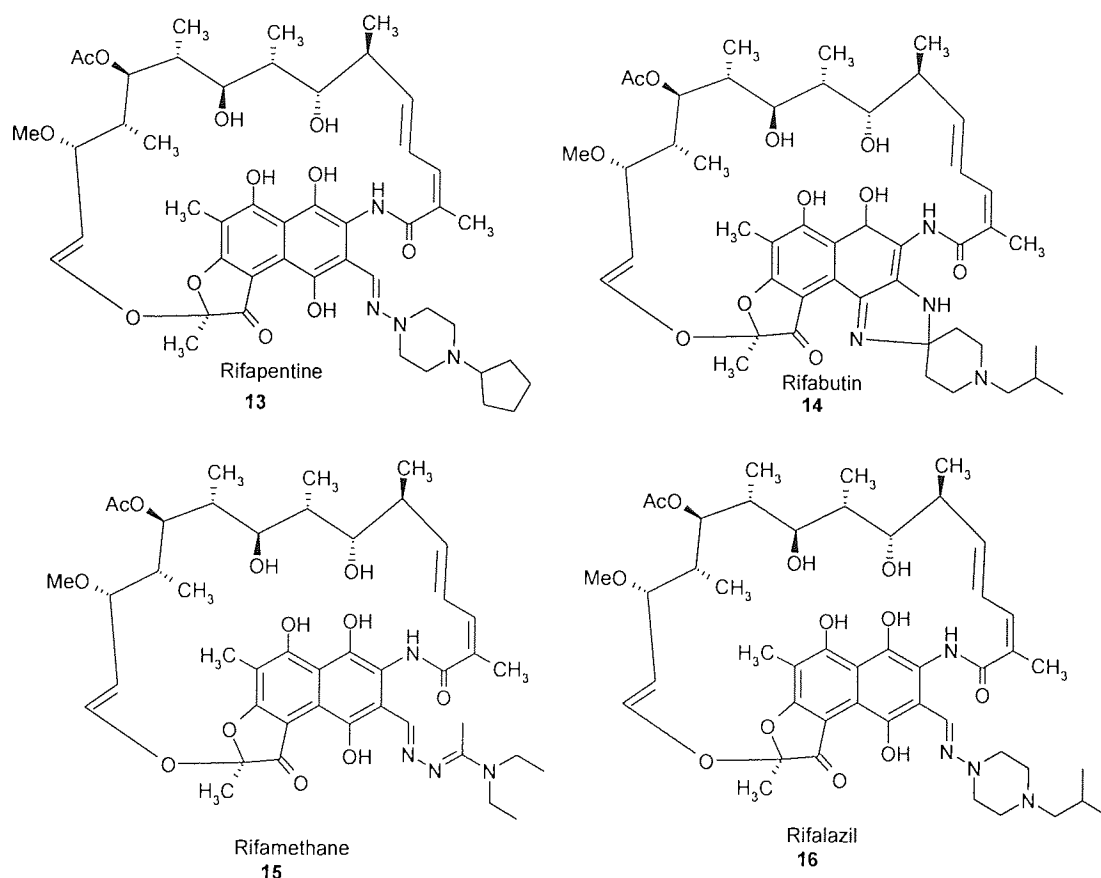


Figure 1.5: Structures of rifampicin derivatives.

1.7.5 Rifabutin (14)

Rifabutin was manufactured by Adria Laboratories, Columbus, Ohio, with the brand name Mycobutin. Rifabutin was approved by FDA for the prevention of MAC (*Mycobacterium avium* complex) disease in people with advanced HIV infection. It is used in combination with others drugs, such as ciprofloxacin (28), ethambutol (6) and amikacin (21) [Gangadharam *et al*, 1987; O'Brien *et al*, 1990].

1.7.6 Rifamethane (SPA-S-565) (15)

Rifamethane (SPA-S-565) is a new semisynthetic analog of rifampin, being manufactured by Societa Prodotti antibiotici (SPA), Milan Italy. The pharmacokinetic profiles of rifamethane were more favourable than that of rifampicin. Currently [Hudson, *et al*, 2003; Porkar, *et al* 1999], SPA is collaborating with Glaxo India to advance rifamethane into phase II trials.

1.7.7 Rifalazil (16).

The benzoxazinorifamycin, or (KRM) 1648) was synthesized at the Kaneka Corporation that possesses potent bactericidal activity against *M. tuberculosis* in vitro and *in vivo*. It was found to be 64-fold more active than rifampin against different *M. tuberculosis* strains. Rifalazil investigated in phase II clinical trials, however, due to severe side effects in the fourth day of the ongoing phase 1 trial, the development of rifalazil was terminated [Saito, *et al*, 1991].

1.7.8 Pyrazinamide (PZA) (4)

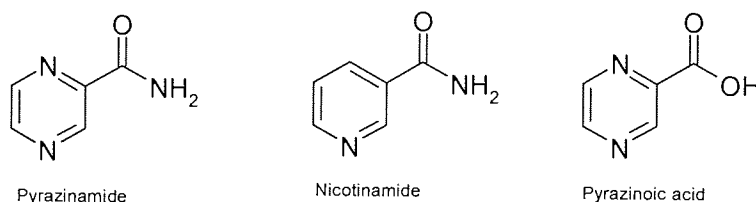


Figure 1.6: Structure of pyrazinamide (4), nicotinamide (17) and pyrazinoic acid (18)

Pyrazinamide 4 (PZA) is a bioisostere of nicotinamide 17 and was discovered while investigating analogs of nicotinamide. PZA is one of the frontline agents prescribed for treatment of *M. tuberculosis*. PZA is considered to be a prodrug of pyrazinoic acid (POA) 18 which is believed to be an active inhibitor of *M. tuberculosis*. It has been reported that PZA is less active against replicating bacilli, but more active against old non-growing bacilli [William and Lemke, 2002]. Activation of PZA to POA is regulated by an enzyme pyrazinamidase present in all PZA sensitive strains of *M. tuberculosis* [Scorpio and Zang, 1996]. Mutation in the pyrazinamidase gene (*pncA*) results in resistant strains of *M. tuberculosis*. Although PZA has been used clinically since the 1950s, its mechanism of action has not been fully understood. The fatty acid synthase-1 (FAS-1) has been proposed as a target of PZA in a study using *M. smegmatis* and 5-Cl-PZA. However, recently Zhang and co-workers proposed that POA disturbs energetic and inhibits membrane transport function in *M. tuberculosis* [Zang, *et al*, 2003] It is well documented that *M. tuberculosis* is uniquely susceptible to PZA, and this unique PZA susceptibility correlates with a deficient POA efflux mechanism in this organism, whereas the naturally PZA resistant *M. smegmatis* has a highly active POA efflux mechanism that quickly extrudes POA out of the cell.

Structural modification of PZA i.e. substitution on the PZA ring or the use of alternative heterocyclic aromatic rings have given compounds with reduced activity [Kushner, *et al*. 1956]. However, two analogs of PZA namely *tert*-butyl 5-chloropyrazinamide (19) and 2-(2-methyldecyl) 5-chloropyrazinamide (20) Figure (1.7) has been prepared with improved activity. The requirements for successful analogs included the provision for hydrophilicity to allow sufficient plasma concentrations

such that the drug can be delivered to the site of infection. In addition, lipophilicity was also considered. This is to allow penetration into the mycobacterial cell and susceptibility to hydrolysis such that the prodrug is unaffected by the extracellular enzymes, but readily hydrolysed at the site of action [Bergmann, *et al.* 1996].

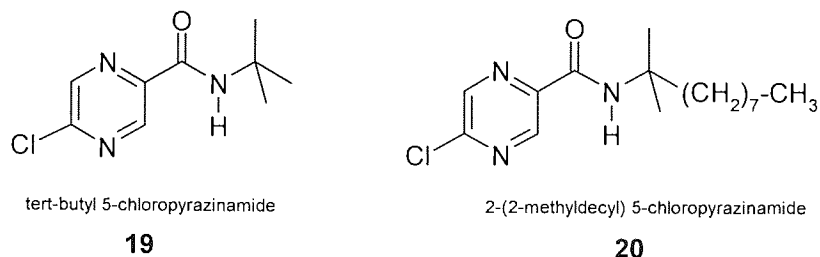
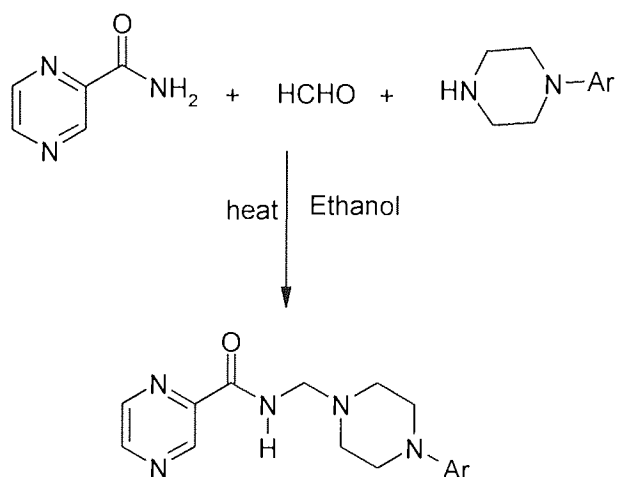


Figure. 1.7: Structure of *tert*-butyl 5-chloropyrazinamide (**19**) and 2-(2-methyldecyl)5-chloropyrazinamide (**20**)

More recently, Mannich base derivatives of PZA have been prepared with improved antimycobacterial activities (Scheme 1.4). Among the synthesised compounds, 1-cyclopropyl-6-fluoro-1,4-dihydro-8-methoxy-7-(3-methyl-4-(pyrazine-2-carboxamido)methyl-piperazin)-4-oxoquinoline-3-carboxylic acid (**21**), Figure (1.8), was found to be the most active compound *in vitro* with MIC of 0.39 and 0.2 $\mu\text{g/mL}$ *M. tuberculosis* H37 RV(MTB) and MDR-TB respectively [Sriram, *et al.* 2006]. The improved mycobacterial activity was thought to be associated the increasing lipophilic character of the compounds. The lipophilicity of the drug is well known to play an important role in the penetration of these compounds into bacterial cells [Wolucka, *et al.* 1994].



Scheme 1.4: Mannich reaction, preparation of pyrazine derivatives.

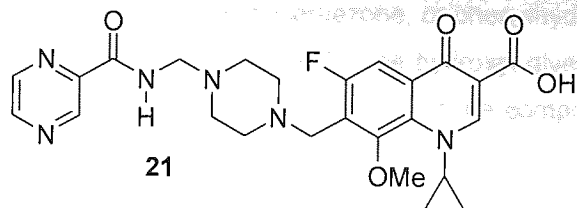


Figure 1.8: Structure of 1-cyclopropyl-6-fluoro-1,4-dihydro-8-methoxy-7-(3-methyl-4-(pyrazine-2-carboxamido)methyl)piperazin)-4-oxoquinoline-3-carboxylic acid (**21**).

1.7.9 Ethambutol (6)

Ethambutol figure (1.3) first reported by Wilkinson and co-worker in the early 1961s, [Thomas *et al*, 1961] is one of the few long-known and reliable front-line antimycobacterial chemotherapeutic agents. The mechanism of action of EMB remains unknown, recently , it could be shown that its biological activity is due to the inhibition of mycobacteria arabinofuranosyl transferases responsible for glycosylation steps in the biosynthesis of lipoarabinomannan (LAM) and arabinogalactan (AG) which are constituents of the mycobacterial cell wall [Wolucka, *et al*. 1994]. A large number of analogs of EMB have been prepared, for example, by extending the ethylene diamine chain, replacing the nitrogen or increasing the size of the nitrogen substituents, moving the location of the alcohol groups all of these changes have abolished antimycobacterial activities [Hausler, *et al*. 2001].

1.7.10 Streptomycin (1)

Streptomycin was isolated by Waksman in 1944, it was the first drug used successfully to treat tuberculosis. Unfortunately, its ototoxicity and the rapid development of resistance have tended to modify its usefulness, and although it still remains a front-line drug against tuberculosis it is usually used in combination with isoniazid and p(4)-aminosalicylic acid. Streptomycin is hydrophilic in nature and is able to diffuse across the outer membrane of *M. tuberculosis* and ultimately penetrate the cytoplasmic membrane through an electron dependent process. It is known that the streptomycin inhibits protein synthesis. Through studies of the mechanism of drug resistance it has been proposed that streptomycin induces a misreading of the genetic code and thus inhibits translational initiation.

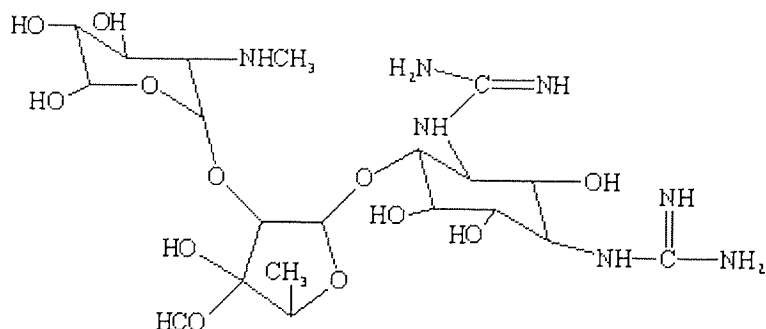


Figure 1.9: Structure of Streptomycin (1).

Modification of the α -streptose portion of streptomycin structure has been extensively studied. For example, reduction of the aldehyde to the alcohol resulted compound dihydrostreptomycin, which had a similar antibacterial action but was more toxic. Oxidation of the aldehyde to a carboxyl group or

conversion to Schiff base derivatives (oxime, semicarbazone, or phenylhydrazone) showed no activity. Oxidation of the methyl group in α -streptose to a methylene hydroxyl gives an active analog but with no advantage over streptomycin modifications in other parts of the compound resulted in decreased activity [Finken, *et al*, 2001].

1.8 Second-line Antituberculosis Drugs

Second-line drugs are usually characterized by lower efficacy or greater toxicity. However, the increase in AIDS-association infections and outbreaks of infections sustained by multidrug-resistant (MDR) *M. tuberculosis* indicate the need for new effective anti-tuberculosis drugs and for alternative therapy regimens. Several tuberculosis control programs have been proposed by WHO to prevent the spread of tuberculosis and MDR *M. tuberculosis* infection. For example, use of multidrug regimens. Several drug combinations have been studied in order to increase the therapeutic efficacy and to reduce the toxicity of anti-mycobacterial agents [Williams and Lemke, 2002]. The drugs normally used to treat MDR-TB are amykacin (**22**), kanamycin (**23**), ethionamide (**24**), protionamide (**25**), cycloserine (**26**), ciprofloxacin (**27**), capreomycin (**28**), ofloxacin (**29**) and *p*-aminosalicylic acid (**30**) (Figure 1.10).

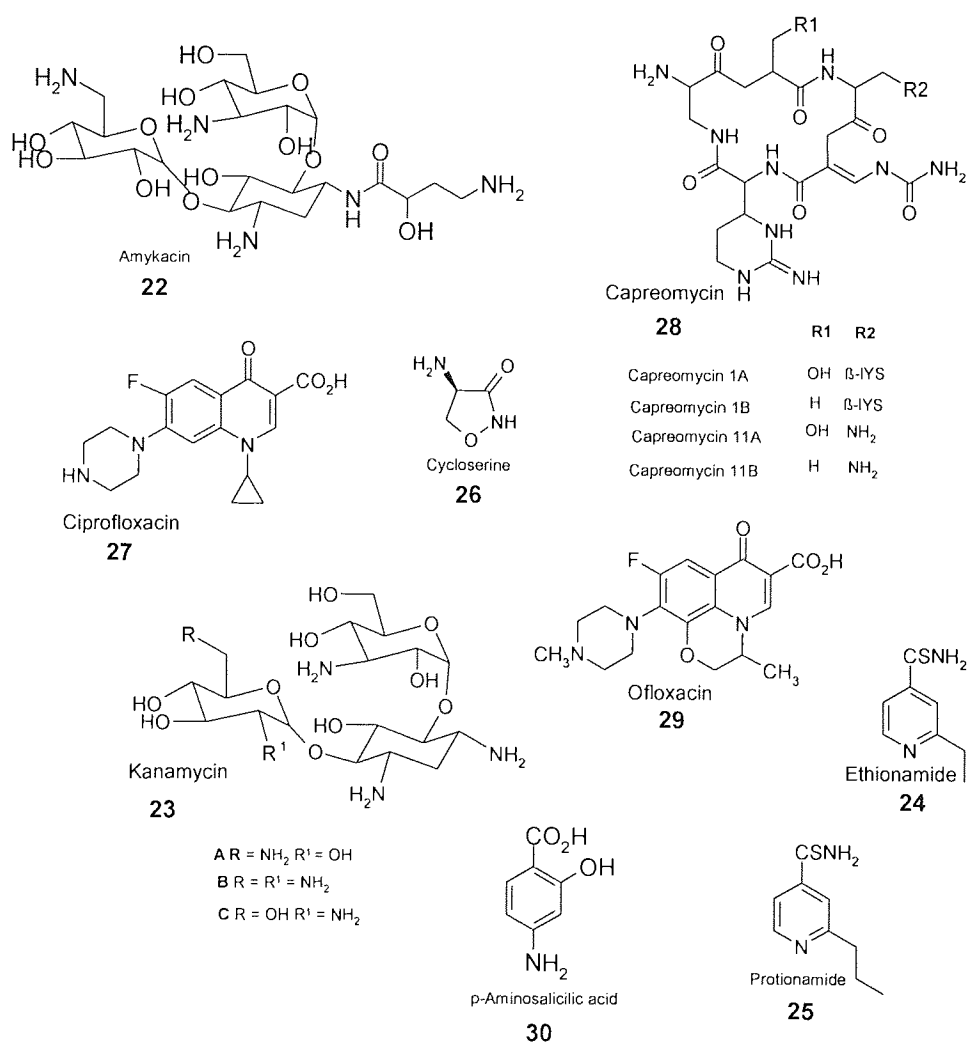
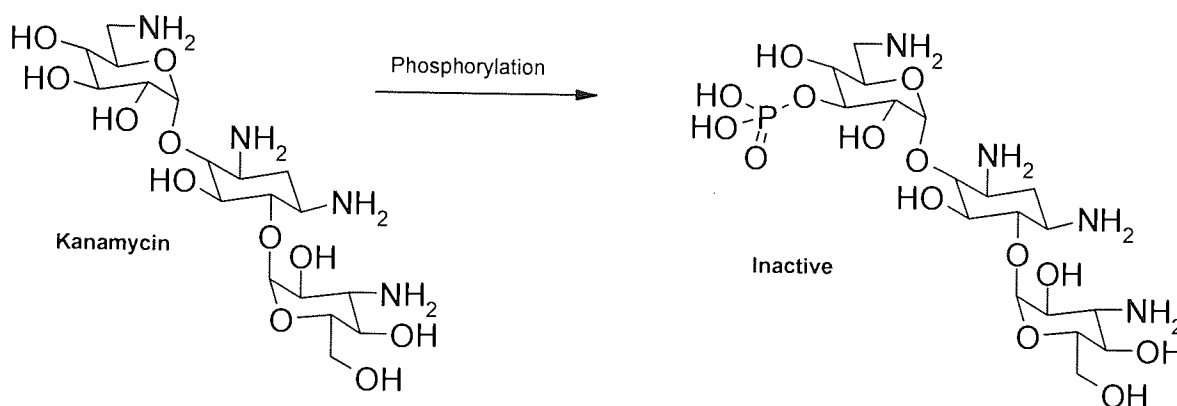


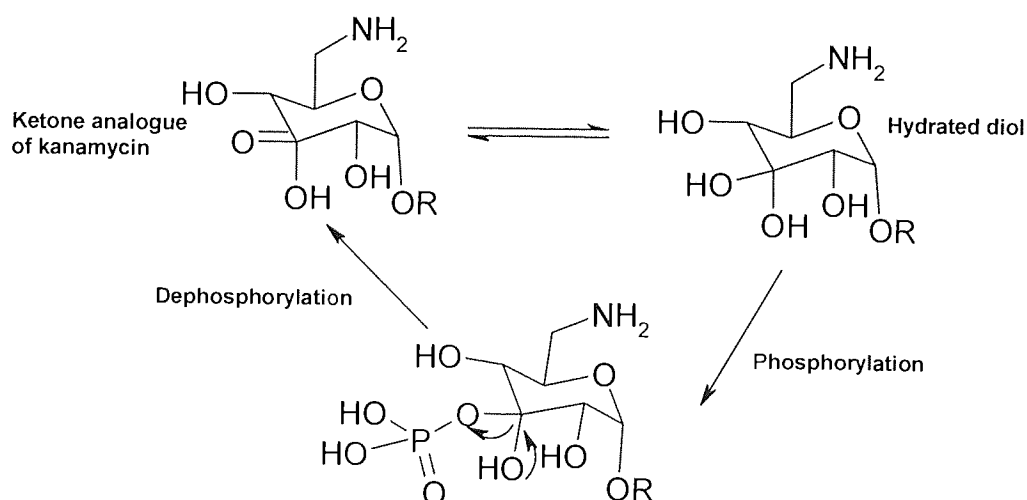
Figure 1.10: Second-line antituberculosis drugs. Amykacin (**22**), Capreomycin (**28**), Ciprofloxacin (**27**), Cycloserine (**26**), Kanamycin (**23**), Ofloxacin (**29**), Ethionamide (**24**), *p*-Aminosalicylic acid (**30**) and Protionamide (**25**).

1.8.1 Kanamycin (23)

Kanamycin was isolated from *streptomyces kanamyceticus* and consists of three components A, B and C, with A being predominate. Kanamycin is no longer used since resistant bacteria can phosphoralate one of the hydroxyl groups present. However, an active analogue has been synthesized which replaces the susceptible alcohol with a ketone. This ketone is in equilibrium with hydrated gem-diol. When phosphorylation occurs on the diol, the phosphate group formed acts as a good leaving group and the ketone is regenerated (**Scheme 1.5**). *In vitro* tests indicated that this agent was active against strains of bacteria which are resistant to kanamycin [Patric, 2005].



Scheme 1.5: Resistance to kanamycin



Scheme 1.6: Analogue of kanamycin resistant to resistance mechanism.

1.8.2 p-aminosalicylic acid (30)

For many years, p-aminosalicylic acid (PAS) was considered a first-line drug for the chemotherapy of tuberculosis and was generally included in combination regimens with isoniazid and streptomycin. Introduction of more effective agents such as rifampin and ethambutol have limited its uses. The mechanism of antibacterial action of PAS is believed to prevent the incorporation of p-aminobenzoic acid (PABA) into the dihydrofolic acid molecule catalyzed by the enzyme dihydrofolate reductase. Structural studies have indicated that the amino and carboxyl groups must be free and *para* to each

other for an effective activity. For an optimal activity the hydroxyl group was preferred to be *ortho* to the carboxyl group [Williams and Lemke, 2002].

1.8.3 Cycloserine (26)

D-Cycloserine (DCS) is produced by *Streptomyces garyphalus* which has a broad spectrum activity. It is a peptidoglycan inhibitor and acts within the cytoplasm to prevent the formation of D-Ala-D-ala. It does this by mimicking the structure of D-Alanine (**Figure 1.11**) and inhibiting the enzymes L-alanine racemase which is responsible for racemizing L-alanine to D-alanine and D-ala-D-Ala ligase responsible for linking two D-Alanine units together. Although very effective against *M. tuberculosis*, DCS is rarely used in the management of this infection due to its high toxicity.

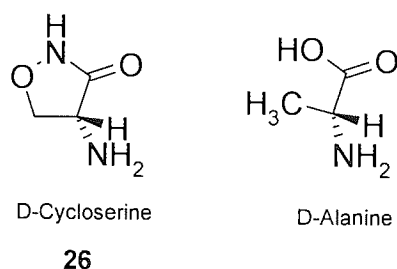


Figure. 1.11: structure of D-Cycloserine (**26**) and D-Alanine

Nevertheless, the worldwide resurgence of tuberculosis, the emergence of multidrug-resistant tuberculosis and the problematic use of available drugs required to treat these infections have resulted in the proposal that DCS now be considered as an alternative therapy [David, 2001].

1.8.4 Ethionamide (ETH) (24) / Prothionamide (PTH) (25).

Ethionamide (ETH) structurally related to INH (**3**) is also a prodrug that is activated by the the enzyme EthA and inhibits the same target InhA as (**3**) of the mycolic acid synthesis pathway [Banerjee, *et al.*, 1994]. ETH is considered a secondary drug for the treatment of tuberculosis. It is used in the treatment of isoniazid-resistant tuberculosis or when the patient is intolerant to isoniazid and other drugs. Prothionamide (**25**) shares almost identical activity as ETH (**24**). Due to the severe side effects (**24**) is no longer listed as being a suitable antitubercular drug [Morlock, *et al.* 2003].

1.9 The promising candidate drugs against TB.

The increasing incidence of *M. tuberculosis* strains resistant to one or more of the standard first-line agents intensifies the need for the identification of novel targets and new drug development. Several promising drug classes are under development including long-lastin rifamycin fluoroquinolones, oxazolidinones nitroimidazoles and others.

1.9.1 Fluoroquinolones

Leshner and co-worker have reported the antibacterial properties of Nalidixic acid (Figure 1.12) in 1962 [Leshner, *et al.* 1962]. Since then a vast number of these compounds have been synthesized as

antibacterial agents. Fluoroquinolones (7-fluoro-4-oxo-1,4-dihydro-quinoline-3-carboxylic acid), (**Figure 1.13**) are an important class of fluorine-containing compounds. This class of antibacterial agents has a wide antibacterial spectrum, though differences exist between compounds in their potency against Gram-positive bacteria, non fermentative bacteria and anaerobic organism [Silva, *et al.* 2003].

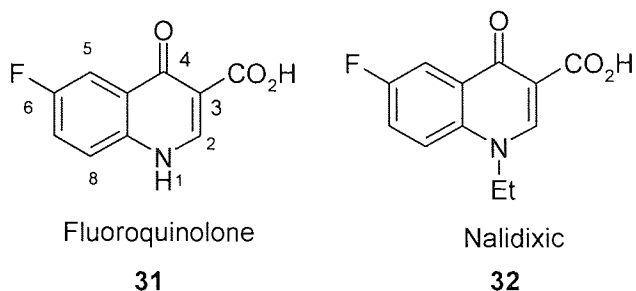


Figure 1.12: Basic structure of fluoroquinolones nucleus (**31**) and nalidixic acid (**32**).

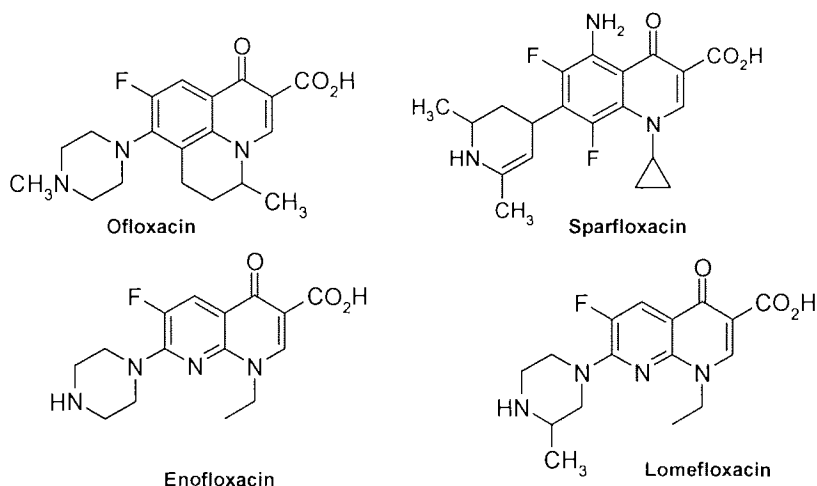


Figure 1.13: Structure of Ofloxacin (**33**), Sparfloxacin (**34**), Enofloxacin (**35**) and Lomefloxacin (**36**).

A large number of fluoroquinolones (**Figure 1.13**) has been synthesized with further improvement, such as the solubility, antimicrobial activity, prolonged serum half-life and lesser adverse side effects. As examples, this can be mentioned ciprofloxacin (**28**), ofloxacin (**33**), sparfloxacin (**34**), enofloxacin (**35**) and lomefloxacin (**36**) [JI, *et al.*, 1995].

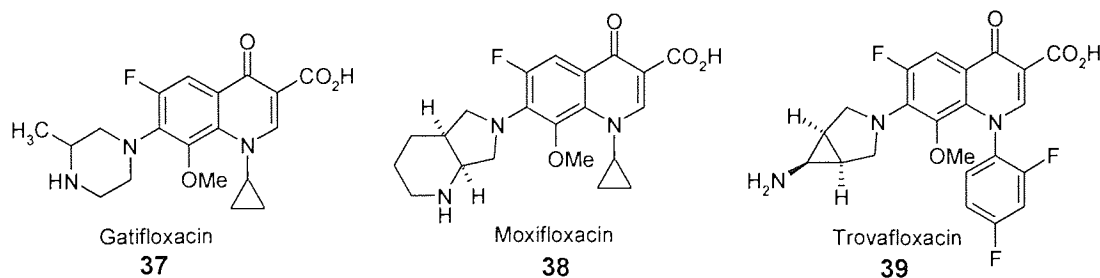


Figure. 1.14: Structure of gatifloxacin (**37**), moxifloxacin (**38**) and Trovafloxacin (**39**).

At present more attention has been paid to the newer fluoroquinolones (**Figure 1.14**) such as gatifloxacin (**37**) [Sriram, *et al.*, 2006], mexifloxacin (BAY12-8039) (**38**) [Miyazaki, *et al.* 1999] and trovafloxacin (**39**). These fluoroquinolones are classified as fourth generation fluoroquinolones due to their fewer toxic effects, improved pharmacokinetic properties, extensive and potent activity against Gram-positive and Gram-negative bacteria including resistant strains, when compared with the earlier fluoroquinolones. Their advantages can be explained in terms of their mechanism of action. For example, the inhibition of bacterial multiplication caused by fluoroquinolones is due to the inhibition of two bacterial enzymes: DNA gyrase (topoisomerase II) and topoisomerase IV enzymes. DNA gyrase is an essential enzyme involved in the replication, transcription and repair of the bacterial DNA. For the Gram-negative organisms, DNA gyrase is the primary target, while in the Gram-positive bacteria, topoisomerase IV is the most affected [LA, 2005]. The efficacy of the new fluoroquinolone in comparison with the earlier fluoroquinolones is due to their dual activity inhibiting both DNA gyrase bacterial type II and topoisomerase IV, which also limits the emergence of fluoroquinolones resistance. The above mentioned biological effects have been attributed to the (C8-OMe) methoxy group at the C-8 position [Tomc, *et al.* 2000]. N-1 cyclopropyl and strongly electro withdrawing fluorine at C-6 were also considered to be an important component of the fluoroquinones drug [Ranau, *et al.* 1996].

1.9.2 Oxazolidinones

The oxazolidinones are a new class of totally synthetic antibacterial agents, active against a variety of clinically important susceptible and resistant Gram positive organism, such as methicillin-resistant *Staphylococcus aureus* (MRSA) and vancomycin-resistant *Enterococcus faecium* (VRE) and penicillin-resistant *Streptococcus pneumoniae* (PRSP). The mechanism of action of oxazolidinone is associated with inhibition of protein synthesis but at a stage different from that of other protein inhibitors.

The oxazolidinones were originally discovered by researchers at DuPont in the late 1980s (Figure 1.15), but the development of DUP-721 (**40**) and DuP-105 (**41**), the drug candidate emerged from early studies, was terminated following Phase 1 clinical trials. In spite of these problems, Upjohn Laboratories and Pfizer continued to study this class of compounds and in 1996, two non-toxic U-100592 (**42**) and U-100766 (**43**) were reported. They were named eperzolid and linezolid respectively [Zurenko *et al.*, 1996; Barbachyn *et al.* 1996; Brickner, *et al.* 1996; Bozdgan and Appelbaum, 2004, Sbardella, *et al.* 2004].

1.9.3 Linezolid (43)

Linezolid was approved by FDA in 2000 and is used to treat infections caused by Gram-positive strains, which are resistant to different antibacterial drugs, such as vancomycin and penicillin. It has reported to possess an effective activity against MDR-TB. Oxazolidinone PNU-100480 (**44**) (Figure 1.15 below) containing thiomorpholine moiety in place of the morpholine unit has been reported to be particularly active against *M. tuberculosis*. A study conducted by Cynamon and co-workers have

confirmed that compound PNU-100480 (**44**) was comparable to isoniazid (**3**) and more active than linezolid (**43**) [Cynamon, *et al.* 1999].

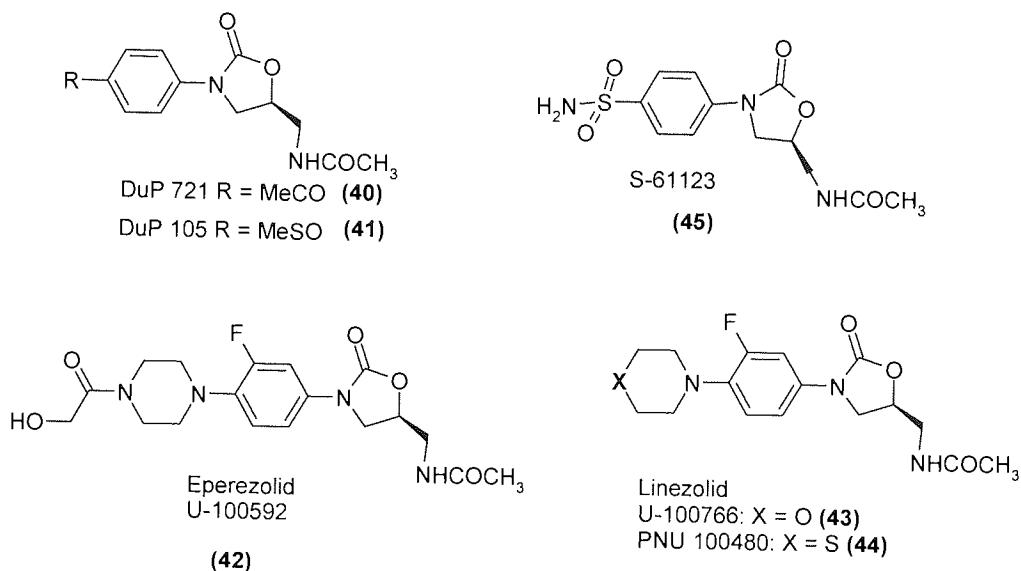


Figure 1.15: The structures of some important linezolid.

1.9.4 Nitroimidazole

Nitroimidazoles were developed by the Ciba-Geigy (Novartis). 5-nitroimidazole derivative CGI 1734 (**46**) (Figure 1.16) showed considerable potential for the treatment of tuberculosis [Ashtekar *et al.*, 2005]. This compound inhibited drug-susceptible and multidrug-resistant strains of *M. tuberculosis* and its activity was superior to streptomycin (**1**), ciprofloxacin (**27**), and the oxazolidinone DuP 721 (**40**). However, despite the above mentioned properties, its development was aborted because of the changes in the company [Lenaerts, *et al.* 2005; Hudson, *et al.* 2003].

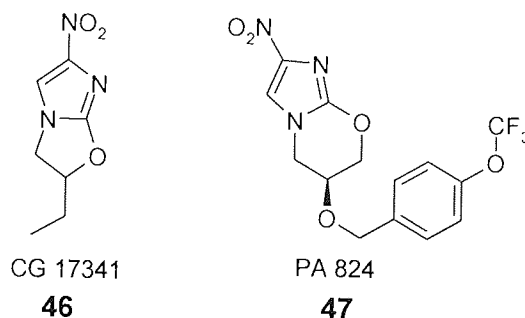


Figure 1.16: Structure of CG-17341 (**46**) and PA 824 (**47**).

Furthermore, PA-824 (**47**) Fig. 1.16 the 5-nitroimidazole derivative, nitroimidazopyrans has been developed by PathoGenesis Corporation in 1995 for cancer treatment [Stover *et al.*, 2000]. However, due to its promising TB activity in 2002 the Global Alliance for TB Drug Development licensed PA-824 and related nitroimidazole compounds for further development. PA-824 shows an excellent sterilize activity compared with isoniazid and rifampin. Due to its important results, PA-824 is under clinical phase [Ashtekar, *et al.* 1993].

1.9.5 Other Classes of Compounds:

1.9.5.1 (a) Azoles

Although the majority of the Structural Activity Relationship (SAR) studies have been done with the above mentioned classes of antimycobacterial agents, there are a number of other classes of compounds which also have antitubercular activity will be briefly mentioned below (**Figure 1.17**). These include azoles (**48**) which are predominantly anti-fungal agents; and recently developed, several analogues of a phenazinamine. For example, B4157 (**49**), closely related to the antileprosy drug clofazimine (**50**) [Reddy, *et al*, 1996; Hudson *et al*, 2003].

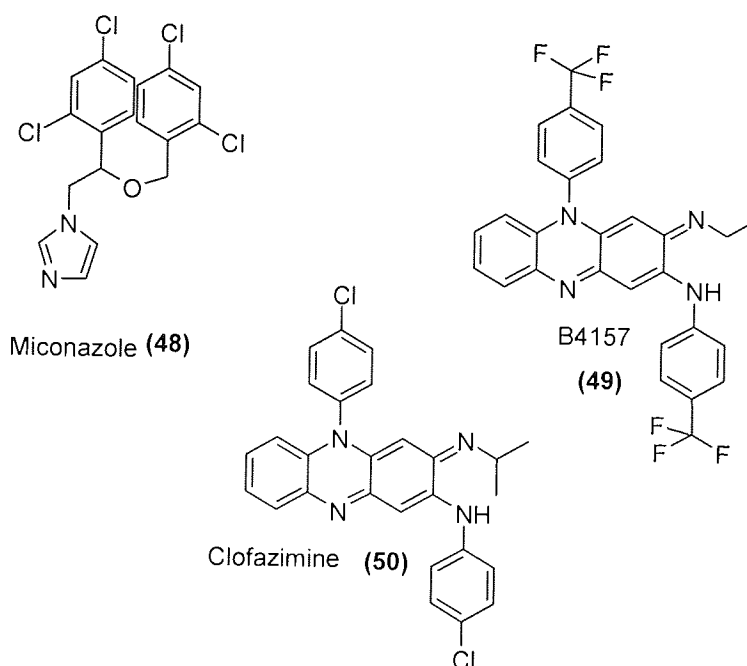


Figure 1.17: The structures of Miconazole (**48**), B4157 (**49**) and Clofazimine (**50**).

1.9.5.2 (b) Amidrazone derivatives

1.9.5.2.1 Discovery of Amidrazones.

Amidrazone derivatives have been described for their *in vitro* antitubercular activity for five decades. Bertrand *et al.* identified the antitubercular activity of some hydrazines in 1956 [Bertrand, *et al.* 1956]. Since then, a vast number of carboxamidrazone derivatives have been synthesized and tested for antibacterial activity. Further investigation into this class of compounds was carried out by Mamalo and coworkers [Mamalo *et al*, 1992, 1993, 1996 and Banfi *et al*, 1993]. They discovered that these compounds have a range of biological and therapeutic actions including antitubercular and antifungal [Vio, *et al*, 1989]. Furthermore, their study showed that some of the *N*¹-benzylideneheteroaryl-carboxamidrazones (Figure 1.18) showed an interesting *in vitro* antimycobacterial activity against

some strain of *Mycobacterium tuberculosis*, some of which were resistant to isoniazid, rifampicin and ofloxacin.

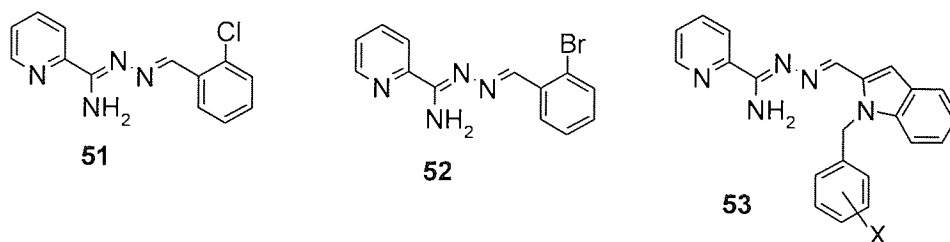


Figure 1.18: The most active compounds discovered by Mamolo *et al.*

The work demonstrated by the Mamolo group produced interesting results, but only a limited number of compounds were made. The Mamolo group drew their conclusions from a small data set of *N'*-benzylideneheteroarylcarboxamidrazones, for example, aldehydes used by aforementioned group only displayed a limited variety of aryl-substituent, such as methyl, methoxy, halogen, nitro and cyano group. However, this work was further investigated at Aston University [Billington *et al.*, 1998, 1998, 2000]. A significant number of aldehydes were incorporated into the study. A large library of carboxamidrazone derivatives was synthesised using robotic techniques. Some of the synthesised compounds (**Figure 1.19**) approach the potency of isoniazid (INH) for antituberculosis bacterial test [Coleman *et al.*, 1999, 1999, 2000, 2001].

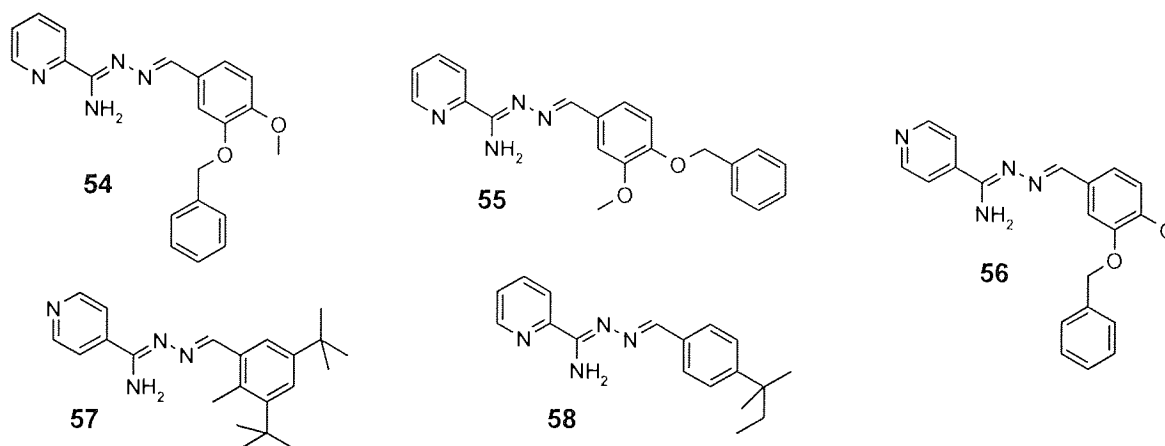


Figure 1.19: The most active compounds discovered by Billington *et al.*

1.9.5.2.2 General Structural Relationship/Requirement for Antimycobacterial Activity

In the light of the progress made in new drug therapies for *M. tuberculosis*, a number of amidrazone derivatives (Figure 1.20) with some of the key features required for the desired biological activity were

identified from aforementioned studies Their investigations indicated that the amidrazone moiety **60** was a necessary structural feature for biological activity.

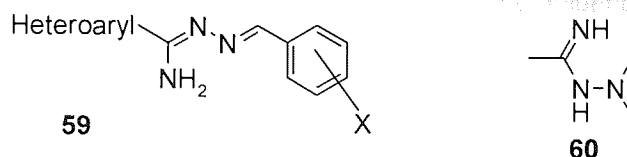


Figure 1.20: The general structure of the N^1 -benzylideneheteroarylcarboxamidrazones (**59**) and amidrazone moiety (**60**).

The second major structural feature considered to achieve the desired biological activity was the nature of the substituted aryl moiety, connected to amidrazone moiety. Preferably, hydrophobic substituent at the *ortho* position was found to be necessary for penetration of the highly lipophilic *Mycobacterium* cell wall [Mamalo *et al* 1992, and Billington 1998].

The presence of a heteroaryl ring, such as pyridine-2- or pyridine-4- was also important for the biological activity. This was demonstrated by Rathbone and Tims [unpublished work]. They investigated the influence of non-nitrogen containing ring on the biological activity of these compounds. In order to keep an electron-withdrawing functionality at the 2- or 4- position, the compounds 2-nitrobenzonitrile (**61**) and 2-chlorobenzonitrile (**62**) were chosen (Figure 1.21) and prepared in the same manner as heteroarylcarboxamidrazones (see section 5.2). It was discovered, that the reaction with 2-chlorobenzonitrile did not proceed. Probably, the chloro-group did not have the necessary electron-withdrawing capacity compared to nitro-group. 2-Nitrobenzenecarboxamidrazone was condensed with a several aldehydes that had previously afforded activity to pyridine-2-carboxamidrazones. The biological activity of 2-nitrobenzenecarboxamidrazone derivatives was lost compared to pyridine-2-carboxamidrazone derivatives indicating that heteroaryl ring was also essential for the biological activity.

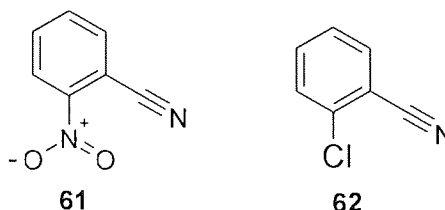


Figure 1.21: The structure of 2-nitrobenzenecarboxamidrazone (**61**) and 2-chlorobenzonitrile (**62**) used in comparison study to see if heteroaryl ring was important for biological activities [Tims, 2002].

Although numerous structural-activity relationship (SAR) studies have been carried on N^1 -benzylideneheteroarylcarboxamidrazone compounds with antitubercular activity [Rathbone *et al*, 2000, 2006; Mamalo *et al*, 1996; Schwalbe, 1998, 1999, 2000 and Coleman *et al*, 2003], there is still scope to design new classes of carboxamidrazone compounds with the desired activity. For example the possible replacement of the imine functional group with other functional groups, such as amide, urea and sulphonamide had not been examined. Hence there was an opportunity to exploit this fact in the

work undertaken here (Figure 1.22). We also proposed that series of novel carboxamidrazone derivatives such as pyridinium salts, methyl-ketimines, pyridine nitrogen oxide and metal complexes (Figure 1.23) were likely to be attractive as synthetic targets. The influence of the various pyridine-bases moiety on the biological activity will also be investigated.

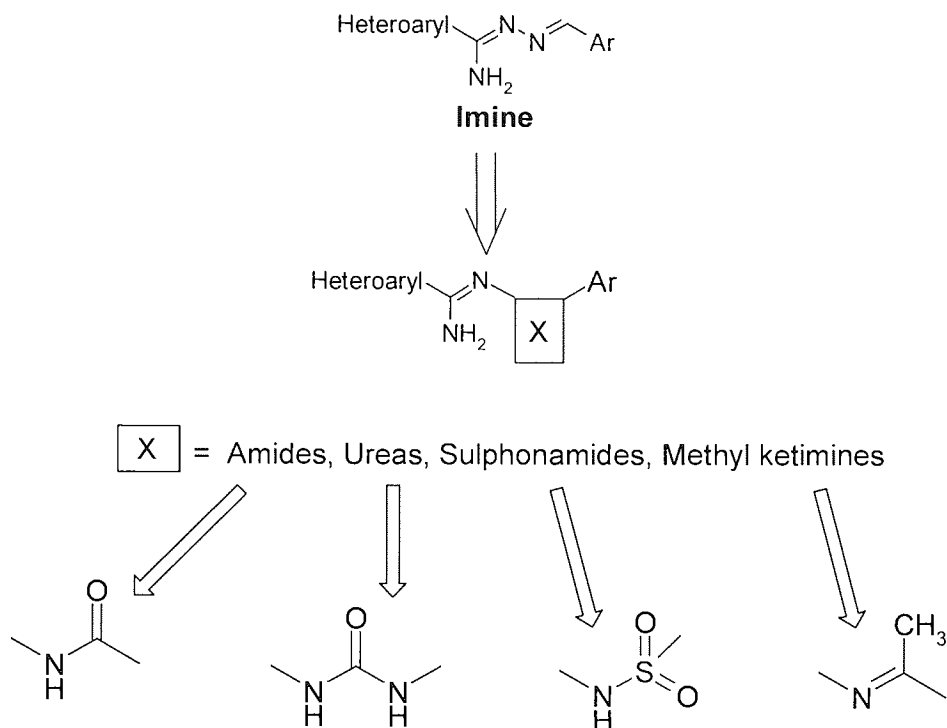


Figure 1.22: The structures of the proposed new classes of heteroarylcarboxamidrazone.

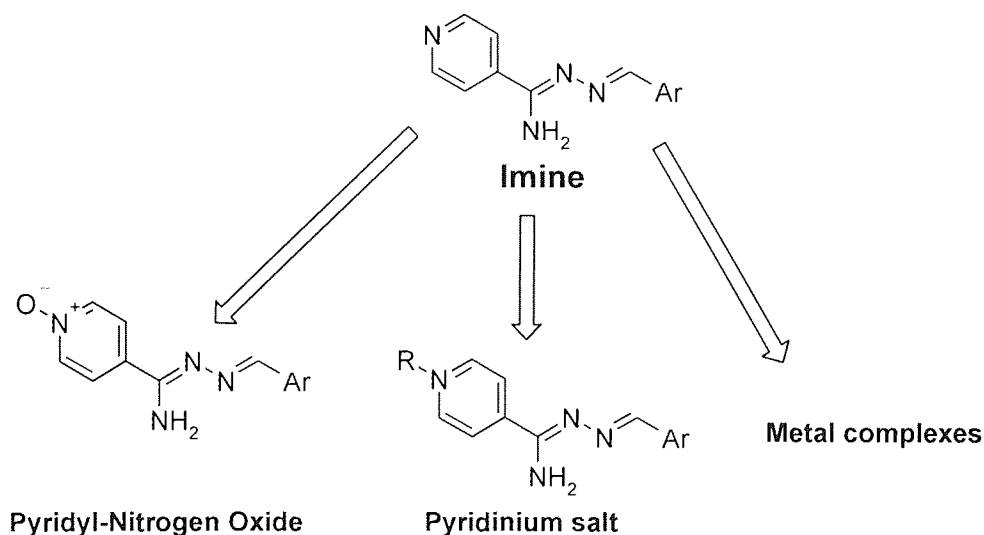


Figure 1.23: The structures of the proposed *N*¹-benzylideneheteroaryl-carboxamidrazone derivatives.

Once these compounds have been synthesized the biological activity will be measured. There are three possibilities: (i) the compound will have less biological activity, (ii) will have equal activity and (iii) will have more activity. In view of this rationale a scientific study was undertaken, the aim of which is given in the following of bullet points.

1.10 Aims and objective

- To investigate the effect upon the biological activity of modification of the imine function of the parent compounds.
- To investigate the effect upon the biological activity of modification to the pyridyl ring.
- To investigate the effect upon the biological activity of conversion of the parent N¹-benzylideneheteroarylcarboxamidrazones to metal complexes.
- To identify potentially active antimicrobial agents.
- To identify common trends characterised by various derivatives of the heteroarylcarboxamidrazones
- To examine the effects of modification of the pyridyl ring in the form of alteration of the nitrogen and N-oxide formation
- To characterise the novel compounds by a variety of spectroscopic methods.
- To screen and evaluate the biological activity of a series of synthesized compounds.

1.11 Conclusions

Tuberculosis TB remains the leading cause of mortality due to the bacterial pathogen, *mycobacterium tuberculosis*. The synergy between tuberculosis and the AIDS epidemic, and the surge of multidrug-resistant clinical isolates of *M. tuberculosis* have reaffirmed tuberculosis as a primary public health threat. No new antimycobacterial drugs with novel mechanisms of action have been developed in the past 40 years. Therefore, there is an urgent need for TB drugs with fewer toxic side effects, improved pharmacokinetics properties, extensive and potent activity against Gram-positive and Gram-negative bacteria, including resistant strains and drugs able to reduce the total duration of treatment.

Due to the demonstrated importance of the need for for new drugs in this field, and as a part of an ongoing programme for the search for a new anti-tuberculosis drug candidate at Aston University, the aim of this research is to modify a series of previously active parent carboxamidrazones and synthesise new classes of carboxamidrazones. In the following chapters of this thesis the syntheses of a variety of carboxamidrazones compounds will be discussed.

2 Preparation of carboxamidrazones derivatives

2.1 Automated and traditional synthesis of carboxamidrazones derivatives.

In a search for novel antimycobacterial structures, a series of amidrazone derivatives was prepared using traditional synthesis and automated liquid handling. A large number of compounds was synthesized and subjected to microbiological screening in order to find active molecules and to elucidate the structure property relationships.

2.2 The heteroarylcarboxamidrazones building blocks

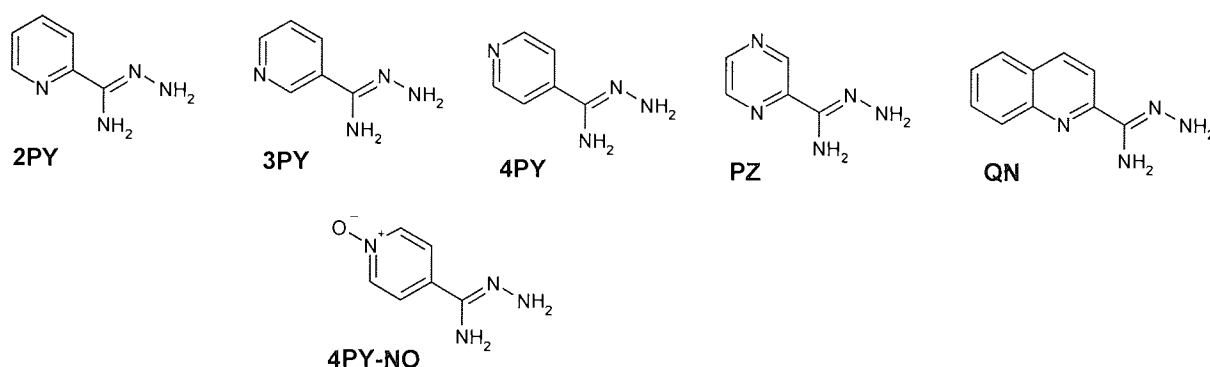
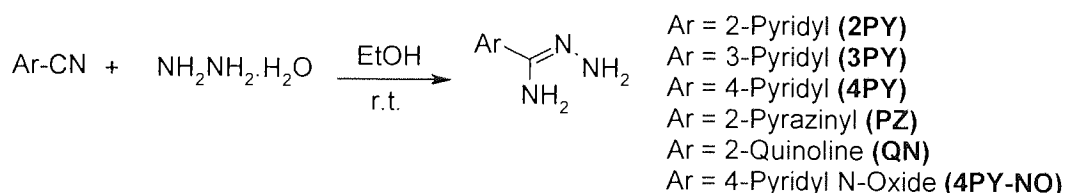


Figure 2.1: Heteroarylcarboxamidrazone building blocks

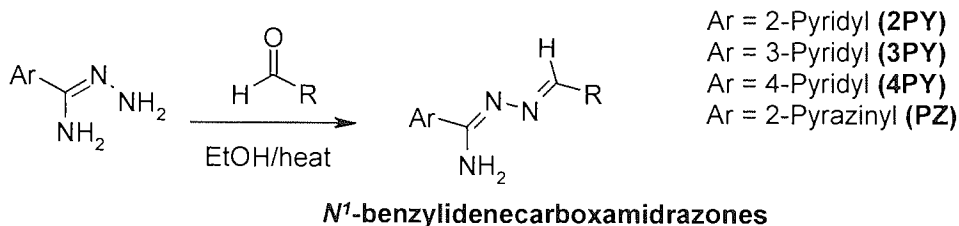


Scheme 2.1: Preparation of heretoarylcarboxamidrazone, the building blocks.

The heteroarylcarboxamidrazones building blocks **2PY**, **3PY**, **4PY**, **PZ**, **QN** and **4PY-NO** (Figure 2.1) were prepared by the action of hydrazine hydrate upon the corresponding cyano compounds (Scheme 2.1). 3-Cyanopyridine and 4-cyanopyridine were expected to be poorly reactive; nevertheless, 3-pyridine (**3PY**) and 4-pyridincarboxamidrazone (**4PY**) were obtained by the reaction of 3- and 4-cynopyridine with hydrazine hydrate under the conditions described in the experimental chapter nine. Pyridine-2-, pyridine-3-, pyridine-4-, pyrazine-2- and quinoline-2-carboxamidrazones were synthesised in order to investigate the biological effect of changing the position of the nitrogen atom. Pyridine-4- and pyrazine-2-carboxamidrazone were used on account of their structural similarity to these compounds, as well as their relationship to the antitubercular agent isoniazid (**3**) and pyrazinamide (**4**) respectively. 4-N-oxide carboxamidrazone was also synthesised in order to investigate the biological effect of introduction of the polar atom and to enhance the solubility of the compounds (see Section 2.16). The structure of these carboxamidrazones was established on the

basis of their $^1\text{H-NMR}$ and MS data, which was consistent with the assigned structure (see experimental section).

2.3 Preparation of N^1 -benzylideneheteroarylcarboxamidrazones



Scheme 2.2: Synthesis of N^1 -benzylideneheteroarylcarboxamidrazone. R= substituted aldehyde residue.

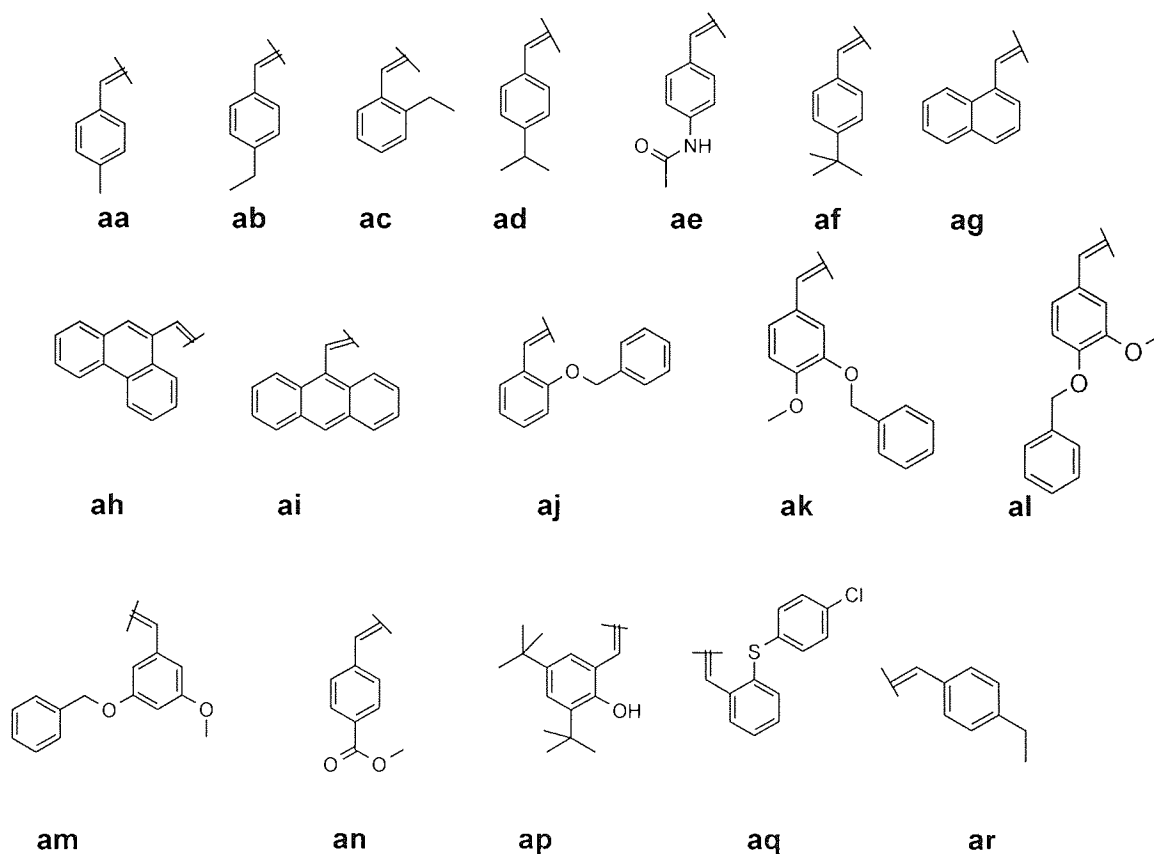


Figure 5.2: Substituted benzaldehyde derived residues used in preparation of N^1 -benzylideneheteroarylcarboxamidrazones

Fifty two previously reported, active N^1 -benzylideneheteroarylcarboxamidrazones were prepared as indicated in **Scheme 2.2**, by methods analogous to those described in the literature [Billinton *et al*, 1995]. The condensation of the heteroarylcarboxamidrazones (**2PY**, **4PY**, **3PY** and **PZ**) with the desired aldehydes in ethanolic solution afforded compounds required for further investigations (For example, an N-alkylation of N^1 -benzylideneheteroarylcarboxamidrazones **Section 2.5** and for the preparation of metal complexes **Section 2.6**). All the N^1 -benzylideneheteroarylcarboxamidrazones compounds gave satisfactory spectral data. The compounds were assigned to be Schiff's bases, because all their ^1H

NMR spectra exhibited the $-\text{CH}=\text{N}$ (azomethine) proton signal at 8.42–9.5 ppm. APCI-Mass spectra of these compounds confirmed their molecular weights.

Spectral investigations also revealed that the pendant amine function present (**Figure 2.3**) was not affected during the synthesis of these compounds, although excess of aldehyde was used in the reactions. In the $^1\text{H-NMR}$ spectra all N^1 -benzylideneheteroarylcarboxamidrazones showed a 2 proton singlet for the NH_2 group. This could be due to the fact that the carboxamidrazone moiety can exist in two tautomeric forms as shown in **Figure 2.3**. Presumably, the compounds in solution tend to stabilise the form **A** intermediate through resonance and therefore the pendant amine is much less reactive.

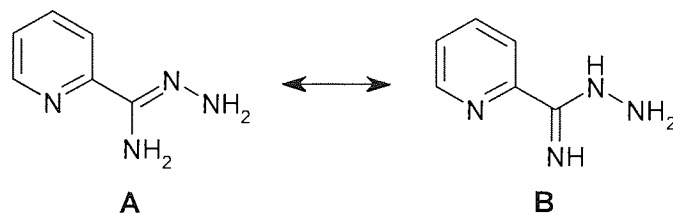
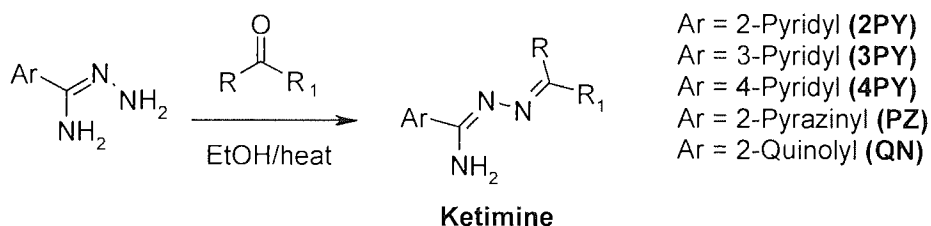


Figure 2.3: Tautomeric forms of pyridine-2-carboxamidrazone

2.4 Automated Synthesis of Carboxamidrazone Ketimines

An initial library of the condensation products of heteroarylcarboxamidrazones and ketones (**Scheme 2.3**) was prepared using automated parallel solution-phase synthesis. A robotic pipetting station was used to transfer stock solutions of previously synthesized heteroarylcarboxamidrazones in ethanol, and stock solutions of ketones in ethanol into a matrix of 90 empty 4mL vials. Within each matrix of 90 vials, each vial contained only one carboxamidrazone building block and only one ketone, to give one product per vial. A heating block was used to heat the matrix of reactions for four days at 75°C . The reaction was followed up by TLC.



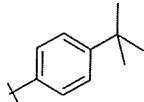
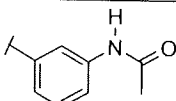
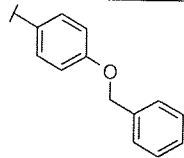
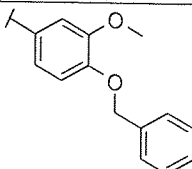
Scheme 2.3: Preparation of carboxamidrazone ketimines.

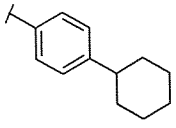
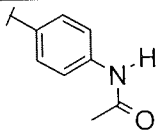
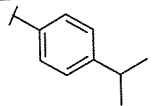
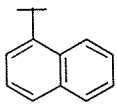
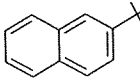
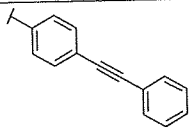
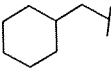
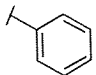
The ethanol was then evaporated to give the crude products. When cool, the purification was performed by robotic trituration (ether or petroleum ether depending upon the lipophilicity of the material). The products were dried under high vacuum prior to analysis. All compounds were characterised by positive atmospheric pressure ionisation mass spectrometry (APCI-MS). Most of the compounds exhibited a dominant $(\text{M}+\text{H})^+$ peak (**Table 2.1a-2.1c**). It has been reported that amidrazones are able to undergo self-condensation at raised temperatures [Neilson *et al*, 1970]. However, this was not observed in the current study. This could be due to the fact that the carbonyl

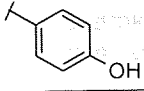
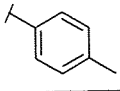
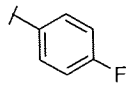
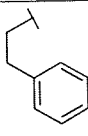
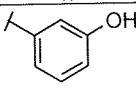
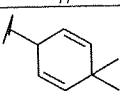
components were assembled at ambient temperature before being heated up relatively slowly to the boiling point of ethanol. It is possible that this procedure together with precipitation of benzylidene products favoured benzylidene formation over the competing self-condensation reaction pathways [Billington *et al*, 1998]. The yields of products ranged (62 –90 %). The crude materials were screened against *M. fortuitum* (NCTC 10394); (discussed in **Section 3.3.1**).

Thirty ketones (k1-k30, Appendix 1) were selected which encompassed a wide range of functional groups to synthesis a library of compounds in an automated fashion. The key reaction was the coupling of the heteroarylcarboxamidrazones with a carbonyl component (**Scheme 2.3**). The product compound codes are such that if pyridine-2-carboxamidrazone **2PY** is reacted with ketone one (**k1**), then the product is called **2PYk1** and so forth. K1-k30 refers to ketone-derived substituent.

Table 2.1a: Represents the data of methylketimines R+R1 = ketone derived residues. Mycobacterial activity was determined against *M. fortuitum*, (+ve = active at 32 µg/mL); (-ve = inactive at 32 µg/mL), s = solid, l = liquid. N/T = reaction was unsuccessful.

Code	Appearance	R	R1	MS (M+H) ⁺	%Yield	MIC <i>M. fortuitum</i> 32µg/mL
2PYk1	greenish yellow (s)	CH ₃		295	44	-
3PYk1	brown (s)	"	"	295	42	-
4PYk1	greenish yellow (s)	"	"	295	84	+
PZk1	"	"	"	296	67	-
QNK1	"	"	"	N/T		
2PYk2	pale yellow (s)	"		296	89	+
3PYk2	yellow (s)	"	"	296	58	-
4PYk2	"	"	"	296	70	-
PZk2	"	"	"	297	78	-
QNK2	"	"	"	345	68	+
2PYk3	"	"		344	42	-
3PYk3	"	"	"	344	56	-
4PYk3	"	"	"	344	29	-
PZk3	"	"	"	345/346	52	-
QNK3	"	"	"	394	65	-
2PYk4	"	"		N/T		
3PYk4	"	"	"	374	33	-
4PYk4	"	"	"	374	88	-
PZk4	"	"	"	375	84	-
QNK4	"	"	"	425	90	-

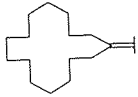
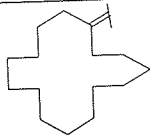
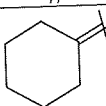
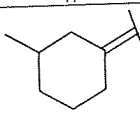
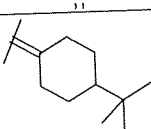
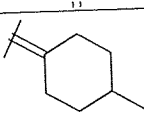
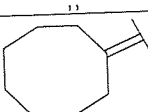
2PYk5	yellow	"		321	96	-
3PYk5	"	"	"	321	89	-
4PYk5	"	"	"	321	34	-
PZk5	"	"	"	322	91	-
QNK5	"	"	"	370	80	-
2PYk6	"	"		296	46	-
3PYk6	"	"	"	296	63	-
4PYk6	"	"	"	296	68	-
PZk6	"	"	"	297	92	-
QNK6	"	"	"	345	93	-
2PYk7	greenish (l)	"		281	50	+
3PYk7	brownish (l)	"	"	281	62	-
4PYk7	greenish (l)	"	"	N/T		
PZk7	"	"	"	N/T		
QNK7	yellow solid	"	"	331	93	-
2PYk9	"	"		289	38	-
3PYk9	"	"	"	288	63	-
4PYk9	"	"	"	N/T		
PZk9	"	"	"	N/T		
QNK9	"	"	"	339	88	-
2PYk10	"	"		289	32	+
3PYk10	"	"	"	289	48	-
4PYk10	"	"	"	289	51	+
PZk10	"	"	"	290	64	-
QNK10	"	"	"	338	91	-
2PYk11	mustard yellow (s)	"		338	35	+
3PYk11	"	"	"	338/339	52	-
4PYk11	"	"	"	338/339	37	-
PZk11	"	"	"	339	63	-
QNK11	"	"	"	388	55	-
2PYk13	"	"		N/T		
3PYk13	"	"	"	259	55	-
4PYk13	"	"	"	259	55	-
PZk13	"	"	"	N/T		
QNK13	"	"	"	390	68	-
2PYk14	yellow (s)	$-\text{CH}_2(\text{CH}_2)_8\text{CH}_3$		350	52	+
3PYk14	"	"	"	350	53	+
4PYk14	"	"	"	351	68	+
PZk14	"	"	"	352	30	-
QNK14	"	"	"	400	75	-

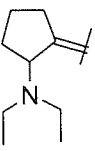
2PYk15	mustard yellow (s)	CH ₃		255	63	+
3PYk15	"	"	"	255	96	+
4PYk15	"	"	"	255	82	-
PZk15	"	"	"	N/T		
QNk15	"	"	"	305	62	-
2PYk16	"	"		253*	44	+
3PYk16	"	"	"	253	64	+
4PYk16	"	"	"	253	72	-
PZk16	"	"	"	254	60	-
QNk16	"	"	"	N/T		
2PYk21	"	"		257	95	-
3PYk21	"	"	"	257	53	-
4PYk21	"	"	"	257	70	-
PZk21	"	"	"	258	66	-
QNk21	"	"	"	307	74	-
2PYk25	brown (s)	"		267	32	+
3PYk25	"	"	"	267	45	-
4PYk25	"	"	"	267	70	-
PZk25	"	"	"	N/T		
QNk25	"	"	"	317	82	-
2PYk26	yellow (s)	"		255	38	+
3PYk26	"	"	"	255	76	-
4PYk26	"	"	"	255	82	-
PZk26	"	"	"	256	85	-
QNk26	"	"	"	305	85	-
2PYk27	mustard yellow (s)	"		267	38	+
3PYk27	"	"	"	267	46	-
4PYk27	"	"	"	267	63	-
PZk27	"	"	"	268	82	-
QNk27	"	"	"	N/T		

Aldehydes generally undergo nucleophilic addition more readily than ketones, due to steric and electronic factors. A ketone contains a second alkyl or aryl group whereas an aldehyde contains a hydrogen atom. Two groups are more effective than one, so there is a bigger barrier to the formation of the transition state for ketone. In addition, alkyl groups release electrons, which will reduce the electrophilic nature of the carbonyl carbon atom, making it less reactive.

In the current study the reaction proceeded normally. **Table 2.1a-2.1c** represents the condensation reaction of aromatic ketones. All the compounds exhibited (M+H)⁺. However, no reaction having taken place for compound **PZk16** and **PZk25**.

Table 2.1b: Represents the data of cycloalkylidenecarboxamidrazones R+R1 = ketone derived residues MIC (+ve = active at 32 µg/mL); (-ve = inactive at 32 µg/mL). N/T = reaction was unsuccessful.

Code	Appearance	R1	R2	MS	%Yield	MIC <i>M. fortuitum</i>
2PYk8	Yellow (s)			343	48	-
3PYk8	"	"	"	342	63	-
4PYk8	yellow (gum)	"	"	N/T	65	-
PZYk8	"	"	"	N/T	75	-
QNYk8	yellow (s)	"	"	393	94	-
2PYk12	brownish yellow (s)			301	31	-
3PYk12	"	"	"	301	38	-
4PYk12	"	"	"	301	96	-
PZk12	"	"	"	302	49	-
QNK12	"	"	"	350/351	29	-
2PYk17	"			217	92	-
3PYk17	"	"	"	217	43	-
4PYk17	"	"	"	217	58	-
PZk17	"	"	"	218	57	-
QNK17	"	"	"	267	88	-
2PYk18	"			231*	73	-
3PYk18	"	"	"	231	36	-
4PYk18	"	"	"	231	52	-
PZk18	"	"	"	232	19	-
QNK18	"	"	"	281	55	-
2PYk19	"			273	68	-
3PYk19	"	"	"	273	41	-
4PYk19	"	"	"	273	99	-
PZk19	"	"	"	274	28	-
QNK19	"	"	"	323	39	-
2PYk20	"			231*	82	-
3PYk20	"	"	"	231*	42	-
4PYk20	"	"	"	231*	20	-
PZk20	"	"	"	232*	17	-
QNK20	"	"	"	281	39	-
2PYk22	yellow (s)			245	96	-
3PYk22	"	"	"	245	30	-
4PYk22	"	"	"	245	58	-
PZk22	"	"	"	246	41	-
QNK22	"	"	"	295	39	-

2PYk23	brownish yellow (s)		276	25	+
3PYk23	„	„	276	26	-
4PYk23	„	„	276	38	-
PZk23	„	„	277	6	-
QNk23	„	„	326	38	-

The syntheses of some cycloalkylidenecarboxamidrazones have been reported previously [Billington *et al*, 1998]. Only three ketones were used in that study, therefore it was required to expand ketone chemistry further. Several cyclic ketones were investigated (see **Table 2.1b**). The reaction proceeded normally. However, compounds denoted by (*), exhibited only weak peak in MS indicating the presence of the product. Many other undesired peaks in MS were also observed.

Table 2.1c: Represents the data of alkylidenecarboxamidrazones R+R1 = ketone derived residues from aliphatic ketones MIC (+ve = active at 32 µg/mL); (-ve = inactive at 32 µg/mL). N/T = reaction was unsuccessful.

Code	Appearance	R1	R2	MS	%Yield	MIC <i>M. fortuitum</i>
2PYk24	brown (gum)	CH ₃	—CCH(CH ₃) ₂	N/T		
3PYk24	brown (s)	„	„	205*	46	-
4PYk24	„	„	„	205*	40	-
PZk24	„	„	„	206*	20	-
QNk24	„	„	„	255*	37	-
2PYk28	„	„	—C(CH ₂) ₅ CH ₃	247	38	-
3PYk28	„	„	„	247	46	-
4PYk28	„	„	„	247*	17	-
PZk28	„	„	„	248	28	-
QNk28	„	„	„	297*	69	-
2PYk29	brown (gum)	„	—C(CH ₂) ₂ CH=CH ₂	N/T		
3PYk29	brown (s)	„	„	217*	40	-
4PYk29	„	„	„	217	35	-
PZk29	„	„	„	218*	37	-
QNk29	„	„	„	267*	77	-
2PYk30	„	„	—CC(CH ₃) ₃	N/T		-
3PYk30	mustard (s)	„	„	N/T		-
4PYk30	„	„	„	219*	38	-
PZk30	„	„	„	N/T		-
QNk30	„	„	„	269	48	-

Table 2.2c represents the results of some aliphatic ketones used in this study. The reaction did not proceed for compounds **2PYk24**, **2PYk29**, **2PYk30**, **3PYk30** and **PZk30**, probably due to the steric hindrance.

The biological activity of the above compounds was determined at the single concentration of (32 µg/mL) and presented in **Table 2.1a - 2.1c**. It will be discussed later in chapter three, **Section 3.3.1**.

2.5

Library of Pyridinium Salts of *N*¹-Benzylidenecarboxamidrazones

A library of 429 quaternary salts was synthesized using automated parallel solution-phase synthesis (**Scheme 2.4**). The aim was to enhance the water solubility and to investigate the effect upon activity of a charged pyridyl N and a variable length chain of the compounds. The moieties of **3PY**, **4PY** and pyrazinyl (**PZ**) *N*¹-benzylidene were alkylated with alkyl halides (**Figure 2.4**). The previously active, thirty nine, *N*¹-benzylidene were prepared by traditional method (**Section 2.3**) and were alkylated with various alkyl halide (**Figure 2.4**).

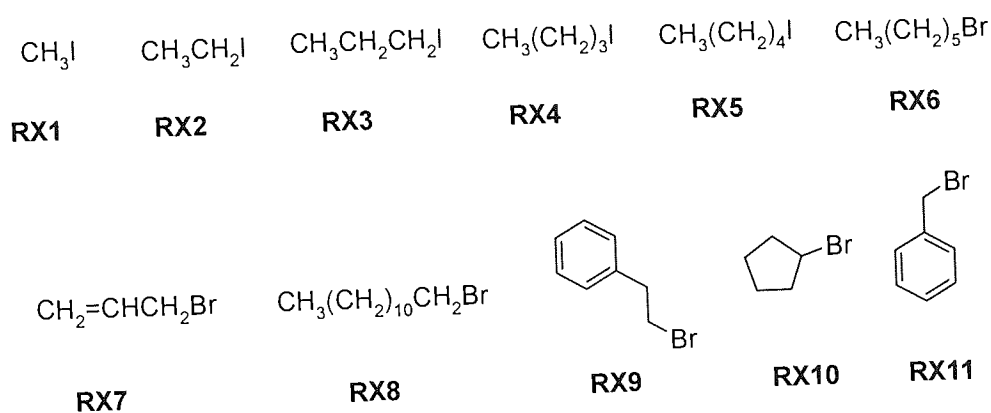
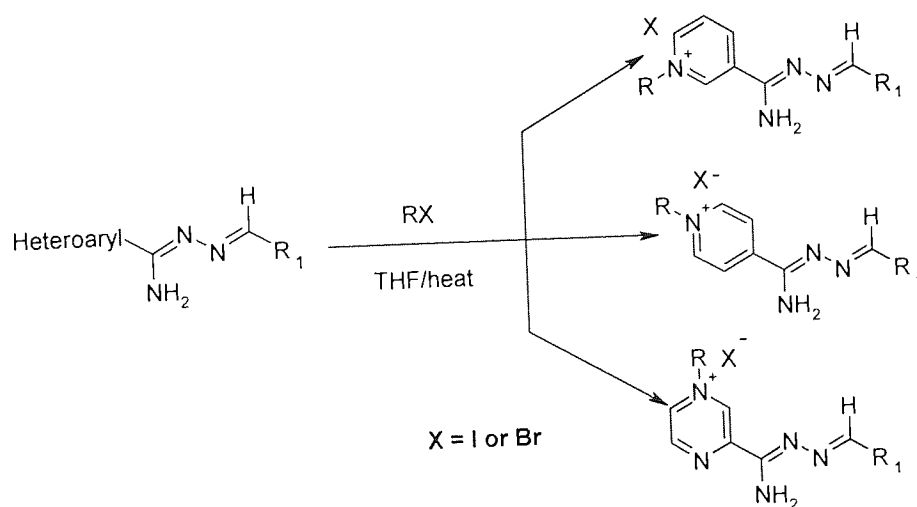


Figure 2.4: Structures of alkyl halides used in automated synthesis.

The reaction mixture was heated in THF at 50 °C for seven days. The THF was evaporated to give the crude products. Purification was performed by robotic trituration (ether or petroleum ether depending upon the lipophilicity of the material). The products were dried under high vacuum prior to analysis. TLC and electrospray positive mass spectrometry analysis showed the reactions were successful with *N*¹-benzylidene- pyridine-3-carboxamidrazones and *N*¹-benzylidene- pyridine-4-carboxamidrazones under the given conditions. In contrast, the reaction between *N*¹-benzylidene- pyrazin-2-carboxamidrazones and the alkyl halides demonstrated problems with most of the compounds. The lack of reactivity was perhaps due to presence of the deactivating nitrogen. The results are presented in **Table 2.2** below:

The biological activity of quaternary pyridinium salts will be discussed in chapter three, **Section 3.3.2**.



Scheme 2.4: The synthetic scheme for alkylating *N*¹-benzylidenecarboxamidrazones.

Table 2.2: Represents the data of pyridinium salts. The product codes are:- if *N*¹-benzylidene-pyridine-3-carboxamidrazone **3PYaa** is reacted with alkyl halide **RX1**, then the product is called **3PYaaRX1**. The biological activity was determined by F. Kusar (final year B.S.c Applied and Human biology project student, Aston University 2004) (+ve indicates that the compound is active against *M. fortuitum* at 32 µg/mL); -ve = inactive at 32 µg/mL. X indicates the reaction was unsuccessful and ** indicates unwanted peaks were present in the mass spec.

Code	% Yield	RMM - X	EI-Mass spec.	MIC 32 µg/mL	Code	% Yield	RMM	EI-Mass spec.	MIC 32 µg/mL	Code	% Yield	EI-Mass spec.
3PYaaRX1	88	253	253	-	4PYaaRX1	51	253	253	-	PZaaRX1	39	254*
3PYaaRX2	62	267	267	-	4PYaaRX2	56	267	267	-	PZaaRX2	97	268*
3PYaaRX3	37	281	281	-	4PYaaRX3	64	281	281	-	PZaaRX3	70	**
3PYaaRX4	44	295	295	-	4PYaaRX4	59	295	295	-	PZaaRX4	57	296
3PYaaRX5	84	309	309	-	4PYaaRX5	60	309	309	-	PZaaRX5	52	310*
3PYaaRX6	88	323	323	+	4PYaaRX6	43	323	323	-	PZaaRX6	46	324
3PYaaRX7	97	279	277*	-	4PYaaRX7	66	279	279	-	PZaaRX7	92	**
3PYaaRX8	88	407	407	-	4PYaaRX8	90	407	407	-	PZaaRX8		
3PYaaRX9	31	357	357	-	4PYaaRX9	46	357	357	-	PZaaRX9		
3PYaaRX10	26	307	307	-	4PYaaRX10					PZaaRX10		
3PYaaRX11	14	329	329	-	4PYaaRX11	34	329	327	+	PZaaRX11	95	**
3PYajRX1	90	345	345	-	4PYajRX1	57	345	345	+	PZajRX1	92	346*
3PYajRX2	24	359	359	-	4PYajRX2	71	359	359	-	PZajRX2	88	**
3PYajRX3	61	373	373	-	4PYajRX3	78	373	373	-	PZajRX3	81	**
3PYajRX4	43	387	387	-	4PYajRX4	73	387	387	-	PZajRX4	65	388*
3PYajRX5	83	401	401	-	4PYajRX5	65	401	401	-	PZajRX5	54	**
3PYajRX6	48	371	371	-	4PYajRX6	95	371	369*	+	PZajRX6	49	**
3PYajRX7	87	499	499	+	4PYajRX7	97	499	499	-	PZajRX7	94	**
3PYajRX8	97	449	449	-	4PYajRX8	64	449	449	-	PZajRX8		
3PYajRX9	77	415	415	-	4PYajRX9	84	415	X		PZajRX9		
3PYajRX10	70	399	399	-	4PYajRX10					PZajRX10		
3PYajRX11	92	421	419*	-	4PYajRX11	34	421	419*	-	PZajRX11	80	**
3PYanRX1	84	297	297	-	N/A					PZanRX1	58	298
3PYanRX2	29	311	311	-	N/A					PZanRX2	57	312
3PYanRX3	84	325	325	-	N/A					PZanRX3	46	**
3PYanRX4	72	339	339	-	N/A					PZanRX4	47	**
3PYanRX5	22	353	353	-	N/A					PZanRX5	64	**
3PYanRX6	90	367	367	+	N/A					PZanRX6	57	**
3PYanRX7	52	322	323*	-	N/A					PZanRX7	79	**
3PYanRX8	89	451	451	-	N/A					PZanRX8		
3PYanRX9	60	401	401	-	N/A					PZanRX9		
3PYanRX10	71	351	351	-	N/A					PZanRX10		
3PYanRX11	64	373	373	-	N/A					PZanRX11	81	374*
3PYalRX1	90	375	375	-	4PYalRX1	30	375	375	-	PZalRX1	71	376
3PYalRX2	64	389	389	-	4PYalRX2	49	389	389	-	PZalRX2	81	**
3PYalRX3	83	403	403	-	4PYalRX3	77	403	403	-	PZalRX3	53	404*
3PYalRX4	24	417	417	+	4PYalRX4	31	417	417	-	PZalRX4	48	**
3PYalRX5	29	431	429*	-	4PYalRX5	75	431	431	-	PZalRX5	56	**
3PYalRX6	24	445	445	-	4PYalRX6	53	445	445	-	PZalRX6	72	446*
3PYalRX7	38	401	401	-	4PYalRX7	38	401	401	-	PZalRX7	72	**
3PYalRX8	31	529	529	-	4PYalRX8	58	529	529	-	PZalRX8		
3PYalRX9	29	479	479	-	4PYalRX9	73	479	479	-	PZalRX9		
3PYalRX10	87	429	429	-	4PYalRX10					PZalRX10		
3PYalRX11	94	451	449	-	4PYalRX11	64	451	451	-	PZalRX11	79	450

3PYadRX1	87	281	X	-	4PYadRX1	38	281	281	-	PZadRX1	86	**
3PYadRX2	80	295	293	-	4PYadRX2	52	295	295	-	PZadRX2	91	**
3PYadRX3	88	309	309	+	4PYadRX3	75	309	309	+	PZadRX3	67	**
3PYadRX4	55	323	323	+	4PYadRX4	89	323	323	-	PZadRX4	62	**
3PYadRX5	99	337	337	-	4PYadRX5	97	337	337	-	PZadRX5	60	**
3PYadRX6	86	351	351	-	4PYadRX6	92	351	351	-	PZadRX6	94	**
3PYadRX7	63	307	305*	-	4PYadRX7	56	307	307	-	PZadRX7	90	**
3PYadRX8	69	418	**	-	4PYadRX8	86	418	**	-	PZadRX8		
3PYadRX9	50	385	385	-	4PYadRX9	66	385	385	-	PZadRX9		
3PYadRX10	70	335	335	-	4PYadRX10					PZadRX10		
3PYadRX11	79	357	355	+	4PYadRX11	54	357	357	-	PZadRX11	90	358*
3PYakRX1	62	296	296	-	4PYakRX1	88	296	296	-	PZakRX1	96	**
3PYakRX2	56	310	310	-	4PYakRX2	63	310	310	-	PZakRX2	47	**
3PYakRX3	47	324	324	-	4PYakRX3	58	324	324	-	PZakRX3	43	**
3PYakRX4	10	338	338	-	4PYakRX4	95	338	338	+	PZakRX4	52	**
3PYakRX5	90	352	352	-	4PYakRX5	31	352	352	+	PZakRX5	65	**
3PYakRX6	89	366	364*	-	4PYakRX6	92	366	366	-	PZakRX6	63	367*
3PYakRX7	41	321	**	-	4PYakRX7	80	321	321	-	PZakRX7	53	**
3PYakRX8	49	450	450	-	4PYakRX8	78	450	450	-	PZakRX8		
3PYakRX9	34	400	400	-	4PYakRX9	45	400	400	-	PZakRX9		
3PYakRX10	39	350	**	-	4PYakRX10					PZakRX10		
3PYakRX11	34	372	**	-	4PYakRX11	25	372	372	-	PZakRX11	35	374*
3PYaerX1	99	297	297	-	4PYaerX1	96	297	297	-	PZaerX1	76	298
3PYaerX2	86	310	310	+	4PYaerX2	88	310	310	-	PZaerX2	90	311
3PYaerX3	86	324	324	-	4PYaerX3	88	324	324	+	PZaerX3	71	325
3PYaerX4	70	338	338	-	4PYaerX4	78	338	338	-	PZaerX4	54	339
3PYaerX5	42	352	352	-	4PYaerX5	75	352	352	-	PZaerX5	51	**
3PYaerX6	81	366	366	-	4PYaerX6	71	366	366	-	PZaerX6	40	367*
3PYaerX7	97	321	321	-	4PYaerX7	89	321	321	-	PZaerX7	92	**
3PYaerX8	45	450	450	+	4PYaerX8	38	450	450		PZaerX8		
3PYaerX9	65	366	366	-	4PYaerX9	75	366	366		PZaerX9		
3PYaerX10	66	350	350	-	4PYaerX10					PZaerX10		
3PYaerX11	70	372	372	-	4PYaerX11	67	372	372	-	PZaerX11	93	373*
3PYacRX1			N/A		4PYacRX1	86	267	267	-	PZacRX1	47	268*
3PYacRX2			N/A		4PYacRX2	63	281	281	-	PZacRX2	60	**
3PYacRX3			N/A		4PYacRX3	37	295	295	-	PZacRX3	41	**
3PYacRX4			N/A		4PYacRX4	96	309	309	-	PZacRX4	47	**
3PYacRX5			N/A		4PYacRX5	76	323	323	-	PZacRX5	84	324*
3PYacRX6			N/A		4PYacRX6	72	337	337	-	PZacRX6	53	338*
3PYacRX7			N/A		4PYacRX7	99	293	293	-	PZacRX7	35	**
3PYacRX8			N/A		4PYacRX8		X			PZacRX8		
3PYacRX9			N/A		4PYacRX9		X			PZacRX9		
3PYacRX10			N/A		4PYacRX10					PZacRX10		
3PYacRX11			N/A		4PYacRX11	68	343	343	-	PZacRX11	49	**
3PYafRX1	95	295	295	-	4PYafRX1	15	295	295	-	PZafRX1	90	296
3PYafRX2	86	309	307*	-	4PYafRX2	64	309	309	-	PZafRX2	35	310
3PYafRX3	82	323	323	-	4PYafRX3	98	323	323	-	PZafRX3	88	**
3PYafRX4	69	337	337	-	4PYafRX4	83	337	337	-	PZafRX4	63	338*
3PYafRX5	67	351	351	-	4PYafRX5	60	351	351	+	PZafRX5	39	352*
3PYafRX6	84	321	321*	-	4PYafRX6	98	321	321	+	PZafRX6	33	**
3PYafRX7	66	449	449	-	4PYafRX7	75	449	449	-	PZafRX7	35	322*
3PYafRX8	90	399	399	-	4PYafRX8	49	399	399	-	PZafRX8		
3PYafRX9	45	365	365	-	4PYafRX9	56	365	365	-	PZafRX9		
3PYafRX10	70	349	349	-	4PYafRX10					PZafRX10		
3PYafRX11	82	371	369*	-	4PYafRX11	72	371	371	-	PZafRX11	32	**
3PYagRX1	99	289	289	-	4PYagRX1	89	289	289	-	PZagRX1	50	290

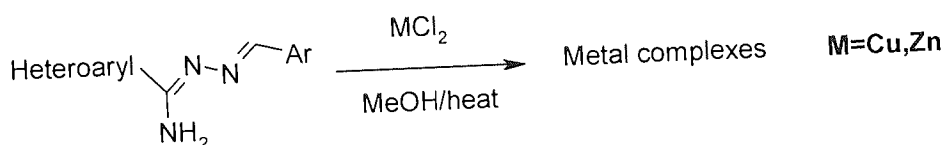
3PYagRX2	86	303	303	-	4PYagRX2	98	303	303	-	PZagRX2	64	304
3PYagRX3	86	317	317	-	4PYagRX3	90	317	317	-	PZagRX3	50	318
3PYagRX4	70	331	331	-	4PYagRX4	86	331	331	+	PZagRX4	80	332*
3PYagRX5	42	345	345	-	4PYagRX5	89	345	345	-	PZagRX5	31	346
3PYagRX6	81	259	259	-	4PYagRX6	78	259	259	-	PZagRX6	36	360
3PYagRX7	97	315	315	-	4PYagRX7	93	315	315	-	PZagRX7	31	**
3PYagRX8	44	443	443	-	4PYagRX8	58	443	443	-	PZagRX8		
3PYagRX9	65	393	393	-	4PYagRX9	42	393	393	-	PZagRX9		
3PYagRX10	66	343	343	-	4PYagRX10					PZagRX10		
3PYagRX11	70	365	365	-	4PYagRX11	60	365	365	-	PZagRX11	47	**
3PYahRX1	51	339	339	-	4PYahRX1	61	339	339	-	PZahRX1	55	340
3PYahRX2	66	353	353	-	4PYahRX2	67	353	353	-	PZahRX2	56	354
3PYahRX3	82	367	367	+	4PYahRX3	69	367	367	-	PZahRX3	55	368
3PYahRX4	71	381	381	-	4PYahRX4	68	381	381	-	PZahRX4	57	382
3PYahRX5	72	395	395	-	4PYahRX5	71	395	395	-	PZahRX5	64	396
3PYahRX6	94	409	409	-	4PYahRX6	74	409	409	+	PZahRX6	29	410*
3PYahRX7	77	365	365	-	4PYahRX7	72	365	365	-	PZahRX7	30	366*
3PYahRX8	29	493	493	-	4PYahRX8	39	493	493	-	PZahRX8		
3PYahRX9	64	443	443	-	4PYahRX9	96	443	443	-	PZahRX9		
3PYahRX10	62	393	393	-	4PYahRX10					PZahRX10		
3PYahRX11	74	415	415	-	4PYahRX11	61	415	415	-	PZahRX11	92	**
3PYaiRX1	89	339	339	-	4PYaiRX1	75	339	339	-	PZaiRX1	56	340
3PYaiRX2	96	353	353	+	4PYaiRX2	91	353	353	-	PZaiRX2	16	354
3PYaiRX3	80	367	367	+	4PYaiRX3	83	367	367	+	PZaiRX3	69	368*
3PYaiRX4	56	381	381	-	4PYaiRX4	88	381	381	-	PZaiRX4	73	382*
3PYaiRX5	68	395	395	-	4PYaiRX5	89	395	395	-	PZaiRX5	6	396*
3PYaiRX6	46	409	409	-	4PYaiRX6	66	409	409	-	PZaiRX6	11	410*
3PYaiRX7	82	365	365	-	4PYaiRX7	65	365	365	+	PZaiRX7	5	**
3PYaiRX8	66	493	493	-	4PYaiRX8	38	493	493	-	PZaiRX8		
3PYaiRX9	68	443	443	-	4PYaiRX9	46	443	443	-	PZaiRX9		
3PYaiRX10	63	393	393	-	4PYaiRX10					PZaiRX10		
3PYaiRX11	88	415	415	-	4PYaiRX11	95	415	415	-	PZaiRX11	42	**
3PYarRX1	48	267	**	-	4PYarRX1	18	267	267	-	PZarRX1	77	268*
3PYarRX2	79	281	**	-	4PYarRX2	87	281	281	-	PZarRX2	42	**
3PYarRX3	56	295	**	-	4PYarRX3	43	295	295	-	PZarRX3	36	**
3PYarRX4	64	309	**	-	4PYarRX4	48	309	309	-	PZarRX4	14	**
3PYarRX5	84	323	**	-	4PYarRX5	94	323	323	-	PZarRX5	32	324*
3PYarRX6	73	337	**	-	4PYarRX6	67	337	337	+	PZarRX6	32	338*
3PYarRX7	36	293	**	-	4PYarRX7	96	293	293	-	PZarRX7	36	**
3PYarRX8	67	421	**	-	4PYarRX8	66	421	421	+	PZarRX8		
3PYarRX9	50	371	**	-	4PYarRX9	75	371	371	-	PZarRX9		
3PYarRX10	59	321	**	-	4PYarRX10					PZarRX10		
3PYarRX11	84	343	**	-	4PYarRX11	67	343	343	-	PZarRX11	65	**

2.6

Library Synthesis of Metal Complexes of *N*¹-Benzylidenecarboxamidrazone

It has been reported that metal conjugation of the carboxamidrazone ligands results in significant enhancement in their anti-tubercular activities against *M. tuberculosis* [Gokhale, 2001 Sandbhor, 2002]. The structural analysis of the benzylidene indicated that the amino group in the side chain promotes formation of hydrogen bonds with the target molecules, via intramolecular N-H-H hydrogen bonding and supplies electron density to other heteroatoms nearby enhances their ability to accept hydrogen

bonds or chelate metals [Schwalbe *et al*, 2000]. It has been imagined that increased liposolubilities of metal complexes, might relative to the uncomplexed metal ions, contribute to their easy permeability through the mycobacterial cell wall. In this context, we were interested to synthesise a library of metal complexes of carboxamidrazone analogs as potential antitubercular agents **Scheme 2.5**.



Heteroaryl = 2-Pyridyl, 3-Pyridyl, 4-Pyridyl and 2-Pyrazinyl

Scheme 2.5: Synthesis of *N*¹-benzylidencarboxamidrazone metal complex.

A library of one hundred of metal complexes of carboxamidrazone derivatives was prepared as described in (**Scheme 2.5**). Glass vials 4mL in a matrix were charged with each of the amidrazones in methanol. This was followed by a solution of metal chloride. The vials were heated in a heating block at 60°C. The methanol was then evaporated to give the crude products. Purification was performed by robotic trituration with deionised water followed by methanol. The products were dried under high vacuum prior to analysis. The yields of products ranged (30-99%). All the crude products were screened against *M. fortuitum*, and will be discussed in chapter three **Section 3.3.3**. The analysis of the metal amidrazone complexes proved to be very difficult, as there were no high through put methods available to characterise them. However, ¹H-NMR and IR were bit helpful in such that ¹H-NMR gave broader peaks if the metal was paramagnetic, whereas the IR showed noticeable shifts in the absorption frequencies between the starting materials and the end products. For exmple, the IR spectrum of **2PYaa** exhibited absorptions around 3481, 3339 cm⁻¹ due to H-bonded NH₂ groups which shifted to lower wave numbers at 3378 cm⁻¹ in **2PYaa CuCl₂** and at 3386 cm⁻¹ in **2PYaa ZnCl₂** due to loss of H-bonding. The bands around 1617 and 1560 cm⁻¹ in the **2PYaa** are due to the -C=N grouping which are shifted to 1635 and 1598 cm⁻¹ in **2PYaa CuCl₂**; 1638 and 1602 cm⁻¹ in **2PYaa ZnCl₂**, respectively confirming the involvement of this group in the metal complexation. IR was promising technique, but it meant that IR had to be done on both, the starting material and the products, which was time consuming. The problem encountered with TLC was finding a suitable solvent to dissolve the product.

Table 2.3 Represents the data of metal complexes of *N*¹-benzylidencarboxamidrazones. The product codes are:- if *N*¹-benzylidene pyridine-2-carboxamidrazone **2PYaa** is reacted with metal halide **CuCl₂**, then the product is called **2PYaaCuCl₂**. The biological activity was determined by N. Ellahi (final year MParm. Project student, Aston University 2005) (+ve indicates that the compound is active against *M. fortuitum* at 32 µg/mL); -ve = inactive at 32 µg/mL. S = solid.

Code	Appearance	% Yield	Activity at 32µg/mL
2PYaa CuCl ₂	Brownish green (s)	52	+
2PYaj CuCl ₂	"	45	+
2PYan CuCl ₂	"	97	+
2PYal CuCl ₂	"	64	+
2PYak CuCl ₂	"	94	+
2PYad CuCl ₂	"	77	+
2PYae CuCl ₂	"	60	+
2PYag CuCl ₂	"	77	+

2PYac CuCl ₂	"	45	+
2PYaf CuCl ₂	"	30	+
2PYah CuCl ₂	"	75	+
2PYai CuCl ₂	"	98	+
2PYar CuCl ₂	"	85	+
3PYaa CuCl ₂	"	58	+
3PYaj CuCl ₂	"	99	+
3PYan CuCl ₂	"	87	-
3PYal CuCl ₂	"	73	+
3PYak CuCl ₂	"	89	+
3PYad CuCl ₂	"	91	-
3PYae CuCl ₂	"	90	+
3PYag CuCl ₂	"	97	+
3PYac CuCl ₂	"	95	+
3PYaf CuCl ₂	"	95	+
3PYah CuCl ₂	"	88	+
3PYai CuCl ₂	"	93	+
3PYar CuCl ₂	"	94	+
4PYaa CuCl ₂	"	91	+
4PYaj CuCl ₂	"	74	+
4PYan CuCl ₂	"	89	+
4PYal CuCl ₂	"	91	+
4PYak CuCl ₂	"	68	+
4PYad CuCl ₂	"	85	+
4PYae CuCl ₂	"	80	+
4PYag CuCl ₂	"	88	+
4PYac CuCl ₂	"	64	+
4PYaf CuCl ₂	"	90	+
4PYah CuCl ₂	"	97	+
4PYai CuCl ₂	"	94	+
4PYar CuCl ₂	"	81	+
PZaa CuCl ₂	"	91	+
PZaj CuCl ₂	"	58	+
PZan CuCl ₂	"	95	+
PZal CuCl ₂	"	78	+
PZak CuCl ₂	"	89	+
PZad CuCl ₂	"	64	+
PZae CuCl ₂	"	80	+
PZag CuCl ₂	"	89	+
PZac CuCl ₂	"	97	+
PZaf CuCl ₂	"	92	+
PZah CuCl ₂	"	93	+
PZai CuCl ₂	"	99	+
PZar CuCl ₂	"	87	+
Zinc Complexes			
2PYaa ZnCl ₂	Yellow (s)	77	+
2PYaj ZnCl ₂	"	53	+
2PYan ZnCl ₂	"	65	-
2PYal ZnCl ₂	"	70	-
2PYak ZnCl ₂	"	81	-
2PYad ZnCl ₂	"	43	+
2PYae ZnCl ₂	"	56	-
2PYag ZnCl ₂	"	38	+
2PYac ZnCl ₂	"	35	+
2PYaf ZnCl ₂	"	83	+
2PYah ZnCl ₂	"	97	+
2PYai ZnCl ₂	"	66	-
2PYar ZnCl ₂	"	37	+

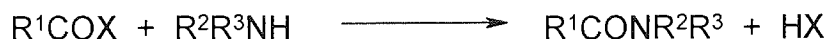
3PYaa ZnCl ₂	Mustard yellow	91	-
3PYaj ZnCl ₂	„	82	+
3PYan ZnCl ₂	„	87	+
3PYal ZnCl ₂	„	42	+
3PYak ZnCl ₂	„	93	+
3PYad ZnCl ₂	„	86	+
3PYae ZnCl ₂	„	92	+
3PYag ZnCl ₂	„	97	+
3PYac ZnCl ₂	„	97	+
3PYaf ZnCl ₂	„	83	+
3PYah ZnCl ₂	„	89	-
3PYai ZnCl ₂	„	72	-
3PYar ZnCl ₂	„	78	+
4PYaa ZnCl ₂	yellow	31	-
4PYaj ZnCl ₂	„	56	+
4PYan ZnCl ₂	„	70	-
4PYal ZnCl ₂	„	94	-
4PYak ZnCl ₂	„	61	+
4PYad ZnCl ₂	„	88	-
4PYae ZnCl ₂	„	82	-
4PYag ZnCl ₂	„	73	-
4PYac ZnCl ₂	„	95	-
4PYaf ZnCl ₂	„	75	+
4PYah ZnCl ₂	„	82	-
4PYai ZnCl ₂	„	82	+
4PYar ZnCl ₂	„	90	-
PZaa ZnCl ₂	„	93	-
PZaj ZnCl ₂	„	70	-
PZan ZnCl ₂	„	94	-
PZal ZnCl ₂	„	60	-
PZak ZnCl ₂	„	44	-
PZad ZnCl ₂	„	72	-
PZae ZnCl ₂	„	80	-
PZag ZnCl ₂	„	78	-
PZac ZnCl ₂	„	99	-
PZaf ZnCl ₂	„	75	-
PZah ZnCl ₂	„	68	-
PZai ZnCl ₂	„	54	-
PZar ZnCl ₂	„	72	+

2.7 Synthesis of new classes of carboxamidrazones

2.8 Carboxamidrazone Amides

A series of novel carboxamidrazone amides, analogs of previously active imines was prepared in a hope that they may provide further novel compounds of pharmaceutical interest. There are many methods available to prepare the amides [Smith and March, 2001; 19 Zabicky, 1970; Sorrel, 2006], but the methods that were used in this research will be described:-

The general preparation of amides from the acylation of amines is shown in **Scheme 2.6**. This represents a nucleophilic substitution at the carbonyl carbon atom.



Scheme 2.6: The general procedure for preparing amides

The treatment of acyl chlorides with ammonia or amines (e.g., X = Cl in **Scheme 2.6**), is a very general reaction for the preparation of amides. The reaction is highly exothermic and must be carefully controlled, usually by cooling. Reaction with ammonia gives unsubstituted amides, whereas primary amines lead to the preparation of 2° amides, and secondary amines react to afford 3° amides. In some cases aqueous alkali is added in accordance with the Schotten-Baumann procedure [Schotten, 1884; Baumann, 1886]. Similarly acylation of amines by anhydrides provides a convenient route to amides. This occurs relatively easily with cyclic anhydrides, to provide a route to the formation of cyclic imides in which two carbonyl groups are attached to the nitrogen [Hargreaves *et al*, 1970].

Acylation of amines by carboxylic acids is less useful as a preparative method for amides compared to the chemical routes described previously. However, the reaction between amines and carboxylic acids can be promoted by the use of coupling agents such as dicyclohexylcarbodiimide. This has been found extensive use in the solid phase synthesis of peptides discovered by Merrifield [Merrifield, 1963].

The conversion of carboxylic acid esters to amides serves as a useful method for the preparation of amides. Many simple esters are found to be poor leaving groups and therefore, for this reason strongly basic catalysis has been used.

2.9 Acylation of carboxamidrazones by acyl halides

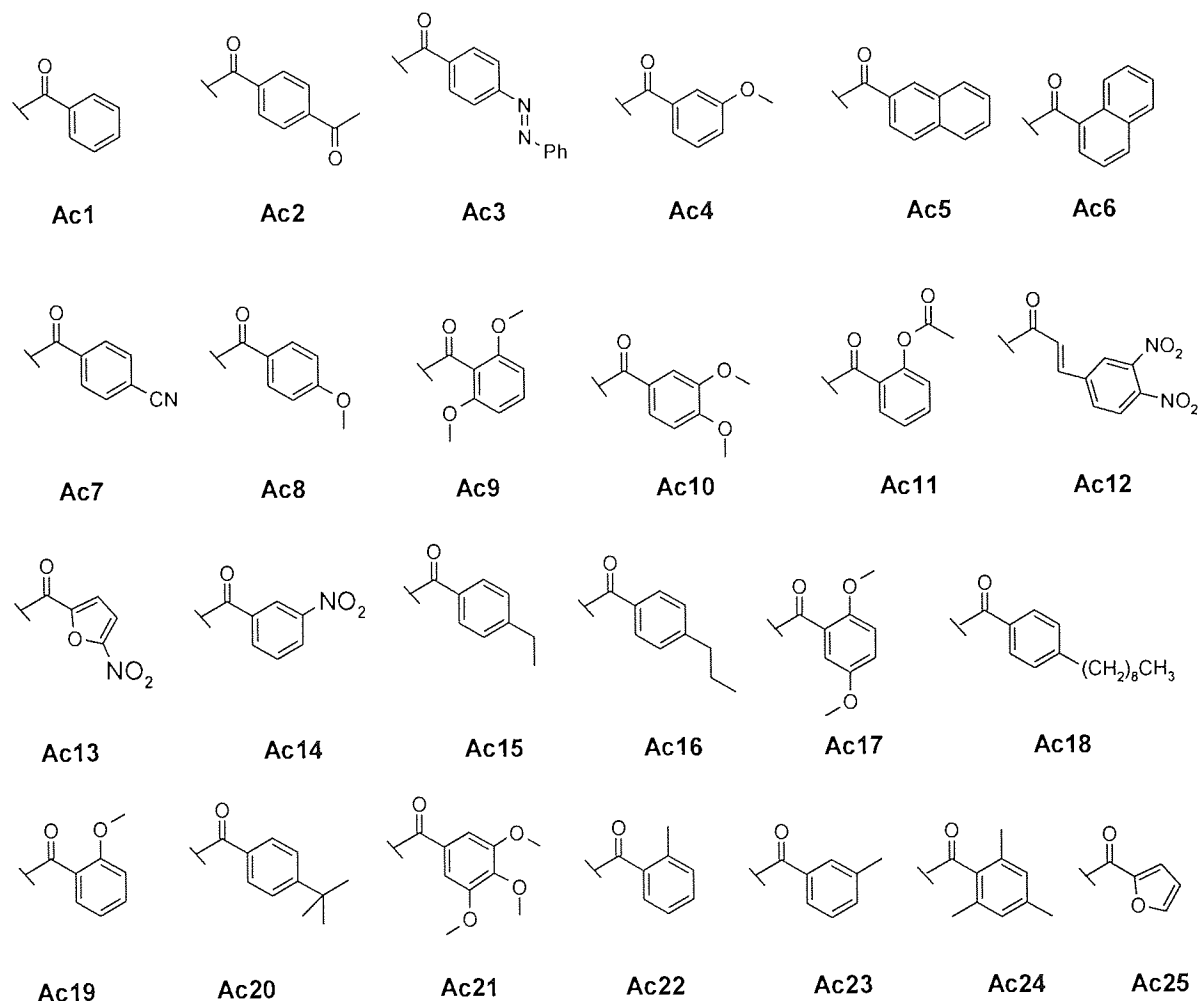
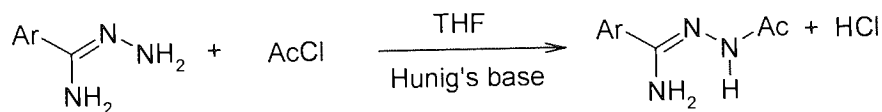


Figure 2.5: Acyl chloride derived residues used in amide synthesis

The most plausible route to synthesis the target carboxamidrazones amides with potential antimycobacterial activity was considered to be the direct acylation of the pyridine-2- and pyridine-4-carboxamidrazones with a range of acyl halides (**Figure 2.5**). The reaction between pyridine-2-carboxamidrazones and excess acyl halide in dry THF at room temperature gave desired products. Since hydrogen chloride was formed in the reaction, Hunig's base was used to neutralize the HCl. Identification of the amide product was achieved by the usual spectroscopic methods ^1H NMR, mass spectrometry and IR.

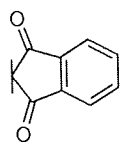


Ar + 2-pyridyl or 4-pyridyl

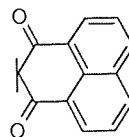
Scheme 2.7: Synthetic scheme for preparation of carboxamidrazones amides

For pyridine-4-carboxamidrazones the reaction conditions were slightly changed because the above mentioned conditions failed to afford the desired compounds (as pyridine-4-carboxamidrazones was partially soluble in THF). Reactions between **4PY** and acyl chlorides were carried out in the mixture of warm THF and dry DMF (10% by volume). This reaction then afforded the desired amide. The pyridine-4-carboxamidrazones amides were susceptible to protonation on the pyridyl nitrogen. Therefore, during work up they were washed with aqueous sodium hydrogen carbonate rather than water. The purification was performed by hot filtration followed by recrystallisation from ethanol/methanol. These compounds were characterised in a similar manner to pyridine-2-carboxamidrazones amides. However, during the course of reaction it was observed that electron-donating methyl group at meta and ortho position reduced the rate of reaction, for example, the compound **2PYAc22** and **2PYAc23** were not obtained upon several attempts. Moreover, the tri-substituted compounds **2PYAc24** and **4PYAc24** also showed the similar trends.

2.10 Synthesis of Carboxamidrazones cyclic imide

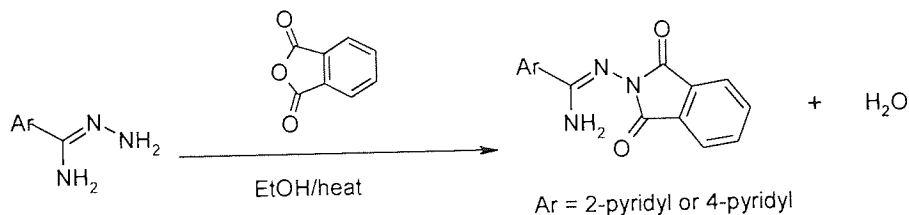


Anh1



Anh2

Figure 2.6: Cyclic acid anhydride derived residues (R) used in carboxamidrazones imide synthesis



Scheme 2.8: Synthetic route to carboxamidrazones imides.

The synthetic route to compounds **2PYAnh1**, **2PYAnh2** and **4PYAnh2** are shown in **Scheme 2.8**. Heteroarylcarboxamidrazone (2PY/4PY) and an appropriate cyclic anhydride were heated at reflux in ethanol to afford the desired compounds. Identification of the carboxamidrazones imide was achieved by ¹H-NMR, IR and MS. Spectral data were consistent with the assigned structures.

2.11 Acylation of Carboxamidrazones by Carboxylic Acids.

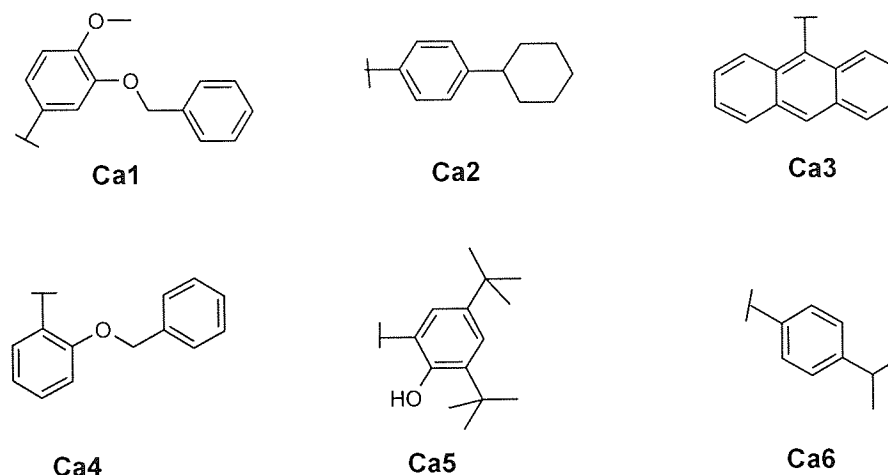
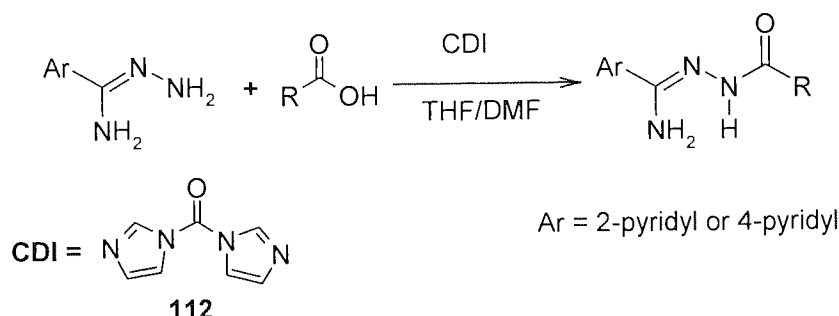


Figure 2.7: Carboxylic acid derived residues (R) used in amide synthesis



Scheme 2.9: Synthetic route for preparation of carboxamidrazones using a coupling reagent.

Although treatment of carboxylic acids with carboxamidrazones does not directly give amides, the reaction was made to proceed by the use of coupling agent *N,N'*-carbonyldiimidazole (**112**) (**Scheme 2.9**). This method was employed because the corresponding acyl chlorides were not commercially available. However, carboxylic acid 4-isopropylbenzoic acid was also commercially unavailable therefore; it was prepared in the laboratory from the commercially available aldehyde (**Section 2.12**).

Staab reagent *N,N'*-carbonyldiimidazole **112** was added to an appropriate carboxylic acid in dry THF to activate an acid. When effervescence ceased, the required carboxamidrazones were added and the reaction was allowed to proceed under argon at room temperature. The resulting solution was evaporated under high vacuum to afford the crude title compound. The mixture was then washed with saturated aqueous sodium hydrogen carbonate followed by water. If necessary the material was purified by recrystallisation. The reaction between **2PY/4PY** did not proceed with **Ca3** probably due to steric hindrance.

Many ways of oxidizing aldehydes to carboxylic acids have been developed. Among many oxidants used, acidic permanganates and chromates are most widely used. Other examples are aqueous potassium permanganate, fuming nitric acids and aqueous sodium hydroxide-silver oxide. In this study isopropyl-benzaldehyde was oxidised by air oxygen, i.e. the cheapest and simplest method. Thus, a mixture of 4-isopropyl-benzaldehyde and ethanol were heated for five days. Air was pumped through the solution and more ethanol was added during five days. The mixture was cooled and the resultant white precipitate was filtered off and treated with aqueous sodium hydrogen carbonate. This solution was extracted twice with chloroform and these extracts were discarded. The aqueous solution was acidified with concentrated hydrochloric acid, precipitating the 4-isopropyl-benzoic acid.

2.13 Attempt to reverse the amide group in a previously discovered active amide-substituted N^1 -benzylidene carboxamidrazone

2.13.1 Aminolysis of N^1 -benzylidene carboxamidrazones containing ester groups.

With the successful preparation of carboxamidrazones amides (above) the attention was turned to preparation of amides where the amide group was reversed and varied its position (**Figure 2.9**). This was stimulated, because in a previous study [Tims, 2002] compound **113** in **Figure 2.10** was found to be active against *M. tuberculosis*. It was decided to attempt to make analogues of this compound by manipulating the nature of the amide functionality in the benzylidene portion. In particular the position of the amide group, its orientation (reversal) and the alkyl chain were to be varied.

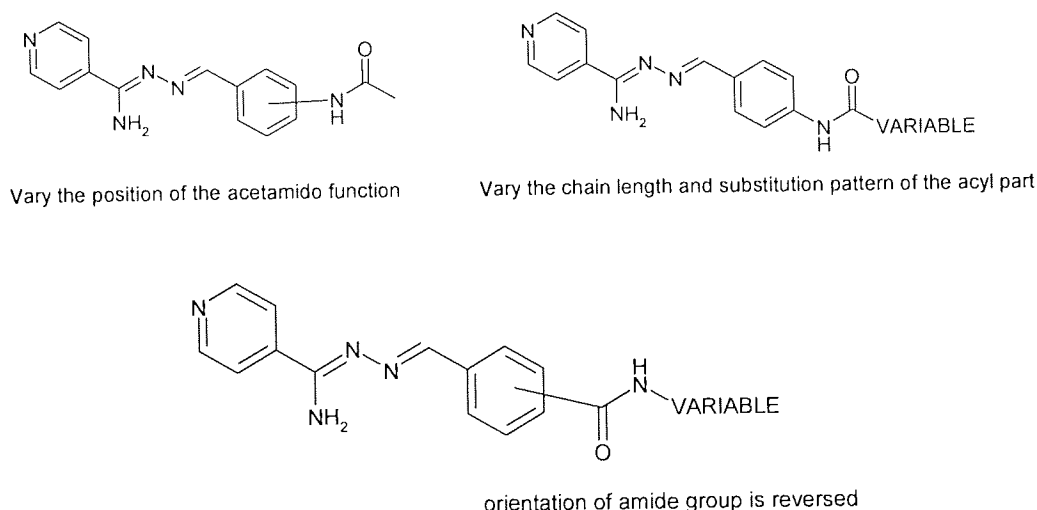


Figure 2.8: Proposed structure for various N^1 -benzylidene carboxamidrazonamide

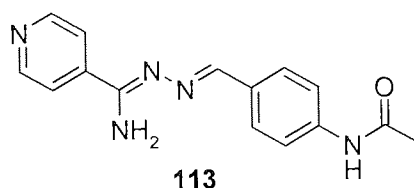


Figure 2.9: Structure of the TB active compound **113** [Tims, 2002].

Initially, attempts to synthesise the reversed amide (**Scheme 2.10**) were made, using *N*¹-benzylidene (**4PYan**) containing ester moiety. **4PYan** was treated with primary amine **114** at room temperature (Method A). The reaction was followed by TLC, but no product could be confirmed. The reaction conditions were changed i.e. the reaction mixture was heated at reflux in chloroform (CHCl₃) for two days and then a catalyst (DBU) was employed, but no product could be confirmed. This route was eventually abandoned and an alternative route was investigated to furnish the desired product.

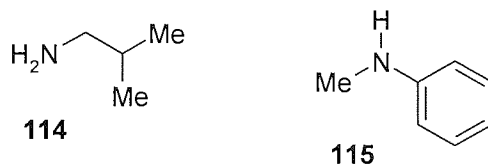
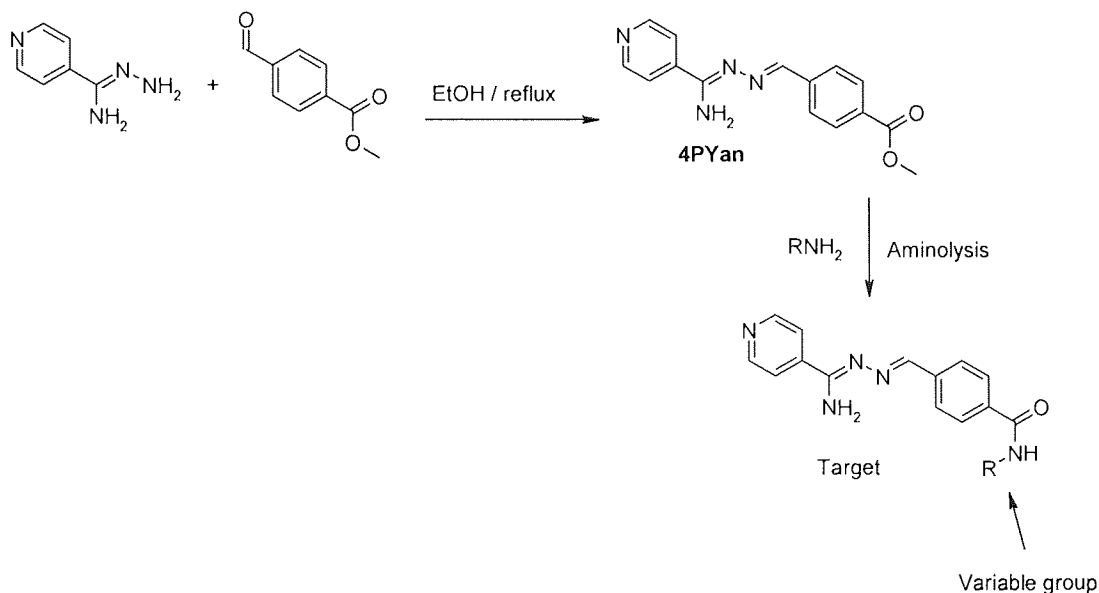


Figure 2.10: The structure of isobutylamine (**114**) and *N*-methylphenylamine (**115**)

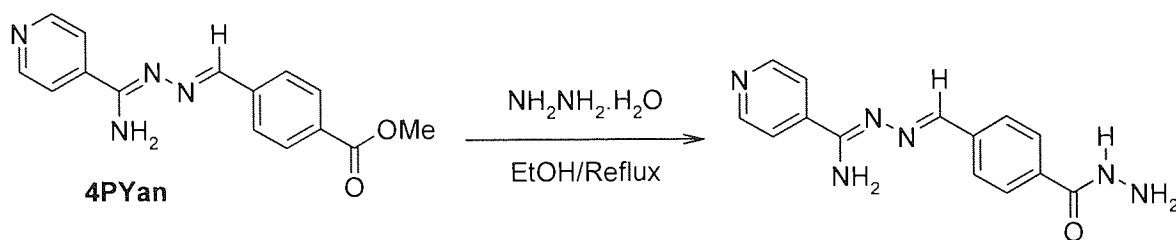
Method B

The *N*¹-benzylidene carboxamidrazone (**4PYan**) mentioned above was treated with secondary amine **115** and heated at reflux in butanol for three days (method B). The reaction was followed by TLC, but no product could be confirmed. The reaction mixture was transferred into a metal pressure vessel (bomb) and heated at 180°C for two days. TLC confirmed starting material. Sodium ethoxide (base) was added and the reaction mixture was sealed and heated for two further days at 180°C. This reaction was not particularly successful. Only starting materials were isolated from the reaction mixture, which was confirmed by APSI-MS.



Scheme 2.10: Synthetic route to aminolysis *N*¹-benzylidene carboxamidrazone

In an attempt to continue the synthesis of carboxamidrazone amides, the method proposed by Mamolo [Mamolo *et al* 2001] was carried out (**Scheme 2.11**). The **4PYan** mentioned above was treated with hydrazine monohydrate in ethanol. The mixture was heated to reflux for five days. A small amount of brown oil was isolated from the reaction mixture, but identification of desired product by ¹H-NMR and MS proved unsuccessful.

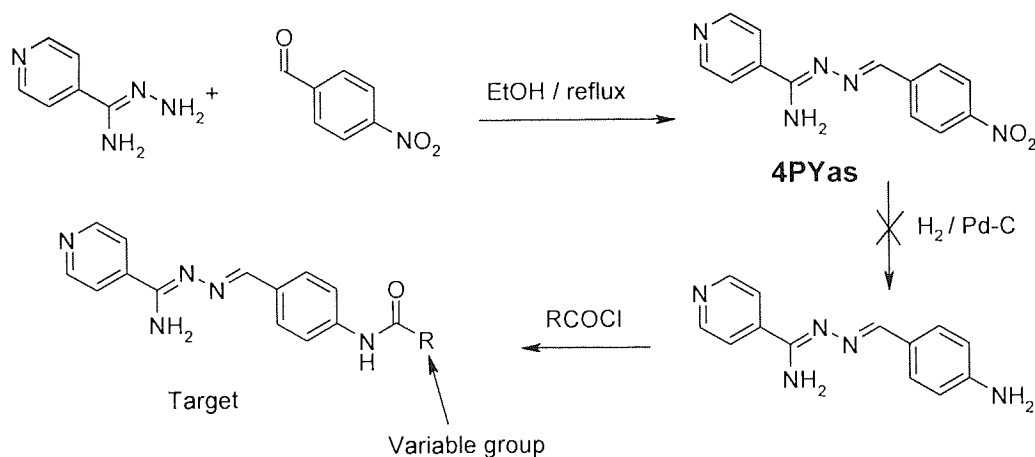


Scheme 2.11: Alternative synthetic route to aminolysis N^1 -benzylidene carboxamidrazone

2.14 Reduction of N^1 -benzylidene carboxamidrazones containing aromatic nitro group.

2.14.1 Attempted Catalytic Hydrogenation Using Palladium-on-Charcoal

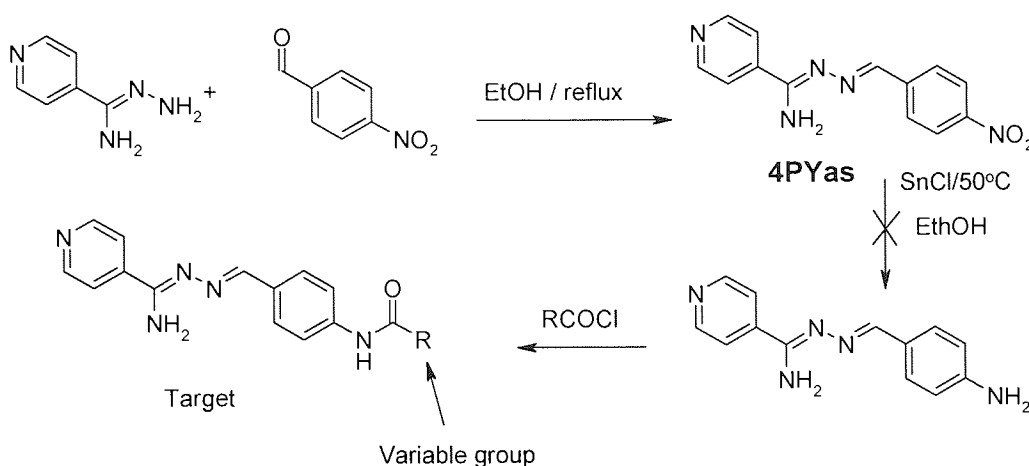
In attempts to synthesise the reversed amidrazone amide, reduction methods were also employed (**Scheme 2.12**). For example, attempts were made for catalytic hydrogenation of aromatic nitro group of N^1 -benzylidenecarboxamidrazone (**4PYas**) with 10% and then 20% Pd-C catalyst, under high pressure (1000 pa).



Scheme 2.12: Schematic synthetic route for hydrogenation of N^1 -benzylidenecarboxamidrazone.

The reaction was followed by TLC, but no product could be confirmed in the reaction mixture. $^1\text{H-NMR}$ and MS was carried out but it did not reveal the desired product. Despite the high pressure, and the long reaction time, the recovered material consisted only of starting material. The initially formed imine (**4PYas**) was also susceptible to reduction to an amine under the given conditions, nevertheless, it was not observed in spectral data. As mentioned earlier the recovered residue was starting material.

2.14.2 Attempted Reduction with Tin (II) Chloride



Scheme 2.13: Possible reduction route for *N*¹-[4-nitrobenzylidene]-pyridine-4-carboxamidrazone

*N*¹-[4-Nitrobenzylidene]-pyridine-4-carboxamidrazone **4PYas**, was heated at 50°C with tin II chloride in ethanol for several days. This failed to afford the desired product (**Scheme 2.13**). This was judged by ¹H-NMR spectroscopy, MS spectrometry and TLC. The MS spectrometry indicated that the product was a starting material **4PYas**.

2.15 Synthesis of Novel Sulphonamides Carboxamidrazone

In an attempt to continue the study of new types of amidrazones, heteroarylcarboxamidrazones **2PY** and **4PY** were reacted with a range of sulphonyl chlorides groups as depicted in (**Figure 2.12**) to afford the corresponding sulphonamide carboxamidrazone (**Scheme 2.14**). Sulphonamide analogues of the amidrazones were synthesised to investigate the effect of the change in the shape of the compound This is will be discussed later in chapter three **Section 3.14**.

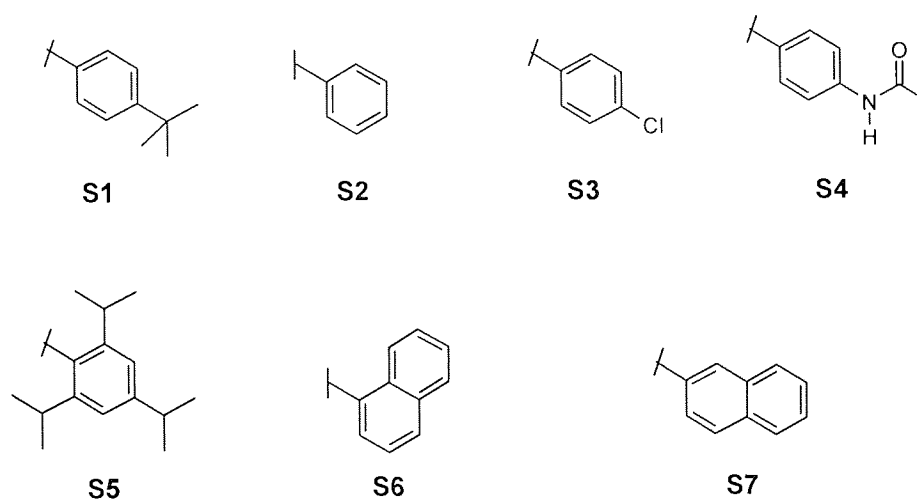
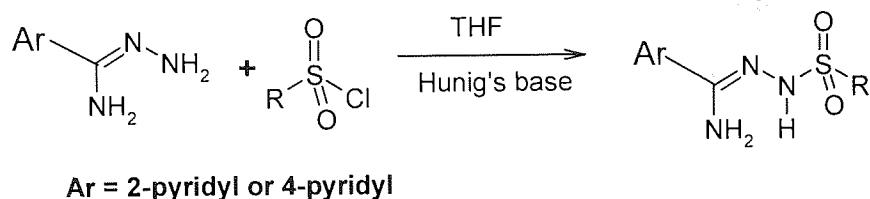


Figure 2.11: Sulphonyl chloride derived residues (R) used in sulphonamide synthesis



Scheme 2.14: Synthetic route for preparation of sulphonamide carboxamidrazones.

The reactions were carried out under argon in dry THF at a room temperature. Hunig's base was selected as a base to neutralize any hydrogen chloride evolved during the reaction. Although analysis of the resulting brown solid by $^1\text{H-NMR}$ and MS, showed identifiable product peaks in some of the compounds, it proved problematic to obtain the pure products with the exception of compounds **2PYS1**, **2PYS2** and **2PYS3**. Increasing the reaction time was met without success. Many solvents were used to recrystallise the target product but it was futile. Chromatography was not performed, because of the poor solubility profile of these compounds. The reactions were also unsuccessful when repeated with **4PY** and were eventually abandoned.

2.16 Synthesis of *N*¹-(Benzylidene)pyridine-4-carboxamidrazone-4-N-Oxides

With the aim to synthesise less toxic, less lipophilic and more selective antimycobacterial agents, a small set of *N*¹-benzylidene-pyridine-4-carboxamidrazone were modified by introduction of an oxygen atom at N1 of pyridine ring. It was established from a previous study that these compounds exhibited antimycobacterial activities; in particular, compound **116** (Figure 2.13). This compound was found to be very potent against panel of Gram-positive bacteria, but unfortunately it was very toxic and very lipophilic [Rathbone *et al*, 2006].

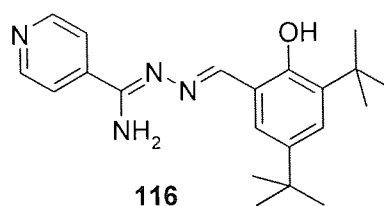
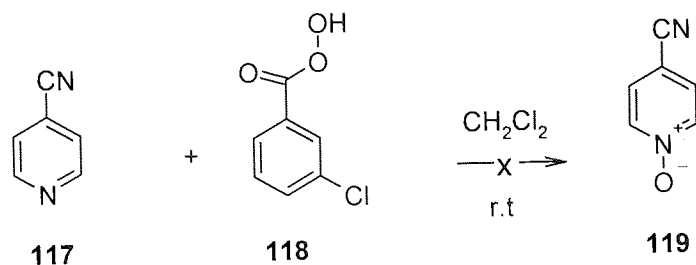


Figure 2.12: The structure of most active antibacterial compound [Rathbone *et al*, 2006].

Therefore, for these reasons and as a continuation of our studies on heteroarylcarboxamidrazone derivatives we modified this particular compound and related compounds by simply introduction of the polar oxygen atom on the pyridine nitrogen with the aims to enhance the water solubility and to reduce the toxicity of the compound.



Scheme 2.15: Preparation of cyano-heteroaryl N-oxide.

An attempt to prepare 4-cyanopyridine N-oxide (**119**) upon treating heteroaryl nitrile (**117**) with m-chloro peroxybenzoic acid (**118**) was unfortunately failed. However, the conversion of 4-cyanopyridine N-oxide served as a useful method for preparation of amidrazone N-oxide (4PY-NO see Section 2.2). An amidrazone N-Oxide (**4PY-NO**) was synthesised from 4-cyanopyridine N-oxide and was condensed with the corresponding aldehyde group (**Figure 2.14**) to afford the desired product (**Scheme 2.15**). The structures were established on the basis of their $^1\text{H-NMR}$ and MS spectral data.

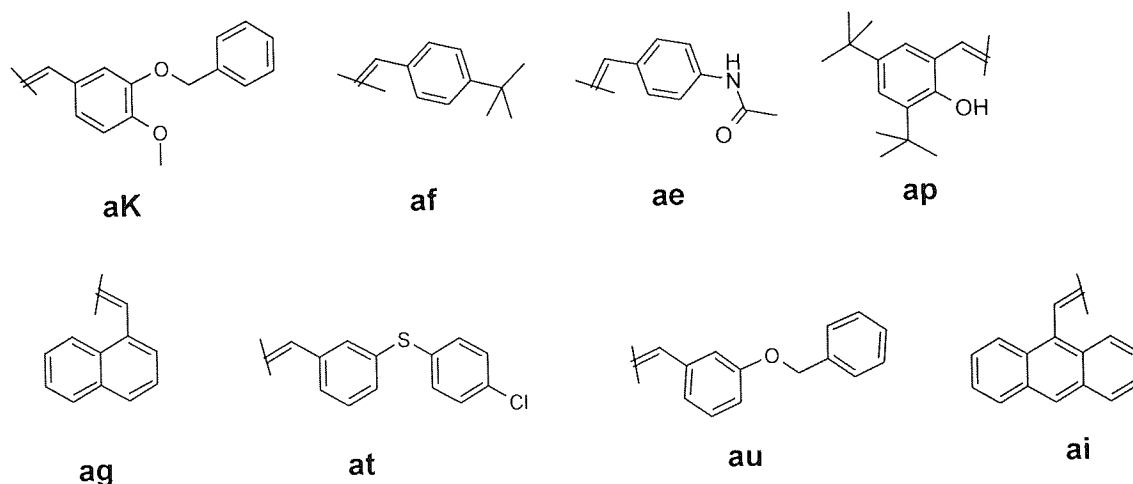
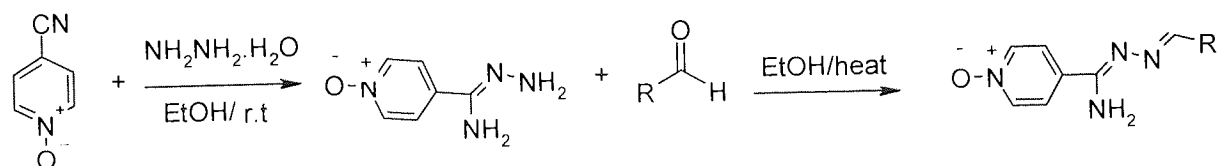


Figure 2.13: The aldehyde derived residues used in preparation of N^1 -benzylidene N-Oxides



Scheme 2.16: Synthetic scheme for preparation of N^1 -benzylidene N-Oxides

2.17 Synthesis of carboxamidrazone Urea

The final series of compounds that was synthesized included compound of the type shown in **Scheme 2.17**. Here, it was intended to replace the imine functionality with the urea functionality to furnish a range of antimycobacterial agents.

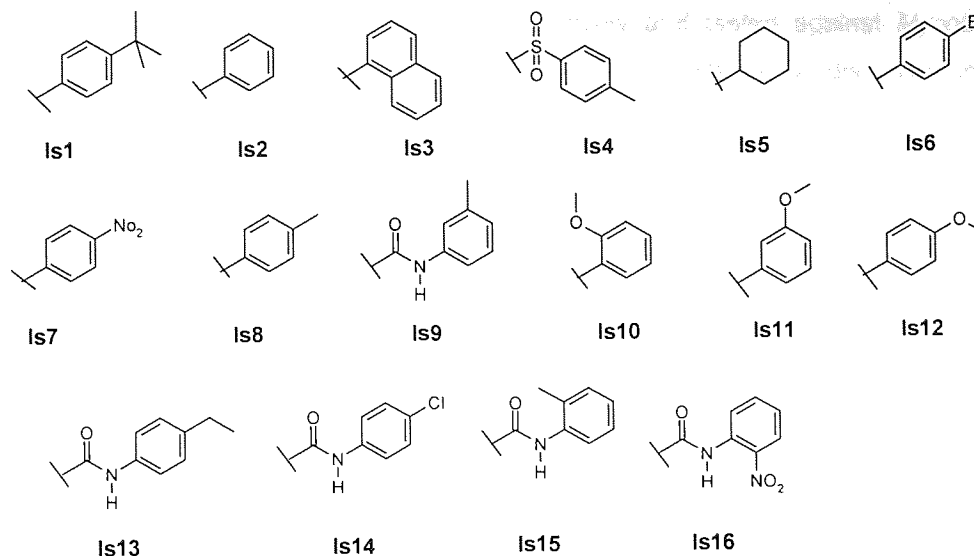


Figure 2.14: Isocyanate derived residues (R) used in urea synthesis.



Ar = 2-pyridyl or 4-pyridyl

Scheme 2.17: Synthetic scheme for preparation of carboxamidrazone ureas.

The amidrazones were transformed into the ureas by reaction with substituted isocyanates (**Figure 2.15**) in dry THF (plus 10% by volume dry DMF in the case of 4PY) under argon. After subsequent purifications the identification of the products was achieved through two principal spectroscopic methods i.e., $^1\text{H-NMR}$ and Mass Spectrometry (MS). (APCI \pm ve)-mass spectra of some of the urea compounds displayed molecular ions two mass units higher than the expected molecular ion. The major fragmentation pathway appeared by the cleavage of the $-\text{CO-NH-R}$ bonds of urea moiety (**Figure 2.16** below). Infra red (IR) spectroscopy was routinely carried out to identify the major functional groups and the purity of the compounds was assessed by melting point determination, TLC and observation of any minor components in the $^1\text{H NMR}$ spectra.

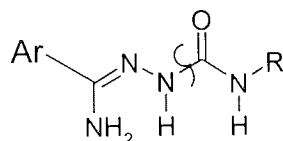


Figure 2.15: The major fragmentation pathway appeared by the cleavage of $-\text{CO-NH-R}$ bond of urea moiety.

2.18 Conclusions

A series of pyridine-2-, pyridine-3-, pyridine-4-, pyrazine-2- and quinoline-2-carboxamidrazones derivatives and novel class of pyridine-2- (**2PY**) and pyridine-4- (**4PY**) carboxamidrazones were

prepared in an automated and traditional fashion respectively and tested against *Mycobacterium fortuitum* and *Mycobacterium tuberculosis* in a rapid screen. The results will be discussed in chapter three.

The condensation of amidrazones with various ketones and substituted benzoic aldehydes afforded the ketimines and *N*¹-benzylidene carboxamidrazones respectively. The *N*¹-benzylidene carboxamidrazones were further alkylated with a range of alkyl halides to afford the new amidrazone derivatives, quaternary pyridinium salts. Alkylating *N*¹-benzylidene-pyridine-3-carboxamidrazone and *N*¹-benzylidene-pyridine-4-carboxamidrazone proceeded smoothly. In contrast, alkylating *N*¹-benzylidene-pyrazin-2-carboxamidrazones demonstrated problems with most of the compounds, probably due to presence of the deactivating nitrogen. The *N*¹-benzylidene carboxamidrazones were also successfully transformed into metal complexes.

An acylation of carboxamidrazones by acyl halides provided a convenient route to the corresponding amides. The reaction was exothermic and the temperature was carefully controlled. In addition, preparation of carboxamidrazone amides from activated carboxylic acids proved to be a convenient route to the desired compounds. ¹H-NMR and MS data were consistent with the assigned structures. Extending this route to prepare the sulphonamides was met with little success. Although the presence of the carboxamidrazone sulphonamides was indicated by ¹H-NMR and MS, but it was not possible to isolate the pure compounds with the exception of **2PYS1**, **2PYS2** and **2PYS3**. An attempt to reverse the amide substituent in a previously active *N*¹-benzylidene carboxamidrazone was disappointing. Finally, the preparation of carboxamidrazone ureas and carboxamidrazone N-oxides was more successful.

The compounds prepared here have undoubtedly highlighted that an enormous range of possible analogues could be produced. The potential for drug development in this area is still enormous, but due to time constraints it was not possible to continue the study. However, it will be useful to further assess the influence upon mycobacterial activity of the isosteric replacement of the oxygen atom of ureas and amides by sulphur. The bioisosteric replacement will change one or more of the following parameters: size, shape, electronic distribution, lipid solubility, water solubility, pK_a, chemical reactivity and hydrogen bonding. In addition, future work would also include replacing the substituent aromatic ring with substituted piperazines.

3 Microbiology

3.1 *Mycobacterium fortuitum* as a screening model for *Mycobacterium tuberculosis*

Antimycobacterial activity of the synthesized compounds was investigated against *M. fortuitum* NCTC 10394, a rapidly growing strain, by the use of microdilution broth susceptibility method. *M. fortuitum* (reference strain NCTC 10394, isoniazid sensitive ($1-2 \mu\text{g mL}^{-1}$)) was used as a model for *M. tuberculosis* for a rapid initial screen, because *M. tuberculosis* was difficult to use, as it is a Hazard Category 3 organism requiring specialized handling facilities. It is also slow growing, taking 12-25 days. *M. fortuitum* on the other hand, is not a virulent human pathogen, can be handled on the laboratory bench and is a rapid grower needing only a 2-3 day incubation time. The synthesized compounds were also screened for inhibition of *Mycobacterium tuberculosis* H₃₇Rv (ATCC 27294) in BACTEC 12B medium [Collins and Franzblau, 1997] conducted by the Tuberculosis Antimicrobial Acquisition and Coordinating Facility (TAACF). It was expected that the result might be different for each species due to the fact that each tested organism is different strain and each species displays its own specificity. The method for testing antimycobacterial activity was also different. However, the large numbers of compounds were expected to be generated in the current study, therefore *M. fortuitum* was thought to be a useful as a primary antitubercular screen because of the rapidity, ease and inexpensiveness and the fact that it is a mycobacterium.

3.2 The antimycobacterial testing

The compounds were screened at a single concentration of $32 \mu\text{g mL}^{-1}$ in Middlebrook 7H9 broth, supplemented with glycerol and Middlebrook ADC enrichment. If a biological activity at $32 \mu\text{g mL}^{-1}$ was observed, the MIC for that compound was measured in broth. The MIC was defined as the lowest concentration inhibiting growth after incubation at 37°C for 72 h.

The *in vitro* antimycobacterial activity of the synthesized compounds against *M. fortuitum*, the structure activity relationship and the comparison of *M. fortuitum* and *M. tuberculosis* results will be discussed in the following sections:

The product compound codes are such that if pyridine-2-carboxamidrazone (**2PY**) is reacted with an acid chloride (**Ac1**), then the product is called **2PYAc1**, if **2PY** is reacted with acid anhydride (**Anh1**) then the product is called **2PYAnh1**, if **2PY** is reacted with an isocyanate (**Is1**), the the product is called **2PYIs1**, if **2PY** is reacted with a sulphonyl chloride (**S1**), the product is called **2PYS1** and if pyridine-4-carboxamidrazone-N-oxide (**4PY-NO**) is condensed with an aldehyde **ak** then the product is called **2PYak-NO**.

3.3 Evaluating antimycobacterial activity of compounds prepared by automated synthesis

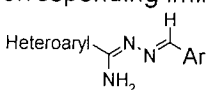
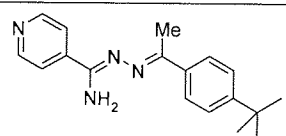
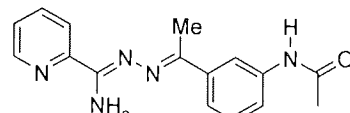
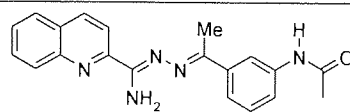
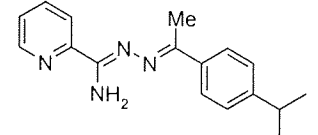
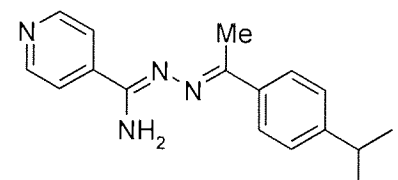
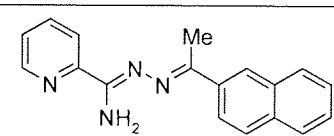
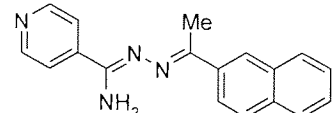
3.3.1 Antimycobacterial activity and structure activity relationship of alkylidencarboxamidrazones (ketimine)

As mentioned in chapter two section 2.4, all the synthesized compounds were subjected to screening against *M. fortuitum* (NCTC 10394) at a single concentration of 32 µg/mL. The results for the complete set of compounds are displayed in **Table 2.1a - 2.1c**.

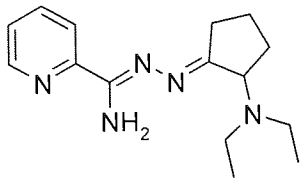
The results for active compounds are presented in **Table 3.1**. MIC data for parent compounds (imines) from previous study are included for comparative purpose.

The code is such that if pyridine-2-carboxamidrazone (**2PY**) is reacted with ketone (**k1**), then the product is called **2PYk1**.

Table 3.1: Represents the biological activity of active methyl ketimine and corresponding imines against *M. fortuitum* (*M. fort.*) The MIC values for imines were provided by Dr. D.L. Rathbone [Tims, 2002]. (+) indicates that compound was active at the concentration of 32 µg/mL⁻¹.

Compound	Structure	<i>M. fort.</i> MIC (32 µg/mL ⁻¹)	<i>M. fort.</i> MIC (µg/mL ⁻¹) Corresponding imine 
4PYk1		+	8-16
2PYk2		+	>32
QNK2		+	>32
2PYk7		+	N/A
4PYk7		+	N/A
2PYk10		+	>32
4PYk10		+	>32

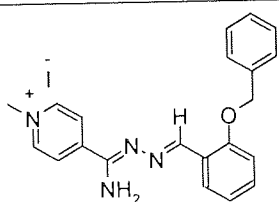
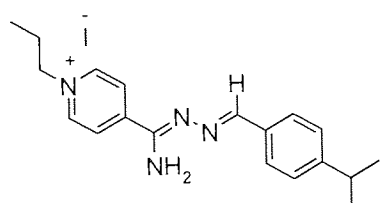
2PYk11		+	N/A
2PYk13		+	N/A
2PYk14		+	>32
3PYk14		+	N/A
4PYk14		+	>32
2PYk15		+	>32
4PYk15		+	N/A
2PYk16		+	16-32
3PYk16		+	>32
2PYk25		+	N/A
2PYk26		+	>32
2PYk27		+	N/A
QNK27		+	N/A

2PYk23		+	N/A
--------	-----------------------------------------------------------------------------------	---	-----

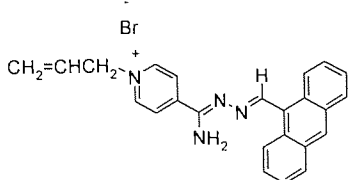
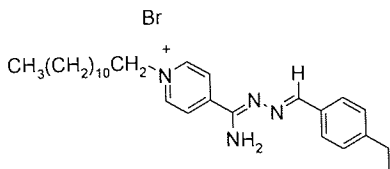
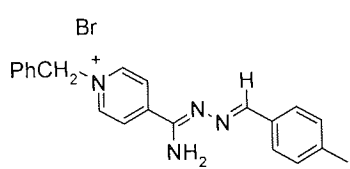
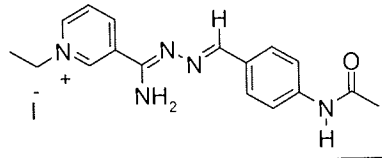
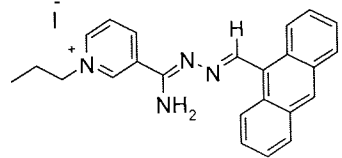
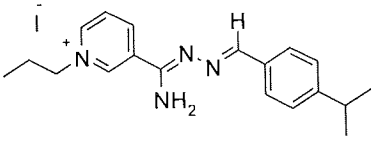
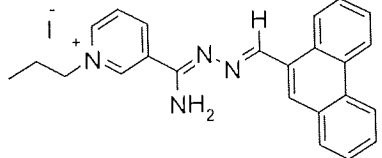
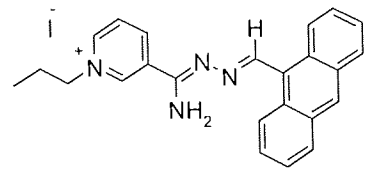
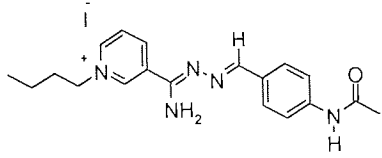
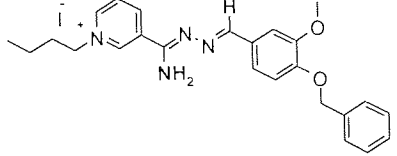
Of the one hundred and fifty tested alkylidenecarboxamidrazones only twenty methyl ketimines were found to be active against *M. fortuitum* (Table 3.1). A general trend observed from these results was that all the aliphatic ketones derivatives were inactive. All the cycloalkylidenecarboxamidrazones were also inactive with the exception of the compound **2PY k23**. Furthermore, when compared to their corresponding imine the introduction of the methyl group enhanced the biological activity for some compounds, for example, **2PYk2**, **Qnk2**, **2PYk10**, **4PYk10**, **2PYk14**, **4PYk14**, **2PYk15**, **3PYk16** and **2PYk26**. In contrast, the antimycobacterial activity against *M. fortuitum* was diminished in case of compounds **4PYk1** and was abolished for the corresponding **2PYk1**. Moreover, most of the compounds which were found to possess activity against *M. fortuitum* were pyridine-2-carboxamidrazone **2PY** derivatives; some of the equivalent pyridine-4-carboxamidrazones **4PY** also displayed the similar activity. The pyrazine-2-carboxamidrazone **PZ**, were inactive, as were most quinoline-2-caboxamidrazone **QN** and pyridine-3-carboxamidrazone **3PY**, with the exception of **Qnk2**, **Qnk27**, **3PYk14** and **3PYk16**. The result demonstrated that the addition of the electron donating substituent (Me) enhanced activity against *M. fortuitum*. Due to the time constrains it was not possible to remake these compounds and obtain full MIC data. The compounds listed in Table 3.1 are worth further investigation.

3.3.2 Evaluating biological activity and structural activity relationship of quaternary pyridinium salts

Table 3.2: Represents the biological activity of active quaternary pyridinium salts and corresponding imine against *M. fortuitum* (*M. Fort.*) The biological activity of quaternary pyridinium salts was determined by F. Kusar (B.Sc. Applied and Human Biology final year project student, Aston University, 2004) and an MIC values for imines were provided by Dr. D.L. Rathbone [Tims, 2002] for comparative purpose. The (+) indicates that compound was active at the concentration of $32 \mu\text{g mL}^{-1}$.

Compound	Structure	<i>M. Fort.</i> MIC ($32 \mu\text{g mL}^{-1}$)	Corresponding imine <i>M. Fort.</i> MIC ($\mu\text{g mL}^{-1}$)
4PYajRX1		+	>32
4PYadRX3		+	>32

4PYaeRX3		+	>32
4PYaiRX3		+	16-32
4PYakRX4		+	5-10
4PYagRX4		+	16-32
4PYakRX5		+	16-32
4PYafRX5		+	8-16
4PYafRX6		+	8-16
4PYahRX6		+	>32
4PYarRX6		+	>32

4PYaiRX7		+	16-32
4PYarRX8		+	>32
4PYaaRX11		+	>32
3PYaeRX2		+	>32
3PYaiRX2		+	>32
3PYadRX3		+	N/A
3PYahRX3		+	>32
3PYaiRX3		+	>32
3PYadRX4		+	>32
3PYaiRX4		+	>32

3PYaaRX6		+	>32
3PYanRX7		+	N/A
3PYaeRX8		+	N/A
3PYadRX11		+	N/A

A library of four hundred and seventeen quaternary pyridinium salts was produced (see chapter two **Section 2.5**). Regrettably, the antimycobacterial activity of pyrazine-2-benzylidene quaternary salts is not available at this point of time. However, one hundred and thirty two pyridine-4-benzylidene quaternary salts and one hundred and twenty one pyridine-3-benzylidene quaternary salts were subjected to screen against *M. fortuitum* at the single concentration of 32 $\mu\text{g/mL}$. The structures of the active compounds are presented in **Table 3.2**. Fourteen out of the one hundred and thirty two pyridinium-4-benzylidene salts exhibited the antimycobacterial activity against *M. fortuitum*. Twelve out of one hundred and twenty one pyridinium-3-benzylidene salts led to the enhancement of the antimycobacterial activity compared to the parent compounds. The activity of compounds **4PYajRX1**, **4PYadRX3**, **4PYaeRX3**, **4PYahRX6**, **4PYarRX6**, **4PYarRX8** and **4PYaaRX11** was also enhanced, in comparison to the equivalent imine (parent compound). This finding is not surprising, since quaternary ammonium compounds are cationic surfactants and classified as disinfectants. It is generally accepted that, in contrast to chemotherapeutic agents, biocides have multiple target sites within the microbial cell and the overall damage to these target sites results in the bactericidal effect [Maillard, 2002]. As the biological testing involved a whole cell system, it is not known how these compounds work against the mycobacteria or what the molecular target is. Furthermore, the presence of the quaternary nitrogen atom suggests that toxicity issues might be a problem. Due to the time constraints it was not possible to remake these compounds and obtain full MIC data. It will be useful to further assess the influence of the lipophilic alkyl chain length for the optimum activity.

3.3.3 Biological activity of the benzylidene heteroaryl carboxamidrazone metal complexes

A library of one hundred *N*¹-benzylidene heteroaryl carboxamidrazone metal complexes was prepared (Chapter two, **Section 2.6**). The compounds were tested for inhibition of *M. fortuitum* at a single concentration of 32 $\mu\text{g/mL}$. The results obtained for the compounds are shown in Table 2.3, which indicated that all copper complexes were active at the concentration of 32 $\mu\text{g/mL}$ with the exception of

compounds **3PYadCuCl₂** and **3PYanCuCl₂**. In contrast, complexation with zinc did not show such a rise in activity. Only twenty-one out of the fifty compounds exhibited antimycobacterial activity against *M. fortuitum*. The significant enhancement in antimycobacterial activity of copper complexes was presumably due to the toxic copper ions.

3.4 Antimycobacterial activity of carboxamidrazone amides compared to their corresponding imines against *M. fortuitum*.

The antimycobacterial activity of the synthesized carboxamidrazone amides is shown in **Appendix 2** and **Appendix 3**. The amide results can be compared to imine results, because both results were determined against the same strain of *M. fortuitum* by the same method.

A careful examination of biological activity data reveals that fourteen compounds showed activity *in vitro* against *M. fortuitum*. Some carboxamidrazone amides i.e. **2PYAc1**, **2PYAc15**, **2PYAc19**, **2PYAc21**, **4PYAc1**, **4PYAc2**, **4PYAc14** and **4PYAc15** were found to have increased in their activity relative to the corresponding imine. It was also observed that compounds **2PYAc6**, **2PYAc8**, **2PYAc14**, **2PYCa1**, **2PYCa6**, **4PYAc5**, **4PYAc25** and **4PYCa1** have diminished their antimycobacterial activities comparing to their corresponding imines. However, some compounds like **2PYAc20** and **2PYCa4** have retained their activities.

3.5 Structural Activity Relationships of Carboxamidrazones Amides

3.5.1 Variation of alkyl substituents

In the present investigation, various pyridine-2-carboxamidrazone *N*¹-(benzoyl)amides and pyridine-4-carboxamidrazones *N*¹-(benzoyl)amides were synthesised and evaluated for *in vitro* antimycobacterial activity against *M. fortuitum* (**Appendix 2** and **Appendix 3**). The alkyl substituents are hydrophobic and may bind with hydrophobic regions of the binding site through van der Waals and hydrophobic interactions. If the alkyl groups interact with a hydrophobic pocket in the binding site, then varying the length and bulk of the alkyl group, for example, ethyl (**2PYAc15**), propyl (**2PYAc16**), heptyl (**2PYAc18**), *tert*-butyl (**2PYAc20**), isopropyl (**2PYCa6**) allows one to probe the depth and width of the pocket. Varying the length of alkyl chain connected to 4-position of aromatic ring (Table 3.3) demonstrated that the ethyl group was the best substituent at that position. Extending the length by an extra methylene group eliminated activity (**2PYAc16**). However, the reduction of the chain length (**2PYAc22**) also abolished the mycobacterial activity of corresponding compounds. Furthermore, the branching of the alkyl chain increased activity (**2PYAc20**). A possible explanation is that branching increases van der Waals interactions to a hydrophobic region of binding site. Alternatively, the lipophilicity of the drug might be increased, allowing easier passage through cell membranes.

Table 3.3: MIC values for alkyl-substituted carboxamidrazone amides against *M. fortuitum*

Code	Structure	MIC ($\mu\text{g mL}^{-1}$)	Code	Structure	MIC ($\mu\text{g mL}^{-1}$)
2PYAc1		16-32	4PYAc1		16-32
2PYAc15		8-16	4PYAc15		16-32
2PYAc16		>32	4PYAc16		>32
2PYAc18		>32	4PYAc18		>32
2PYAc22		N/A	4PYAc22		>32
2PYAc23		>32	4PYAc23		>32
2PYAc24		>32	4PYAc24		>32
2PYCa6		>32	4PYCa6		>32
2PYAc20		8-16	4PYAc20	X	

3.5.2

Variation alkoxy substituents

Table 3.4: MIC values for methoxy-substituted carboxamidrazone amides against *M. fortuitum*

Code	Structure	MIC ($\mu\text{g mL}^{-1}$)	Code	Structure	MIC ($\mu\text{g mL}^{-1}$)
2PYAc19		4-8	4PYAc19		>32
2PYAc4		>32	4PYAc4		>32
2PYAc8		>32	4PYAc8		>32
2PYAc9		>32	4PYAc9		>32
2PYAc21		16-32	4PYAc21		>32
2PYAc10		>32	4PYAc10		>32

Substituents having different steric, hydrophobic and electronic properties were also investigated to see if these factors have any effect on activity. The position of substituents on aromatic ring was varied to find better binding interactions, resulting in increased activity, for example, the substitution pattern of methoxy groups on the aromatic ring was altered (Table 3.4 above). The best activities were found if the methoxy group was at an ortho position of the aromatic ring for the compound **2PYAc19**, ($4-8 \mu\text{g mL}^{-1}$) but for the equivalent pyridine-4- compound the activity was lost. Similarly, tri-methoxy substituted compound **2PYAc21** displayed activity ($16-32 \mu\text{g mL}^{-1}$), whereas the equivalent pyridine-4- compound **4PYAc21** was inactive. The methoxyl containing aryl group which decreases the lipophilicity of the compound is also the bulkiest group; therefore, the activity could be due to a combination of steric and electronic factors.

The effect of benzyloxy-substituents was also studied. Adding a benzyloxy substituent to **2PYAc8** to give **2PYCa1** improved the activity, resulting in an MIC $16-32 \mu\text{g mL}^{-1}$ (Table 3.5). However, having a single benzyloxy substituent at position 2 **2PYCa4**, the compound retained activity. The corresponding pyridine-4-compounds **4PYCa1** and **4PYCa4** did not follow the same trend indicating that the positioning of the nitrogen atom also plays an important part in the biological activity of the compounds.

Table 3.5: MIC values for benzoyloxy and alkoxy-substituted carboxamidrazone amides against *M. fortuitum*

Code	Structure	MIC ($\mu\text{g mL}^{-1}$)	Code	Structure	MIC ($\mu\text{g mL}^{-1}$)
2PYCa1		16-32	4PYCa1		>32
2PYCa4		16-32	4PYCa4		>32

3.5.3 Replacing the benzene ring

Table 3.6: MIC values for various ring-substituted carboxamidrazone amides against *M. fortuitum*

Code	Structure	MIC ($\mu\text{g mL}^{-1}$)	Code	Structure	MIC ($\mu\text{g mL}^{-1}$)
2PYAc5		>32	4PYAc5		>32
2PYAc6		>32	4PYAc6		>32
2PYAnh2		>32	4PYAnh2		>32
2PYAnh1		>32			

The benzene ring of the benzoyl portion of the parent amide structure was replaced with a range of other bicyclic rings of different ring size and different isomers (Table 3.6) above. Aromatic rings are planar, hydrophobic structures, commonly involved in van der Waals and hydrophobic interactions with flat hydrophobic regions of binding sites. From the current study it was observed that replacing

the benzene ring by bulkier rings was not beneficial for *M. fortuitum* inhibition. This could have been due to the steric nature of these compounds.

Table 3.7: MIC values for 5-nitro substituted furanyl carboxamidrazone amide against *M. fortuitum*.

Code	Structure	MIC ($\mu\text{g mL}^{-1}$)	Code	Structure	MIC ($\mu\text{g mL}^{-1}$)
2PYAc13		0.1-2	4PYAc13		>32
2PYAc25		>32	4PYAc25		>32

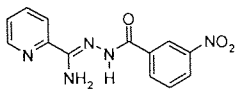
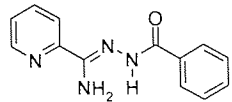
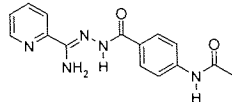
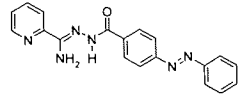
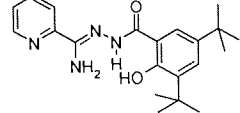
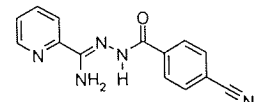
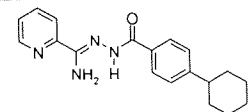
Substituting the benzene ring by a furanyl group was also investigated. If one considers **Table 3.7**, the 5-nitro substituted furanyl compound **2PYAc13** is most active with an MIC of 0.1-2 $\mu\text{g mL}^{-1}$ compared to that of isoniazid (MIC 1-2 $\mu\text{g mL}^{-1}$). Note the activity was much greater in one of the isomers than it was in the other i.e **4PYAc13** MIC (>32 $\mu\text{g mL}^{-1}$). It was expected that pyridine-4- **4PY** compounds' activity would be similar to those of the corresponding pyridine-2- **2PY** compounds as reported by the Mamolo group [1993]. This trend, however, was not observed in this study.

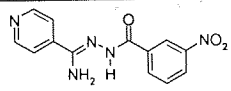
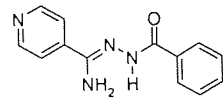
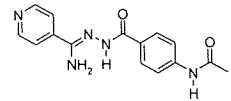
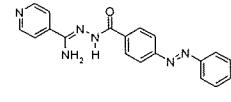
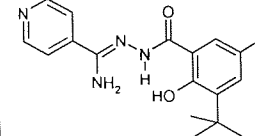
Furthermore, as well as the 2-pyridinecarboxamidrazone component, the 5-nitro-2-furanyl moiety also seems to be important for the antimycobacterial activity of compound **2PYAc13**, as the corresponding unsubstituted furanyl compounds **2PYAc25** and **4PYAc25** were inactive.

3.6 Evaluating miscellaneous carboxamidrazone amides against *M. fortuitum*

As mentioned previously, substituents having different electronic, hydrophilic and steric properties were investigated in this study. The results in Table 3.8 below indicate that the electron-withdrawing nitro substituent at 3-position of the benzoyl ring exhibited moderate activity for **4PYAc14** whereas the equivalent 2-pyridine compound **2PYAc14** was inactive against *M. fortuitum*. However, compound **2PYAc3** was more potent (4-8 $\mu\text{g mL}^{-1}$) than corresponding **4PYAc3** (16-32 $\mu\text{g mL}^{-1}$).

Table 3.8: MIC values for miscellaneous carboxamidrazone amides against *M. fortuitum*.

Code	Structure	MIC ($\mu\text{g mL}^{-1}$)
2PYAc14		>32
2PYAc1		16-32
2PYAc2		>32
2PYAc3		4-8
2PYCa5		>32
2PYAc7		>32
2PYCa2		>32

Code	Structure	MIC ($\mu\text{g mL}^{-1}$)
4PYAc14		16-32
4PYAc1		16-32
4PYAc2		16-32
4PYAc3		16-32
4PYCa5		>32

3.7 Antimicrobial Activity of Carboxamidrazone Amides

A small library of the synthesised carboxamidrazone amides was also tested *in vitro* for its antimicrobial activity against panel of various Gram-positive and Gram-negative bacteria to investigate the possibility of any broad spectrum activity. Although these new classes of carboxamidrazones were synthesised as antimycobacterial agents, it was thought to be useful to test them against the MRSA strains which are currently causing concern in hospitals. Furthermore, it was hoped that these results would also shed some light on the selectivity of the tested compounds.

The microdilution method was used and activities expressed as minimum inhibition concentration (MIC $\mu\text{g/mL}$) are summarised in **Appendix 4**. (The MIC was determined by the placement student S. Chauhan). The compounds were tested against the panel of following microorganisms: *S. aureus* (NCTC 6571), *B. subtilis* (ATCC 6633), *E. faecalis* (NCTC 5957), *E. coli* (ATCC 27325), *P. aeruginosa* (ATCC 15692) and *K. pneumoniae* (1082E).

None of the compounds tested in the present study was found to have antimicrobial activity against the microorganisms listed in **Appendix 4**. Interestingly, compounds **2PYCa1**, **2PYCa2**, **2PYCa4**,

2PYCa5, **2PYCa6**, **2PYAnh1** and **4PYCa5** exhibited an antimycobacterial activity (90-100% Inh) against the strain *M. tuberculosis* H37Rv. In contrast, these particular compounds were inactive against other strains listed in **Appendix 4**. This could be that the higher lipophilicity of these compounds aids the passage of the molecule through the lipophilic cell wall affording greater activity to the compound. It is well documented, that the structure, chemical composition and thickness of the cell wall differ in gram-positive and gram-negative bacteria. Gram-positive bacteria have a single, very thick cell wall, consisting largely of peptidoglycan whereas Gram-negative bacteria have a very thin inner membrane consisting of only 1-5% peptidoglycan, surrounded by an outer membrane consisting of a large amount of lipoproteins and lipopolysaccharides. Probably these differences account for different in activity [Rathbone *et al*, 2006].

3.8 Comparison of the *M. fortuitum* results with *M. tuberculosis* results

In this study *M. fortuitum* (reference: NCTC 10394) was used as a surrogate for *M. tuberculosis* for the aforementioned reasons stated above (Section 3.1). It is however, difficult to compare the two sets of mycobacterial results directly, since their activity is measured in different ways, i.e. an MIC measurement for *M. fortuitum* and a percentage inhibition for *M. tuberculosis*. Moreover, the TAACF only consider compounds with an inhibitory activity of 90% or more, at a concentration of 6.25 $\mu\text{g mL}^{-1}$, worthy of further investigation into their potential as antitubercular drugs. Of the ninety two compounds selected to be tested for *M. tuberculosis* only the results of sixty eight compounds had been received from TAACF. The rest of the compounds were said to exhibited fluorescence and will be tested at a later date. Unfortunately, it is not possible to present the full findings at this point of time. However, of the 68 compound tested in this study are listed in **Appendix 5**, 15 compounds were found to be active and worthy of further investigation **Table 3.9** and **Table 3.19**.

3.9 Comparison of the *M. fortuitum* results with *M. tuberculosis* results for carboxamidrazone amides and cyclic imides

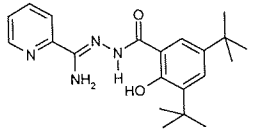
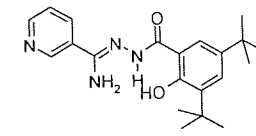
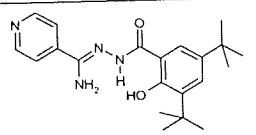
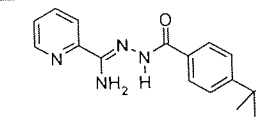
The activity of all the synthesised compounds was investigated by the preliminary *M. fortuitum* screen. A set of sixty eight compounds was screen against both organisms. Of the fifteen compounds which exhibited the greatest inhibition (90-100 %) for *M. tuberculosis*; six of the compounds were also active against *M. fortuitum*. The *M. fortuitum* screen did not predict the activity of nine compounds that were highly active against *M. tuberculosis*. From this study it has been conveyed that in order to minimise the possibility of missing potentially active compound, it would be worth submitting the compounds for screening against *M. tuberculosis*, even if they were inactive against *M. fortuitum*. However, the active compounds against *M. tuberculosis* in this study were highly lipophilic and this could be one of the reasons that they were not predicted by *M. fortuitum*. The lipophilicity may present problems in terms of solubility, as well as direct and biotransformational toxicity [Coleman *et al* 2000].

Table 3.9: Comparison of *M. fortuitum* MIC, with *M. tuberculosis* H37Rv (*M. tuber*) MIC and %Inhibition results

Code	Structure	MIC <i>M. fort</i> $\mu\text{g mL}^{-1}$	MIC <i>M. tuber</i> $\mu\text{g mL}^{-1}$	%Inh
4PYAc18		>32	<6.25	100
2PYCa5		>32	<6.25	100
2PYAnh 1		>32	<6.25	99
2PYCa2		>32	<6.25	97
4PYAc3		16-32	<6.25	95
4PYCa5		>32	<6.25	94
2PYAc16		>32	<6.25	93
2PYAc18		>32	<6.25	93
2PYCa1		16-32	<6.25	93
2PYAc3		4-8	<6.25	92
2PYAc20		8-16	<6.25	91
2PYCa4		16-32	<6.25	90
2PYCa6		>32	<6.25	90

From the obtained results it was observed that for compounds **2PYCa5** and **4PYCa5** the 3,5-di-*tert*-butyl-2-hydroxy-benzoyl moiety was important for the antimycobacterial activity **Table 3.10**. However, the 2-pyridinecarboxamidrazone component appears also responsible for the antimycobacterial potency (100% inhibition) for compound **2PYCa5**, because the corresponding 4-pyridinecarboxamidrazone derivative **4PYCa5** retained antimycobacterial activity, but the potency was diminished (94% inhibition). The presence of the 3-pyridinecarboxamidrazone moiety in compound **3PYCa5** practically abolishes the antimycobacterial potency (64% inhibition). It seems that the electronic properties of the heteroaryl ring are important for activity. Furthermore, in case of mono-substituted derivative **2PYAc20** ie *tert*-butyl group at 4-position of the benzoyl ring, the antitubercular activity of the compound was retained (91% inhibition), suggesting that the branching alkyl group was also important for antitubercular activity.

Table 3.10: Comparison of *M. fortuitum* MIC, with *M. tuberculosis* H37Rv (*M. tuber*) MIC and % Inhibition results for *tert*-butyl substituted carboxamidrazone amides

Code	Structure	MIC <i>M. fort</i> $\mu\text{g mL}^{-1}$	MIC <i>M. tuber</i> $\mu\text{g mL}^{-1}$	%Inh
2PYCa5		>32	<6.25	100
3PYCa5		>32	>6.25	64
4PYCa5		>32	<6.25	94
2PYAc20		8-16	<6.25	91

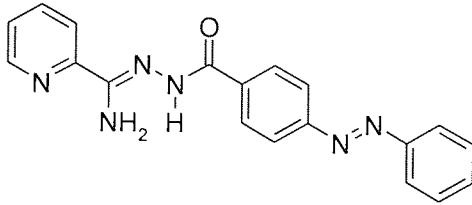
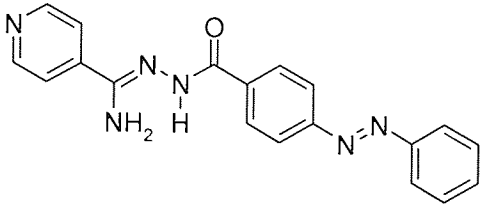
Considering compounds **2PYAc18** and **4PYAc18**, **Table 3.11** below it appeared that extending the length of side chain at 4-position by methylene group was beneficial for antitubercular activity. The peak antitubercular activity occurred with 4-heptyl-substituted derivatives. The 4-pyridinecarboxamidrazone derivative **4PYAc18** was more potent (100% inhibition) than the corresponding 2-pyridinecarboxamidrazone derivative (93% inhibition). These compounds did not exhibit any activity against *M. fortuitum*. Similarly, compound **2PYAc16** having a propyl group attached at 4-position, displayed activity against *M. tuberculosis* (93% inhibition), whereas the corresponding **4PYAc16**, abolished the antimycobacterial activity (58% inhibition). On the other hand, 4-ethyl substituted derivatives **2PYAc15**, **4PYAc15** (34% inhibition) and hydrogen substituted derivatives **2PYAc1** and **4PYAc1** (46% inhibition) have greatly reduced the antitubercular activities against *M. tuberculosis*, but these compounds were active against *M. fortuitum*. Furthermore, the 2-pyridinecarboxamidrazone derivative, **2PYCa6**, possessing an isopropyl moiety at the 4-position was

also active against *M. tuberculosis* (90% inhibition). In contrast the equivalent **4PYCa6** had no activity (53 % inhibition). Both of the compounds were inactive against *M. fortuitum*.

Table 3.11: Comparison of *M. fortuitum* MIC, with *M. tuberculosis* H37Rv (*M. tuber*) MIC and %Inhibition results for alkyl-substituted carboxamidrazone amides

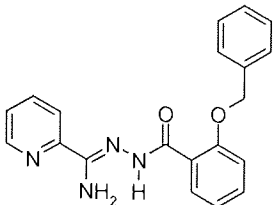
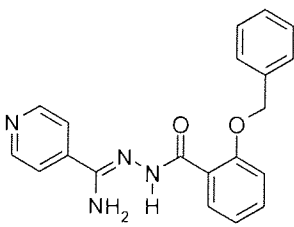
Code	Structure	MIC <i>M. fort</i> $\mu\text{g mL}^{-1}$	MIC <i>M. tuber</i> $\mu\text{g mL}^{-1}$	%Inh
2PYAc1		16-32	N/A	N/A
4PYAc1		16-32	>6.25	46
2PYAc15		8-16	N/A	N/A
4PYAc15		16-32	>6.25	34
2PYAc16		>32	<6.25	93
4PyAc16		>32	>6.25	11
2PYAc18		>32	<6.25	93
4PYAc18		>32	<6.25	100
2PYCa6		>32	<6.25	90
4PYCa6		>32	>6.25	53

Table 3.12: Comparing MIC values and %Inhibition of **2/4PYAc3** against *M. tuberculosis* and *M. fortuitum*

Code	Structure	<i>M. Fort.</i> MIC $\mu\text{g mL}^{-1}$	<i>M. Tuber.</i> MIC $\mu\text{g mL}^{-1}$	% Inh
2PYAc3		4-8	<6.25	92
4PYAc3		16-32	<6.25	95

Other compounds of interest in the series were **2PYAc3** and **4PYAc3** Table 3.12. The conjugated azobenzoyl substituent, displayed a significant amount of potency against *M. tuberculosis* as well as against *M. fortuitum*. It was interesting to note that compound **4PYAc3** (95% inhibition) was more potent than compound **2PYAc3** (92% inhibition) against *M. tuberculosis* and compound **2PYAc3** (MIC 4-8 $\mu\text{g mL}^{-1}$) was more potent than **4PYAc3** (MIC 16-32 $\mu\text{g mL}^{-1}$) against *M. fortuitum*.

Table 3.13: Comparing MIC values and %Inhibition of **2/4PYCa4** against *M. tuberculosis* and *M. fortuitum*

Code	Structure	<i>M. Fort.</i> MIC $\mu\text{g mL}^{-1}$	<i>M. Tuber.</i> MIC $\mu\text{g mL}^{-1}$	% Inh
2PYCa4		16-32	<6.25	90
4PYCa4		>32	>6.25	55

The antimycobacterial activity of the compounds **2PYCa4** and **4PYCa4** (Table 3.13) bearing a benzyloxybenzoyl substituent at the *ortho* position was also assessed. It was discovered that **2PYCa4** was not only active against *M. tuberculosis* (90% inhibition), but was also active against *M. fortuitum* (MIC 16-32 $\mu\text{g mL}^{-1}$). The corresponding **4PYCa4** (55% inhibition) was inactive against both the organisms. However, addition of a methoxy group at the *para* position and exchanging the benzyloxy group from the *ortho* to the *meta* position to give compounds **2PYCa1** and **4PYCa1** Table 3.14 was

encouraging. The potency of **4PYCa1** (81% inhibition) was also increased significantly against *M. tuberculosis*, which was reasonable, but not high enough to be considered worthy of further investigation according to TAACF. This change was not beneficial against *M. fortuitum*.

Table 3.14: Comparing MIC values and %Inhibition of **2/4PYCa1** against *M. tuberculosis* and *M. fortuitum*.

Code	Structure	<i>M. Fort.</i> MIC $\mu\text{g mL}^{-1}$	<i>M. Tuber.</i> MIC $\mu\text{g mL}^{-1}$	% Inh
2PYCa1		16-32	<6.25	93
4PYCa1		>32	>6.25	81

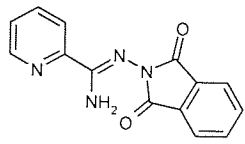
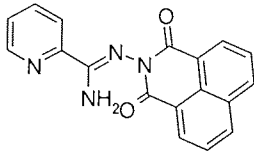
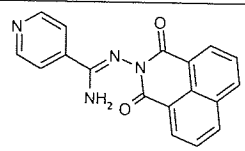
In case of compound **2PYCa2** (Table 3.15) the introduction of the bulkier cyclohexane ring at the 4-position, aimed at increasing the lipophilicity resulted in increased activity against *M. tuberculosis* (97% inhibition). In addition to lipophilicity, the steric factor may have been responsible for the increased antitubercular activity. However, the activity of this compound was not predicted by the preliminary *M. fortuitum* screen.

Table 3.15: MIC values and %Inhibition of **2PYCa2** against *M. tuberculosis* and *M. fortuitum*

Code	Structure	<i>M. Fort.</i> MIC $\mu\text{g mL}^{-1}$	<i>M. Tuber.</i> MIC $\mu\text{g mL}^{-1}$	% Inh
2PYCa2		>32	<6.25	97

Furthermore, substituting benzene ring by a cyclic anhydride (Table 3.16) below, for example, in compound **2PYAnh1** was more effective. The antitubercular activity was enhanced (99 % against *M. tuberculosis*) probably by constraining the ring into a particularly favourable conformation. However, introduction of polycyclic ring into compounds **2PYAnh2** and **4PYAnh2** may have constrained the molecules into the unfavourable conformation, and potency could have been dropped.

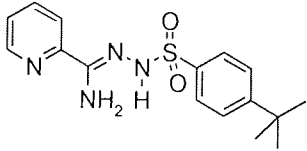
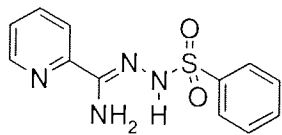
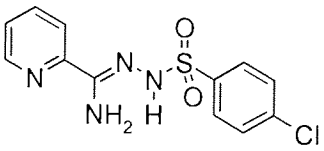
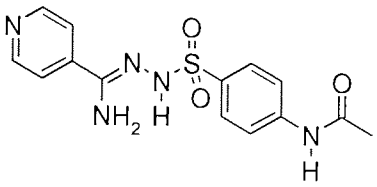
Table 3.16: MIC values and % Inhibition of carboxamidrazone imides against *M. tuberculosis* and *M. fortuitum*.

Code	Structure	<i>M. Fort.</i> MIC $\mu\text{g mL}^{-1}$	<i>M. Tuber.</i> MIC $\mu\text{g mL}^{-1}$	% Inh
2PYAnh 1		>32	<6.25	99
2PYAnh2		>32	N/A	N/A
4PYAnh2		>32	>6.25	47

3.10 Evaluating antimycobacterial activities of carboxamidrazone sulphonamides.

The synthesized carboxamidrazone sulphonamides (**Table 3.17**), were screened against *M. fortuitum* to investigate if they possessed any activity. Unfortunately they were found to be inactive against *M. fortuitum*. It remains to be established whether these compounds possessed any anti-tubercular activity.

Table 3.17: Antimycobacterial activity of various carboxamidrazone *N*¹-(benzoyl)sulphonamide against *M. fortuitum* The biological activity was determined by F. Kusar (B.Sc Applied and Human Biology final year project student, Aston University, 2004).

Code	Structure	MIC ($\mu\text{g mL}^{-1}$)
2PYS1		>32
2PYS2		>32
2PYS3		>32
4PYS4		>32

4PYS5		>32
4PYS2		>32

3.11 Antimicrobial testing results versus *M. fortuitum* and *M. tuberculosis* for *N*¹-benzenlidene-4-pyridinecarboxamidrazones nitrogen oxides

A series of pyridine-4-carboxamidrazone-N-oxide has been synthesised with the aim of evaluating their antimicrobial activity **Table 3.18** toward a strain of *M. tuberculosis* H₃₇Rv and *M. fortuitum*. It was demonstrated that the introduction of an electron-withdrawing substituent at N1 position on pyridine ring resulted in loss of activity against *M. tuberculosis*. With the exception of **4PYauN-O** and **4PYafN-O** the rest of compounds had either diminished or abolished the activity against *M. fortuitum*. Having said that, this conclusion was drawn from a small set of compounds and should be evaluated further in more-extensive studies.

Table 3.18: Antimicrobial testing results versus *M. fortuitum* (*M.fort*) and *M. tuberculosis* (*M.tuber*) for various *N*¹-benzenlidene-4-pyridinecarboxamidrazones nitrogen oxides and their corresponding imine. An MIC for imine was obtained from thesis (TIMS 2002) and an MIC for *N*¹-benzenlidene-4-pyridinecarboxamidrazones nitrogen oxides was determined by project students F. Kusar (B.Sc Applied and Human Biology final year project student, Aston University, 2004). Results against *M. tuberculosis* strain H₃₇Rv was provided by the TAACF. (+) indicates that, the compound is active at the single concentration of 32 µg mL⁻¹, (-) indicates that the compound is not active.

Compound	Structure	<i>M. Fort.</i>	<i>M. fort.</i> MIC (µg mL ⁻¹)	<i>M. fort.</i> MIC (µg mL ⁻¹) Corresponding imine	<i>M.tuber</i> %Inh
4PYakN-O		-	>32	4-8	67
4PYafN-O		+	16-32	8-16	11
4PYaeN-O		-	>32	>32	30

4PYapN-O		+	16-32	>32	49
4PYagN-O		-	>32	16-32	0
4PYatN-O		-	>32	16-32	76
4PYauN-O		+	8-16	16-32	88
4PYaiN-O		-	>32	16-32	66

3.12 Antimicrobial activity of pyridine-4-carboxamidrazone-4-N-oxides

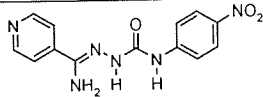
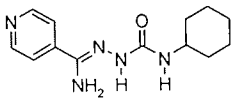
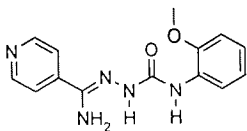
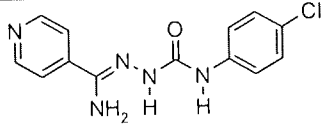
Pyridine-4-carboxamidrazone-4-N-oxides were also tested against a panel of Gram-positive and Gram-negative microbacteria for any broad-spectrum activity (**Appendix 6**). The antimicrobial activities of the compounds were determined by Laura Wheedon (the microbiology research student, at Aston University, 2006) using the microdilution broth susceptibility method. With the exception of the compound **4PYakN-O** which was active at $16-32 \mu\text{g mL}^{-1}$ against Gram-negative *M. catarrhalis* the rest of the tested pyridine-4-carboxamidrazones-4-N-oxide was inactive against panel of Gram-negative bacteria. None of the tested compounds exhibited any *M. tuberculosis* inhibition at $6.25 \mu\text{g mL}^{-1}$. Compound **4PYaeN-O** exhibited activity against *B. subtilis* and *B. cereus* at a concentration of $8-16 \mu\text{g mL}^{-1}$ and $16-32 \mu\text{g mL}^{-1}$ respectively. In addition, **4PYafN-O** has exhibited activity against *M. roseus* and *B. subtilis* at a concentration of $16-32 \mu\text{g mL}^{-1}$, whereas **4PYagN-O** exhibited activity against the microorganism *B. cereus* at a concentration of $16-32 \mu\text{g mL}^{-1}$.

Overall, the introduction of polar atom at the pyridine ring reduced the lipophilicity of the compounds and perhaps this factor is responsible for loss of activities against *M. tuberculosis*.

3.13 Comparison of the *M. fortuitum* results with *M. tuberculosis* results for carboxamidrazone ureas

The next series of compounds to be discussed are the heteroarylcarboxamidrazone ureas. In the course of this work, thirty two compounds with different substituents are prepared. The compounds were subjected to mycobacterial activity assays as mentioned above section 3.2 and the results are summarized in **Appendix 7** and **Appendix 8**. The results demonstrated that all the synthesized pyridine-2-carboxamidrazone ureas were inactive against both of the organisms, namely, *M. fortuitum* and *M. tuberculosis*. The results obtained for the pyridine-4-carboxamidrazone ureas showed different trends than those of their corresponding pyridine-2-carboxamidrazone compounds. Of the sixteen compounds, four compounds exhibited antimycobacterial activity (**Table 3.19**).

Table 3.19: MIC values for active pyridine-4-carboxamidrazone ureas against *M. fortuitum* and *M. tuberculosis*.

Code	Structure	MIC <i>M. Fort</i> ($\mu\text{g mL}^{-1}$)	<i>M. tuber.</i> % Inh
4PYIs7		16-32	100
4PYIs5		>32	94
4PYIs10		8-16	55
4PYIs14		4-8	69

The nitro substitution at the 4-position gave a very active compound **4PYIs7** against *M. tuberculosis* (100% inhibition) whereas the nitro group at 2-position for **4PYIs16** reduced antitubercular activity (73% inhibition) suggesting that positioning of nitro group was important for antitubercular activity. The MIC of the compound **4PYIs7** against *M. fortuitum* was predicted to be ranging from 16-32 $\mu\text{g mL}^{-1}$. The halogen substitution at the 4-position gave compound **4PYIs14**, which was very active against *M. fortuitum* having an MIC value of 4-8 $\mu\text{g mL}^{-1}$. This compound was inactive against *M. tuberculosis* (69% inhibition). The 4-Br compound **4PYIs6** was inactive against both organisms.

The 2-methoxy substituted compound **4PYIs10** exhibited activity against *M. fortuitum* having a MIC value of 8-16 $\mu\text{g mL}^{-1}$. In contrast it was inactive against *M. tuberculosis*.

Substituting the benzene ring of **4PYIs4** with a cyclohexane ring in compound **4PYIs5** enhanced the potency of compound (from 50% to 94% inhibition) against *M. tuberculosis*.

3.14 Crystal Structure of New Classes of Carboxamidrazones

As a continuation of our studies on new classes of heteroarylcarboxamidrazones, the crystal structure determination of pyridine-2-carboxamidrazone amide (**2PYAc20**), urea (**2PYIs1**) and sulphonamide (**2PYS1**) has been carried out [Cox *et al*, 2003]. It was of interest to investigate the structures of new types of amidrazones Figure 7.1 with a hydrogen atom on N9 causing N-H...H-N stereoelectronic clash. It was also of interest to find out why the structurally similar compounds display different biological activities. For this reason a suitable X-ray quality crystals of these compounds were obtained by a slow evaporation from an appropriate solvents and subjected to an X-ray analysis. The results were compared with the parent compound **120**, Figure 3.1.

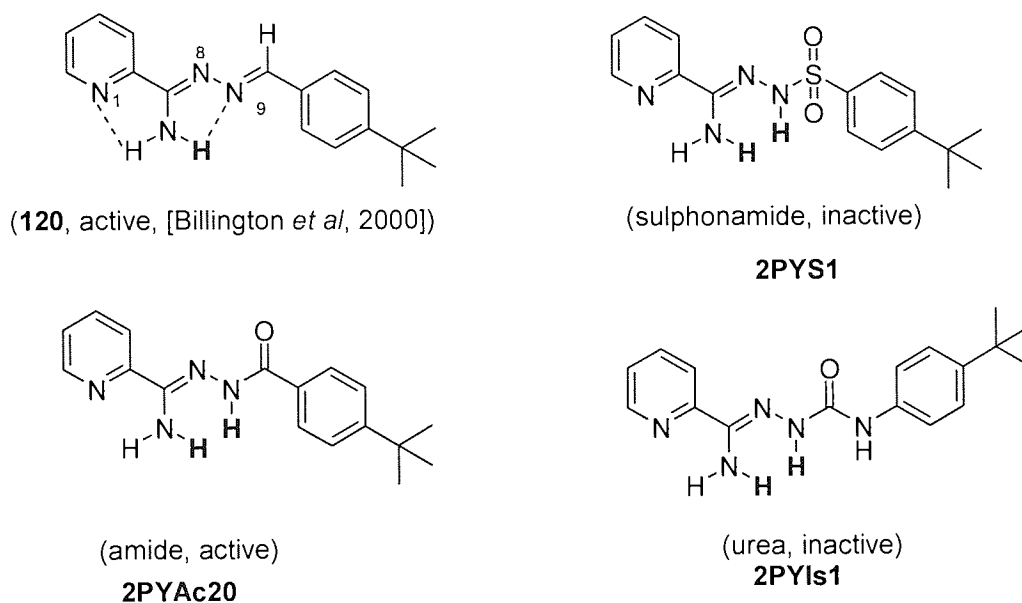
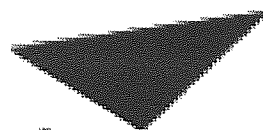


Figure 3.1: Structure of imine (*N*¹-benzylidene heteroarylcarboxamidrazones the parent compound **120**) MIC (8-16 $\mu\text{g}/\text{mL}$), amide **2PYAc20**, MIC (8-16 $\mu\text{g}/\text{mL}$), urea **2PYIs1** MIC (>32 $\mu\text{g}/\text{mL}$) and sulphonylamide **2PYS1** MIC (>32 $\mu\text{g}/\text{mL}$) against *M. fortuitum*.

Previous crystallographic studies have established that *N*¹-benzylidene-2-carboxamidrazones **120** (**Figure 3.1**) exist as the E-isomer in the solid state [Billington *et al*, 2000]. It is also known that unhindered intramolecular hydrogen bonding can occur between the amino hydrogen atoms and the pyridine N1 atoms causing the molecule to adopt a reasonably planar conformation. The X-ray analysis also reveals that partial intermolecular hydrogen bonds between the adjacent molecules were also important in the stabilization of the crystal structure. However, in the present study, the presence of a hydrogen atom at N9 caused a different pattern of molecular packing. For example, these molecules are fairly flat, but not as flat as the parent compound **120** with exception of amide which was quite linear resembling the parent compound. Structural study indicates that due to the involvement of the hydrogen atom on N9, the bond length C7=N9 is significantly increased (0.036 Å). The longer bonds suffer greater twists about N8-N9, for example, in case of urea compound **2PYIs1**. Due to the extra NH group the angle C7-N8-N9 is reduced and the molecule is slightly bent probably causing molecule to contact a different part of the receptor. The amino groups participate in an intramolecular interaction to pyridine N1 with N-H...H and N-H...N angles of 95-114°.



Aston University

Illustration removed for copyright restrictions

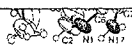


Figure 3.2: Superimposed structures of imine, amide, urea and sulphonamide adapted from reference [Cox, *et al*, 2003]

Furthermore, in both amide and urea one amino H atom and one nearby NH bite onto the carbonyl atom of the neighboring molecule, whereas sulphonyl O atoms act as hydrogen bond acceptors, sometime for amino H atoms and sometimes for NH. The staggered bonds to sulphur make **2PYS1** an L-shaped molecule. The difference in the biological activities of these compounds was probably due to the difference in shapes of these compounds. Hence, urea and sulphonamide are bent and L-shaped respectively and both are inactive. In contrast, imine and amide are both linear and are active; this difference in shape perhaps accounts for their activity.

3.15 Conclusions

The present studies have revealed that most of the compounds which were found to possess activity against *M. tuberculosis* and *M. fortuitum* were pyridine-2-carboxamidrazones (**2PY**) derivatives, while some of the equivalent pyridine-4-carboxamidrazones also displayed similar activities. Another interesting trend observed from this study was that pyridine-2-carboxamidrazones urea (**2PY**) derivatives (**Appendix 7**) displayed no activity against *M. fortuitum* or *M. tuberculosis*. In contrast, four compounds from the pyridine-4-carboxamidrazones urea series (**Appendix 8**) demonstrated good activity against *M. fortuitum* and *M. tuberculosis*. It would be interesting to investigate the effect on biological activities by modifying carboxamidrazones to their corresponding carboxamidrazones thioureas.

It is of interest that most of the carboxamidrazones which displayed activity against *M. tuberculosis* were highly lipophilic. Increasing the carbon chain length of the substituents or the

addition of bulkier substituents, at the 4-position of the aryl substituent, improved the activity of the compounds for *M. tuberculosis*, while this change abolished the activity for *M. fortuitum*. It may be predicted that increased lipophilicity contributes to their easy permeability through the mycobacterial cell wall. It is not known how these compounds work inside the mycobacteria or what the molecular target is. However, if the target is an enzyme, then the molecule has to reach that enzyme, by first penetrating the lipophilic cell wall. These results were consistent with the observations of Mamalo *et al* [1992] and Billington *et al* [1998]. They stated, that lipophilicity was important for antimycobacterial activity and that decreasing lipophilicity of the compounds resulted in reduced activity. Another important observation made from this study was that the compounds which displayed activity against *M. tuberculosis* in this study were in fact specific for mycobacteria and were inactive against Gram-positive or Gram-negative bacteria. Furthermore, structural analysis of these compounds indicated that the shape, the volume and the length of the molecule also contribute for their biological activity. In addition, solubility, electronic factors and the nature and positioning of substituents at the aromatic ring tend to have an influence on the activity.

It is noteworthy that MIC value for compound **2PYAc13** against *M. fortuitum* was found to be in the range of 0.1-2 µg/mL, which was comparable to those observed for isoniazid which is the clinically used first-line antitubercular drug. It remains to be established whether **2PYAc13** possess any anti-tubercular activity. The compound should be assessed in further tests in comparison with other anti-tuberculosis drugs. The positive activity of **2PYAc13** also shows that the nitro substituted furan ring may replace the benzyl substituent in the carboxamidrazone amide series. However, the presence of the nitro substituents in compound **2PYAc13** raises concerns about the possibility of toxicity and this issue remains to be addressed. This is primarily due to the fact that the eradication of tuberculosis requires a lengthy course of treatment, and the need for an agent with a high margin of safety becomes a primary concern.

Moreover, fifteen compounds were found to be active against *M. tuberculosis* H37Rv and the TAACF is to conduct further tests into the suitability of these compounds as potential drug candidates. It would be highly desirable to compare all potential candidates for further progression in a standard series of tests, for example, efficacy, ADME (absorption, distribution, metabolism and elimination), toxicity studies in mice and *in vitro* tests v resistant strains of *M. tuberculosis*.

In this study attempts have been made to uncover trends in the structure activity relationships for the various carboxamidrazone derivatives in their antimicrobial and antimycobacterial activities. This has been possible with particular compound groups and certain molecular features have been found to be important or limiting. This, however, is only a partial view. Since drug-receptor interactions are multi-factorial in their structure activity relationships, the next step in this study would be to use molecular modelling (property calculations) and statistical methods to derive quantitative structure activity relationships. By this approach it may be possible to uncover multi-factorial features necessary for good antimycobacterial activity across the entire dataset.

The results obtained from this study have established that carboxamidrazones possess an interesting activity within them and if they are investigated further, then still more molecules possessing antitubercular activity closer to existing tuberculosis drug regimens could be generated.

CHAPTER 4

4 Introduction to Dihydrofolate Reductase

The appearance of drug-resistant *Mycobacterium tuberculosis* emphasises the need for new drugs to treat these infections. Also, effective chemotherapy of persons with AIDS who are also infected with *M. tuberculosis*, especially multidrug-resistant *M. tuberculosis*, can be difficult. A good biochemical target to accomplish this is the enzyme dihydrofolate reductase (DHFR). DHFR catalyses the NADPH-dependent reduction of dihydrofolate (FH₂) (**63**) to tetrahydrofolate (FH₄) (**64**), which is the reduced form of folate (**65**) that is involved in a variety of biochemical functions involving single-carbon transfers at various oxidation states Figure 4.1.

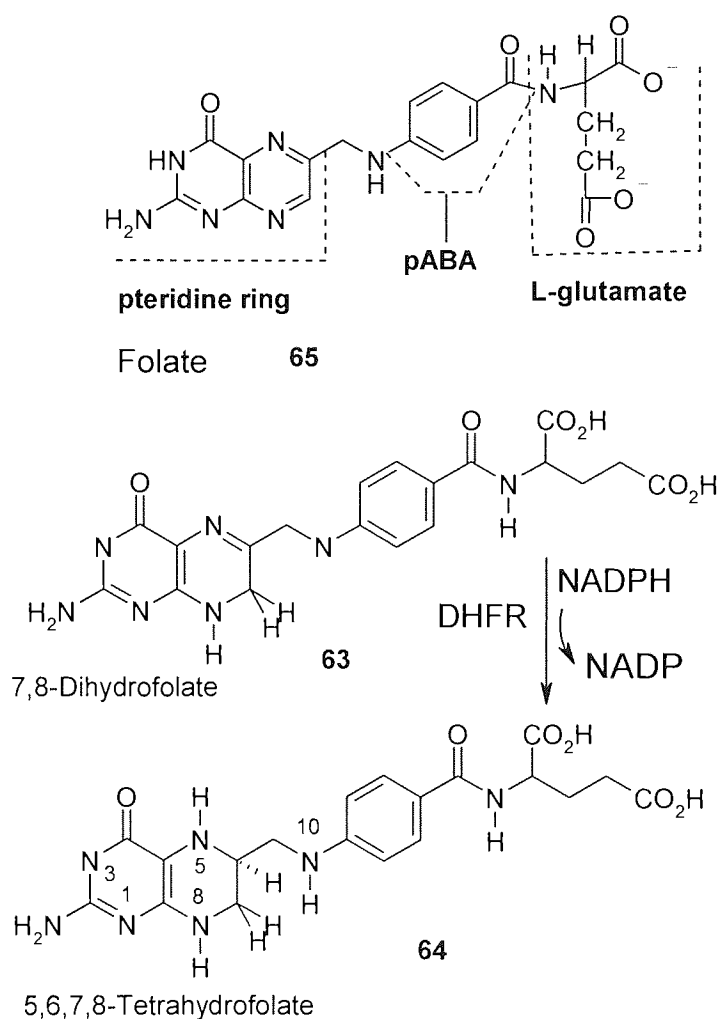


Figure 4.1: The substrate (**63**), 7,8-dihydrofolate, product (**64**), 5,6,7,8-tetrahydrofolate and folate (**65**)

These coenzymes of folate are involved in the biosynthesis of thymidilate, purine nucleotides, serine and methionine, as well as other metabolites. Inhibitors of DHFR reduce the intracellular level of tetrahydrofolate resulting in aberrant cellular metabolism. In rapidly dividing cells, the inhibition of DNA, RNA and protein synthesis leads to cell death. Therefore, DHFR is an important target for drug development against cancer and a variety of infectious diseases caused by bacteria, protozoa and fungi.

The recognition of the importance of these enzymes and the routine availability of protein crystallography led to an explosion of information of 3-D structures of DHFRs from human, protozoal, fungal and bacterial sources with numerous ligands and cofactors bound in their active centres. A detailed comparison of the *M. tuberculosis* and the human enzyme should provide needed data for the design of drugs with high potency as well as selectivity for effective therapy. For example, the atomic structure of human DHFR complexed with NADPH and two lipophilic antifolates, the 3D-structure of the *M. tuberculosis* DHFR complexed with several inhibitors, and many others including a variety of DHFRs from clinically important Gram-positive and Gram-negative bacterial pathogen are reviewed by Kompis and co-workers [Kompis *et al*, 2005]. The X-ray structure of the enzyme from *M. tuberculosis* was solved recently by Li and co-workers [Li *et al*, 2000]. The binary complex with NADP and ternary complexes with NADP and different inhibitors were determined at 1.7-2.0 Å resolution. These complexes identified a number of key interactions involved in inhibitors binding, and shed light on aspects of differences between the enzymes from host and pathogen. It was revealed that, despite only 26% sequence identity with the human DHFR, the overall fold was similar. However, there were significant differences; in particular, the presence of a glycerol molecule in the crystal structure of the *M. tuberculosis* complex suggests additional binding interactions which have prompted us to synthesise novel inhibitors for the *M. tuberculosis* DHFR (see Section 4.7, 4.7.3 and 4.8) for a more detailed description).

4.1 Agents Acting on the Folate Pathway

Many micro-organisms, including *M. tuberculosis* cannot take in preformed folates from their environment and therefore must synthesise folates from p-aminobenzoic acid, glutamic acid, and a pterin formed from GTP. In contrast, mammalian cells lack the folate biosynthetic enzymes and cannot synthesise folate. Therefore, mammals must take folate from dietary sources. This fundamental difference in metabolism creates potential targets for species-specific effects. Various strategies have been used in the design of antimicrobials. Some interrupt microbial metabolic pathways which are not possessed by host cells. The first example of this was the development of sulphonamides by Domagk [Domagk, 1935]. These compounds mimic para-amino benzoic acid (PABA) (**26**) and competitively inhibit the conversion of PABA into dihydropteroic acid, which is an essential precursor of folate. Bacteria rely on this metabolic pathway, as they are unable to take preformed folate from the host and folate is essential substrate in the synthesis of DNA. Further down the same pathway, trimethoprim and pyrimethamine inhibit the activity of dihydrofolate reductase, which converts dihydrofolate into tetrahydrofolate (**Figure 4.2**). This also reduces tetrahydrofolate concentrations. These two groups of agents can be used together in the treatment of bacterial infections (trimethoprim-sulphamethoxazole) or parasitic infections such as toxoplasmosis (pyrimethamine and sulphadiazine) [Bannister *et al* 1996].

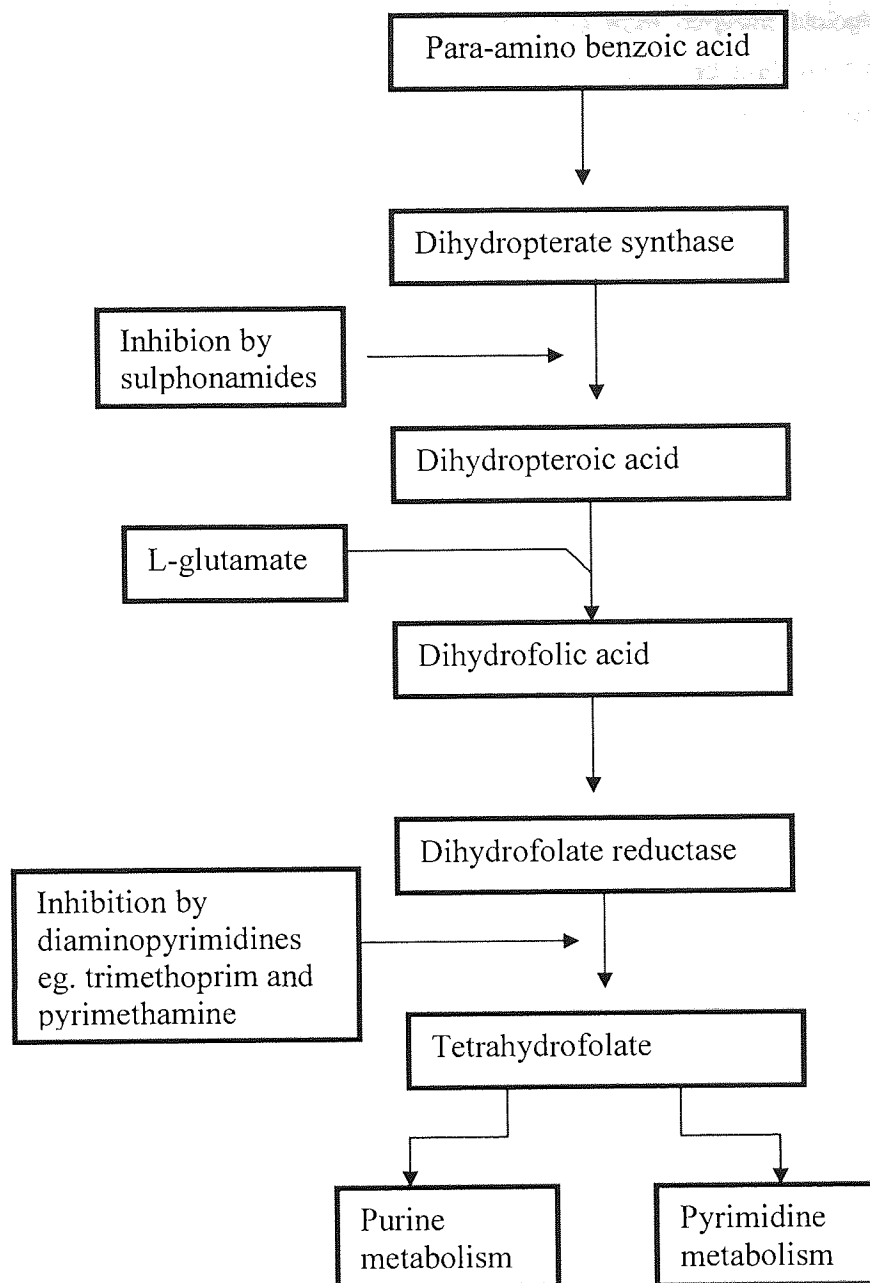


Figure 4.2: The actions of sulphonamides and trimethoprim [Adapted from Bannister *et al* 1996]

4.2 Inhibitors of Dihydrofolate Reductase

A large family of compounds has been discovered which inhibit DHFR, most of which contain a 2,4-diaminopyrimidine nucleus (Figure 4.3). The activity of DHFR inhibitors is due to the presence of the N-C(NH₂)-N-C(NH₂)- fragment in 2,4-diaminopyrimidine like moieties (Figure 4.3).

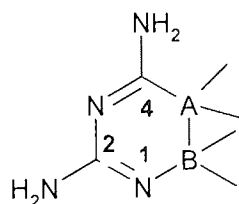


Figure 4.3: Structure of nitrogen-containing heterocyclic ring, where A B is C=C, N-C, or C=N.

It is believed that both of the amino group nitrogen atoms on the 2,4-diaminopyrimidine ring (Figure 2.3) play a role in the inhibition process [Perault and Pullman, 1961; Kuyper *et al* 1996]. The

combination of X-ray crystallography of numerous enzymes from different biological sources and molecular modeling [Li *et al.*, 2000; Mattioni *et al.*, 2003] has revealed that the conformations and binding modes of the inhibitors containing the aforementioned 2,4-aminopyrimidine nucleus bind essentially in the same pocket and their nitrogen containing heterocyclic rings position in the same orientation via hydrogen bonding. However, the other moieties of the inhibitors bind to quite different protein residues [Li *et al.*, 2000].

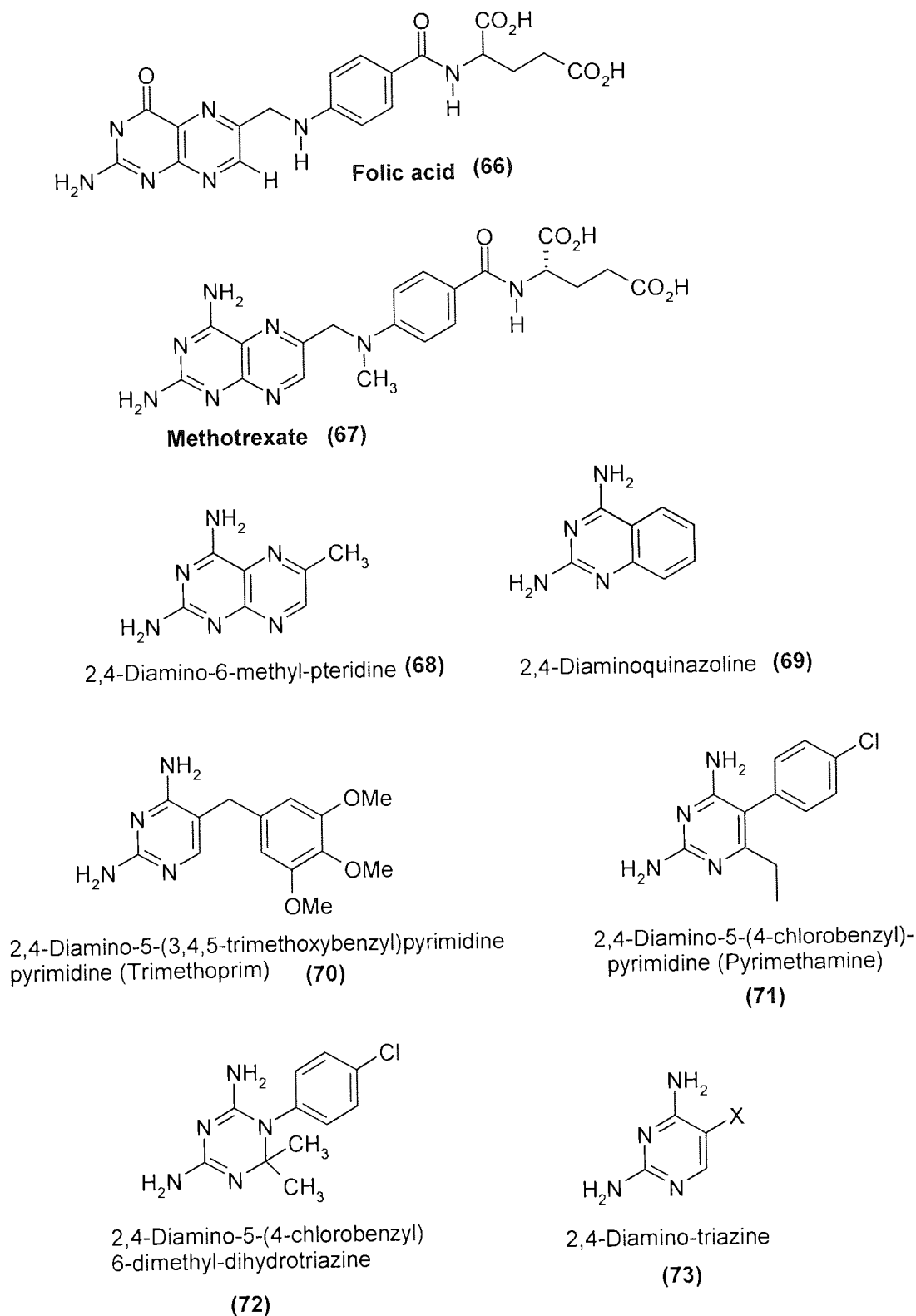


Figure 4.4: Structures of Folic Acid Antagonists (DHFR Inhibitors).

Perault and Pullman [Perault and Pullman, 1961] have discussed at some length the relation of the molecular structure to the distribution of electric charges in the atoms of folic acid analogues, using molecular orbital calculations. They concluded that in folic acid antagonists (inhibitors) the most basic nitrogen is in the 1-position while in the natural substrates it is in the 5- or 8-position; the 2-NH₂ is also more basic in the inhibitors than in the substrates. It was considered that the increased basicity of the 1-N and the 2-NH₂ accounted for the increased affinity of the inhibitors compared with that of the substrates for DHFR. For example, methotrexate (**67**), a compound much used in the treatment of cancer, inhibits the human enzyme through competitive tight binding to the active site, and is a potent inhibitor of the DHFR from most other sources. The antibacterial compound trimethoprim (**70**) is a potent inhibitor of bacterial DHFR and has been therapeutically useful because it binds only weakly to human DHFR.

Inhibitors of DHFR are classified as either 'classical' or 'non-classical' antifolates. Classical agents, such as methotrexate (**67**), contain side chains with a polar glutamic acid moiety and hence require a carrier mediated transport system to enter cells. Nonclassical inhibitors of DHFR do not possess the glutamic acid side chain, but rather have lipophilic side chains. These drugs are able to penetrate the cells by passive diffusion, thus circumventing the requirement for the carrier-mediated active transport system(s) needed for the uptake of classical antifolates [Gangjee *et al* 1999].

4.3 New Drugs and Drugs in Development (Antibacterials)

4.3.1 Novel Inhibitors of bacterial DHFR

4.4.1.1 Recent diaminopyrimidines

In addition to the established antifolate drugs (**Figure 4.4**), several new investigational drugs are at different stages of development (**Figure 2.5**). Intensive research, performed at Roche, led to the synthesis of various novel diaminopyrimidine compounds. Although many of these diaminopyrimidines do not possess superior microbiological activity compared to trimethoprim (TMP), several did possess properties that were considered to be potentially advantageous. For example, brodimoprim (**72**) (**Figure 4.5**) possess the similar antibacterial and toxicological properties to those of TMP. Brodimoprim has a long elimination half life of (32-35 h), which permitted once daily dosing as compared with the bi-daily dosing for TMP and co-trimoxazole. Brodimoprim was initially marketed for the treatment of respiratory tract infections, but did not find wide acceptance and was withdrawn from the market in 2000 due to severe side effects [Hawser *et al*, 2006].

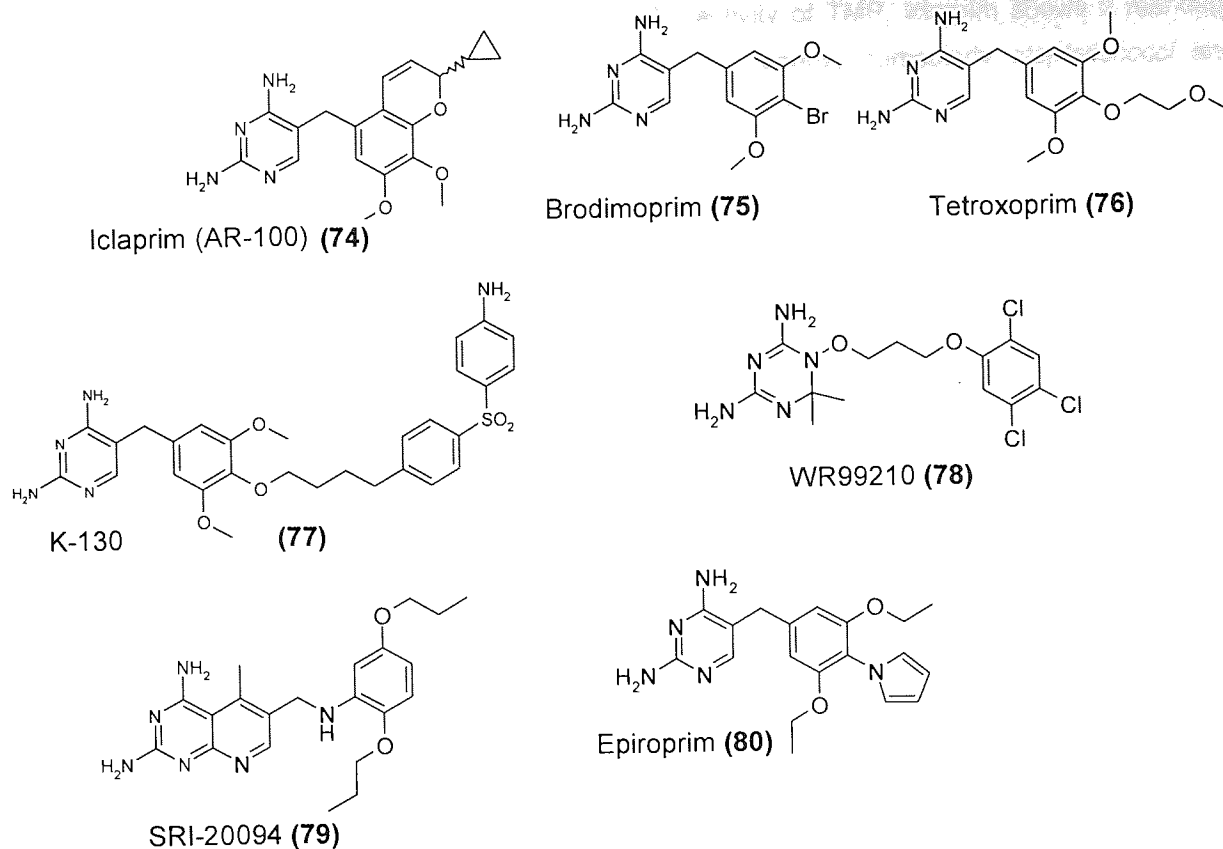


Figure 4 5: Structures of novel and in development Inhibitors of DHFR

Epiroprim (**80**) is a diaminopyrimidine antibiotic that is more lipophilic than TMP. Epiroprim (Ro 11-8958) possess attractive properties for the treatment of Gram-positive infections and has recently been evaluated against various *M. tuberculosis* strains [Dhople, 2002] and found to exhibit weak activity. However, the anti-mycobacterial activity of epiroprim was too weak to develop the drug for this indication. The triazine DHFR inhibitor WR99210 has been shown to exhibit reasonable activity against *M. tuberculosis*, but the selectivity was not sufficient for use as an antimicrobial agent. Therefore, novel DHFR inhibitors would need to show much better activity than epiroprim and WR99210. One example of a novel molecule with better activity is the diaminopyrimidine K-130 (**Figure 2.5**) which when coupled to dapsone was found to potently inhibit the DHFR from *Mycobacterium lufu* [Dhople, 1999].

In addition to WR99210 and K-130, a series of 2,4-diamino-5-deazapteridine derivatives synthesised at the Southern Research Institute, SRI-20094 exhibits significant activity against *M. avium* complex. Other close analogues of this compound were shown to be selective for the *mycobacterial* DHFR with activity ratios of >100 as compared with human DHFR. However, the activity of the compounds against *M. tuberculosis* is not as good as their activity against *M. avium* and although the overall characteristics of the compounds are encouraging further improvements in terms of anti-mycobacterial activity are required [Hawser *et al*, 2006].

Moreover, a novel diaminopyrimidine iclaprim (**Figure 4.5**) shows marked differences in activity as compared with TMP. Iclaprim (formerly AR-100 and Ro 48-2622) was discovered at Roche and has been licensed by Arpida which has developed this compound through pre-clinical and clinical trails. Iclaprim, like TMP, specifically and selectively inhibits Gram-positive and Gram-negative DHFRs at sub-micromolar concentrations with little or no inhibition of the human enzyme at over five orders of

magnitude higher concentration. As compared with the activity of TMP, iclaprim shows a markedly more potent activity against the major Gram-positive pathogens, particularly *staphylococci* and *streptococci* and including many strains that are resistance to TMP.

4.5 DHFR structure and ligand binding site

Many dihydrofolate reductases from various sources have been purified and the determination of their amino acid sequences [Hitching and Smith, 1980] has confirmed the differences in the characteristics of DHFR from different sources that the inhibition studies had detected. DHFR has been classified as a doubly wound mixed β -sheet in which the central eight-stranded β -sheet is protected on either side by two alpha helices [Richardson *et al*, 1981]. The individual strands of the β -sheet are designated A-H in order of their occurrence in the linear protein sequence [Matthews *et al*, 1977]. All the DHFR structures exhibit the same general fold.

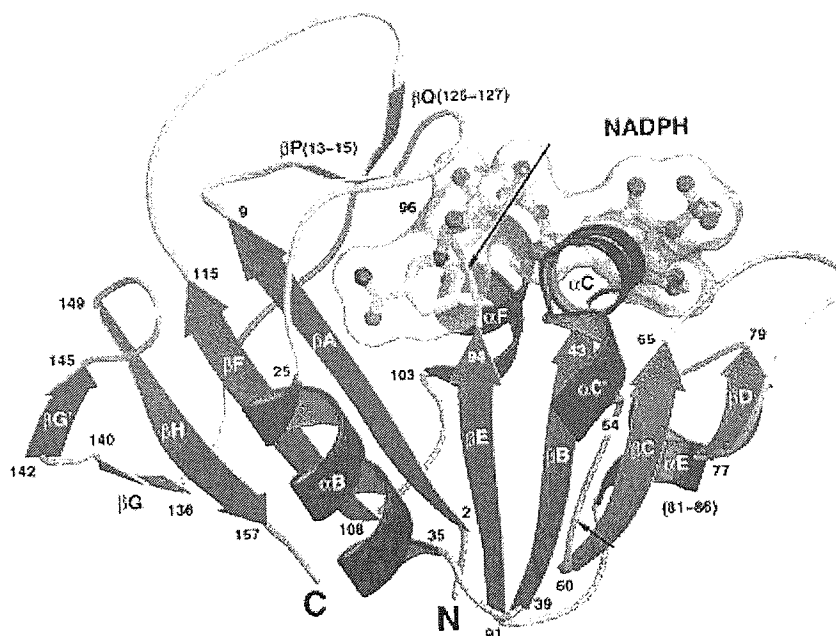


Figure 4.6: Structure of *M. tuberculosis* DHFR adapted from [Li *et al*, 2000].

A deep cleft exists on the enzyme surface between alpha helices B and C, and this cavity serves as the binding site for the diaminopyrimidine-type inhibitors and probably the substrate dihydrofolic acid. The nicotinamide portion of the cofactor also binds in this cleft, in a position to transfer its hydride equivalent to the adjacent substrate. The central portion of the inhibitor binding cleft of DHFR is lined with hydrophobic residues and is flanked at both ends by polar regions. Several hydrogen bonding sites are located at one end, deep within the cleft. The most important of these is a carboxyl group from an aspartate residue in the bacterial enzymes and a glutamate in the enzymes of vertebrate origin.

4.5.1 Aspects of Drug-Enzyme Interactions

The three-dimensional structure of the *M. tuberculosis* DHFR complexed with several inhibitors and NADPH (**Figure 4.7**) have been solved, and the enzyme has been characterised [Li *et al*, 2000]. They

have provided vital information on inhibitor binding, conformational changes, enzyme-inhibitor-cofactor complexes and exploitable differences between the parasite and host enzyme. Although the general fold of the protein was found to be the same as that of the human enzyme, a number of differences was detected, which could be exploited for inhibitor design. The binding mode of the inhibitors MTX, TMP and Br-WR99210 in three ternary complexes revealed that three inhibitors containing heterocyclic rings bind in the same region via set of strong hydrogen bonds, whereas the other moieties of the inhibitors bind to different protein residues.

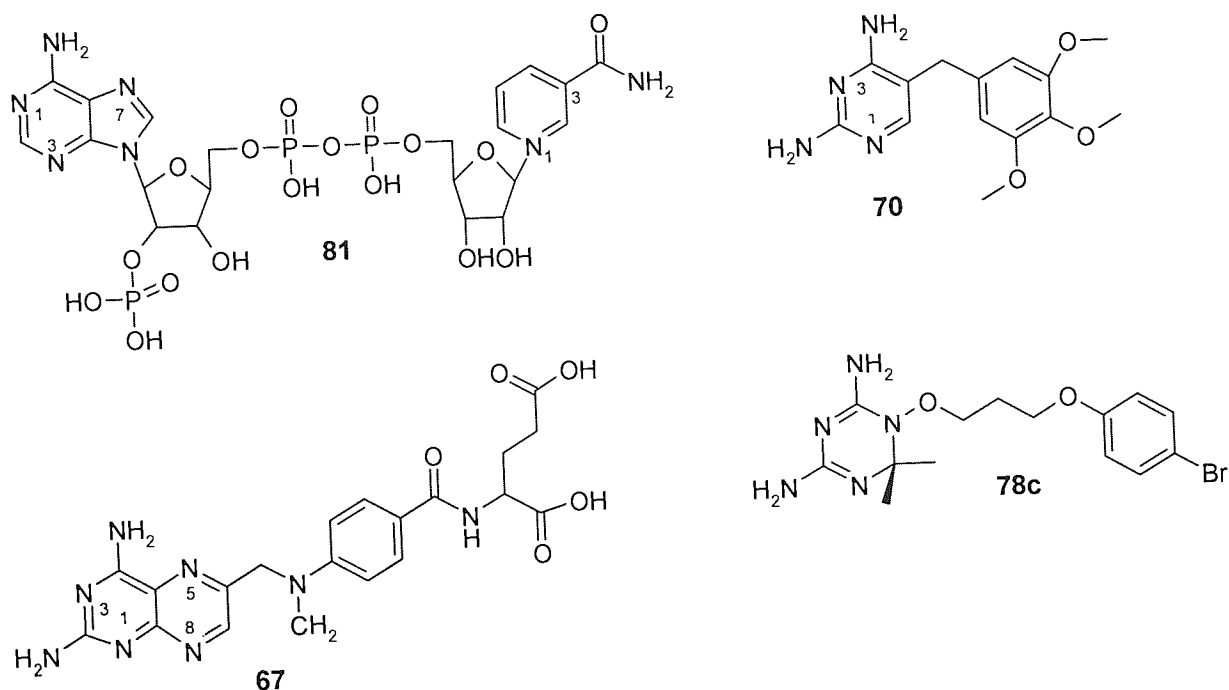


Figure 4.7: Chemical structures of coenzyme NADP (**81**) and three inhibitors: trimethoprim (**70**); methotrexate (**67**) and Br-WR99210 (**75c**), used in the structure determinations of *M. tuberculosis* dihydrofolate reductase binary and ternary complexes.

4.5.2 NADP binding to *M. tuberculosis* DHFR

The interactions of NADP with *M. tuberculosis* DHFR are indicated in **Figure 4.8**. The cofactor (NADP) was bound to *M. tuberculosis* DHFR in an extended conformation. The adenine ring contacts the protein through hydrophobic interactions involving Leu65 and Leu102 on one side and through stacking interactions with the side chain of Arg67 on the other side. In addition, the adenine ring contacts residues Ser66, Gly80 and Gln98. The O^{2'}-phosphate of the adenosyl ribose interacts with *M. tuberculosis* DHFR through five H-bonds involving side chains of Ser66, Gln68, Arg44 and the main chain of Arg67. The pyrophosphate moiety forms a salt-bridge with Arg45, while the amide group of the nicotinamide ring forms three hydrogen-bonds with main-chain atoms of Ala7 and Ile14. Two hydrophobic residues, Ile14 and Ile20 also approached nicotinamide ring from the opposite side.

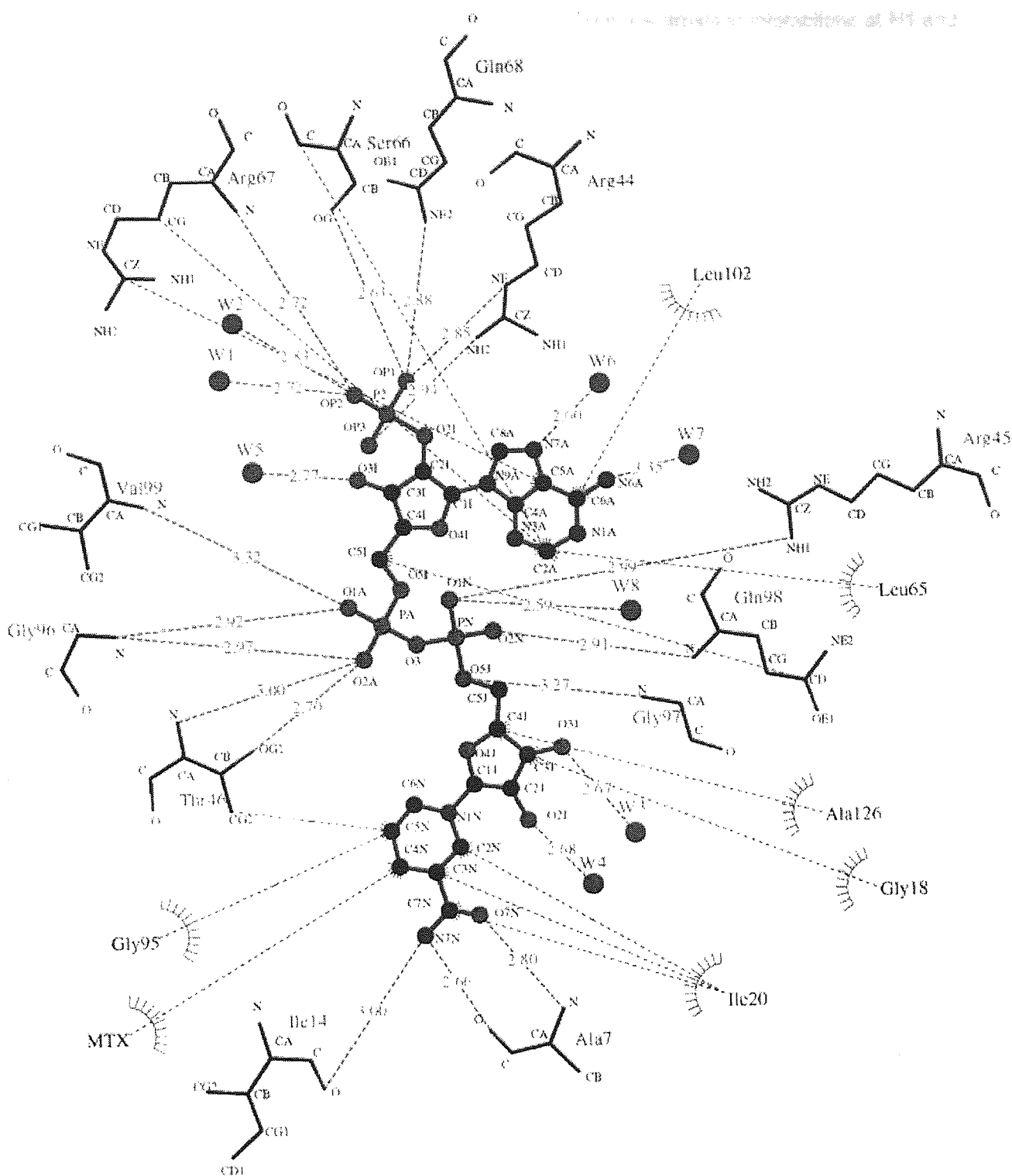


Figure 4.8: Shows Interactions between the *M. tuberculosis* DHFR and NADP molecule [Adapted from Li, *et al* 2000]

4.5.3 Methorexate binding to to *M. tuberculosis* –DHFR.

MTX is bound to *M. tuberculosis*-DHFR via contacts with strands β -A, β -E and two helices, α B and α C. The 2,4-pteridine ring of MTX interacts with the acidic residue Asp27, via two hydrogen bonds with N1 and the 2-amino group. The other hydrogen of the 2-amino group is associated with a buried water molecule. The negatively charged Asp27 is highly conserved and critical for catalysis [Howell *et al*

1986] The 4-amino group is involved in hydrogen bonding with the carbonyl groups of Ile-4 and Ile-94 (Figure 4.9) which is conserved in the bacterial enzymes, through electrostatic interactions at N1 and the 2-amino group.

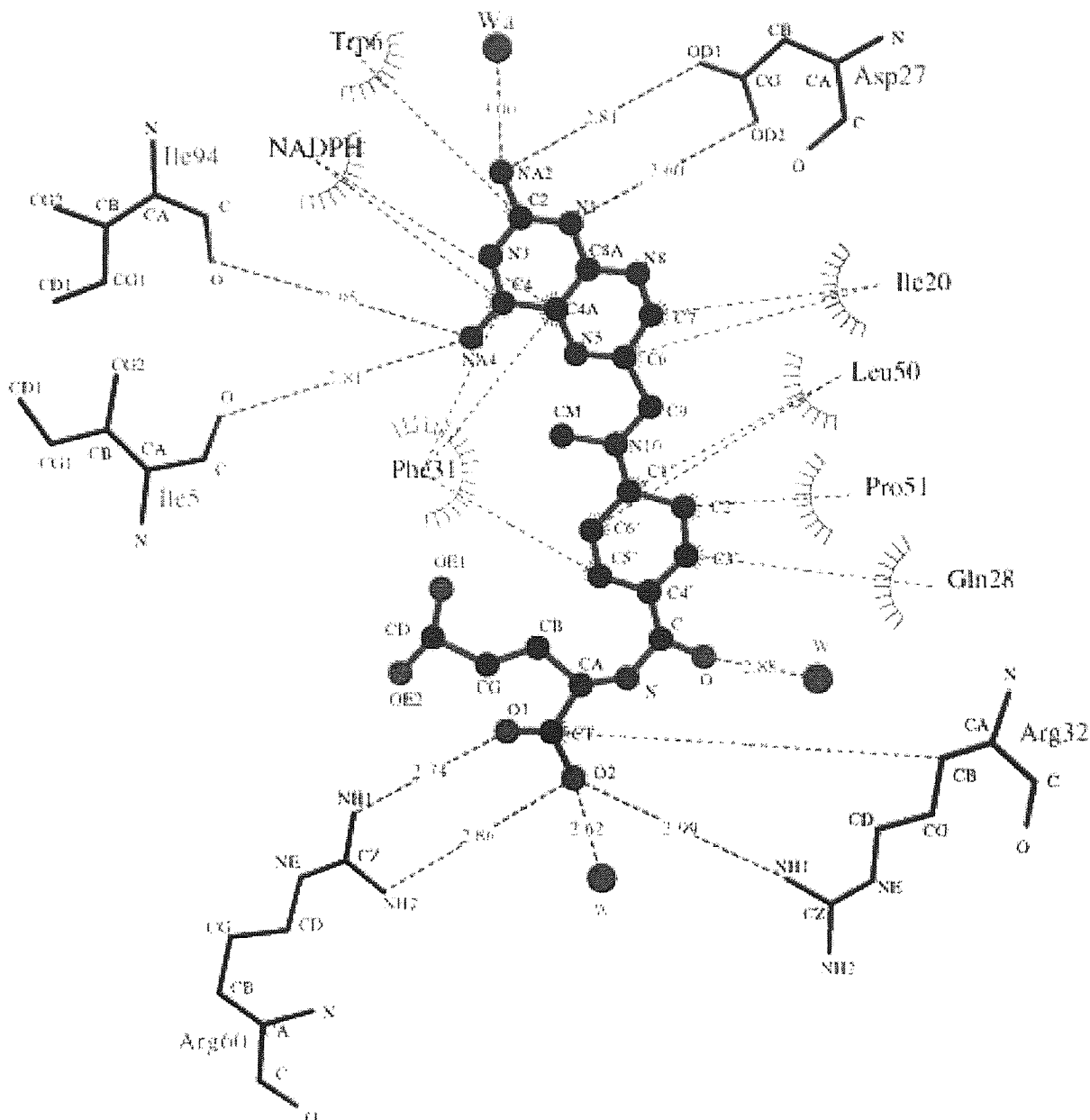


Figure 4.9: Shows Interactions between the *M. tuberculosis* DHFR and inhibitor methotrexate [Adapted from Li *et al*, 2000]

The aminopteridine ring also interacts with the protein through many hydrophobic interactions. On the side facing the nicotinamide ring of the cofactor, the aminopteridin ring is in contact with Trp6, Ala7 and Ile20. The other side of the aminopteridin ring interacts with Phe31, Ile5, Ile94 and Gln28. The *p*-aminobenzoyl ring of MTX is in contact with Ile50, Pro51, Ile54, Ile57, Gln28 and Phe31, which provide a hydrophobic environment for the phenyl group. The glutamate moiety of the MTX lies near the surface of the protein and interacts with Gln28, Ala29 and Arg32. The salt bridge interaction of the α -carboxyl group of MTX was observed with Arg32 and Arg60.

4.5.4 Trimethoprim binding to *M. tuberculosis* -DHFR

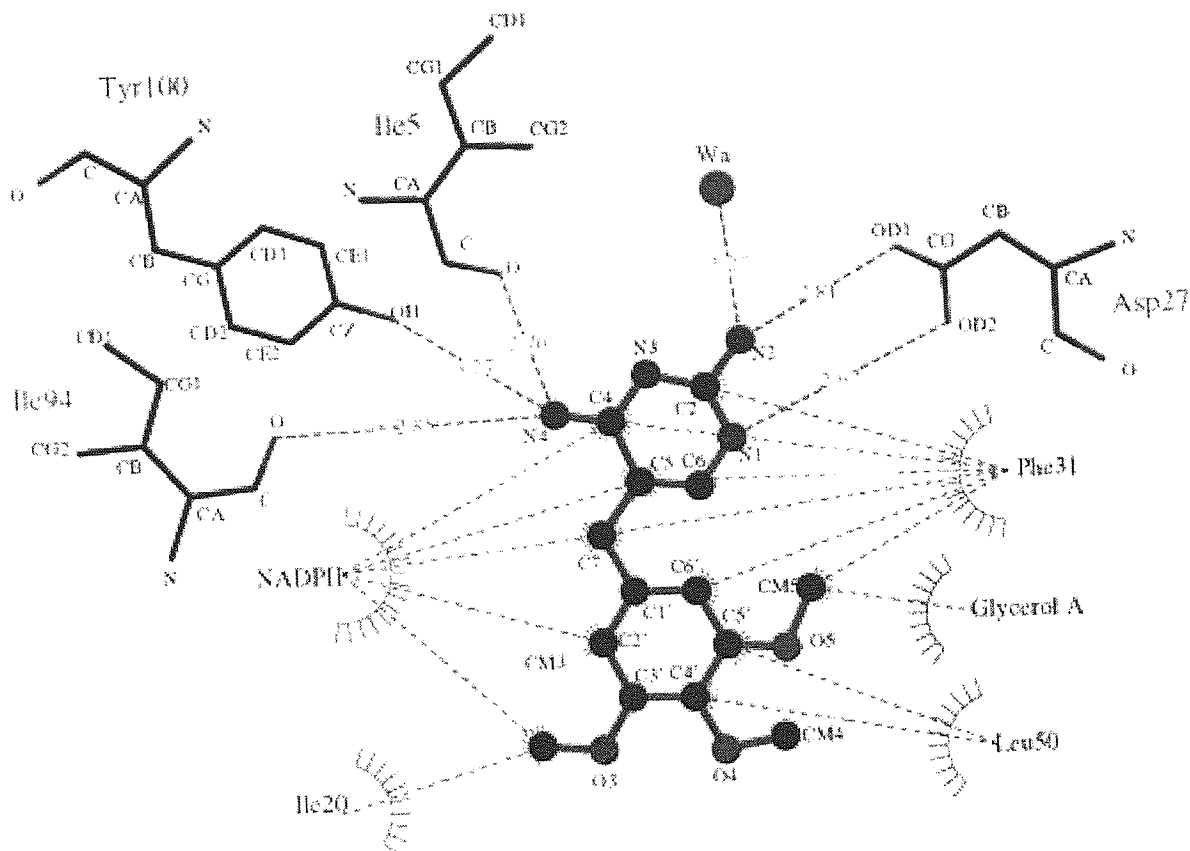


Figure 4.10: Interactions between *M. tuberculosis* DHFR and inhibitor trimethoprim, adapted from [Li *et al*, 2000]

Since trimethoprim, in contrast to methotrexate, is a selective inhibitor of bacterial DHFR it is of considerable interest to know how the selectivity arises. In early studies (Volz *et al*, 1982; Matthews *et al*, 1985, Kuyper *et al*, 1996) of the binding of trimethoprim to the vertebrate enzyme revealed that it binds to chicken liver DHFR in a conformation that is different from that in the *E. coli* DHFR complex. This different conformation of trimethoprim can be adopted because the active site in chicken liver enzyme was somewhat wider than that in the bacterial enzyme; the wider site does not provide the appropriate hydrophobic interactions to optimize this mode of binding. Detailed NMR work [Birdsall *et al*, 1983] leads to the same conclusion. Li and co-workers [Li *et al*, 2000] provided the first information on the crystal structure of the trimethoprim-*M. tuberculosis*-DHFR complex. TMP binds at the active site of *M. tuberculosis*-DHFR with its pyrimidine ring being held in the interior of the deep cleft through hydrogen bonds with the residue Asp-27, Ile-94, Ile-5 and Tyr-100; and van der Waals contact with Phe31, Ile5, Ala6, Ala7 and Ile94. The methoxy-benzyl side chain extends out towards the entrance of the binding pocket, making van der Waals contacts with Phe-31, Ile-20, and Leu-50 near the active site. The inhibitor also contacts NADP and a glycerol molecule. TMP has two principal degrees of conformational freedom. The three methoxy groups can adopt in-plane and out-of-plan conformations with torsion angles of 0° and -180° , resulting in a conformation that positions the two aromatic rings of the inhibitor nearly perpendicular to each other.

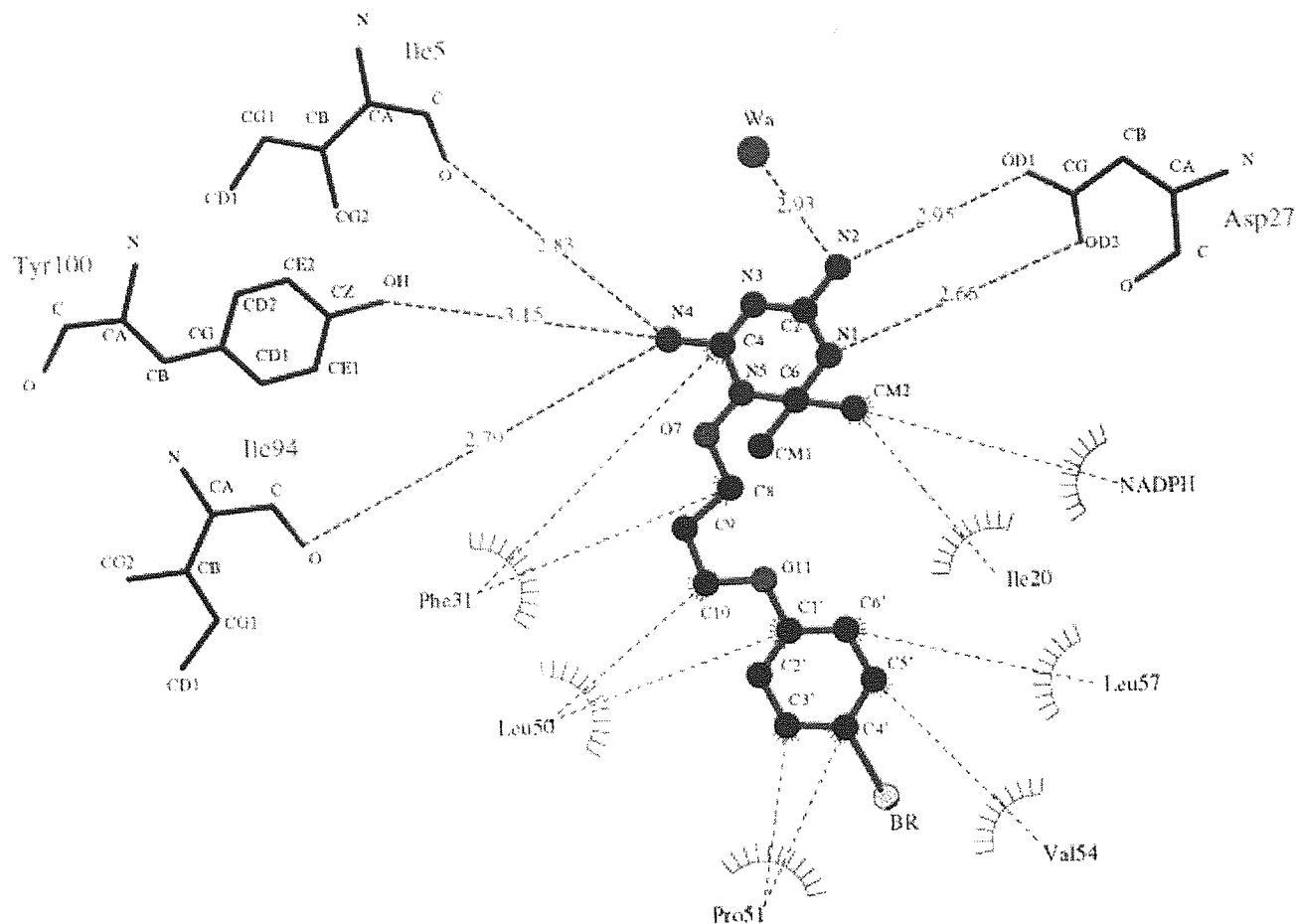
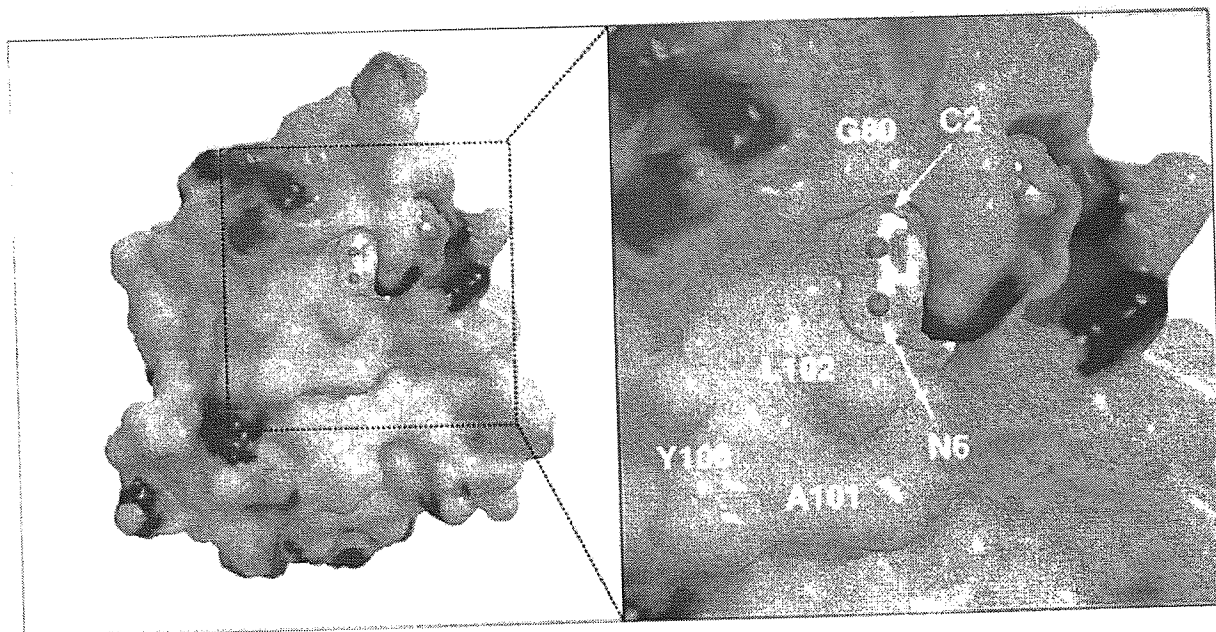
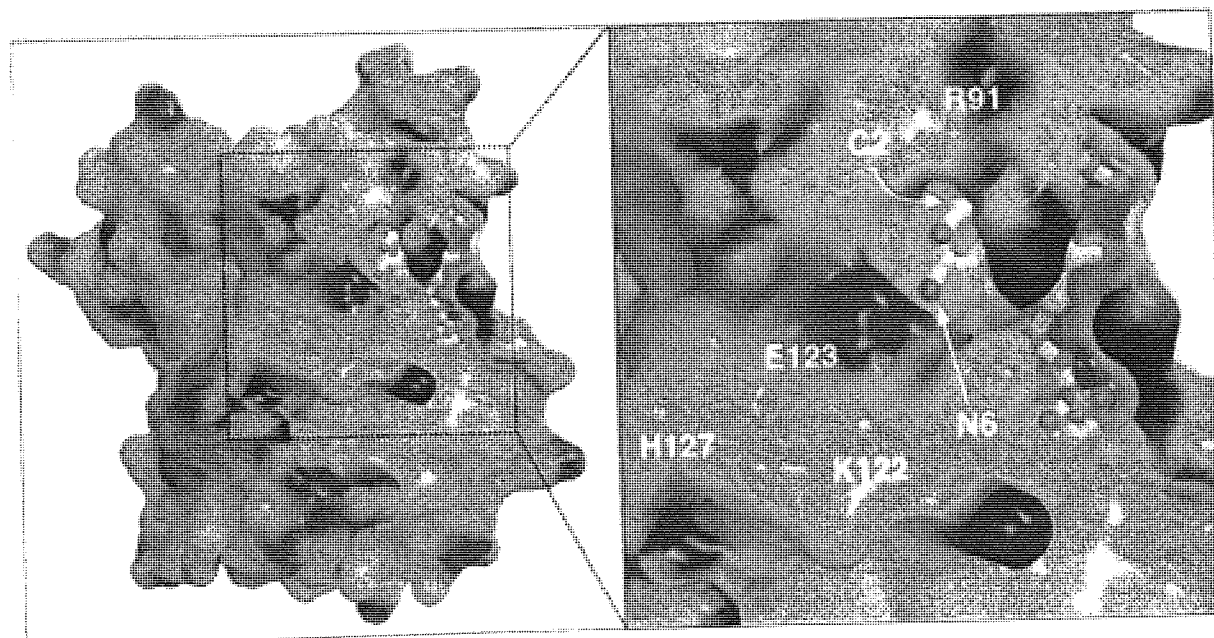


Figure 4.11: Shows Interactions between the *M. tuberculosis* DHFR and inhibitor Br-WR99210

The Br-WR99210 complex with *M. tuberculosis* DHFR revealed that the two amino groups interact with Ile5, Asp27, Ile94 and Tyr100 to form four hydrogen bonds. In addition the axial methyl group on C1 of Br-WR99210 interacts with Ala7, Ile20 and the amide of the nicotinamide while the equatorial methyl group interacts with Glu28. The 1,3-dioxypropyl linking group interact with hydrophobic Phe31, Thr46 and Leu50 whereas the 4-bromophenyl group contacts several hydrophobic residues in a similar way as observed for MTX. The bromine atom of Br-WR99210 points toward the Lys53 which is about 4Å away from the inhibitor. (**Figure 4.11-4.17**).

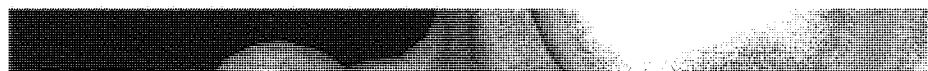
NADPH binding sites***M. tuberculosis* DHFR****Human DHFR****Figure 4.12:** Comparison of *M. tuberculosis* DHFR and Human DHFR [Adapted from Li *et al* 2000]

In contrast to *M. tuberculosis* DHFR, the human DHFR active site is larger than that of *M. tuberculosis* DHFR and displays the structural differences which could be exploited for the design of therapeutic compounds that would selectively bind to the *M. tuberculosis* protein and would not affect the normal function of the human enzyme. **Figure 4.12** shows the comparison of NADP binding site close to the adenine ring which indicates the differences in size and shape of the human and mycobacterial enzymes. Near to the N6 amino group of NADP of human are two hydrophilic residues Lys122 and

Glu123 whereas the equivalent residues in *M. tuberculosis* enzyme are hydrophobic i.e. Ala 101 and Leu102. Extension of the N6 amino group of NADP with hydrophobic substituents could lead to TB-specific inhibitors. An additional difference in the NADP binding site between the enzymes from *M. tuberculosis* and human exists close to the C2 of the adenine ring. There was an extended groove in *M. tuberculosis*-DHFR, which is blocked in human DHFR by the residue Arg91. This difference also allows for creating NADPH variants and adenosine C2 substitutes which bind to this opening.

4.6.1 The glycerol binding pocket present in *M. tuberculosis*-DHFR

Another major difference identified by comparing the crystal structure of *M. tuberculosis*-DHFR to human DHFR was the existence of a glycerol molecule. **Figure 4.13** indicates the presence of glycerol molecule in *M. tuberculosis* DHFR crystal structure whereas the equivalent site in human enzyme does not contain glycerol but is packed with three hydrophobic side chain residues, Leu22, Pro26 and Phe31. The study performed by Li and co-worker [Li *et al*, 2000] revealed that the glycerol molecule occurs close to aminopterin ring of methotrexate, the aminopyrimidine ring of TMP and the aminotriazine ring of Br-WR99210 in *M. tuberculosis* DHFR. However, the γ -carboxylate region of methotrexate is quite different in proteins. The two residues Leu22 and Phe31 near the N8 of and C7 of methotrexate were shown to restrict its accessibility to the human enzyme binding site as they are separated by 3.8 Å whereas the *M. tuberculosis*-DHFR residues Leu20 and Gln28 are separated by about 6.5 - 9.4 Å (**Figure 4.12**). This suggests that the analogues of methotrexate with an additional group connected to N8 and C7 with the binding mode of the glycerol may produce selective inhibitors for *M. tuberculosis* DHFR.



Aston University

Illustration removed for copyright restrictions



Figure 2.13: Shows the presence of a glycerol molecule in the *M. tuberculosis* crystal structure IDF7. Furthermore, the glycerol pocket near N8 of MTX is also in the immediate vicinity of TMP and Br-WR99210 and these inhibitors can also be extended by hydrophilic substituents which could bind in the glycerol pocket and further reduce the affinity for the human enzyme. [Li *et al*, 2000].

Figures 4.13 and 4.14 show the arrangement of the *M. tuberculosis* DHFR active site residues and their interactions with methotrexate.

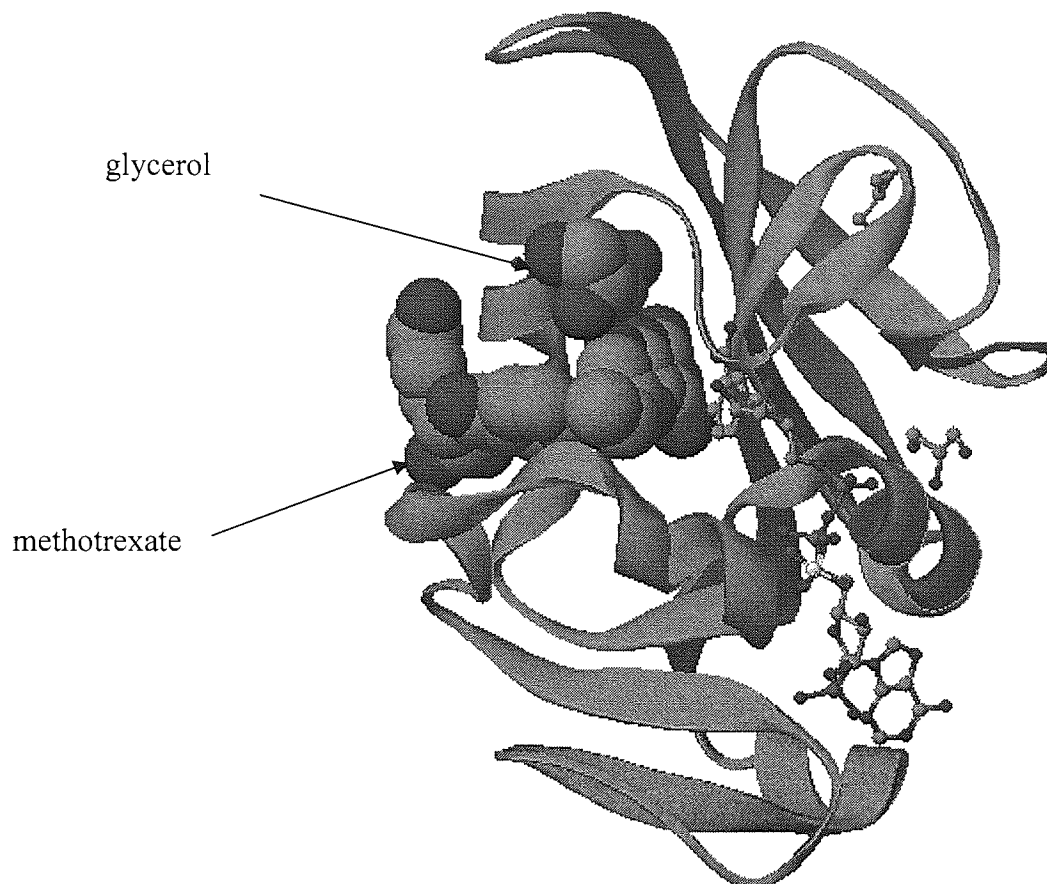


Figure 4.14: Shows methotrexate and the adjacent glycerol molecule. View from the *M. tuberculosis* DHFR crystal structure IDF7

Also present in this structure was a molecule of glycerol bound close to the N8 position of methotrexate, presumably arising from the crystallisation process. The glycerol was bound to the Asp27, Gln28 and Leu24 through three hydrogen bonds with all hydroxyl groups (**Figure 4.15 - 4.16**). This glycerol molecule was also observed weakly in the electron density map of the ternary Br-WR99210 complex (**Figure 4.17**) and was absent in the TMP complex. This was probably due to the presence of hydrophobic Gln28 which led the α -carboxyl group of methotrexate to be oriented in a different direction. However, the appearance of glycerol molecule in the crystal structure was adventitious and suggested additional binding interactions which prompted us to synthesis new mycobacterial DHFR inhibitors (**Section 4.8.1**).

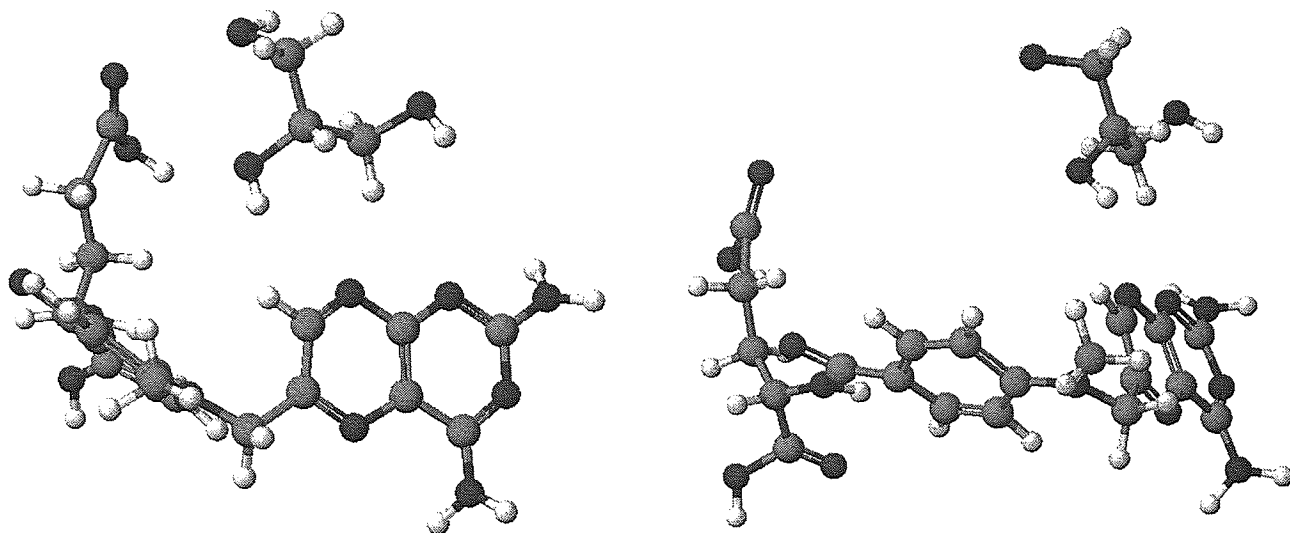


Figure 4.15: Ball and stick diagram showing the preferred conformation of the methotrexate and the glycerol molecule viewed from different orientations

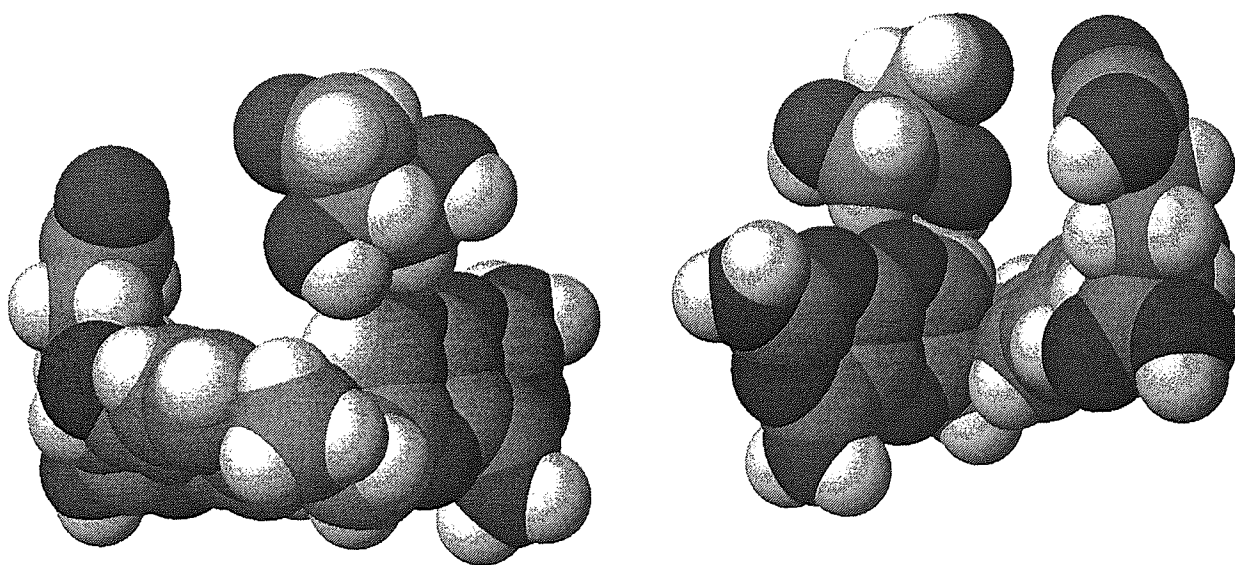


Figure 4.16: Space-filling diagram for the MTX and the glycerol molecule

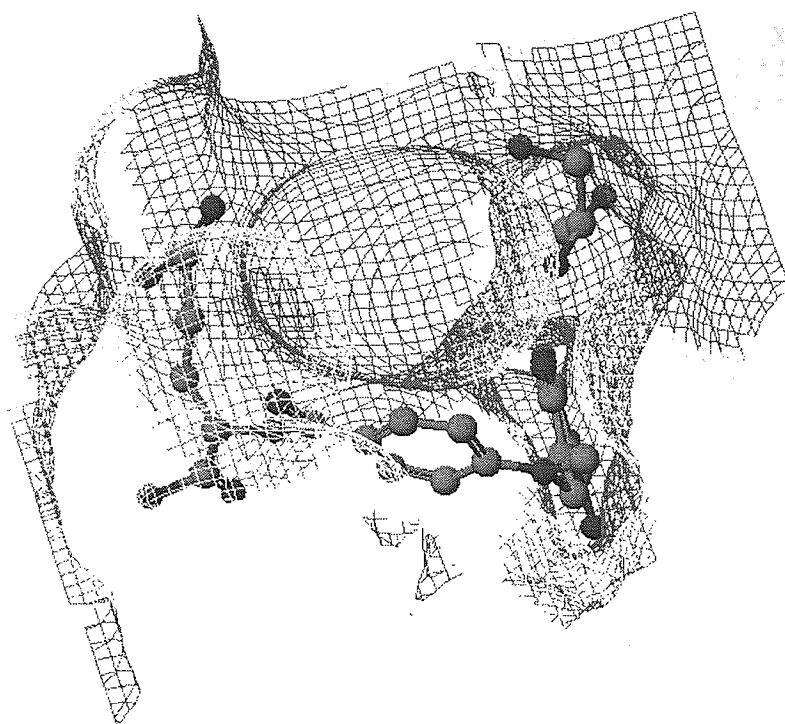


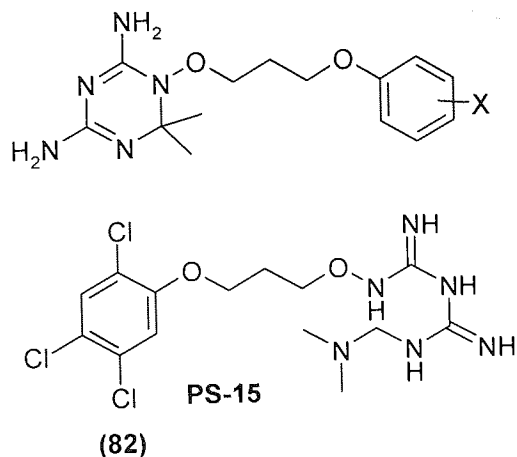
Figure 4.17: The electron density map of the ternary Br-WR99210 complex with the *M. tuberculosis* DHFR

4.7 Design and Synthesis of new inhibitors of *M. tuberculosis* DHFR

Dihydrofolate reductase is an essential bacterial enzyme necessary for the maintenance of intracellular folate pools in a biochemically active reduced state. DHFR from *M. tuberculosis* is also considered an important target for drug design. In view of the fact that some antimalarial agents such as WR99210 [Gerum *et al*, 2002; Shah *et al*, 1996] and pyrimethamine [Shah *et al* 1996; Opravil *et al*, 1995] also show antimycobacterial activity, it was thus decided to explore the potential antitubercular activity of the derivatives of pyrimethamine. In addition to indications that WR99210 is effective against several mycobacteria, the crystal structure of the *M. tuberculosis* DHFR was solved with the brominated analogue of WR99210 bound in the active site (**Section 4.5.6, Figure 4.11 and 4.17**). Taking this into account it was suggested a detailed study of the inhibition of *M. tuberculosis* by other antimalarial compounds such as pyrimethamine would be productive.

4.7.1 WR99210

The triazine DHFR inhibitor WR99210 has been shown to exhibit reasonable in vitro activity against *M. tuberculosis*, as well as against other mycobacteria [Gerum *et al*, 2002]. A series of analogs have been synthesised and tested and showed activity comparable to the lead molecule. Yuvaniyama *et al* proposed that the flexible side chain of WR99210 enables this compound to adopt a conformation that fits into the mutant active site, effectively inhibiting the enzyme].



Compd no.	X
78 (WR99210):	2,4,5-Cl ₃
78a:	2,4,Cl ₂
78b:	2,3-C ₄ H ₄
78c:	4-Br

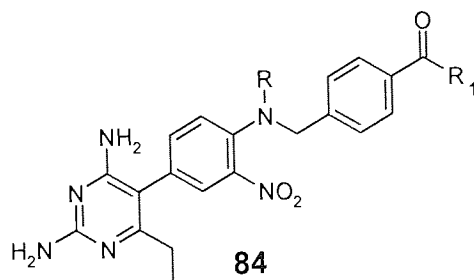
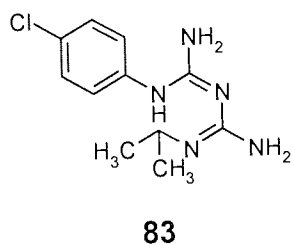
Figure 4.18: Analogues of WR99210

However, the selectivity of WR99210 is not sufficient for use as an antimicrobial agent with the major disadvantage being problems of poor gastrointestinal tolerance associated with designed (the molecule [Canfield, 1993]. In 1985, a prodrug form of WR99210 was designed (**Figure 4.18**). This agent, *N*-[3-(2,4,5-trichlorophenoxy)propoxy]-*N'*-(1-methylethyl)imidocarbonimidic diamide hydrochloride, designated **PS-15 (82)**, showed more potency than WR99210 in an *in vitro* activity against clinical *Mycobacterium avium* complex isolates [Meyer *et al*, 1995].

4.7.2 Pyrimethamine (71)

Pyrimethamine belongs to the 2,4-diaminopyrimidine derivative family. It was synthesised and tested as analogues of folic acid in the treatment of tumours in 1940s [Hitchings *et al* 1950]. However, Falco and coworkers [Falco *et al*, 1951] observed that the structures of these compounds and proguanil (**83**) were similar (**Figure 4.19**) and hypothesised that 2,4-diaminopyrimidine could have antimalarial activity. The screening of their antimalarial activity led to the identification of pyrimethamine as a therapeutic antimalarial agent and has been the most widely used antimalarial antifolate agent so far.

Several derivatives of 2,4-diamino-5-[4'-(substituted)-3'-nitrophenyl]-6-ethyl-pyrimidines (**Figure 4.16**), **84a - 84e**, have been synthesized and evaluated as inhibitors of *P. carinii* and *T. gondii* DHFR [Robson *et al* 1997]. The compounds exhibit potent inhibitory activity against the *T. gondii*, but were relatively weak inhibitors of the *P. carinii*.



Compd	R	R ₁
84a:	H	OH
84b:	Me	OH
84c:	H	NH ₂
84d:	H	NHMe
84e:	H	NH-L-Glu

Figure 2.19: The structure of proguanil (**83**) and an analogues of pyrimetamine.

4.7.3 Novel analogues of pyrimethamine that might interact with *Mycobacterium tuberculosis* DHFR.

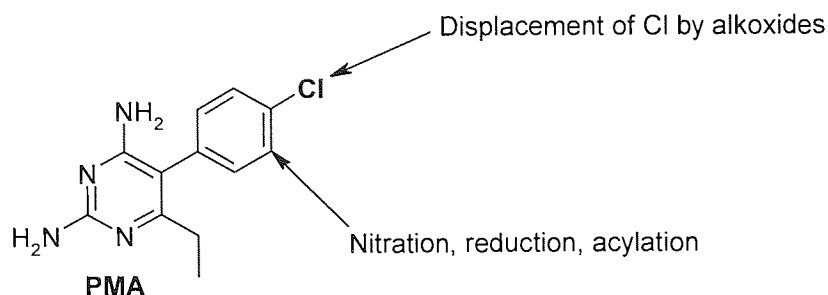
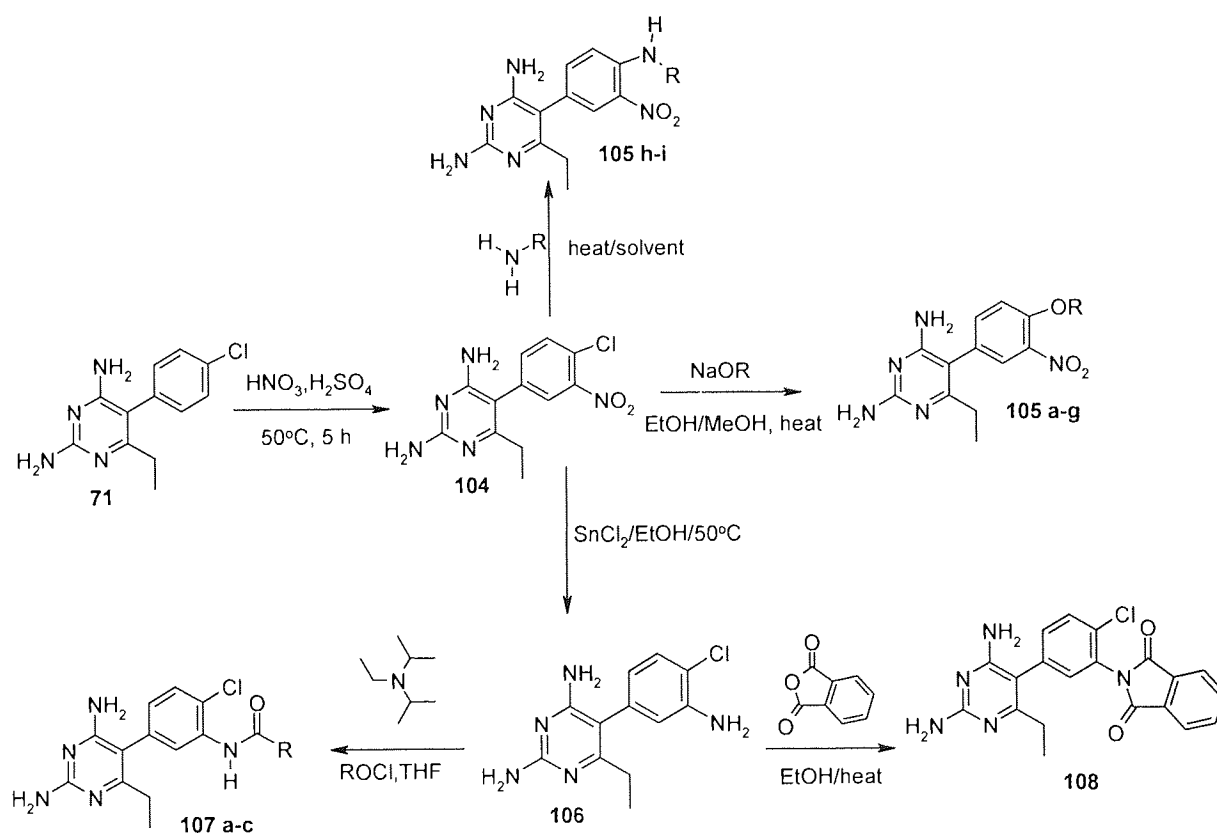


Figure 4.20: The structure of 2,4-diamino-5-aryl-6-ethylpyrimidine and its analogues to be synthesised in this study.

4.8 Chemistry

4.8.1 Preparation of Analogues of Pyrimethamine

In an effort to discover more active and selective antifolates for *M. tuberculosis* DHFR, it was decided to prepare and evaluate a series of analogues of 2,4-diamino-5-[4'-(substituted)-3'-nitrophenyl]-6-ethyl-pyrimidines, and 2,4-diamino-5-[4'-chloro-3'-(substituted)]-6-ethyl-pyrimidines **Scheme 4.1**.



Scheme 4.1: Synthetic scheme for preparation of various analogues of 2,4-diamino-5-aryl-6-ethylpyrimidine (pyrimethamine) (**71**).

Based on the analysis of the structure of the *M. tuberculosis* DHFR, a variety of polar groups was embraced at the 3 and 4 positions of the 5-aryl ring (**Scheme 4.1 - 4.5**). It was hoped to identify novel

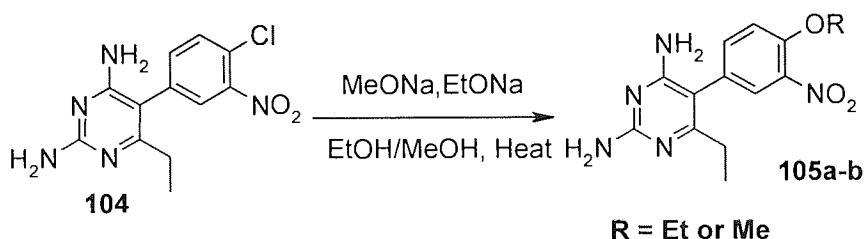
lipophilic diaminopyrimidines that would interact with the glycerol binding pocket and the residues of Aps27, Gln28 and Leu24 in an active site of the *M. tuberculosis* enzyme [Li *et al*, 2000].

4.8.2 Preparation 2,4-diamino-5-[4'-chloro-3-nitrophenyl]-6-ethyl-pyrimidine **104**

The starting material for most of the synthetic structures was the commercially available antimalarial drug pyrimethamine (**71**). The first step was to nitrate the pyrimethamine to afford 2,4-diamino-5-[4'-chloro-3-nitrophenyl]-6-ethyl-pyrimidine (**104**) **Scheme 4.1**. This was carried out by means of a mixture of concentrated nitric acid and concentrated sulphuric acid (1:1) according to the method published by [Griffin, *et al*.1985]. After purification, the structure of the synthesised compound (**104**) was confirmed by ¹H NMR and MS.

4.8.3 Preparation of 2,4-diamino-5-[4'-chloro-3-nitrophenyl]-6-ethylpyrimidine ethers.

4.8.4 Reaction of 2,4-diamino-5-[4'-chloro-3-nitrophenyl]-6-ethylpyrimidine with sodium alkoxide



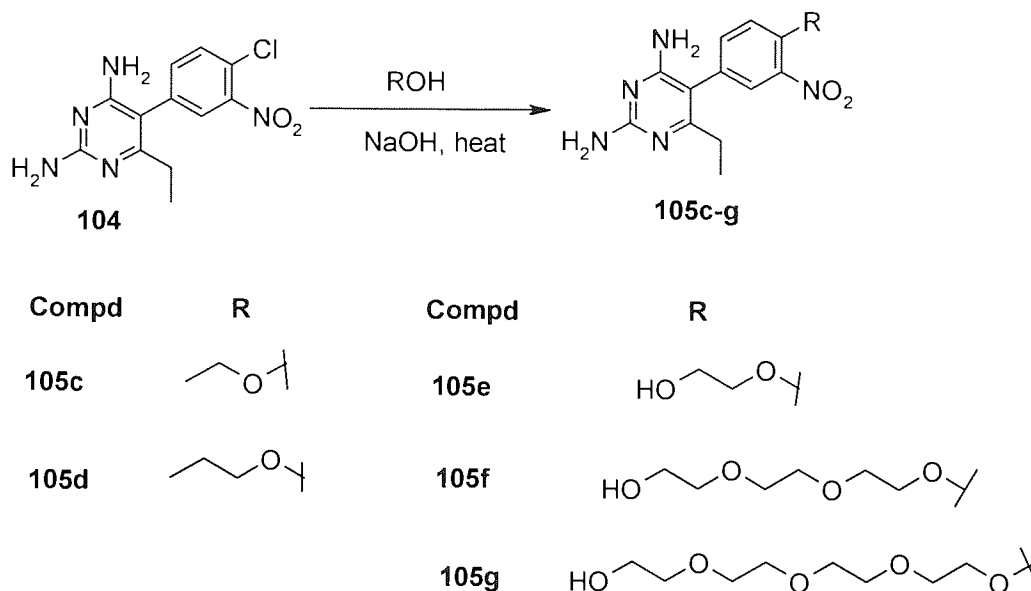
Scheme 4.2: Synthesis of NPMA ethers where R = Et, Me

Subsequent reaction of **104** was then carried out with various sodium alkoxide (**Scheme 4.2**). For example **104** was heated at reflux with sodium methoxide **109** in methanol (as the base, which was generated *in situ* from metallic sodium in methanol) for several days at 120°C in a sealed, metal container. The reaction mixture was concentrated *in vacuo* and a brown solid was obtained. Although ¹H-NMR and MS indicated the desired compound **105a** was present it could not be isolated as a pure product. Many solvents including ethanol, ethyl acetate and toluene were used to attempt to recrystallise the product, but unfortunately all attempts failed to show the desired product. Purification by chromatography was not performed due to the poor solubility profile of the pyrimethamine derivatives.

Compound **104** was also treated with sodium ethoxide **110** in ethanol. The reaction mixture was heated at reflux for several days and the reaction was followed by TLC. The reaction mixture was concentrated *in vacuo* and the light brown solid was obtained. Although ¹H-NMR and MS indicated the presence of the compound (**105b**); attempts to recrystallise the product from various solvents was met without success.

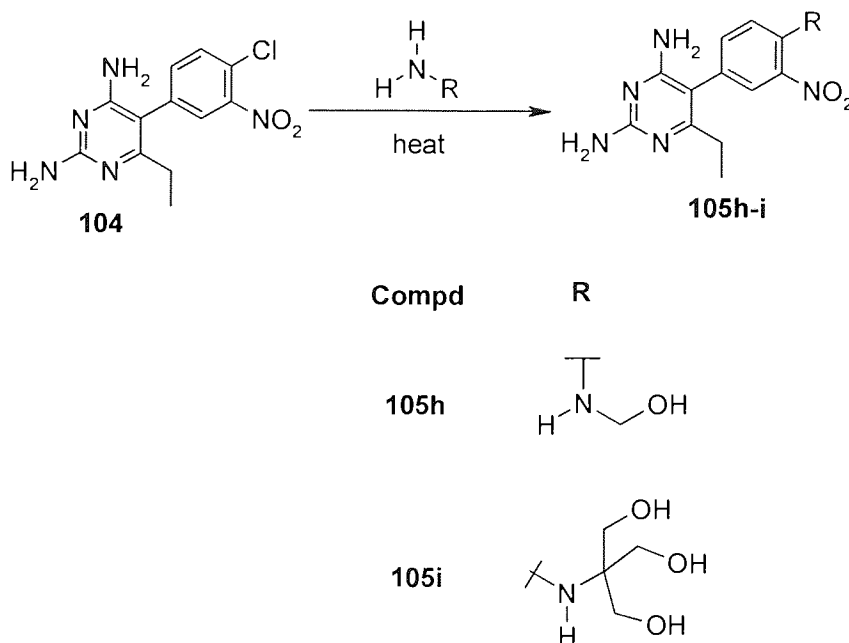
4.8.5 Reaction of 2,4-diamino-5-[4'-chloro-3-nitrophenyl]-6-ethyl-pyrimidine (104) with alcohols

In an attempt to continue the study of series of analogues, compound **104** was then reacted with a range of selected alcohols (including a range of ethylene glycols) as depicted in (Scheme 4.3), employing sodium hydroxide as a base. The reaction mixture was heated at reflux for several days to afford compounds **105c - g**.



Scheme 4.3: Synthesis of 2,4-diamino-5-[4'-chloro-3-nitrophenyl]-6-ethyl-pyrimidine ethers where R = alcohol or an ethyleneglycol derived residues.

4.8.6 Reaction of 2,4-diamino-5-[4'-chloro-3-nitrophenyl]-6-ethyl-pyrimidine with an amines



Scheme 4.4: Synthesis of NPMA amine where R = amine derived residues.

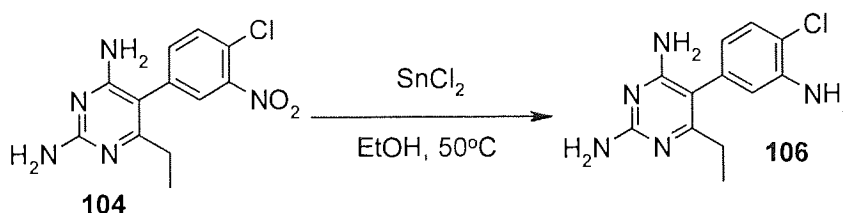
Compound **104** was reacted with ethanolamine (reagent and solvent) at 100°C for five days. The resultant brown gum was dissolved in water and then neutralised to pH7 hoping to obtain a precipitate, which was unsuccessful. The mixture was then extracted with EtOAc affording a brown gum. ¹H-NMR and MS analysis did not confirm the presence of the desired compound **105h**.

A similar situation was encountered when this reaction was repeated with 2-amino-2-(hydroxyl methyl)propane-1,3-diol (tris) to afford **105i**. Thus a mixture of **104** and tris in 1-methyl-2-pyrrolidone was heated at 190°C for seven days. The reaction mixture was poured on water and then extracted with EtOAc to afford a brown solid. Attempts to purify the compound further by flash chromatography eluting with EtOAc and MeOH 8:2 respectively, afforded an unknown complex mixture. The nucleophilic aromatic substitution for halogen atom has been unsuccessful. This could have been due to the poor solubility of **104** coupled with the ineffective reaction conditions.

4.9 Synthesis and Reactions of Amino Pyrimethamine (106)

4.9.1 Preparation of 2,4-diamino-5-[4'-chloro-3'-aminophenyl]-6-ethyl-pyrimidines (106).

During the course of the studies, to search for a potent inhibitor for *M. tuberculosis* DHFR it was decided to prepare pyrimethamine amides. The synthetic procedures employed for the preparation of the target compounds are outlined in **Scheme 4.1**. A key starting material for the synthesis of diaminopyrimidines bearing an amine substituent in the 3-aryl ring was 2,4-diamino-5-[4'-chloro-3'-nitrophenyl]-6-ethyl-pyrimidine **104**. The subsequent reaction of compound **104** with tin (II) chloride dihydrate in ethanol at 50°C furnished the reduction of aromatic nitro substituent to an amine **106** **Scheme 4.5**. This method was adapted from Griffin and co-worker [Griffin, *et al.* 1989].

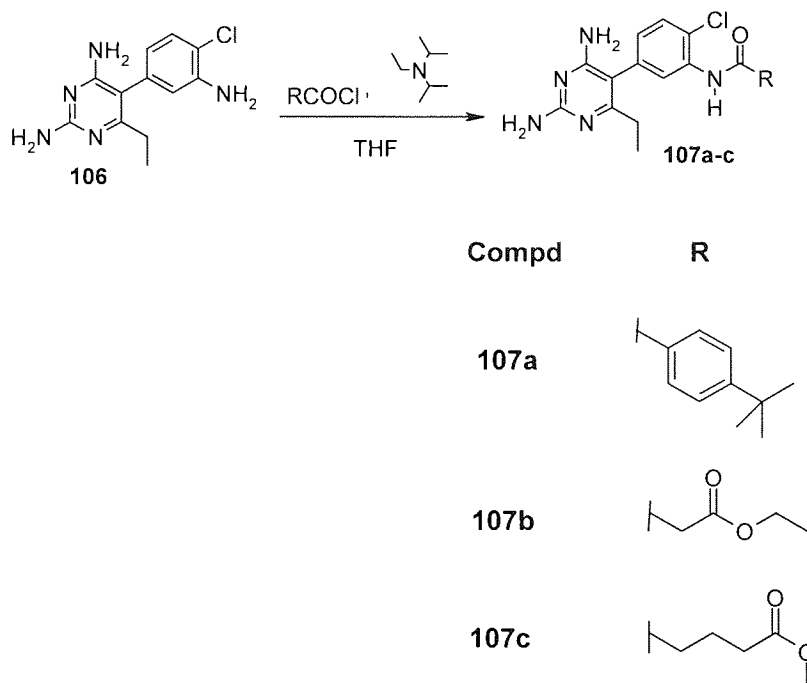


Scheme 4.5: The synthesis of amino pyrimethamine (**106**)

4.9.2 Reaction of 2,4-diamino-5-[4'-chloro-3'-aminophenyl]-6-ethyl-pyrimidines with carboxylic acid chlorides

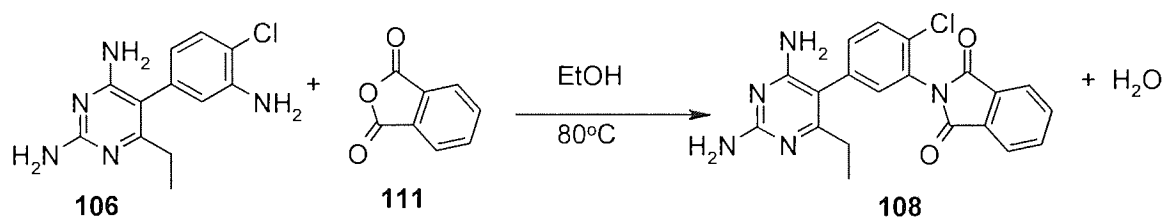
It was attempted to acylate compound **106** with the acid chlorides as depicted in Scheme 4.6. Reaction between **106** and appropriate acid chlorides in the presence of a Hunig's base was carried out in dry THF under an argon atmosphere to afford the corresponding pyrimethamine amide **107a-c** (Scheme 4.6). The presence of the compound was confirmed by the mass spectrometry and ¹H-NMR spectra, but the pure compound could not be isolated. It was attempted to recrystallise the products

from a combination of solvents including EtOH, MeOH, toluene and THF, but this proved to be unsuccessful. Flash chromatography was not carried out because of the poor solubility profiles of the title compounds. The failure of these reactions was perhaps due to the poor solubility of the pyrimethamine derivatives under the given conditions.



Scheme 4.6: Preparation of pyrimethamine amides R= acyl chloride derived residue.

4.9.3 Preparation of 2-[2-Chloro-5-(2,4-diamino-6-ethylpyrimidin-5-yl)-phenyl]isoindole-1,3-dione (108)



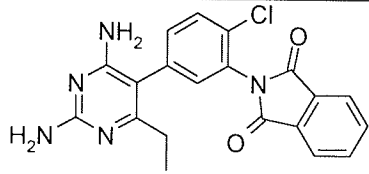
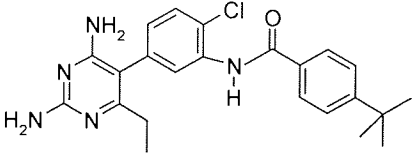
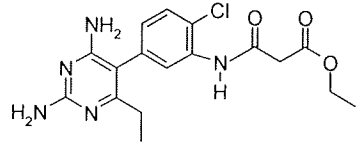
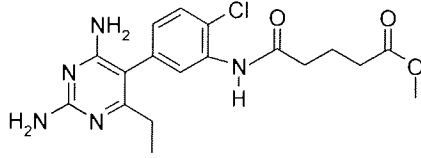
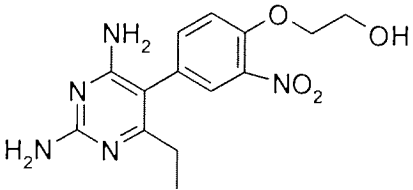
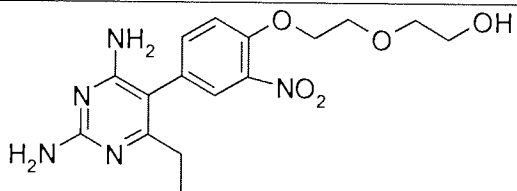
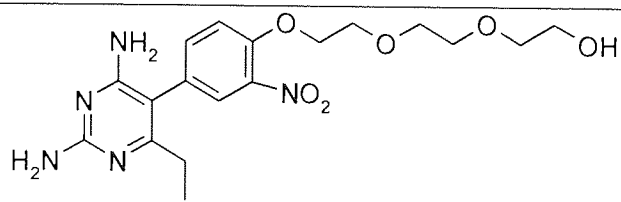
Scheme 4.7: Synthesis of 2-[2-Chloro-5-(2,4-diamino-6-ethylpyrimidin-5-yl)-phenyl]isoindole-1,3-dione (108)

Finally, the nucleophilic acyl substitution reaction between **106** and acid anhydride **111** proceeded smoothly to afford product **108** as white solid (**Scheme 4.7**). The reaction mixture was heated at reflux in ethanol to afford the the title compound. Recrystallisation from ethyl acetate afforded compound 2-[2-chloro-5-(2,4-diamino-6-ethylpyrimidin-5-yl)-phenyl]isoindole-1,3-dione (**108**) which was identified by $^1\text{H-NMR}$, MS and IR.

4.10 Evaluating antimycobacterial activity of the pyrimethamine derivatives

The only clean compound that was isolated from series of pyrimethamine derivative was compound **108**. The compound was inactive against both mycobacteria, namely, *M. tuberculosis* and *M. fortuitum* (Table 4.1 below). Although the rest of the synthesized pyrimethamine derivatives seemed to show some impurities, they were still subjected to screen against *M. fortuitum* to probe if they possessed any activity. Unfortunately, they were found to be inactive.

Table 4.1: Antimycobacterial activity of pyrimethamine derivatives. An MIC of the compounds was determined by project students N. Ellahi (MPharm final year project student, Aston University, 2005) and F. Kusar (B.Sc Applied and Human Biology final year project student, Aston University, 2004).. Results against *M. tuberculosis* strain H₃₇Rv was provided by TAACF.

Compound	Structure	<i>M. Fort.</i> MIC (µgmL ⁻¹)	<i>M. tuber.</i> % Inh
108		>32	57
107a		>32	N/A
107b		>32	N/A
107c		>32	N/A
105e		>32	N/A
105f		>32	N/A
105g		>32	N/A

4.11 Conclusions

The X-ray structures of DHFR from mammalian DHFR and *Mycobacterium tuberculosis* were found to have differences in substrate binding site. These differences from pathogen to host provide opportunities to design selective inhibitors of the pathogen enzyme. In this study we have explored this idea by synthesising analogues of pyrimethamine (2,4-diamino-5-(4-chlorophenyl)-6-ethylpyrimidine) by extending the phenyl moiety and incorporating alcohols and other polar functional groups that it might be able to interact with the *M. tuberculosis* DHFR glycerol binding pocket (Figure 4.20).

Unfortunately all attempts failed to afford compounds **105h-i**. The mass spectrometry and ¹H NMR analysis indicated the presence of 2,4-diamino-5-[4'-chloro-3-nitrophenyl]-6-ethylpyrimidine ethers **105a-g**, but it was not possible to isolate the clean compounds. A series of 2,4-diamino-5-[4'-chloro-3'-benzamide]-6-ethyl-pyrimidines **107a-c** were also prepared. The only clean compound obtained from this series of compound was 4-*tert*-butyl-N-[2-chloro-5-diamino-6-ethylpyrimidine-5-yl]-phenyl]benzamide (**107a**). Although the mass spectrometry and ¹H NMR indicated the presence of compounds **107b-c** it was not possible to purify them. The failure of these reactions was perhaps due to the poor solubility of the compounds. However, the subsequent reaction between **106** and **111** was successful and afforded clean compound 2-[2-chloro-5-(2,4-diamino-6-ethylpyrimidin-5-yl)-phenyl]isoindole-1,3-dione (**108**). The pure compounds and the other crude mixtures were screened against *M. fortuitum*. No antimycobacterial activity was observed. Owing to time constraints and the lack of antimycobacterial activity no further attempts were made to purify or re-synthesise these compounds.

In this study *M. fortuitum* has been used as a model for *M. tuberculosis* for the reasons for which are discussed in **Section 3.1**. It is apparent from **Appendix 5** that although many compounds were inactive against *M. fortuitum*, they were nevertheless potent antitubercular agents. There is a possibility that they may have been found false negatives at this stage. It is recommended that the above compounds should be prepared, purified and tested against *M. tuberculosis*.

5 Introduction to the use of molecular imprinting to guide a chemical synthesis of potential inhibitors of mycobacterial dihydrofolate reductase.

5.1 Introduction

This chapter describes the development and use of molecular imprinting as a means for preparation of anti-idiotypic imprint matrices. The so formed preparations can be used in a vast variety of applications for example, new drugs, inhibitors or new affinity materials. A brief background is given first in order to lay out the aims and objectives of of this part of the thesis. Thereafter the background material is covered in greater detail.

5.2 Molecular Recognition

Molecular recognition is a fundamental requirement of living systems. At the cellular and sub-cellular level, the fundamental processes of life, information transfer and reaction catalysis rely on the specific interaction of low molecular weight molecules with macromolecular "hosts." In the majority of such events the macromolecule is a protein. Processes as diverse as neural transmittance, respiration, immune defense, cellular differentiation and nutrition all rely on the basic principle of specific molecular recognition [Sellergren and Allender, 2005]. Non-covalent interactions are highly prevalent in biological systems and are found in enzymes, DNA, proteins, antibodies, membranes and receptors. The remarkable specificity, reaction control, and rate accelerations observed in nature are also the result of non-covalent intermolecular interactions. All of these examples illustrate the importance of molecular recognition to the properties of life, providing pressing reasons for studying how molecules interact.

5.3 Synthetic Molecular Recognition

Although biological systems are often very highly slective, the practical applications of protein based assays faces many difficulties due to their instability against high temperature, organic solvents, drastic pH conditions and they are expensive. Therefore scientists have invested huge amounts of time and effort, in trying to mimic these properties in synthetic materials. A number of synthetic approaches has been developed that aim to mimic the dynamic non-covalent molecular recognition approach favoured by biology.

The modern field of molecular recognition began in 1967 with Pederson's synthesis of crown ethers. These man-made macrocyclic receptors were capable of binding alkali metals with amazing efficiency and selectivity. Since then, synthetic receptors such as crown ethers [Pederson, 1967], cryptates [Lehn, 1969], cyclophanes and molecular clefts [Rebek, 1990] have found utility as synthetic reagents. The field has also accumulated a number of names including: host-guest chemistry and

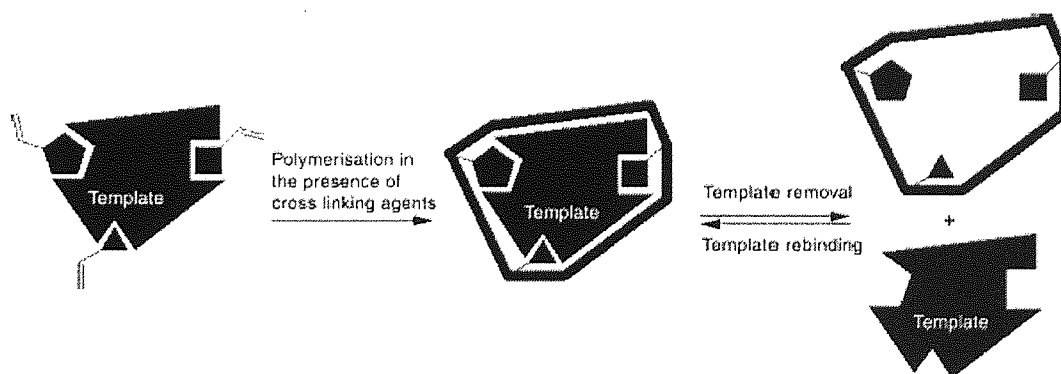
supramolecular chemistry. In 1987, the emerging multi-disciplinary field was acknowledged with a Nobel Prize.

5.4 Molecular Imprinting

One of the most promising areas of biomimetics and synthetic receptors is molecular imprinting, which has attracted significant interest from a large number of areas within chemistry and analytical science. Constructing molecular imprints is crucially different from guest-host chemistry. The main difficulty in preparing a synthetic host is often not the design of its recognition elements but the chemical effort required to combine precisely these elements into a single receptor molecule. Imprinting overcomes this problem by holding the recognition elements in place, owing to their interactions with the template, while they are connected to a macromolecular scaffold via growing polymer chains. This allows the pathways between neighbouring groups in the recognition site to be of virtually any length through the crosslinked matrix, precisely matching the template's requirements. An analogy can be made with the structure of antibodies, where amino acid residues at the binding site are brought together by folding the protein chain. Linus Pauling once speculated that antibodies were synthesised to complement the 'template' antigen [Pauling, 1940]. This insight proved to be incorrect, but was the first description of molecular imprinting.

5.4.1 Principle of molecular imprinting

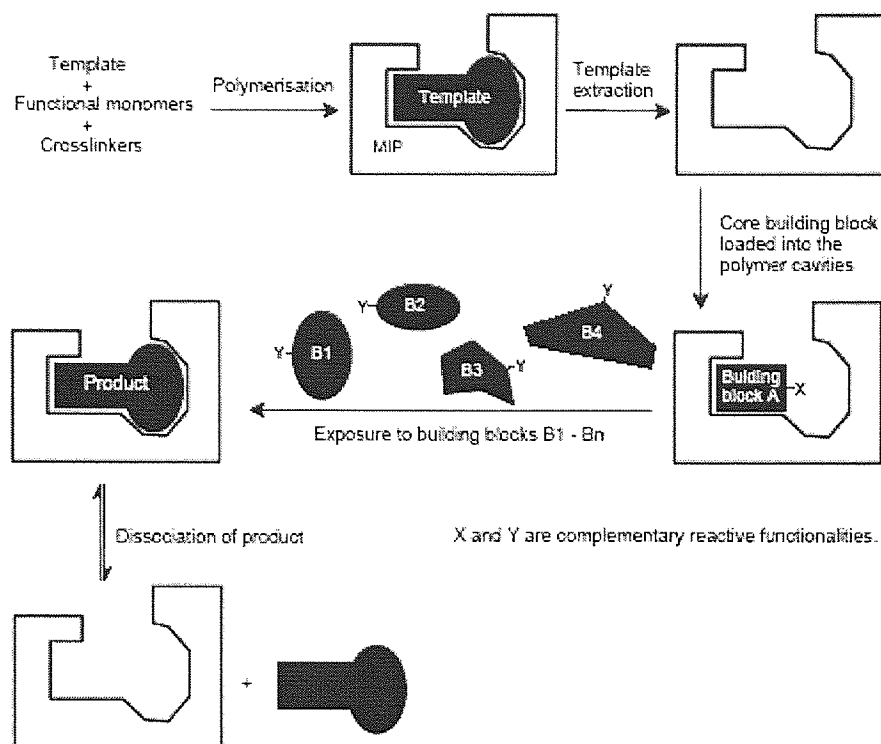
The principle underlying molecular imprinting is the assembly of a cross-linked polymer matrix around a template; when the template is removed, recognition sites are created which should be complementary to the template (**Scheme 5.1**).



Scheme 5.1: General scheme for MIP construction adapted from Rathbone *et al*, 2005

Schematic representation of a molecular imprinting process. Preassembly of functional monomers is driven by their complementary interactions with the template. Polymerisation 'freezes' binding groups within a template-defined 'cavity'. Removal of the template by solvent extraction or chemical cleavage affords binding sites specific to the original template.

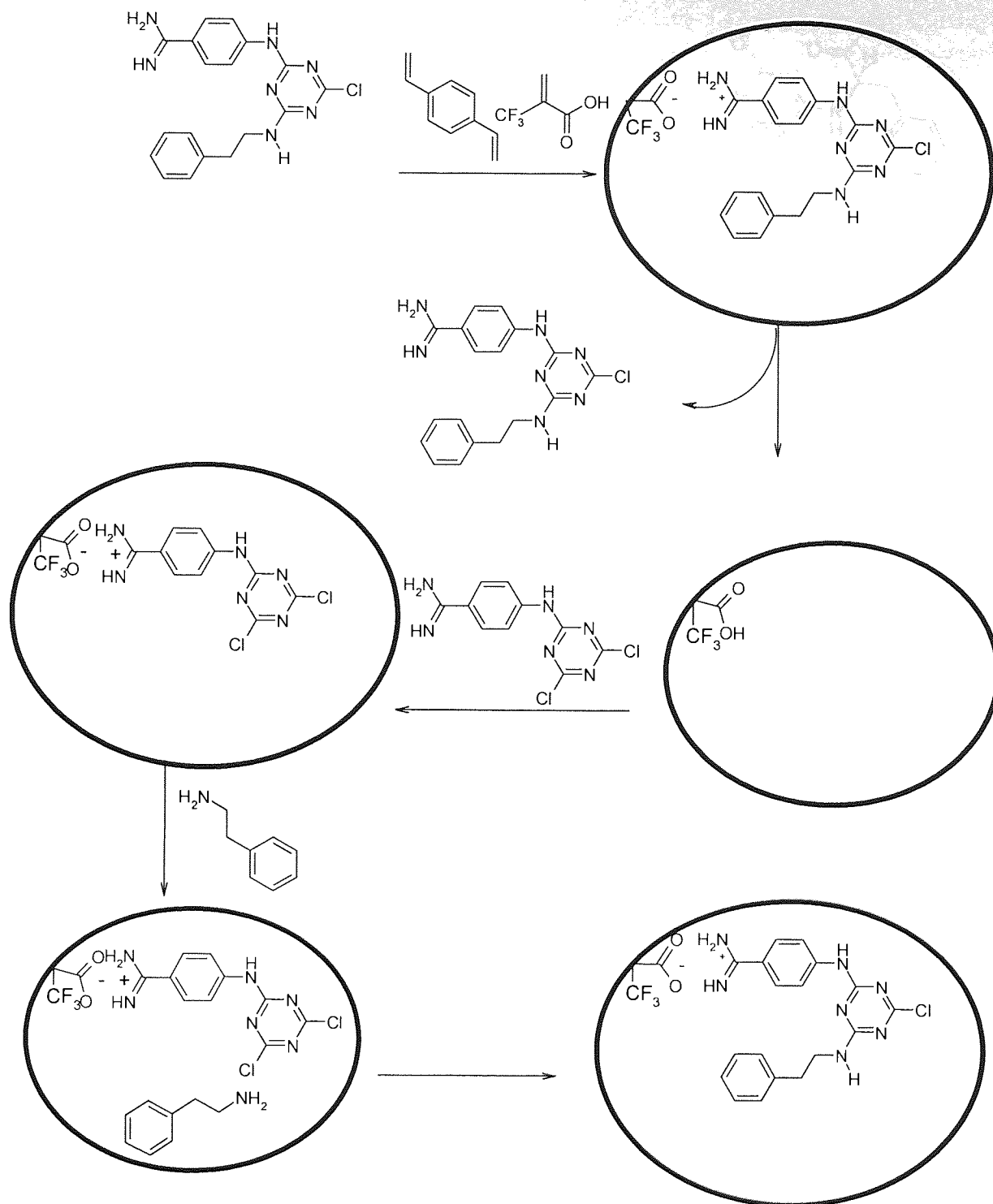
5.5 An Anti-idiotypic Approach, a Step toward the Next Generation of Molecular Imprinting



Scheme 5.2: The process of anti-idiotypic imprinting adapted from Rathbone 2005. Structure of the imprinted polymer (a) after removal of the template from the MIP, the binding cavity can be used to direct the assembly of the reactants to give products mimicking the original template.

As a further step in its development, which could be described as the next generation of molecular imprinting, double or anti-idiotypic imprints have been made, involving two steps: (i) making an imprint of the template in the polymer i.e. micro-reactor, (ii) the obtained cavities of such original imprints can be used as mould leading to the creation of new molecules (mimics); anti-idiotypic imprints or images of the original imprints. The resulting images would resemble the original imprint species in shape and functionality. The principle is schematically described in **scheme 5.2** and **5.3**.

To demonstrate the method (**Scheme 5.3**), Mosbach and co-workers use the protease kallikrein as their test case. The researchers made a polymeric "mould" that fit around a known inhibitor of the clinically interesting enzyme kallikrein [Mosbach *et al* 2001; Yu, *et al.* 2002]. They removed the inhibitor, leaving a molecularly imprinted polymer with a cavity shaped like the inhibitor. Condensation reactions between pairs of small building-block compounds capable of binding to opposite halves of the cavity were then used to form addition products that resembled the shape and activity of the inhibitor.



Scheme 5.3: The process of anti-idiotypic imprinting.

The inhibitor (**Figure 5.1**) containing a guanidine headgroup and a hydrophobic benzylic tail was used as a template to establish MIP binding sites with structural similarity to the enzyme's active site. The functional monomer trifluoromethylacrylic acid and the cross-linker DVB were chosen in order to establish acid-base and hydrophobic π - π interactions in the cavities of the resultant polymers.

Illustration removed for copyright restrictions

Figure 5.1: Templates (inhibitors) and core building block used in anti-idiotypic imprinting. [Mosbach *et al* 2000]

Moreover, this approach requires suitable chemistry and chemical building blocks for use inside the MIP cavity. For example, Mosbach and co-workers replaced the template by the related reactive building block (2-(4-amidinophenylamino)-4,6-dichloro-s-triazine) (**Figure 5.1**). This compound was reacted with various nucleophilic amines (**Figure 5.2**) to give the aminotriazine products as shown in **scheme 5.4**. Once the reaction had attained complete conversion, acetic acid was added to liberate the products from the polymers. The compound formed using phenylethylamine (R3) was found to have an affinity for kallikrein close to that of original inhibitor (template 1).

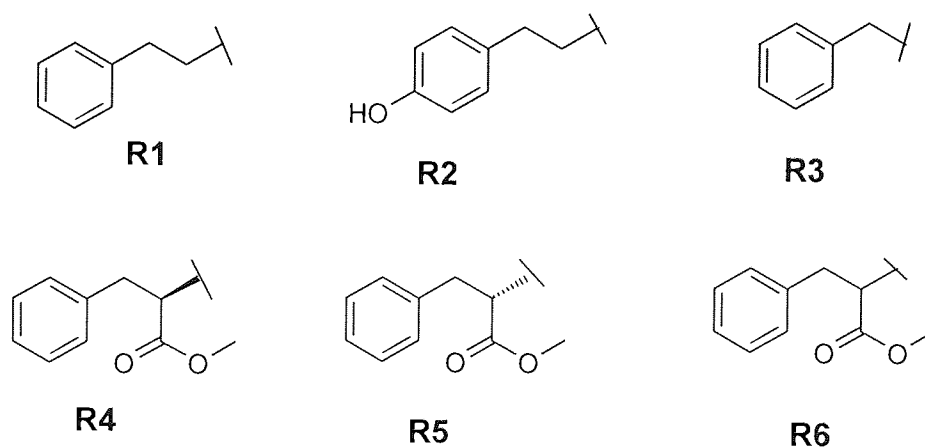
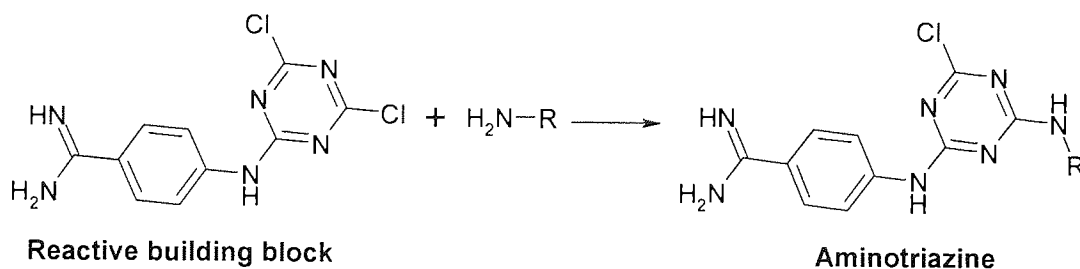


Figure 5.2: Nucleophilic substituted amines residues used in anti-idiotypic imprinting.



Scheme 5.4: Aminotriazine formation.

However, the compound with amine (**R6**) was not formed. This could be explained in terms of steric hindrance, i.e. the MIP1 was able to discriminate against the rather bulky nucleophile (**R6**) i.e. carboxymethyl ester derivative. When the bulkier and a chiral template 2 (**Figure 5.1**) was used to create MIP2, it was then possible to form products with nucleophile (**R6**) as well as with smaller nucleophiles (**R1**) and (**R3**) owing to the larger cavity size. MIP2 was further investigated for an entiospecific synthesis inside the MIP's binding cavities. It was observed that since MIP2 cavities were chiral they were able to direct the 67% of the synthesis of products with the same stereochemistry as the initial template; showing that the templating process displays stereoselectivity [Yu, *et al.*, 2002].

The anti-idiotypic strategy is useful in situations where a known inhibitor is already available. This approach can be used to generate analogs of known drugs with the need to create large combinatorial libraries of candidate structures. Moreover, the molecularly imprinted polymers are not only used as artificial receptors for screening synthetic compounds; in the anti-idiotypic approach, the molecularly imprinted polymers can also be used to find out useful reactants (or reaction conditions) leading to active products. This approach has the advantage of saving considerable synthetic efforts, since only the hit reactions need to be scaled up for further investigation.

5.6 Design of a molecularly imprinted polymers (MIPs) with affinity for compounds containing the 2,4-diaminopyrimidine group

As part of a drug discovery program for the treatment of *M. tuberculosis* at Aston University, it was decided to develop an anti-idiotypic approach to the synthesis of potential inhibitors of mycobacterial dihydrofolate reductase. The first step in that process is the design and synthesis of MIPs capable of binding compounds containing the 2,4-diaminopyrimidine unit. The overall concept is expanded later in chapter eight. In the first step, the design of MIPs capable of recognizing the 2,4-diaminopyrimidine group, it was proposed to use a polymerisable barbituric acid derivative as the functional monomer (**85**, **Figure 5.3**). This unit would have the possibility to make three hydrogen bonds with 2,4-diaminopyrimidine unit.

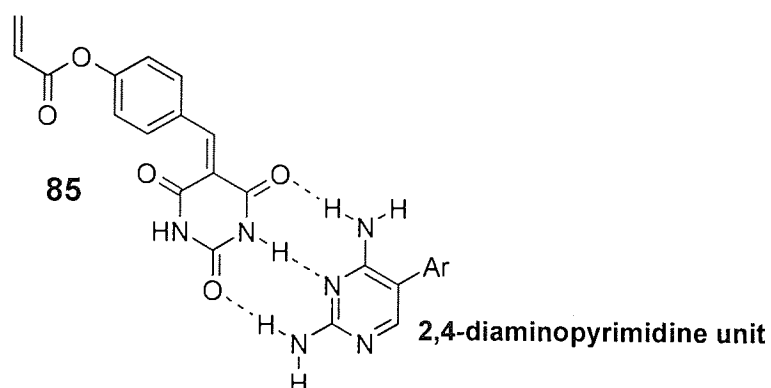


Figure 5.3: The structure of the proposed polymerisable 'receptor' that has the possibility to recognise 2,4-diaminopyrimidine unit.

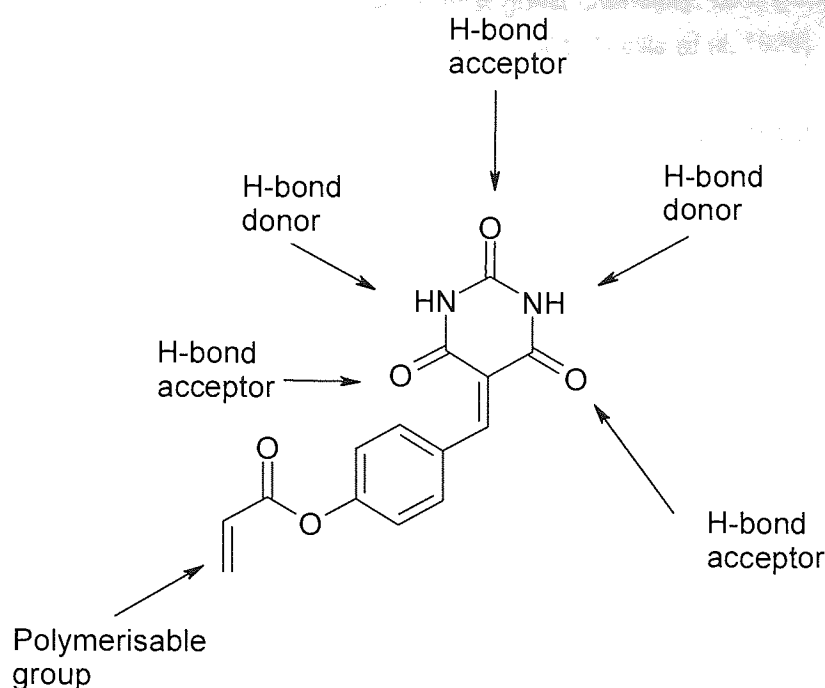


Figure 5.4: Structure of the proposed functional monomer (acrylic acid 4-(2,4,6-trioxo-tetrahydro-pyrimidin-5-ylidenemethyl)-phenyl ester (**85**).

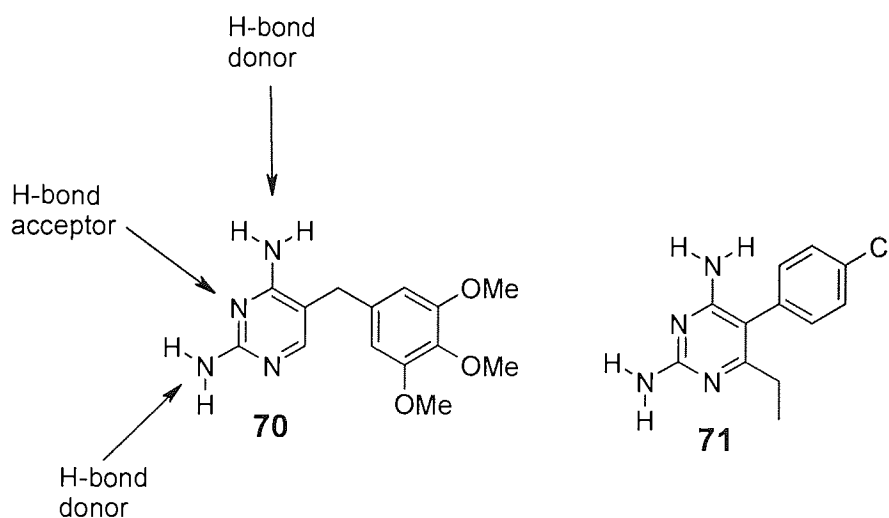


Figure 5.5 The structures of the DHFR inhibitors selected to be used as templates in the current study.

A key element in the design of a specific receptor concerns the incorporation of several recognition features (eg. hydrogen bonding, hydrophobic or electrostatic) that complement the chemical characteristics of the target. This multiple point binding is dramatically seen in the enzyme DHFR that binds a diaminopyrimidine containing substrate *via* hydrogen bonding interactions [Li, 2000; Quaglia, 2001].

The barbiturate derivatives can generally hydrogen bond with various groups in 2,4-diaminopyrimidine. For example, the carboxylic amide groups of barbituric acid can form strong hydrogen bonds with

amine groups of 2,4-diaminopyrimidine containing inhibitors. To date, barbiturates have been used as analytes in various studies. For example, Tanabe *et al* [1995] and Kubo *et al* [2003] have reported an imprinted polymer using 2,6-bisacrylamidopyridine as a functional monomer and various barbiturates as template. Barbiturates have been also employed in host-guest chemistry, as a guest compound in variety of studies [Chang and Hamilton, 1991, Hamilton *et al*, 1991, Tecilla *et al*, 1995].

Moreover, the existence of non-covalent interactions between the 2,4-diamino-5-(3,4,5-trimethoxybenzyl)pyrimidine (**70**) and 5,5-diethyl barbituric acid (**86**) are evident from its crystal structure Figure 5.6-5.7) [Shimizu and Nishigaki, 1982].

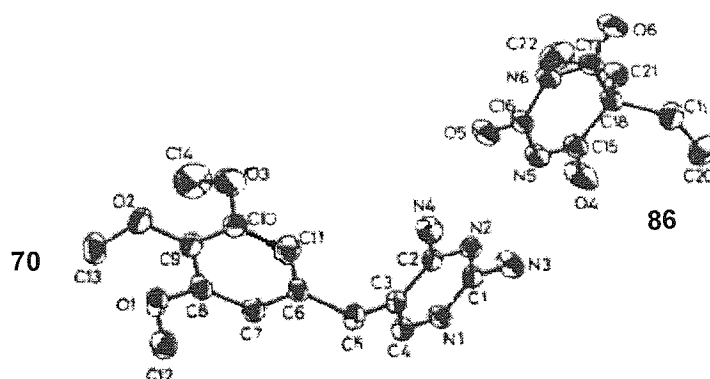


Figure 5.6: Molecular structure of TMP (**70**) and 5,5-diethyl barbituric acid (**86**), adapted from Shimizu and Nishigaki, 1982

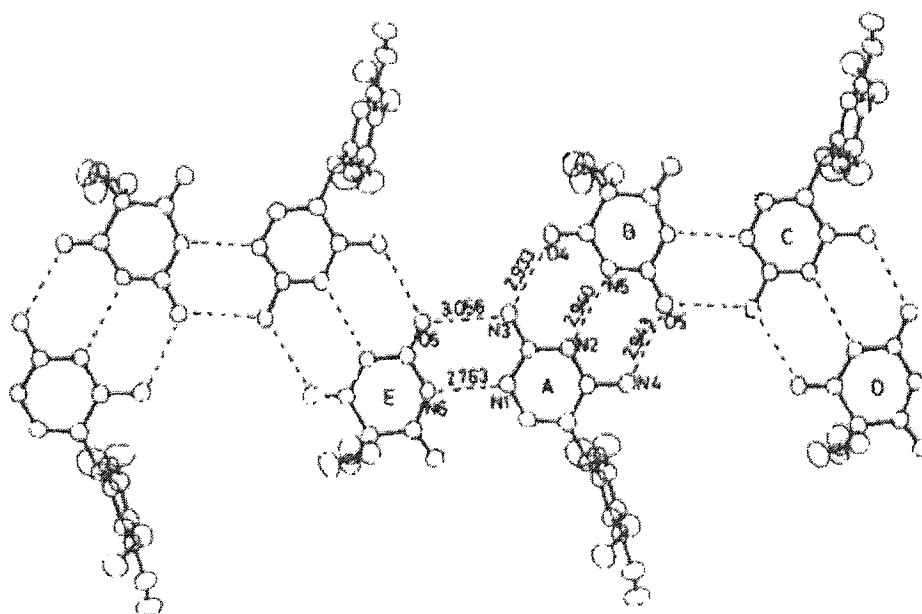


Figure 5.7: Packing diagram of the title compound **70** and **86**, adapted from Shimizu and Nishigaki, 1982

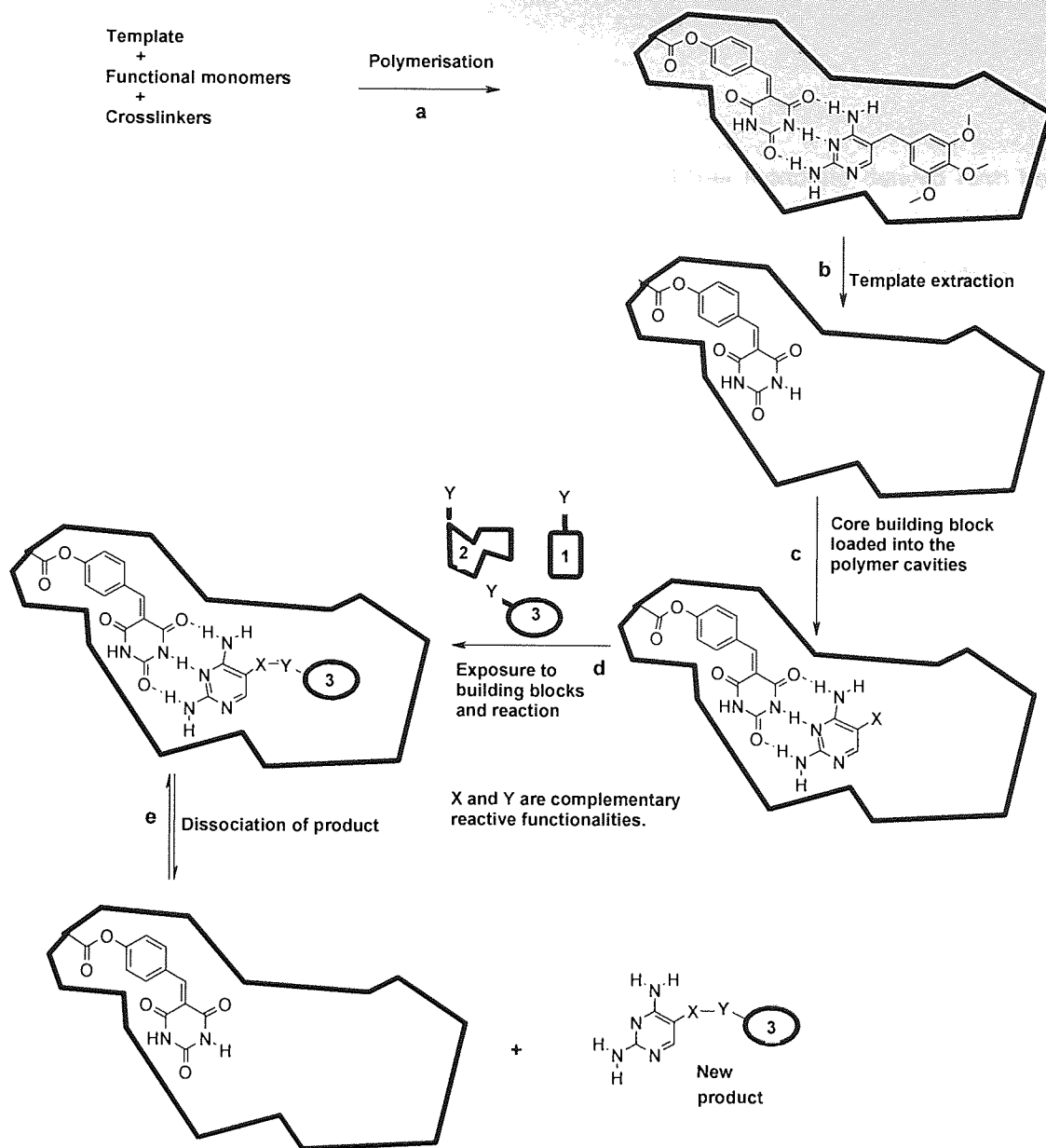
The crystal structure revealed that the TMP and 5,5-diethyl barbituric acid (1:1) were alternately linked by hydrogen bonds to form a crystalline hetero-dimers by characteristic hydrogen bonds, which apparently contribute to the stabilization of the crystal. Earlier studies carried out by Koetzle and

Williams in 1976 found that TMP (**70**) has a tendency to form crystalline homo-dimers. Similarly, compound **86** also has a tendency to form homo-dimers [Craven *et al*, 1969]. In contrast no contacts between molecules of the same kind were observed in the crystal structure of 2,4-diamino-5(3,4,5-trimethoxybenzyl)pyrimidine-5,5-diethylbarbituric acid (**Figure 5.7**) [Shimizu and Nishigaki, 1982].

Quaglia and co-worker selected 2,4-diamino-5(3,4,5-trimethoxybenzyl)pyrimidine (TMP) as a template for the synthesis of molecularly imprinted polymers using methacrylic acid as a functional monomer. In their study, chromatography and ¹HNMR were used in order to characterize the polymer-template interaction. The results demonstrated that the polymer imprinted with TMP showed the highest selectivity among the MIPs in an organic mobile-phase system. It also shown to associate strongly with the methacrylic acid in CDCl₃ in ¹HNMR studies.[Quaglia *et al*, 2001].

Furthermore, in the present study we have proposed a polymerisable functional monomer that possesses a barbiturate moiety containing carbonyl and amide groups that will be incorporated into scaffold of the polymer to serve as hydrogen bond donor/acceptor. I.E. the carboxylic group of barbiturate may act as hydrogen bond and proton donor as well as hydrogen bond acceptor (**Figure 5.4**). Templates **70** and **71** containing 2,4-diamino-pyrimidine nucleus were selected as they have both hydrogen-bond donor and acceptor sites as illustrated in (**Figure 5.5**). In DHFR the 2,4-diamino pyrimidine ring appears to be a key component for an activity and play a role in the binding between the enzyme and the substrate. Additionally, **70** and **71** are small, basic, lipophilic and have much higher solubility in organic solvents compare to other DHFR inhibitors, for example, methotrexate (**67**). On the other hand, diaminopyrimidine was an attractive model for the purpose of this investigation on account of its molecular features, namely the presence of an aromatic π-electron system, which renders the molecule fluorescent and the presence of amine and nitrogen groups for intermolecular interactions with the functionalized monomers during non-covalent imprinting.

The main goal of this research was to incorporate the proposed functional monomer into the scaffold of a polymer for binding the 2,4-diaminopyrimidine nucleus as the first stage in MIP-guided synthesis of potential mycobacterial DHFR inhibitors **Scheme 5.5**. As follow up work to this current research, the imprinted polymers containing cavities shaped to bind 2,4-diaminopyrimidine could be used as molecular-scale reaction vessels for synthesising new types of substrate (inhibitors) for a active site of mycobacterium DHFR.



Scheme 5.5: Schematic representation of an anti-idiotypic imprinting process. **(a)** Preassembly of functional monomers is driven by their complementary interactions with the template. Polymerisation 'freezes' binding groups within a template-defined 'cavity'. **(b)** Removal of the template by solvent extraction affords binding sites specific to the original template **(c)** Loading of the polymer with building blocks containing the 2,4-diaminopyrimidine moiety. **(d)** Selective binding of reagents that fit the cavity and show association with a 2,4-diaminopyrimidine **(e)** Dissociation of new product from the polymer.

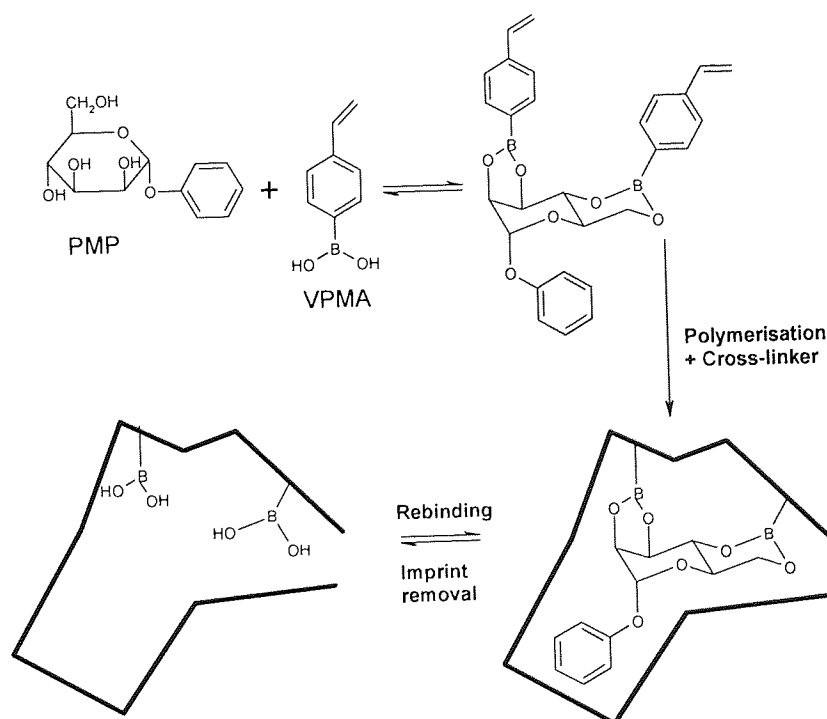
5.7 Aim of this work

The aim of this part of the research was to pave the way for the use of molecular imprinting to produce micro-reactors which would be able to direct the synthesis of potential inhibitors of mycobacterial DHFR. This work took its inspiration from the studies published by Mosbach *et al* in the field of anti-idiotypic molecular imprinting [Mosbach *et al*, 2001; Yu *et al* 2002]. The details of this work will be discussed in chapter 6.

polymerisation. The covalent bonding system employs a template-monomer complex which is formed by covalent, but reversible, bonding. An important feature of imprinting with covalent interactions is that it allows the structure of imprinted cavities to be probe in detail. However, the covalent system is not very flexible in terms of the choices of functional monomer(s) and template species and removal of the template molecule is tedious (chemical cleavage). Finally, the third method is based on the sacrificial spacer approach that was first introduced by Whitcombe and co-workers [Whitcombe, 1995]. This approach involves the use of reversible covalent bond in the imprinting step, and non-covalent interactions in the rebinding step; taking advantage of faster rebinding kinetic.

5.9.1 Covalent methods

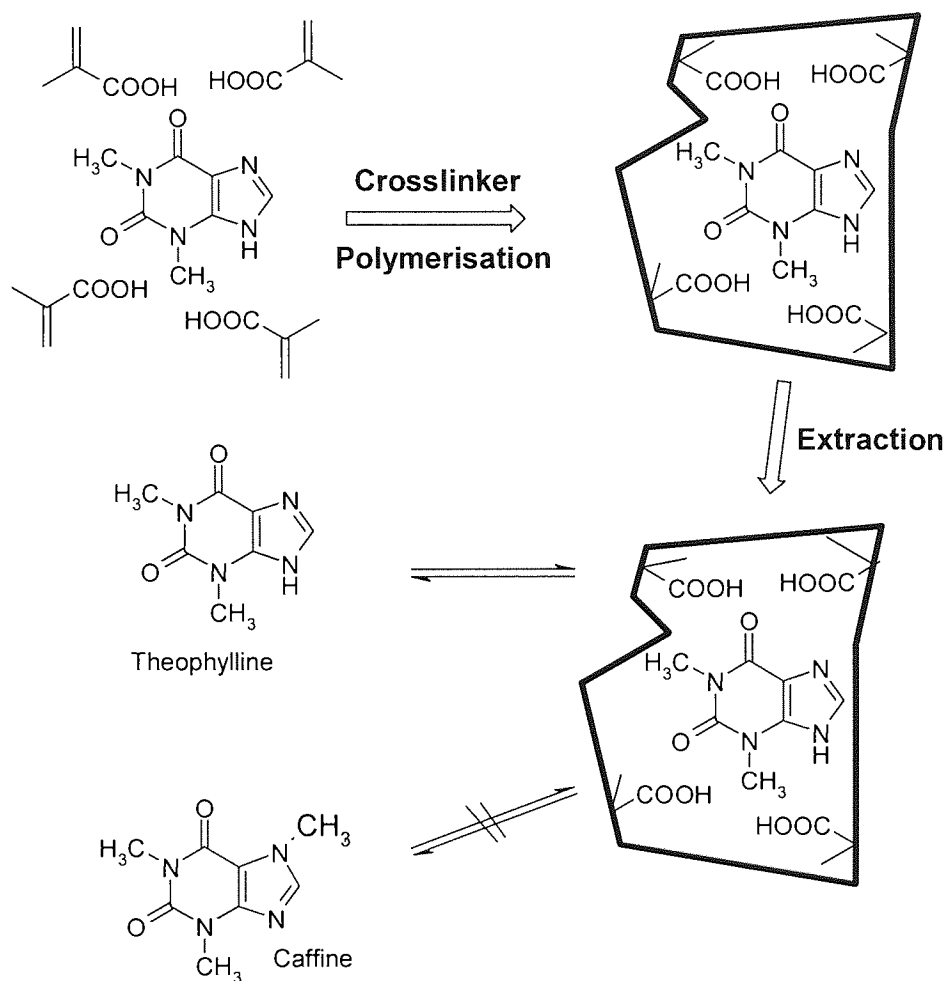
The covalent imprinting was pioneered by Günter Wulff and coworkers. The aim of this method is to produce an 'exact fit' recognition site, in which the same chemical bonds in the initial templatemonomer complex reform during any subsequent binding of the imprinted polymer cast. For this to be true, it must be possible to form a labile, reversible bond between the template and the polymer. Wulff and co-workers have synthesized the boronate di-ester of phenyl- α -D-mannopyranoside (PMP) using 4-vinylphenylboronic acid (VPBA) [Wulff, 1997]. The boronate sugar was then co-polymerised with a large amount of an acrylic cross-linking monomer to give a macroporous polymeric product (**Scheme 5.6**). Removing the template from the resulting polymer requires only mild hydrolysis with, for example, aqueous methanol, leaving a polymer cavity containing boronic acid residues in the exact spatial arrangement necessary to rebind the template. Besides boronate esters [Wulff and Sarhan, 1972], the formation of ketals [Shea and Dougherty, 1986] and Schiff's bases [Wulff *et al*, 1984] also involves reversible covalent bond formation, giving rise to a useful, although somewhat restricted, range of functional groups (diols, aldehydes, ketones and primary amines) for covalent imprinting.



Scheme 5.6: Boronic ester approach to covalent molecular imprinting of PMP using VPMA

5.9.2 Non-covalent Methods

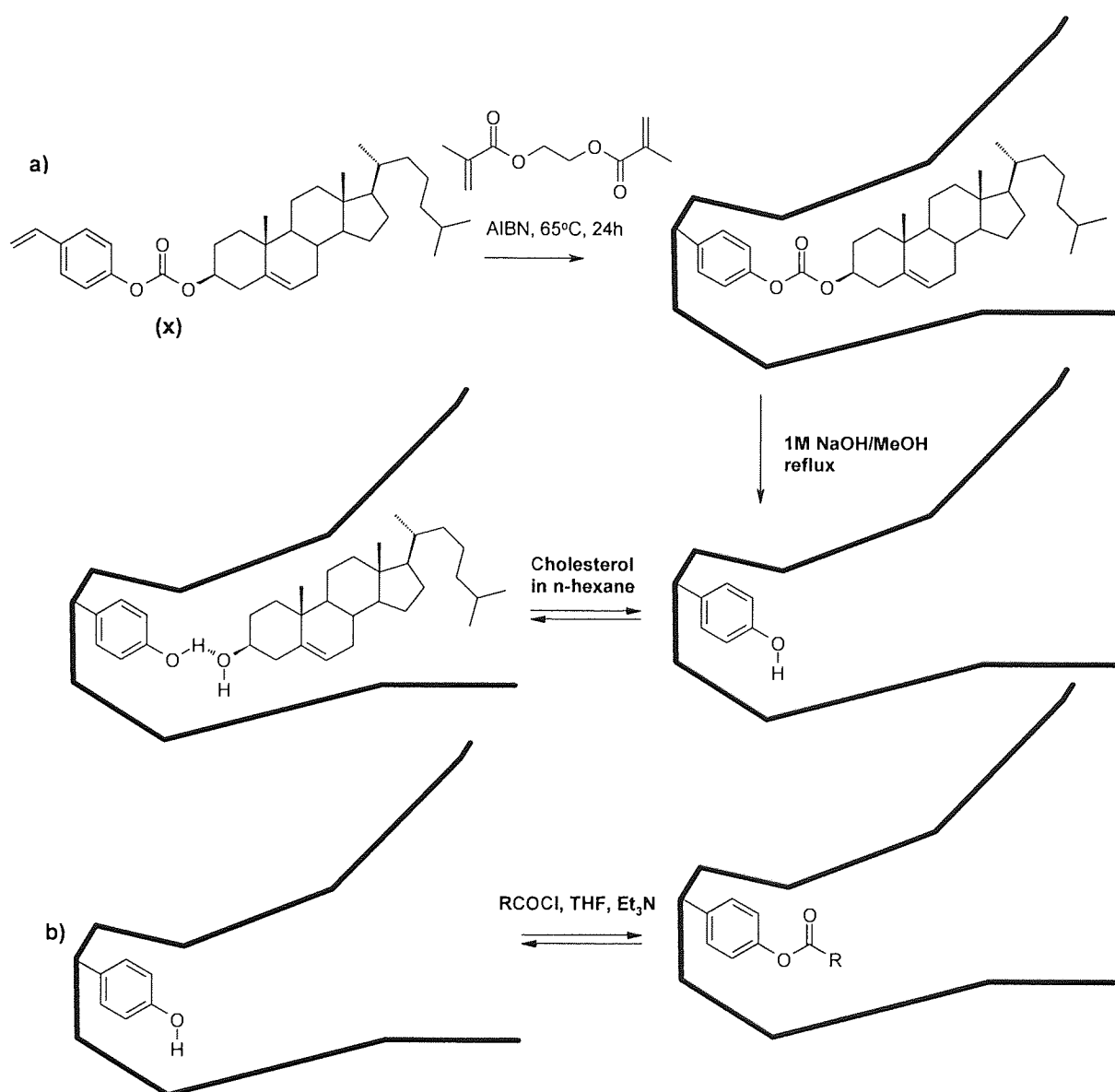
Non-covalent imprinting was pioneered by Klaus Mosbach's group. It has been applied to a much wider range of template molecules including amino acid derivatives, [Wulff and Haarer, 1991] peptides [Kempe, *et al.* 1995], β -blockers, [Fischer *et al.* 1991] diazepam and theophylline [Vlatakis *et al.*, 1993; Ye, *et al.* 1999]. It relies on self-assembling functional monomers around the template in the polymerisation mixture (**Scheme 5.7**) and, because no covalent bonds form between the template and polymer, template removal involves simply washing the polymer repeatedly with a suitable solvent.



Scheme 5.7: Non-covalent molecular imprinting of theophylline adapted from [Vlatakis *et al.*, 1999].

Although a range of functional monomers is used, methacrylic acid and vinylpyridine are among the most common. Again, the rebinding of non-covalently imprinted polymers is an 'exact-fit' process, since the interactions between the polymer and its target ligand (usually a drug or other metabolite) will be the same as those holding together the template-monomer complexes. As a result, factors that tend to increase the stability of the initial complex will improve imprinting efficiency, while those that destabilise it will produce an inferior polymer. Binding to these polymers can be very rapid, because covalent bond formation is not involved in recognition.

The semi covalent strategy involves using the covalent bonds for imprinting that allows the functional groups to be fixed within the MIP and the non-covalent bonds to be used for the rebinding step. The approach of combining both has improved binding site homogeneity, reduced non-specific binding and improved kinetics. Sellergren and co-worker reported the imprinting of structural analogue of *p*-amino-phenylalanine-ethyl-ester, *N*²-propionyl-L-2-amino-3-(4-hydroxyphenyl)-1-propanol which was covalently to a polymerisable group via an ester linkage. After basic hydrolysis, two carboxyl groups remained in the polymer matrix capable of forming hydrogen bonds and ionic interactions with the amino group of the amino acid. However, the polymer preferred binding of the D-form rather than the L-form that was used in this study [Sellergren and Andersson, 1990].



Scheme 5.8: Imprinting cholesterol by the sacrificial spacer method. (a) Preparation of cholesterol-imprinted polymers using cholesteryl (4-vinyl)phenyl carbonate (x), and (b) Chemical modification of the recognition site by acylation [Whitcomb *et al* 1995].

The semi covalent approach was further developed by Whitcombe and co-workers [Whitcomb *et al* 1995]. In their study a cholesterol-specific polymer was prepared by imprinting with chloesteryl (4-

vinyl)phenylcarbonate as the template monomer. Hydrolytic cleavage of the carbonate ester with the loss of 'sacrificial' CO₂, led to a recognition site bearing a phenolic residue (**Scheme 5.8**). The resulting polymers showed preferential binding of cholesterol over epi-cholesterol, cholest-5-ene-3-one and cholesteryl acetate. Remarkably, they also bound cholesterol with a single dissociation constant, thus displaying characteristics similar to true biological receptors or synthetic hosts.

5.10 The functional Monomer

The functional monomer undergoes a regiospecific, weak and complementary interaction with template. The polymerisable unit enables the template-monomer complex to be incorporated into the polymer matrix. The functional monomer has a variety of functional groups (e.g. hydrogen bond donors, acceptors, possibly acidic or basic groups, or aliphatic or aromatic groups). One or more of these groups can interact with the imprint molecule via specific hydrogen bonds. Thus, functional groups complementary to the template are one of the basis for the selection of the functional monomer. For example, methacrylic acid (MAA) is a typical functional monomer for a template with basic functional groups.

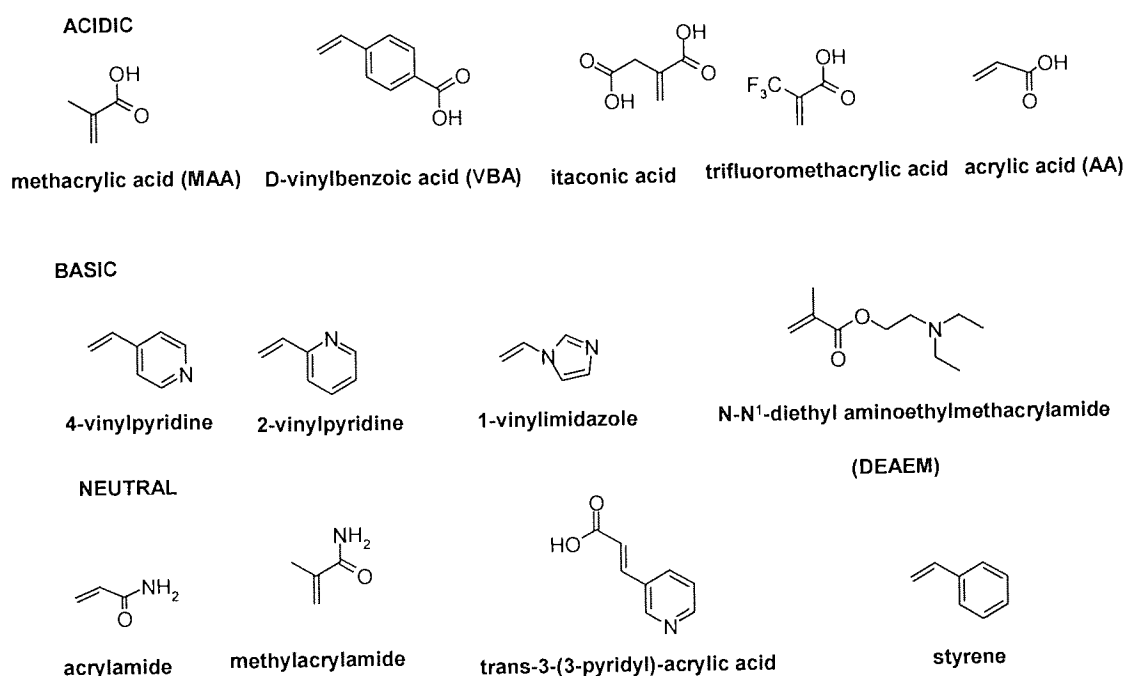


Figure 5.8: Selection of functional monomers used in non-covalent molecular imprinting

For templates with acidic functional groups, basic functional monomers such as 2-vinylpyridine [Wulff and Vietmeier, 1989], 4-vinylpyridine [Wulff and Akelah, 1984], 1-vinylimidazole [Damen and Neckers, 1980] have been commonly used. For templates with acid functional group as well as a basic functional group for example, amino acids and peptides, the combination of MAA and vinyl pyridine [Ramstrom, *et al.* 1993] have been shown to improve MIP performance. The structures of some functional monomers employed in non-covalent molecular imprinting are displayed in (**Figure 5.8**). Furthermore, the choice of monomer can also be influenced by factors such as solubility, stability and

the ability of polymerisation. The monomeric molecules can be made to polymerize to form a rigid or semi-rigid polymer in order to improve affinity and kinetics respectively.

In summary, the choice of functional monomer should be based upon the functionality of the molecule to be imprinted. The general approach of the technique is to combine the desired "imprint" molecule with a solution of small monomeric molecules which has several desired features: They have a variety of functional groups (e.g. hydrogen bond donors, acceptors, possibly acidic or basic groups, or aliphatic or aromatic groups). One or more of these groups can specifically interact with the imprint molecule (e.g. they can form specific hydrogen bonds). The imprint molecule is soluble in the monomer solution. The monomers, either in solution or during the polymerization process, do not form covalent bonds with the imprint molecule (the interaction is strictly non-covalent).

5.11 The Template

In molecular imprinting a target molecule acts as a template around which interacting and cross-linking monomers are arranged and co-polymerized to form a cast-like shell. In order to be successfully imprinted, a template must be soluble in a non-polar solvent and contain a certain level of functionality that can be paired with reciprocating moieties present on a polymerisable unit. In general, small, multi-functional, templates give rise to highly specific imprints whilst larger, mono-functional, templates produce imprinted sites which are less specific [Bowman *et al.* 1998]. By employing the non-covalent approach a diverse number of templates have been successfully imprinted. For instance steroids [Cheong *et al.*, 1997], proteins [Shi *et al.*, 1999], peptides [Rachkov and Minoura, 2001], amino acids [Sellergren *et al.*, 1985; Andersson *et al.*, 1984; Andersson and Mosbach, 1990; Kempe and Mosbach, 1995], drugs [Suedee *et al.*, 2000], dyes [Arshady and Mosbach, 1981] and nucleosides [Spivak and Shea, 2001]. In contrast the covalent approach entails more specific requirements that leads to the limited number of templates utilised.

5.12 Solvent/Porogens

The solvent plays an important role in the outcome of a molecular imprinting process. As porogen in the polymerisation, the solvent governs the strength of non-covalent interactions in addition to its influence on the polymer morphology. Generally, the more polar the porogen, the weaker the resulting recognition effect becomes, as a consequence of the influence of the solvent polarity on non-covalent interactions [Sellergren, 1993]. The best imprinting porogens for accentuating the binding strengths are solvents of very low dielectric constant, such as toluene, chloroform, dichloromethane and benzene. The use of more polar solvents will inevitably weaken the interaction forces formed between the print species and the functional monomers resulting in poorer recognition [Nicholls; 1995; Sellergren, 1985; Matsui; 1996].

In the recognition step similar questions about the choice of solvent arise. Since all non-covalent forces are influenced by the properties of the solvent, non-polar solvents normally lead to the best recognition. When applying the polymers to gradually more polar solvents, the recognition is

diminished. Also, the morphology is affected since the swelling of the polymers is dependent on the surrounding medium.

The swelling is most pronounced in chlorinated solvents, such as chloroform and dichloromethane, as compared to acetonitrile and tetrahydrofuran. This swelling behaviour may lead to changes in the three-dimensional conformation of the functional groups taking part in the recognition in the sites resulting in poorer binding capability. As a general rule, the best choice of recognition solvent should be more or less identical to the imprinting porogen in order to avoid any swelling problems, although this is not necessarily a prerequisite. On the whole, the recognition complexes of a majority of non-covalent molecular imprinted systems have been shown to rely primarily on electrostatic interactions [Sellergren *et al*; 1988; Andersson *et al*; 1990; Nicholls *et al*; 1995; Andersson *et al*; 1996], which have necessitated the use of non-polar, aprotic solvents for both polymer synthesis and template rebinding.

5.13 Crosslinkers

One of the main roles of the crosslinking monomer is to form a three-dimensional structure that remains unchanged after removal of the template. Therefore, the type and amount of crosslinker in the polymeric matrix are very important in order to have high selectivity. Since a very high degree of crosslinking (70-90%) is necessary for achieving specificity, only a limited number of crosslinkers have been utilised (Figure 5.9). The solubility of the crosslinker itself in the pre-polymeric solution and the solubility of the monomerised template species reduce the number of possible alternatives.

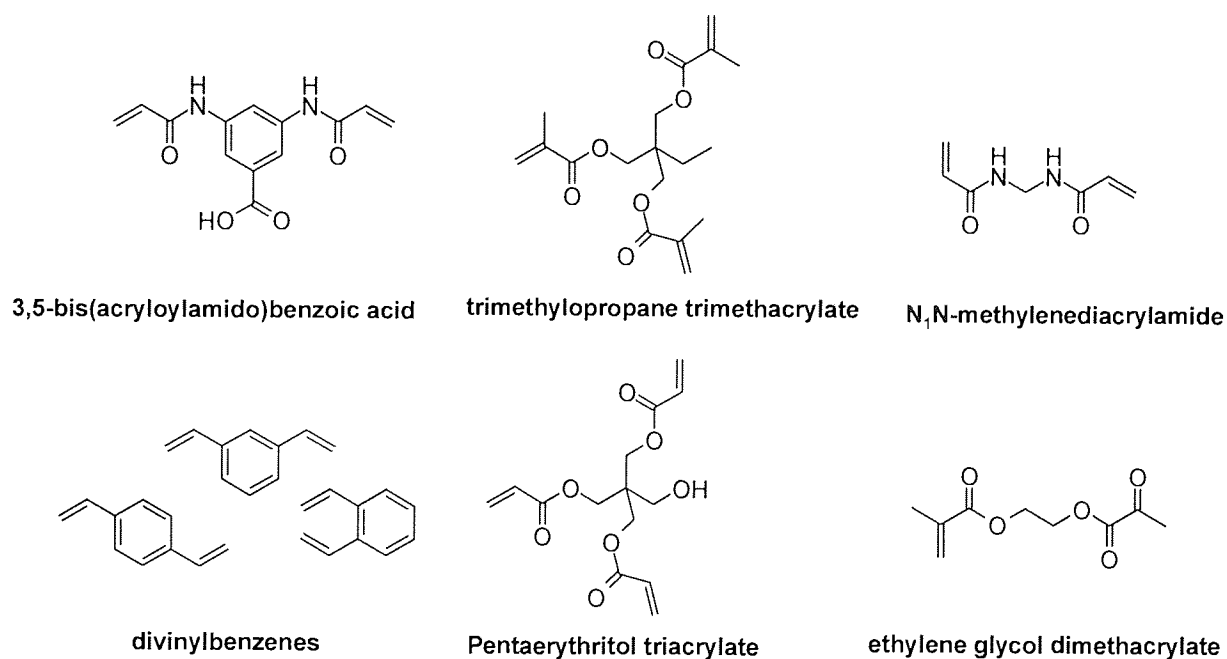


Figure 5.9: Selection of the cross-linking monomers used in molecular imprinting

Nevertheless, several different crosslinkers have been tried with different degrees of success. Originally, isomers of divinylbenzene were used for crosslinking of styrene and other functional monomers into polystyrenes. Later, it was found that acrylic or methacrylic acid based systems could be prepared with much higher specificity. Ethylene glycol dimethacrylate (EDMA) [Wulff, 1995, 1982; Kempe, 1995] and trimethylolpropane trimethacrylate (TRIM) are presently commonly employed.

Recently, several other crosslinkers have been studied. Thus, tri- and tetra functional acrylate crosslinkers, such as pentaerythritol triacrylate (PETRA) and pentaerythritol tetraacrylate (PETEA) [Kempe and Mosbach, 1995; Keepe, 1996] have been used for the preparation of peptide-selective molecularly imprinted polymers.

5.14 Proportions of Monomer:Template:Porogen

The relative proportions of the constituents of a MIP affect both the morphology and the function of the polymer. The polymer morphology and structure from the imprinting process is important for the dynamic binding properties of the synthetic receptor sites. The ideal properties of the cross-linked polymer matrix with embedded binding sites are a compromise between structural rigidity of the matrix maintaining the integrity of the binding sites and sufficient flexibility facilitating access to the binding pockets [Matsui, 1995]. The amount of cross-linker present during co-polymerisation with a functional monomer will largely determine the rigidity of the imprinted polymer matrix [Wulff *et al.* 1995; Sellergren, 1989]. A high degree of cross-linker is necessary for maintaining the structural integrity of the cavities formed during imprinting of the target analyte. Sellergren showed that the internal surface area of the polymer was proportional to the percentage of cross-linker, which correlated well with selectivity [Sellergren, 1993; 1989]. Besides the structural flexibility of the polymer matrix, porosity, is another parameter affecting access to embedded binding pockets. However, this can be overcome by selecting the appropriate polymerisation method, i.e. preparing MIPs in different formats such as micro and nano-spheres and polymer films.

The effect of the ratio of porogen to monomer was investigated extensively by Wulff's group who concluded that an approximate ratio of 1:1 (mL:g) gave rise to optimal selectivity and affinity [Wulff 1986]. Other studies have broadly agreed [Fischer *et al.*, 1991].

The final important ratio to consider is that of template:functional monomer. An elegant approach considerably reducing non-specific binding in non-covalent imprinting based on 'stoichiometric non-covalent imprinting' has been presented by Wulff. In this approach, a 1:1 or 1:2 molar ratio between template and functional monomer is used. It has shown that more than 90% of the complex can be stabilised [Wulff and Knorr, 2002]. Sellergren proposed a 2:1 model for the MAA:L-PheNHph complex, but suggested a 4:1 ratio should be used to maximise the number of interactions at a given time [Sellergren, 1988].

5.15 Development of Improved Crosslinking Monomers for Molecularly Imprinted Materials

The field of molecular imprinting has been dominated by the use of methacrylic acid (MAA) as the functional monomer and EGDMA or DVB as the crosslinking monomers. In search for the most effective monomers and cross-linkers for molecular imprinting the Spivak group [Sibrian and Spivak, 2004] has proposed a much simpler approach (OMNiMIP = one monomer molecularly imprinted polymers) to MIP formation which utilize a single cross-linking monomer, *N,O*-bismethacryloyl ethanolamine (NOBE, Figure 5.10), in addition to template, solvent and initiator. Basically, this approach eradicates variables such as choice of functional monomer and cross-linker, the ratio of

functional monomer/cross-linker and the ratio of functional monomer/template which normally complicate MIP design.

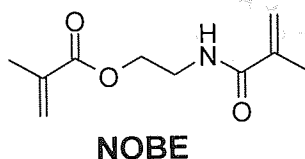


Figure 5.10: The structure of the novel crosslinking monomer that was used in OMNiMIP approach.

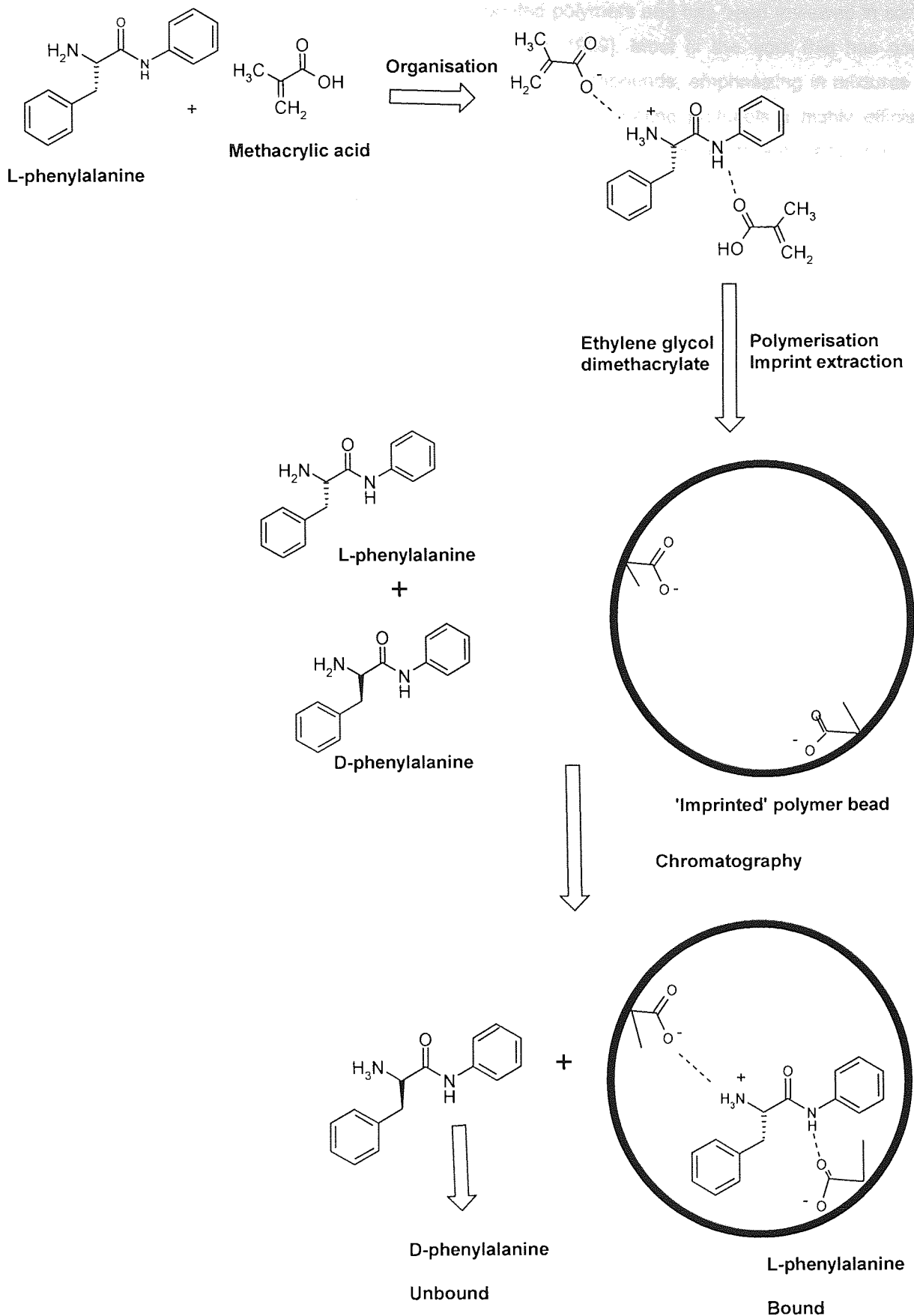
The binding and the selectivity scope of the polymers formulated with NOBE was compared with polymers imprinted with the traditionally used MIP formulation EGDMA/MAA. The results showed the OMNiMIP approach using NOBE exhibited improved or similar results for enantioselective recognition in organic and aqueous media in comparison to the traditionally used MIP. The origin of the improved molecular recognition observed in organic media was due to the hydrogen bonding interaction. The amide functionality in the cross-linker NOBE interacts adequately with most templates containing more than one functional group capable of forming hydrogen bonds with the amide group in NOBE with the exception of amines. The low selectivity for amine templates by the NOBE MIPs was presumably due to the weak hydrogen-bonding interactions of amine groups with the amide group on NOBE. Furthermore, incorporation of another functional monomer into the polymeric network of NOBE tends to interfere with good binding site interactions giving as a result MIPs with lower selectivity.

Moreover, a cross-linking monomer derived from an L-asparatic acid was also reported from the same group [Spivak, 2001]. The molecularly imprinted polymer formulated with L-asparatic acid derived monomer mimics more closely the scaffolding of proteins, and thus provided more protein-like selectivity. Chromatographic results revealed a more than seven-fold improvement in polymers imprinted using the new monomer versus a traditionally formulated polymer imprinted with methacrylic acid as the functional monomer.

Another example of this class of monomers is the 2,6-bis(acrylamido)pyridine **99** (Figure 5.15). This monomer incorporates a donor-acceptor-donor motif that mimics interactions found in DNA via multiple hydrogen bonds for binding the template [Kubo *et al*, 2003 see Section 5.17.]. This study indicated that the crosslinkers can also serve as the complexing functionality required to form the pre-polymerisation complex and provide affinity for the template.

5.16 Applications of MIP technology

Molecular imprinted polymers have been investigated for a number of applications since their conception. The specificity of these imprinted networks is sufficiently high and due to their advantages in term of ease of preparation, cost and durability they have established for a variety of novel applications:



Scheme 5.9: Use of the imprinted polymer as a chromatographic resin to preferentially achieve the enantiomeric selection of L-phenylalanine from a racemic mixture of L- and D-phenylalanine [Søllergren, 1994]

The use of MIPs as a stationary phase for analytical chromatographic and electrophoretic separation is by far the most extensively studied application of printed polymers and has been reviewed in some excellent literatures [Kempe and Mosbach, 1995; Remcho, 1999]. Most of the work that has been performed with MIPs has been focused on the separation of compounds, emphasizing in mixtures of racemate [Kempe and Mosbach, 1995]. Using self-assembly imprinting protocols a highly efficient chirally discriminating phase may be produced (**Scheme 5.9**). For example, there are many drugs on the market which are optically active, about 90% of these are administered as racemic mixtures. The official authorities concerning drug preparation and administration (Food and Drugs Agency) requires that for optically active drugs both enantiomers must be treated as separate substances in pharmacokinetic and toxicology profiling. Therefore, there is a great need for preparative methods of enantiomer separations. This approach has been applied for a variety of separations, for example, amino acids and peptides [Andersson, *et al.* 1990; Sellergren and Shea, 1993; Mayes and Mosbach 1996; Kempe, 1993] nucleotide bases [Shea, 1993], drugs [Fischer *et al.* 1991; Haginaka *et al.* 1998; Ramstrom and Mosbach, 1996], sugars [Wulff and Minarik, 1990; Mayes *et al.* 1994, Nilsson *et al.* 1995; Kugimiya *et al.*, 1996], and steroids [Ramstrom *et al.*, 1998; 1996; Sreenivasan, 1998; Asanuma *et al.* 1997].

Characteristic of these materials is the elution order of the enantiomers, only depending on which enantiomeric form was used in as print molecule. For instance, when the L-enantiomer is used as template, the D-form will be eluted first and vice versa if the D-enantiomer is used as the template.

5.16.2 Solid Phase Extraction

The high affinity and selectivity of MIPs can be exploited in solid phase extraction, where these polymers find application in the selective extraction, preconcentration and clean-up of analytes prior to further analysis such as HPLC or LC-MS. The basic concept for the application of the MIPs in solid-phase extraction (MISPE) is that the chromatographic parameters are tuned such that the MISPE column traps only the analytes, or a group of structurally related compounds, whereas the other interfering compounds in the sample mixture were washed without retention. The first molecularly imprinted polymer used for solid phase extraction was reported by Sellergren in 1994 [Sellergren, 1994]. The high selectivity of the polymer allowed pentamidine (a drug used to treat AIDS-related pneumonia) to be sufficiently enriched even when present in low concentration in a diluted human urine sample.

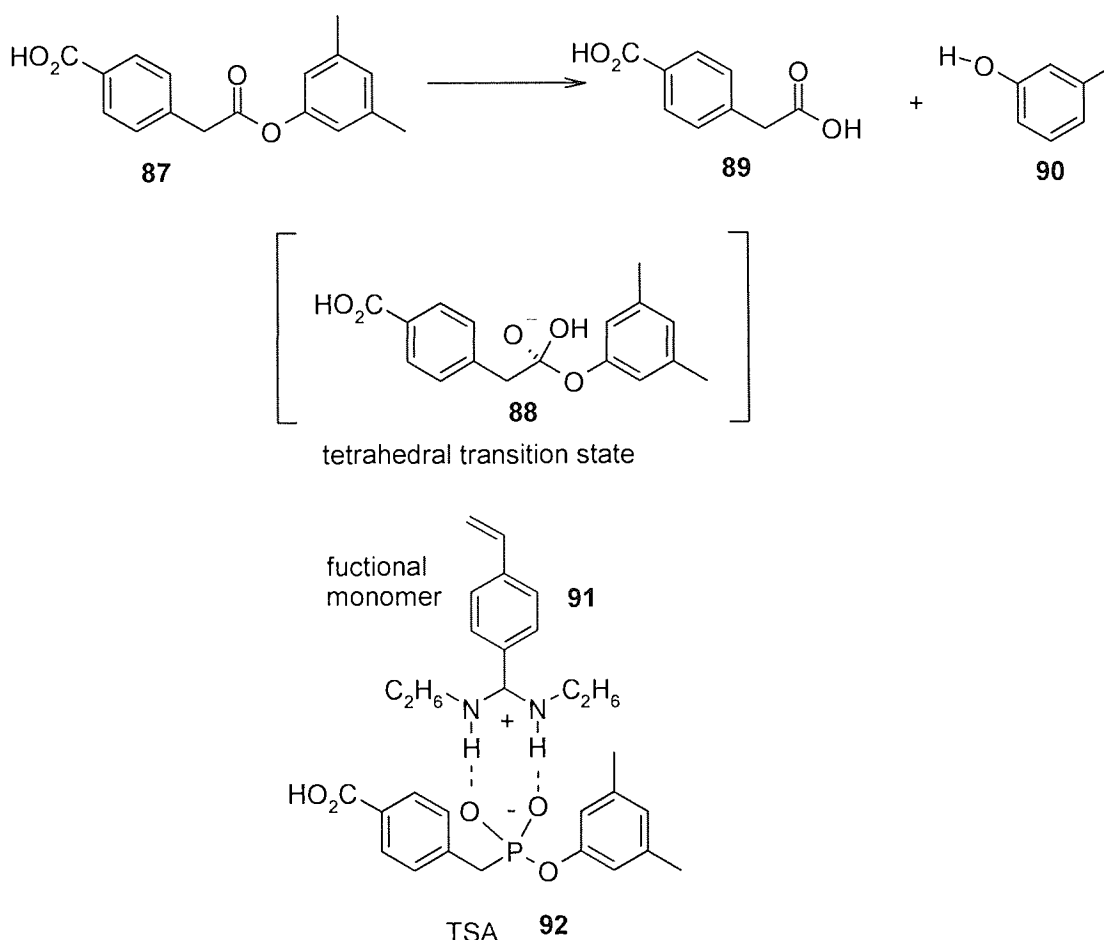
The application of MIP cross-reactivity has also been exploited in the extraction of given classes of pharmaceutically active compounds from decoction of plant materials. The flavonoids quercetin and kaempferol have been extracted from *Ginkgo biloba* leaves using a quercetin imprinted polymer [Jianchun, *et al.* 2001]. The polymer showed good affinity for structural analogues of the template and demonstrated the possibility of using polymer to extract a given class of pharmacologically active compounds.

5.16.3 Imprinted polymers as enzyme mimics

MIPs have also been used as catalysts and enzyme mimics. Based on the mechanism of enzymatic catalysis, several requisites must be fulfilled in order to obtain a synthetic material showing enzyme-

like behaviour. These requisites include the presence of a cavity with the shape of the substrate or the transition state of the reaction, and the functional groups that act as binding sites, coenzyme analogues or catalytic groups within the cavity in a defined stereochemistry [Wulff, 2002].

Two different imprinting methodologies have been used to synthesise enzyme mimics: (I) imprinting of the substrate or product analogue and (II) imprinting with a transition state analogue (TSA). Imprinting of the substrate or product analogue essentially produces a cavity to be used as a micro-reactor for regio- and stereoselective reaction; remarkable results have been obtained using this approach. In contrast, if imprints are prepared against transition state analogues, the MIP will stabilize the transition state and resulting enhanced catalytic rates. MIPs using a TSA as the print molecule have made use of different types of binding site interactions to create a catalytic site. These binding interactions include non-covalent, covalent, stoichiometric non-covalent and metal coordination for bond formation [Motherwell *et al.*, 2001].



Scheme 5.10: Phosphonic monoesters mimics of the transition state of ester hydrolysis [Wulff *et al.*, 1997].

However, artificial catalysts prepared using the molecular imprinting approach showed only limited catalytic activity compared to native enzyme. Wulff and co-workers, recognized that TSA binding alone was not enough to confer catalytic activity. They designed their system to contain an appropriately positioned amidine catalytic group **91** (Scheme 5.10) [Wulff, *et al.*, 1997]. This group mimics the active arginine residue in the catalytic antibody equivalent and was shown to bind strongly to phosphonic acid monoesters such as the TSA (**92**). Phosphonic monoesters such as **92** are well established

mimics of the transition state of ester hydrolysis representing the tetrahedral geometry of the ester intermediate **88**. The MIPs formed with **91** as imprint molecule caused a 100 fold rate acceleration of the hydrolysis of ester **87** with typical Michaelis-Menten kinetics.

5.16.4 Drug Development

The rational approach to drug design has been used to generate candidate species able to act as inhibitors of the proteinase kallikrein (see **Section 5.4**).

5.16.5 Antibody receptor binding mimics

Over the last few years, several studies have demonstrated that molecularly imprinted polymers can serve as artificial binding mimics of natural antibodies and can be used as recognition elements in immunoassay-type analyses. The polymeric nature of molecularly imprinted polymers results in several advantages over natural antibodies. For instance, the physical and chemical resistance of imprinted polymers leads to the possibility of sterilising the polymers, the high durability ensures a high stability of the recognition properties, and the production cost is considerably lower. Another advantage is the obviation of the need for host animals in the antibody production.

To detect the assay product it is usually necessary to use a label which is attached either to the antibody or antigen. This label can be fluorescent, luminescent, radioactive, an enzyme or an electrochemically active group. Although immunoassays can be used for the quantitative detection of extremely small amounts of analytes in complex samples mixture, they are quite time consuming to perform. Parallel to this development, the technique of molecular imprinting has emerged, which provides synthetic polymers with specific binding properties.

The first molecularly imprinted absorbent assay (MIA) was based on a competitive radioligand-binding measurement. This format is analogous to solid-phase radio immunoassay, except that the immobilised antibody is replaced by a molecularly imprinted polymer [Vlatakis 1993]. MIPs made against theophylline and diazepam showed strong binding and cross reactivity profiles similar to those of antibodies. The sensitivity and accuracy was comparable to the result obtained by a traditional radioimmunoassay technique. Other assays developed later have used the same principle, for example, Haupt 1998 prepared a MIA for the herbicide, 2,4-dichlorophenoxyacetic acid and so forth. However, these radio assays involved the handling of radioactive materials and produce radioactive waste, which led to the development of other assays based on other labelling and detection methods. Piletsky and co-worker reported fluorescence label where as Haupt, 1998 and Kroger, 1999 employed electrochemical probes for detection. MIPs have been also used in ELISA-type assays where the analyte was labelled with an enzyme peroxidase and was detected by colorimetric and chemiluminescence. In the ELISA type assays the use of enzyme-labelled template is less practical in MIP assays for two reasons: primarily due the enzyme only functioning in aqueous buffer, where as most of the MIPs function in organic solvents: secondly, the accessibility of the template to the binding

site can be affected due to the hydrophobic nature of the MIPs and enzyme labels are large in size compare to the template.

Furthermore, Piletsky and co-worker [Piletsky, 2001] have reported a new technique that involved coating microtitre plates with MIPs. The MIPs synthesised were specific for low molecular weight analytes such atrazine, epinephrine and proteins. The MIPs were prepared by oxidation polymerisation in the presence of a template molecule.

3-aminophenylboronic acid, 3-thiopheneboronic acid and aniline were polymerised in water. Then the MIPs were finally grafted onto the polystyrene surface of the microplates. These MIP-coating generated antibody-like binding properties and served an alternative to conventional antibodies or receptors that are employed in ELISA.

3.16.6 Sensors

The possibility to detect the binding between an analyte and an MIP by transduction into a specific signal has led to the development of MIP sensors. They exhibit good specificity for various compounds of medical, environmental and industrial interest. Their recognition properties are unaffected by acid, base, heat or organic phase treatment. Detection methods include measurement of mass change, field-effect capacitance or conductivity, luminescence and fluorescence.

Upon binding, the transducer translates the chemical event into a quantifiable output signal. When the analyte interacts with the recognition element, a change in one or more physicochemical parameters associated with the interaction occurs. This change may produce ions, electrons, gases, heat, mass changes, or light, and the transducer converts these parameters into an electrical output signal that can be amplified, processed and displayed in a suitable form.

The type of molecular recognition reaction determines the form of the transducer used. For example, enzymatic reactions often involve an electron transfer. This electrical activity can be measured with *amperometric*, *potentiometric* or *conductometric* sensors. If the bioreaction includes the generation of H^+ or OH^- ions, then a pH sensitive dye in combination with an optical device can be used. For antibody-antigen binding, the mass change on the surface of the transducer can be detected with a piezoelectric device. Exothermic or endothermic reactions can be followed with temperature sensors.

Moreover, MIP sensors have also been designed on the basis that the analyte itself carries a specific property such as fluorescence [Kriz *et al*, 1995; Dickert 1999] or electrochemical activity [Kriz, 1995]. Kriz and co-worker reported using an optical-fibre-like device in which a fluorescent amino acid derivative (dansyl-L-phenylalanine) binds to the polymer particles, resulting in fluorescent signals that vary as the function of the concentration of the derivative (**Figure 5.11**). Chiral selectivity was shown by using the corresponding D-enantiomer as a control. However, the response was dependent on concentration, and enantiomeric form was slow, hence this approach is only suitable for naturally fluorescent analytes. If the analyte lacks such property, a competitive or displacement sensor format may be used. Turner and co-workers, have developed a voltametric sensor for the herbicide 2,4-dichlorophenoxyacetic acid [Kroger, 1999] where the electroactive compound 2,5-dihydroxyphenylacetic acid was used as a probe.

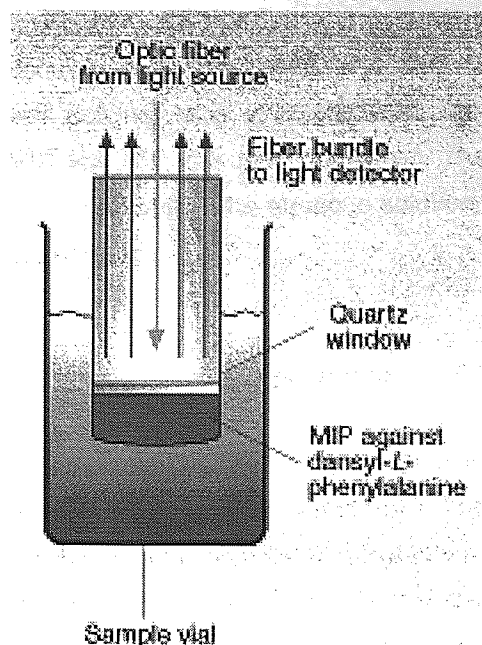


Figure 5.11: Biomimetic sensor in which an MIP selective for the fluorescently labelled amino acid dansyl-L-phenylalanine was applied as a layer on the tip of the fibre-optic sensing device [Kirz *et al* 1995]

A similar approach was preceded by Levi [Levi *et al.*, 1997] where the sensors have also been prepared on the basis of competitive displacement where fluorescence and HPLC were used as detecting systems for chloramphenicol. Here a competitive displacement of a chloramphenicol-methyl red (CAP-MR) dye conjugate from specific binding cavities in an imprinted polymer by the analyte was performed and the HPLC with a mobile phase containing CAP-MR were used as the detection system. In the same manner, Liao and co-workers [Liao *et al* 1999] synthesised a fluorescent sensor for L-tryptophan by using a fluorescent functional monomer (FFM). The sensor's dansyl moiety however had low sensitivity to the binding event. This led researchers to use an external quencher (p-nitrobenzaldehyde) to study binding of the fluorescent polymer. Displacement of the quencher from the binding cavities by L-tryptophan caused a concentration dependent change in fluorescence and therefore counteracted the problem successfully.

Rachkov *et al* 2000 reported development of a fluorescence sensing system to determine β -estradiol (an intrinsically fluorescent template) by combining MIPs with HPLC whereas Diaz-Garcia (2000) prepared a selective MIP for 3-hydroxyflavone (flavonol-afluorescence template) by using the non-covalent imprint approach.

Recently, He and co workers [He *et al*, 2005] have proposed molecular imprinting-chemiluminescence (CL) method to determine the analyte directly in complicated samples. In their study, the trimethoprim-imprinted polymer was prepared by using methacrylic acid (MAA) as functional monomer and ethylene glycol dimethacrylate (EGDMA) as cross-linker in the presence of a template molecule of trimethoprim. The trimethoprim-imprinted polymer was used as the molecular recognition material and the CL reaction of trimethoprim with potassium permanganate in acidic medium was used as the detection system. In the process, the MIP was packed into a glass column and was connected into the flow CL system for the selective and temporary adsorption of trimethoprim. The combined stream of acidic potassium permanganate solution and sodium hyposulfite solution was then flowed through the

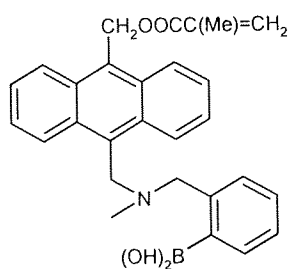
MIP column and reacted with trimethoprim adsorbed on the polymer to generate CL. During the CL reaction, the trimethoprim molecules were destroyed and the cavities were left for a new determination. The non imprinted polymer was also prepared using the same procedure. The adsorption performance of the MIP and NIP was then compared. The results showed that both the MIP and the NIP can adsorb the trimethoprim in the aqueous solution, but the adsorption capacity of the MIP was higher than that of the NIP.

5.17 Fluorescent molecularly imprinted polymers

The incorporation of the signalling system into the polymer structure has also been developed. Fluorescent molecularly imprinted polymers have the benefit of a fluorophore in their cavities which may respond to the presence of bound test compound by a change in the fluorescence output. Another advantage of using fluorescent imprinting polymers is that lower template loading is required. This can be very important when the template is expensive or has been prepared at small quantities.

In 1998, a fluorescent dye monomer was reported by Turkewitsch. This monomer was employed as an integral part of the recognition cavity and served as the recognition element as well as measuring element for the detection of cAMP in aqueous media. The fluorescence of the MIP quenched in the presence of the template cAMP, but no effect was observed in the presence of structurally similar molecule, cGMP [Turkewitsch *et al*, 1999].

Similarly, Wang and co-workers reported the preparation of MIP-based fluorescent sensor for D-fructose based on the covalent interaction of boric acid containing anthracene derivative with a *cis*-diol (**93**, Figure 5.12). This approach resulted in fluorescence enhancement upon substrate binding to the MIP cavities via suppression of a fluorescence quenching mechanism [Wang *et al*, 1999].



Functional monomer (**93**)

Figure 5.12: Representation of the functional monomer (**93**) for D-fructose-boronic acid complex (Wang *et al*, 1999).

In another related approach, Matsui and co-workers have employed a metalloporphyrin based monomer **94** (Figure 5.13) as the recognition element for 9-ethylamine (9-EA). The resultant MIP showed fluorescence quenching if the template was rebound and the degree of the quenching depended on the concentration of 9-EA. The structurally related adenine and 4-aminopyridine mimicking a partial structure of 9-EA however showed higher rebinding than the template Matsui *et al* (2000).

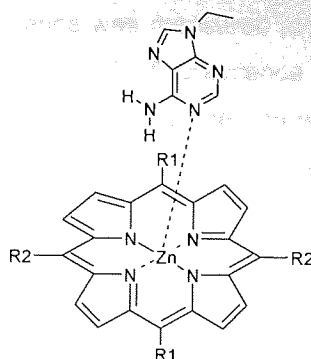


Figure 5.13: The structure of metallophorphyrine monomer (**94**)

A further work in the field of fluorescent sensors was carried out by Rathbone and co-workers [Rathbone *et al*, 2000]. In this study four fluorescent hydrogen-bonding monomers were synthesized (**Figure 5.14**) to prepare imprinted polymers that exhibited binding dependent fluorescence. Of the four polymers, **95** and **96** gave the larger fluorescent output.

In further study [Rathbone and Ge, 2001] FFM 3-acrylamidorhodanine **97** (**Figure 5.14**) was used to prepare fluorescent polymers imprinted with various *N*¹-benzylidene pyridine-2-carboxamidrazones which were evaluated for their recognition of the original template and cross-reactivity to similar molecules. Dramatic quenching of fluorescence approaching background level was observed for most cases where the 'empty' MIP was re-exposed to its template. Molecules that were large in size compared with the cavity could not enter the cavity and gave no reduction of fluorescence. A general trend that observed from their study was that relatively inflexible molecule such as the polycyclic aromatics were more easily discriminated against those more flexible alkoxy-substituted benzylidene compounds.

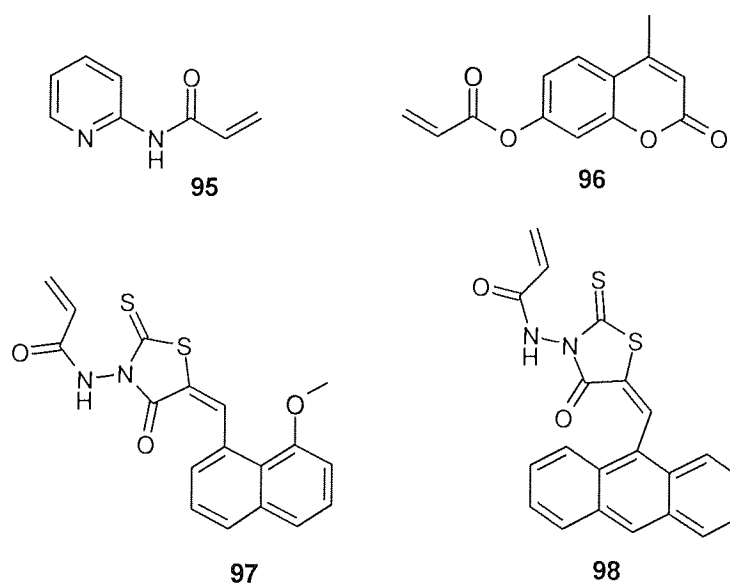


Figure 5.14: The structures of the fluorescence monomers [Rathbone, *et al* 2000]

In addition, a ratiometric approach was conveyed in this study, which was established to be more suitable for automated high-throughput screening. This approach offers a rapid analysis method where

no weighing was required. The fluorescence was measured at two wavelengths, one wavelength for which the polymer exhibits a totally non-specific fluorescence and the other wavelength exhibits a specific fluorescence for the template binding. Finally, the non-specific and specific wavelengths were compared to the non-specific emission wavelengths i.e. the ratiometric approach.

A further example in development of fluorescence sensors was demonstrated by Kubo *et al* 2003. A multiple hydrogen bonding based fluorescent imprinted polymer for cyclobarbital was prepared with FFM 2,6-bis(acrylamido)pyridine (**99**, Figure 5.15).

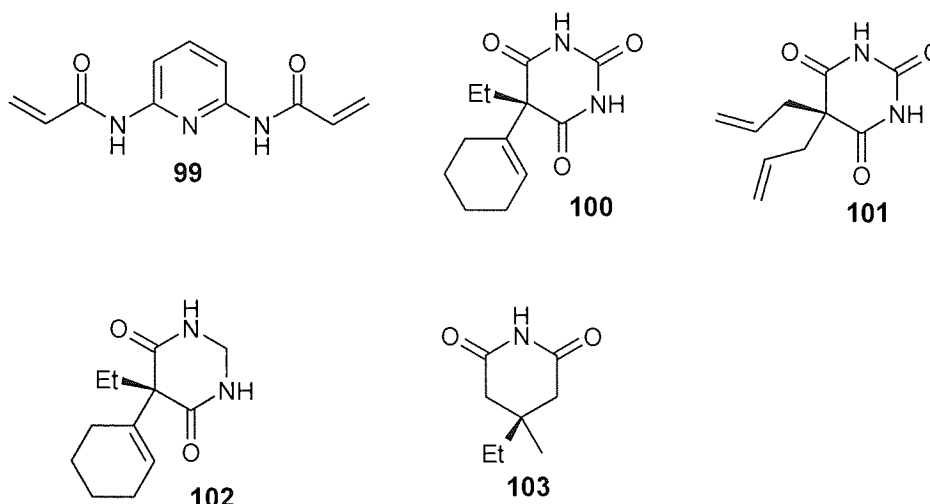


Figure 5.15: The structures of the FFM (**94**), template (**95**) and the test compounds (**96-98**).

The polymer showed not only selective binding of cyclobarbital but also enhancement of fluorescence intensity, suggesting that the polymer could be utilised as a selective fluorescence probe. This was shown by evaluating the polymer by chromatographically comparing the retention time of **100** (template) to structurally related compounds (**101-103**). The results from the chromatography and the fluorescence studies indicated that the more points of connection between the monomer and template, the stronger the interaction and more stable the complex formed [Kubo *et al*, 2003].

5.18 Conclusions

Molecular imprinting is a methodology used for the creation of selective recognition sites in synthetic polymers. Formation of a pre-polymerisation complex, between complementary monomers and the template molecule, followed by polymerisation in the presence of a crosslinker, in a porogenic environment, produces a molecularly imprinted polymer capable of specific molecular recognition. Subsequent removal of the imprint molecule by solvent extraction reveals binding sites that are complementary in size and shape to the analyte. In this way, a molecular memory is introduced into the polymer, which is now capable of rebinding the analyte with high selectivity. Advantages of molecularly imprinted polymers lie in the durability, low cost and ease of formation.

An anti-idiotypic imprints have been also developed which can use to act as a micro-reactor, i.e. the obtained cavities of original imprints can be used as moulds leading to generate analog of known drugs.

Two different approaches using covalent and non-covalent interactions for molecular imprinting have been developed. Of these two approaches, the non-covalent imprinting seem to be more efficient system for mimicking the interactions presents in nature (hydrogen bonding, electrostatic interactions etc.). Molecularly imprinted polymers are widely considered as potential alternatives to relatively unstable antibodies, receptors and enzymes. They have also been used in biosensors technology.

6.1 Preparation of polymers capable of recognising 2,4-diaminopyrimidines

As mentioned in chapter five, Mosbach and co-workers [Mosbach *et al* 2000, 2002] have developed an anti-idiotypic approach to generate analogs of known drugs with the need to create large combinatorial libraries of candidate structures. This approach requires two steps: (i) making an imprint of the template in the polymer i.e. micro-reactor, (ii) using the obtained cavities as molds leading to create new molecules (anti-idiotypic imprints or images of the original imprints). The resulting images would resemble the original imprint species in shape and functionality. The principle is schematically described in chapter five (**Section 5.5 schemes 5.2-5.3 and 5.5**).

A part of this work was to design and synthesise an imprinted polymer that would recognise the 2,4-diaminopyrimidine moiety. A functional monomer presenting a donor-acceptor hydrogen bonding array (see **Section 5.5.1**) was prepared and used in the preparation of molecularly imprinted polymers targeted towards 2,4-diaminopyrimidine. The molecularly imprinted polymers were prepared using the non covalent approach. As a follow up work, the binding cavity can be used to direct assembly of the reactants to give products mimicking the original template (see **Scheme 5.5**). The molecular recognition properties of the materials were investigated *via* fluorescence spectroscopy. The affinity of the proposed functional monomer for 2,4-diaminopyrimidine was investigated by ¹H-NMR monitored titrations using a model compound.

6.2 Preparation of Barbiturates

To investigate the feasibility of our plan, it was decided to perform reactions with the extensively studied compound pyrimidine-2,4,6-trione (**121**) (Barbituric acid). Barbituric acid is a pyrimidine derivative and it exists in several tautomeric forms including one with an aromatic ring (**Figure 6.1**). Its reaction with various aromatic aldehydes (**Table 6.1**) was carried out in ethanol under reflux in the presence of piperidine (**Scheme 6.1**). After workup of the reaction mixtures only a single product was isolated in each case. Barbiturates (**122**, **123** and **124**) bearing hydroxyl group were synthesized and employed in attempts to prepare polymerisable monomers that would be soluble in non-polar solvents.

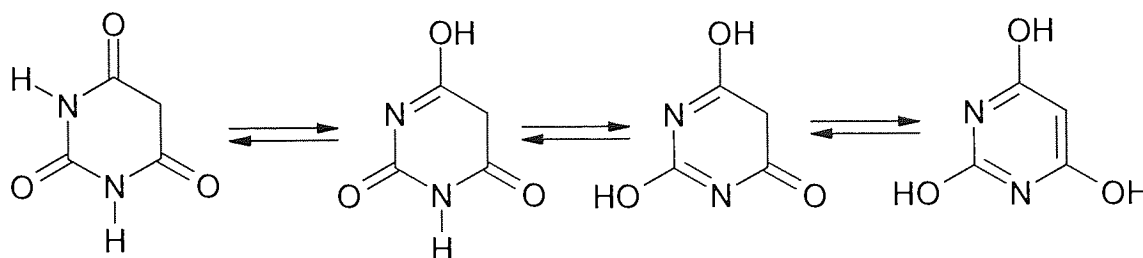
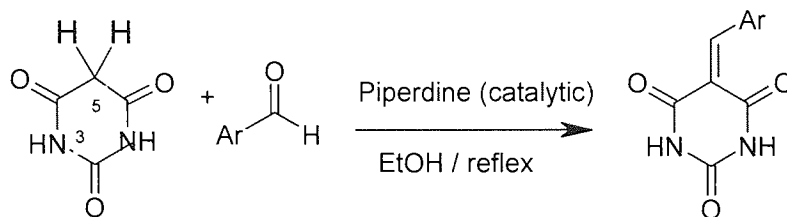


Figure 6.1: Structure of barbituric acid (**121**) and several tautomers

Synthetic routes are outlined in **Scheme 6.2-6.4**. Compounds (**125**, **126** and **127**) bearing anthryl, naphthyl and pyrene groups respectively were prepared in an attempt to derive a barbiturates that

would be soluble in non-polar solvent and because these groups are well known as fluorophores, they would be quite useful for recognition and selectivity studies in fluorescence spectroscopy. Compound (**128**, **129** and **130**) were prepared and used as model receptor for the substrate diaminopyrimidines in $^1\text{H-NMR}$ studies



Scheme 6.1: General procedure for preparation of pyrimidine-2,4,6-triones.

Table 6.1: Substituted aldehydes (Ar) used in Scheme 6.1

Compound	Ar	Compound	Ar
122		127	
123		128	
124		129	
125		130	
126			

The reaction (**scheme 8.1**) represents an example of a Knoevenagel condensation reaction. A Knoevenagel condensation is a nucleophilic addition of an active hydrogen compound to carbonyl group followed by an elimination reaction in which a molecule of water is lost (hence condensation). The products were conjugated pyrimidine-2,4,6-triones.

6.3 The interaction of Template and a Model Functional Monomer Monitored by $^1\text{H-NMR}$ Titrations

Proton NMR spectroscopy was used to study the interactions between the template and the functional monomer. Interactions between functional groups of the template and the functional monomer can result in chemical shift changes in the NMR spectrum [Selligren *et al*, 1988] and provides a convenient way to study the extent of monomer-template interactions. The observation of bond formation during self-assembly in solution aids in predicting the suitability of a functional monomer for association with a particular target species.

In the present study a simple $^1\text{H-NMR}$ titration experiment was performed to quickly identify the interaction/binding between the model functional monomer (**130**) to a template molecule trimethoprim (**70**) i.e. a 2,4-diaminopyrimidine. The template (**70**) molecule was capable of forming three interactions with a model receptor functional monomer (**130**), (Figure 6.2) similar to the Watson-Crick binding mode of guanine with cytosine found in the double helix of DNA (Figure 6.3). Deuterated THF was used as the solvent as these aromatic compounds were poorly soluble in other solvents. However, the compounds **128** and **129** were not employed in this study as they were not soluble in THF.

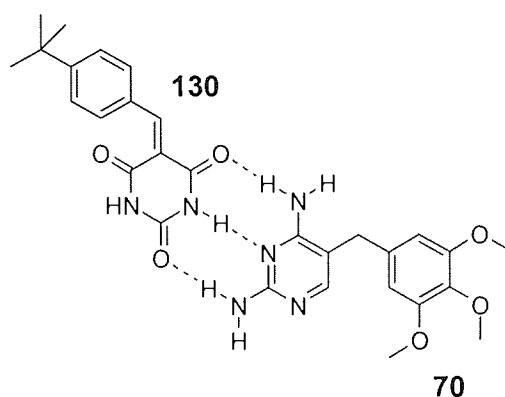


Figure 6.2: A model receptor (**130**) shown associated with trimethoprim (**70**)

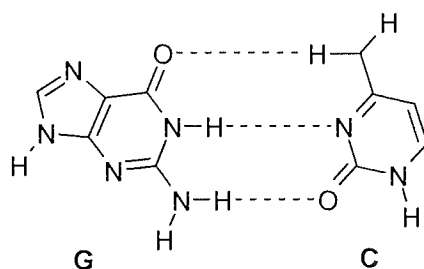


Figure 6.3: Watson-Crick binding mode between guanine and cytosine in the double helix of DNA

6.3.1 NMR titration studies

In the NMR titration study, measurements were performed at variable concentrations of one component **130** ranging from (0.0184 – 0.0015 mM) and at a fixed concentration of the other component **70**. The changes in NMR chemical shifts of independent signals were used to monitor

complex formation. Thus, the $^1\text{H-NMR}$ spectra were recorded and the chemical shifts of the significant protons were followed.

Prior to this, samples of 0.6 mL of the **70** containing 0.0086 mM and **130** containing 0.0184 mM in THF-D_8 were run on their own. The $^1\text{H-NMR}$ spectra revealed the expected peaks and the integration ratios **Figure 6.4 - 6.6**.

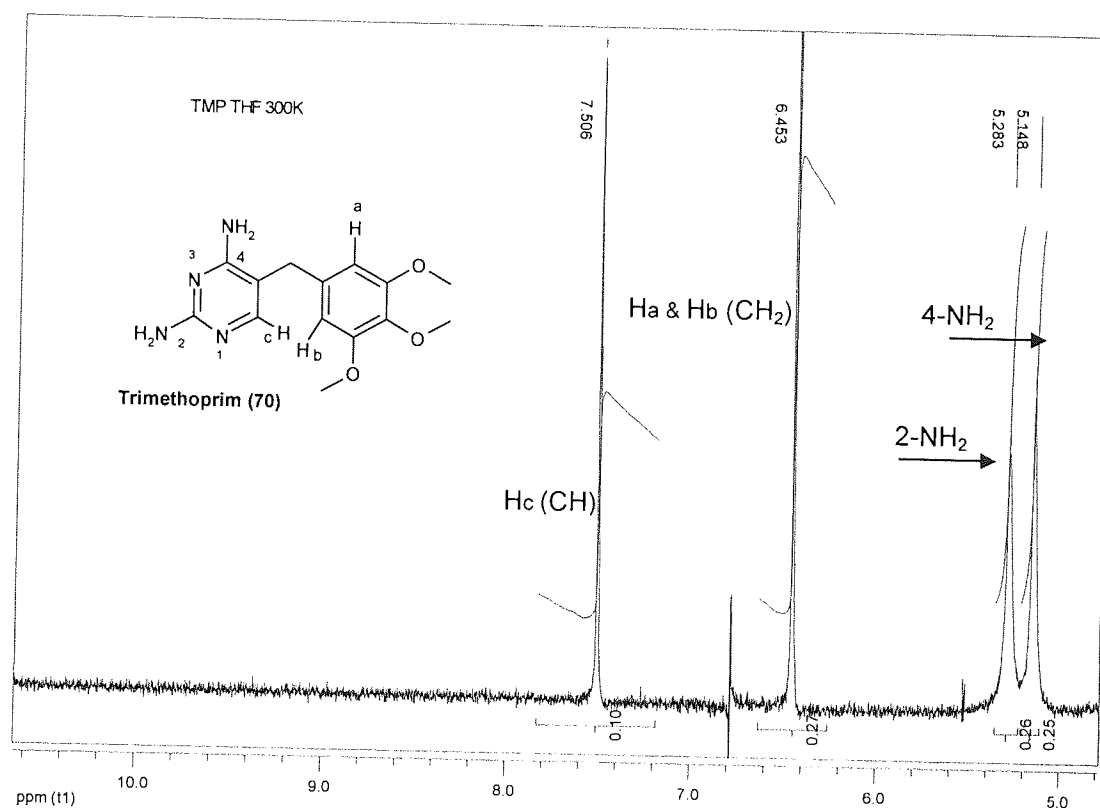


Figure 6.4: The $^1\text{H-NMR}$ spectrum of trimethoprim (TMP) on its own in $\text{D}_8\text{-THF}$ at 300K, along with the structural assignment. THE signals for 3 x (OCH_3) and (CH_2) are not shown in spectrum.

Figure 6.4 (above) shows the $^1\text{H-NMR}$ spectrum of TMP (**70**) in $\text{D}_8\text{-THF}$ at a concentration of 0.0086 mM acquired at 300K. The reference was set with the $\text{D}_8\text{-THF}$ peak at 3.580 ppm. Four signals are shown in the $^1\text{H-NMR}$ spectrum. The singlet at (7.506 ppm) corresponds to Hc proton of diaminopyrimidine ring and the singlets at (6.453 ppm) correspond to the aromatic protons of TMP. The two broad peaks at 5.283 and 5.15 ppm were assigned for the two amino groups.

Figure 6.5 (below) shows the $^1\text{H-NMR}$ spectrum of **130**. The two broad peaks at low field (10.420 ppm and 10.322 ppm) correspond to the amides NHs. A singlet at 8.371 ppm was assigned to H7 ($\text{C} = \text{CH}$). The two doublets at 8.238 ppm and 7.500 ppm were due to the aromatic protons of **130**. **Figure 6.6** (below) shows the superimposed spectra of **70** and **130**.

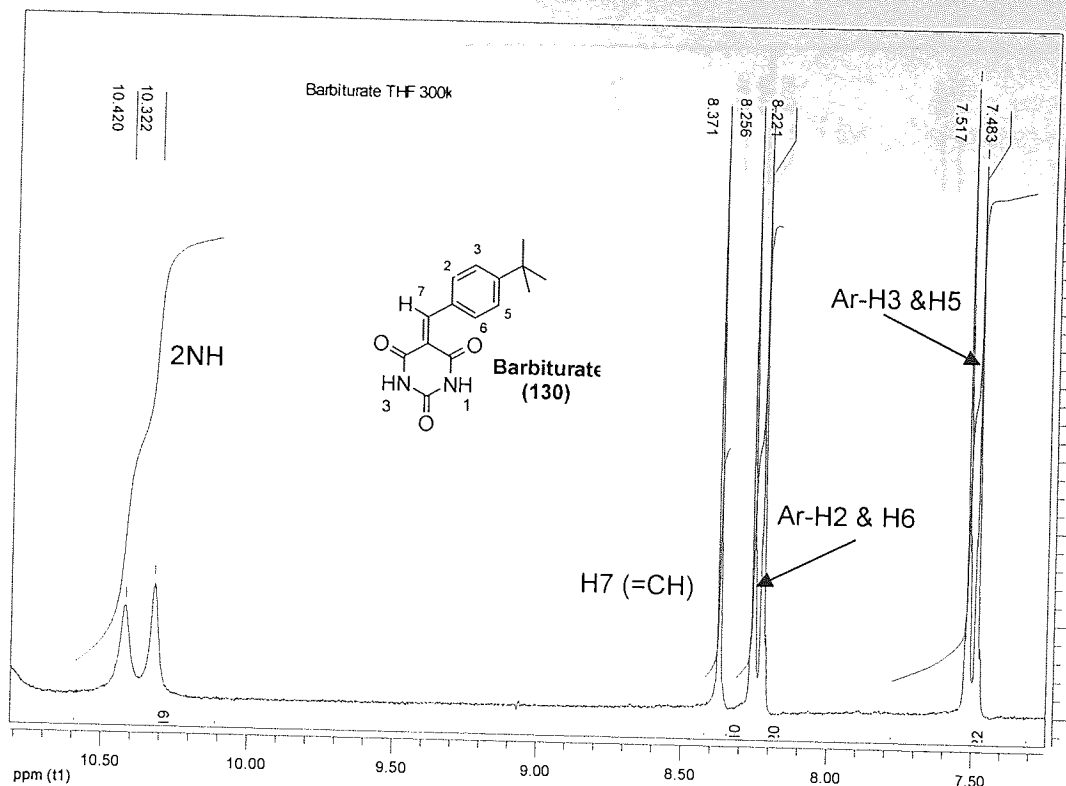


Figure 6.5: The $^1\text{H-NMR}$ spectrum of (130) on its own in $\text{D}_8\text{-THF}$ at 300K. The signal for the $\text{C}(\text{CH}_3)_3$ is not shown.

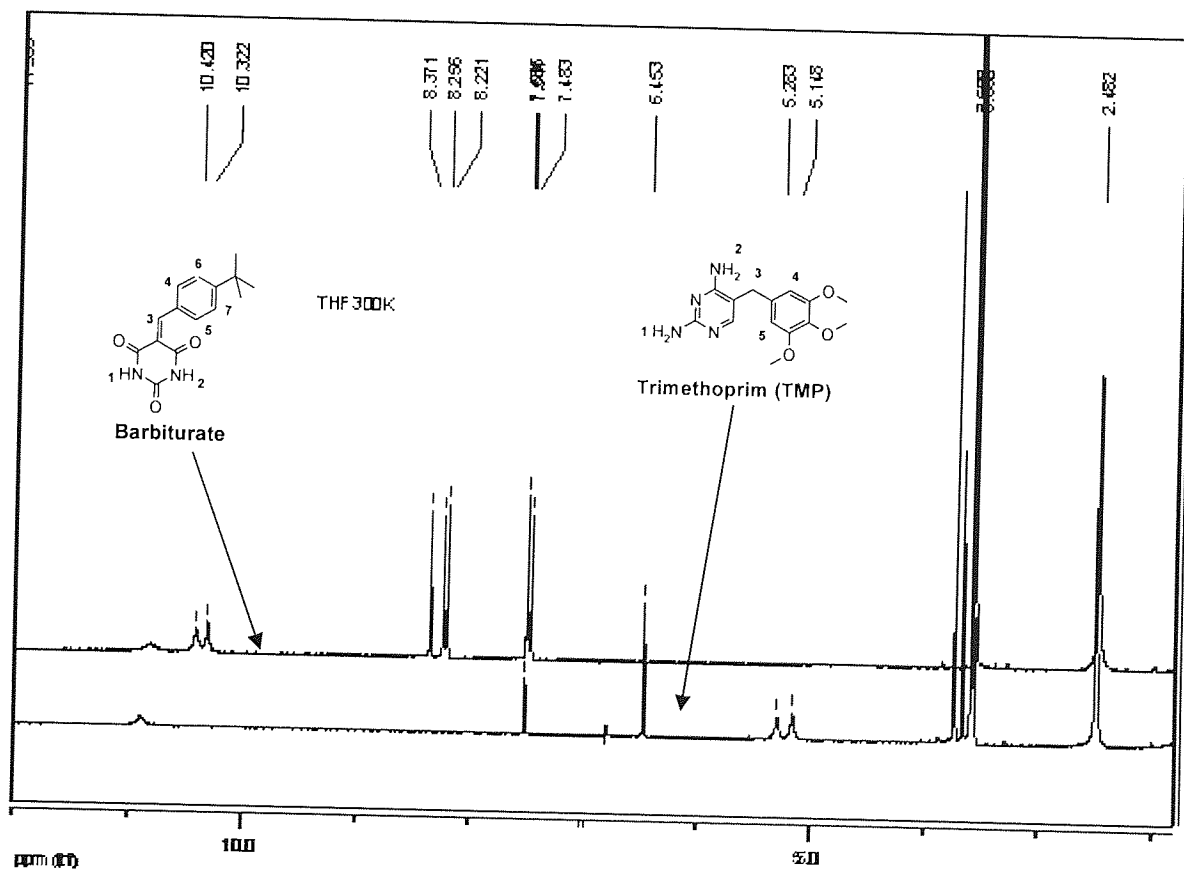


Figure 6.6: The $^1\text{H-NMR}$ spectra of (130) (0.0184 mM) and (70) (0.0086 mM) superimposed in $\text{D}_8\text{-THF}$ at 300K

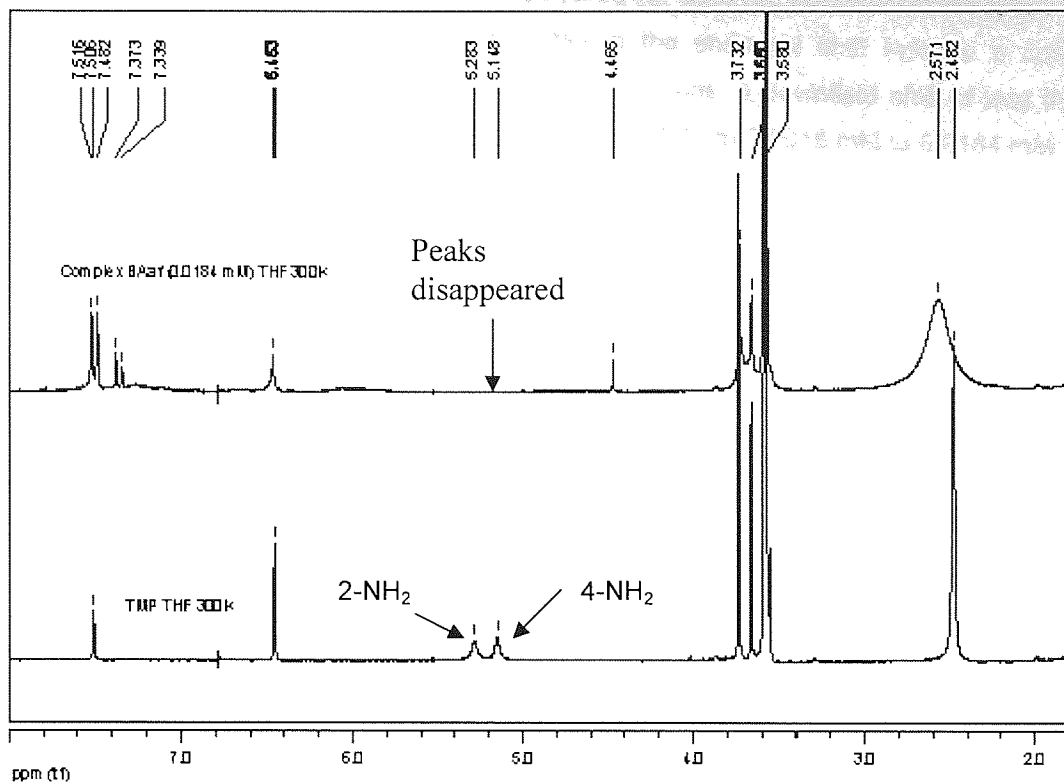


Figure 6.7: The $^1\text{H-NMR}$ spectrum of the complex formation between **(70)** (0.0086 mM) and **(130)** (0.0184 mM), superimposed on the $^1\text{H-NMR}$ spectrum of TMP **(70)** on its own.

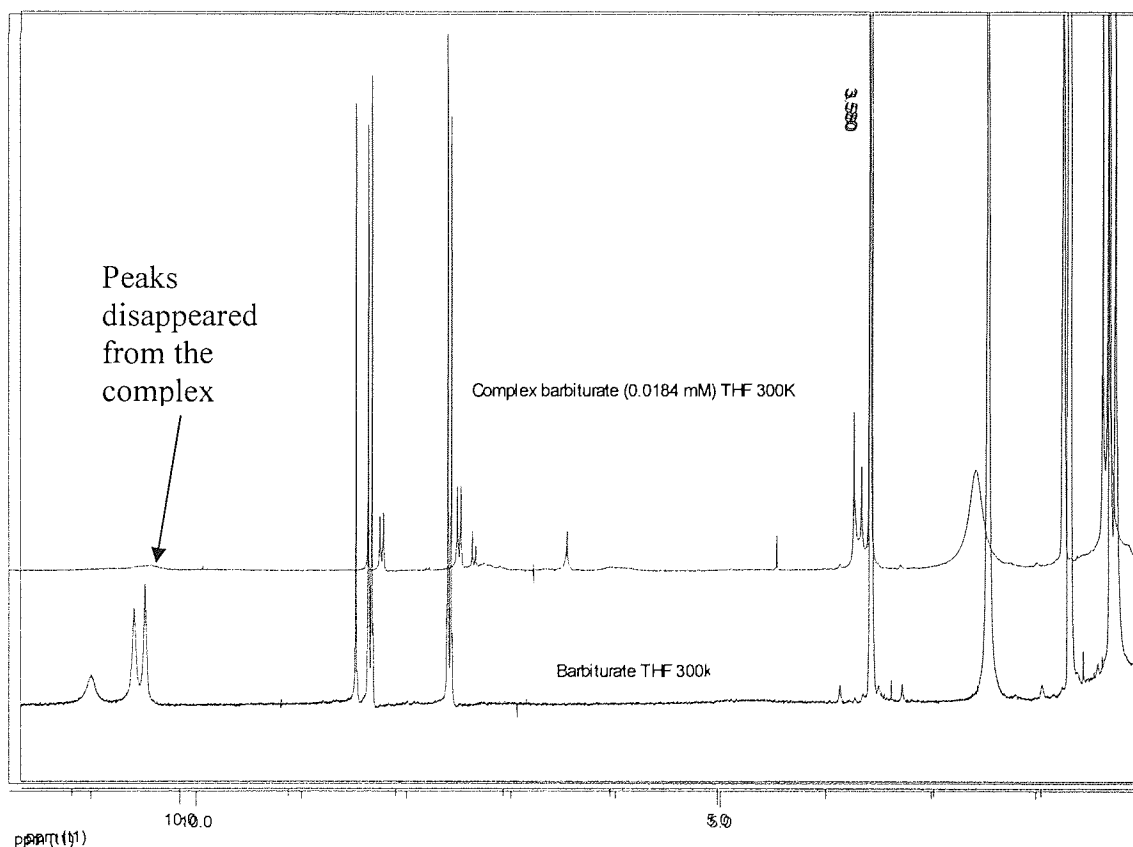


Figure 6.8: The $^1\text{H-NMR}$ spectrum of the complex formation between **(70)** (0.0086 mM) and **(130)** (0.0184 mM), superimposed on the $^1\text{H-NMR}$ spectrum of Barbiturate **(130)** on its own.

Figures 8.7 – 8.8 showed the large change in the chemical shifts of the amino protons on **70** with the addition of **130**. The amino protons of **70** (hydrogen donor) were shifted down field and the acidic

protons from **130** (hydrogen acceptor) were disappeared i.e. were not observed in the spectrum, as **70** was increasingly protonated. These large changes in the chemical shift indicate a considerable association between the **70** and **130**. For the aromatic protons, a downfield shift of less than 0.002 ppm was observed upon increasing **130** concentration of **130** from 0.0015 mM to 0.0184 mM.

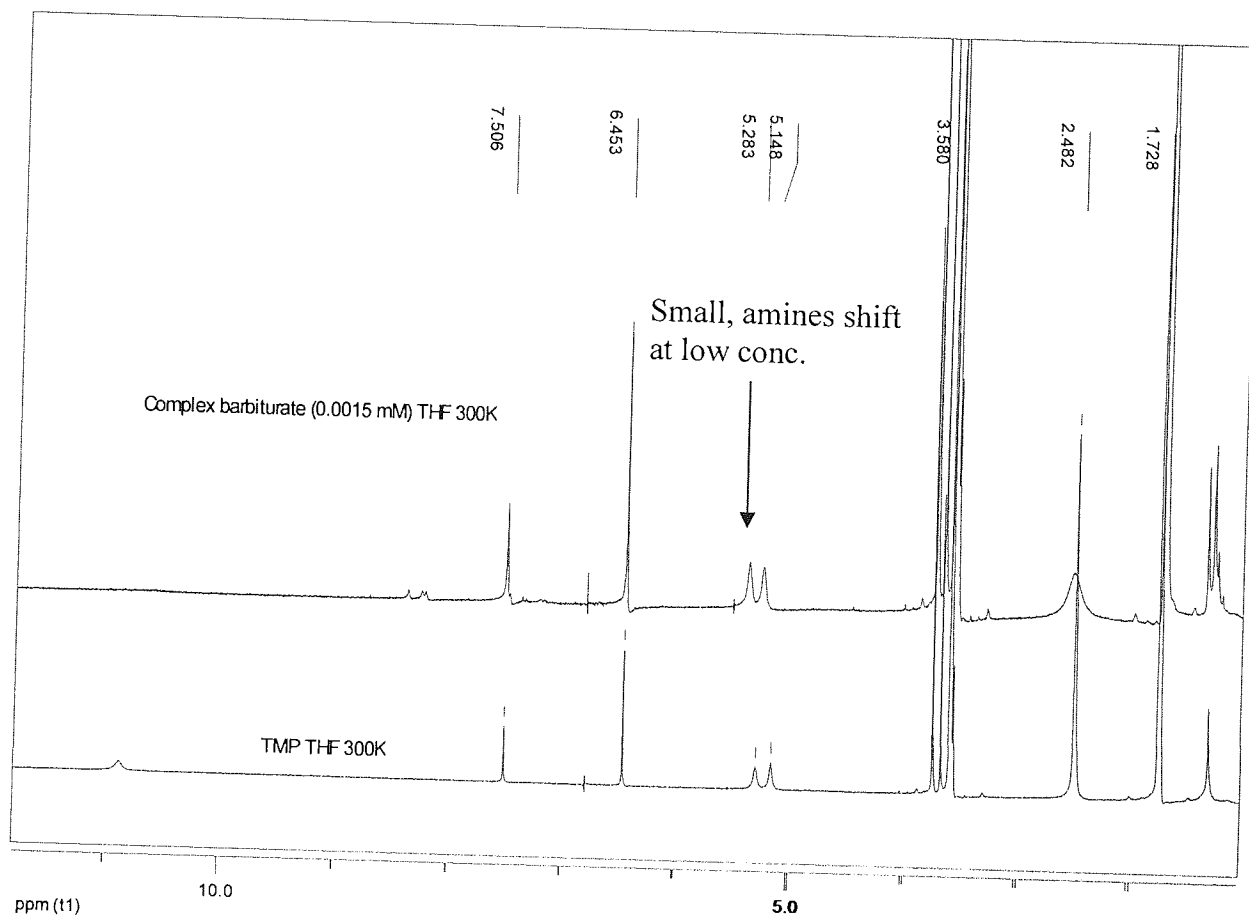


Figure 6.9: The ¹H-NMR spectrum of the complex formation between **70** (0.0086 mM) and **130** (0.0015 mM), superimposed on the ¹H-NMR spectrum of TMP (**70**).

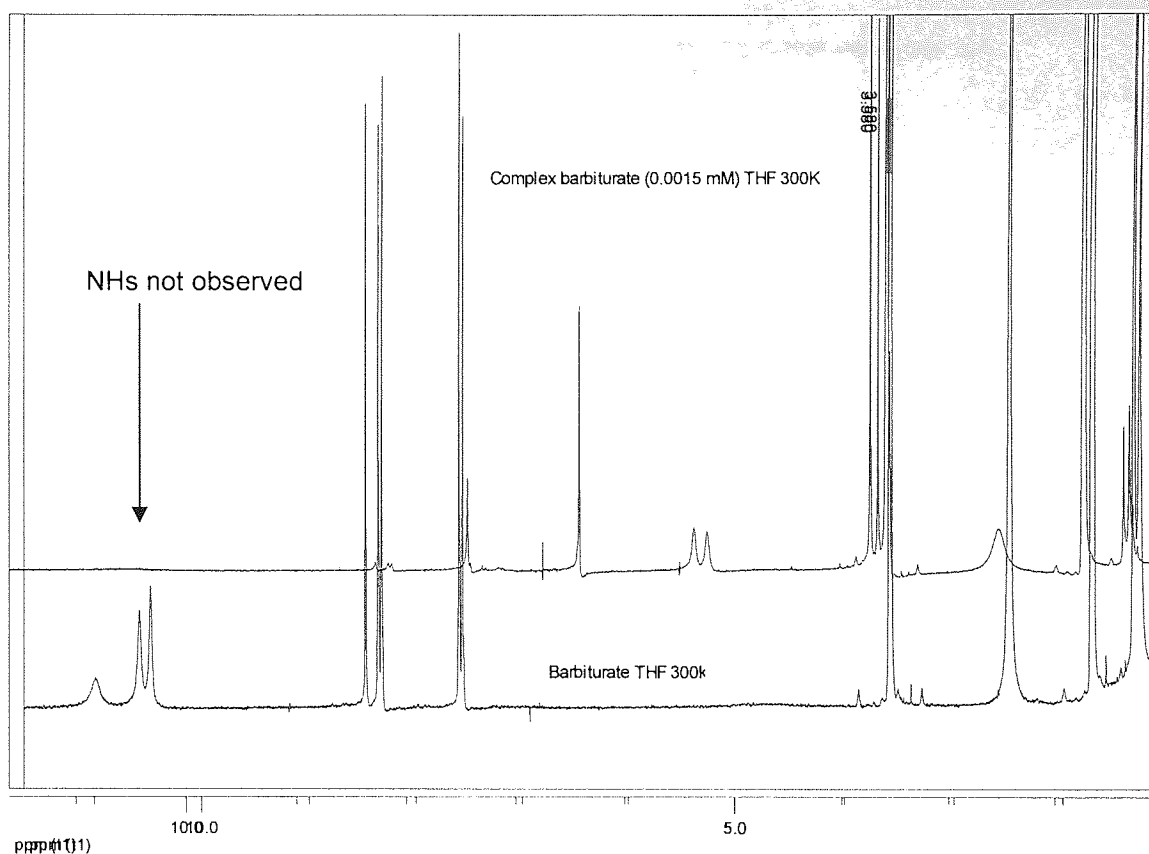


Figure 6.10: The ¹H-NMR spectrum of the complex formation between **70** (0.0086 mM) and **130** (0.0015 mM), superimposed on the ¹H-NMR spectrum of **130**.

Figures 8.9 – 8.10 indicated that as the concentration of **130** was decreased the changes in chemical shifts of amino groups of **70** and amide NHs of **130** were negligible. **Table 8.3** shows the complexation induced shifts of amino protons of **70** obtained in the titration of **70** with **130**.

Table 6.2: Complexation induce shifts from the NMR titration experiments.

Concentration of (70) mM	Concentration of (130) mM	2-NH ₂ Δδ (ppm)	4-NH ₂ Δδ (ppm)
0.0086	0.00	0.00	0.00
0.0086	0.0015	0.095	0.105
0.0086	0.0023	0.143	0.163
0.0086	0.0031	0.139	0.167
0.0086	0.0046	0.207	0.231
0.0086	0.0061	0.259	0.292
0.0086	0.0092	0.371	0.440
0.0086	0.0123	0.412	0.478
0.0086	0.0184	0.775	0.872

Complexation-induced shifts of the amino protons of TMP (**70**), (0.0086 mM) versus total concentration of **130** in THF

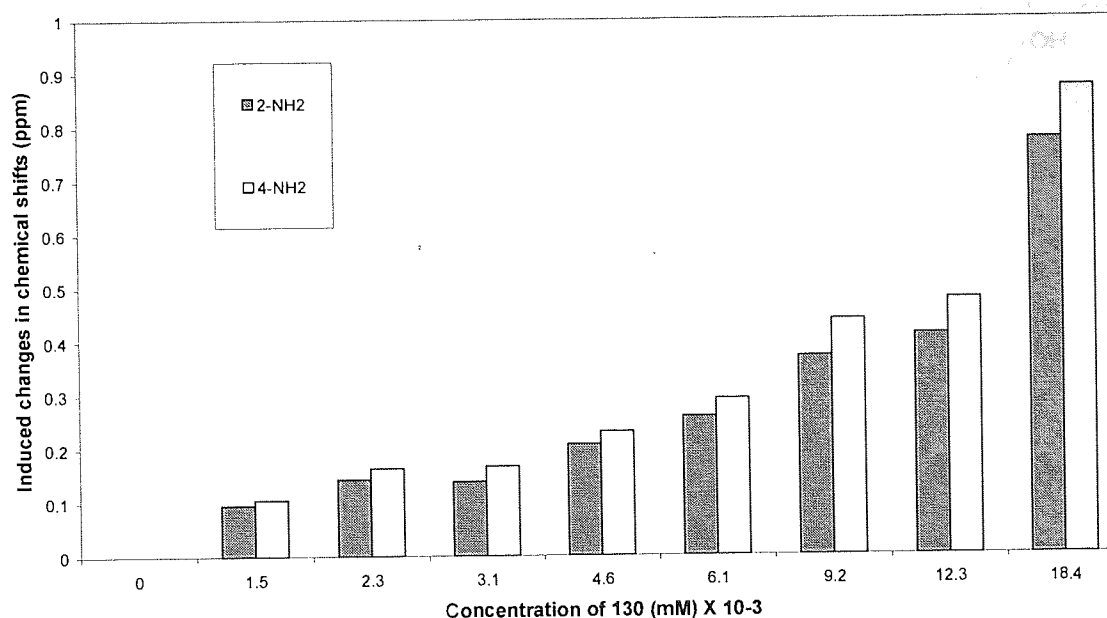


Figure 6.11: Complexation-induced shifts ($\Delta\delta$) of the amino protons of TMP (**70**), (0.0086 mM) versus total concentration of **130** in THF at 300K.

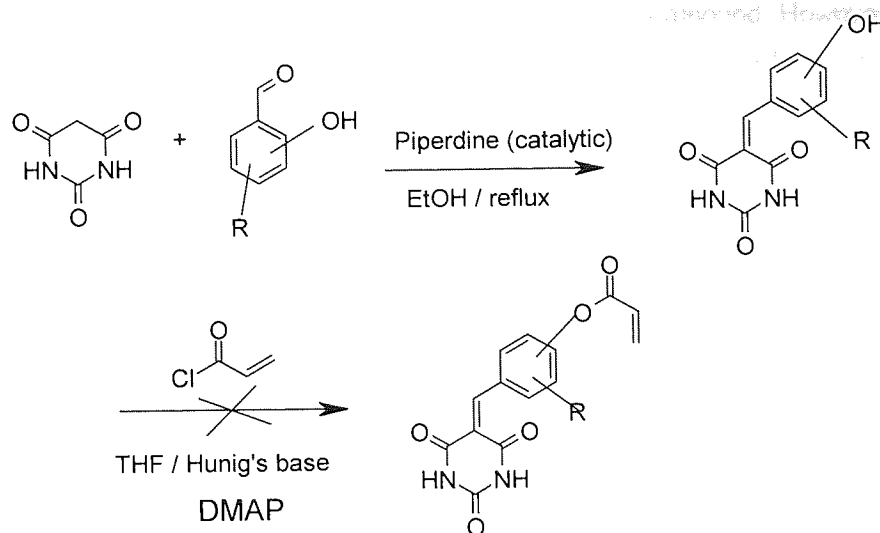
The ¹H-NMR study has demonstrated that the addition of **130** to a solution of **70** resulted in large down field shifts of both amino protons of the **70** Table 8.3, Figure 8.11 In general, the extent of the observed change of chemical shifts is proportional to the strength of the interactions. Thus this example of binding between the barbiturate (**130**) and 2,4-diaminopyrimidine (**70**) was a good indicator of its potential to pre-organise polymerisable barbiturates in a pre-polymerisation complex for molecular imprinting. The ¹H-NMR studies have also indicated that the proposed model receptor **130**, Figure 6.2 may form complexes with **70** via strong hydrogen bonds at three sites. The most stable of these was observed to involve the basic N3 nitrogen, leading to the larger shift of 4-NH₂ protons in contrast to 2-NH₂ protons.

6.4 Synthesis of a functional monomer for the recognition of 2,4-diaminopyrimidine.

6.4.1 Synthesis of acrylic acid 4-(2,4,6-trioxotetrahydropyrimidin-5-ylidenemethyl)phenyl ester (**85**).

Recognition of 2,4-diaminopyrimidine derivative was based on the barbiturate moiety with acceptor-donor-acceptor hydrogen bond triad. At the first instance, three barbiturate derivatives **122**, **123** and **124** bearing hydroxy groups were prepared (Section 6.2). The choice of the barbiturate to use was restricted due to solubility problem. These compounds were poorly soluble in non-polar solvents. Subsequent reaction of above barbiturates with acryloyl chloride in dry THF or DMF was unsuccessful on several occasions. The desired compound was neither identified by ¹H-NMR, nor by mass spectrometry. Usually one would expect that an acrylate ester would be prepared by the acylation of an alcohol with acryloyl chloride as portrayed in Scheme 6.2, but this was not the case in the present

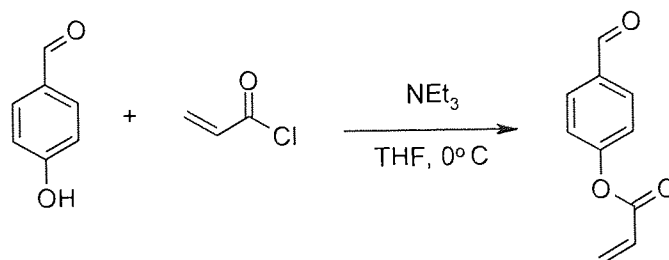
reaction. Acryloyl chloride was taken as a typical acyl chloride and was reacted with 5-(4-hydroxybenzylidene)pyrimidine-2,4,6-trione (**124**) under normal acylating conditions.



Scheme 6.2: Attempted synthesis of acrylic acid 4-(2,4,6-trioxotetrahydropyrimidin-5-ylidenemethyl)phenyl ester (**85**).

For example, **124** was treated with acryloyl chloride (**131**) in the presence of N,N-diisopropyl ethylamine (Hunig's base) or triethylamine and a catalytic amount of DMAP (4-(Dimethyl amino)pyridine) in dry THF or DMF. The reaction mixture was poured onto cold stirred water and the resultant solid was filtered and dried under high vacuum. Analysis of the resulting solids showed no assignable peaks by $^1\text{H-NMR}$ spectroscopy or mass spectrometry. Several attempts to purify the product by chromatography or the solvent extraction were failed. No desired product was isolated. It is possible that the product may have been polymerised since a broad peak was observed in $^1\text{H-NMR}$ spectrum.

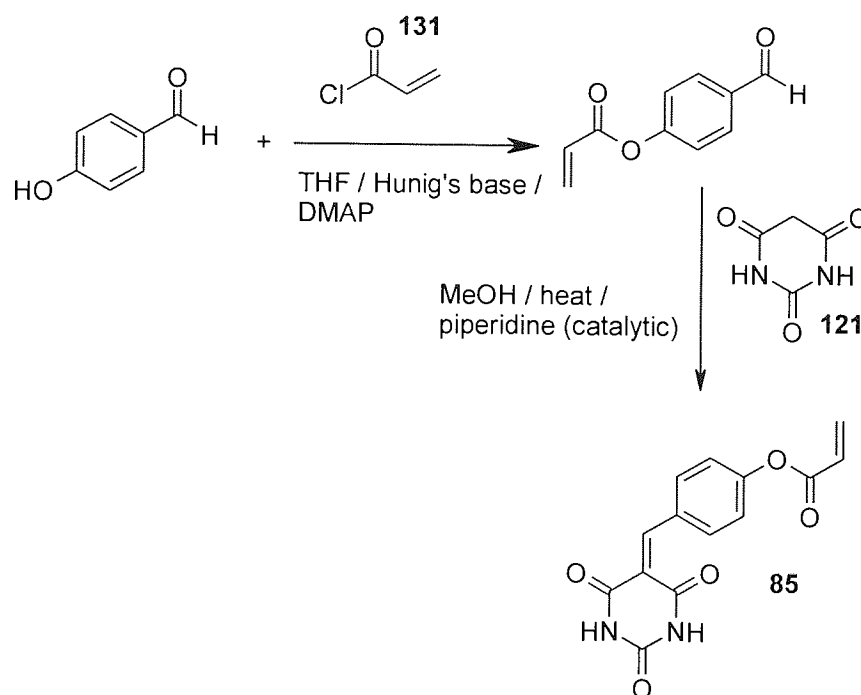
Neither of these outlined attempts worked. Due to this drawback an alternative method was attempted (**Scheme 6.3**). The synthetic sequence was reversed. 4-hydroxybenzaldehyde was acrylated instead of 5-(4-hydroxybenzylidene)pyrimidine-2,4,6-trione (**124**). The reaction was proceeded according to **Scheme 8.3**. Unfortunately, upon several attempts, the desired compound have not been isolated.



Scheme 8.3: Attempted synthesis of acrylic acid 4-formylphenyl ester.

It was then considered, to employ an alternative route (**Scheme 6.4**). In this reaction the Hunig's base and a catalytic amount of dmap was added to a solution of 4-hydroxybenzaldehyde and acryloyl

chloride in dry THF under argon. The reaction was stirred at 0°C with constant monitoring by TLC. The crude product generated *in situ* was stirred with barbituric acid and catalytic amount of piperidine in methanol at 50 0°C. The resulting product was collected by filtration and washed with cold EtOAc. The ¹H-NMR analysis indicated that this product was not the desired compound. However, the remaining filtrate was evaporated under vacuum at ambient temperature to give a brown sticky liquid. The brown sticky liquid was stirred in ice cold water to gave the title compound as pale yellow solid (0.815g). The title compound was collected by filtration and stored below 5°C.

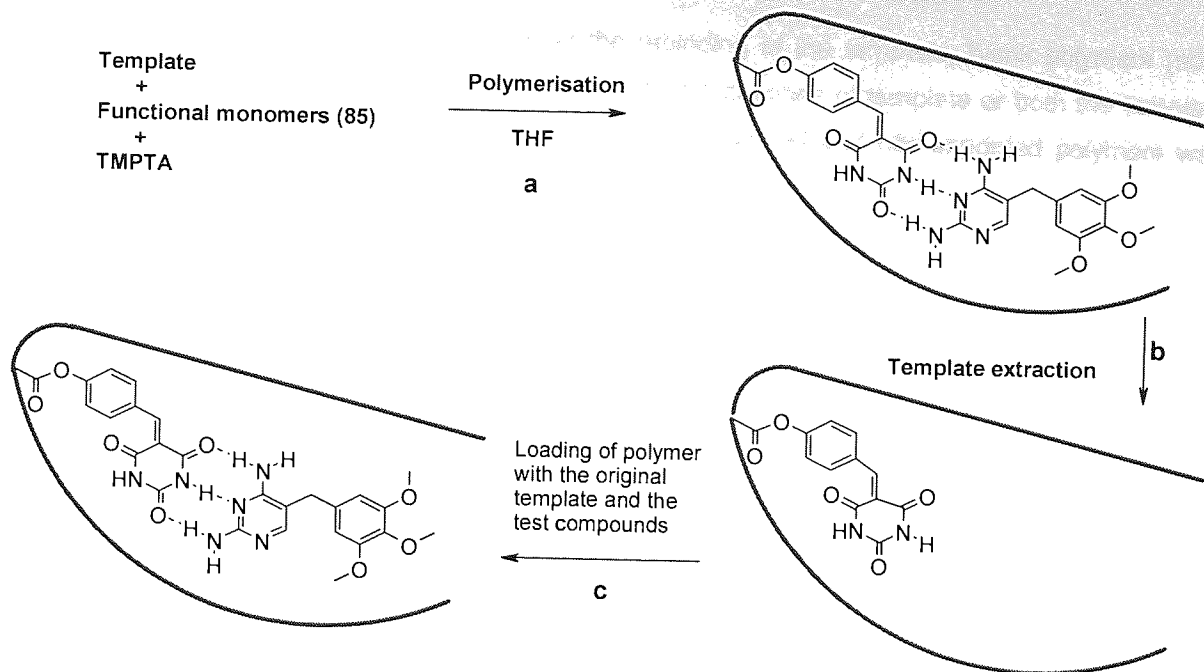


Scheme 6.4: Synthesis of acrylic acid 4-(2,4,6-trioxotetrahydropyrimidin-5-ylidene)methylphenyl ester (85).

6.5 Selectivity studies

6.5.1 Preparation of Polymers

To examine the selectivity/cross-reactivity profiles generated by the functional monomer (85) molecularly imprinted polymers were prepared using the non-covalent approach (Scheme 6.5) Timethoprim (70) and pyrimethamine (71) shown in Figure 8.12 were used as the templates. As mentioned previously, the functional groups present in these templates, provide fluorescence as well as points for electrostatic and hydrogen-bonding interactions for the complex formation prior to polymerisation. The templates were complexed with the functional monomer 85 in THF and then copolymerised with the cross-linker (TMPTA) using AIBN as the initiator. The molar ratio of the monomer:template (M:T) was 2:1. After polymerisation the particles were sieved and subjected to extensive extraction with chloroform or ethanol in a soxhlet extractor and dried.



Scheme 6.5: Schematic representation of molecular imprinting process (a) complex formation of the template (print) molecule with the functional monomer and excess of a cross-linking agents in THF binding sites specific to the original template, (b) Removal of template molecule by extraction affords the binding sites specific to the original template, (c) Loading of polymer with the original template and the test compounds.

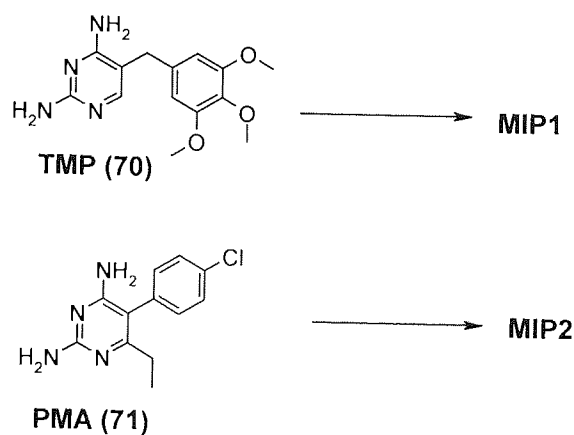


Figure 6.12: The structures of the templates: TMP (70) and PMA (71).

Table 6.3: Shows a series of MIPS and the blank polymers 3 and 4 synthesised to investigate the binding performance of MIPS

Polymer	Monomer	Template	Crosslinker	M:T	Solvent	Initiator
Polymer 1 (MIP1)	(85)	TMP (70)	TMPTA	2:1	THF	AIBN
Polymer 2 (MIP 2)	(85)	PMA (71)	TMPTA	2:1	THF	AIBN
Polymer 3 (NIP)	(85)	–	TMPTA	–	THF	AIBN
Polymer 4	–	–	TMPTA	–	THF	AIBN

To see the influence of the polymer matrix on the rebinding of the template, blank polymers (non-MIPs) were also prepared by the same procedure with the absence of template or both the template and the monomer see **Table 6.3**. The selectivity of the imprinted and non-imprinted polymers was determined by fluorescence spectroscopy.

6.6 Investigation into the binding selectivities of the imprinted polymers.

One strategy to investigate the binding performance of the MIP was based on fluorescence experiments. Fluorescent probes have played an important role in the elucidation of physical properties of polymers. For example, when the sensing element interacts with the analyte, it undergoes physicochemical transformations that change its optical property. This transduction mechanism generates a light signal that can be correlated with the analyte concentration. The major advantage of fluorescence-based detection is that a very little sample is required for analysis and sub-micromolar concentrations may be detected. The analytes (**Figure 6.12**) used in the current study exhibit intrinsic fluorescence; therefore, fluorescence-based detection was applicable to monitor the binding of specific ligand to their respective imprint.

6.7 Exposure of imprinted polymers and the control polymers to the templates and the test compounds followed by fluorescence measurements:

Prior to fluorescence measurements each synthesised polymer was exposed to the solution of its imprinting molecule and a series of other test compounds. The structures of the test compounds are given in **Figure 6.13**. All the polymers were then collected by filtration, briefly washed with THF and dried under vacuum. The resulting powders were weighed accurately in triplicate, into black polystyrene 96 well plates. A layer of polyethylene glycol (PEG) was added to each well and the MIPs were examined by fluorescence. The results are presented as relative fluorescence counts per milligram of MIP (RFU/mg). For example, in a graph (**Figure 6.14**) when MIP1 was re-exposed to its template, the fluorescence results are given as relative fluorescence unit per milligram (RFU/mg). In contrast, the PEG-only results shown in the graphs for comparison are raw RFU plots and as such appear to be greater than they really are in comparison to the polymer data, typically by a factor of five.

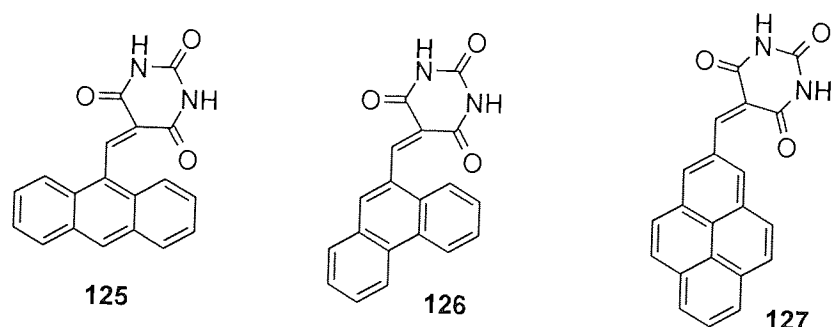


Figure 6.13: The structures of the test compounds.

6.8 Fluorescence results for MIP1

6.8.1. MIP1 re-exposed to its template (TMP)

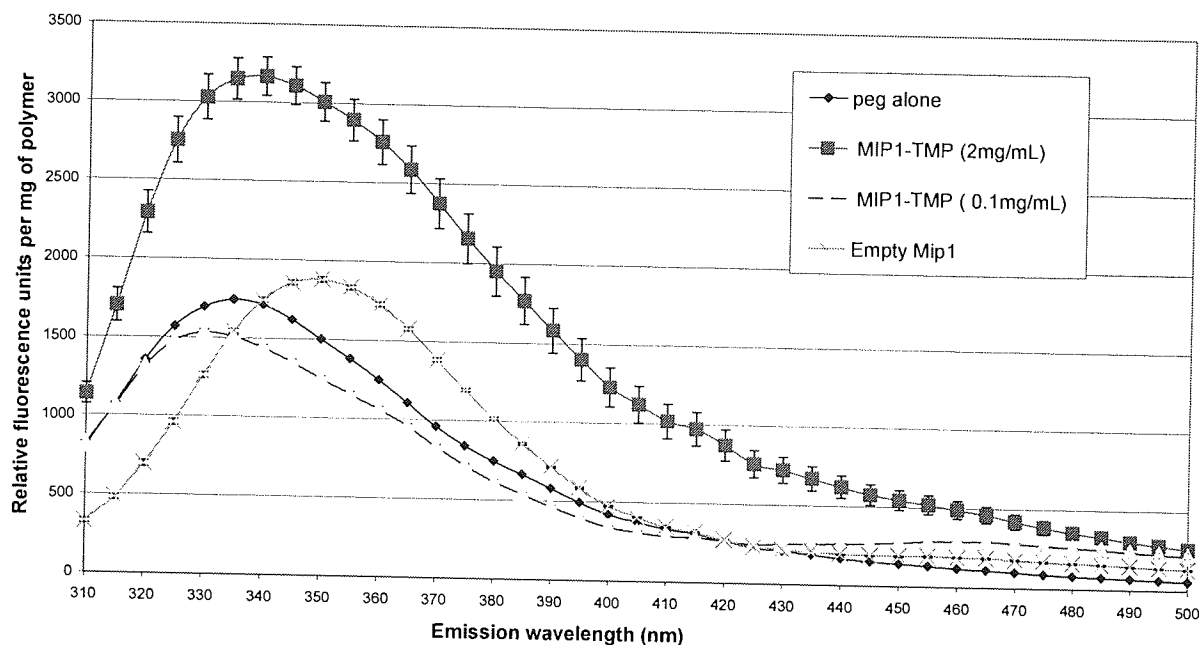


Figure 6.14: Fluorescence spectra for MIP1 re-exposed to its template TMP (**70**) at concentrations of 2 mg/mL and 0.1 mg/mL. The quoted errors are the standard deviations of triplicate wells ($\lambda_{\text{ex}} = 290$ nm)

Figure 6.14 above shows the binding of the template TMP (**70**) to MIP1. The fluorescence spectra were taken at the observed optimum excitation wavelength of 290 nm. Maximum fluorescence emission was observed at 340 nm after exposure to a 2mg/mL solution of **70**. It can be seen from the **Figure 6.14** that when the empty MIP1 was re-exposed to solution of its own template (0.1 mg/mL, 2.0 mg/mL) a dose-dependent fluorescence enhancement was observed. Moreover, the maximum fluorescence emission for empty MIP was observed at 350 nm (1899 RFU/mg). In contrast, the maximum fluorescence emission for MIP1 was observed to be (3165 RFU/mg) at 340 nm.

6.8.2 A blank polymer 3 (NIP) exposed to (70)

A blank polymer 3 (NIP) was also exposed to TMP (70) Figure 6.15 and the result was compared Figure 6.16-6.17

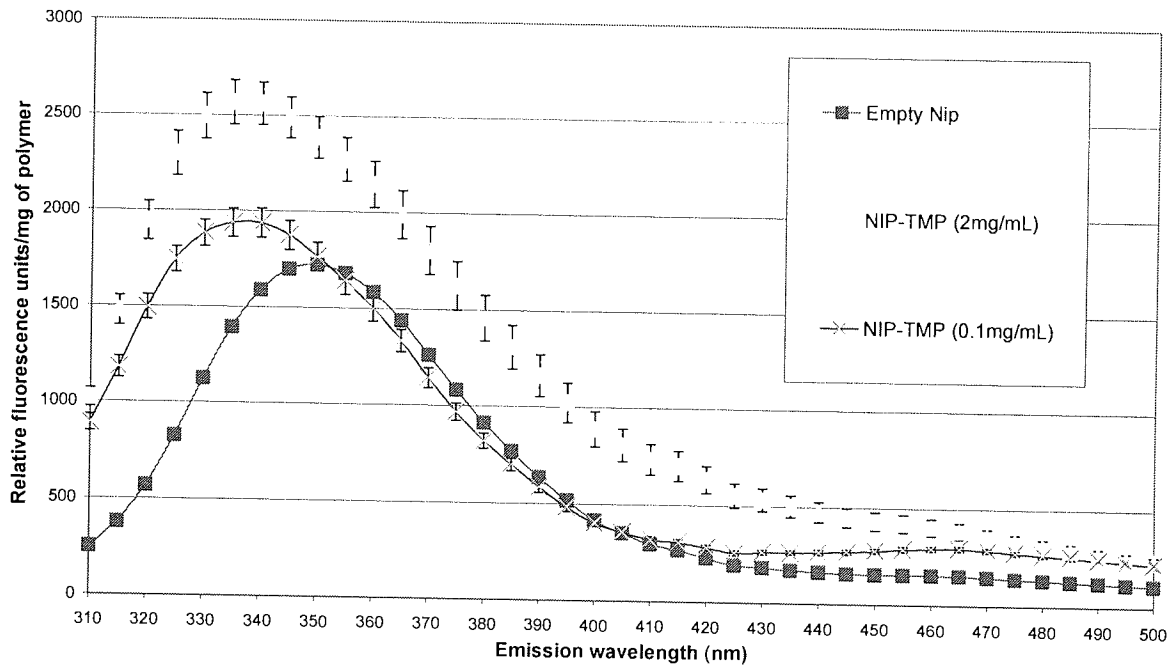


Figure 6.15: Dose-dependent fluorescence spectra for blank polymer 3 (NIP) when exposed to solutions of TMP (70) The quoted errors are the standard deviations of triplicate wells ($\lambda_{ex} = 290$ nm).

6.8.3 Comparison of MIP1 and polymer 3 (NIP) when exposed to TMP (70)

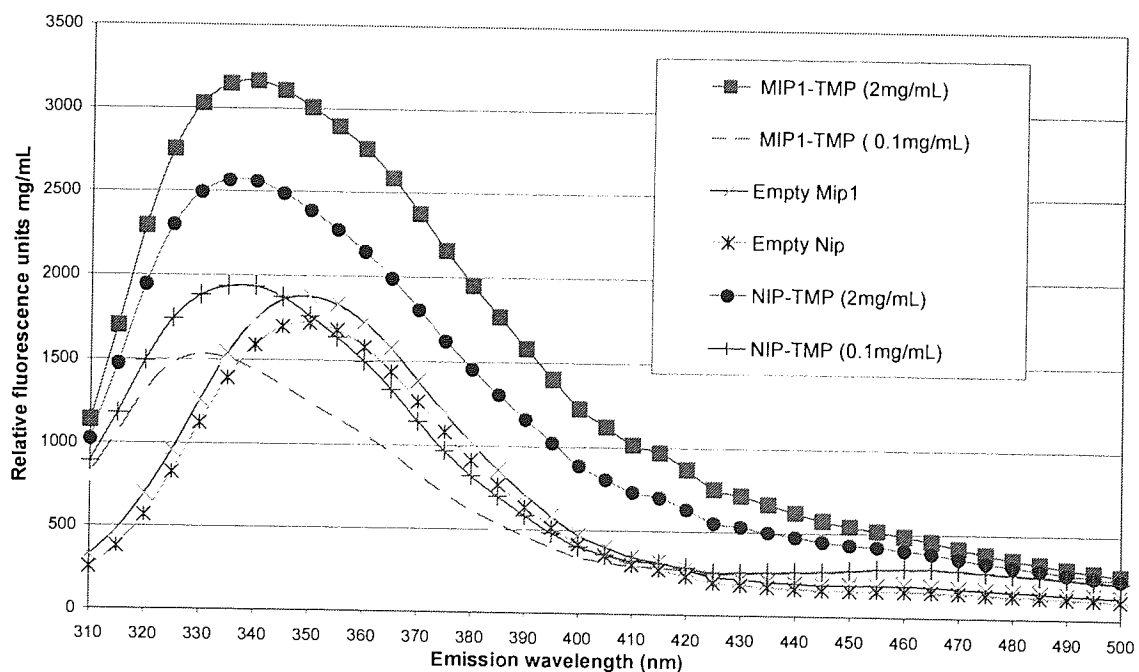


Figure 6.16: Fluorescence spectra for MIP1 and NIP re-exposed to TMP (70) at concentrations of 2 mg/mL and 0.1 mg/mL ($\lambda_{ex} = 290$ nm).

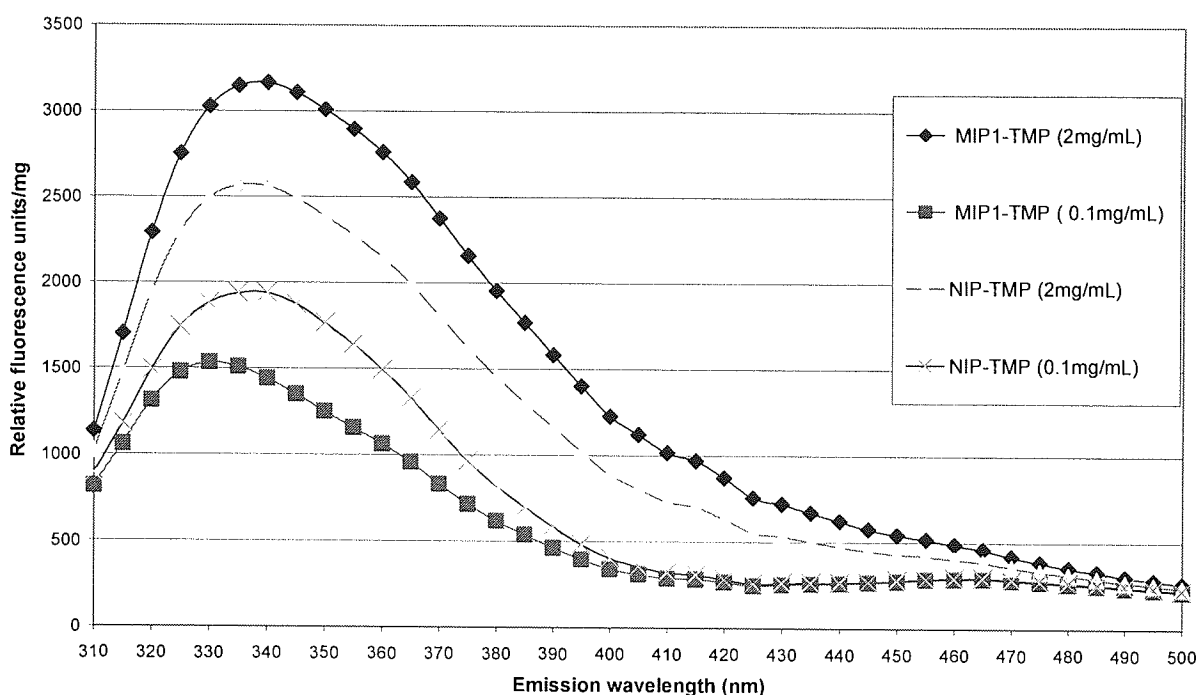


Figure 6.17: More expanded fluorescence spectra for MIP1 and NIP re-exposed to TMP (**70**) at concentrations of 2 mg/mL and 0.1 mg/mL ($\lambda_{\text{ex}} = 290 \text{ nm}$).

The maximum fluorescence enhancement was observed when MIP1 was re-exposed to its template TMP (**70**) at the concentration of 2.0 mg/mL at an emission wavelength of 340 nm (**Figure 6.17**). It was also apparent that both MIP1 and the NIP can adsorb trimethoprim (**70**) from the solution, but the adsorption capacity of the MIP was higher (3165 RFU/mg) at the solution concentration of 2 mg/mL than that of the NIP (2561 RFU/mg). It was assumed that this high absorption capacity of MIP1 could be due to the cavities formed during the imprinting process. Another observation made from these results was that when the MIP1 and NIP were exposed to TMP (**70**) in solution at the concentration of 0.1 mg/mL the absorption capacity of the MIP1 was lower (1442 RFU/mg) than that of NIP (1937 RFU/mg). Moreover, it was expected that an empty MIP1 and the NIP should exhibit the same level of fluorescent output, but this was not the case. The empty MIP1 exhibited slightly higher level of fluorescence output (1742 RFU/mg) than the NIP (1588 RFU/mg); this was most likely caused by inadequate extraction of the template i.e. it is very likely that the little amount of template was still trapped in the MIP1 cavity. Moreover, the maximum fluorescence for both empty MIP1 and the NIP was observed at emission wavelength of 350 nm.

The next step was to investigate the size of the cavities and discover how tight the polymer matrix was formed around the template molecule. It was assumed if the matrix was formed well enough around the template (**70**) the bigger ligand would not be able to get into the cavity to form hydrogen bonds and as a result the MIP1 would show the lower binding in contrast to the **70**.

However, to demonstrate this, the MIP1 and NIP were re-exposed to structurally similar compound to TMP, for example, pyrimethamine (**71**) and to other synthesised test compounds **Figure 6.13**. A synthesised compound **127** was not used in this study due to its poor solubility profile. The rebinding

experiments for the test compounds were performed under the same conditions as for the template (70). The results are presented in (Figure 6.18 - 6.21).

6.8.4 MIP1 exposed to test compound PMA (71)

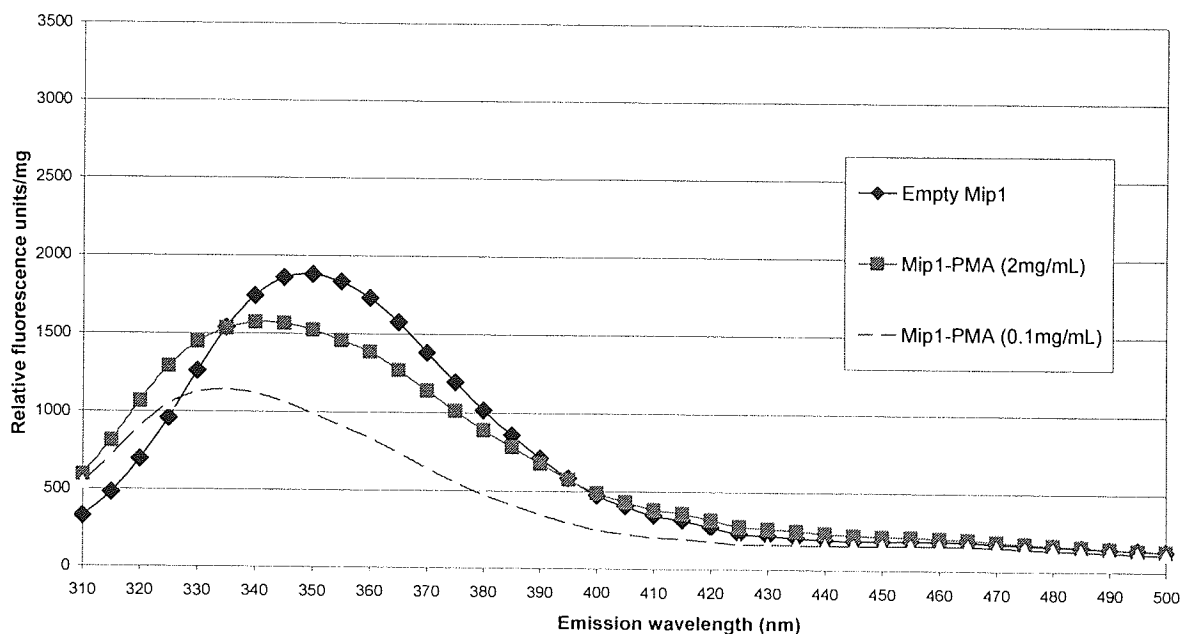


Figure 6.18: Fluorescence spectra for MIP1 re-exposed to PMA (71) at concentrations of 2 mg/mL and 0.1 mg/mL ($\lambda_{ex} = 290$ nm). The quoted errors are the standard deviations of triplicate wells ($\lambda_{ex} = 290$ nm).

Figures 6.18 to 6.21 show the result of TMP imprinted polymer MIP1 and non-imprinted polymer 3 (NIP) exposed to a solution of a structurally related 2,4-diaminopyrimidine molecule i.e. pyrimethamine (71) solution at the concentrations of 2 mg/mL and 0.1 mg/mL. A dose dependent enhancement was observed for MIP1. However, no significant absorption of 71 was seen for MIP1 at either concentration (1574 RFU/mg and 1121 RFU/mg respectively), suggesting that MIP1 had rejected 71 see Figure 6.18.

6.8.5

A blank polymer 3 (NIP) exposed to test compound PMA (71)

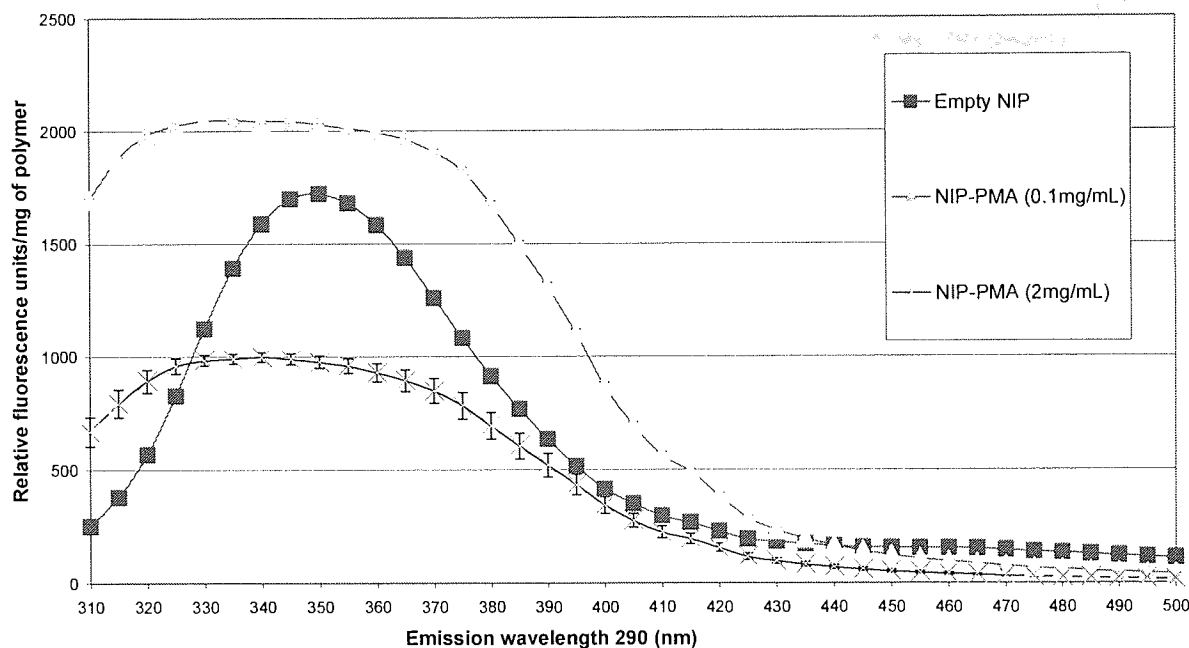


Figure 6.19: Fluorescence spectra for NIP re-exposed to PMA (71) at concentrations of 2 mg/mL and 0.1 mg/mL. The quoted errors are the standard deviations of triplicate wells ($\lambda_{\text{ex}} = 290 \text{ nm}$).

6.8.6

Comparison of MIP1 and polymer 3 (NIP) when exposed to PMA (71)

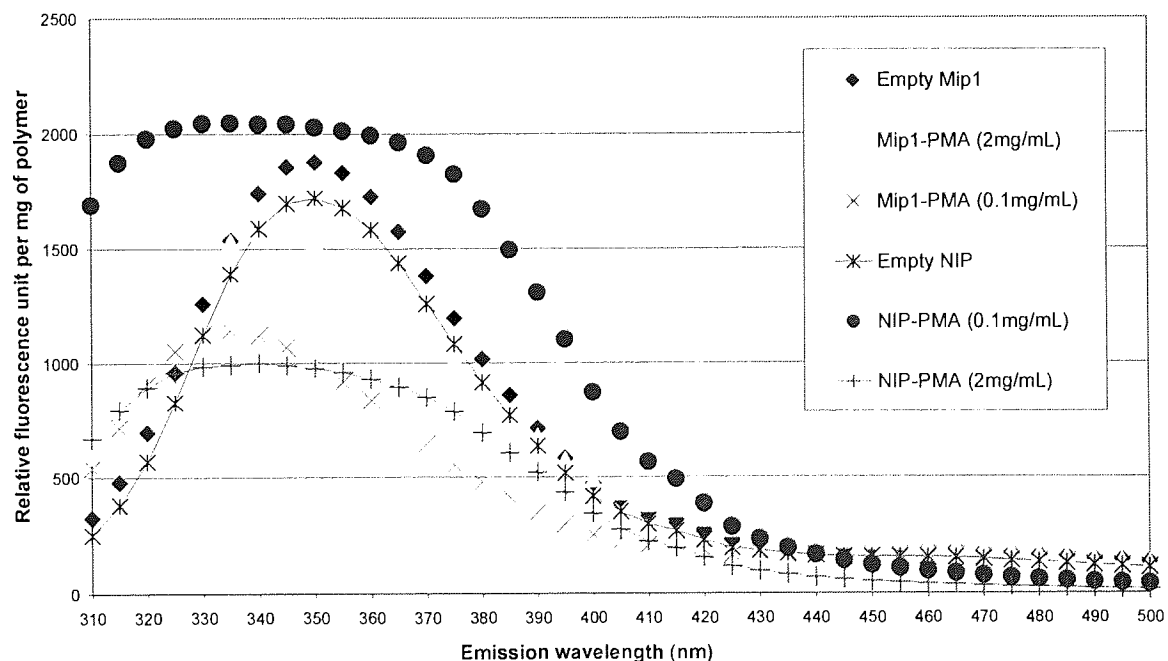


Figure 6.20: Fluorescence spectra for MIP1 and NIP exposed to PMA at concentrations of 2 mg/mL and 0.1 mg/mL ($\lambda_{\text{ex}} = 290 \text{ nm}$).

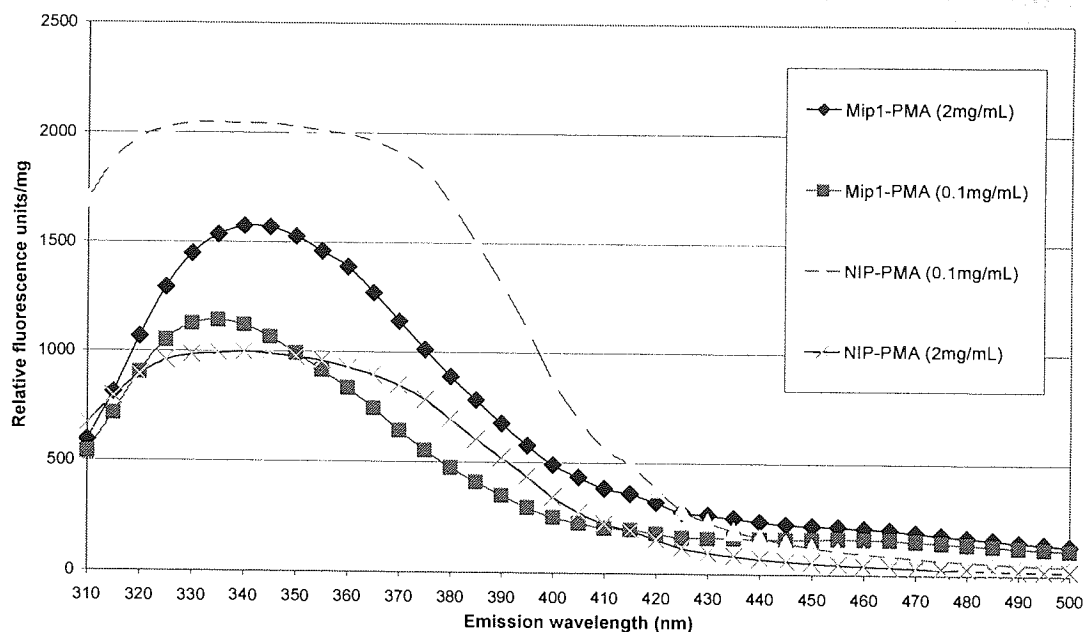


Figure 6.21: Expanded version of fluorescence spectra for MIP1 and NIP exposed to **71** at concentrations of 2 mg/mL and 0.1 mg/mL ($\lambda_{ex} = 290$ nm).

The similar trend was not observed for the blank polymer 3 (NIP) (Figure 6.19 - 6.21 above). In fact a larger absorption was seen at 0.1 mg/mL (2043 RFU/mg) relative to the 2.0 mg/mL (998 RFU/mg) for a NIP. In addition, the NIP formed a plateau at a region of 325 to 360 emission wavelength and then the fluorescence out-put falls at 360 nm. This peak broadening was probably due to the non-specific absorptions, probably at the surface of the NIP. This behaviour was not observed for MIP1. To demonstrate the specificity of the MIP1 it was further exposed to compounds **125** and **126**.

6.8.7 MIP1 and the blank polymer 3 (NIP) exposed to compound **125**

The results obtained for exposure of **125** to MIP1 and the polymer 3 (NIP) are presented in Figure 6.22 - 6.26. Compound **125** displayed similar behaviour to **71**. MIP1 in that it did not show the recognition for compound **125**. A similar trend was observed for NIP. A relatively larger absorption was observed for NIP at lower concentrations 0.1 mg/mL (1176 RFU/mg) in contrast to 2mg/mL (792 RFU/mg). It was difficult to draw any conclusion from this result. The MIP1 and the NIP were then exposed to compound **126**.

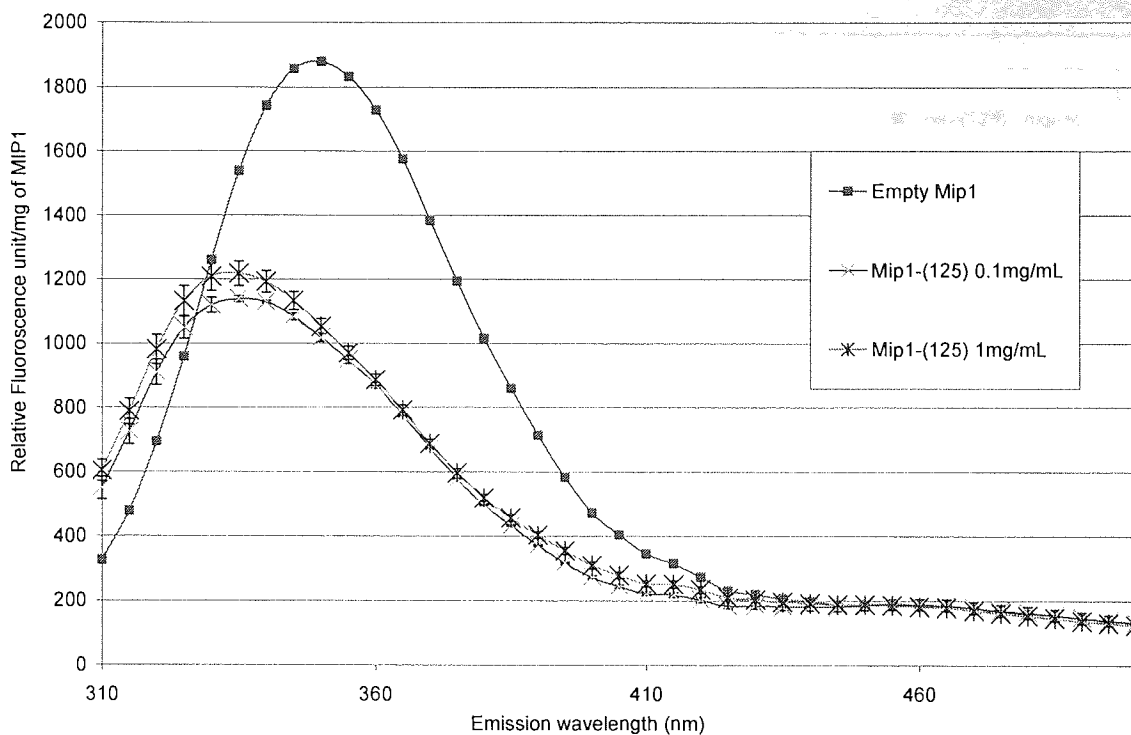


Figure 6.22: Fluorescence spectra for MIP1 exposed to compound **125** at concentrations of 1 mg/mL and 0.1 mg/mL. The quoted errors are the standard deviations of triplicate wells ($\lambda_{ex} = 290$ nm).

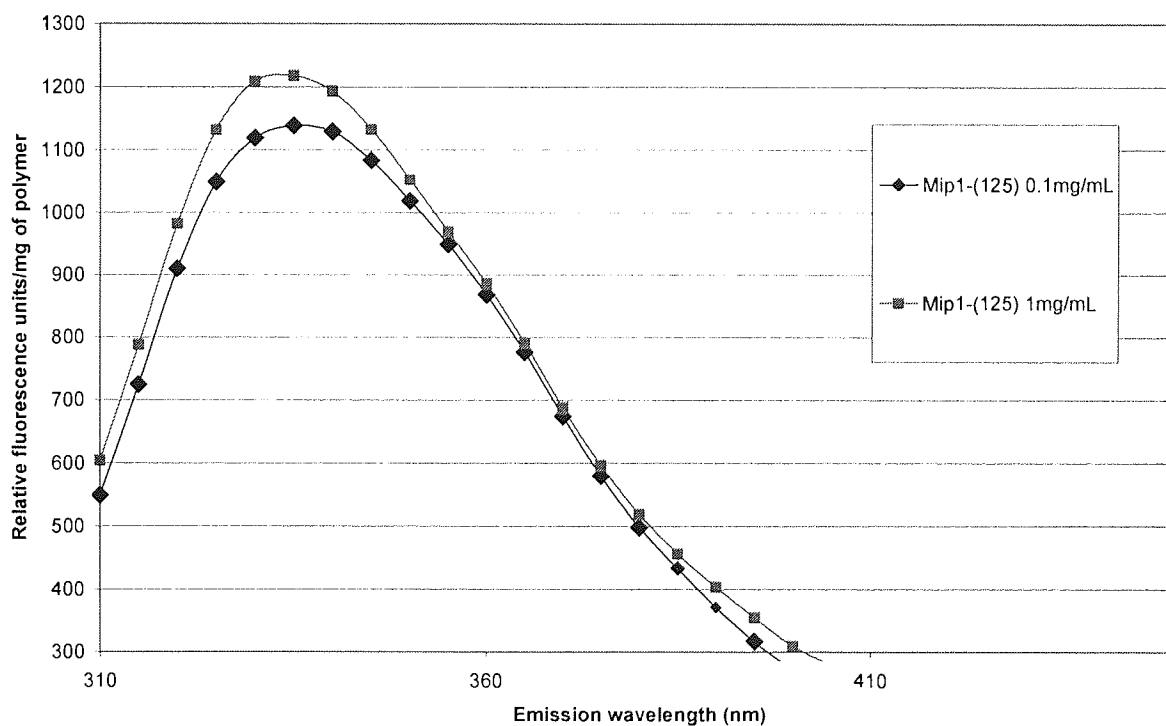


Figure 6.23: Expanded version of Fluorescence spectra for MIP1 when exposed to **125** at the concentrations of 1 mg/mL and 0.1 mg/mL ($\lambda_{ex} = 290$ nm).

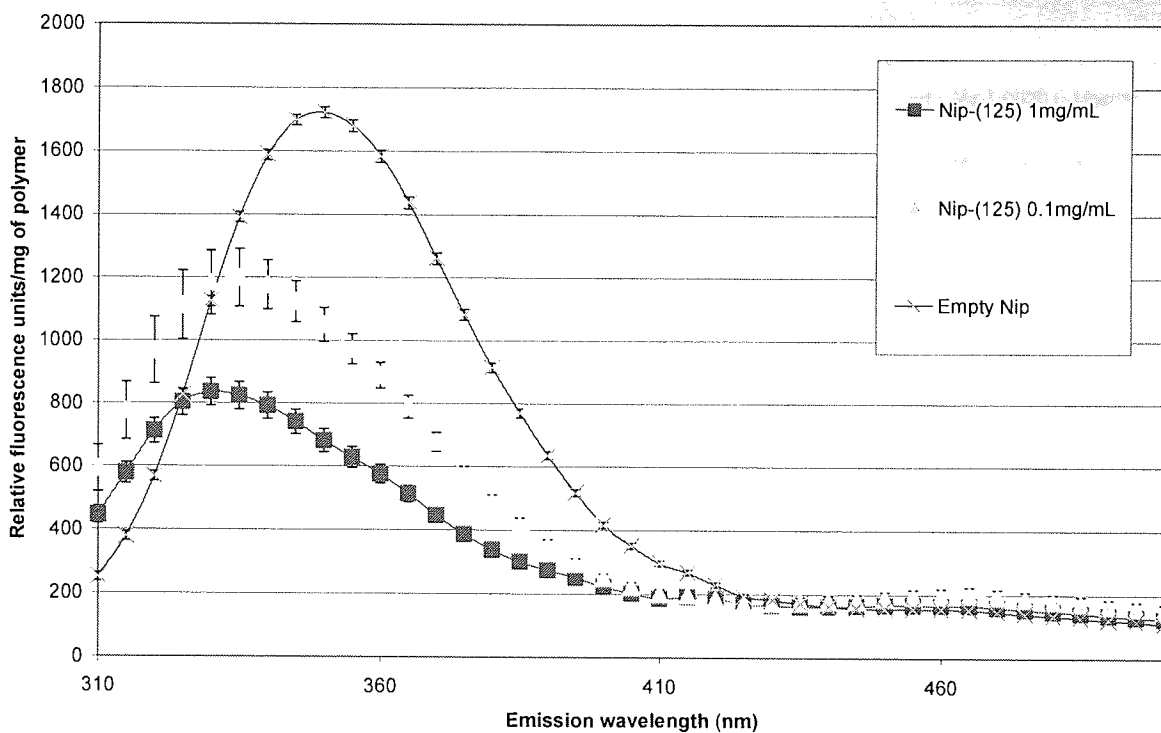


Figure 6.24: Fluorescence spectra for NIP exposed to compound **125** at concentrations of 1 mg/mL and 0.1 mg/mL. The quoted errors are the standard deviations of triplicate wells ($\lambda_{\text{ex}} = 290 \text{ nm}$).

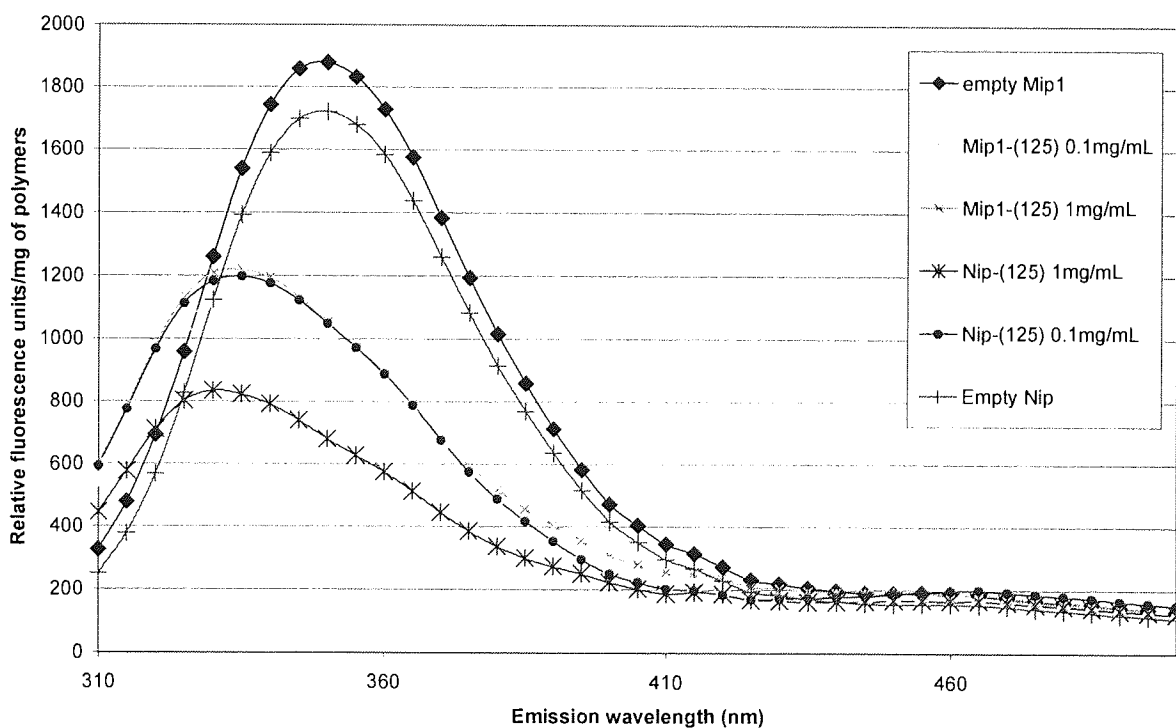


Figure 6.25: Fluorescence spectra for MIP1 and NIP exposed to compound **129** at concentrations of 1 mg/mL and 0.1 mg/mL. ($\lambda_{\text{ex}} = 290 \text{ nm}$).

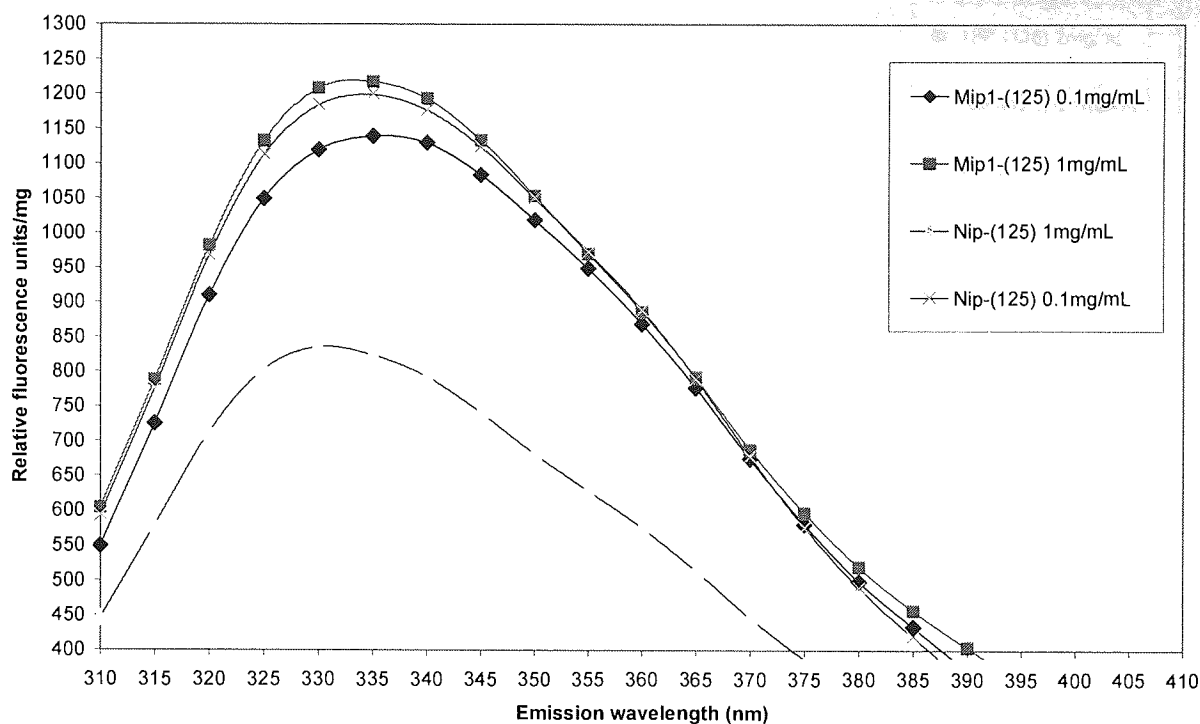


Figure 6.26: Expanded version of fluorescence spectra for MIP1 and NIP re-exposed to compound **125** at concentrations of 1 mg/mL and 0.1 mg/mL ($\lambda_{ex} = 290$ nm).

6.8.8 MIP1 and the blank polymer 3 (NIP) exposed to compound 126

The performance of the MIP1 was further assessed by exposing the MIP1 and the polymer 3 (NIP) to the compound **126**. The results are presented in **Figures 6.27** to **6.30**.

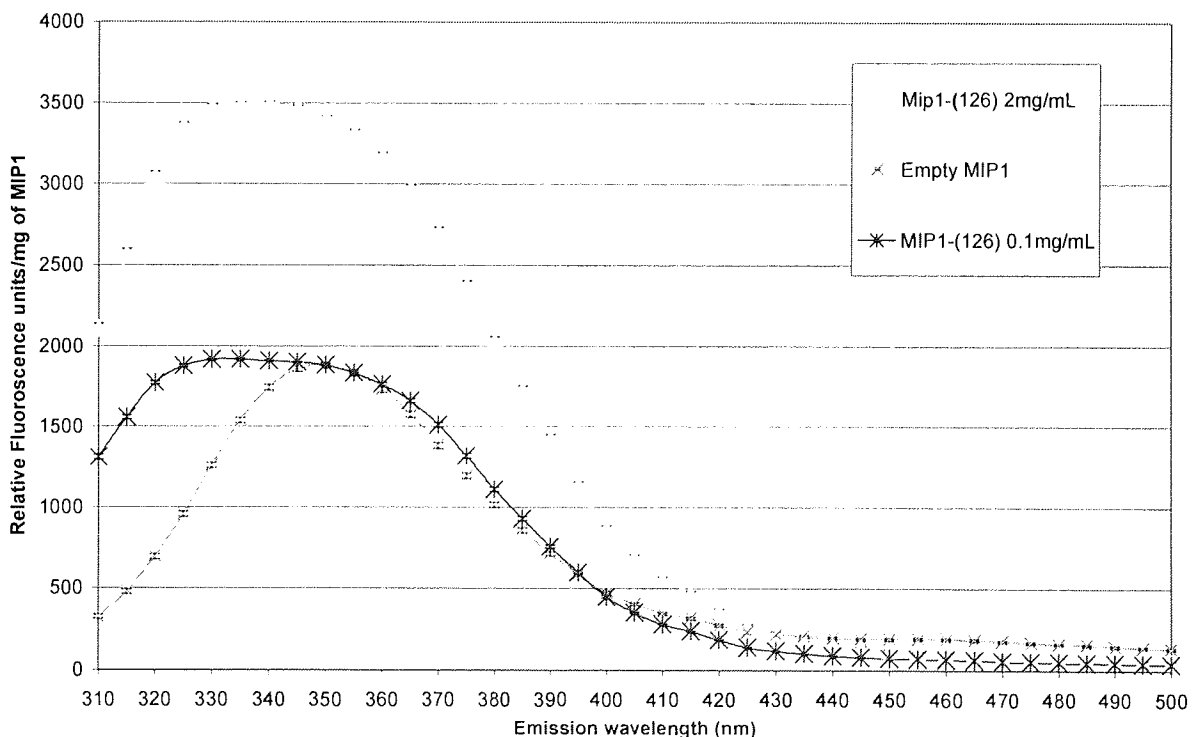


Figure 6.27: Fluorescence spectra for MIP1 exposed to compound **126** at concentrations of 2 mg/mL and 0.1 mg/mL. The quoted errors are the standard deviations of triplicate wells ($\lambda_{ex} = 290$ nm).

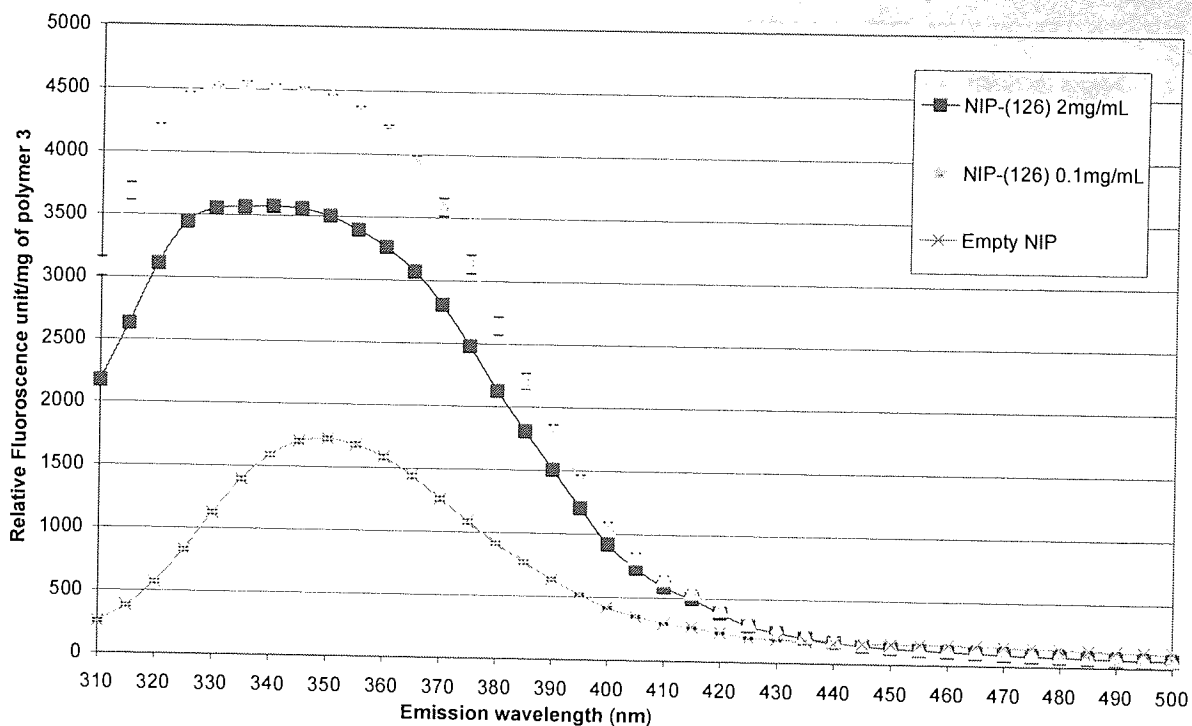


Figure 6.28: Fluorescence spectra for NIP exposed to compound **126** at concentrations of 2.mg/mL and 0.1 mg/mL. The quoted errors are the standard deviations of triplicate wells ($\lambda_{ex} = 290$ nm).

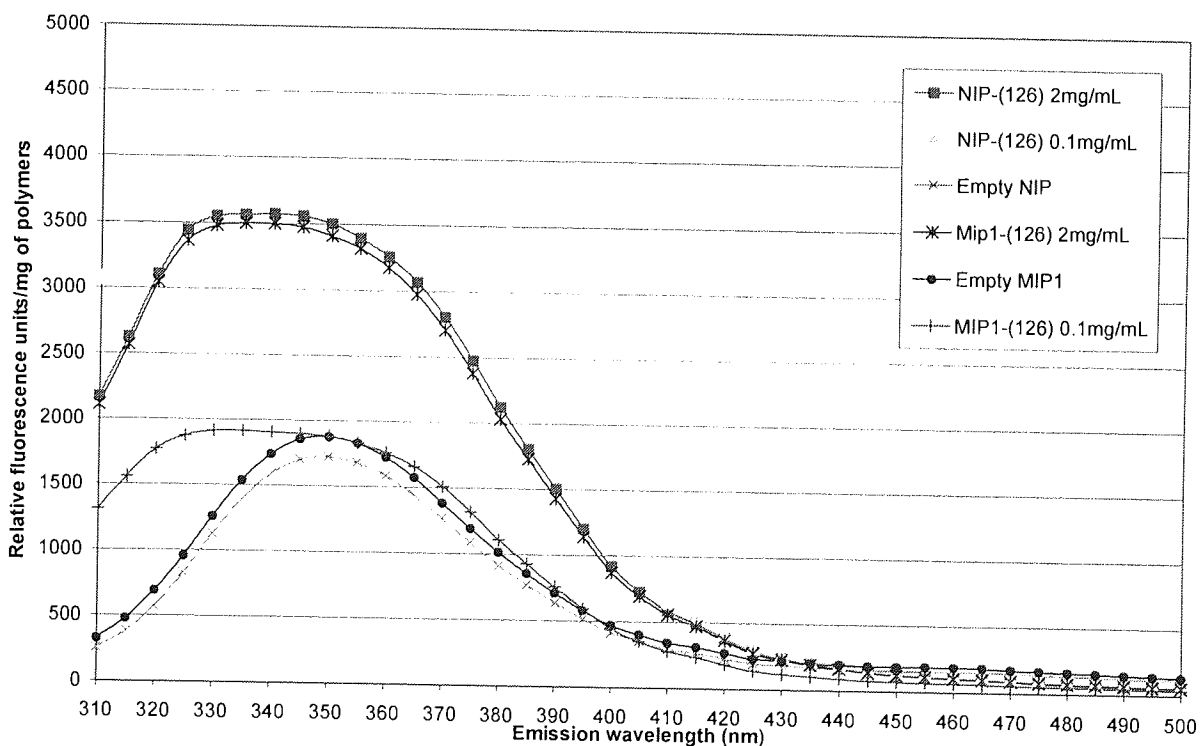


Figure 6.29: Fluorescence spectra for MIP1 and NIP exposed to compound **126** at concentrations of 2 mg/mL and 0.1 mg/mL ($\lambda_{ex} = 290$ nm).

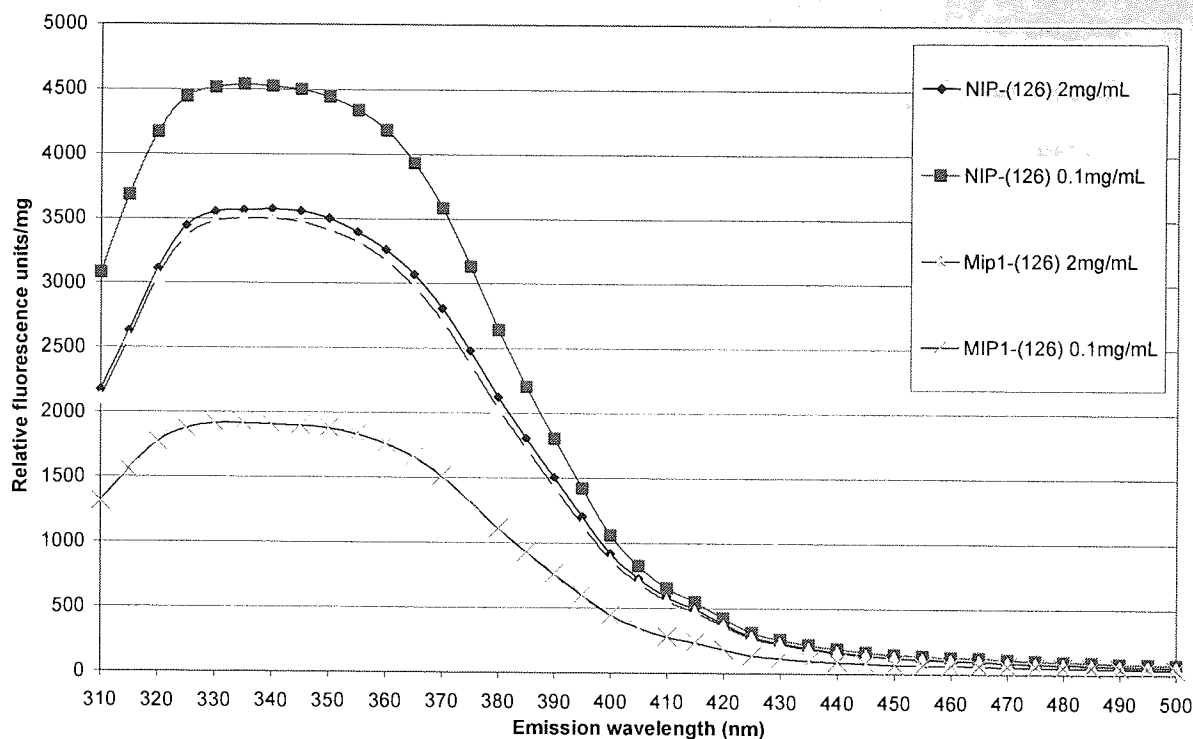


Figure 6.30: Expanded version of fluorescence spectra for MIP1 and NIP exposed to compound **126** at concentrations of 2 mg/mL and 0.1 mg/mL ($\lambda_{ex} = 290$ nm).

The graph (**Figures 6.27 to 6.30**) showed the dose dependent enhancement of fluorescent emission for MIP1. There was a large amount of absorption exhibited by MIP1 (3499 RFU/mg), suggesting that compound **126** was probably more fluorescence than the template TMP (**70**). In contrast polymer 3 (NIP) once again showed tremendous amount of fluorescence at the lower concentrations of test solution i.e. at 0.1mg/mL (4540 RFU/mg). It can be seen from the above results that the polymer 3 (NIP) did not turn out to be a good control polymer for the comparative purpose. It could be that the polymer 3 NIP had the functional groups derived from the functional monomer randomly distributed throughout its matrix. To investigate this factor and to validate our results, it was decided to prepare another blank polymer 4 (TMPTA), without both the template and the functional monomer see **Table 6.3** The rebinding experiment for the test compound **70**, **71**, **125** and **126** were repeated with the polymer 4 (TMPTA) under the same conditions as for the TMP (**70**) imprinted polymer and the blank polymer 3 NIP. The results are presented in **Figures 6.31 to 6.32** below.

6.8.9 Comparison of MIP1 Polymer 3 (NIP) and Polymer 4 (TMPTA) Results

Figure 6.31 below indicated that the relative fluorescence output of the polymer 4 (TMPTA) was negligible (524 RUF) at 325 nm relative to MIP1 and NIP (1879 and 1722 RUF respectively) at 350 nm. This difference could have been due the presence of functional monomer. MIP1 and NIP have had functional monomer in their composition (**Table 6.3**) and exhibited fluorescence at higher wavelength compared to TMPTA.

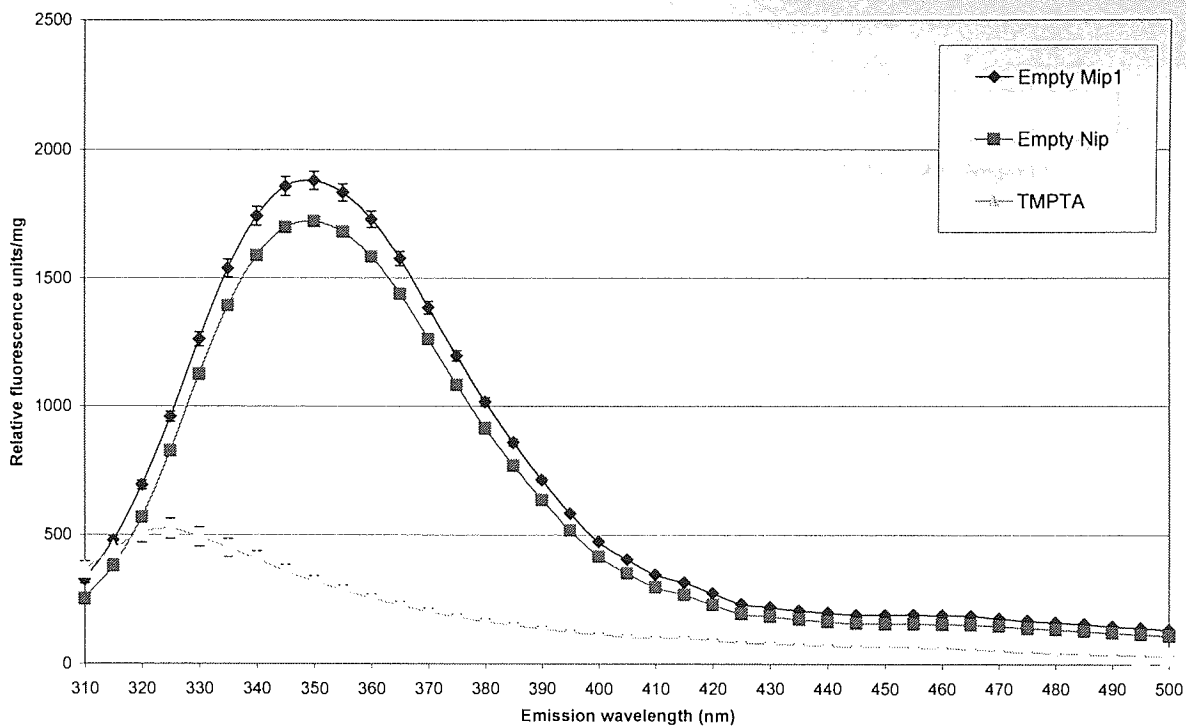


Figure 6.31: Fluorescence spectra for TMPTA , empty NIP and empty MIP1. The quoted errors are the standard deviations of triplicate wells ($\lambda_{ex} = 290$ nm).

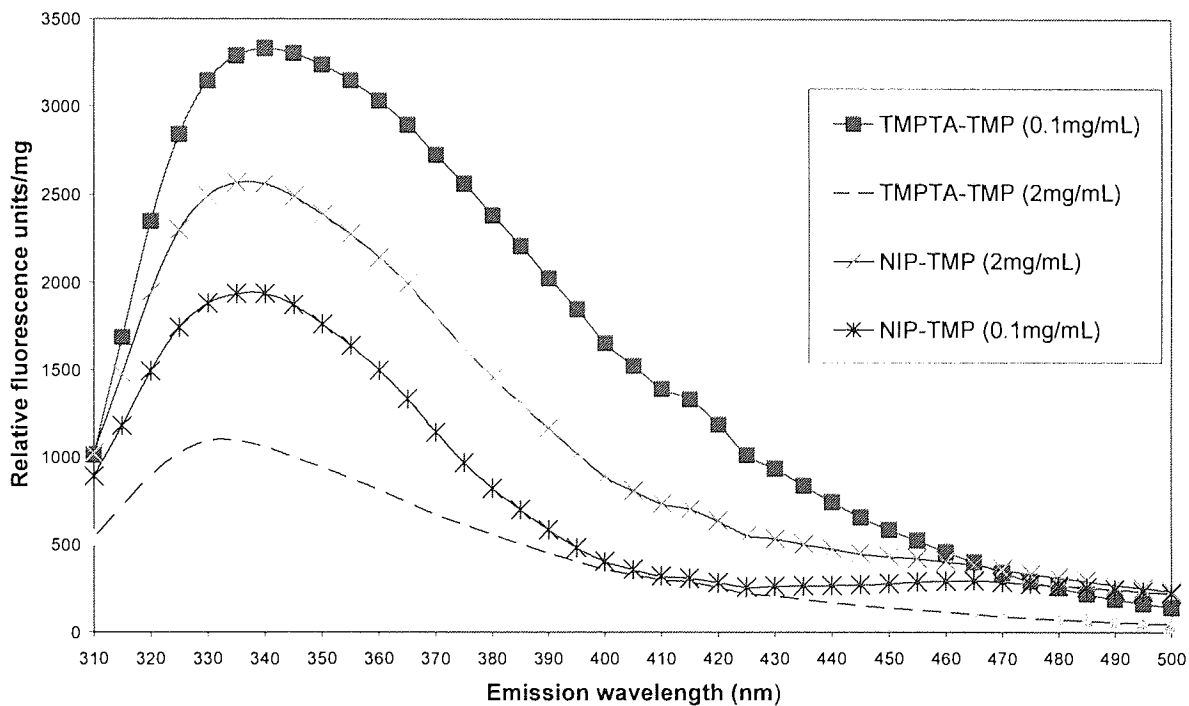


Figure 6.32: Fluorescence spectra for polymer 4 TMPTA and polymer 3 (NIP) exposed to compound 70 at concentrations of 2 mg/mL and 0.1 mg/mL ($\lambda_{ex} = 290$ nm).

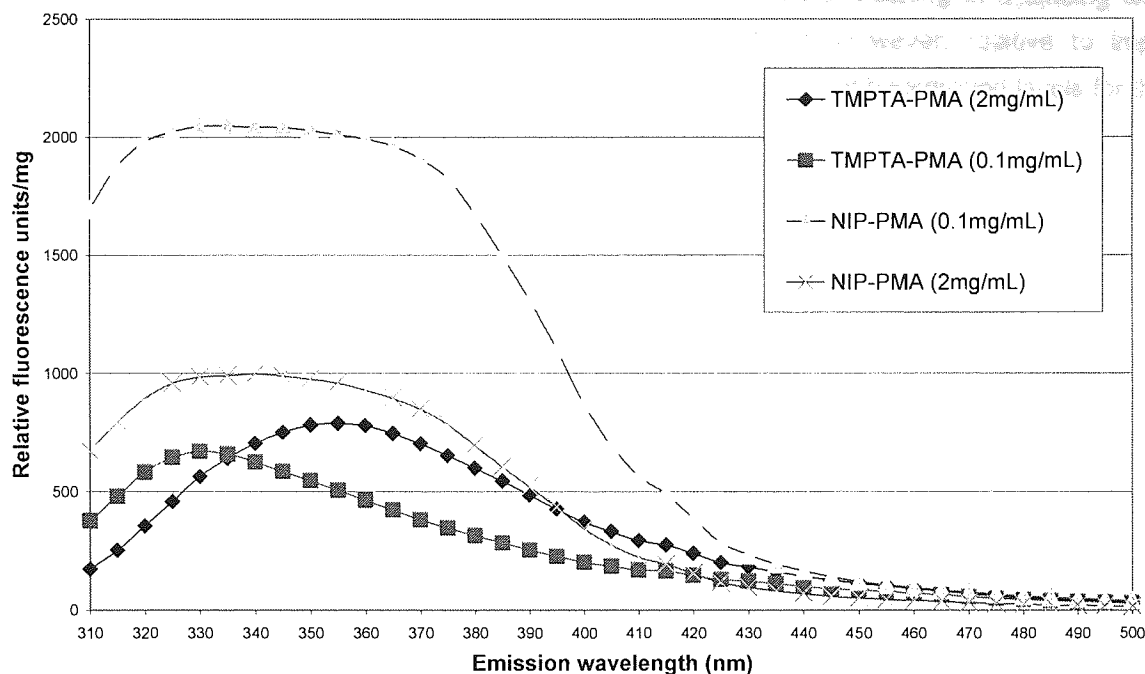


Figure 6.33: Fluorescence spectra for polymer 4 (TMPTA) and polymer 3 (NIP) exposed to compound 71 at concentrations of 2 mg/mL and 0.1 mg/mL. ($\lambda_{ex} = 290$ nm).

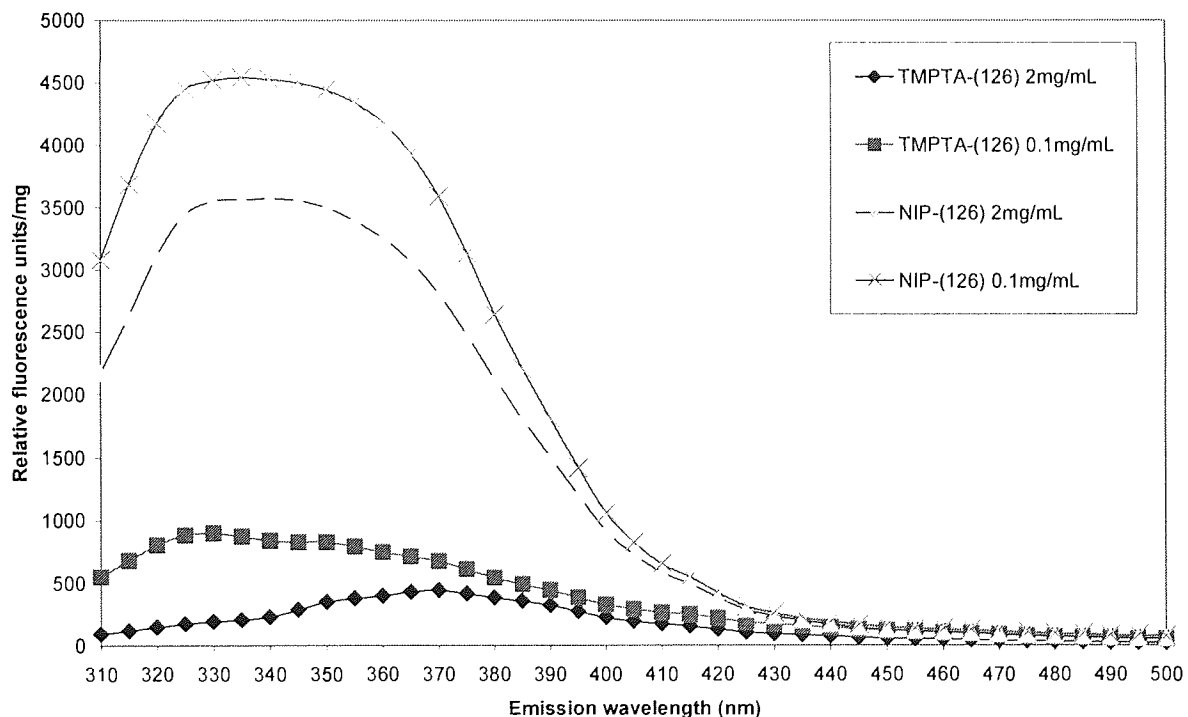


Figure 6.34: Fluorescence spectra for polymer 4 (TMPTA) and polymer 3 (NIP) exposed to compound 126 at concentrations of 2 mg/mL and 0.1 mg/mL. ($\lambda_{ex} = 290$ nm).

It can be seen from **Figures 6.32 to 6.34** that both type of blank polymers 3 (NIP) and 4 (TMPTA) gave almost identical fluorescence profiles when exposed to a lower concentrations. With the exception of **70**, which exhibited dose dependent enhancements with NIP, the rest of the compounds **71**, **125** and **126** showed larger fluorescent outputs at the lower concentrations relative to the corresponding higher concentrations. This suggested that, probably, the non-imprinted polymers 3 (NIP) and 4 (TMPTA) had no well defined binding sites i.e. cavities, therefore, the test compounds

were randomly distributed in the polymers matrix with no specific positioning in a binding site and showed the self-quenching effects at the higher concentrations. However, relative to imprinted polymers and NIP, the TMPTA exhibited very low absorption capacity at background levels for the test compounds with the exception of compound **70** (Figure 6.32).

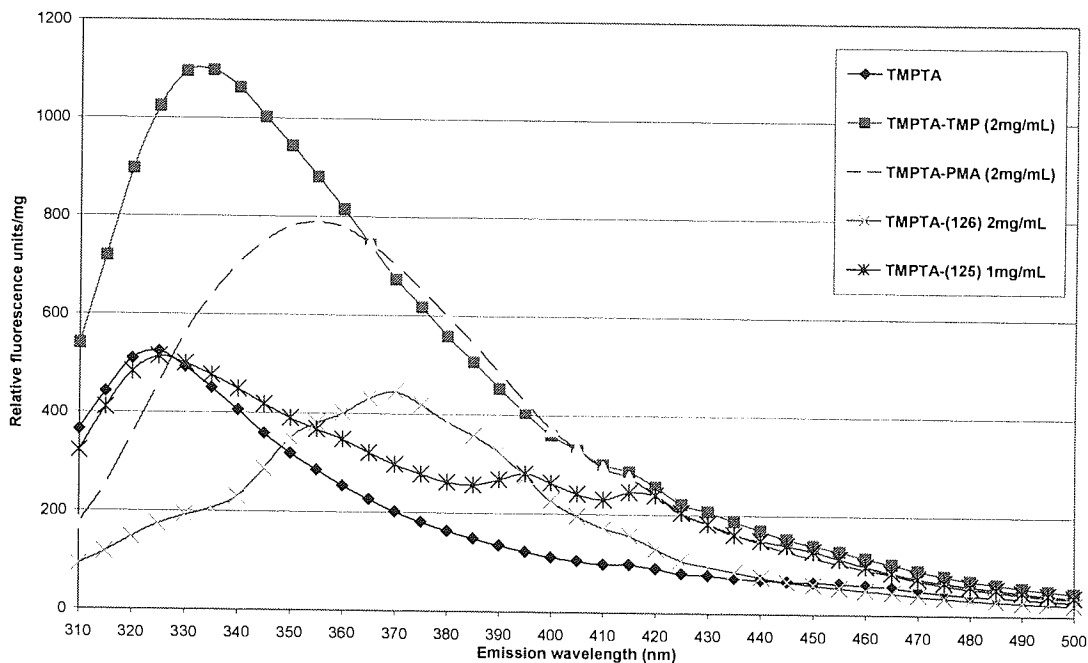


Figure 6.35: Fluorescence spectra for TMPTA exposed to test compounds **70**, **71**, **125** and **126** at concentrations of 2 mg/mL ($\lambda_{ex} = 290$ nm).

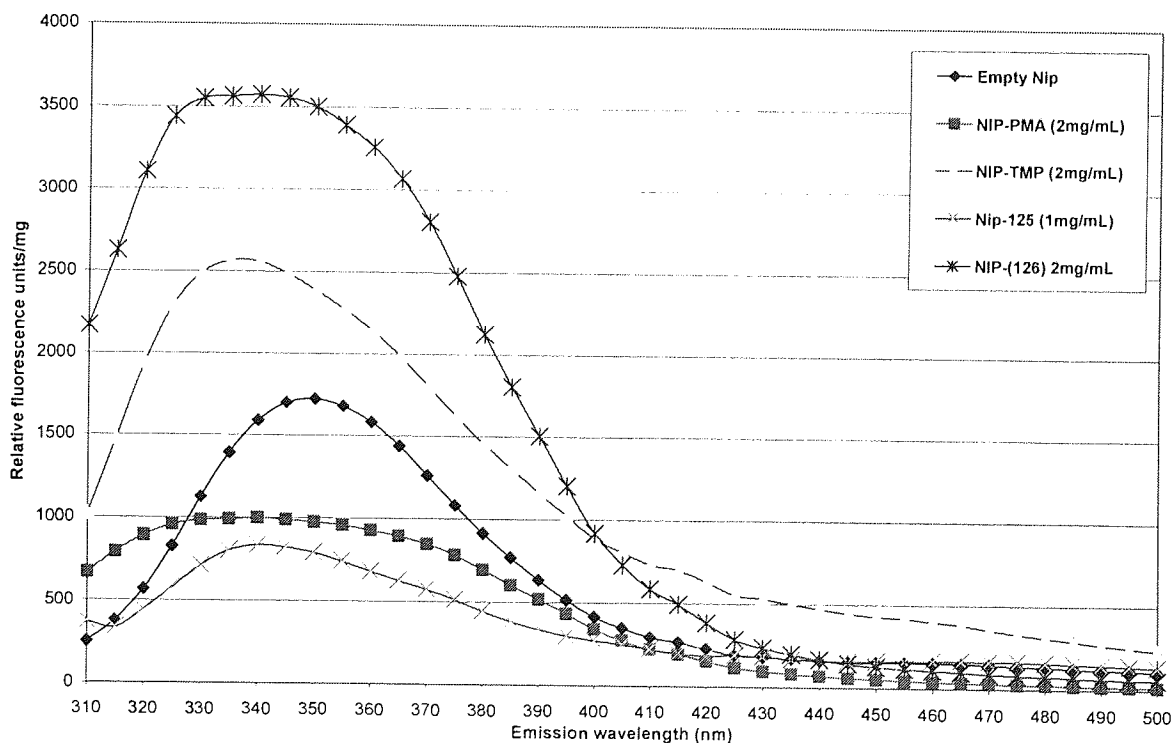


Figure 6.36: Fluorescence spectra for polymer 3 (NIP) exposed to test compounds **70**, **71**, **125** and **126** at concentrations of 2 mg/mL ($\lambda_{ex} = 290$ nm).

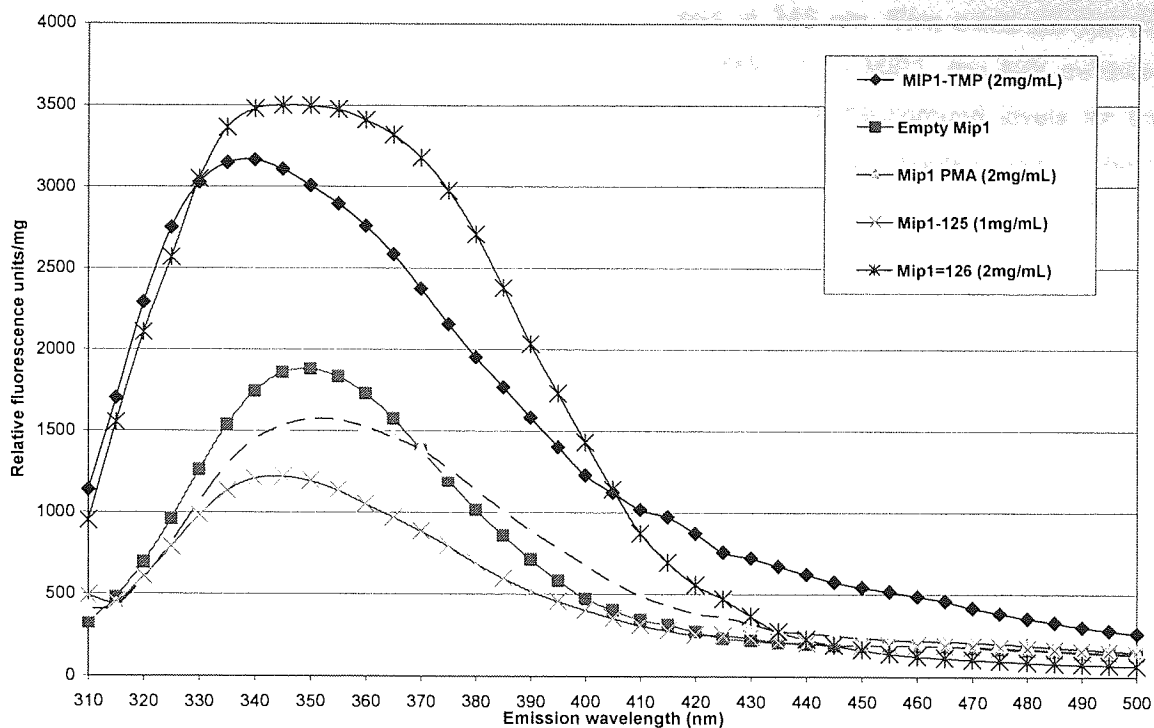


Figure 6.37: Fluorescence spectra for MIP1 exposed to test compounds **70**, **71**, **125** and **126** at concentrations of 2 mg/mL ($\lambda_{ex} = 290$).

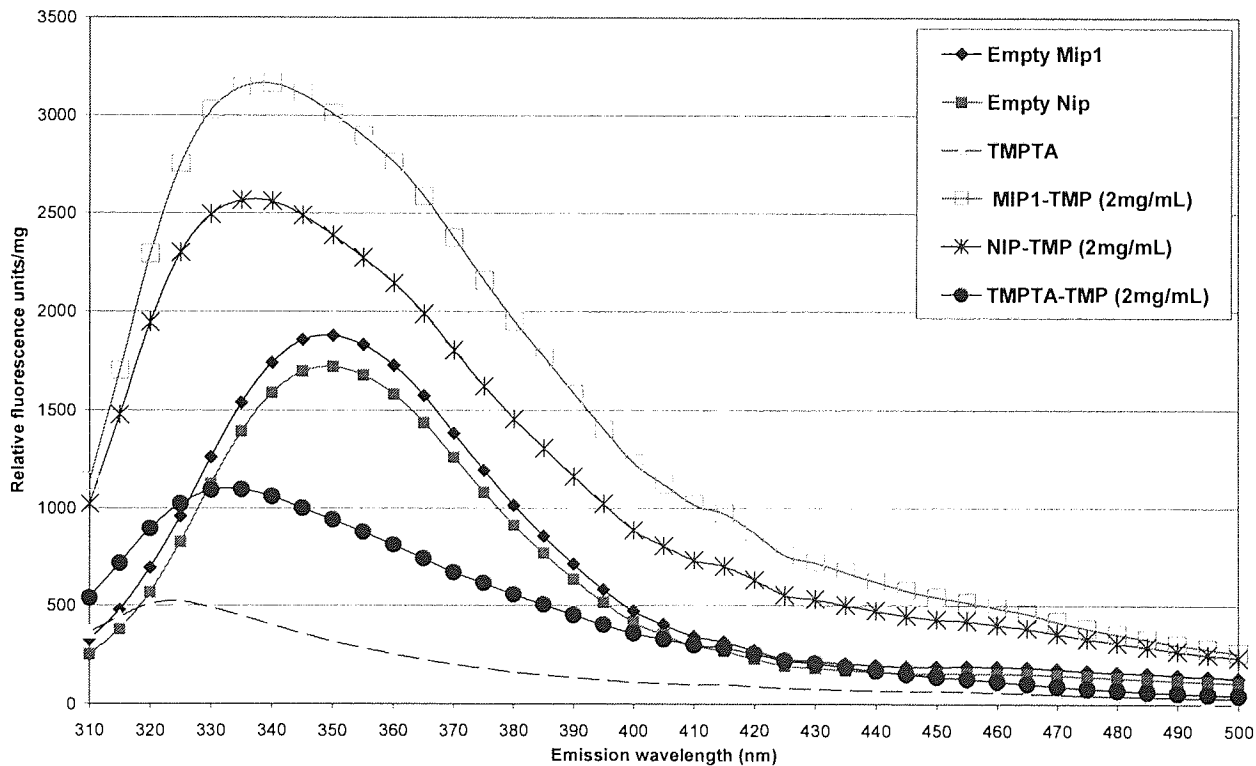


Figure 6.38: Fluorescence spectra for MIP1, NIP and TMPTA when exposed to compound **70** at concentrations of 2 mg/mL ($\lambda_{ex} = 290$).

Figure 6.38 demonstrated that when MIP1 was re-exposed to its template the relative fluorescence out put was maximum at 340 nm whereas maximum fluorescence out put for Nip was at 335 nm and

in contrast maximum fluorescence output for TMPTA was at 335 nm. This could be that the test compound was in different environments in each case. Relative to MIP1, the NIP exhibited low absorption capacity. In contrast, TMPTA exhibited fluorescence at background levels for the test compound TMP. Furthermore, empty MIP1 and NIP exhibited maximum fluorescence at the higher wavelength of 350 nm probably due to the presence of functional monomer in their composition.

When the polymers were exposed to compound **71** (PMA) **Figure 6.39** below the fluorescence emission for MIP1 was lower than that of empty MIP1. In contrast, a broad peaks were observed for polymer 3 (NIP) and polymer 4 (TMPTA). Furthermore, the absorption capacity for the non-imprinted polymers NIP and TMPTA was also lower than that of imprinted polymer MIP1. The broadening of the emission peaks for the NIP and polymer 4 (TMPTA) relative to the imprinted polymer may be because of differences in the environments of the bound test compounds in these three polymers. In the case of MIP1 it is expected that the test compounds will be associated with functionalised cavities created by the imprinting process. The NIP contains functional groups arising from the functional monomer and these are assumed to be scattered throughout the polymer matrix. As a result the test compound may adhere to the NIP randomly and in a variety of environments (ie. in a much wider range of environments than was the case with the MIP1). Each different environment for the bound test compound may result in a slightly different emission maximum in the fluorescence spectrum. Taken together, this range of environments may have resulted in an observed broadening of the fluorescence output relative to the same test compound bound to the MIP1.

In the case of Polymer 4, there was no imprinting and no included functionality. Here there may have been non-specific binding of the test compounds into a range of environments, but not so wide a range of environments as was the case with the NIP. This may be behind the observed level of broadening in the fluorescence spectrum that was intermediate between the MIP1 and NIP.

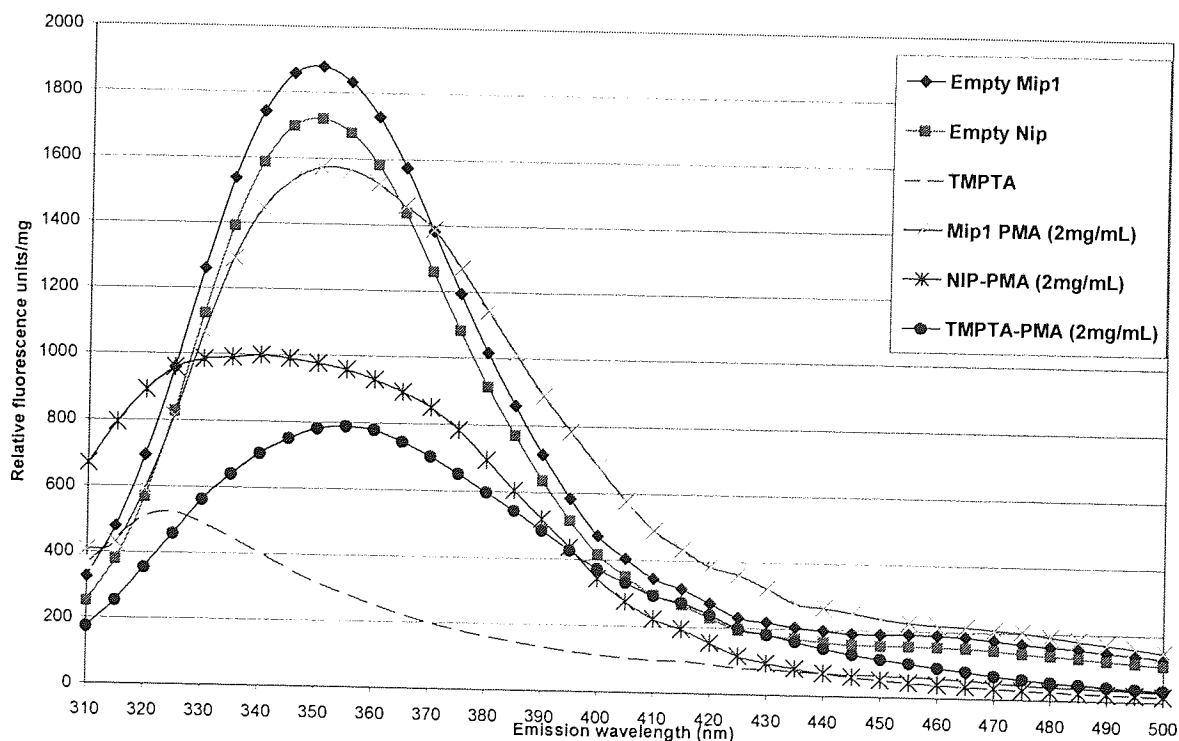


Figure 6.39: Fluorescence spectra for MIP1, NIP and TMPTA when exposed to compound **71** (PMA) at concentrations of 2 mg/mL ($\lambda_{ex} = 290$).

Figure 6.40 (below) showed that when the compound **125** was exposed to MIP1, NIP and TMPTA, no absorption was observed for TMPTA. In contrast small amount of absorption was seen for NIP and MIP1 at the higher wavelength indicating that this difference was perhaps to the presence of functional monomer present in NIP and MIP1.

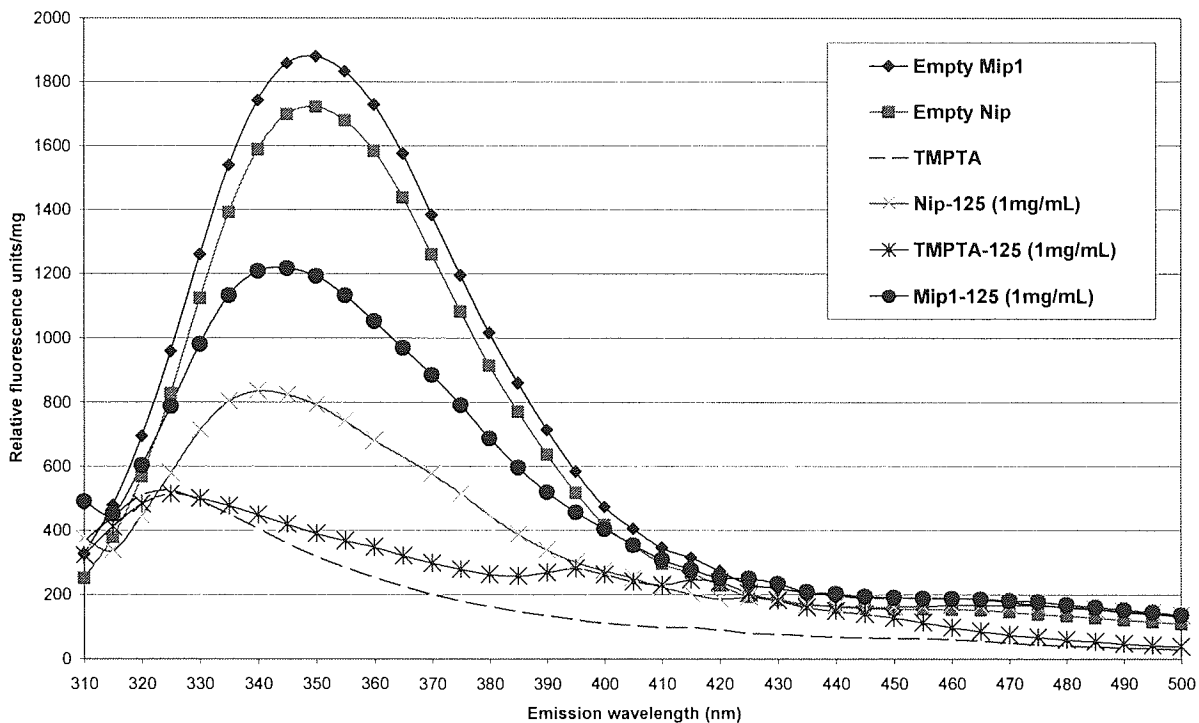


Figure 6.40: Fluorescence spectra for MIP1, NIP and TMPTA when exposed to compound **125** at concentrations of 1 mg/mL ($\lambda_{ex} = 290$).

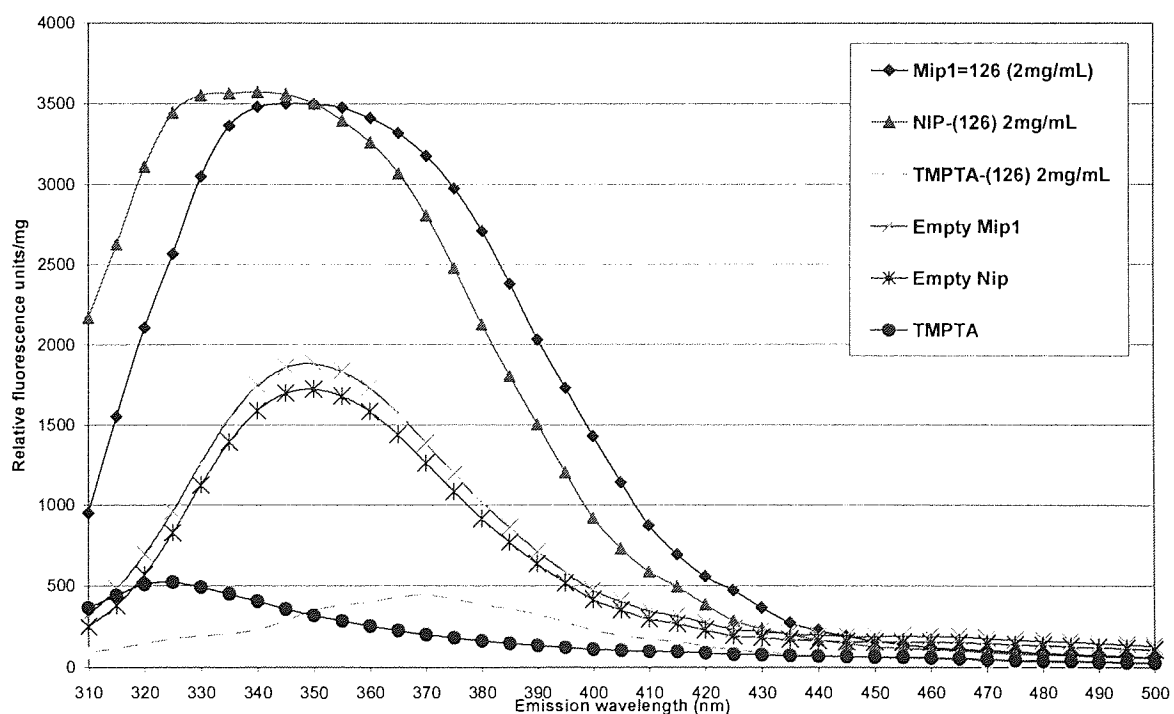


Figure 6.41: Fluorescence spectra for MIP1, NIP and TMPTA when exposed to compound **126** at concentrations of 2 mg/mL ($\lambda_{ex} = 290$).

Figure 6.41 (above) indicates that compound **126** was highly fluorescence. In contrast to TMPTA the fluorescence output of NIP and MIP1 was extremely high.

However, to investigate the performance of MIP1 and to study the results further, the pyrimethamin imprinted polymer MIP2 was also prepared and the results were compared. MIP2 was prepared in THF and with TMPTA as the crosslinker using the same procedure as for the MIP1 see Table 6.4. The ability of the of the imprinted polymer MIP2 to recognise its template pyrimethamine (**71**) and other test compounds (Figure 6.13.) was determined under the same procedure and conditions as for MIP1 and the blank polymers 3 and 4. The results are shown below.

6.8.10 MIP2 -exposed to its template (**71**) and the test compounds

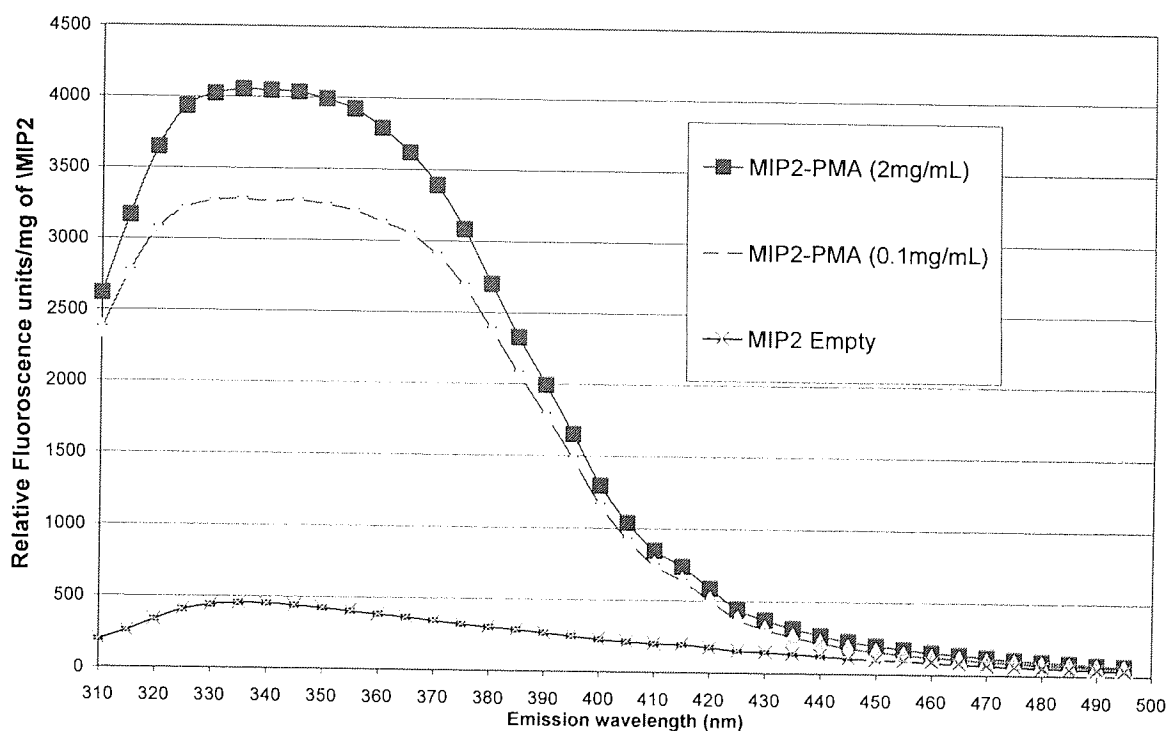


Figure 6.42: Fluorescence spectra for MIP2 re-exposed to its template (**71**) at concentrations of 2 mg/mL and 0.1 mg/mL ($\lambda_{ex} = 290$).

Figure 6.42 shows the rebinding of **71** to its imprinted polymer MIP2. A dose dependent enhancement was observed. A large amount of fluorescence out-put was seen suggesting that MIP2 cavity has probably recognised its template. To investigate the specificity of the imprinted polymer MIP2; it was exposed to **70**. It was assumed that the bigger compound **70** would not be able to get into the cavity and consequently would show lower fluorescence output in contrast to **71**.

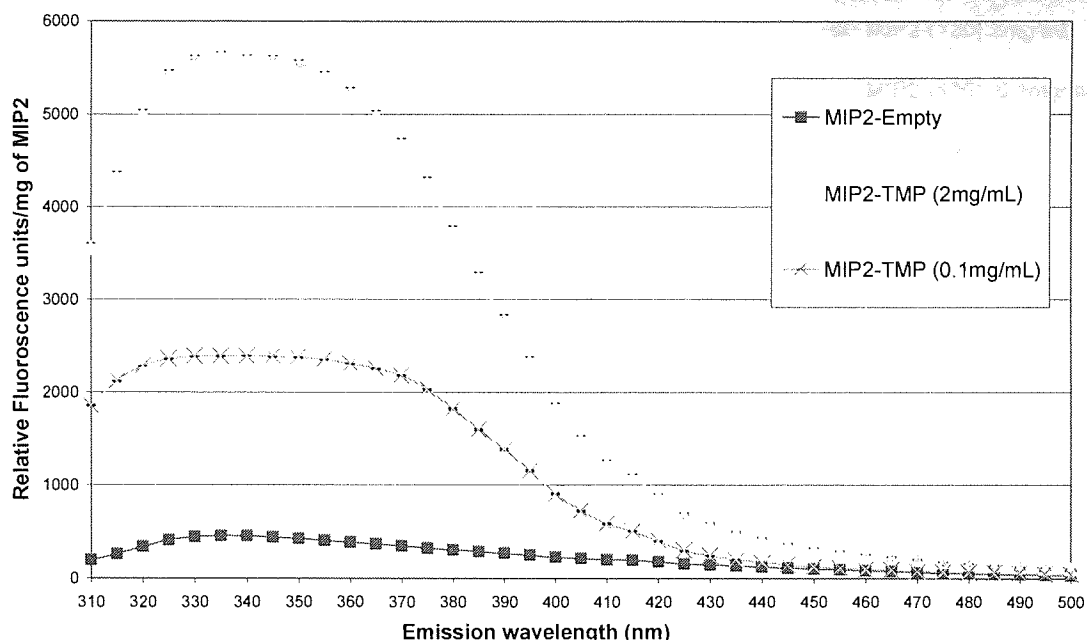


Figure 6.43: Fluorescence spectra for MIP2 exposed to compound **70** at concentrations of 2 mg/mL and 0.1 mg/mL. The quoted errors are the standard deviations of triplicate wells ($\lambda_{ex} = 290$ nm).

Figure 6.43 shows the binding of the test compound **70** to MIP2. A dose dependent enhancement was observed. A significant amount of fluorescent emission was observed indicating that MIP2 had in fact, accommodated **70**. Similarly, when MIP2 was exposed to compound **125** a dose dependent enhancement was observed (**Figure 6.44**) and surprisingly MIP2 did not show any discrimination against this compound as was observed for MIP1 (**Figure 6.22**).

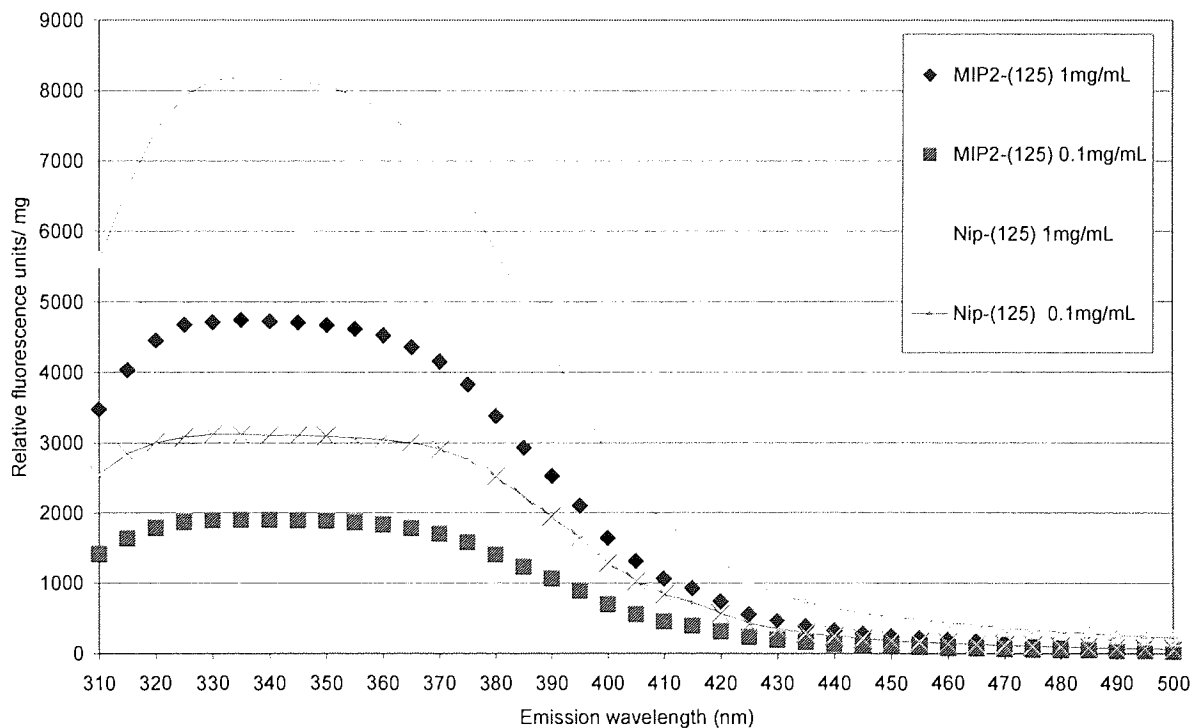


Figure 6.44: Fluorescence spectra for MIP2 exposed to **125** at concentrations of 2 mg/mL and 0.1 mg/mL. The quoted errors are the standard deviations of triplicate wells ($\lambda_{ex} = 290$ nm).

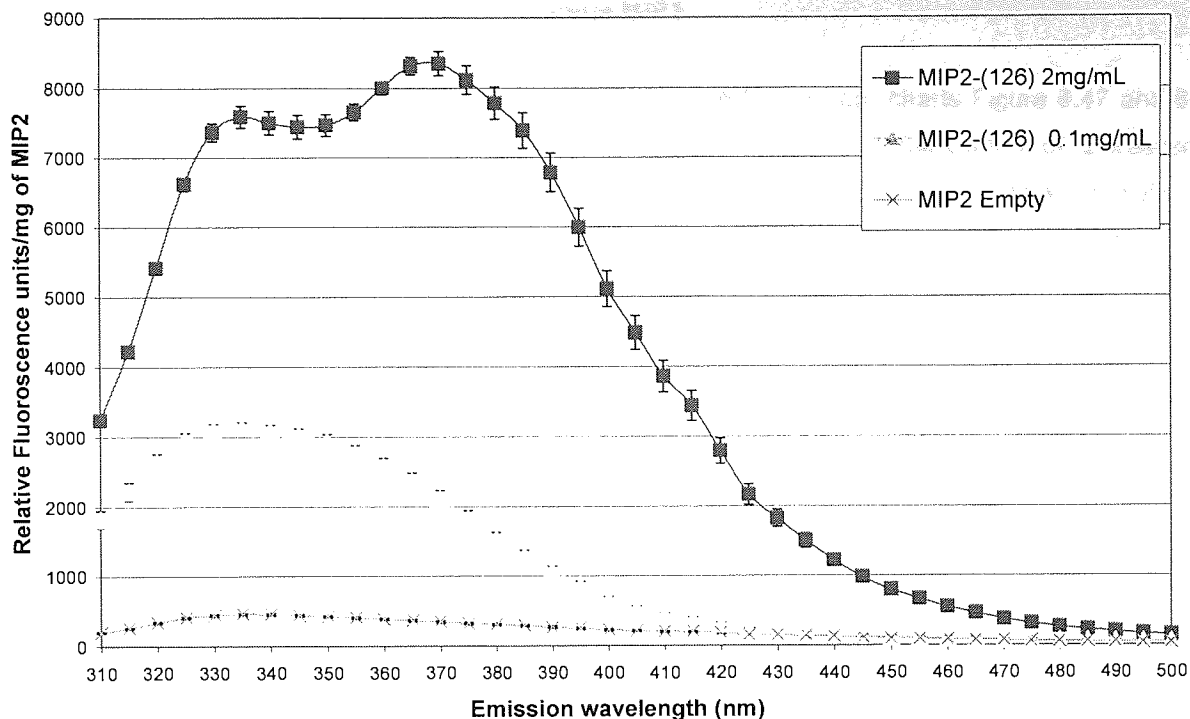


Figure 6.45: Fluorescence spectra for MIP2 exposed to compound **126** at concentrations of 2 mg/mL and 0.1 mg/mL. The quoted errors are the standard deviations of triplicate wells ($\lambda_{ex} = 290$ nm)

As seen in **Figure 6.45** the fluorescence spectra corresponding to MIP2 displayed emission maxima at 335 nm, stronger intensities were also observed at higher wavelengths with a shoulder at 370 nm for the concentration of 2mg/mL. Moreover, the dose dependent enhancements were observed on re-exposure of **126**. The fluorescence out-put has indicated that MIP2 was able to accommodate **126** too. Moreover, the peaks for test compounds **70**, **71** and **125** were broad probably due to the inspecific interactions **Figure 6.46**.

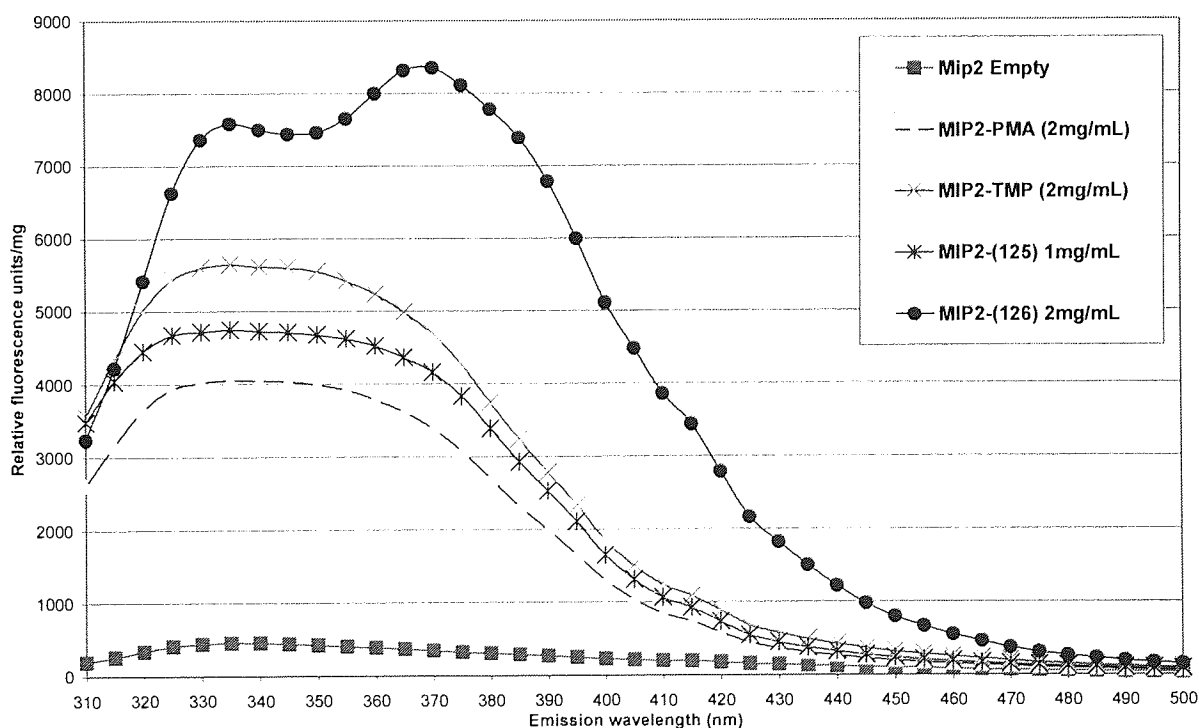


Figure 6.46: Fluorescence spectra for MIP2 exposed to compounds **70**, **71**, **126** and **125** at concentrations of 2 mg/mL and 1 mg/mL respectively ($\lambda_{ex} = 290$ nm).

6.8.11 The performance of MIP1 versus MIP2

The performances of MIP1 and MIP2 were compared in the form of bar charts Figure 6.47 and 6.48 respectively at the emission wavelength of 340 nm. A dose dependent enhancement of fluorescence intensity was observed for both MIP1 and MIP2. MIP1 was more sensitive to its original template and rejected **71** and **125**. This indicates that some binding sites were probably well defined and were able to rebind TMP but too small for the more bulky compounds such as **125**. Moreover, MIP1 has showed a stronger affinity for **126**; this may have been due to the hydrophobic interactions of this highly aromatic compound possessing higher fluorescence.

6.8.11.1 MIP1 re-exposed to its template and the test compounds

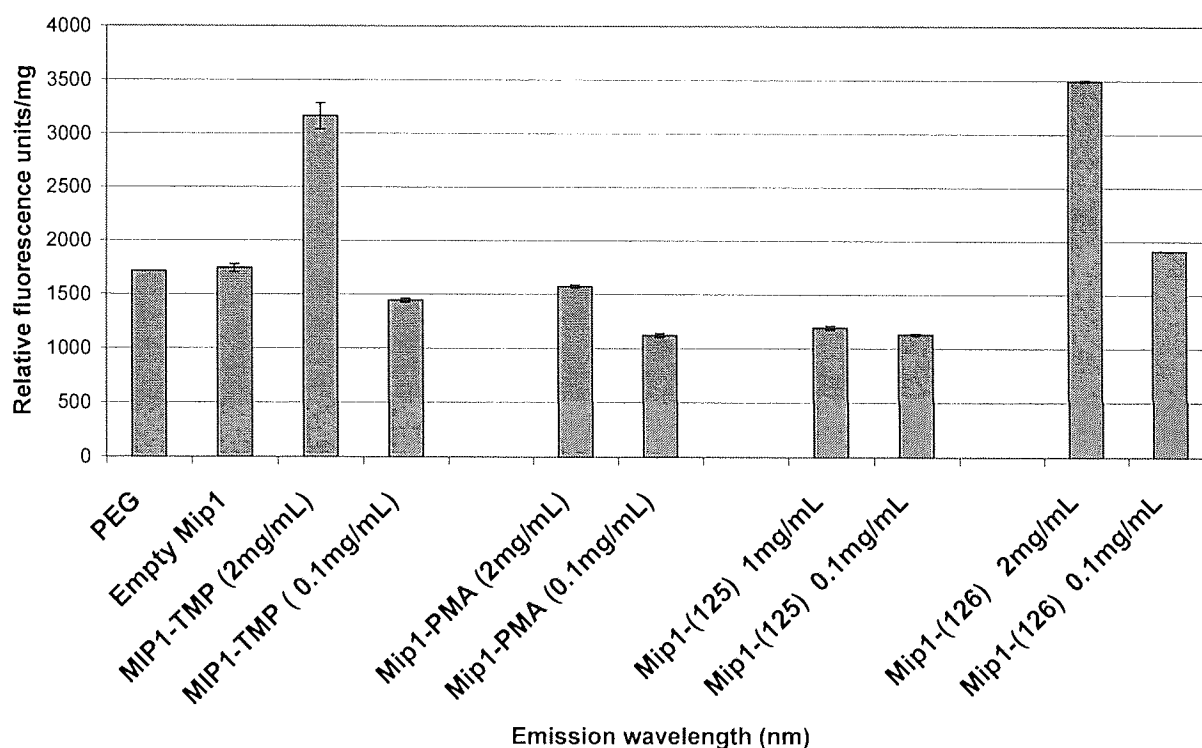


Figure 6.47: Fluorescence output of a MIP1 exposed to solutions of its template **70** and the test compounds **71**, **125** and **126** at 2 mg/mL and 0.1 mg/mL respectively. The quoted errors are the standard deviations of triplicate wells $\lambda_{ex} = 290$ nm, $\lambda_{em} = 340$ nm.

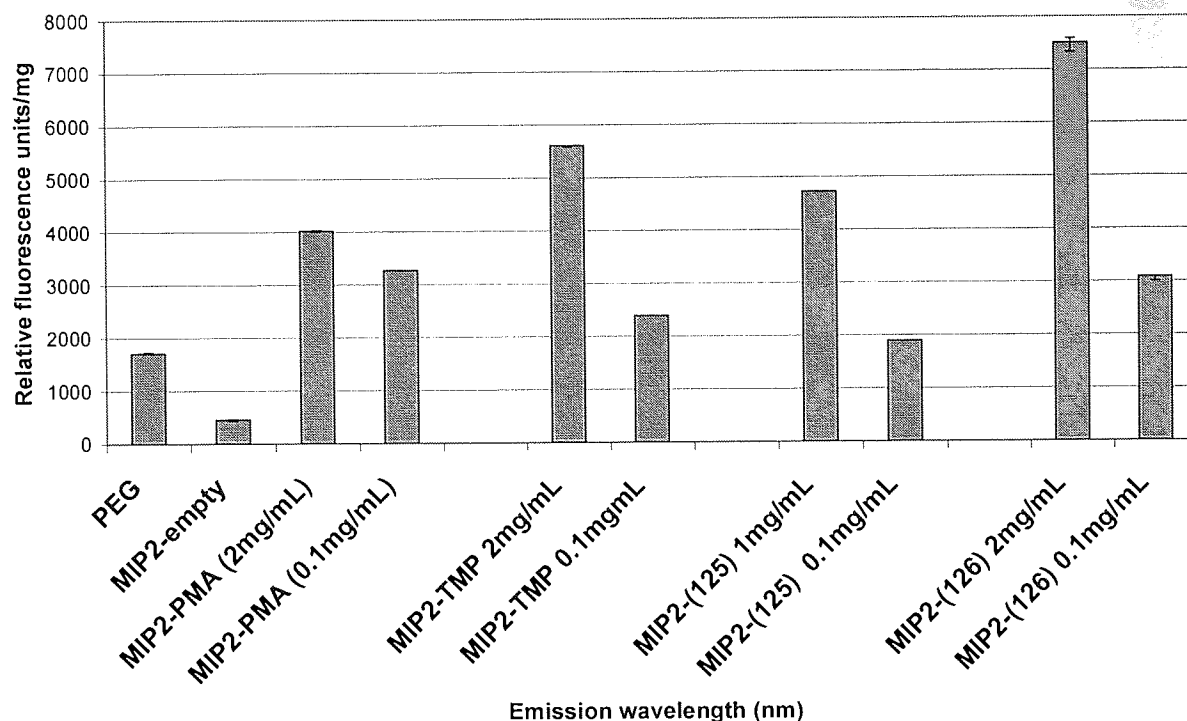


Figure 6.48: Fluorescence output of a MIP2 exposed to solutions of its template **71** and the test compounds **70**, **125** and **126** at 2 mg/mL and 0.1 mg/mL respectively. The quoted errors are the standard deviations of triplicate wells $\lambda_{ex} = 290$ nm, $\lambda_{em} = 340$ nm.

The fact that the pyrimethamine (**71**) imprinted polymer MIP2 bound to a greater extent to all the tested compounds suggested that the binding sites were not of the optimum geometry to discriminate on size of the tested compounds. In addition the uptakes of **70** and **125** were higher than **71** suggesting that the size and electronic factor of the template may have influenced the selectivity performance of the MIP2. In general MIP2 was not specific towards its own template (**71**), hence it recognised/accepted all the tested compounds.

6.8.11.3 Polymer 3 (NIP) exposed to the test compounds

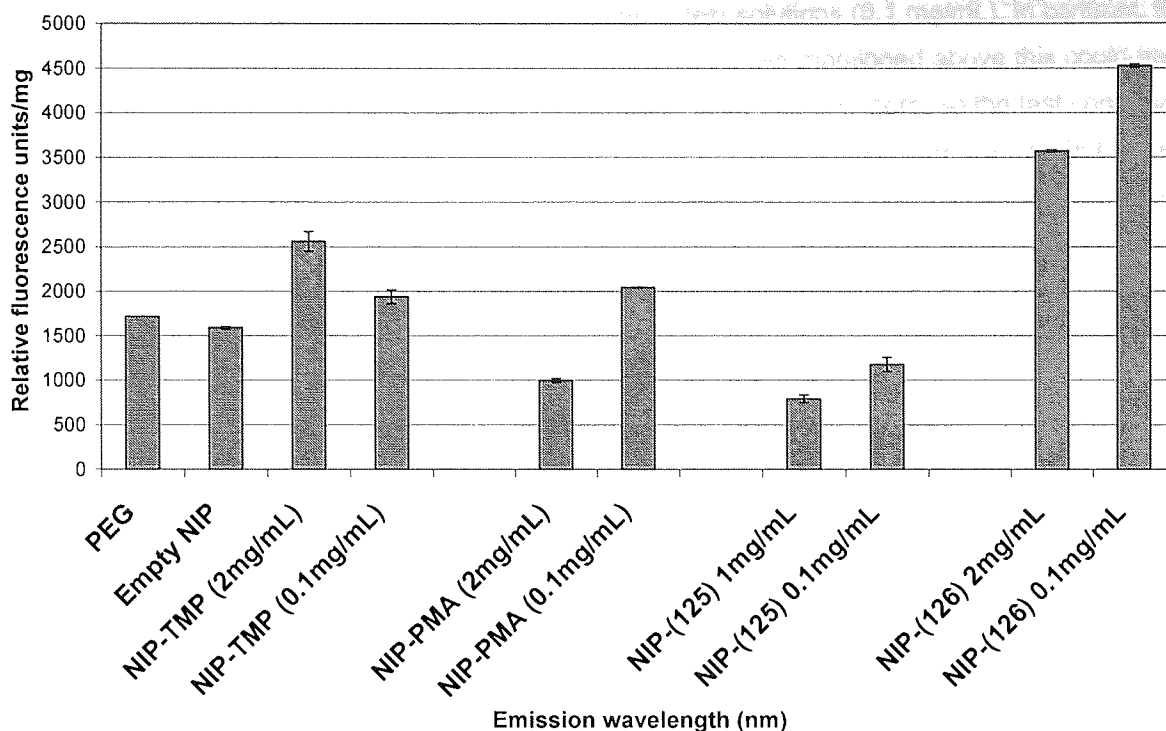


Figure 6.49: Fluorescence output of a blank polymer 3 (NIP) exposed to solutions of test compounds 70, 71, 125 and 126 at 2 mg/mL and 0.1 mg/mL respectively. The quoted errors are the standard deviations of triplicate wells $\lambda_{ex} = 290$ nm, $\lambda_{em} = 340$ nm.

6.8.11.4 Polymer 4 (TMPTA) re-exposed to the test compound

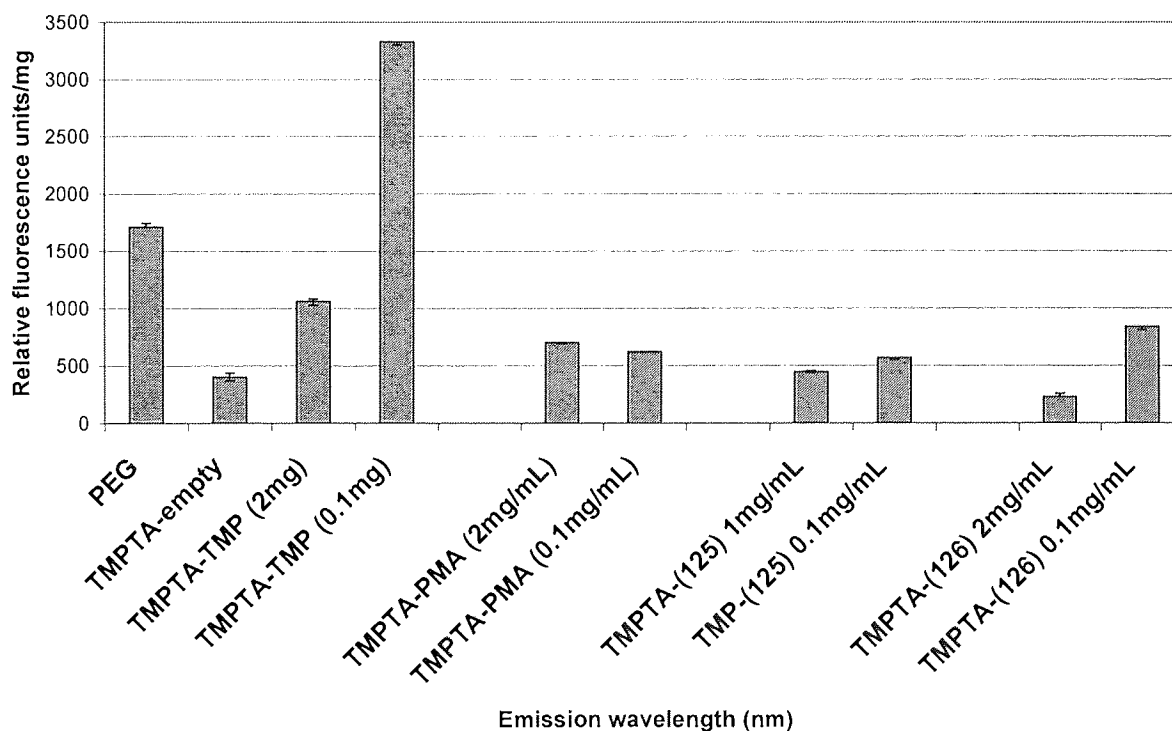


Figure 6.50: Fluorescence output of a blank polymer 4 (TMPTA) exposed to solutions of test compounds 70, 71, 125 and 126 at 2 mg/mL and 0.1 mg/mL respectively. The quoted errors are the standard deviations of triplicate wells $\lambda_{ex} = 290$ nm, $\lambda_{em} = 340$ nm.

The blank polymers 3 and 4 showed a similar trend (Figure 6.20c-d); hence the overall uptake of the tested compounds was seen at the lower concentrations of test solutions (0.1 mg/mL). In contrast, this trend was not followed for the imprinted polymers MIP1 or MIP2. As mentioned above this could have been due to the fact that there was no defined cavity in non-imprinted polymers, so the test compound were distributed randomly in the polymers matrix, therefore the fluorescence was probably self-quenched at the higher concentrations. In this study it appeared that the polymer 4 (TMPTA) was a better control polymer, this is because it showed less absorption of the test compounds in contrast to the polymer 3 (NIP) which contained a functional monomer in its matrix.

8.9 Conclusions

Molecularly imprinted polymers have been prepared using bioactive templates containing the 2,4-diaminopyrimidine unit that possess binding sites mimicking those of the corresponding biological target dihydrofolate reductase, This work has taken its inspiration from Mosbach [Mosbach *et al* 2002]. An anti-idiotypic approach is in its preliminary stage. Due to the time constraints, this study has only demonstrated the principle that the binding sites can be created in the polymers for recognition of 2,4-diaminopyrimidines. The possibility of using this approach would be to facilitate chemical reactions with in the MIP. The artificial sites could be used to control synthetic reactions, so the desired bioactive product can be prepared. For, instance, the binding cavity within the polymer formed would be able to direct synthesis of both the original templates from simpler component molecules and also of related analogues.

The 2,4-diaminopyrimidine containing compounds (trimethoprim and pyrimethamine) were imprinted via the non-covalent approach with acrylic acid 4-(2,4,6-trioxotetrahydropyrimidin-5-ylidenemethyl)phenyl ester (**85**) as a new functional monomer and TMPTA as cross linking monomer in tetrahydrofuran as porogen. Non imprinted polymers were also prepared. Both of the imprinted polymers showed to absorbed direct templates and exhibited dose dependent fluorescence emissions to a greater extent than the control polymers. MIP1 was able to discriminate between different sized ligands, in contrast, non-specific binding was observed for MIP2. This could be that template (**71**) had an electron withdrawing group (chlorine) i.e. para-substituted phenyl attached at position 5 of the 2,4-diaminopyrimidine which decreased the basicity of the N3 ring nitrogen, thereby, making it a weaker hydrogen bond acceptor. Based on these results it could be said that the recognition of 2,4-diaminopyrimidine by the imprinted polymers is dependent on several parameters, including the size of the template, hydrogen bonding, hydrophobic interactions and electrostatic forces.

Although the polymer 3 (NIP) and the polymer 4 (TMPTA) were not very good control polymers they did show some common trends, which must be highlighted, for example, they showed mostly large enhancements at the lower concentrations (0.1 mg/mL) in contrast to 2 mg/mL possibly because of self-quench of the fluorescence at the higher test solution concentration. Although the data has presented some obvious trends a further investigation needs to be done. For example, MIPs and NIPs should be exposed to a wide range of test compounds at lower solution concentrations. In addition they could be prepared using different polymerisation methods with a range of different crosslinkers and different template to functional monomer ratio.

7 Forward To Experimental

7.1 Instrumentation:

Robotic procedures were performed using a Tecan 5072 robotic sampler processor. Proton NMR spectra were obtained on a Bruker AC 250 instrument operating at 250 MHz as solution in d_6 -DMSO and referenced from δ DMSO = 2.5ppm. Infrared were recorded as KBr discs on a Mattson 3000 FTIR spectrophotometer. Atmospheric pressure chemical ionization mass spectrometry (APCI-MS) was carried out a Hewlett-Packard 5989B quadrupole instrument connected to an electrospray 59987A unit with an APCI accessory automatic injection using a Hewlett-Packard 1100 series autosampler. Melting points were obtained using a Reichert-Jung Thermo Galen hot stage microscope and are corrected by calibration against a compound of known melting point. Thin layer chromatography (TLC) was carried out on aluminium silica gel 60 F₂₅₄ plated (Merck). B.D.H. silica gel (MFC) (Merck) Kieselgel Art 7736 was employed for medium pressure or flash column chromatography. Anhydrous magnesium sulphate was used as a drying agent for solutions in organic solvent. Fluorescence analyses were performed in polystyrene standard format 96-well microplates in a molecular Devices SpectraMax Geminix TM dual-scanning microtitre plate spectrofluorometer.

The abbreviations for the NMR spectra are: bs = broad, dd = doublet, d = doublet, m = multiplet, t = triplet, td = triplet of doublet, dt = doublet of triplet, ov = over lapping.

7.1.2 Synthesis of the Heteroarylcarboxamidrazone

7.1.3 Pyridine-2-carboxamidrazone (2PY)

An appropriate cynopyridine (29.99g, 288.4 mmol) was suspended in ethanol (90mL) and treated with hydrazine monohydrate (60 mL) and stirred at ambient temperature for two days. The solvent was then removed by rotary evaporation, at 30°-40°C. The solid material was collected by filtration, washed with hexane (3 x 50 mL) and dried under vacume to give the product as a white crystalline solid.

Yield 36.76 g, 270 mmol, 93.7%. R.f.[EtOAc:MeOH (2:1)]: 0.10.

MS (APCI +ve) m/z = 137 (M+H)⁺

¹H NMR: 5.24 (bs, 2H, NH₂); 5.71 (bs, 2H, NH₂); 7.31 (td, 1H, J=4.9, 1.2 Hz, Pyr-H4); 7.74 (td, 1H, J=6.92, 1.8 Hz, Pyr-H5); 7.91 (m, 1H, Pyr-H3); 8.48 (m, 1H, Pyr-H6) ppm.

7.1.4 Pyridine-3-carboxamidrazone (3PY)

Prepared same as pyridine-2-carboxamidrazone except, that the reaction mixture was stirred at ambient temperature for eleven day. The solid material was collected by filtration, washed with petrol (40-60°C) (3 x 50 mL) and dried under vacume to give the product as brown crystalline solid.

Yield 39.079g , 287 mmol (99%). R.f. [EtOAc:MeOH (2:1)] 0.10.

MS (APCI +ve) m/z = 137 (M+H)⁺

¹H-NMR: 4.26 (bs, 2H, NH₂); 5.73 (bs, 2H, NH₂); 7.34 (m, 1H, Pyr-H5); 8.01 (dt, 1H, J= 2.0, 3.7 Hz, Pyr-H4); 8.48 (d, 1H, J= 4.7Hz, Pyr-H6); 8.86 (d, H, J=2.1 Hz, Pyr-H2) ppm.

7.1.5 Pyridine-4-carboxamidrazone (4PY)

Prepared in the same manner as described for 3-pyridincarboxamidrazone. Brown crystalline solid.

Yield: 36.09g, 265 mmol, (92%). R.f. [EtOAc:MeOH (2:1)]: 0.18.

MS (APCI +ve) m/z = 137 (M+H)⁺

¹H-NMR: 5.33 (bs, 2H, NH₂); 5.71 (bs,2H, NH₂); 7.63 (d, 2H, J=6.3 Hz, Pyr-H5 and H3); 8.51 (d, 2H, J=6.3 Hz, Pyr-H2 and H6) ppm.

7.1.6 Pyrazinyl-2-carboxamidrazone (PZ)

Prepared in the same manner as described for pyridin-2-carboxamidrazone.

Yellow crystalline solid.

Yield 8.72g, 63.6 mmol, (68%). R.f. [EtOAc:MeOH (9:1)]: 0.23.

MS (APCI +ve) m/z = 138 (M+H)⁺

¹H-NMR 5.57 (bs, 2H, NH₂); 5.75 (bs, 2H, NH₂); 8.50 (s, 2H, PZ-H5 and H6); 9.01 (s,1H, PZ-H3) ppm.

7.1.7 Quinoly-2-carboxamdrazone (QN)

Prepared in the same manner as described for pyridin-2-caboxamidrazone. Yellow crystalline solid.

Yield 9.0g, 48.4 mmol, 83%. R.f. [EtOAc:MeOH (9:1)]: 0.39.

MS (APCI +ve) m/z = 187 (M+H)⁺

¹H-NMR: 4.78 (bs,2H, NH₂); 5.48 (bs,2H, NH₂); 7.68 (ddd, 1H, J=6.9Hz, QN-H6 or H7); 7.73 (ddd, 1H, J=6.9 Hz, QN-H6 or H7); 7.85 (d,1H, J=8.4Hz, QN-H5 or H8); 8.09 (td, 3H, J=8.8, 8.8Hz, QN-H3 and H4).

7.1.8 Pyridine-4-carboxamidrazone-4-N-oxide (4PY-NO)

1-Oxy-isonicotinonitrile (14.516 g, 121 mmol) was suspended in ethanol (45 mL) and treated with hydrazine monohydrate (30 mL) and stirred at ambient temperature for nine days. The solid material was collected by filtration, washed with ethanol (3 x 30 mL) and dried under vacuum to give the product as a yellow crystalline solid.

Yield 15.46 g, 102 mmol, 84%.

MS (APCI +ve) m/z = 153 (M+H)⁺

¹H NMR: 5.32 (bs, 2H, NH₂), 5.71 (bs, 2H, NH₂), 7.64 (d, 2H, J=7.2Hz, Pyr-H2 and H6), 8.13 (d, 2H, J=7.2Hz, Pyr-H3 and H5) ppm.

7.2. Synthesis of the *N*¹-Arylidene-pyridinecarboxamidrazone

7.2.1 General method for the preparation of *N*¹-Arylidene-pyridinecarboxamidrazone

A mixture of heteroarylcarboxamidrazone (1.0 g, 7.35 mmol) and an appropriate benzylaldehyde (1.1 eq.) in ethanol (20 ml) was refluxed at the boil for 12 h. The resultant mixture was cooled, filtered and washed with ethanol (15 ml) three times. If necessary the material was purified by recrystallisation.

7.2.2 Characterisation of *N*¹-arylidene-pyridine-2-carboxamidrazone

7.2.3. *N*¹-(4-Methylbenzylidene)-pyridine-2-carboxamidrazone (2PYaa).

Recrystallised from ethanol to give yellow crystalline solid. Yield 1.5583 g, 6.55 mmol, 89%; R.f. [EtOAc : MeOH 8:2]: 0.49

MP 122.2-123.8 °C

MS (APCI +ve) *m/z* = 239 (M+H)⁺ 118 (M-PyrNH₂CN=N)⁺

¹H NMR: 2.36 (s, 3H, Me), 7.03 (bs, 2H, NH₂), 7.26 (d, 2H, J=8.0 Hz, Ar-3H and 5H), 7.53 (m, 1H, Pyr-H4), 7.81 (d, 2H, J= 8.0 Hz, Ar-2H and 6H), 7.92 (td, 1H, J= 7.7, 1.8 Hz, Pyr-H5), 8.24 (d, 1H, 8.0 Hz, Pyr-3H), 8.46 (s, 1H, N=CH), 8.65 (d, 1H, J= 5.5 Hz, Pyr-H6) ppm.

7.2.4 *N*¹-(4-Ethylbenzylidene)-pyridine-2-carboxamidrazone (2PYab).

Recrystallised from ethanol to give yellow crystalline solid. Yield (0.898g, 3.56 mmol, 49%. R.f. [EtOAc]: 0.54.

MS (APCI +ve) *m/z* 253 (M+H)⁺ 132 (M-PyrNH₂CN=N)⁺

¹H NMR: 1.17 (t, 3H, J= 7.5 Hz, Me), 2.50-2.67 (m, 2H CH₂), 7.04 (bs, 2H, NH₂), 7.27 (d, 2H, J= 8.0 Hz, Ar-H3 and H5), 7.50 (m, 1H, Pyr-H4), 7.80 (d, 2H, J= 8.3 Hz, Ar-H2 and H6), 7.91 (td, 1.5, 7.8 Hz, Pyr-H5), 8.20 (d, 1H, J= 7.8 Hz, Pyr-H3), 8.63 (s, 1H, N=CH), 8.65 (d, 1H, J= 5.5 Hz, Pyr-H6) ppm.

7.2.5 *N*¹-(2-Ethylbenzylidene)-pyridine-2-carboxamidrazone (2PYac)

Recrystallised from ethanol twice to give yellow crystalline solid. Yield 1.334g, 5.29 mmol (72%). R.f. [EtOAc]: 0.53

MS (APCI +ve) *m/z* = 253 (M+H)⁺, 132 (M-PyrNH₂CN=N)⁺

¹H NMR: 1.18 (t, 3H, J= 7.5 Hz, Me), 2.50-2.67 (m, 2H, CH₂), 7.03 (bs, 2H, NH₂), 7.27 (d, 2H, J= 8.0 Hz, Ar-H3 and H5), 7.49-7.55 (m, 1H, Pyr-H4), 7.80 (d, 2H, J= 8.0 Hz, Ar-H4 and H6), 7.91 (td, 1H, 1.8 and 7.8 Hz, Pyr-H5), 8.20 (d, 1H, J= 8.0 Hz, Pyr-H3), 8.44 (s, 1H, N=CH), 8.63-8.67 (m, 1H, Pyr-H6) ppm.

7.2.6 *N*¹-(4-Isopropylbenzylidene)-pyridine-2-carboxamidrazone (2PYad)

Recrystallised from ethanol to give yellow crystalline solid. Yield 0.884g, 3.32 mmol, (45%) R.f. [EtOAc]: 0.55

MP 65.5-67.2 °C

MS (APCI +ve) *m/z* = 267 (M+H)⁺, 146 (M-PyrNH₂CN=N)⁺

¹H NMR: 1.18 (s, 3H, Me), 1.21 (s, 3H, Me), 2.85-2.96 (m, 1H, CMe₂), 7.03 (bs, 2H, NH₂), 7.30 (d, 2H, J= 8.3 Hz, Ar-H3 and H5), 7.50-7.55 (m, 1H, Pyr-H4), 7.81 (d, 2H, J= 8.3 Hz, Ar-H2 and H6), 7.91 (td, 1H, J= 1.8 and 7.8 Hz, Pyr-H5), 8.20 (d, 1H, J= 8.8 Hz, Pyr-H3), 8.44 (s, 1H, N=CH), 8.64 (d, 1H, J= 5.8 Hz, Pyr-H6) ppm.

7.2.7 *N*¹-(4-Acetamidobenzylidene)-pyridine-2-carboxamidrazone.(2PYae)

Recrystallised from the mixture of MeOH and EtOH (2:8) respectively to afford yellow crystalline solid. Yield 1.594g, 5.67 mmol (77)% yield.

MS (APCI +ve) *m/z* = 282 (M+H)⁺, 161 (M-PyrNH₂CN=N)⁺, 238 (M-CO₂)⁺

¹H NMR: 2.04 (s, 3H, =Ome), 7.02 (bs, 2H, NH₂), 7.48-7.54 (m, 1H, Pyr-H4), 7.62 (d, 2H, J= 8.5 Hz, Ar-H2 and H6), 7.82 (d, 2H, J= 8.5 Hz, Ar-H3 and H5), 7.90 (td, 1H, J= 1.8 and 7.8 Hz, Pyr-H5), 8.18 (d, 1H, 8.0 Hz, Pyr-H3), 8.39 (s, 1H, N=CH), 8.63 (d, 1H, J, 4.8 Hz, Pyr-H6), 10.18 (bs, 1H, NH) ppm.

7.2.8 *N*¹-(4-*tert*-Butylbenzylidene)-pyridine-2-carboxamidrazone (2PYaf)

Recrystallised from ethanol twice to give yellow crystalline solid. Yield 1.907g, 6.81 mmol (93%) yield. R.f. [EtOAc]: 0.64

MP 122.6-124.1 °C

MS (APCI +ve) *m/z* = 281 (M+H)⁺, 160 (M-PyrNH₂CN=N)⁺

¹H NMR: 1.29 (s, 9H, CMe₃), 7.03 (bs, 2H, NH₂), 7.46 (d, 2H, J= 8.5 Hz, Ar-H3 and H5), 7.51-7.55 (m, 1H, Pyr-H4), 7.82 (d, 2H, J=8.5 Hz, Ar-H2 and H6), 7.92 (dt, 1H, J= 1.7 and 7.1 Hz, Pyr-H5), 8.21 (d, 1H, J=8.0 Hz, Pyr-H3), 8.44(s, 1H, N=CH), 8.66 (d, 1H, J= 4.8 Hz, Pyr-H6) ppm.

7.2.9 *N*¹-(1-Naphthylidene)-pyridine-2-carboxamidrazone (2PYag)

Recrystallises from a mixture of ethanol and ethyl acetate (40:60) respectively to give yellow crystalline solid. Yield 1.821g, 6.65 mmol (80%). R.f. [EtOAc]: 0.52

MP 111.9-115.1 °C

MS (APCI +ve) *m/z* = 275 (M+H)⁺, 154 (M-PyrNH₂CN=N)⁺

¹H NMR: 7.12 (bs, 2H, NH₂), 7.53-7.68 (ov.m, 4H, Pyr-4H and 3Ar-H), 7.92-8.03 (m, 3H, 3Ar-H), 8.22-8.31 (ov.m, 2H, Pyr-H5 and Ar-H), 8.68 (d, 1H, J= 4.8 Hz, Pyr-H3), 8.86 (d, 1H, J= 8.3 Hz, Pyr-H6), 9.19 (s, 1H, N=CH) ppm.

7.2.10 *N*¹-(9-Phenanthrene)-pyridine-2-carboxamidrazone (2PYah)

Recrystallised from ethanol three times to afford yellow crystalline solid. Yield (1.979g, 6.11 mmol (91%).

MS (APCI +ve) *m/z* = 325 (M+H)⁺, 204 (M-PyrNH₂CN=N)⁺

¹H NMR: 7.18 (bs, 2H, NH₂), 7.54-7.59 (m, 1H, Pyr-H4), 7.65-7.79 (m, 3H, 3Ar-H), 7.96 (td, 1H, J= 1.5 and 7.5 Hz, Pyr-H5), 8.09 (d, 2H, J= 7.8 Hz, 2Ar-H), 8.32 (d, 1H, J= 8.0 Hz, Ar-H), 8.56 (s, 1H, Ar-H),

8.62 (d, 1H, J= 4.0 Hz, Ar-H), 8.82-8.91 (m, 2H, Pyr-H3 and Ar-H), 9.02-9.06 (m, 1H, Pyr-H6), 9.20 (s, 1H, N=CH) ppm.

7.2.11 *N*¹-(9-Anthrylidene)-pyridine-2-carboxamidrazone (2PYai)

Recrystallised from MeOH to afford yellow crystalline solid. Yield 2.117g, 6.53mmol, (89%).

MS (APCI +ve) m/z = 325 (M+H)⁺, 204 (M-PyrNH₂CN=N)⁺

¹H NMR: 7.02-7.09 (bs, 2H, NH₂), 7.51-7.66 (ov.m, 5H, Pyr-H4 and 4Ar-H), 7.99 (td, 1H, J= 1.8 and 7.5 Hz, Pyr-H5), 8.15 (d, 2H, 7.8 Hz, Pyr-H3 and Ar-H), 8.38 (d, 1H, j= 8.0 Hz, Ar-H), 8.70 (d, 4H, J= 8.3 Hz, Pyr-H6 and 3Ar-H), 9.67 (s, 1H, N=CH) ppm.

7.2.12 *N*¹-(2-Benzyloxybenzylidene)-pyridine-2-carboxamidrazone (2PYaj)

Yellow crystalline solid. Yield 2.069g, 6.27 mmol, 85 %. R.f. [EtOAc]: 0.49

MS (APCI +ve) m/z = 331 (M+H)⁺, 209 (M-PyrNH₂CN=N)⁺

¹H NMR: 5.19 (s, 2H, OCH₂Ph), 6.98-7.06 (ov.m, 3H, NH₂ and Ar-H5), 7.27 (d, 1H, J= 8.5 Hz, Pyr-H4), 7.43 (m, 5H, 5Phenyl-H) 7.89 (td, 1H, J= 1.8, 7.8 Hz, Pyr-H5), 8.19(d, 3H, J= 7.8 Hz, Pyr-H3, Ar-H2 and H3), 8.64 (d, 2H, J= 5.3 Hz, Pyr-H6 and Ar-H5), 8.77 (s, 1H, N=CH) ppm.

7.2.13 *N*¹-(3-Benzyloxy-4-methoxybenzylidene)-pyridine-2-carboxamidrazone (2PYak)

Yellow crystalline solid. Yield 2.147g, 5.96 mmol (81%). R.f. [EtOAc]: 0.51

MP 149.2-151.9 °C

MS (APCI +ve) m/z = 361 (M+H)⁺, 240 (M-PyrNH₂CN=N)⁺

¹H NMR: 3.79 (s, 3H, OMe), 5.15 (s, 2H, OCH₂Phenyl), 7.05 (d, 1H, 8.3 Hz, Ar-H5), 7.07 (bs, 2H, NH₂), 7.29-7.52 (ov.Ar-H6m and H, 5Phenyl-H), 7.75 (d, 1H, J= 1.8 Hz, Pyr-H4), 7.91 (td, 1H, J= 1.8, 7.8 Hz, Pyr-H5), 8.8.20 (d, 1H, J= 8.0 Hz, Pyr-H3), 8.38 (s, 1H, N=CH), 8.65 (d, 1H, J= 4.8 Hz, Pyr-H6) ppm.

7.2.14 *N*¹-(4-Benzyloxy-3-methoxybenzylidene)-pyridine-2-carboxamidrazone (2PYal)

Recrystallised from ethanol to give yellow crystalline solid. Yield 1.082g, 3.0 mmol, (41%). R.f. [EtOAc]: 0.47

MP 143.6-144.8 °C

MS (APCI +ve) m/z = 361 (M+H)⁺, 240 (M-PyrNH₂CN=N)⁺

¹H NMR: 3.86 (s, 3H, OMe), 5.12 (s, 2H, OCH₂Ph), 7.08 (d, 1H, J= 8.3 Hz, Ar-H2), 7.28 (d, 1H, 8.3 Hz, Ar-H6), 7.37-7.55 (ov.m, 8H, NH₂, 5Phenyl-H, Pyr-H4), 7.64 (m, 1H, Ar-H5), 7.91 (td, 1H, J= 1.8, 7.5 Hz, Pyr-H5), 8.20 (d, 1H, 8.8 Hz, Pyr-H3), 8.38 (s, 1H, N=CH), 8.65 (d, 2H, J= 5.0 Hz, Pyr-H6) ppm.

7.2.15 *N*¹-(4-Formyl-benzoic acid methyl ester)-pyridine-2-carboxamidrazone (2PYan)

Yellow crystalline solid. Yield 1.069g, 3.79 mmol (52%).

MS (APCI +ve) m/z = 283 (M+H)⁺, 162 (M-PyrNH₂CN=N)⁺

¹H NMR: 3.99 (s, 3H, OMe), 6.65 (bs, 2H, NH₂), 7.45 (m, 1H, Pyr-H4), 7.80 (td, 1H, J= 1.8, 7.5 Hz, Pyr-H5), 7.91 (d, 2H, J= 6.3 Hz, Ar-H2 and H6), 8.09 (d, 2H, J= 6.7 Hz, Ar-H3 and H5), 8.36 (d, 2H, J= 7.5 Hz, Pyr-H3 and H5), 8.48 (s, 1H, N=CH), 8.63 (d, 1H, J= 5.1, Pyr-H6) ppm.

7.3 Characterisation of *N*¹-Arylidene-pyridine-3-carboxamidrazone

7.3.1 *N*¹-(4-Methylbenzylidene)-pyridine-3-carboxamidrazone (3PYaa)

Yellow crystalline solid. Yield 2.401g, 10.0 mmol (69%).

MS (APCI +ve) *m/z* = 239 (M+H)⁺, 118 (M-Pyr-NH₂C=N)⁺

¹H NMR: 2.35 (s, 3H, Me), 7.15 (bs, 2H, NH₂), 7.26 (d, 2H, J= 8.0 Hz, Ar-H3 and H5), 7.49 (m, 1H, Pyr-H5), 7.80 (d, 2H, J= 8.3 Hz, Ar-H2 and H6), 8.26 (dt, 1H, J= 1.8, 4.0 Hz, Pyr-H4), 8.42 (s, 1H, N=CH), 8.65 (dd, 1H, J= 1.5, 4.8 Hz, Pyr-H6), 9.10 (d, 1H, J= 1.6 Hz, Pyr-H2) ppm.

7.3.2 *N*¹-(4-Ethylbenzylidene)-pyridine-3-carboxamidrazone (3PYab)

Yellow crystalline solid. Yield 2.864g, 11.3 mmol (77%).

MS (APCI +ve) *m/z* 253 (M+H)⁺ 132 (M-PyrNH₂CN=N)⁺

¹H NMR: 1.33 (t, 3H, Me), 3.34 (s, 2H, CH₂), 7.14 (bs, 2H, NH₂), 7.49 (ov.m, 3H, Ar-H3, H5 and Pyr-H5), 7.83 (d, 2H, J= 8.3 Hz, Ar-H2 and H6), 8.28 (dt, 1H, J= 1.5, 3.8 Hz, Pyr-H4), 8.43 (s, 1H, N=CH), 8.66 (dd, 1H, J= 1.8, 4.8 Hz, Pyr-H6), 9.11 (d, 1H, J= 2.3 Hz, Pyr-H2) ppm.

7.3.3 *N*¹-(4-Isopropylbenzylidene)-pyridine-3-carboxamidrazone (3PYad)

Yellow crystalline solid. Yield 2.796g, 10.50 mmol (97%).

MS (APCI +ve) *m/z* = 267 (M+H)⁺

¹H NMR: 1.19 (m, 6H, 2Me), 2.93 (m, 1H, isoprop-H), 7.14 (bs, 2H, NH₂), 7.31 (d, 2H J= 8.3 Hz, Ar-H3 and H5), 7.48 (m, 1H, Pyr-H5), 7.82 (d, 2H, J= 8.3 Hz, Ar-H2 and H6), 8.28 (dt, 1H, J= 2.0, 8.3 Hz, Pyr-H4), 8.43 (s, 1H, N=CH), 8.66 (d, 1H, J= 6.5 Hz, Pyr-H6), 9.10 (d, 1H, J= 2.3 Hz, Pyr-H2) ppm.

7.3.4 *N*¹-(4-Acetamidobenzylidene)-pyridine-3-carboxamidrazone (3PYae)

Yellow crystalline solid. Yield 2.768g, 9.85 mmol (79%).

MS (APCI +ve) *m/z* = 282 (M+H)⁺, 161 (M-PyrNH₂CN=N)⁺, 238 (M-CO₂)⁺

¹H NMR: 2.06 (s, 3H, Me), 7.13 (bs, 2H, NH₂), 7.47 (m, 1H, Py-H5), 7.64 (d, 2H, J= 8.5 Hz, Ar-H2 and H6), 7.84 (d, 2H, J= 8.5 Hz, Ar-H2 and H6 Hz), 8.27 (dt, 1H, J= 1.3, 4.5 Hz, Pyr-H4), 8.39 (s, 1H, N=CH), 8.60 (bs, 1H, NH), 8.65 (dd, 1H, J= 1.8, 4.8 Hz, Pyr-H6), 9.09 (d, 1H, J= 2.0 Hz, Pyr-H2) ppm.

7.3.5 *N*¹-(4-*tert*-Butylbenzylidene)-pyridine-3-carboxamidrazone (3PYaf)

Yellow brown crystalline solid. Yield 2.397g, 8.56 mmol (58%).

MS (APCI +ve) *m/z* = 281 (M+H)⁺, 160 ((M-Pyr-NH₂C=N)⁺

¹H NMR: 1.29 (s, 9H, CMe₃), 7.13 (bs, 2H, NH₂), 7.49 (ov.m, 3H, Ar-H3, H5 and Pyr-H5), 7.81 (m, 2H, Ar-H2 and H6), 8.27 (dt, 1H, J= 1.7, 7.1 Hz, Pyr-H4), 8.43 (s, 1H, N=CH), 8.66 (d, 1H, J= 6.3 Hz, Pyr-H6), 9.09 (d, 1H, J= 2.0 Hz, Pyr-H2) ppm.

7.3.6 *N*¹-(1-Naphthylidene)-pyridine-3-carboxamidrazone (3PYag)

Yellow crystalline solid. Yield 2.599g, 9.48 mmol, (89%).

MS (APCI +ve) *m/z* = 275 (M+H)⁺ 154 (M-PyrNH₂CN=N)⁺

¹H NMR: 7.24 (bs, 2H, NH₂), 7.59 (m, 5H, 5Ar-H), 8.00 (dd, 2H, J= 2.9, 8.1 Hz, 2Ar-H), 8.35 (m, 1H, Pyr-H5), 8.69 (bs, 1H, N=CH), 8.83 (d, 1H, J= 8.3 Hz, Pyr-H4), 9.20 (bs, 2H, Pyr-H6 and H2) ppm.

7.3.7 *N*¹-(9-Phenanthrene)-pyridine-3-carboxamidrazone (3PYah)

Yellow crystalline solid. Yield 2.520g, 11.25 mmol (77%).

MS (APCI +ve) *m/z* = 325 (M+H)⁺, 204 (M-PyrNH₂CN=N)⁺

¹H NMR: 7.32 (bs, 2H, NH₂), 7.55 (m, 1H, Ar-H), 7.67-7.80 (m, 4H, 4Ar-H), 8.10 (d, 1H, J= 7.5 Hz, Pyr-H5), 8.35 (dt, 1H, J= 2.0, 3.8 Hz, Pyr-H4), 8.59 (s, 1H, N=CH), 8.70 (d, 1H, J= 4.5 Hz, Ar-H), 7.72-7.80 (m, 3H, 3Ar-H), 9.18 (d, 2H, J= 8.3 Hz, Pyr-H2 and H6) ppm.

7.3.8 *N*¹-(2-Benzyloxybenzylidene)-pyridine-3-carboxamidrazone (3PYaj).

Yellow crystalline solid. 2.541g, 7.70 mmol (73%).

MS (APCI +ve) *m/z* = 331 (M+H)⁺, 209 (M-PyrNH₂CN=N)⁺

¹H NMR: 5.19 (s, 2H, OCH₂Ph), 7.01 (t, 1H, J= 7.5 Hz, Ar-H5), 7.20 (ov.m, 3H, NH₂ and Ar-H4), 7.34-7.51 (ov.m, 7H, 5Phenyl-H, Ar-H6 and H3), 8.25 (m, 2H, Pyr-H5 and Pyr-H4), 8.65 (dd, 1H, J= 1.5, 4.8 Hz, Pyr-H6), 8.76 (s, 1H, N=CH), 9.08 (bs, 1H, Pyr-H2) ppm.

7.3.9 *N*¹-(3-Benzyloxy-4-methoxybenzylidene)-pyridine-3-carboxamidrazone (3PYak)

Yellow crystalline solid. Yield 2.810g, 7.80 mmol (77%).

MS (APCI +ve) *m/z* = 361 (M+H)⁺, 240 (M-PyrNH₂CN=N)⁺

¹H NMR: 3.80 (s, 3H, OMe) 5.1 (s, 2H, OCH₂Ph), 7.01 (d, 1H, J= 8.3 Hz, Ar-H5), 7.18 (bs, 2H, NH₂), 7.28-7.51 (ov.m, 7H, 5Phenyl-H, Ar-H2 and H6), 7.77 (s, 1H, Pyr-H5), 8.25 (dt, 1H, J= 2.0, 3.8 Hz, Pyr-H4), 8.36 (s, 1H, N=CH), 8.66 (d, 1H, J= 4.8 Hz, Pyr-H6), 9.08 (s, 1H, Pyr-H2) ppm.

7.3.10 *N*¹-(4-Benzyloxy-3-methoxybenzylidene)-pyridine-3-carboxamidrazone (3PYal)

Yellow crystalline solid. 68% yield.

MS (APCI +ve) *m/z* = 361 (M+H)⁺, 240 (M-PyrNH₂CN=N)⁺

¹H NMR: 3.85 (s, 3H, OMe), 5.12 (s, 2H, OCH₂Ph), 7.10 (d, 1H, J= 8.3 Hz, Ar-H2), 7.21 (bs, 2H, NH₂), 7.26-7.33 (ov.m, 7H, 5Phenyl-H, Ar-H6 and H5), 7.66 (d, 1H, J= 1.8 Hz, Pyr-H5), 8.25 (dt, 1H, J= 1.8, 3.8 Hz, Pyr-H4), 8.37 (s, 1H, N=CH), 8.66 (d, 1H, J= 4.8 Hz, Pyr-H6), 9.08 (s, 1H, Pyr-H2) ppm.

7.4 Characterisation of *N*¹-Arylidene-pyridine-4-carboxamidrazone.

7.4.1 *N*¹-(4-Methylbenzylidene)-pyridine-4-carboxamidrazone (4PYaa).

Recrystallised from ethanol to give a yellow crystalline solid. Yield 2.648g, 11.12 mmol (71%).

MS (APCI +ve) *m/z* = 239 (M+H)⁺ 118 (M-PyrNH₂CN=N)⁺

¹H NMR: 2.35 (s, 3H, Me), 7.17 (s, 2H, NH₂), 7.25 (d, 2H, J= 8.0 Hz, Ar-H3 and H5), 7.81 (d, 2H, J= 8.0 Hz, Ar-H2 and H6), 7.88 (d, 2H, J= 6.3 Hz, Pyr-H3 and H5), 8.44 (s, 1H, =CHAr), 8.68 (d, 2H, J= 6.3 Hz, Pyr-H2 and H6) ppm.

7.4.2 *N*¹-(4-Ethylbenzylidene)-pyridine-4-carboxamidrazone (4PYab).

Yellow crystalline solid. Yield 3.451g, 13.69 (93%).

MS (APCI +ve) *m/z* = 253 (M+H)⁺, 132 (M-PyrNH₂CN=N)⁺

¹H NMR: 1.20 (t, 3H, J= 7.5 Hz, Me), 2.58-2.96 (m, 2H, CH₂), 7.17 (bs, 2H, NH₂), 7.28 (d, 2H, J= 8.3 Hz, Ar-H3 and H5), 7.83 (d, 2H, J= 8.3, Ar-H2 and H6), 7.88 (d, 2H, J= 6.3 Hz, Pyr-H3 and H5), 8.44 (s, 1H, N=CH), 8.67 (d, 2H, J= 6.3 Hz, Pyr-H2 and H6) ppm.

7.4.3 ***N*¹-(2-Ethylbenzylidene)-pyridine-4-carboxamidrazone (4PYac).**

Yellow crystalline solid. Yield 3.510g, 13.92 mmol (95%).

MS (APCI +ve) $m/z = 253$ (M+H)⁺, 132 (M-PyrNH₂CN=N)⁺

¹H NMR: 1.19 (t, 3H, J= 7.5 Hz, Me), 2.59-2.68 (m, 2H, CH₂), 7.16 (bs, 2H, NH₂), 7.27 (d, 2H, J= 8.3 Hz, Ar-H4 and H5), 7.83 (d, 2H, J= 8.3 Hz, Ar-H3 and H6), 7.88 (d, 2H, J= 6.3, Pyr-H3 and H5), 8.44 (s, 1H, N=CH), 8.67 (d, 2H, J= 6.3, Pyr-H2 and H6) ppm.

7.4.4 ***N*¹-(4-Isopropylbenzylidene)-pyridine-4-carboxamidrazone (4PYad)**

Yellow crystalline solid. Yield 3.858g, 14.50 mmol (98%).

MS (APCI +ve) $m/z = 267$ (M+H)⁺, 146 (M-PyrNH₂CN=N)⁺

¹H NMR: 1.20 (s, 3H, Me), 1.23 (s, 3H, Me), 2.86-2.97 (m, 1H, CH), 7.16 (bs, 2H, NH₂), 7.30 (d, 2H, J= 8.0 Hz, Ar_H3 and H5), 7.83 (d, 2H, J=8.3 Hz, Ar-H2 and H6), 7.89 (d, 2H, J= 6.0 Hz, Pyr-H3 and H5), 8.44 (s, 1H, N=CH), 8.68 (d, 2H, J= 6.0 Hz, Pyr-H2 and H6) ppm.

7.4.5 ***N*¹-(4-Acetamidobenzylidene)-pyridine-4-carboxamidrazone (4PYae)**

Yellow crystalline solid. Yield 2.989g, 10.63 mmol (72%).

MP 236.6-238 °C

MS (APCI +ve) $m/z = 282$ (M+H)⁺

¹H NMR: 2.06 (s, 3H, Me), 7.14 (bs, 2H, NH₂), 7.64 (d, 2H, J= 8.5 Hz, Ar-H2 and H6), 7.82 (d, 2H, J= 7.5 Hz, Ar-H-3 and H5), 7.87 (d, 2H, J= 6.3 Hz, Pyr-H3 and H5), 8.39 (s, 1H, N=CH), 8.66 (d, 2H, J= 4.5 Hz, Pyr-H2 and H6), 10.12 (bs, 1H, NH) ppm.

7.4.6 ***N*¹-(4-*tert*-Butylbenzylidene)-pyridine-4-carboxamidrazone (4PYaf)**

Yellow crystalline solid. Yield 3.422g, 12.22 mmol (83%).

MS (APCI +ve) $m/z = 281$ (M+H)⁺, 160 (M-PyrNH₂CN=N)⁺

¹H NMR: 1.30 (s, 9H, CMe₃), 7.19 (bs, 2H, NH₂), 7.45 (d, 2H, J= 8.3 Hz, Ar-H3 and H5), 7.83 (d, 2H, J= 8.3 Hz, Ar-H2 and H6), 7.88 (dd, 2H, J= 1.5 and 4.5 Hz, Pyr-H3 and H5), 8.43 (s, 1H, N=CH), 8.67 (d, 2H, J= 6.3 Hz, Pyr-H2 and H6) ppm.

7.4.7 ***N*¹-(1-Naphthylidene)-pyridine-4-carboxamidrazone (4PYag)**

Yellow crystalline solid. Yield 2.818g, 10.28 mmol (70%).

MS (APCI +ve) $m/z = 275$ (M+H)⁺, 154 (M-PyrNH₂CN=N)⁺

¹H NMR: 7.24 (bs, 2H, NH₂), 7.53-7.67 (m, 3H, 3Ar-H), 7.94 (d, 2H, J= 4.5 Hz, Pyr-H3 and H5), 7.98-8.04 (m, 2H, 2Ar-H), 8.30 (d, 1H, J= 7.3 Hz, Ar-H), 8.71 (d, 2H, J= 4.5 Hz, Pyr-H2 and H6), 8.83 (d, 1H, J= 8.3 Hz, Ar-H), 9.20 (s, 1H, N=CH) ppm.

7.4.8 **4PYah *N*¹-(9-Phenanthrene)-pyridine-4-carboxamidrazone**

Yellow crystalline solid. Yield 2.986g, 9.21 mmol (62%).

MS (APCI +ve) $m/z = 325$ (M+H)⁺, 204 (M-PyrNH₂CN=N)⁺

¹H NMR: 7.33 (bs, 2H, NH₂), 7.67-7.78 (m, 4H, 4Ar-H), 7.96 (d, 2H, J= 6.0 Hz, Pyr-H3 and H5), 8.08 (d, 1H, J= 9.3, Ar-H), 8.62 (s, 1H, Ar-H), 8.72 (d, 2H, J= 6.0 Hz, Pyr-H2 and H6), 8.84-9.01 (m, 3H, 3Ar-H), 9.21 (s, 1H, N=CH) ppm.

7.4.9 *N*¹-(9-Anthrylidene)-pyridine-4-carboxamidrazone (4PYai)

Yellow crystalline solid. Yield 3.694g, 11.40 mmol (77%).

MS (APCI +ve) *m/z* = 325 (M+H)⁺, 204 (M-PyrNH₂CN=N)⁺

¹H NMR: 7.16 (bs, 2H, NH₂), 7.54-7.65 (m, 4H, 4 Ar-H), 7.99(d, 2H, J= 6.0 Hz, Pyr-H3 and H5), 8.15 (d, 2H, J= 9.5 Hz, 2 Ar-H), 8.66 (s, 1H, Ar-H), 8.71 (ov.d, 4H, j=.5.3 and 13.8 Hz, Pyr-H2 and H6, and 2Ar-H), 9.65 (s, 1H, =CHAr) ppm.

7.4.10 *N*¹-(2-Benzyloxybenzylidene)-pyridine-4-carboxamidrazone (4PYaj)

Yellow crystalline solid. Yield 3.689g, 11.17 mmol (76%).

MS (APCI +ve) *m/z* = 331 (M+H)⁺

¹H NMR: 5.20 (s, 2H, OCH₂Ph), 7.01 (t, 1H, J= 7.8 Hz, Ar-H), 7.19 (bd, 2H, NH₂), 7.35-7.51 (m, 7H, 5Phenyl-H and 2Ar-H), 7.87 (d, 2H, J= 6.3 Hz, Pyr-H3 and H5), 8.24 (d, 1H, J= 7.8 Hz, Ar-H), 8.65 (d, 2H, J= 6.3 Hz, Pyr-H2 and H5), 8.76 (s, 1H, N=CH) ppm.

7.4.11 *N*¹-(3-Benzyloxy-4-methoxybenzylidene)-pyridine-4-carboxamidrazone (4PYak)

Recrystallised from ethanol to give a yellow crystalline solid. Yield 3.301g, 9.17 mmol (62%). R.f. [EtOAc]: 0.4

MP 158.7-160.2 °C

MS (APCI +ve) *m/z* = 361 (M+H)⁺, 240 (M-PyrNH₂CN=N)⁺

¹H NMR: 3.81 (s, 3H, OMe) 5.17 (s, 2H, CH₂Ph), 7.03 (d, 1H, J= 8.3 Hz, Ar-H), 7.15 (bs, 2H, NH₂), 7.31-7.52 (m, 6H, 5Phenyl-H and Ar-H), 7.78 (d, 1H, J= 1.8 Hz, Ar-H), 7.88 (d, 2H, J= 6.3 Hz, Pyr-H3 and H5), 8.38 (s, 1H, N=CH), 8.67 (d, 2H, J= 6.0 Hz, Pyr-H2 and H6) ppm.

7.4.12 *N*¹-(4-Benzyloxy-3-methoxybenzylidene)-pyridine-4-carboxamidrazone (4PYal)

Recrystallised from ethanol to give yellow crystalline solid. Yield 2.899g, 8.05 mmol (55%).

MS (APCI +ve) *m/z* = 361 (M+H)⁺, 240 (M-PyrNH₂CN=N)⁺

¹H NMR: 3.86 (s, 3H, OMe), 5.14 (s, 2H, OCH₂Ph), 7.09 (d, 1H, J= 8.3 Hz, Ar-H), 7.15 (bs, 2H, NH₂), 7.28-7.48 (m, 6H, 5phenyl-H and Ar-H), 7.67 (d, 1H, J= 1.8 Hz, Ar-H), 7.88 (d, 2H, J= 6.3 Hz, Pyr-H3 and H5), 8.38 (s, 1H, N =CH), 8.67 (d, 2H, J= 6.0 Hz, Pyr-H2 and H6) ppm.

7.4.13 *N*¹-(4-Formyl-benzoic acid methyl ester)-pyridine-4-carboxamidrazone (4PYan).

Yellow crystalline solid. Yield 3.629g, 12.86 mmol (87%).

MS (APCI +ve) *m/z* = 283 (M+H)⁺, 162 (M-PyrNH₂CN=N)⁺

¹H NMR (D6-DMSO; δDMSO = 2.50ppm), 3.87 (s, 3H, OMe), 7.39 (bs, 2H, NH₂), 7.89 (d, 2H, J= 6.3 Hz, Pyr-H3, H5), 8.04 (dd, 4H, J= 8.5 and 17.8 Hz, 4Ar-H), 8.53 (s, 1H, N =CH), 8.69 (d, 2H, J= 6.3 Hz, Pyr-H2 and H6) ppm.

7.4.14 *N*¹-(4-Nitrobenzylidene)-pyridine-4-carboxamidrazone (4PYar).

Yellow crystalline solid. Yield 2.163g, 8.04 mmol (55%).

MS (APCI +ve) *m/z* = 270 (M+H)⁺.

¹H NMR: 7.51 (bs, 2H, NH₂), 7.90 (d, 2H, J= 6.3 Hz, Pyr-H3 and H5), 8.24 (dd, 4H, J= 8.8 and 18.8 Hz, 4Ar-H), 8.59 (s, 1H, N=CH), 8.70 (d, 2H, J= 5.0 Hz, Pyr-H2 and H6) ppm.

7.5 Characterisation of *N*¹-Arylidene-pyrazin-2-carboxamidrazone

7.5.1 *N*¹-(4-Methylbenzylidene)-pyrazin-2-carboxamidrazone (PZaa).

Yellow crystalline solid. Yield 3.258g, 13.63 mmol (93%).

MS (APCI +ve) *m/z* = 240 (M+H)⁺, 132 (M-PZNH₂CN=N)⁺

¹H NMR: 2.35 (s, 3H, Me), 7.10 (bs, 2H, NH₂), 7.26 (d, 2H, J= 8.0 Hz, Ar-H3 and H5), 7.83 (d, 2H, J= 8.0 Hz, Ar-H2 and H6), 8.48 (s, 1H, N=CH), 8.74 (dd, 2H, J= 2.5 and 11.5 Hz, PZ-H5 and H6), 9.37 (s, 1H, PZ-H3) ppm

7.5.2 *N*¹-(4-Ethylbenzylidene)-pyrazin-2-carboxamidrazone (PZab)

Yellow crystalline solid. Yield 3.162g, 12.49 mmol (86%)

MS (APCI +ve) *m/z* = 254 (M+H)⁺, 132 (M-PZNH₂CN=N)⁺

¹H NMR: 1.20 (t, 3H, J= 7.5 Hz, Me), 2.60-2.69 (m, 2H, CH₂), 7.11 (bs, 2H, NH₂), 7.29 (d, 2H, J= 8.3 Hz, Ar-H3 and H5), 7.85 (d, 2H, J= 8.0 Hz, Ar-H2 and H6), 8.48 (s, 1H, N=CH), 8.74 (dd, 2H, J= 2.5 and 10.0 Hz, PZ-H5 and H6), 9.38 (s, 1H, PZ-H3) ppm.

7.5.3 *N*¹-(2-Ethylbenzylidene)-pyrazin-2-carboxamidrazone (PZac)

Yellow crystalline solid. Yield 2.619g, 10.35 mmol (70%).

MS (APCI +ve) *m/z* = 254 (M+H)⁺, 132 (M-PZNH₂CN=N)⁺

¹H NMR (D₆-DMSO; δDMSO = 2.50ppm), 1.20 (t, 3H, J= 7.5 Hz, Me), 2.60-2.69 (m, 2H, CH₂), 7.11 (bs, 2H, NH₂), 7.29 (d, 2H, J= 8.0 Hz, Ar-H3 and H5), 7.85 (d, 2H, J= 8.0 Hz, Ar-H4 and H6), 8.48 (s, 1H, N=CH), 8.74 (dd, 2H, J= 2.5 and 9.8 Hz, PZ-H5 and H6), 9.37 (s, 1H, PZ-H3) ppm.

7.5.4 *N*¹-(4-Isopropylbenzylidene)-pyrazin-2-carboxamidrazone (PZad)

Yellow crystalline solid. Yield 2.85g, 10.58 mmol (72%)

MS (APCI +ve) *m/z* = 268 (M+H)⁺, 146 (M-PZNH₂CN=N)⁺

¹H NMR: 1.21 (s, 3H, Me), 1.24 (s, 3H, Me), 2.88-2.99 (m, 1H, CH), 7.10 (bs, 2H, NH₂), 7.32 (d, 2H, J= 8.0 Hz, Ar-H3 and H5), 7.85 (d, 2H, J= 8.3 Hz, Ar-H2 and H6), 8.49 (s, 1H, N=CH), 8.77 (dd, 2H, J= 2.5 and PZ-H5 and H6), 9.38 (s, 1H, PZ-H3) ppm.

7.5.5 *N*¹-(4-Acetamidobenzylidene)-pyrazin-2-carboxamidrazone (PZae)

Yellow crystalline solid. Yield 1.785g, 6.33 mmol (43%).

MS (APCI +ve) *m/z* = 283 (M+H)⁺, 161 (M-PZNH₂CN=N)⁺ 239 (M-CO₂)⁺

¹H NMR: 2.07 (s, 3H, Me), 7.09 (bs, 2H, NH₂), 7.66 (d, 2H, J= 8.5 Hz, Ar-H2 and H6), 7.87 (d, 2H, J= 8.5 Hz, Ar-H3 and H5), 8.44 (s, 1H, N=CH), 8.72 (dd, 2H, J= 2.5 and 9.8 Hz, PZ-H5 and H6), 9.37 (s, 1H, PZ-H3), 10.12 (bs, 1H, NH) ppm.

7.5.6 *N*¹-(4-*tert*-Butylbenzylidene)-pyrazin-2-carboxamidrazone (PZaf)

Yellow crystalline solid. 3.241g, 11.53 mmol (79%).

MS (APCI +ve) *m/z* = 282 (M+H)⁺, 160 (M-PZNH₂CN=N)⁺

¹H NMR: 1.30 (s, 9H, CMe₃), 7.10 (bs, 2H, NH₂), 7.46 (d, 2H, J= 8.3 Hz, Ar-H3 and H5), 7.86 (d, 2H, J= 8.3 Hz, Ar-H2 and H6), 8.49 (s, 1H, N=CH), 8.74 (dd, 2H, J= 2.5 and 12.8 Hz, PZ-H5 and H6), 9.38 (s, 1H, PZ-H3) ppm.

7.5.7 N^1 -(1-Naphthylidene)-pyrazin-2-carboxamidrazone (PZag)

Yellow crystalline solid. Yield 3.650g, 13.27 mmol (91%).

MS (APCI +ve) $m/z = 276 (M+H)^+$, $154 (M-PZNH_2CN=N)^+$

1H NMR: 7.18 (bs, 2H, NH_2), 7.58-7.69 (m, 3H, 3Ar-H), 8.02 (t, 2H, $J = 8.0$ Hz, 2Ar-H), 8.29 (d, 1H, $J = 7.3$ Hz, Ar-H), 8.75 (dd, 3H, $J = 2.5$ and 10.0 Hz, PZ-H5 and H6), 8.89 (d, 1H, $J = 8.3$ Hz, Ar-H), 9.23 (s, 1H, N=CH), 9.46 (s, 1H, PZ-H3) ppm.

7.5.8 N^1 -(9-Phenanthrene)-pyrazin-2-carboxamidrazone (PZah).

Yellow crystalline solid. Yield 2.897g, 8.85 mmol (61%).

MS (APCI +ve) $m/z = 326 (M+H)^+$, $204 (M-PZNH_2CN=N)^+$

1H NMR: 7.25 (bs, 2H, NH_2), 7.67-7.79 (m, 3H, 3Ar-H), 8.09 (d, 1H, $J = 7.8$ Hz, Ar-H), 8.63 (s, 1H, N=CH), 8.76-8.93 (ov.m, 3H, PZ-H5 and H6, and Ar-H), 9.03-9.07 (m, 1H, Ar-H), 9.25 (s, 1H, Ar-H), 9.49 (s, 1H, PZ-H3) ppm.

7.5.9 N^1 -(9-Anthrylidene)-pyrazin-2-carboxamidrazone (PZai).

Yellow crystalline solid. Yield 3.105g, 9.55 mmol (65%).

MS (APCI +ve) $m/z = 326 (M+H)^+$, $204 (M-PZNH_2CN=N)^+$

1H NMR: 7.09 (bs, 2H, NH_2), 7.55-7.67 (m, 4H, 4Ar-H), 8.16 (d, 2H, $J = 7.5$ Hz, 2Ar-H), 8.73-8.77 (m, 3H, 3Ar-H), 8.80 (dd, 2H, $J = 2.5$ and 11.8 Hz, PZ-H5 and H6), 9.55 (s, 1H, N=CH), 9.73 (s, 1H, PZ-H3) ppm.

7.5.10 N^1 -(2-Benzyloxybenzylidene)-pyrazin-2-carboxamidrazone (PZaj)

Yellow crystalline solid. Yield 2.712g, 8.19 mmol (56%)

MS (APCI +ve) $m/z = 332 (M+H)^+$, $210 (M-PZNH_2CN=N)^+$

1H NMR: 5.21 (s, 2H, OCH_2Ph), 6.99-7.21 (ov.m, 4H, NH_2 and 2Ar-H), 7.35-7.52 (m, 6H, 5Phenyl-H and Ar-H), 8.26 (d, 1H, 6.0 Hz, Ar-H), 8.71 (dd, 2H, $J = 7.8$ and 10.3 Hz, PZ-H5 and H6), 8.81 (s, 1H, N=CH), 9.37 (s, 1H, PZ-H3) ppm.

7.5.11 N^1 -(3-Benzyloxy-4-methoxybenzylidene)-pyrazin-2-carboxamidrazone (PZak).

Yellow crystalline solid. 2.983g, 8.23 mmol (57%).

MS (APCI +ve) $m/z = 362 (M+H)^+$, $240 (M-PZNH_2CN=N)^+$

1H NMR: 3.82 (s, 3H, OMe), 5.18 (s, 2H, OCH_2Ph), 7.04 (d, 1H, 8.5 Hz, Ar-H), 7.15 (bs, 2H, NH_2), 7.33-7.52 (m, 6H, 5phenyl-H and Ar-H), 7.82 (s, 1H, Ar-H), 8.43 (s, 1H, N=CH), 8.76 (dd, 2H, $J = 2.5$ and 13.0 Hz, PZ-H5 and H6), 9.37 (s, 1H, PZ-H3) ppm.

7.5.12 N^1 -(4-Benzyloxy-3-methoxybenzylidene)-pyrazin-2-carboxamidrazone (PZal).

Yellow crystalline solid. Yield 3.125g, 8.66 mmol (59%).

MS (APCI +ve) $m/z = 362 (M+H)^+$, $240 (M-PZNH_2CN=N)^+$

1H NMR: 3.87 (s, 3H, OMe), 5.15 (s, 2H, OCH_2Ph), 7.08-7.49 (ov.m, 9H, NH_2 , 5Phenyl-H and 2Ar-H), 7.70 (s, 1H, Ar-H), 8.43 (s, 1H, N=CH), 8.75 (dd, 2H, $J = 2.5$ and 11.8 Hz, PZ-H5 and H6), 9.38 (s, 1H, PZ-H3) ppm.

7.6 Automated Synthesis

7.6.1 The *N*¹-Benzylideneheteroarylcarboxamidrazone Library

Glass 4ml vials in a matrix were charged with each of the amidrazones (0.544g, 0.2mmol) in ethanol (20ml), with the exception of 2-quinolylcarboxamidrazone, which was insoluble, so had to be weighed manually. This was followed by a solution of ketone (0.2mmol, 1ml, 1.1eq. in ethanol). The vials were heated in a heating block at 75°C for seven days. The ethanol was then evaporated to give the crude products. Purification was performed by robotic titration (3x3ml ether or petroleum ether depending upon the lipophilicity of the material). The products were dried under high vacuum prior to analysis. All compounds were analysed by positive APCI-MS. The yields of products ranged (62–90 %).

7.6.2 Automated Synthesis of the *N*¹-Benzylideneheteroarylcarboxamidrazone-Pyridium Salts

Glass 4ml vials in a matrix were charged with each of the 3-pyridyl, 4-pyridyl and pyrazinyl amidrazones (0.15 mmol) in THF 1 (1mL), This was followed by a solution of alkyl halide 200µl, The vials were heated in a heating block at 50°C for seven days. The THF was then evaporated to give the crude products. Purification was performed by robotic trituration (3x3ml ether or petroleum ether depending upon the lipophilicity of the material). The products were dried under high vacuum prior to analysis. All compounds were analysed by MS, positive Electro Spray [ES]. The yields of products ranged (35-88 %).

7.6.3 Automated Synthesis of the *N*¹-Benzylideneheteroarylcarboxamidrazone Metal Complexes

Glass 4ml vials in a matrix were charged with each of the amidrazones (0.2 mmol) in methanol (1ml), This was followed by a solution of metal chloride (0.2 mmol in water). The vials were heated in a heating block at 60°C for two days. The methanol was then evaporated to give the crude products. Purification was performed by robotic trituration (3x3ml deionised water followed by methanol). The products were dried under high vacuum prior to analysis. The compounds were analysed by TLC or IR. The yields of products ranged (45-99 %).

7.7 Synthesis of the New Classes of Carboxamidrazones

7.7.1 Synthesis of the Carboxamidrazone Amides

7.7.2 General method for the preparation of carboxamidrazone Amide

A mixture of appropriate carboxamidrazone (1g, 7.35 mmol) and anhydrous THF (20 mL) was stirred for 15 min. Then 2mL of Hunig's base was added to this reaction mixture followed by drop-wise addition of the required carboxylic acid chloride (1.1 eq.) in anhydrous THF (10 mL) over the period of 5-10 min. The reaction mixture was stirred at room temperature over the period of 6-12h under argon atmosphere. The crude product was filtered and washed with the aqueous sodium hydrogen carbonate followed by water. If necessary the material was purified by recrystallisation.

7.7.3 Synthesis of the Pyridin-2-carboxamidrazone Amides

7.7.4 Characterisation of pyridine-2-carboxamidrazone amides

7.7.4.1 Pyridine-2-carboxamidrazone *N*¹-(benzoyl)amide (2PYAc1)

White crystalline solid. Yield 1.713g, 12.20 mmol (97%) R.f. [EtOAc:MeOH, 8:2]: 0.41

MP 233.5-234.6 °C

MS (APCI +ve) *m/z* = 241 (M+H)⁺, 224 (M-H₂O)⁺

IR (KBr disc) ν = 3401 (N-H), 3208, 3060, 1671, 1690 (C=O), 1548, 1456, 1393 cm⁻¹

¹H NMR 6.94 (bs, 2H, NH₂), 7.50 (d, 4H, J = 7.2, Ar-H3, H4, H5 and Pyr-H4), 7.89 (d, 3H, J = 7.5, Ar-H2, H6 and Pyr-H5), 8.1 (d, 1H, J = 8.0 Hz, Pyr-H3), 8.61 (s, 1H, Pyr-H6), 10.20 (bs, 1H, NH).

7.7.4.2 Pyridine-2-carboxamidrazone *N*¹-(4-acetamidobenzoyl)amide (2PYAc2)

Pale yellow crystalline solid. Yield 0.872g, 2.93 mmol (40%). R.f. [MeOH:EtOAc, 9:1]: 0.37

MP 248.9-250 °C

MS (E+) [C₁₅H₁₆N₅O₂] = Mass 298.1304, calculated mass = 298.1304 [M=Na]⁺ [-7.0 ppm]

IR (KBr disc) ν = 3411, 3330 (N-H), 3272, 3178, 1665, 1629 (C=O), 1598, 1519, 1469, 1396 1312 cm⁻¹

¹H NMR: 2.08 (s, 3H, Me), 6.92 (bs, 2H, NH₂), 7.47 (t, 1H, J = 5.4 Hz, Pyr-H4), 7.66 (d, 2H, J = 8.6 Hz, Ar-H2 and H6), 7.83-8.15 (m, 3H, Ar-H3, H5 and Pyr-H5), 8.17 (d, 1H, J = 7.9 Hz, Pyr-H3), 8.59 (d, 1H, J = 4.5 Hz, Pyr-H6), 1.18 (bd, 2H, 2NH).

7.7.4.3 Pyridine-2-carboxamidrazone *N*¹-(4-phenylazo-benzoyl)amide (2PYAc3)

Orange crystalline solid. Yield 1.609g, 4.68 mmol (64%). R.f. [MeOH]: 0.45

MP 263.7-264.4 °C

MS (APCI +ve) *m/z* = 345 (M+H)⁺, 327 (M-H₂O)⁺

IR (KBr disc) ν = 3416, 3312 (N-H), 3214, 3056, 1629 (C=O), 1590, 1567, 1534, 1473, 1438 cm⁻¹

¹H NMR: 7.01 (bd, 2H, NH₂), 7.50 (t, 1H, J = 6.2 Hz, Pyr-H4), 7.62 (d, 3H, J = 7.2 Hz, Ar'-3H, H4 and 5H), 7.93-7.99 (ov.m, 5H, Ar-H2, H6, Ar'-H2, H6 and Pyr-H5), 8.13 (d, 2H, J = 8.5 Hz, Ar-H3 and H5), 8.21 (d, 1H, J = 8.0, Pyr-H3), 8.63 (d, 1H, J = 5.5 Hz, Pyr-H6), 10.37 (bs, 1H, NH).

7.7.4.4 Pyridine-2-carboxamidrazone *N*¹-(3-methoxy-benzoyl)amide (2PYAc4)

Recrystallised from methanol to give beige crystalline solid. Yield 1.030g, 3.82 mmol (52%). R.f. [MeOH:EtOAc, 9:1]: 0.59

MP 248.9-250.2 °C

MS (E+) [C₁₄H₁₅N₄O₂] = Mass 271.1181, calculated mass = 271.1195 [M=Na]⁺ [-5.2 ppm]

IR (KBr disc) ν = 3424 (N-H), 3173, 3129, 2994, 2954 1625 (C=O), 1577, 1569, 1477, 1393, 1317 cm⁻¹

¹H NMR: 3.82 (s, 3H, OMe), 6.92 (bs, 2H, NH₂), 7.10 (d, 1H, J = 8.3 Hz, Pyr-H4), 7.36-7.48 (m, 4H, Ar-H2, H4, H5 and H6), 7.90 (t, 1H, J = 6.9 Hz, Pyr-H5), 8.17 (d, 1H, J = 7.7 Hz, Pyr-H3), 8.58 (d, 1H, J = 4.5 Pyr-H6), 10.15 (bs, 1H, NH).

7.7.4.5 Pyridine-2-carboxamidrazone *N*¹-(2-naphthalene)amide (2PYAc5)

White crystalline solid. Yield 1.796g, 6.19 mmol (84%). R.f. [EtOAc:MeOH, 8:2]: 0.37

MP 229.9-230.5 °C

MS (E+) [C₁₇H₁₅N₄O] = Mass 291.1233, calculated mass = 291.1246 [M=Na]⁺ [-4.5 ppm]

IR (KBr disc) $\nu = 3405, 3341$ (N-H), 3212, 3054, 1665, 1634, 1610 (C=O), 1580, 1548, 1474, 1448, 1393, 1309 cm^{-1}

^1H NMR: 6.98 (bd, 2H, NH_2), 7.49 (t, 1H, $J = 5.4$, Pyr-H4), 7.58-7.62 (m, 2H, 2Ar-H), 7.88-8.07 (ov.m, 4H, 3Ar-H and Pyr-H5), 8.21 (d, 1H, $J = 8.0$ Hz, Pyr-H3), 8.50 (s, 1H, Ar-H), 8.60 (d, 1H, $J = 4.1$ Hz, Pyr-H6), 10.34 (bs, 1H, NH).

7.7.4.6 Pyridine-2-carboxamidrazone N^1 -(1-naphthalene)amide (2PYAc6)

Recrystallised from ethanol to give cream crystalline solid. Yield 1.9124g, 6.59 mmol (89%).

MP 263.5-264.7 $^{\circ}\text{C}$

MS (E+) [$\text{C}_{17}\text{H}_{15}\text{N}_4\text{O}$] = Mass 291.1228, calculated mass = 291.1246 [$\text{M}=\text{Na}$] $^+$ [-6.2 ppm]

IR (KBr disc) $\nu = 3727, 3419$ (N-H), 3204, 2921, 1629 (C=O), 1559, 1532, 1465, 1401, 1291 cm^{-1}

^1H NMR: 6.83 (bs, 2H NH_2), 7.47-7.61 (m, 4H, 4Ar-H), 7.72 (d, 1H, $J = 6.4$ Hz, Pyr-H4), 7.89-8.07 (ov.m, 3H, Pyr-H5 and 2Ar-H), 8.17-8.24 (m, 2H, Pyr-H3 and Ar-H), 8.60 (d, 1H, $J = 4.9$ Hz, Pyr-H6), 10.42 (bs, 1H, NH) ppm.

7.7.4.7 Pyridine-2-carboxamidrazone N^1 -(4-cyno-benzoyl)amide (2PYAc7)

White crystalline solid. Yield 1.547g, 5.84 mmol (79%). R.f. [EtOAc:MeOH, 1.1] 0.70

MP 264.7-265.8 $^{\circ}\text{C}$

MS (E+) [$\text{C}_{14}\text{H}_{12}\text{N}_5\text{O}$] = Mass 266.1028, calculated mass = 266.1042 [$\text{M}=\text{Na}$] $^+$ [-5.3 ppm]

IR (KBr disc) $\nu = 3413$ (N-H), 3200, 3048, 1623 (C=O), 1553, 1538, 1475, 1405, 1297, 1280 cm^{-1}

^1H NMR: 6.70 (bs, 2H, NH_2), 7.51 (m, 1H, Pyr-H4), 7.96 (d, 2H, $J = 8.0$ Hz, Ar-H2 and H6), 7.98 (ov.m, 3H, Ar-H3, H5 and Pyr-H5), 8.18 (d, 1H, $J = 8.0$ Hz, Pyr-3), 8.62 (s, 2H, Pyr-H6), 10.38 (bs, 1H, NH).

7.7.4.8 Pyridine-2-carboxamidrazone N^1 -(4-methoxy-benzoyl)amide (2PYAc8)

White crystalline solid. Yield 0.614g, 2.27 mmol (31%). R.f. [MeOH:EtOAc, 9:1] 0.46

MP 220.3-221.7 $^{\circ}\text{C}$

MS (E+) [$\text{C}_{14}\text{H}_{15}\text{N}_4\text{O}_2$] = Mass 291.1233, calculated mass = 298.1246 [$\text{M}=\text{Na}$] $^+$ [-4.5 ppm]

IR (KBr disc) $\nu = 3330, 3391$ (N-H), 3202, 3056, 2834, 1631 (C=O), 1588, 1550, 1471, 1393, 1259 cm^{-1}

^1H NMR: 3.82 (s, 3H, OMe), 6.90 (bs, 2H, NH_2), 7.01 (d, 2H, $J = 9.0$ Hz, Ar-H3 and H5) 7.48 (m, 1H, Pyr-H4), 7.87 (ov.m, 3H, $J = 8.5$ Hz, Ar-H2, H6 and Pyr-H5), 8.16 (d, 1H, $J = 10.3$ Hz, Pyr-H3), 8.59 (d, 1H, $J = 4.5$ Hz, Pyr-H6), 10.05 (bs, 1H, NH).

7.7.4.9 Pyridine-2-carboxamidrazone N^1 -(2-acetoxybenzoyl)amide (2PYAc11)

Recrystallised from ethyl acetate to give white crystalline solid. Yield 1.133g, 3.30 mmol (43%).

MP 172.9-174.2 $^{\circ}\text{C}$

MS (APCI +ve) $m/z = 298$ found $m/z = 297$ ($\text{M}-1\text{H}$) $^+$, 279 ($\text{M}-\text{H}_2\text{O}$) $^+$ (2 mass units less).

IR (KBr disc) $\nu = 3492$ (N-H), 3121, 3071, 3021, 2919, 2836, 2778, 1600 (C=O), 1569, 1486, 1430 cm^{-1}

^1H NMR: 2.34 (s, 3H, Me), 7.23 (d, 1H, $J = 8.2$ Hz, Ar-H4), 7.22-7.57 (ov.m, 3H, Ar-H2, H3 and Pyr-H4), 8.02 (td, 1H, 1.7 and 7.5 Hz, Pyr-H5), 8.11-8.18 (ov.m, 2H, Pyr-H3 and Ar-H5), 8.73 (d, 1H, $J = 3.7$ Hz, Pyr-H6) ppm. NH_2 and NH peaks were not observed, probably shifted down field.

7.7.4.10 Pyridine-2-carboxamidrazone *N*¹-(5-nitro-2-furoyl)amide (2PYAc13).

Recrystallised from DMF and water to give rust red crystalline solid. Yield 1.135g, 4.12 mmol (43%).

R.f. [MeOH:EtOAc, 9:1]: 0.5

MP 244.6-245.9 °C

MS (APCI +ve) $m/z = 276 (M+H)^+$, $259 (M-H_2O)^+$

IR (KBr disc) $\nu = 3441, 3370 (N-H), 3284, 2919, 1683, 1611 (C=O), 1563, 1513, 1463, 1391, 1336 \text{ cm}^{-1}$

¹H NMR: 7.08 (bd, 2H, NH₂), 7.477 (ov.m, 2H, Pyr-H4 and Furan-H5), 7.78 (m, 1H, Pyr-H5), 8.19 (d, 1H, J= 8.0 Hz, Pyr-H3), 8.66 (d, 1H, J= 2.8 Hz, Pyr-H6) ppm.

7.7.4.11 Pyridine-2-carboxamidrazone *N*¹-(3-nitro-benzoyl)amide (2PYAc14)

Yellow crystalline solid. Yield 1.847g, 6.48 mmol (88%).

MP 261.9-262.8 °C

MS (APCI +ve) $m/z = 286 (M+H)^+$, $269 (M-H_2O)^+$

IR (KBr disc) $\nu = 3386 (N-H), 3255, 3255, 3095, 3008, 1689, 1633 (C=O), 1582, 1567, 1546, 1482, 1459, 1426, 1351 \text{ cm}^{-1}$

¹H NMR: 6.99 (bd, 2H, NH₂), 7.55 (m, 1H, Pyr-H4), 7.80 (d, 1H, J= 7.8 Hz Ar-H6), 7.94 (m, 1H, Pyr-H5), 8.20 (d, 1H, J= 8.0 Hz, Ar-H5), 8.37 (d, 2H, J= 8.0 Hz, Ar-H2 and H4), 8.38 (d, 1H, J= 8.6 Hz, Pyr-H3), 8.73 (s, 1H, Pyr-H6), 10.55 (bs, 1H, NH) ppm

7.7.4.12 Pyridine-2-carboxamidrazone *N*¹-(ethyl-benzoyl)amide (2PYAc15)

Recrystallised from ethanol twice to give white crystalline solid. Yield 0.922g, 3.44 mmol (47%).

MP 200.1-2001.1 °C

MS (APCI +ve) $m/z = 269 (M+H)^+$, $150 (M-Ph-C_2H_5C=ONH)^+$

IR (KBr disc) $\nu = 3411, 3345 (N-H), 3204, 3062, 2964, 1665, 1637, 1602 (C=O), 1580, 1548, 1474, 1448, 1399 \text{ cm}^{-1}$

¹H NMR 1.20 (t, 3H, J= 7.5 Hz, Me), 2.62-2.71 (m, 2H, CH₂), 6.90 (bs, 2H, NH₂), 7.31 (d, 2H, J= 8.2 Hz, Ar-H3 and H5), 7.44-7.49 (m, 1H, Pyr-H4), 7.80 (d, 2H, J= 8.2 Hz, Ar-H2 and H6), 7.86-7.93 (m, 1H, Pyr-H5), 8.17 (d, 1H, J= 7.5Hz, Pyr-H3), 8.59 (d, 1H, J= 4.5 Hz, Pyr-H6), 10.10 (bs, 1H, NH) ppm.

7.7.4.13 Pyridine-2-carboxamidrazone *N*¹-(4-propyl-benzoyl)amide (2PYAc16)

Recrystallised from ethanol twice to give white crystalline solid. Yield 1.821g, 4.46 mmol (88%). R.f.

[MeOH:EtOAc, 9:1]: 0.56

MP 221.7-223.3 °C

MS (APCI +ve) $m/z = 283 (M+H)^+$, $265 (M-H_2O)^+$

IR (KBr disc) $\nu = 3409, 3342 (N-H), 3210, 3060, 3025, 2956, 2925, 2869, 1663, 1635, 1600 (C=O), 1583, 1550, 1474, 1448, 1399, 1313 \text{ cm}^{-1}$

¹H NMR: 0.90 (t, 3H, J= 7.2 Hz, CMe), 1.54-1.69 (m, 2H, CH₂), 2.62 (t, 2H, J= 7.7 Hz, CH₂), 6.91 (bs, 2H, NH₂), 7.80 (d, 2H, J= 8.0 Hz, Ar-H3 and H5), 7.90 (t, 1H, J= 8.0 Hz, Pyr-H4), 8.18 (d, 2H, J= 8.0 Hz, Ar-H2 and H6), 7.90 (t, 1H, J= 7.4 Hz, Pyr-H5), 8.16 (d, 1H, J= 4.5 Hz, Pyr-H3), 8.60 (d, 1H, J= 4.6 Hz, Pyr-H6), 10.12 (bs, 1H, NH) ppm.

7.7.4.14 Pyridine-2-carboxamidrazone *N*¹-(2,5-dimethoxy-benzoyl)amide (2PYAc17)

Recrystallised from DMF and petrol to give yellow crystalline solid. % yield.R.f. [MeOH:EtOAc, 9:1]: 0.55.

MP 225.7-226.9 °C

MS (APCI +ve) m/z m/z = 299 (M-1H)⁺, 282 (M-H₂O)⁺

IR (KBr disc) ν = 3422, 3314 (N-H), 3283, 3216, 3023, 2832 1643 (C=O), 1587, 1562, 1504, 1396, 1286, 1228 cm⁻¹

¹H NMR: 3.71 (m, 6H, 2OMe), 6.60 (bs, 2H, NH₂), 6.68 (bs, 1H, NH), 6.78 (m, 2H, 2Ar-H), 7.45 (m, 1H, Pyr-H4), 7.84 (m, 1H, Pyr-H5), 8.08 (d, 1H, J= 8.7 Hz, Pyr-H3), 8.56 (m, 1H, Ar-H), 9.96 (d, 1H, J= 8.2 Hz, Pyr-H6) ppm.

7.7.4.15 Pyridine-2-carboxamidrazone *N*¹-(4-heptyl-benzoyl)amide (2PYAc18)

peach crystalline solid. Yield 1.405g, 4.16 mmol (56%). R.f. [MeOH:EtOAc, 8:2]: 0.28.

MP 260-261.6 °C

MS (APCI +ve) m/z = 339 (M+H)⁺, 321 (M-H₂O)⁺

IR (KBr disc) ν = 3405 (N-H), 3208, 2927, 2856, 1631 (C=O), 1548, 1474, 1448, 1403, 1301 cm⁻¹

¹H NMR: 0.86 (t, 3H, J= 5.0 Hz, Me), 1.27 (s, 8H, (CH₂)₄), 1.58 (s, 2H, CH₂), 2.63 (t, 2H, J= 7.5 Hz, CH₂), 6.92 (bs, 2H, NH₂), 7.29 (2H, J= 7.7 Hz, Ar-H3 and H5), 7.47 (t, 1H, 5.7, Pyr-H4), 7.80 (d, 2H, J= 8.0Hz, Ar-H2 and H6), 7.90 (t, 1H, J= .8 Hz, Pyr-H5), 8.17 (d, 1H, J= 7.7 Hz, Pyr-H3), 8.59 (d, 1H, J= 4.5 Hz, Pyr-H6), 10.11 (bs, 1H, NH).

7.7.4.16 Pyridine-2-carboxamidrazone *N*¹-(2-methoxy-bezoyl)amide (2PYAc19)

Cream crystalline solid. Yield 1.147g, 4.25 mmol (58%). R.f. [MeOH:EtOAc, 5:5]: 0.57

MP 222.3-223 °C

MS (APCI +ve) m/z = 271 (M+H)⁺, 253 (M-H₂O)⁺

¹H NMR: 3.85 (s, 3H, OMe), 6.72 (bs, 2H, NH₂), 7.01 (t, 1H, J= 7.3 Hz, Ar-H5), 7.08 (d, 1H, J= 6.1 Hz, Ar-H4), 7.43-7.50 (m, 2H, Ar-H3 and H6), 7.56 (d,d, 1H, J= 1.7 and 7.5 Hz, Pyr-H4), 7.90 (td, 1H, j= 1.7 and 7.7 Hz, Pyr-H5), 8.16 (d, 1H, J= 8.0 Hz, Pyr-H3), 8.59 (d, 1H, J= 5.5 Hz, Pyr-H6), 10.10 (bs 1H, NH) ppm.

7.7.4.17 Pyridine-2-carboxamidrazone *N*¹-(4-tert-butyl-benzoyl)amide (2PYAc20)

Recrystallised from mixture of ethanol and ethyl acetate (6:4) to give white crystalline solid. Yield 1.935g, 6.54 mmol (89%).

MP 228.9-231 °C

MS (APCI +ve)m/z = 296 found m/z = 295 (M-2H)⁺ (2 mass unit less than expected), 277 (M-H₂O)⁺

IR (KBr disc) ν = 3405, 3349 (N-H), 3226, 3033, 2961, 1673, 1639 (C=O), 1589, 1546, 1474, 1448, 1400, 1285 cm⁻¹

¹H NMR: 1.31 (s, 9H, (CMe)₃), 6.911 (bs, 2H, NH₂), 7.50 (ov.m, 3H, J= 8.2 Hz, Ar-H3, H5 and pyr-H4), 7.81 (d, 2H, 8.2 Hz, Ar-H2 and H6), 7.90 (t, 1H, J= 7.7 Hz, Pyr-H5), 8.18 (d, 1H, J= 7.7 Hz, Pyr-H3), 8.60 (d, 1H, J= 4.5 Hz, Pyr-H6), 10.13 (bs, 1H, NH) ppm.

7.7.4.18 Pyridine-2-carboxamidrazone *N*¹-(3,4,5-trimethoxy-benzoyl)amide (2PYAc21)

Recrystallised from methanol three times to give white crystalline solid. Yield 1.979g, 5.99 mmol (82%).

MP 123.9-126.3 °C

MS (APCI +ve) *m/z* = 331 (M+H)⁺, 313 (M-H₂O)⁺

IR (KBr disc) ν = 3423 (N-H), 3297, 3189, 2987, 2936, 2834, 1666, 1623 (C=O), 1567, 1496, 1465, 1411, 1346 cm⁻¹

¹H NMR: 3.73 (s, 3H, OMe), 3.87 (s, 6H, (OMe)₂), 7.26 (s, 2H, Ar-H2 and H6), 7.62 (m, 1H, Pyr-H4), 8.02 (t, 1H, J= 7.5 Hz, Pyr-H5), 8.24 (d, 1H, J= 8.0 Hz, Pyr-H3), 8.71 (d, 1H, J= 4.3 Hz, Pyr-H6), 10.69 (bs, 1H, NH) ppm.

7.7.4.19 Pyridine-2-carboxamidrazone *N*¹-(2-furoyl)amide (2PYAc25)

Recrystallised from a mixture of ethanol and methanol (3:1) respectively to give white crystalline solid. Yield 1.492g, 6.51 mmol (88%).

MP 227.9-229.5 °C

MS (APCI +ve) *m/z* = 231 (M+H)⁺, 214 (M-H₂O)⁺

IR (KBr disc) ν = 3411 (N-H), 3201, 3044, 1663, 1641, 1607 (C=O), 1594, 1544, 1474, 1399, 1297 cm⁻¹

¹H NMR: 6.67 (bs, 1H, Furan-H5), 6.99 (bs, 2H, NH₂), 7.24 (bs, 1H, Fur-H4), 7.48 (m, 1H, Pyr-H4), 7.88-7.94 (ov.m, 2H, Furan-H3 and Pyr-H5), 8.15 (d, 1H, J= 8.0 Hz, Pyr-H3) 8.60 (d, 1H, J= 5.7 Hz, Pyr-H6), 10.14 (bs, 1H, NH,) ppm.

7.8 Synthesis of the Pyridin-4-carboxamidrazone Amides

7.8.1 Characterisation of pyridine-4-carboxamidrazone

7.8.1.1 Pyridine-4-carboxamidrazone *N*¹-(4-acetamidobenzoyl)amide (4PYAc2)

Yellow crystalline solid. 0.326g, 1.03 mmol (56%).

MP 277-279.5 °C

MS (APCI +ve) *m/z* = 299 (M+H)⁺

IR (KBr disc) ν = 3413, 3327 (N-H), 3275, 3175, 1672, 1627 (C=O), 1596, 1521, 1471 cm⁻¹

¹H NMR: 2.08 (s, 3H, Me), 6.8 (bs, 2H, NH₂), 7.66 (d, 2H, J= 8.7 Hz, Ar-H3 and H5), 7.79 (d, 2H, J= 5.5 Hz, Pyr-H3 and H5), 7.84 (d, 2H, J= 8.5 Hz, Ar-H2 and H6), 8.64 (d, 2H, J= 5.7 Hz, Pyr-H2 and H6), 10.06 (bs, 1H, NH), 10.18 (bs, 1H, NH) ppm.

7.8.1.2 Pyridine-4-carboxamidrazone *N*¹-(4-phenylazo-benzoyl)amide (4PYAc3)

Orange crystalline solid. Yield 0.837g, 2.43 mmol (33%). R.f. [MeOH]: 0.58.

MP 276.3-278.2 °C

MS E(+) [C₁₉H₁₇N₆O] = mass 345.1453, calculated mass = 345.1464 [M+Na]⁺ [-3.2 ppm].

IR (KBr disc) ν = 3424, 3306 (N-H), 3218, 3173, 1673, 642 (C=O), 1592, 1538, 1395, 1289 cm⁻¹

¹H NMR: 7.00 (bd, 2H, NH₂), 7.62 (d, 3H, J= 7.0 Hz, Ph-H3, H4 and H5), 7.82 (d, 2H, J= 5.7 Hz, Ar-H2 and H6), 7.92-7.97 (ov.m, 4H, Ar-H3, H5, Ph-H2 and H6), 8.13 (d, 2H, J= 8.2 Hz,), 8.65 (d, 2H, J= 5.5 Hz, Pyr-H2 and H6), 10.45 (bs, 1H, NH) ppm.

7.8.1.3 Pyridine-4-carboxamidrazone *N*¹-(3-methoxy-benzoyl)amide (4PYAc4)

Recrystallised from a mixture of ethyl acetate and methanol (9:1) to give beige brown crystalline solid.

Yield 0.993g, 3.68 mmol (50%). R.f. [MeOH]: 0.54

MP 184.2-186.3 °C

MS E(+) [C₁₄H₁₅N₄O₂] = mass 271.1192, calculated mass = 271.1195 [M+Na]⁺ [-1.1 ppm].

IR (KBr disc) ν = 3351 (N-H), 3156, 2996, 2834, 1635, 1602 (C=O), 1540, 1471, 1413, 1307 1237 cm⁻¹

¹H NMR 3.82 (s, 3H, OMe), 6.93 (bs, 2H, NH₂), 7.10 (d, 1H, J = 9.0 Hz, Ar-H5), 7.36-7.48 (m, 3H, Ar-H2, H4 and H6), 7.79 (d, 2H, J = 5.5 Hz, Pyr-H3 and H5), 8.65 (d, 2H, 5.5 Hz, Pyr-H2 and H6), 10.15 (bs, 1H, NH) ppm.

7.8.1.4 Pyridine-4-carboxamidrazone *N*¹-(2-naphthalene)amide (4PYAc5)

Pale Yellow crystalline solid. 0.558g, 1.92 mmol (26%). R.f. [EtOAc:MeOH, 8:]: 0.29.

MP 295.6-297.5 °C

MS E(+) [C₁₇H₁₅N₄O] = mass 291.1241, calculated mass = 291.1246 [M+Na]⁺ [-1.7 ppm].

IR (KBr disc) ν = 3397, 3322 (N-H), 3064, 1636, 1602 (C=O), 1538, 1496, 1403, 1309 cm⁻¹

¹H NMR: 7.00 (bs, 2H, NH₂), 7.59-7.64 (m, 2H, 2Ar-H), 7.81 (d, 2H, J = 6.0 Hz, Pyr-H3 and H5), 7.95-8.07 (m, 4H, 4Ar-H), 8.52 (s, 1H, Ar-H), 8.66 (d, 2H, J = 5.7 Hz, Pyr-H2 and H6), 10.34 (bs, 1H, NH) ppm.

7.8.1.5 Pyridine-4-carboxamidrazone *N*¹-(1-naphthalene)amide (4PYAc6)

Yellow crystalline solid. Yield 1.215g, 4.19 mmol (57%). R.f. [EtOAc:MeOH, 8:2]: 0.34

MS E(+) [C₁₇H₁₅N₄O] = mass 291.1234, calculated mass = 291.1246 [M+Na]⁺ [-4.1 ppm].

¹H NMR: 6.80 (bd, 2H, NH₂), 7.55-7.61 (m, 3H, 3Ar-H), 7.73 (d, 1H, J = 8.0 Hz, Ar-H), 7.82 (d, 2H, J = 6.0 Hz, Pyr-H3 and H5), 7.98-8.07 (m, 2H, Ar-H), 8.16-8.20 (m, 1H, Ar-H), 8.66 (d, 2H, J = 6 Hz, Pyr-H2 and H6), 10.35 (bs, 1H, NH) ppm. (19% impurities).

7.8.1.6 Pyridine-4-carboxamidrazone *N*¹-(4-methoxy-benzoyl)amide (4PYAc8)

Cream crystalline solid. Yield 1.289g, 4.77 mmol (65%). R.f. [EtOAc:MeOH, 9:1]: 0.19

MP 209.9-211.5 °C

MS E(+) [C₁₄H₁₅N₄O₂] = mass 271.1183, calculated mass = 271.1195 [M+Na]⁺ [-4.4 ppm].

IR (KBr disc) ν = 3187, 2840, 1631, 1608 (C=O), 1544, 1503, 1440, 1413, 1320, 1257 cm⁻¹

¹H NMR: 3.82 (s, 3H, OMe), 6.88 (bs 2H, NH₂), 7.43 (d, 2H, J = 9.0 Hz, Ar-H2 and H6), 7.78 (d, 2H, J = 5.2 Hz, Pyr-H3 and H5), 7.88 (d, 2H, 8.7, Ar-H3 and H5), 8.63 (d, 2H, J = 6.0 Hz, Pyr-H2 and H6), 10.06 (bs, 1H, NH) ppm.

7.8.1.7 Pyridine-4-carboxamidrazone *N*¹-(2,6-dimethoxy-benzoyl)amide (4PYAc9)

Beige crystalline solid. Yield 1.501g, 5.0 mmol (68%). R.f. [EtOAc:MeOH, 8:2]: 0.29

MP 234.9-236.7 °C

MS E(+) [C₁₅H₁₇N₄O₃] = mass 301.1295, calculated mass = 301.1301 [M+Na]⁺ [-2.0 ppm].

IR (KBr disc) ν = 3353 (N-H), 3202, 2934, 2834, 1650 (C=O), 1592, 1540, 1475, 1405, 1295, 1247 cm⁻¹

^1H NMR: 3.75 (s, 6H, (OMe)₂), 6.62 (bd, 2H, NH₂), 6.71 (d, 3H, J= 8.5 Hz, Ar-H3, H4 and H5), 7.25-7.36 (m, 1H, Pyr-H3 or H5), 7.75 (d, 1H, 6.0 Hz, Pyr-H3 or H5), 8.63 (d, 2H, J= 6.5 Hz, Pyr-H2 and H6), 10.03 (bs, 1H, NH) ppm.

7.8.1.8 Pyridine-4-carboxamidrazone *N*¹-(5-nitro-2-furoyl)amide (4PYAc13)

mustard orange crystalline solid. Yield 1.161g, 4.22 mmol (44%). R.f. [MeOH]: 0.54

MP 273.3-274.6 °C

MS (APCI +ve) *m/z* = 274 (M-H)⁺, 257 (M-H₂O)⁺

IR (KBr disc) ν = 3428, 3365 (N-H), 3201, 3021, 1699, 1600 (C=O), 1505, 1359 1025 cm⁻¹

^1H NMR 6.96 (bs, 1H, NH₂), 7.17 (bs, 1H, NH₂), 7.50 (d, 1H, J= 3.7 Hz, Furan-H4), 7.64-7.80 (ov.m, 3H, Furan-H3, Pyr-H3 and H5), 8.67 (2H, J= 6.0 Hz, Pyr-H2 and H6), 10.61 (bs, 1H, NH) ppm.

7.8.1.9 Pyridine-4-carboxamidrazone *N*¹-(3-nitro-benzoyl)amide (4PYAc14).

Beige crystalline solid. Yield 0.648g, 2.27 mmol (31%). R.f. [MeOH]: 0.48

MP 290.8-293.2 °C

MS E(+) [C₁₃H₁₂N₅O₃] = mass 286.0928, calculated mass = 2286.0940 [M+Na]⁺ [-4.2 ppm].

IR (KBr disc) ν = 3403 (N-H), 3178, 3070, 1636 (C=O), 1598, 1525, 1407, 1347, 1320 cm⁻¹

^1H NMR: 7.07 (bd, 2H, NH₂), 7.64-7.82 (ov.m, 3H, Pyr-H3, H5 and Ar-H6), 8.37 (d, 2H, J= 8.0 Hz, Ar-H5, Ar-H2 or H4), 8.67 (d, 2H, J= 6.0 Hz, Pyr-H2 and H6), 8.72 (s, 1H, Ar-H2 or H4), 10.52 (bs, 1H, NH) ppm.

7.8.1.10 Pyridine-4-carboxamidrazone *N*¹-(4-ethyl-benzoyl)amide (4PYAc15).

Recrystallised from ethanol twice to give white crystalline solid. Yield 1.687g, 6.29 mmol (86%). R.f. [EtOAc:MeOH, 8:2]: 0.55

MP 209-210.5 °C

MS E(+) [C₁₅H₁₇N₄O] = mass 269.1391, calculated mass = 269.1402 [M+Na]⁺ [-4.1 ppm].

IR (KBr disc) ν = 3359 (N-H), 3195, 2961, 2927, 1644 (C=O), 1596, 1532, 1496, 1393, 1309, 1292 cm⁻¹

^1H NMR: 1.20 (t, 3H, J= 7.5 Hz, Me), 2.62-2.71 (m, 2H, CH₂), 6.86 (bs, 2H, NH₂), 7.31 (d, 2H, J= 8.0 Hz, Ar-H3 and H5), 7.79 (d, 4H, J= 8.1 Hz, Ar-H2, H6, Pyr-H3 and H5), 8.64 (d, 2H, J= 5.7 Hz, Pyr-H2 and H6), 10.03 (bs, 1H, NH) ppm.

7.8.1.11 Pyridine-4-carboxamidrazone *N*¹-(4-propyl-benzoyl)amide (4PYAc16)

Recrystallised from ethanol twice to give white crystalline solid. Yield 1.389g, 4.92 mmol (67%). R.f. [MeOH]: 0.51.

MP 208.9-210 °C

MS E(+) [C₁₆H₁₉N₄O] = mass 283.1560, calculated mass = 283.1559 [M+Na]⁺ [0.4 ppm].

IR (KBr disc) ν = 3299, 3154, 2955, 2933, 2873, 1671, 1627 (C=O), 1594, 1540, 1499, 1413, cm⁻¹

^1H NMR: 0.90 (t, 3H, J= 7.3 Hz, Me), 1.57-1.65 (m, 2H, CH₂), 2.61 (t, 2H, J= 7.3 Hz, CH₂), 6.86 (bs, 2H, NH₂), 7.29 (2H, J= 7.8 Hz, Ar-H3 and H5), 7.79 (d, 4H, 7.2 Hz, Ar-H2, H6, Pyr-H3 and H5), 8.63 (d, 2H, J= 4.9 Hz, Pyr-H2 and H6), 10.07 (bs, 1H, NH) ppm.

7.8.1.12 Pyridine-4-carboxamidrazone *N*¹-(4-heptyl-benzoyl)amide (4PYAc18).

Light brown crystalline solid. Yield 1.093g, 3.23 mmol (44%). R.f. [MeOH]: 0.57

MP 261.2-263 °C

MS E(+) [C₂₀H₂₆N₄O] = mass 339.2185, calculated mass = 339.2185 [M+Na]⁺ {-4.4 ppm}.

¹H NMR 0.85 (t, 3H, J= 6.7 Hz, CH₃), 1.25-1.28 (m, 8H, (CH₂)₄), 1.55-1.61 (m, 2H, CH₂), 2.63 (t, 2H, J= 7.2 Hz, CH₂), 6.95 (bs, 2H, NH₂), 7.28 (d, 2H, J= 8.0 Hz, Ar-H3 and H5), 7.81 (d, 4H, J= 8.0 Hz, Ar-H2, H6, Pyr-H3 and H5), 8.64 (d, 2H, J= 5.5 Hz, Pyr-H2 and H6), 10.14 (bs, 1H, NH) ppm.

7.8.1.13 Pyridine-4-carboxamidrazone N¹-(3,4,5-trimethoxy-benzoyl)amide (4PYAc21)

Yellow crystalline solid. Yield 0.734g, 2.22 mmol (30%). R.f. [EtOAc:MeOH, 8:2]: 0.56

MP 219.9-220.7 °C

MS (APCI +ve) m/z = 328 (M+H)⁺, 311 (M-H₂O)⁺

IR (KBr disc) ν= 3450, 3301 (N-H), 3199, 3008, 2938, 1666, 1641 (C=O), 1542, 1496, 1455, 1339 cm⁻¹

¹H NMR: 3.71 (s, 3H, OMe), 3.86 (s, 6H, OMe₂), 6.93 (bs, 2H, NH₂), 7.20 (s, 2H, Ar-H2 and H6), 7.80 (d, 2H, J= 5.3 Hz, Pyr-H3 and H5), 8.66 (d, 2H, 5.8 Hz, Pyr-H2 and H6), 10.14 (bs, 1H, NH) ppm.

7.8.1.14 Pyridine-4-carboxamidrazone N¹-(2-methyl-benzoyl)amide (4PYAc22)

Yellow crystalline solid. Yield 0.325g, 1.28 mmol (17%). R.f. [EtOAc:MeOH, 9:1]: 0.25.

MS (APCI +ve) m/z = 255 (M+H)⁺, 237 (M-H₂O)⁺

¹H NMR: 2.36 (s, 3H, Me), 6.75 (bs, 2H, NH₂), 7.34 (m, H4, 4Ar-H), 7.77 (d, 2H, J= 6.1 Hz, Pyr-H3 H5), 8.62 (d, 2H, J= 6.1 Hz, Pyr-H2 and H6), 10.18 (bs, 1H, NH) ppm.

7.8.1.15 Pyridine-4-carboxamidrazone N¹-(3-methyl-benzoyl)amide (4PYAc23).

Recrystallised from a mixture of ethanol and methanol (6:4) to give cream crystalline solid. Yield 0.486g, 1.91 mmol (26%). R.f. [MeOH:EtOAc, 8:2]: 0.24

MP 203.9-204.8 °C

MS (APCI +ve) m/z = 255 (M+H)⁺, 237 (M-H₂O)⁺

IR (KBr disc) ν= 3394 (N-H), 31, 64, 3025, 2990, 2838, 1650 (C=O), 1582, 1538, 1411, 1311 cm⁻¹

¹H NMR: 2.36 (s, 3H, Me), 6.89 (bs, 2H, NH₂), 7.35 (s, 2H, Ar-H4 and H5), 7.67 (s, 2H, Ar-H2 and H6), 7.78 (d, 2H, J= 5.4 Hz, Pyr-H3 and H5), 8.62 (d, 2H, J= 5.5 Hz, Pyr-H2 and H6), 10.09 (bs, 1H, NH) ppm.

7.8.1.16 Pyridine-4-carboxamidrazone N¹-(2,4,6-trimethyl-benzoyl)amide (4PYAc24).

Brown crystalline solid. Yield 0.465g, 1.65 mmol (22%) yield.

MS (APCI +ve) m/z = 282 (M+H)⁺, (M-H₂O)⁺

¹H NMR: 3.71 (s, 3H, Me), 3.55 (s, 6H, (Me)₂), 6.93 (bs, 2H, NH₂), 7.20 (s, 2H, A-H3 and H5), 7.80 (d, 2H, J= 5.2 Hz,), 8.65 (d, 2H, J= 5.7 Hz, Pyr-H2 and H6), 10.13 (bs, 1H, NH) ppm.

7.8.1.17 Pyridine-4-carboxamidrazone N¹-(2-furoyl)amide (4PYAc25)

Recrystallised from ethanol twice, to give yellow crystalline solid. Yield 1.235g, 5.36 mmol (73%).

MP 229.8-230.6 °C

MS (APCI +ve) m/z = 231 (M+H)⁺, 214 (M-H₂O)⁺

IR (KBr disc) ν= 3405 (N-H), 3292, 2927, 2856, 1631 (C=O), 1548, 1474, 1448, 1403, 1301 cm⁻¹

¹H NMR: 6.67 (bs, 2H, NH₂), 6.95 (bs, 1H, Furan-H 4), 7.23 (d, 2H, J= 3.0 Hz, Pyr-H3 and H5), 7.77 (d, 1H, J= 4.3 Hz, Furan-H3), 7.89 (d, 2H, J= 7.3 Hz, Pyr-H2 and H6), 8.65 (d, 1H, J= 5.8 Hz, Furan-H2), 10.34 (bs, 1H, NH) ppm.

7.9 Synthesis of Amides from Carboxylic Acid

7.9.1 General method for the preparation of carboxamidrazone Amide

7.9.2 Synthesis of the pyridine-2-carboxamidrazone amides

N,N'-carbonyldiimidazole (1.622g, 10.0 mmol) was added to required carboxylic acid (10.0 mmol 1eq) in dry THF (10 mL) at room temperature. When effervescence stopped, the 2PY (1.36g, 10.0 mmol 1eq dissolved in 2 mL of dry THF) was then added and the reaction was allowed to proceed under argon at room temperature. After 4-6 hours the resulting solution was evaporated under high vacuum to afford the title compound. The compound was then washed with saturated bicarbonate and water. If necessary the material was purified by recrystallisation.

7.9.3 Characterisation of Pyridine-2-carboxamidrazone Amides

7.9.3.1 Characterisation of pyridine-2-carboxamidrazone *N*'-(3-benzyloxy-4-methoxy-benzoyl)amide (2PYCa1)

Recrystallised from a mixture of ethanol and methanol (8:2) to give white crystalline solid. Yield 0.599g, 1.59 mmol (43%). R.f. [MeOH:EtOAc, 5:5]: 0.12

MP 209.9-211.6 °C

MS (APCI +ve) m/z = 377 (M+H)⁺, 241 (M-Pyr-CHN₂NH₂)⁺

IR (KBr disc) ν = 3426, 3338 (N-H), 3208, 3060, 3035, 2937, 2842, 1627, 1604 (C=O), 1577, 1548, 1515, 1446, 1427, 1268 cm⁻¹

¹H NMR: 3.85 (s, 3H, OMe), 5.16 (s, 2H, PhenyIOCH₂), 6.89 (bs, 2H, NH₂), 7.08 (d, 1H, J= 8.5 Hz, Ar-H), 7.34-7.57 (ov.m, 8H, 5H-Phenyl, 2Ar-H and Pyr-H4), 7.90 (t, 1H, J= 7.3 Hz, Pyr-H5), 8.17 (d, 1H, 7.5 Hz, Pyr-H3), 8.60 (d, 1H, J= 4.7 Hz, Pyr-H6), 10.04 (bs, 1H, NH) ppm.

7.9.3.2 Pyridine-2-carboxamidrazone *N*'-(4-cyclohexyl-benzoyl) amide (2PYCa2)

White crystalline solid. Yield 2.069g, 6.43 mmol (87%).

MP 237.9-239.1 °C

MS (APCI +ve) m/z = 323 (M+H)⁺, 305 (M-H₂O)⁺, 187 (M-Pyr-CN₂NH₂)⁺

IR (KBr disc) ν = 3411, 3328 (N-H), 2923, 2854, 1656, 1619 (C=O), 1559, 1544, 1472, 1395, 1313 cm⁻¹

¹H NMR: 1.21-1.80 (m 10H, cyclohexan (CH₂)₅), 2.57 (m, 1H, cyclohexan-H), 6.88 (bs, 2H, NH₂), 7.31, (d, 2H, J= 8.2 Hz, Ar-H3 and H5), 7.44-7.49 (m, 1H, Pyr-H4), 7.78 (d, 2H, J=8.0, Ar-H2 and H6), 7.88 (t, 1H, J= 7.0 Hz, Pyr-H5), 8.16 (d, 1H, J= 7.5 Hz, Pyr-H3), 8.58 (d, 1H, J= 4.7 Hz, Pyr-H6), 10.08 (bs, 1H, NH) ppm.

7.9.3.3 Pyridine-2-carboxamidrazone *N*'-(2-benzyloxy-benzoyl)amide (2PYCa3)

Recrystallised from methanol three times to give white crystalline solid. Yield 0.669g, 1.93 mmol (52%).

MP 187.1-188.4 °C

MS (APCI +ve) $m/z = 347 (M+H)^+$, $163 (M-PhOCH_2Ph)^+$

IR (KBr disc) $\nu = 3413, 3332 (N-H), 3299, 3199, 3062, 1639 (C=O), 1552, 1474, 1448, 1312, 1241 \text{ cm}^{-1}$

$^1\text{H NMR}$: 5.18 (s, 2H, OCH_2Ph), 6.64 (bd, 2H, NH_2), 7.01-7.1 (m, 1H, Ar-H), 7.19-7.55 (ov.m, 9H, 5H-Phenyl, 3Ar-H and Pyr-H4), 7.87 (td, 1H, $J = 1.7, 7.7 \text{ Hz}$, Pyr-H5), 8.12 (d, 1H, $J = 8.0$, Pyr-H3), 8.57 (d, 1H, $J = 5.0 \text{ Hz}$, Pyr-H6), 10.11 (bs, 1H, NH) ppm.

7.9.3.4 Characterisation of pyridine-2-carboxamidrazone N^1 -(3,5-di-tert-butyl-2-hydroxy-benzoyl)amide (2PYCa5).

Yellow crystalline solid. Yield 0.613g, 1.67 mmol (45%). R.f. [MeOH]: 0.58.

MP 225.4-227.1 °C

MS E(+) [$\text{C}_{21}\text{H}_{29}\text{N}_4\text{O}_2$] = Mass 369.2278, calculated mass 369.2291 [M + Na]⁺ [-3.5 ppm]

IR (KBr disc) $\nu = 3447, 3347 (N-H), 3150, 2958, 2865, 1660, 1600 (C=O), 1567, 1519, 1474, 1438, 1388, 1366 \text{ cm}^{-1}$

$^1\text{H NMR}$: 1.20 (s, 9H, CMe_3), 1.43 (s, 9H, CMe_3), 7.23 (d, 1H, $J = 2.5 \text{ Hz}$, Ar-H4), 7.27 (bs, 2H, NH_2), 7.43-7.48 (m, 1H, Pyr-H4), 7.73 (d, 1H, $J = 2.0 \text{ Hz}$, Ar-H6), 7.97 (d, 1H, $J = 4.5 \text{ Hz}$, Pyr-H3), 8.03 (t, 1H, $J = 9.0 \text{ Hz}$, Pyr-H5), 8.23 (d, 1H, $J = 8.5 \text{ Hz}$, Pyr-H6), 13.94 (bs, 1H, NH) ppm.

7.9.3.5 Characterisation of pyridine-2-carboxamidrazone N^1 -(4-isopropyl-benzoyl)amide (2PYCa6)

Recrystallised from a mixture of ethyl acetate and methanol (7:3) to give a white crystalline solid. Yield 0.512g, 1.82 mmol (49%).

MP 223.5-224 °C

MS (APCI +ve) $m/z = 283 (M+H)^+$, $285 (M-H_2O)^+$

IR (KBr disc) $\nu = 3397, 3343, 3303 (N-H), 3216, 3046, 3027, 2964, 2865, 1667, 1635 (C=O), 1546, 1481, 1444, 1395, 1307 \text{ cm}^{-1}$

$^1\text{H NMR}$: 1.22 (s, 3H Me), 1.24 (s, 3H, Me), 2.90-3.01 (m, 1H, isp-H), 6.91 (bs, 2H, NH_2), 7.35 (d, 2H, $J = 8.0 \text{ Hz}$, Ar-H3 and H5), 7.47-7.50 (m, 1H, Pyr-H4), 7.81 (d, 2H, $J = 8.0 \text{ Hz}$, Ar-H2 and H6), 7.90 (t, 1H, $J = 7.7 \text{ Hz}$, Pyr-H5), 8.17 (d, 1H, $J = 7.7 \text{ Hz}$, Pyr-H3), 8.60 (d, 1H, $J = 4.5 \text{ Hz}$, Pyr-H6), 10.11 (bs, 1H, NH) ppm.

7.9.4 Synthesis of pyridine-4-carboxamidrazone amides

N,N' -carbonyldiimidazole (1.622g, 10.0 mmol) was added to required carboxylic acid (10.0 mmol 1eq) in dry THF (10 mL) at room temperature. When effervescence stopped, the 4PY (1.36g, 10.0 mmol 1eq dissolved in 2 mL of dry THF and 2 mL of dry DMF) was then added and the reaction was allowed to proceed under argon at room temperature. After 4-6 hours the resulting solution was evaporated under high vacuum to afford the title compound. The compound was then washed with saturated bicarbonate. Inorganic impurities were removed by hot filtration in MeOH or EtOH and then the solution was allowed to recrystallise at room temperature.

7.9.5 Characterisation of pyridine-4-carboxamidrazones amide

7.9.5.1 Pyridine-4-carboxamidrazone *N*¹-(3-Benzyloxy-4-methoxy-benzoyl)amide (4PYCa1)

Recrystallised from ethanol to give cream crystalline solid. Yield 0.501g, 1.33 mmol (36%).

MP 209.9-211.6 °C

MS (APCI +ve) $m/z = 377 (M+H)^+$, $359 (M-H_2O)^+$ found 375

IR (KBr disc) $\nu = 3441 (N-H)$, 3268, 3148, 3031, 1638, 1600 (C=O), 1575, 1526, 1403, 1303, 1268, 1226 cm^{-1}

¹H NMR: 3.83 (s, 3H, OMe), 5.14 (s, 2H, OCH₂Ph), 6.84 (bs, 2H, NH₂), 7.30 (d, 1H, J= 8.3 Hz, Ar-H), 7.33-7.56 (ov.m, 7H, 5Phenyl-H, 2Ar-H), 7.78 (d, 2H, J= 5.1 Hz, Pyr-H3 and H5), 8.64 (d, 2H, J= 5.8 Hz, Pyr-H2 and H6), 9.98 (bs, 1H, NH) ppm.

7.9.5.2 Pyridine-4-carboxamidrazone *N*¹-(2-Benzyloxy-benzoyl)amide (4PYCa4)

Cream crystalline solid. Yield 0.308g, 0.89 mmol (24%).

MP 133.9-134.8 °C

MS (APCI +ve) $m/z = 347 (M+H)^+$, $329 (M-H_2O)^+$ found 345 (2 mass units less than expected).

IR (KBr disc) $\nu = 3467$, 3432, 3318 (N-H), 3107, 3031, 1644, 1602 (C=O), 1532, 1482, 1449, 1393, 1297, 1270 cm^{-1}

¹H NMR: 5.20 (s, 2H, PhenyIOCH₂), 6.73 (bs, 2H, NH₂), 7.06 (t, 1H, J= 7.4 Hz, Ar-H), 7.20-7.57 (ov.m, 7H, 5Phenyl-H and 2Ar-H), 7.76 (d, 2H, J= 6.1 Hz, Pyr-H3 and H5), 8.63 (d, 2H, J= 6.1 Hz, Pyr-H2 and H6), 10.05 (bs, 1H, NH)

7.9.5.3 Pyridine-4-carboxamidrazone *N*¹-(3,5-Di-tert-butyl-2-hydroxy-benzoyl)amide (4PYCa5)

Recrystallised from a mixture of ethanol and methanol (1:1) to give pale yellow crystalline solid. Yield 0.503g, 1.37 mmol (37%). Yield.R.f. [EtOAc:MeOH, 8:2]: 0.35.

MP 210-211.9 °C.

MS E(+) [C₂₁H₂₉N₄O₂] = mass 369.2288, calculated mass = 369.2291 [M+Na]⁺ [-0.8ppm].

IR (KBr disc) $\nu = 3366 (N-H)$, 3222, 2962, 2911, 2873, 1633 (C=O), 1575, 1540, 1440, 1396, 1365 cm^{-1}

¹H NMR: 1.30 (s, 9H, Me₃), 1.38 (s, 9H, Me₃), 7.10 (bs, 2H, NH₂), 7.35 (bs, 1H, Ar-H4), 7.76 (bs, 1H, Ar-H6), 7.82 (d, 2H, J= 6.0 Hz, Pyr-H3 and H5), 8.70 (d, 2H, J= 5.8 Hz, Pyr-H2 and H6), 10.57 (bs, 1H, NH) ppm.

7.9.5.4 Pyridine-4-carboxamidrazone *N*¹-(4-Isopropyl-benzoyl)amide (4PYCa6)

Beige crystalline solid. Yield 0.3911g, 1.39 mmol (38%).

MP 205.9-207.9 °C

MS (APCI +ve) $m/z = 283 (M+H)^+$, $265 (M-H_2O)^+$ found 281 (2 mass unit less than expected).

IR (KBr disc) $\nu = 3477$, 3424, 3361 (N-H), 3205, 2962, 1677, 1636 1600 (C=O), 1532, 1484, 1413 cm^{-1}

¹H NMR: 1.21 (s, 6H, Me₂), 2.86-3.00 (m, 1H, isop-H), 6.93 (bs, 2H, NH₂), 7.33 (d, 2H, J= 8.2 Hz, Ar-H3 and H5), 7.81 (ov.d, 4H, J= 8.0, Ar-H2, H6, Pyr-H3 and H5), 8.64 (d, 2H, 5.7 Hz, Pyr-H2 and H6), 10.16 (bs, 1H, NH) ppm.

7.10 Characterisation of pyridine-3-carboxamidrazone *N*¹-(3,5-Di-*tert*-butyl-2-hydroxy-benzoyl)amide (3PYCa5)

Beige crystalline solid. 0.319 g, 8.66 mmol (24%).

MP 218.7-220.3 °C

MS (APCI +ve) *m/z* = 369 (M+H)⁺

IR (KBr disc) ν = 3353 (N-H), 3220, 3046, 2962, 2907, 2869, 1666, 1614 (C=O), 1579, 1546, 1481, 1434, 1336, cm^{-1}

¹H NMR: 1.30 (s, 9H, Me₃), 1.38 (s, 9H, Me₃), 7.09 (bs, 2H, NH₂), 7.33 (bs, 1H, Ar-H4), 7.50 (m, 1H, Pyr-H5), 7.79 (bs, 1H, Ar-H6), 8.21 (d, 1H, J = 7.5 Hz, Pyr-H4), 8.68 (d, 1H, J = 4.3 Hz, Pyr-H6), 9.03 (s, 1H, Pyr-H2), 10.67 (bs, 1H, NH), 13.54 (bs, 1H, OH) ppm.

7.11 Synthesis of Carboxamidrazoe Imides

7.11.1 General procedure for preparation of carboxamidrazone Imides

A mixture of **2PY** (1.150 g, 8.45 mmol) and phthalic anhydride Anh1 (1.1 eq) in ethanol (30 mL) was heated to refluxed with stirring for 12 h at 80 °C. The resultant solution was evaporated under high vacuum to give a precipitate. The precipitate was collected by filtration, washed with a little cold ethanol and dried under vacuum. If necessary the material was purified by recrystallisation

7.11.2 Characterisation of Carboxamidrazoe Imides

7.11.2.1 Pyridine-2-carboxamidrazone *N*¹-phthalimide (2PYAnh1)

Recrystallisation from EtOAc afforded the title compound as white crystalline solid. Yield (1.1099 g, 4.13 mmol) 56%. R.f. [EtOAc:MeOH, 9:1]: 0.67.

MP 196.2-197.5 °C

IR (KBr disc) ν = 3417, 3314 (N-H), 3060, 1702, 1661, 1623 (C=O), 1584, 1567 1482, 1336, 1235 cm^{-1}

¹H NMR: 7.40 (bs, 2H, NH₂), 7.60-7.65 (m, 1H,), 7.86 (t, 2H, J = 8.0 Hz,), 7.97-8.04 (m, 1H,), 8.33 (d,d 1H, J = 7 Hz,), 8.45 (t, 4H, J = 6.7 Hz,), 8.70 (d,1H, J = 5.7 Hz,)

7.11.2.2 Pyridine-2-carboxamidrazone *N*¹-1,8-Naphthalimide (2PYAnh2)

Recrystallisation from EtOAc afforded the title compound as white crystalline solid.

White crystalline solid. Yield (1.109 g, 3.50 mmol) 48% R.f. [EtOAc:MeOH, 9:1]: 0.75.

MP 269.9-270.6 °C

MS (APCI +ve) *m/z* = 317 (M+H)⁺, 299 (M-H₂O)⁺

IR (KBr disc) ν = 3345, 3299 (N-H), 3060, 1584, 1561, 1467, 1444, 1388, 1285 cm^{-1}

¹H NMR: 7.50-7.55 (m, 2H, 2Ar-H), 7.88-7.98 (m, 4H, 4Ar-H), 8.63 (d, 2H, J = 4.7 Hz, Pyr-H4 and H5), 8.96 (s, 2H, Pyr-H3 and H6) ppm.

7.11.3 Synthesis and Characterisation of Pyridine-4-carboxamidrazone *N*¹-1,8-Naphthalimide (4PYAnh2).

7.11.3.1 Pyridine-4-carboxamidrazone *N*¹-1,8-naphthalimide (4PYAnh2).

4PYAnh2 was prepared in the same manner as described for 2PYAnh (Section 9.12.1). The crude material was recrystallised from the mixture of MeOH and THF 80:20 respectively.

White crystalline solid. Yield (0.873 g, 0.23 mmol) 38% .R.f. [EtOAc: MeOH 9:1]: 0.19

MP 225.1-226 °C

MS (APCI +ve) *m/z* = 317 (M+H)⁺, 299 (M-H₂O)⁺

IR (KBr disc) ν = 3413, 3328 (N-H), 3179, 3060, 1768, 1743, 1704, 1658 (C=O), 1580, 1538, 1405 cm⁻¹

¹H NMR: 7.37 (bs, 2H, NH₂), 7.85 (m, 4H, 4Ar-H), 8.45 (t, 2H, J = 6.9 Hz, Pyr-H3 and H5), 8.56 (m, 2H, 2Ar-H), 8.75 (d, 2H, J = 6.0 Hz, Pyr-H2 and H6) ppm.

7.12 Synthesis of the 4-Isopropyl-benzoic acid

A mixture of 4-Isopropyl-benzaldehyde (10 g, 67.6 mmol) and ethanol (200 mL) were heated at 78 °C for five days. Air was allowed to enter the system and more ethanol was added during five days. The mixture was cooled and the resultant white precipitate was filtered off and treated with aqueous sodium hydrogen carbonate. This solution was extracted twice with chloroform (50 mL), and these extracts were discarded. The aqueous solution was acidified with concentrated hydrochloric acid, precipitating the 4-Isopropyl-benzoic acid.

White crystalline solid. Yield 1.457 g, 8.88 mmol (13.14%).

MS (APCI -ve) *m/z* = 163 (M-H)⁺, 119 (M-CO₂)⁺

¹H NMR: 1.180 (s, 3H, Me), 1.26 (s, 3H, Me), 2.96 (m, 1H, isoprop-H), 7.36 (d, 2H, J = 8.3 Hz, Ar-H3 and H5), 7.86 (d, 2H, J = 8.2 Hz, Ar-H2 and H6), 12.78 (bs, 1H, OH) ppm.

7.13 Preparation of Carboxamidrazones Sulphonamide.

7.13.1 General method for the preparation of carboxamidrazones sulphonamide.

2-Pyridylcarboxamidrazone (0.5 g) was dissolved in THF (5ml) and Hunig's base 1(ml) was added. 4-tert-butyl benzenesulfonyl chloride (1.1 eq) was dissolved in dry THF and added drop wise in the same manner as urea. The crude product was brown liquid, which was concentrated in high vacuum and was washed with water followed by ether.

7.13.2 Characterisation of Carboxamidrazones Sulphonamide

7.13.2.1 Pyridine-2-carboxamidrazone *N*¹-(4-tert-butylbenzoyl)sulphonamide (2PYS1)

Recrystallised from ethanol to gave brown crystalline solid. Yield obtained was 1.164 g (97%).

MS (APCI +), *m/z*: 332, Found (*m*⁺¹) 333.

¹H-NMR 1.36 (s, 9H, C(Me)₃); 5.57 (bs, 2H, NH₂); 7.59 (m, 4H, Ar-H3, Ar-H5 and Pyr-H4 and H5), 7.45 (d, 2H, J = 8.6 Hz, Ar-H2 and H6), 8.69 (d, 2H, J = 6.3 Hz, Pyr-H3 and H6) ppm. NH was not observed in the spectrum.

7.13.2.2 Pyridine-2-carboxamidrazone *N*¹-(benzoyl)sulphonamide (2PYS2)

Recrystallised from ethanol twice to gave light brown crystalline solid.

MS (APCI +ve) $m/z = 277 (M+H)^+$, $136 (M-PhSO_2)^+$

1H -NMR: 7.71 (m, 4H, Pyr-H4, Ar-H3, H4 and H5), 7.92 (d, 2H, $J = 9.5$ Hz, Ar-H2 and H6), 8.04 (d, 2H, Pyr-H3 and H5), 8.72 (d, 1H, $J = 4.5$ Hz, Pyr-H6), 9.13 (bs, 1H, NH) ppm.

7.13.2.3 Pyridine-2-carboxamidrazone N^1 -(4-chlorobenzoyl)sulphonamide (2PYS3)

Recrystallised from ethanol to gave brown crystalline solid.

MS (APCI +ve) $m/z = 310, 312 (M+H)^+$, $130 (M-ClC_6H_4SO_2)^+$

1H -NMR: 6.53 (bs, 2H, NH_2), 7.44 (td, 1H, $J = 1.9, 4.63$ Hz, Pyr-H4), 7.68 (d, 2H, $J = 8.7$ Hz, Ar-H2 and H6), 7.84 (d, 2H, $J = 6.6$ Hz, Ar-H3 and H5), 7.89 (d, 2H, $J = 5.5$ Hz, Pyr-H3 and H5), 8.54 (d, 1H, $J = 3.6$ Hz, Pyr-H6), 9.65 (bs, 1H, NH) ppm.

7.13.2.4 Pyridine-4-carboxamidrazone N^1 -(4-acetamidobenzoyl)sulphonamide (4PYS4)

Recrystallised from ethanol to gave brown crystalline solid.

MS (APCI +ve) $m/z = 258 (M+H)^+$

1H -NMR: 2.04 (s, 3H, Me), 5.18 (bs, 2H, NH_2), 6.4.4 (d, 2H, $J = 8.5$ Hz, Ar-H2 and H6), 7.26 (d, 2H, $J = 8.5$ Hz, Pyr-H2 and H6), 7.52 (m, 4H, Ar-H3, H5 and Pyr-H3 and H5), 8.65 (bs, 1H, NH), 10.20 (bd, 1H, HN) ppm. Peaks due to the impurity were also observed in the spectrum.

7.13.2.5 Pyridine-4-carboxamidrazone N^1 -(2,4,6-isopropylbenzoyl)sulphonamide (4PYS5)

Recrystallised from ethanol and methanol several time to give a brown crystalline solid.

MS (APCI +ve) $m/z = 403 (M+H)^+$, $136 (M-(CH_3CH)_3C_6H_2SO_2)^+$

1H -NMR: 1.17 (s, 6H, Me_2), 1.19 (s, 12H, $2Me_2$), 2.88 (m, 1H, isopro-CH), 4.31 (m, 2H, 2 isopro-CH), 6.4 (bs, 2H, NH_2), 7.18 (s, 2H, Ar-H3 and H5), 7.56 (d, 2H, 6.3 Hz, Pyr-H2 and H6), 8.52 (d, 2H, $J = 6.3$ Hz, Pyr-H3 and H5) ppm. Peak for NH was not observed in the spectrum. 1H -NMR spectrum of the compound also indicated some impurities.

7.14 N^1 -Arylidene-pyridine-4-carboxamidrazone-4-N-oxides

7.14.1 General method for the preparation of N^1 -arylidene-pyridine-4-carboxamidrazone-4-N-oxides

A mixture of the pyridine carboxamidrazone N-oxide and an appropriate aldehyde (1.1 – 1.3 molar equivalents) in ethanol (20 mL/g of carboxamidrazone N-oxide) was stirred at reflux for 18 h. The starting materials dissolved once heating commenced. After cooling, the precipitated material was collected by filtration, washed with a little cold ethanol and dried under vacuum. The material obtained at this point was generally found to contain a single component as judged by thin layer chromatography. If necessary the material was purified by recrystallisation.

7.14.2 Characterisation of N^1 -Arylidene-pyridine-4-carboxamidrazone-4-N-oxides

7.14.2.1 N^1 -(3,5-Di-tert-butyl-2-hydroxybenzylidene) pyridinecarbox amidrazone-4-N-oxide (4PYap-N-O).

Yellow crystalline solid. 68% yield.

MP 277.2 – 278.9 °C

MS (APCI +ve) $m/z = 369 (M+H)^+$

IR (KBr disc) $\nu = 3458, 3273, 3114, 2955, 1635, 1622, 1542, 1500, 1438, 1399, 1356, 1247 (N-O), 1177 \text{ cm}^{-1}$

$^1\text{H NMR}$: 1.28 (s, 9H, CMe_3), 1.43 (s, 9H, CMe_3), 7.12 (bs, 2H, NH_2), 7.30 (d, 1H, $J=2.4\text{Hz}$, Ar'-H), 7.33 (d, 1H, $J=2.4\text{Hz}$, Ar'-H), 7.94 (d, 2H, $J=7.3\text{Hz}$, Pyr 2-H and Pyr 6-H), 8.30 (d, 2H, $J=7.3\text{Hz}$, Pyr 3-H and Pyr 5-H), 11.57 (s, 1H, N=CH) ppm

7.14.2.2 N^1 -(1-Naphthylidene)pyridine-4-carboxamidrazone-4-N-oxide (4PYag-N-O).

Yellow crystalline solid. 78% yield.

MP 225.3 – 227.7 °C

MS (APCI +ve) $m/z = 291 (M+H)^+$, $273 (M-H_2O)^+$

IR (KBr disc) $\nu = 3406, 3220, 3094, 1615, 1492, 1436, 1241 (N-O), 1181 \text{ cm}^{-1}$

$^1\text{H NMR}$: 7.22 (bs, 2H NH_2), 7.55-7.70 (ov.m, 3H, 3Ar-H), 7.98-8.04 (ov.m, 4H, 2Ar-H, Pyr-H2 and H6), 8.27-8.34 (ov. m, 3H, Pyr-H3, H5 and Ar-H), 8.81 (d, 1H, $J=8.3\text{Hz}$, ArH), 9.19 (s, 1H, N=CH) ppm

7.14.2.3 N^1 -(4-Acetamidobenzylidene)pyridine-4-carbox-amidrazone-4-N-oxide (4PYae-N-O)

Yellow crystalline solid. 75% yield.

MP 232.9 – 234.1 °C

MS (APCI +ve) $m/z = 298 (M+H)^+$, $280 (M-H_2O)^+$

IR (KBr disc) $\nu = 3412, 3280, 3207, 3154, 1674, 1618, 1601, 1562, 1539, 1509, 1492, 1412, 1376, 1327, 1244 (N-O), 1171 \text{ cm}^{-1}$

$^1\text{H NMR}$: 2.06 (s, 3H, Me), 7.13 (bs, 2H, NH_2), 7.63 (d, 2H, $J=8.6\text{Hz}$, Ar 2'-H and Ar 6'-H), 7.83 (d, 2H, $J=8.6\text{Hz}$, Ar 3'-H and Ar 5'-H), 7.93 (d, 2H, $J=7.3\text{Hz}$, Ar 2-H and Ar 6-H), 8.27 (d, 2H, $J=7.3\text{Hz}$, Ar 3-H and Ar 5-H), 8.37 (s, 1H, N=CH), 10.12 (bs, 1H, NH) ppm

7.14.2.4 N^1 -(4-tert-Butylbenzylidene)pyridine-4-carboxamidrazone-4-N-oxide (4PYaf-N-o).

Yellow crystalline solid. 90% yield.

MP 216.1 – 218.2 °C

MS (APCI +ve) $m/z = 297 (M+H)^+$, $279 (M-H_2O)^+$

IR (KBr disc) $\nu = 3450, 3324, 3095, 3060, 3029, 2962, 2944, 2898, 2864, 1616, 1527, 1500, 1445, 1400, 1362, 1345, 1330, 1320, 1245 (N-O), 1195 \text{ cm}^{-1}$

$^1\text{H NMR}$: 1.31 (s, 9H, $\text{C}(\text{CH}_3)_3$), 7.14 (bs, 2H, NH_2), 7.46 (d, 2H, $J=8.4\text{Hz}$, Ar 3'-H and Ar 5'-H), 7.83 (d, 2H, $J=8.4\text{Hz}$, Ar 2'-H and Ar 6'-H), 7.94 (d, 2H, $J=7.3\text{Hz}$, Ar 2-H and Ar 6-H), 8.29 (d, 2H, $J=7.3\text{Hz}$, Ar 3-H and Ar 5-H), 8.42 (s, 1H, N=CH), 10.12 (bs, 1H, NH) ppm

7.14.2.5 N^1 -(3-Benzyloxy-4-methoxybenzylidene)pyridine-4-carboxamidrazone-4-N-oxide (4PYak-N-O)

Yellow crystalline solid. 84% yield.

MP 227.9 – 229.7 °C

MS (APCI +ve) $m/z = 377 (M+H)^+$

¹H NMR: 3.80 (s, 3H, OCH₃), 5.16 (s, 2H, OCH₂), 7.02 (d, 1H, J=8.4Hz, Ar 5'-H), 7.13 (bs, 2H, NH₂), 7.30-7.52 (overlapping m, 6H, Ar-H), 7.75 (d, 1H, J=2.2Hz, Ar 2'-H), 7.93 (d, 2H, J=7.3Hz, Ar 2-H and Ar 6-H), 8.29 (d, 2H, J=7.3Hz, Ar 3-H and Ar 5-H), 8.35 (s, 1H, N=CH) ppm

7.14.2.6 *N*¹-(2-(4-Chlorophenyl)thio)benzylidene)pyridine-4-carboxamidrazone-4-N-oxide (4PYaq-N-O)

Yellow crystalline solid. 52% yield.

MP 175.8 – 178.0 °C

MS (APCI +ve) m/z = 383/385 (M+H)⁺, 365/367 (M-H₂O)⁺

IR (KBr disc) ν = 3371, 3275, 3174, 3092, 1637, 1625, 1617, 1610, 1603, 1560, 1543, 1527, 1509, 1493, 1476, 1458, 1437, 1340, 1285, 1237 (N-O), 1177 cm⁻¹

¹H NMR: 7.23 (d, 2H, J=8.5Hz, ArH), 7.29 (bs, 2H, NH₂), 7.33-7.52 (overlapping m, 5H, ArH), 7.93 (d, 2H, J=7.3Hz, Ar 2-H and Ar 6-H), 8.27 (d, 2H, J=7.2Hz, Ar 3-H and Ar 5-H), 8.35 (m, 1H, ArH), 8.80 (s, 1H, N=CH) ppm

7.14.2.7 *N*¹-(9-Anthrylylidene)pyridine-4-carboxamidrazone-4-N-oxide (4PYai-N-O)

Yellow crystalline solid. 58% yield.

MP 227.8 – 228.9 °C

MS (APCI +ve) m/z = 340 (M+H)⁺, 323 (M-H₂O)⁺

¹H NMR: 7.27 (d, 2H, J=8.5Hz, ArH), 7.68-7.85 (overlapping m, 4H, Anthryl-H), 8.02 (d, 2H, J=7.2Hz, Ar 2-H and Ar 6-H), 8.08 (d, 1H, J=7.5Hz, Anthryl-H), 8.33 (d, 2H, J=7.2Hz, Ar 3-H and Ar 5-H), 8.59 (s, 1H, Anthryl 10-H), 8.85 (d, 1H, J=7.9Hz, Anthryl-H), 8.94 (overlapping m, 2H, Anthryl-H), 9.19 (s, 1H, N=CH) ppm

7.14.2.8 *N*¹-(3-Benzyloxybenzylidene)pyridine-4-carboxamidrazone-4-N-oxide (4PYas-N-O)

Yellow crystalline solid. 89% yield.

MP 179.3 – 180.9 °C

MS (APCI +ve) m/z = 347 (M+H)⁺, 329 (M-H₂O)⁺

IR (KBr disc) ν = 3431, 3275, 3155, 3105, 1614, 1601, 1570, 1490, 1433, 1392, 1260 (N-O), 1181 cm⁻¹
¹H NMR: 5.17 (s, 2H, OCH₂), 7.65 (m, 1H, Ar-H), 7.23 (bs, 2H, NH₂), 7.31-7.51 (overlapping m, 7H, Ar-H), 7.67 (m, 1H, Ar-H), 7.94 (d, 2H, J=7.3Hz, Pyridyl 2-H and Pyridyl 6-H), 8.29 (d, 2H, J=7.3Hz, Pyridyl 3-H and Pyridyl 5-H), 8.42 (s, 1H, N=CH) ppm.

7.15 Synthesis of the Carboxamidrazone Urea

7.15.1 Preparation of pyridid-2-carboxamidrazone-urea

7.15.2 General method for the preparation of pyridine-2-carboxamidrazone urea

A mixture of pyridin-2-carboxamidrazone (**2PY** 1 g, 7.35 mmol), dry THF (20 mL) was stirred under argon until the **2PY** had dissolved. Then an appropriate isocyanate (1.2 eq) in dry THF (10 mL) was added drop-wise over the period of ten minutes. The reaction mixture was left stirred at room

temperature for two days. The resultant precipitate was collected by filtration and washed with THF (2 x 20 mL). If necessary the material was purified by Recrystallisation.

7.15.3 Characterisation of Carboxamidrazone urea

7.15.3.1 Pyridine-2-carboxamidrazone *N*¹-(4-*tert*-butyl-phenyl)urea (2PYIs1)

Recrystallised from ethanol to give white crystalline solid. Yield 1.146 g, 3.68 mmol (64%)

MP 280.2-281 °C

MS (APCI +ve) *m/z* = 312 (M+H)⁺, 163 (M-NH-Ph-(C Me)₃)⁺

IR (KBr disc) ν = 3434, 3360, 3332 (N-H), 3195, 3062, 2948, 2925, 1677, 1644 (NHCO), 1595, 1525, 1471, 1396, 1318, 1297 cm⁻¹

¹H NMR 1.25 (s, 9H, CMe₃), 6.55 (bs, 2H, NH₂), 7.23 (d, 2H, J= 13.6 Hz, Ar-H3 and H5), 7.27-7.30 (m, 1H, Pyr-H4), 7.39 (d, 2H, J= 1.0 Hz, Ar-H2 and H6), 7.422 (td, 1H, J= 1.8, 7.8 Hz, Pyr-H5), 8.45 (d, 1H, J= Hz, Pyr-H3), 8.54 (d, 1H, J= 4.2 Hz, Pyr-H6), 8.66 (bs, 1H, NH), 9.13 (bs, 1H, NH) ppm.

7.15.3.2 Pyridine-2-carboxamidrazone *N*¹-(1-phenyl) urea (2PYIs2).

Recrystallised from ethanol to give cream crystalline solid. Yield 0.581g, 2.27 mmol (62%).

MP 284.3-286.1 °C

MS (APCI +ve) *m/z* = 256 (M+H)⁺, 163 (M-PhHN)⁺

IR (KBr disc) ν = 3445, 3345 (N-H), 3214, 3067, 2932, 1689, 1655, 1610 (NHCO), 1588, 1538, 1477, 1440, 1397 cm⁻¹

¹H NMR 6.58 (bs, 2H, NH₂), 6.99 (t, 1H, J=8.9 Hz, Ar-H4), 7.28 (t, 2H, J= 7.7 Hz, Ar-H3 and H5), 7.41-7.46 (m, 1H, Pyr-H4), 7.67 (d, 2 H, J= 8.7, Ar-H2 and H6), 7.87 (td, 1H, J= 2.5 and 8.3 Hz, Pyr-H3), 8.49 (d, 1H, J= 8.2 Hz, Pyr-H3), 8.57 (d, 1H, J= 5.0 Hz, Pyr-H6), 8.76 (bs 1H, NH), 9.21 (bs, 1H, NH) ppm.

7.15.3.3 Pyridine-2-carboxamidrazone *N*¹-(1-naphthalene)urea (2PYIs3)

Recrystallised from the mixture of EtOH and MeOH (8:2) to give cream crystalline solid. Yield 1.382 g, 4.53 mmol (62%).

MP 268.9-270.3 °C

MS (APCI +ve) *m/z* = 305 (M+H)⁺, 163 (M-naph-NH)⁺

IR (KBr disc) ν = 3445, 3353 (N-H), 3083, 2937, 1685, 1654 (NHCO), 1532, 1471, 1351, 1287 cm⁻¹

¹H NMR 6.63 (bs, 2H, NH₂), 7.42-8.01 (m, 9H, 7Ar-H and Pyr-H4 and H5), 8.49 (d, 1H, J= 8.0, Pyr-H3), 8.59 (d, 1H, J= 4.1 Hz, Pyr-H6), 9.18 (bs, 1H, NH), 9.41 (bs, 1H, NH) ppm.

7.15.3.4 Pyridine-2-carboxamidrazone *N*¹-(4-methyl-benzenesulfonyl)urea (2PYIs4)

Recrystallised from the mixture of EtOH and MeOH (7:3) three times to give pale yellow crystalline solid. Yield 1.526 g, 4.58 mmol (62%).

MP 167.4-168.8 °C

MS (APCI +ve) *m/z* = 333 (M+H)⁺, 163 (M-PhMeSO₂NH)⁺

IR (KBr disc) ν = 3405 (N-H), 3219, 3093, 1615 (NHCO), 1525, 1492, 1436, 1240, 1180 (SO₂), 960 (S-N) cm⁻¹

¹H NMR 2.38 (s, 3H, Me), 6.62 (bs, 2H, NH₂), 7.38-7.47 (ov.m, 3H, Ar-H3, Ar-H5 and Pyr-H4), 7.85-8.46 (ov.m, 3H, Ar-H2, Ar-H6 and Pyr-H5), 8.46 (s, 1H, Pyr-H3), 8.54 (s, 1H, Pyr-H6), 9.50 (bs, 1H, NH), 10.86 (bs, 1H, NH).

7.15.3.5 Pyridine-2-carboxamidrazone *N*'-(4-cyclohexyl)urea (2PYIs5)

Recrystallised from aqueous DMF to give white crystalline solid. Yield 0.954 g, 3.65 mmol (50%).

MP 178-178.9 °C

MS (APCI +ve) m/z = 263 (M+H)⁺, 137 (M-cyclohex-CONH)⁺

IR (KBr disc) ν = 3451, 3401, 3355, 3328 (N-H), 3257, 3222, 3077, 2938, 2851, 1675, 1636 (C=O), 1582, 1536, 1467, 1253 cm⁻¹

¹H NMR 1.09-1.80 (m, 10H, cyclohex (CH₂)₅), 3.53 (s, 1H, cyclohex H1), 6.40 (bs, 2H, NH₂), 6.47 (d, 1H, J= 8.5 Hz, Pyr-H4), 7.38-7.43 (m, 1H, Pyr-H 3), 7.82 (td, 1H, J=2.5 and 9.2 Hz, Pyr-H5), 8.25 (d, 1H, J= 8.0Hz, Pyr-H6), 8.54 (m, 1H, NH), 8.75 (bs, 1H, NH) ppm.

7.15.3.6 Pyridine-2-carboxamidrazone *N*'-(4-bromo-phenyl)urea (2PYIs6)

Recrystallised from EtOH to give yellow crystalline solid. Yield 1.078 g, 3.22 mmol (44%) yield.

MP 281.1-282.4 °C

MS (APCI +ve) m/z = 335 (M+H)⁺

IR (KBr disc) ν = 3455, 3353 (N-H), 3208, 3075, 2933, 1683, 1652, 1602 (NHCO), 1580, 1527, 1469, 1394, 1311, 1234 cm⁻¹

¹H NMR 6.60 (br, 2H, NH₂), 7.41-7.48 (m, 3H, Ar-H3, Ar-H5 and Pyr-H4), 7.66-7.72 (m, 2H, Ar-H2 and H6), 7.86 (td, 1H, J=1.75, and 7.7 Hz, Pyr-H5), 8.53 (d, 1H, J= 8.3 Hz, Pyr-H3), 8.56 (d, 1H, J= 4.5 Hz, Pyr-H6), 8.89 (br, 1H, NH), 9.30 (br, 1H, NH) ppm.

7.15.3.7 Pyridine-2-carboxamidrazone *N*'-(4-nitro-phenyl)urea (2PYIs7)

Recrystallised from mixture of MeOH and THF (6:4) yellow crystalline solid. Yield 1.07 g, 3.59 mmol (49%).

MP 224.6-225.9 °C

MS (APCI +ve) m/z = 300 (M+H)⁺, 162 (M-PhNO₂NH)⁺

IR (KBr disc) ν = 3459, 3342 (N-H), 3214, 1700, 1663, 1606 (C=O), 1534, 1395, 1332 (NO₂), 1239 cm⁻¹

¹H NMR 6.67 (bs, 2H, NH₂), 7.43-7.49 (m, 1H, Pyr-H4), 7.89 (td, 1H, J= 1.75, and 15.2 Hz, Pyr-H5), 8.01 (d, 2H, J= 7.2 Hz, Ar-H2 and H6), 8.18-8.22 (m, 2H, Ar-H3 and H5), 8.50-8.58 (m, 2H, Pyr-H3 and H6), 9.38 (bs, 1H, NH), 9.56 (bs, 1H, NH) ppm.

7.15.3.8 Pyridine-2-carboxamidrazone *N*'-(4-methyl-phenyl)urea (2PYIs 8)

Recrystallised from EtOH to give white crystalline solid. Yield 0.592 g, 2.20 mmol (30%).

MP 282.6-283.9 °C

MS (APCI +ve) m/z = 269 (M+H)⁺, 163 (M-PhMeNH)⁺

IR (KBr disc) ν = 3428, 3357, 3320 (N-H), 3194, 3069, 2925, 1685, 1654 (C=O), 1588, 1526, 1471, 1320 cm⁻¹

¹H NMR: 2.25 (s, 3H, Me), 6.56 (bs, 2H, NH₂), 7.08 (d, 2H, J= 8.3 Hz, Ar-H3 and H5), 7.40-7.45 (m, 1H, Pyr-H4), 7.54 (d, 2H, J= 8.3 Hz, Ar-H2 and H6), 7.85 (td, 1H, J= 1.6, and 7.7 Hz, Pyr-H5), 8.47 (d, 1H, J= 8.0 Hz, Pyr-H3), 8.55 (d, 1H, J= 8.0 Hz, Pyr-H6), 8.67 (bs, 1H, NH), 9.15 (bs, 1H, NH) ppm.

7.15.3.9 Pyridine-2-carboxamidrazone *N*¹-(3-methyl-phenyl)urea (2PYIs9)

Recrystallised from the mixture of EtOAc and EtOH (5:5) to give yellow crystalline solid. Yield 0.772 g, 2.87 mmol (39%).

MP 281.5-282.4 °C

MS (APCI -ve) *m/z* = 268 (M-H)⁺, 135 (M-PhMeNHCO)⁺

IR (KBr disc) ν = 3441, 3360 (N-H), 3181, 3073, 2927, 1683, 1641 (NHCO), 1538, 1469, 1395, 1287, 1251 cm⁻¹

¹H NMR 2.29 (s, 3H, Me), 6.58 (bs, 2H, NH₂), 6.81 (d, 1H, J= 7.6Hz, Ar-H4), 7.16 (t, 1H, J= 7.95 Hz, Ar-H5), 7.41-7.49 (ov.m, 3H, Ar-H2, Ar-H6 and Pyr-H4), 7.86 (td, 1H, J= 1.7, and 7.6 Hz, Pyr-H5), 8.46 (d, 1H, J= 8.0, Hz, Pyr-H3), 8.55 (d, 1H, J=5.6 Hz, Pyr-H6), 8.73 (bs, 1H, NH), 9.19 (bs 1H, NH) ppm.

7.15.3.10 Pyridine-2-carboxamidrazone *N*¹-(2-methoxy-phenyl)urea (2PYIs10)

Recrystallised from EtOH to give white crystalline solid. Yield 1.198 g, 9.20 mmol (57%).

MP 282.8-284.5 °C

MS (APCI -ve) *m/z* = 284 (M+H)⁺, 162 (M-PhOMeNH)⁺

IR (KBr disc) ν = 3463, 3359 (N-H), 3216, 2940, 1685, 1658, 1604 (NHCO), 1545, 1461, 1337 cm⁻¹

¹H NMR 3.94 (s, 3H, OMe), 6.62 (bs, 2H, NH₂), 6.87-7.00 (m, 3H, Ar-H3, H4 and H5), 7.44-7.49 (m, 1H, Pyr-H4), 7.96 (td, 1H, 1.7 and 4.9 Hz, Pyr-H 5), 8.08 (d, 1H J= 8.0 AR-H 6), 8.17 (d,d, 1H, J= 1.9 and 2.1 Hz, Pyr-H 3), 8.59 (d, 1H, J= 4.7 Hz, Pyr-H6), 9.02 (bs, 1H, NH), 9.39 (bs, 1H, NH) ppm

7.15.3.11 Pyridine-2-carboxamidrazone *N*¹-(3-methoxy-phenyl)urea (2PYIs11)

Recrystallised from EtOH twice to give white crystalline solid. Yield 1.073 g, 3.76 mmol (51%).

MP 182-184.4 °C

MS (APCI +ve) *m/z* = 284 (M+H)⁺, 163 (M-PhOMeNH)⁺

IR (KBr disc) ν = 3461, 3357 (N-H), 3212, 3090, 2928, 1691, 1636, 1606 (NHCO), 1542, 1312, cm⁻¹

¹H NMR 3.74 (s, 3H, OMe), 6.55 (Ov.m, 3H, J= 1.6 Hz, Ar-H4 and NH₂), 7.4-7.28 (m, 2H, Ar-H3 and H5), 7.36 (t, 1H, J= 2.1 Hz, Ar-H 6), 7.41-7.46 (m, 2H, Pyr-H4), 7.86 (td, 1H, J= 1.65 Hz, Ar-H5), 8.49 (d, 1H, J= 8.0, PYr-H3), 8.56 (d, 1H, J= 4.7 Hz, Pyr-H6), 8.73 (bs, 1H, NH), 9.20 (bs, 1H, NH) ppm.

7.15.3.12 Pyridine-2-carboxamidrazone *N*¹-(4-methoxy)urea (2PYIs12)

Recrystallised from methanol to give white crystalline solid. Yield 1.192 g, 4.18 mmol (57%).

MP 287.6-288.3 °C

MS (APCI +ve) *m/z* = 284 (M+H)⁺, 163 (M- PhOMeNH)⁺

IR (KBr disc) ν = 3441, 3399, 3337 (N-H), 3206, 3075, 2940, 1681, 1650 (NHCO), 1598, 1532, 1473, 1398, 1292, 1241 cm⁻¹

¹H NMR 3.72 (s, 3H, OMe), 6.54 (bs, 2H, NH₂), 6.88 (d, 2H, J= 12.3 Hz, Ar-H2 and H6), 7.40-7.55 (m, 1H, Pyr-H4), 7.53 (d, 2H, J= 8.9Hz, Ar-H3 and H5), 7.84 (td, 1H, J= 1.5 and 1.6 Hz, Pyr-H5), 8.48 (d, 1H, J= 8.0 Hz, Ar-H3), 8.55 (d, 1H, J= 3.1 Hz, Pyr-H6), 8.64 (bs, 1H, NH), 9.11 (bs, 1H, NH) ppm.

7.15.3.13 Pyridine-2-carboxamidrazone N¹-(4-chloro-phenyl)urea (2PYIs14).

Recrystallised from EtOH to give pale yellow crystalline solid. Yield 1.198 g, 4.15 mmol (56%).

MP 232.3-233.2 °C

MS E(+) [C₁₃H₁₃N₅OCl] = mass 290.0800, calculated mass 290.0809 [M+Na]⁺ {-2.9 ppm}.

IR (KBr disc) ν = 3455, 3355, 3330 (NH), 3216, 3100, 2930, 1702, 1658, 1602 (NHCO), 1532, 1436 1395, 1309 cm⁻¹

¹H NMR 7.01 (bs, 2H, NH₂), 7.05 (td, 1H, J= 1.5 and 8.0 Hz, Pyr-H5), 7.33 (t, 1H, J= 8.3 Hz, Pyr-H4), 7.44-7.52 (m, 2H, Ar-H2 and H6), 7.93 (td, 1H, J= 1.8, and 8.0 Hz, Pyr-H3), 8.14 (d, 1H, J=9.0 Hz, Ar-H3 or H5), 8.30 (d, 1H, J= 8.9 Hz, Ar-H3 or H5), (d, 1H, J= 6.5 Hz, Pyr-H6), 9.11 (bs, 1H, NH), 9.59 (bs, 1H, NH) ppm.

7.15.3.14 Pyridine-2-carboxamidrazone N¹-(2-methyl-phenyl)urea (2PYIs15)

Recrystallised from mixture of EtOH and EtOAc to give white crystalline solid. Yield 0.673 g, 2.50 mmol (34%).

MP 246.6-247.8 °C

MS (APCI +ve) m/z = 270

IR (KBr disc) ν = 3417, 3351 (N-H), 3212, 2921, 1695, 1634 (NHCO), 1532, 1442, 1395, 1307 cm⁻¹

¹H NMR 2.30 (s, 3H, Me), 6.60 (bs, 2H, NH₂), 6.98 (t, 1H, J= 7.4 Hz, Ar-H4), 7.09-7.22 (m, 2H, Ar-H5 and H3), 7.41-7.46 (m, 1H, Pyr-H4), 7.68 (ov.m, 2H, Pyr-H5 and Ar-H6), 8.27 (d, 1H, J= 7.8 Hz, Pyr-H3), 8.55 (d, 2H, J= 4.9 Hz, Pyr-H6), 8.5 (bs, 1H, NH), 9.28 (bs, 1H, NH) ppm

7.15.3.16 Pyridine-2-carboxamidrazone N¹-(2-nitro-phenyl)urea (2PYIs16)

Recrystallised from aqueous DMF to give cream crystalline solid. Yield 1.061 g, 3.54 mmol (48%) yield.

MP 283.8-285.1 °C

MS (APCI +ve) m/z = 301 (M+H)⁺, 163 (M-PhNO₂NH)⁺

MS E(+) [C₁₃H₁₃N₆O₃] = mass 301.1048, calculated mass = 301.1041 [M+Na]⁺ {2.3 ppm}.

IR (KBr disc) ν = 3405 (N-H), 3274, 1679, 1617 (NHCO), 1594, 1532, 1484, 1403, 1363 cm⁻¹

¹H NMR: 6.75 (bs, 2H, NH₂), 7.19 (t, 1H, J= 7.2 Hz, Ar-H4), 7.45-7.50 (m, 1H, Pyr-H4), 7.72 (t, 1H, J= 8.6 Hz, Ar-H6), 7.95 (td, 1H, J= 1.6 and 7.6 Hz, Pyr-H5), 8.21 (d, 1H, J= 9.9 Hz, Ar-H3 or H5), 8.36 (d, 1H, J= 8.1 Hz, Pyr-H3), 8.60 (d, 1H, J= 4.8 Hz, Pyr-H6), 8.78 (d, 1H, J= 9.6 Hz, Ar-H3 or H5), 9.78 (bs, 1H, NH), 11.29 (bs, 1H, NH) ppm.

7.16 Preparation of Pyridine-4-carboxamidrazone-Urea

7.16.1. General method for the preparation of pyridine-4-carboxamidrazone-urea

A mixture of pyridin-4-carboxamidrazone **4PY** (1 g, 7.35 mmol), dry THF (20 mL) and DMF (2-3 mL) was stirred under argon until the **4PY** had dissolved. Then an appropriate isocyanate (1.2 eq) in THF (10 mL) was added drop-wise over the period of ten minutes. The reaction mixture was left stirred at

room temperature for two days. The white precipitate was collected by filtration and washed with THF (2 x 20 mL). If necessary the material was purified by recrystallisation.

7.16.2 Characterisation of pyridine-4-carboxamidrazones Urea

7.16.2.1 Pyridine-4-carboxamidrazone *N*¹-(4-*tert*-butyl-phenyl)urea (4PYIs1)

Recrystallised from the mixture of EtOH and MeOH (8:2) to give pale yellow crystalline solid. Yield 0.917 g, 2.95 mmol (40%). R.f. [EtOAc:MeOH, 9:1]: 0.09.

MP 381.9-383.5 °C

MS E(+), [C₁₇H₂₂N₅O] = mass 312. 1815, calculated mass = 312.1824 [M+ Na]⁺ [-2.9 ppm].

IR (KBr disc) ν =

¹H NMR 1.27 (s, 9H, CMe₃), 6.57(bs, 2H, NH₂), 7.29 (d, 2H, J= 8.5 Hz, Ar-H3 and H5), 7.53 (d, 2H, J= 8.5 Hz, Ar-H2 and H6), 7.91(d, 2H, J= 6.2 Hz, Pyr-H3 and H5), 8.6 (d, 2H, J= 4.5 Hz, Pyr-H2 and H6), 8.62 (bs, 1H, NH), 9.10 (bs, 1H, NH) ppm.

7.16.2.2 Pyridine-4-carboxamidrazone *N*¹-(1-phenyl)urea (4PYIs2)

Orange crystalline solid (1.031 g, 4.03 mmol (55%)). R.f. [EtOAc:MeOH, 8:2]: 0.72

MP 260.2-262.2 °C

MS (APCI +ve) m/z = 256 (M+H)⁺, 239 (M-H₂O)⁺

IR (KBr disc) ν = 3733, 3443 (N-H), 3277, 1748, 1698, 1644 (NHCO), 1533, 1428, 1218 cm⁻¹

¹H NMR 6.57 (bs, 2H, NH₂), 6.99 (t, 1H, J= 7.3 Hz, Ar-H4), 7.28 (t, 2H, J= 7.5 Hz, Ar-H3 and H5), 7.64 (d, 2H, J=7.6 Hz, Ar-H2 and H6), 7.92 (d, 2H, J=6.1 Hz, Pyr-H3 and H5), 8.61 (d, 2H, J= 6.1 Hz, Pyr-H2 and H6), 8.70 (bs, 1H, NH), 9.16 (bs, 1H, NH) ppm.

7.16.2.3 Pyridine-4-carboxamidrazone *N*¹-(1-naphthalene)urea (4PYIs3)

The crude material was recrystallised from the mixture of MeOH and EtOH (7:3) several time to give beige crystalline solid. Yield 1.274 g, 4.18 mmol (57%) The 1H-NMR and MS analysis showed the complex mixture.

7.16.2.4 Pyridine-4-carboxamidrazone *N*¹-(4-methylbenzenesulfonyl)urea (4PYIs4).

Yellow crystalline solid. Yield 1.772 g, 5.32 mmol (72%).

MP 184.2-185 °C

MS (APCI +ve) m/z = 333 (M+H)⁺, 163 (M-PhMeSO₂NH)⁺ (M-H₂O)⁺

¹H NMR 2.24 (s, 3H, Me), 6.55 (bs, 2H, NH₂), 7.08 (d, 2H, J= 8.5 Hz, Ar-H3 and H5), 7.51 (d, 2H, J= 8.5, Ar-H2 and H6), 7.84 (d, 2H, J= 6.0 Hz, Pyr-H3 and H5), 8.60 (ov.m, 3H, J= 6.3 Hz, Pyr-H2, H6 and NH), 9.12 (bs, 1H, NH) ppm.

7.16.3.5 Pyridine-4-carboxamidrazone *N*¹-(4-cyclohexyl)urea (4PYIs5)

Yellow crystalline solid. Yield 0.865 g, 3.31 mmol (45%). R.f. [EtOAc:MeOH 9:1]: 0.31

MP 263.5-265.5 °C

MS (APCI +ve) m/z = 262 (M+H)⁺, 137 (M-cyclohex-CONH)⁺

IR (KBr disc) ν = 3411 (N-H), 3214, 3071, 2927, 2852, 1704, 1652 (NHCO), 1596, 1532, 1404 cm⁻¹

¹H NMR 1.08-1.76 (m, 10H, cyclohexane), 3.51 (s, 1H, cyclohex), 6.38 (bs, 2H, NH₂), 6.41 (bs, 1H, NH), 7.78 (d, 2H, *J* = 6.0 Hz Pyr-H₃ and H₅), 8.58 (d, 2H, *J* = 6.0 Hz, Pyr-H₂ and H₆), 8.71 (bs, 1H, NH) ppm.

7.16.3.6 Pyridine-4-carboxamidrazone *N*¹-(4-bromo-phenyl)urea (4PYIs6)

Off white crystalline solid. Yield 1.408 g, 4.22 mmol (57%).

MP 356.9-358.5 °C

MS (APCI +ve) *m/z* = 334/336 (M+H)⁺,

IR (KBr disc) ν = 3428, 3368 (N-H), 1689, 1658 (NHCO), 1584, 1521, 1388, 1309 1222 cm⁻¹

¹H NMR 6.58 (2H, NH₂), 7.44 (d, 2H, *J* = 8.9 Hz, Ar-H₂ and H₆), 7.66 (d, 2H, *J* = 8.9 Hz, Ar-H₃ and H₅), 7.92 (d, 2H, *J* = 6.2 Hz, Pyr-H₃ and H₅), 8.60 (d, 2H, *J* = 6.1 Hz, Pyr-H₂ and H₆), 8.83 (bs, 1H, NH), 9.24 (bs, 1H, NH) ppm.

7.16.3.7 Pyridine-4-carboxamidrazone *N*¹-(4-nitro-phenyl)urea (4PYIs7)

Recrystallised from MeOH twice to give yellow crystalline solid. Yield 1.297 g, 4.32 mmol (59%). R.f.

[EtOAc: Petrol 60-80°C 7:3]: 0.44

MP 292.9-295 °C

MS (APCI +ve) *m/z* = 301 (M+H)⁺, 162 (M-PhNO₂NH)⁺

IR (KBr disc) ν = 3445, 3366, (N-H), 1733, 1642 (NHCO), 1594, 1496 (NO₂), 1334, 1320 cm⁻¹

¹H NMR 6.59 (bs, 2H, NH₂), 7.46 (d, 2H, *J* = 9.0 Hz, Ar-H₂, and H₆), 7.68 (d, 2H, *J* = 8.8 Hz, H₃ and H₅), 7.94 (d, 2H, *J* = 6.3 Hz, Pyr-H₃ and H₅), 8.63 (d, 2H, *J* = 6.3 Hz, Pyr-H₂ and H₆), 8.85 (bs, 1H, NH), 9.26 (bs, 1H, NH) ppm.

7.16.3.8 Pyridine-4-carboxamidrazone *N*¹-(3-methyl-phenyl)urea (4PYIs9)

Peach crystalline solid. Yield 0.699 g, 2.60 mmol (35%).

MP 218.8-219 °C

MS (APCI +ve) *m/z* = 270 (M+H)⁺, 253 (M-H₂O)⁺

IR (KBr disc) ν = 3415, 3337 (N-H), 3239, 2917, 1704, 1644 (NHCO), 1532, 1452, 1386, 1309 cm⁻¹

¹H NMR 2.28 (s, 3H, Me), 6.57 (bs, 2H, NH₂), 6.80 (d, 1H, Ar-H₄), 7.15 (t, 1H, *J* = 7.4 Hz, Ar-H₅), 7.44 (d, 2H, Ar-H₂ and H₆), 7.91 (d, 2H, *J* = 6.2, Pyr-H₃ and H₅), 8.61 (d, 2H, *J* = 6.2, Pyr-H₂ and H₆), 8.63 (bs, 1H, NH), 9.16 (bs, 1H, NH) ppm.

7.16.3.9 Pyridine-4-carboxamidrazone *N*¹-(2-methoxy-phenyl)urea (4PYIs10)

Yellow crystalline solid. Yield 1.534 g, 5.38 mmol (73%). R.f. [EtOAc:MeOH, 9:1]: 0.35

MP 288-289.5 °C

MS (APCI +ve) *m/z* = 286 (M+H)⁺, 162 (M-PhOMeNH)⁺ (M-H₂O)⁺

IR (KBr disc) ν = 3416, 3345 (N-H), 3216, 3095, 2940, 1696, 1658 (NHCO), 1596, 1542, 1486, 1465, 1344, 1295, 1245 cm⁻¹

¹H NMR 3.91 (s, 3H, OMe), 6.64 (bs, 2H, NH₂), 6.89-7.06 (m, 3H, Ar-H 3, H₄ and H₅), 7.75 (d, 2H, *J* = 6.0 Hz, Pyr-H₃ and H₅), 8.16 (d, 1H, *J* = 9.5 Hz, Ar-H₆), 8.67 (d, 2H, *J* = 6.0 Hz, Pyr-H₂ and H₆), 8.99 (bs, 1H, NH), 9.35 (bs, 1H, NH) ppm.

7.16.3.10 Pyridine-4-carboxamidrazone *N*¹-(3-methoxy-phenyl)urea (4PYIs11)

Recrystallised from DMF to give yellow crystalline solid 0.872 g, 3.06 mmol (42%). R.f. [EtOAc:MeOH, 9:1]: 0.07

MP 357.9-359.5 °C

MS (APCI +ve) *m/z* = 286 (M+H)⁺

IR (KBr disc) ν = 3430, 3351 (N-H), 3218, 3090, 2935, 2832, 1704, 1664, 1606 (NHCO), 1546, 1492, 1461, 1396, 1309, 1289 cm⁻¹

¹H NMR 3.73 (s, 3H, OMe), 6.57 (d, 1H, *J* = 7.3 Hz, Ar-H6), 6.67 (bs, 2H, NH₂), 7.14-7.25 (m, 2H, Ar-2 and H4), 7.33 (s, 1H, Ar-H5), 7.93 (s, 2H, Pyr-H3 and H5), 8.64 (s, 2H, Pyr-H2 and H6), 8.69 (bs, 1H, NH), 9.17 (bs, 1H, NH) ppm.

7.16.3.11 Pyridine-4-carboxamidrazone *N*¹-(4-methoxy phenyl)urea (4PYIs12)

Recrystallised from DMF to give cream crystalline solid. Yield 0.982 g, 3.45 mmol (47%).

MP 354.9-356.8 °C

MS (APCI +ve) *m/z* = 286 (M+H)⁺, 269 (M-H₂O)⁺

IR (KBr disc) ν = 3359 (N-H), 3231, 3071, 2934, 1700, 1662 (NHCO), 1594, 1531, 1515, 1397, 1292, 1224 cm⁻¹

¹H NMR 3.72 (s, 3H, OMe), 6.53 (bs, 2H, NH₂), 6.85 (d, 2H, *J* = 9.0 Hz, Ar-H2 and H6), 7.51 (d, 2H, *J* = 9.0 Hz, Ar-H3 and H6), 7.92 (d, 2H, *J* = 6.3 Hz, Pyr-H3 and H5), 8.59 (s, 2H, Pyr-H2 and H6), 8.61 (bs, 1H, NH), 9.07 (bs, 1H, NH) ppm.

7.16.3.12 Pyridine-4-carboxamidrazone *N*¹-(4-chloro-phenyl)urea (4PYIs14)

Recrystallised from MeOH to give yellow crystalline solid. Yield 1.361 g, 4.71 mmol (64%). R.f. [EtOAc:MeOH, 9:1]: 0.35

MP 348.2-349.4 °C

MS (APCI +ve) *m/z* = 290 (M+H)⁺, 273 (M-H₂O)⁺

IR (KBr disc) ν = 3418, 3376 (N-H), 3235, 3081, 2936, 1708, 1665 (NHCO), 1592, 1531, 1496, 1398, 1315, 1282 cm⁻¹

¹H NMR 6.65 (bd, 2H, NH₂), 7.33 (d, 2H, *J* = 8.8 Hz, Ar-H2 and H6), 7.71 (d, 2H, *J* = 9.0 Hz, Ar-H Ar-H3 and H5), 7.94 (d, 2H, *J* = 6.0, Pyr-H3 and H5), 8.64 (d, 2H, *J* = 5.0 Hz, Pyr-H2 and H6), 8.85 (bd, 1H, NH), 9.24 (bs, 1H, NH) ppm.

7.16.3.13 Pyridine-4-carboxamidrazone *N*¹-(2-methyl-phenyl)urea (4PYIs15).

Recrystallised from a mixture of DMF and ether (6:4) to give pale yellow crystalline solid. Yield 0.528 g, 1.96 mmol (27%).

MP 350.6-351.2 °C

MS (APCI +ve) *m/z* = 270 (M+H)⁺, 253 (M-H₂O)⁺

IR (KBr disc) ν = 3420, 3355 (N-H), 3218, 3099, 2935, 1698, 1661, 1604 (NHCO), 1590, 1536, 1463, 1415, 1309, 1287 cm⁻¹

¹H NMR: 2.27 (s, 3H, Me), 6.60 (bs, 2H, NH₂), 6.98 (s, 1H, Ar-H4), 7.13-7.21 (m, 2H, Ar-H3 and H5), (ov.m, 3H, Pyr-H3, H5 and Ar-H6), 8.49 (bs, 1H, NH), 8.62 (d, 2H, *J* = 5.9 Hz, Pyr-H2, H6), 9.25 (bs, 1H, NH) ppm.

7.16.3.14 Pyridine-4-carboxamidrazone *N*'-(2-nitro-phenyl)urea (4PYIs16).

Recrystallised from DMF and ether (6:4) to give an orange crystalline solid. Yield (0.869 g, 2.89 mmol (39%).

MP >350 °C

MS (APCI +ve) $m/z = 301 (M+H)^+$, $163 (M-PhNO_2NH)^+$

1H NMR 7.16-7.22 (m, 1H, Ar-H4), 7.71-7.77 (m, 1H, Ar-H6), 7.89 (d, 2H, $J = 6.3$ Hz Pyr-H3 and H5), 8.21 (d,d, 1H, $J = 1.5$ and 8.5 Hz, Ar-H3 or H5), 8.67 (d, 2H, $J = 6.3$ Hz, Pyr-H2 and H6), 8.75 (dd, 1H, $J = 1.3$ and 8.5 Hz, Ar-H3 or H5), 9.74 (bs, 1H, NH), 11.21 (bs, 1H, NH) ppm.

7.17 Synthesis of the Derivatives of Pyrimethamine

7.17.1 Synthesis of 5-(4-chloro-3-nitro-phenyl)-6-ethyl-pyrimidine-2,4-diamine (104) (Nitro-pyrimethamine)

Pyrimethamine (**71**) (10 g, 43.85 mmol) was added in small portion (10-15 min) to a stirred mixture of conc. nitric acid (30 mL) and conc. sulphuric acid (30 mL). The mixture was heated to 50 °C for 1 h and then kept at 25 °C for 20 h. The syrupy golden solution was then poured into the concentrated aqueous ammonia containing ice (300 mL + ice) and the resultant precipitate was filtered off, and washed with ether. Recrystallisation from the mixture of ethanol and methanol (2:1) respectively furnished yellow crystals.

Yellow crystalline solid.(8.4023 g, 28.67 mmol) 65% yield.

MP 199.9-202.7 °C

MS (APCI +ve) $m/z = 294,296 (M+H)^+$.

IR (KBr disc) $\nu = 3482, 3316, NH_2, 1344, N-H, 1550, NO_2$ cm^{-1} .

1H NMR 0.97(t, 3H, $J = 7.50$ Hz (CH₃), 2.11 (m, 2H, CH₂), 5.82 (bs, 2H, NH₂), 5.96 (bs, 2H, NH₂), 7.49 (d, 1H, $J = 2.0$ Hz, Ar-H6), 7.77 (d, 1H, $J = 8.2$ Hz, Ar-H2 or Ar-H5).7.84 (d, 1H, $J = 2.0$ Hz, Ar-H2 or Ar-H5) ppm.

7.17.2 Synthesis of 2,4-diamino-6-ethyl-5-(4-methoxy-3-nitrophenyl)pyrimidine (105a)

A mixture of nirtopyrimethamine (**104**) (2.50 g, 8.532 mmol) and sodium methoxide (5.75 g, 106.48 mmol) in methanol (75 mL) was heated in a metal bomb at 90 °C for three days. The mixture was cooled by ice bath and the methanol was removed under reduced pressure. Recrystallised from ethanol three times.to gave a brown crystalline solid. The mass spectrometry indicted the presence of the product whereas the 1H -NMR spectrum had showed some impurities.

Brown crystalline solid (1.8709 g, 6.75 mmol) 79% yield.

MS (APCI +ve) $m/z = 290 (M+H)^+$, $149 (M-2,4-Ph NO_2, OMe)^+$

1H NMR: 1.25-0.94 (m, 3H, Me), 2.11(m, 2H, CH₂), 3.81 (m, 3H, OCH₃), 4.71 (bs 2H, NH₂), 5.74 (bs, 2H, NH₂), 7.18-7.70 (m, 3H, Ar-H2, Ar-H5 and Ar-H6).Plus extra peak at 2.11 ppm.

7.17.3 Preparation of 5-(4-ethoxy-3-nitro-phenyl)-6-ethyl-pyrimidine-2,4-diamine (105c)

A mixture of 104, (1 g, 3.41 mmol) in ethanol (40 mL) and sodium hydroxide (0.4 g, 10 mmol) was refluxed with stirring for 3 days. The mixture was cooled to room temperature, the ethanol solvent was removed under reduced pressure. Recrystallisation from EtOAc several times afforded light brown solid. The mass spectrometry indicated the presence of the product, but ¹H NMR spectrum showed impurities.

Brown crystalline solid.(0.547 g, 1.80 mmol), 53% yield.

MS (APCI +ve) m/z = 304 (M+H)⁺, 285 (M-H₂O)⁺

¹H NMR: 1.60 (s, 6H, 2Me), 2.12 (m, 2H, CH₂), 4.22 (m, 2H, OCH₂), 5.81 (m, 2H, Ar-H 5 and H6), 7.31(m, 1H, Ar-H2) ppm, and some extra peaks due to impurities.

7.17.4 Preparation of 2-[4-(2,4-diamino-6-ethyl-pyrimidin-5-yl)-2-nitro-phenoxy]ethanol (105e).

A mixture of (104), (1 g, 3.41 mmol) and sodium hydroxide (0.4 g, 10 mmol) in ethylene glycol (40 mL) was heated at 100 °C with stirring for 10 days. The brown mixture was cooled to room temperature and was poured onto water. The reaction mixture was adjusted to pH 7 by the addition of the few drops of HCl. The resultant mixture was extracted with ethyl acetate (3 x 50 mL). The ethyl acetate layer was dried over magnesium sulphate and the solvent was removed under reduced pressure to give the yellow solid. Recrystallisation form ether three times afforded yellow crystalline solid. The product was identified by mass spectrometry and ¹H-NMR.

Yellow crystalline solid, (0.1684 g, 0.53 mmol) 15% yield.

MS (APCI +ve) m/z = 320 (M+H)⁺, 276 (M-CH₂CH₂O)

¹H NMR: 0.97 (t, 3H, J= 15 Hz, CH₃), 2.10 (m, 2H, CH₂), 3.55 (s, 2H, CH₂), 3.76 (s, 2H, CH₂), 4.21 (t, 2H, OCH₂), 4.91 (bs, 1H, OH), 5.77 (bs, 4H, 2NH₂), 7.41 (s, 2H, H5 and H6), 7.61 (s, 1H, H2) ppm

7.17.5 6-Ethyl-5-[3-nitro-4-(2-propoxy-ethoxy)-phenyl]-pyrimidine-2,4-diamine (105f)

The same method for the preparation of 105e was repeated.

Yellow crystalline solid.(0.587 g, 1.61 mmol). 47% yield.

MS (APCI +ve) m/z = 364 (M+H)⁺, 276 (M-OCH₂CH₂ OCH₂CH₂)⁺

¹H NMR: 0.96 (t, 3H, J= 7.25 Hz, Me), 2.06-2.15 (m, 2H, CH₂), 3.17 (m, 2H, CH₂), 3.78 (m, 2H, CH₂), 4.51-4.30 (ovbd, (OCH₂)₂), 5.73 (bs, 2H, NH₂), 5.90 (bs, 2H, NH₂), 7.24 (m, 2H, Ar-H5 and H6), 7.62 (s, 1H, Ar-H2) ppm.

7.17.6 6-Ethyl-5-[3-nitro-4-[2-(2-propoxy-ethoxy)-ethoxy]-phenyl]-pyrimidine-2,4-diamine (105g)

The same method for the preparation of 105e and 105f was repeated.

Yellow crystalline solid.(0.2088 g, 0.513 mmol), 15% yield.

MS (APCI +ve) m/z = 408 (M+H)⁺, 276 (M-(OCH₂)₃)⁺

¹H NMR: 0.96 (t, 3H, J= 7.5 Hz, Me), 2.07-2.15 (m, 2H, CH₂), 3.43-3.53 (ovm, 6H, (CH₂)₃), 3.79 (s, 2H, OCH₂), 3.78 (t, 2H, OCH₂), 4.30 (s, 2H, OCH₂), 4.58 (s, 2H, OCH₂), 5.79 (bs, 4H, 2NH₂), 7.41 (s, 2H, Ar-H5 and H6), 7.62 (s, 1H, Ar-H2) ppm.

7.18. Synthesis of 5-(3-amino-4-chloro-phenyl)-6-ethyl-pyrimidine-2,4-diamine (106) (APMA)

Tin (II) chloride (5 mol eq) was added in small portions (30 min) to a stirred suspension of the 104, (5 g, 17.06 mmol) in ethanol (100 mL) and was heated at 50°C for 3h. The reaction mixture was cooled and the syrupy yellow residue was dissolved in hot water, cooled, and basified to pH 12 with 10M aqueous sodium hydroxide solution. The white precipitate was filtered, washed with water and dried under high vacuum. Recrystallisation from the mixture of EtOAc and EtOH (2:1) respectively afforded white crystalline solid.

White crystalline solid. (4.067 g, 15.46 mmol), 90% yield.

MP 212.4-214 °C

MS (APCI +ve) m/z = 264 (M+H)⁺

IR (KBr disc) ν = 3461, 3376, 3310 (N-H), 3158, 2965, 1623 (C=O), 1557, 1442, 1278 cm⁻¹

¹H NMR: 0.973 (t, 3H, J= 7.5 Hz, CH₃), 2.08-2.17 (m, 2H, CH₂), 5.41 (bs, 4H, 2NH₂), 5.80 (bs, 2H, NH₂), 6.32 (dd, 1H, J= 1.75, 1.75 Hz, Ar-H₃ or Ar-H₆), 6.60 (d, 1H, J= 1.75 Hz, Ar-H₃ or Ar-H₆), 7.20 (d, 1H, J= 8.0 Hz, Ar-H₅) ppm.

7.19 General procedure for preparation of derivatives of 106 (i.e. Amides)

A mixture of **106** (1 g, 3.80 mmol) and anhydrous THF (20 mL) was stirred for 15 min. Then 2mL of Hunig's base was added to this reaction mixture followed by drop-wise addition of the required carboxylic acid chloride (1.1 eq.) in anhydrous THF (10 mL) over the period of 5-10 min. The reaction mixture was stirred at room temperature over the period of 6h under argon atmosphere. The crude product was filtered and washed with the aqueous sodium hydrogen carbonate followed by water. The title compound was further recrystallised in hot ethanol or methanol to give the compound as white crystalline solid. The mass spectrometry indicated the desired compounds **107a-c** was present, but unfortunately they were not pure with the exception of **107a**. ¹H NMR analysis indicated the presence of some impurities.

7.19.1 Characterisation of 4-tert-butyl-N-[2-chloro-5-(2,4-diamino-6-ethyl-pyrimidin-5-yl)-phenyl]-N-methyl-benzamide (107a)

Recrystallised from ethanol twice to gave white crystalline solid (0.622 g, 1.48 mmol) 62% yield.

MS (APCI +ve) m/z = 424 (M+H)⁺

¹H NMR: 1.077 (t, 3H, J= 7.5, 7.5 Hz, Me), 1.32 (s, 9H, CMe₃), 2.23-2.32 (m, 2H CH₂), 7.16 (d, 1H, J= 1.75 Hz, Ar-H₆), 7.61 (d, 2H, J= 8.4 Hz, Ar'-3 and H₅) 7.66 (d, 2H, J= 9.8 Hz, Ar'-H₂ and H₆), 7.92 (d, 2H, J= 8.4 Hz Ar-H₅ and H₂), 9.97 (bs, 1H, NH) ppm. Peak for 2NH₂ was not observed in the spectrum.

7.19.2 Preparation of N-[2-Chloro-5-(2,4-diamino-6-ethyl-pyrimidin-5-yl)-phenyl]-4-ethoxy-3-oxo-butylamide (107b)

White crystalline solid (0.563 g, 1.49 mmol) 39% yield.

MS (APCI +ve) m/z = 378,380 (M+H)⁺, 264,266 (M-COCH₂COOC₂H₅)⁺

¹H NMR: 1.06 (t, 3H, J= 7.5 Hz, Me), 1.19 (t, 3H, J= 7.0 Hz, Me), 2.23 (m, 2H, CH₂), 3.62 (ovs, 2H, OCH₂), 4.11 (m, 2H, CH₂), 7.07 (d, 2H, j= 9.5 HZ, Ar-H2 and H6), 7.61 (bd, 2H, NH₂), 7.77 (s, 1H, Ar-H5), 8.15 (bs, 2H, NH₂), 9.95 (bs, 1H, NH) ppm.

7.19.3 Preparation of 4-[2-Chloro-5-(2,4-diamino-6-ethyl-pyrimidin-5-yl)-phenylcarbamoyl]-butyric acid methyl ester (107c).

White crystalline solid (0.358 g, 0.916 mmol) 25% yield.

MS (APCI +ve) m/z = 392 (M+H)⁺

¹H NMR: 1.08 (t, 3H, J= 7.3 Hz, Me), 1.28 (m, 6H, 3CH₂), 1.83 (m, 2H, CH₂), 3.59 (s, 3H, OMe), 7.07 (d, 2H, J= 2.0 Hz, Ar-H6 and H2), 8.15-7.57 (ovbm, 4H, 2NH₂), 9.61 (s, 1H, Ar-H5), 12.94 (bs, 1H, NH) ppm.

7.20 Preparation of 2-[2-Chloro-5-(2,4-diamino-6-ethyl-pyrimidin-5-yl)-phenyl]-isoindole-1,3-dione (108)

A mixture of **106**, (1 g, 3.78 mmol) and 116 (1.1 eq) in ethanol (30 mL) was refluxed with stirring for 12 h. The mixture was cooled to room temperature; the ethanol solvent was removed under reduced pressure to give the white precipitate. Recrystallisation from EtOAc afforded the title compound as white crystalline solid.

White crystalline solid. 0.723 g, 2.75 mmol) 72% yield.

MP 221-222.8 °C

MS (APCI +ve) m/z = 264 (M+H)⁺.

IR (KBr disc): ν = 3169, (NH₂), 1655, 1627 (C=O) cm⁻¹.

¹H NMR: 1.053 (m, 3H, Me), 2.23 (m, 2H, CH₂), 5.48 (bs, 2H, NH₂), 6.38 (dd, 1H, J= 1.95, 8.08 Hz, H5 or H6), 6.61 (d, 1H, J= 1.93 Hz, H5 or H6), 7.04 (bs, 2H, NH₂), 7.27 (d, 1H, J= 8.05 Hz, Ar-H6), 7.50 (m, 2H, H4 and H7), 8.18 (m, 2H, Ar-H2 and H5) ppm.

7.21 Microbiology

7.21.1 Testing of compounds at 32 $\mu\text{g}\cdot\text{ml}^{-1}$

The medium used was Middlebrook 7H9 broth, supplemented with glycerol (0.2%) and Middlebrook ADC enrichment (10%). A DMSO solution of the test compound (0.64 mg.ml⁻¹, 50 μl) was added to the medium (1 ml), which was then inoculated with *M. fortuitum* (10 μl , 10⁶CFU), and incubated at 37°C for four days. Control tubes containing broth and inoculum, and broth alone were also set up. The compound was recorded as active at this concentration if a 99% reduction of mycobacterial growth was observed, as judged by appearance.

7.21.2 Minimum Inhibitory Concentrations (MICs)

The MICs were determined using the broth dilution method. The medium used was Middlebrook 7H9 broth, supplemented with glycerol (0.2%) and Middlebrook ADC enrichment (10%). Serial two-fold dilutions of the heteroarylcarboxamidrazone stock solution (5.1 mg.ml⁻¹ solution in DMSO) with broth were carried out to give solutions of 32, 16, 8, 4, 2, 1 $\mu\text{g}\cdot\text{ml}^{-1}$. Each tube was inoculated with *M. fortuitum* (10 μl , 10⁶CFU), and incubated at 37°C for four days. Control tubes containing broth and inoculum, and broth alone were also set up. The MIC values were recorded as the minimum concentration which resulted in a 99% reduction of mycobacterial growth, based on appearance.

7.22 Preparation of Molecularly Imprinted Polymers I

7.22.1 Synthesis of the Barbiturates (monomers and the test compounds)

7.22.2 General procedure for the preparation of the barbiturates

A mixture of barbituric acid (**121**) (1.00 g, 7.807 mmol), an appropriate aldehyde (1.2 – 1.2 molar equivalents) and 5 drops of piperidine (catalytic) in ethanol (50 mL) was stirred at reflux for 2 days. After cooling, the precipitated material was collected by filtration, washed with a little cold ethanol and dried under vacuum. The material obtained at this point was generally found to contain a single component as judged by thin layer chromatography. If necessary the material was purified by recrystallisation.

7.22.3 5-(4-Benzyloxy-2-hydroxy-benzylidene)pyrimidine-2,4,6-trione (**122**)

Recrystallised from MeOH to give orange yellow crystalline solid 0.715 g, 2.128 mmol) 71% yield. MP 103.5 -105 °C

MS (APCI -ve) $m/z = 337 (M-H)^+$, 229 (PhCH₂O)⁺

¹H NMR: 5.17(s, 3H, OMe), 6.57 (d, 2H, CH₂), 7.35-7.48 (m, 5H, Ar'), 8.69 (t, 2H, J= Hz), 11.09 (bs, 2H, NH) ppm.

7.22.4 5-(3,5-Di-*tert*-butyl-4-hydroxy-benzylidene)-pyrimidine-2,4,6-trione (**123**)

Recrystallised from EtOAc:EtOH (3:1) to give yellow crystalline solid (1.395 g, 4.06 mmol). 52% yield. MP 171.7-172.7 °C

MS (APCI +ve) $m/z = 345 (M+H)^+$, 235 ()⁺

¹H NMR: 1.41 (s, 18H, CMe₃), 8.23 (s, 1H, C=CH), 8.30 (s, 2H, Ar-H₂ and H₆), 10.12 (bs, 2H, NH) ppm.

IR (KBr disc) $\nu = 3419$ (OH), 2956, 1735, 1669 (C=O), 1595, 1543, 1427, 1385, 1200, 1100 cm⁻¹.

7.22.5 5-(4-Hydroxy-benzylidene)-pyrimidine-2,4,6-trione (**124**)

Recrystallised from EtOAc : EtOH (3:1) to give yellow crystalline solid .0.933 g, 4.06 mmol) 55% yield. MP 227.8-229.2 °C

MS (APCI -ve) $m/z = 231 (M-H)^+$.

¹H NMR: 6.851 (d, 2H, J=9.0 Hz, Ar-2H and Ar-6H), 8.19 (s, 1H, C=C-H), 8.33 (d, 2H, J=8.75 Hz, Ar-3H and Ar-5H), 11.13 (bs, 2H, NH)

IR (KBr disc) $\nu = 3271$ (b, OH), 3194, 1718, 1669, 1613 (C=O), 1533, 1507, 1408, 1287 cm⁻¹

7.22.6 5-Anthracen-9-ylmethylene-pyrimidine-2,4,6-trione (**125**)

Recrystallised from EtOH:MeOH (1:1) to gave red crystalline solid (0.786 g, 2.49 mmol) 32% yield.

MP 326-328.6 °C

MS (APCI -ve) $m/z = 315 (M-H)^+$.

IR (KBr disc) $\nu = 3412, 3217$ (NH), 1746, 1676 (C=O), 1569, 1436, 1379 cm⁻¹.

^1H NMR: 7.57-7.47 (m, 4H, Anth-2CH, 3CH, 6CH and 7CH), 7.96-7.92 (m, 2H, Anth-4H and Anth-5H), 8.11-8.25 (m, 2H, Anth-H5 and Anth-H8), 8.65(s, 1H, C=C-H), 8.98 (s, 1H, Anth-10H), 11.07 (bs, 1H, NH), 11.52 (bs, 1H, NH) ppm.

7.22.7 5-Phenanthren-9-ylmethylene-pyrimidine-2,4,6-trione (126)

Yellow crystalline solid (0.491 g, 1.56 mmol) 20% yield.

MP 286.6-287.6 °C

MS (APCI -ve) m/z = 315 (M-H)⁻.

IR (KBr disc) ν = 3404 (NH), 3199, 3058, 2858, 1746, 1677 (C=O), 1561, 1426, 1399, 1366 cm^{-1} .

^1H NMR: 8.25-7.45 (ovm, 8H, phenanth-H2, H3, H4, H5, H6, H7 and H8), 8.93-8.69 (m, 2H, phenanth-H10 and C=CH), 9.99 (bs, 2H, NH) ppm.

7.22.8 5-Pyren-1-ylmethylene-pyrimidine-2,4,6-trione (127)

Orange red crystalline solid (1.352 g, 3.98 mmol) 51% yield.

MP 260.-261.8 °C.

MS (APCI -ve) m/z = 339 (M-H)⁺.

IR (KBr disc) ν = IR (KBr) ν = 3403 (NH), 3159, 3079, 2850, 1741, 1665 (C=O), 1549, 1443, 1415, 1399, 1347, 1324 cm^{-1} .

^1H NMR: 8.09-8.40 (m, 9H, Pyren-1-9H), 9.10 (s, 1H, C=C-H), 11.19 (bs, 1H, NH), 11.49 (bs, 1H, NH) ppm.

7.22.9 5-(4-Octyloxy-benzylidene)-pyrimidine-2,4,6-trione (128)

Recrystallised from DMF and water to gave yellow crystalline solid (1.127 g, 3.28 mmol) 42% yield.

MP 227.8-229.6 °C.

MS (APCI +ve) m/z = 345 (M+H)⁺.

IR (KBr disc) ν = 3405, 3220 (NH), 2924, 1749, 1665 (C=O), 1547, 1441 cm^{-1} .

^1H NMR: 0.85 (t, 3H, Me), 1.25-1.43 (m, 10H, (CH₂)₅), 1.72 (m, 2H, CH₂), 4.08 (t, 2H, J= 6.4 Hz, CH₂), 7.03 (d, 2H, J= 8.82 Hz, Ar-3H and Ar-5H), 8.23 (s, 1H, C=C-H), 8.34 (d, 2H, J= 8.95, Ar-2H and Ar-6H), 11.16 (bs, 1H, NH), 11.28 (bs, 1H, NH) ppm.

7.22.10 5-(4-Benzyloxy-benzylidene)-pyrimidine-2,4,6-trione (129)

Yellow crystalline solid (1.780 g, 5.53 mmol), 71% yield.

MP 235.9-238.1 °C

MS (APCI +ve) m/z = 323 (M+H)⁺.

IR (KBr disc) ν = 3058, 2857, 1756, 1702, 1659 (C=O), 1507, 1417, 1399 cm^{-1}

^1H NMR: 5.23 (s, 2H, OCH₂), 7.13 (d, 2H, J=8.93 Hz, Ar-2H and 6H), 7.37-7.46 (m, 5H, Ar'-2-6H), 8.23 (s, 1H, C=C-H), 8.35 (d, 2H, J= 8.95 Hz, Ar-3H and 5H), 10.22 (bs, 2H, NH) ppm..

7.22.11 5-(4-tert-Butyl-benzylidene)-pyrimidine-2,4,6-trione (130)

Recrystallised from ethanol to gave pale yellow crystalline solid (0.381 g, 1.40 mmol) 18% yield.

MP 238.2-240.5 °C

MS (APCI -ve) m/z = 271 (M-H)⁺.

IR (KBr disc) ν = 3216, 3079 (NH), 3079, 2961, 2866, 1744, 1678 (C=O), 1574, 1417 cm^{-1} .

¹H NMR: 1.31 (s, 9H, CMe₃), 7.50 (d, 2H, J=8.5 Hz, Ar-H3 and H5), 8.11 (d, 2H, J= 8.5 Hz, Ar-H2 and H6), 8.26 (s, 1H, C=C-H), 11.21 (bs, 1H, NH), 11.35 (bs, 1H, NH) ppm.

7.23 ¹H-NMR titration experiments

A stock solutions of the template **70** (TMP) 5 mg/mL (17.24 mM) and the functional monomer **130** 10 mg/mL (36.76 mM) were prepared by dissolving appropriate amounts of the TMP and the **130** in D8-THF.

A samples of 0.6 mL of the TMP containing 0.0086 mM and **130** containing 0.0184 mM in D8-THF were first run on their own. The ¹H-NMR spectra revealed the expected peaks The solvent shift for D8-THF is evident at 3.580 ppm

Aliquotes of the template (**70**) solution (0.3 mL, 0.0086 mM) were pipetted into clean NMR tubes, and different concentration of **130** and D8-THF were added in order to obtain molar ratios of **130** to template, ranging from (0.0184 - 0.0015 mM) in a total volume of 0.6 mL (**Table 7.1**). The ¹H-NMR spectra were recorded and the shifts of the significant protons were taken **Table 7.2**

Table 7.1 Shows the concentration of TMP (**70**) was 0.0086 mM and **130** was added from 0.0184 mM to 0.0015 mM, X = component was absent

(70) conc. mM	(130) conc mM
0.0086	x
x	0.0184
0.0086	0.0184
0.0086	0.0123
0.0086	0.0092
0.0086	0.0061
0.0086	0.0046
0.0086	0.0031
0.0086	0.0023
0.0086	0.0015

Table 7.2 Amino induced shifts in the titration of **130** with **70**.

Concentration of (70) mM	Concentration of (130) mM	2-NH ₂ Δδ (ppm)	4-NH ₂ Δδ (ppm)
0.0086	0.00	0.00	0.00
0.0086	0.0015	0.095	0.105
0.0086	0.0023	0.143	0.163
0.0086	0.0031	0.139	0.167
0.0086	0.0046	0.207	0.231
0.0086	0.0061	0.259	0.292
0.0086	0.0092	0.371	0.440
0.0086	0.0123	0.412	0.478
0.0086	0.0184	0.775	0.872

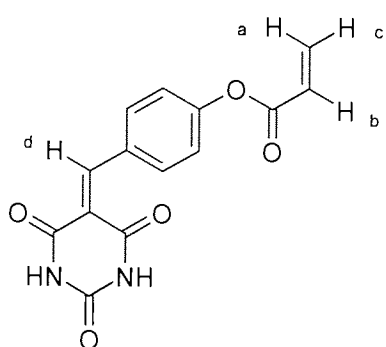
Table 7.3 Complexation induced shifts in the titration of **130** with **70**.

H	TMP(70) (mM)	130 (mM)	δ_{start} ppm	δ_{end} ppm	$\Delta\delta$ ppm
TMP(70) 2-NH ₂	0.0086	x	5.283		
4-NH ₂	„	x	5.148		
130 N-H	x	0.0184	10.420		
N-H	x	„	10.322		
TMP (70) 2-NH ₂	0.0086	0.0184	5.283		
4-NH ₂	„	„	5.148		
130 N-H	„	„	10.420	2.571	7.849
N-H	„	„	10.322	2.571	7.751
New peak		„			
TMP (70) 2-NH ₂	0.0086	0.0123	5.283	5.654	0.371
4-NH ₂	„	„	5.148	5.588	0.44
130 N-H	„	„	10.420	2.563	7.857
N-H	„	„	10.322	2.563	7.759
New peak		„			
TMP(70) 2-NH ₂	0.0086	0.0092	5.283	5.659	0.412
4-NH ₂	„	„	5.148	5.626	0.478
130 N-H	„	„	10.420	2.525	7.895
N-H	„	„	10.322	2.525	7.797
New peak		„			
TMP (70) 2-NH ₂	0.0086	0.0061	5.283	5.542	
4-NH ₂	„	„	5.148	5.440	
130 N-H	„	„	10.420	2.547	
N-H	„	„	10.322	2.547	
New peak		„			
TMP (70) 2-NH ₂	0.0086	0.0046	5.283	5.49	
4-NH ₂	„	„	5.148	5.379	
130	„	„	10.420	2.577	

N-H					
N-H	"	"	10.322	2.577	
New peak		"			
TMP (70) 2-NH ₂	0.0086	0.0031	5.283	5.422	
4-NH ₂	"	"	5.148	5.315	
130 N-H	"	"	10.420	2.526	
N-H	"	"	10.322	2.526	
New peak		"			
TMP (70) 2-NH ₂	0.0086	0.0023	5.283		
4-NH ₂	"	"	5.148		
130 N-H	"	"	10.420		
N-H	"	"	10.322		
New peak		"			
TMP(70) 2-NH ₂	0.0086	0.0015	5.283	5378	
4-NH ₂	"	"	5.148	5.253	
130 N-H	"	"	10.420	2.533	
N-H	"	"	10.322	2.533	
New peak		"			

7.24 Synthesis of the Functional Monomer

7.24.1 Preparation of Acrylic acid 4-(2,4,6-trioxo-tetrahydro-pyrimidin-5-ylidenemethyl)phenyl ester (85)



Acryloyl chloride (5 mL, mmol 5eq) was added dropwise over 10 min to a solution of 4-hydroxy-benzylaldehyde **124** (3 g, 24.57 mmol), *N,N*-diisopropyl ethylamine (6 mL, 6 eq) and DMAP (75 mg) in dry THF (60 mL). The mixture was stirred at 0 °C for 5 h. The crude product (6.382 g, 2.5 eq) was stirred *in situ* with barbituric acid **121** (11.228 g, 87.66 mmol) and piperidine (5 drops) in methanol (200 mL) at 50 °C for 8 h and then at room temperature for 2 days. The resulting product (0.427 g) was collected by

filtration and washed with cold EtOAc. The $^1\text{H NMR}$ analysis indicated that this product was not the desired compound. The remaining filtrate was evaporated under vacuum at ambient temperature to give a brown sticky liquid. The brown sticky liquid was poured onto small amount of cold water and stirred for 40 min at 0°C to give the title compound as pale yellow solid. The title compound was collected by filtration and stored below 5°C . Yield (0.815g)

Yellow crystalline solid. (0.815 g, 2.85 mmol) 12% yield.

MP $294.8\text{--}297.6^\circ\text{C}$

MS (APCI +ve) $m/z = 287 (\text{M}+\text{H})^+$, $233 (\text{M}-\text{CH}_2=\text{CH}_2\text{C}=\text{O})^+$

IR (KBr disc) $\nu = 3465 (\text{N-H})$, 3225 , $3095 (\text{C}=\text{CH}_2)$, 2825 , 1741 , $1669 (\text{C}=\text{O})$, 1561 , 1509 , 1436 cm^{-1}

$^1\text{H NMR}$: $6.18 (\text{dd}, 1\text{H}, J = 1.75 \text{ and } 10.0 \text{ Hz}, \text{Hc})$, $6.42 (\text{dd}, \text{H}, J = 9.75, 17.0 \text{ Hz}, \text{Hb})$, $6.57 (\text{dd}, 1\text{H}, 1.75, 17.25 \text{ Hz}, \text{Ha})$, $7.29 (\text{d}, \text{H}, J = 8.75 \text{ Hz}, \text{Ar-H5 and H3})$, $8.18 (\text{d}, 2\text{H}, J = 9.0 \text{ Hz}, \text{Ar-H2 and H6})$, $8.27 (\text{s}, 1\text{H}, \text{Hd})$, $11.27 (\text{bs}, 1\text{H}, \text{NH})$, $11.41 (\text{bs}, 1\text{H}, \text{NH})$ ppm.

7.25 General procedure for the preparation of imprinted polymers

7.25.1 Preparation of Polymer 1 (MIP1)

A solution of Acrylic acid 4-(2,4,6-trioxo-tetrahydro-pyrimidine-5-ylidenemethyl)-phenyl ester (**85**) (14.3 mg, 0.05 mmol), the template trimethoprim (**70**) (7.25 mg, 0.025 mmol), AINB (50 mg) and the crosslinker TMPTA (5 g) in THF (5 mL) was de-oxygenated by alternative application of vacuum and argon (6x) with rapid stirring. The solution was stirred at 55°C for 48 h under an argon atmosphere. The resulting polymer monolith was collected by filtration and washed with THF (2 x 30 mL). The crude material was dried under vacuum and then crushed using a mortar and pestle. The powder was graded by sieving and the 100-250 μm fraction was extracted exhaustively with chloroform in a soxhlet apparatus and dried under vacuum.

7.25.2 Preparation of Polymer 2 (MIP2)

A solution of Acrylic acid 4-(2,4,6-trioxo-tetrahydro-pyrimidine-5-ylidenemethyl)-phenyl ester (**85**) (14.3 mg, 0.05 mmol), the template perimethamine (**71**) (6.21 mg, 0.025 mmol), AINB (50 mg) and the crosslinker TMPTA (5 g) in THF (5 mL) was de-oxygenated by alternative application of vacuum and argon (6x) with rapid stirring. The solution was stirred at 55°C for 48 h under an argon atmosphere. The resulting polymer monolith was collected by filtration and washed with THF (2 x 30 mL). The crude material was dried under vacuum and then crushed using a mortar and pestle. The powder was graded by sieving and the 100-250 μm fractions was extracted exhaustively with ethanol in a soxhlet apparatus and dried under vacuum.

7.25.3 Preparation of Reference Polymer 3 (NIP)

A solution of Acrylic acid 4-(2,4,6-trioxo-tetrahydro-pyrimidine-5-ylidenemethyl)-phenyl ester (**85**) (mg,mmol), AINB (50 mg) and the crosslinker TMPTA (5 g) in THF (5 mL) was de-oxygenated by alternative application of vacuum and argon (6x) with rapid stirring. The solution was stirred at 55°C for 48 h under an argon atmosphere. The resulting polymer monolith was collected by filtration and washed with THF (2 x 30 mL). The crude material was dried under vacuum and then crushed using a

mortar and pestle. The powder was graded by sieving and the 100-250 μm fraction was extracted exhaustively with chloroform in a soxhlet apparatus and dried under vacuum.

7.25.4 Preparation of Reference Polymer 4 (TMPTA)

A solution of AINB (50 mg) and trimethylolpropane triacrylate TMPTA (5g), AINB (50 mg) in THF (5mL) was de-oxygenated by alternative application of vacuum and argon (6 x) with rapid stirring. The solution was stirred at 55°C for 48 h under an argon atmosphere. The resulting polymer monolith was collected by filtration and washed with THF (2 x 30 mL). The crude material was dried under vacuum and then crushed using a mortar and pestle. The powder was graded by sieving and the 100-250 μm fraction was extracted exhaustively with chloroform in a soxhlet apparatus and dried under vacuum.

7.26 Exposure of imprinted polymers to templates and test compounds followed by fluorescence measurements

7.26.1 General procedure

Each polymer (MIP1, MIP2, NIP and TMPTA) was exposed to imprinting molecule and a series of other test compounds. The polymers (0.05 g) were shaken with the test solution (2.0 and 0.1 mg/mL in THF) for 1 day, collected by filtration, washed very briefly with THF (5 mL) dried under vacuum. The resulting powders were weighed accurately (about 5 mg per well) in triplicate into black polystyrene 96 well plates. A layer of polyethyleneglycol (0.2 mL) was added to each well and the MIPs were examined by fluorescence. The results are presented as fluorescence counts per milligram of MIP.

REFERENCES

- Andersson L.I., Sellergren B., Mosbach K. Imprinting of amino-acid derivatives in macroporous polymers. *Tetrahedron Lett.* **1984**, 25, 5211-5214.
- Andersson, L.I., Mosbach, K. Enantiomeric resolution on molecularly imprinted polymers prepared with only noncovalent and nonionic interactions. *Journal Of Chromatography.* **1990**, 516, 313-322.
- Andersson, L.I. Application of molecular imprinting to the development of aqueous buffer and organic solvent based radioligand binding assays for (S)- propranolol. *Analytical Chemistry.* **1996**, 68, 111-117
- Arshady, R., Mosbach, K. Synthesis of substrate-selective polymers by host-guest polymerization. *Macromolecular Chemistry And Physics-Makromolekulare Chemie.* **1981**, 182, 687-692.
- Asanuma, H., Kakazu, M., Shibata, M., Hishiya, T., Komiyama, M. Molecularly imprinted polymer of beta-cyclodextrin for the efficient recognition of cholesterol. *Chemical Communications.* **1997**, 1971-1972.
- Ashtekar, S.R., *et al.* *In vitro* and *in vivo* activities of the nitroimidazol CGI 17341 against *Mycobacterium tuberculosis*. *Antimicrobial Agents and Chemother.* **1993**, 37, 183-86.
- Ashtekar, D.R., Costa-Perira, R., Nagrajan, K., Vishvanathan, N., Bhatt, A.D. *In vitro* and *in vivo* activities of nitroimidazole CG I7341 against *Mycobacterium tuberculosis*. *Antimicrobial Agents Chemother.* **1993**, 37, 183-86.
- Banerjee, A., Dubnau, E., Quemard, A., Balasubramanian, V., Um, K.S. *inhA*, a gene encoding a target for isoniazid and ethionamide in *Mycobacterium tuberculosis*. *Science.* **1994**, 263, 227-30.
- Banfi, E., Mamalo, M.G., Vio, L., Predominato, M. *In-vitro* antimycobacterial activity of new synthetic amidrazone derivatives. *J. Chemother.* **1993**, 5 (3), 164-167.
- Bannister, B.A, Worman, T.B. *Infectious diseases.* Blackwell Science. **1996**.
- Barbachyn, M.R., *et al.* Identification of a novel oxazolidinone (U-100480) with potent antimycobacterial activity. *Journal of Medicinal Chemistry,* **1996**, 39(3), 656-80
- Bergmann, K.E., Cynamon, M.H., Welch, J.T. Quantitative Structure-Activity Relationships for the *In Vitro* Antimycobacterial Activity of Pyrazonoic Acid Esters. *J. Med. Chem.* **1996**, 3394-3400.
- Bertrand, G, Doberitz, C., Beerens, H. *Bull. Soc. Pharm. Lille. J.* **1956**, 39, 1; *C.A.,* **1957**, 51, 1168.
- Billington, D.C., Coleman, M.D., Ibiabuo, J., Lambert, P.A., Rathbone, D.L., Tims, K.J. Synthesis and antimycobacterial activity of some heteroarylcarboxamidrazone derivatives. *Drug Design Discov.* **1998**, 15, 269-2
- Billington, D.C., Tims, K.J., Rathbone, D.L. Automated synthesis and antimycobacterial activity of a series of 2-heteroarylcarboxamidrazones and related compounds. *J. Pharm. Pharmacol.* **1998**, 50 (Suppl), 262.

- Billington, D.C., Lowe, P.R., Rathbone, D.L., Schwalbe, C.H. A new amidrazone derivative with antimycobacterial activity. *Acta Cryst.* **2000**, C56, e211-e212.
- Birdsall, B. Roberts, G.C., Feeney, J., Dann, J.D., Burgen, A.S. Trimethoprim binding to bacterial and mammalian dihydrofolate: Comparison by proton and carbon-13-nuclear magnetic resonances. *Biochemistry*, **1983**, 22, 22(24), 5597-5604.
- Birdsall, B., DeGram, J., Feeney, J., Hammond, S., Searte, M.S., Roberts, G.C.K., Colwell, W., G.C.K., Colwell, W.T., Grase, J., *FEBS Lett.*, **1987**, 217, 106-110.
- Brickner, S.J., Hutchinson, D.K., Barbachym, M.R. Synthesis and antibacterial activity of U-100592 and U-100766, two oxazolidinone antibacterial agents for potential treatment of multidrug resistant gram-positive bacterial infections. *J. Med Chem.* **1996**, 39: 673-679.
- Bowman, M.A.E., Allender, C.J., Heard, C.M., Brain, K.R. *Meth. Surv.* **1998**, 25, 37-43.
- Bozdogan, B., Appelbaum, P.C. Oxazolidinones: activity, mode of action and mechanism of resistance. *Int. J. Antimicrob. Agents*, **2004**, 23: 113-119.
- Canfield, C. J., Milhous, W. K., Ager, A. L., Rossan, R. N., Sweeney, T. R., Lewis N. J., Lewis, Jacobus, D.P. PS-15: a potent, orally active antimalarial from a new class of folic acid antagonists. *Am. J. Trop. Med. Hyg.* **1993**, 49, 121-126.
- Chan, D.C., Loughton, C.A., Queener, S.F., Stevens, M.F. *J. Med. Chem.* **2001**, 44, 255.
- Chang, S.K., Engen, D.V., Fan, E., Hamilton, A.D. Hydrogen Bonding and Molecular Recognition: Synthetic, Complexation, and Structural Studies on Barbiturate Binding to an Artificial Receptor. *J. Am. Chem. Soc.* **1991**, 113, 7640-7645.
- Cheong, S.H., McNiven, S., Yano, K., Karube, I. Development of steroid sensors using molecularly imprinted polymers. *Abstracts Of Papers Of The American Chemical Society.* **1997**, 213, 31-IEC.
- Cody, V., Chan, D., Galitsky, N., Rak, D., Luft, J.R., Pangborn, W., Queener, S.F., Loughton, C.A., Stevens, M. *Biochemistry.* **2000**, 39, 3556.
- Coleman, M.D., Rathbone, D.L., Chima, R., Lambert, P.A., Billington, D.C. Preliminary *in-vitro* toxicological evaluation of a series of 2-pyridylcarboxamidrazone candidate anti-tuberculosis compounds: III. *Environ. Tox. Pharmacol.* **2001**, 9, 99-102.
- Coleman, M.D., Rathbone, D.L., Abberly, L., Lambert, P.A., Billington, D.C. Preliminary *in-vitro* toxicological evaluation of a series of 2-pyridylcarboxamidrazone candidate anti-tuberculosis compounds. *Environ. Tox. Pharmacol.* **1999**, 7, 59-65.
- Craven, B.M., Vizzini, E.A., Rodrigues, M.M. *Acta Cryst.* **1969**, B25, 1978-1993.

- Cynamon, M.H., Klemens, S.P., Sharpe, C.A., Chase, s. Activities of Several Novel Oxazolidinones against *Mycobacterium tuberculosis* in Murine Model, *Antimicrobial Agents and Chemotherapy*, **1999**, 1189-1191.
- Cox, N.D., Schwalbe, C.H., Rathbone, D.L., Khan, N.B., Parker, K.J. Shape changes, H..H contacts and hydrogen bonds in derivatives of antimycobacterial compounds. *J. Pharm. Pharmacol.* **2003**, 55(suppl.), S-22.
- Damen, J., Neckers, D.C. *Tetrahedron Lett.* **1980**, 21, 1913.
- David, S. Synergy activity of D-Cycloserine and β -chloro-D-alanine against *Mycobacterium tuberculosis*. *J. Antimicrobial Chemother.* **2001**, 47, 203-206.
- Dhople, A.M. *In vitro* and *in vivo* activity of epiroprim, a dihydrofolate reductase inhibitor, singly and in combination with dapson, against *Mycobacterium leprae*. *Int. J. Antimicrob Agents.* **2002**, 19, 71-74
- Dhople, A.M. *In vitro* and *in vivo* activity of K-130, a dihydrofolate reductase inhibitor, against *Mycobacterium leprae*. *Arazneim Forsch/Drug Res.* **1999**, 49, 267-271.
- Dickert, F.L., Tortschanoff, M., Bulst, W.E., Fischerauer, G., Molecularly imprinted sensor layers for the detection of polycyclic aromatic hydrocarbons in water. *Analytical Chemistry.* **1999**, 71, 4559-4563.
- Domagk, G. *Dtsch. Med. Wochenschr.*, **1935**, 61, 250.
- Duncan, K. Progress in TB drug development and what is still needed, *Tuberculosis.* **2003**, 83 201-207.
- Emergence of *Mycobacterium Tuberculosis* with Extensive Resistance to Second-Line Drugs- Worldwide, 2000-2004. *Astma/Respiration News.* Article Date 30th March, **2006**.
- Falco, E.A., Goodwin, L.G., Hichings, G.H. 2,4-diaminopyridimidines a new series of antimalarials. *Br J. Pharmacol Chemother*, **1951**, 6, 185-200.
- Finken, M., Kireschner, P., Meier, A. Molecular Basis of a streptomycin Resistance in *Mycobacterium tuberculosis*. Alterations of the Ribosomal Protein S12 Gene and Point Mutations Within a Functional 16S Ribosomal RNA pseudoknot. *Mol. Microbiol.* **1993**, 9, 1230-1246.
- Fischer, L., Müller, R., Ekberg, B., Mosbach, K. Direct enantioseparation of beta-adrenergic blockers using a chiral stationary phase prepared by molecular imprinting. *Journal Of The American Chemical Society.* **1991**, 113, 9358-9360.
- Floss, H.G., Yu, T.W. Rifamycin – Mode of action, resistance and biosynthesis. *Chem Rev* **2005**, 105, 621-32.
- Fox, H.H., Gibas, J.T. Synthetic Tuberculostats. X1. Trialkyl and Other derivatives of Isonicotinylhydrazine. *J Org. Chem* **1956**, 21, 356-361.

Gangadharam, P.R.J., Perumal, V.K., Jairam, B.T., Rao, P.N., Nguyen, A.K., Farhi, D.C., Iseman, M.D. Activity of rifabutin alone or in combination with clofazimine or ethambutol or both against acute and chronic experimental *Mycobacterium intracellulare* infections. *Am. Rev. Respir. Dis.* **1987**; 136, 329-33.

Gangjee, A., Adair, O., Queener, S.F. *Pneumocystis carinii* and *Toxoplasma gondii* Dihydrofolate Reductase Inhibitors and Antitumor Agents: Synthesis and Biological Activities of 2,4-Diamino-5-methyl-6-[(monosubstituted aniline)methyl]-pyrido[2,3-d]pyrimidines. *J. Med. Chem.* **1999**, 42, 2447-2455.

Gerum, A.B., Ulmer, J.E., Jacobus, D.P., Jensen, N.P., Sherman, D.R., Sibley, C.H. Novel *Saccharomyces cerevisiae* screen identifies WR99210 analogues that inhibit *Mycobacterium tuberculosis* dihydrofolate reductase. *Antimicrobial Agents Chemother.* **2002**, 46, 3362-3369.

Gokhale, N., Padhye, S., Rathbone, D.L., Billington, D., Lowe, P., Schwalbe, C., Newton, C. The crystal structure of first Copper (II) complex of a pyridine-2-carboxamidrazone-a potential antitumor agent. *Inorganic Chemistry Communications.* 2001, 4, 26-29.

Griffin, R.J., Schwalbe, C.H., Stevens, M.F.G., and Wong, K.P. Structural Studies on Bio-active Compounds. Part 3.1 Re-examination of the Hydrolysis of the Antimalarial Drug Pyrimethamine and Related Derivatives and Crystal Structure of a Hydrolysis Product. *J. Chem. Soc. Perkin Trans. 1* **1985**, 2267-2276..

Griffin, R.J., Meek, M.A., Schwalbe, C.H., and Stevens, M.F.G. Structural Studies on Bioactive Compounds. 8.¹ Synthesis, Crystal Structure, and Biological Properties of a New Series of 2,4-Diamino-5-aryl-6-ethylpyrimidine Dihydrofolate Reductase Inhibitors with in Vivo Activity against a Methotrexate-Resistant Tumor Cell Line. *J. Med. Chem.* **1989**, 32, 2468-2474.

<http://www.who.int/tb/en/>. August, **2005**.

<http://www.medicalnewstoday.com>. 23 December, **2006**.

<http://www.who.tuberculosisfactsheet.com>. March, **2006**.

Haginaka, J., Sakai, Y., Narimatsu, S. Uniform-sized molecularly imprinted polymer material for propranolol. Recognition of propranolol and its metabolites. *Analytical Sciences.* **1998**, 14, 823-826.

Hamilton, A.D. *Bioorganic Chemistry Frontiers.* **1991**, 2, 115.

Hargreaves, M.K., Pritchard, J.G., Dave, H.R. Cyclic carboxylic monoimides. *Chemical Reviews.* 1970, 70(4), 439.

Haupt, K., Dzugoev, A., Mosbach, K. Assay system for the herbicide 2,4-dichlorophenoxyacetic acid using a molecularly imprinted polymer as an artificial recognition element. *Analytical Chemistry.* **1998**, 70, 628-631.

- Hausler, H., Kawakami, R. P., Mlaker, E., Severn, W. B. ethambutol Analogues as Potential Antimycobacterial Agents. *Bioorganic & Medicinal Chemistry Letters*. **2001**, 11 1679-1681
- Hawser, S., Lociuro, S., Islam, K. Dihydrofolate reductase inhibitors as antibacterial agents. *Biochemical Pharmacology*. **2006**, 71, 941-948.
- He, Y., Lu, J., Liu, M., Du, J. Molecular imprinting-chemiluminescence determination of trimethoprim using trimethoprim-imprinted polymer as recognition material. *Analyst*. **2005**, 103, 1032-1037.
- Hitchings, G.H, Elion, G.B., Falco, E.A. Antagonists of nucleic acid derivatives. i. The *Lactobacillus casei* model. *J. Biol. Chem.* **1950**, 183, 1-9.
- Hitchings, G.H., Smith, S.L. Dihydrofolate Reductases as targets for inhibitors. *Adv. Enzyme Regul.* G. Weber, Ed., Oxford, Pergamon, 1980, 18, 349-371.
- Howell, E. E., Villafranca, J. E., Warren, M. S., Oatley, S. J., Kraute, J. Functional role of aspartic acid-27 in dihydrofolate reductase revealed by mutagenesis. *Science*, **1986**, 231, 1123-1128.
- Hudson, A. Imamura, T., Guutteride, W. Kanyok, T. Nunn, P. The current anti-TB drug research and development pipeline. **2003**, http://www.who.int/tdr/publications/publications/anti-tb_drug.htm.
- Jahnsson, K., Schultz, P.G. Mechanistic Studies of the Oxidation of Isoniazid by the Catalase Peroxidase from *Mycobacterium tuberculosis* *J. Am. Chem. Soc.* **1994**, 116, 7425-7426.
- Jl, B., Lounis, N., Truffot, C.P., Grosset, J. In *Vitro* and in *Vivo* Activities of Levofloxacin against *Mycobacterium tuberculosis*. *Antimicrobial Agents and Chemotherapy*. **1995**, 39(6): 1341-1344.
- Jianchun, X., Lili, Z., Hongpeng, L., Li, Z., Chongxi, L., Xiaojie, X. *J. Chromatogr. A*. **2001**, 1, 934.
- Johnsson, K., King, D.S., Schultz, P.G. Studies on the Mechanism of Action of Isoniazid and Ethionamide in the Chemotherapy of Tuberculosis. *J. Am. Chem. Soc.* **1995**, 117, 5009-5010.
- Kempe, M., Fischer, L., Mosbach, K. Chiral separation using molecularly imprinted heteroatomic polymers. *Journal Of Molecular Recognition*. **1993**, 6, 25-29.
- Kempe, M., Mosbach, K. Separation of amino-acids peptides and proteins on molecularly imprinted stationary phases. *Journal of Chromatography A*. **1995**, 691, 317-323.
- Kempe, M., Mosbach, K. Receptor-binding mimetics - a novel molecularly imprinted polymer. *Tetrahedron Letters*. **1995**, 36, 3563-3566.
- Koetzle, T.F, William, G.J.B. *J. Am. Chem. Soc.* **1976**, 98, 2074-2078.
- Kompis, I.V., Islam, K., Then, R.L. DNA and RNA Synthesis: Antifolates. *Chem. Rev.* **2005**, 105, 593-620
- Kong, S.K., Lee, J.H., Lee, Y.c., Kim, C.H. Catalase-peroxidase of *Mycobacterium bovis* BCG converts isoniazid to isonicotinamide, but Not to isonicotinic acids: Differentiation parameter between

enzyme of *Mycobacterium bovis* BCG and *Mycobacterium tuberculosis*. *Biochemica et Biophysica Acta*, **2006**, 1760 724-729.

Kriz, D., Ramström, O., Svensson, A., Mosbach, K. Introducing biomimetic sensors based on molecularly imprinted polymers as recognition elements. *Analytical Chemistry*. **1995**, 67, 2142-2144.

Kriz, D., Mosbach, K. Competitive amperometric morphine sensor-based on an agarose immobilized molecularly imprinted polymer. *Analytica Chimica Acta*. **1995**, 300, 71-75.

Kröger, S., Turner, A.P.F., Mosbach, K., Haupt, K. Imprinted polymer based sensor system for herbicides using differential-pulse voltammetry on screen printed electrodes. *Analytical Chemistry*. **1999**, 71, 3698-3702.

Kubo, H., Nariai, H., Takuechi, T. Multiple hydrogen bonding-bases fluorescent imprinted polymers for cyclobutal prepared with 2,6-bis(acrylamide)pyridine. *Chem. Commun.* **2003**, 2792-2793.

Kugimiya, A., Takeuchi, T., Matsui, J., Ikebukuro, K., Yano, K., Karube, I. Recognition in novel molecularly imprinted polymer sialic acid receptors in aqueous media. *Analytical Letters*. **1996**, 29, 1099-1107.

Kushner, S., Dalalian, H., Sanjurjo, J.L. Epeirmental Chemotherapy of tuberculosis. II. The synthesis of pyrazinamides and Related Compounds. *J. Am. Chem. Soc.* **1952**, 74, 3617-3621.

Kuyper, L.F., Garvey, J.M., Baccanari, D.P., Champness, J.N., Stammers, D.K., Beddell, C.R. Pyrrolo[2,3-d]pyrimidines and Pyrido[2,3-d]pyrimidines as Conformationally Restricted Analogues of the Antibacterial Agent Trimethoprim. *J. Med. Chem.* **1996**, 4, No.4, 593-602.

LA, M. Topoisomerase Inhibitors: Quinolone and Pyridone. *Antibacterial Agents Chem Chem Rev.* **2005**, 105: 559-92.

Lee, A.S.G., Teo, A.S.M., Wong, S.Y., Novel mutation in *ndh* in Isoniazid- Resistant *Mycobacterium tuberculosis* Isolates. *Antimicrob Agents and Resistant *Mycobacterium tuberculosis* Isolates. Antimicrob Agents and Chemotherapy*, **2001**, 45(7): 2157-2159.

Lehn, J-M., Dietrich, B., Sauvage, J-P. *Tetrahedron Lett.* **1969**, 34, 2885-2888.

Lehn, J-M., Dietrich, B., Sauvage, J-P. *Tetrahedron Lett.* **1969**, 34, 2889-2892.

Lenaerts, A. J., Gruppo, V., Marirtta, K. S., Johnson, C.M., Driscoll, D.K., Tompkins, N.M., Rose, J.D., Reynolds, R.C., Orme. Preclinical Testing of the Nitroimidazopyran PA-824 for Activity against *Mycobacterium tuberculosis* in a Series of *In Vitro* and *In Vivo* Models. *Antimicrob Agents Chemother*, **2005**, 49(6): 2294-2301.

Levi, R., McNiven, S., Piletsky, S. A. Cheong S. H. Yano K. Karube I. Optical detection of chloramphenicol using molecularly imprinted polymers. *Analytical Chemistry*. **1997**, 69, 2017-2021.

- Leshner, G.Y., Froelich, E.J., Gruett, M.D., Bailey, J.H., Brundage, R.P. J. Med. Pharm. Chem. **1962**, 5, 1063.
- Levinson, W. Jawetz, E. Medical microbiology and immunology, 6th ed; McGraw-Hill International Editions, **2001**.
- Liao, Y., Wang, W., Wang, B. Building Fluorescent Sensors by Template Polymerization: The Preparation of a Fluorescent Sensor for -Tryptophan. Bioorganic Chemistry. **1999**, 27, 463-476.
- Li, P.A. Reith, M.K. Rasmussen, A. Gorski, J.C. Hall, S.D. Xu, L. Kaminski, D. L. Cheng, L.K. Primary human hepatocytes as a tool for Evaluation of structure-activity relationship in cytochrome p450 induction potential of xenobiotics: evaluation of rifampin, rifapentine and rifabutin. Chemico-Biological Interactions. **1997**, 107, 17-30
- Li, R., Sirawaraporn, R., Chitnumsub, P., Sirawaraporn, W., Wooden, J., Athappilly, S.T., Hol, W.G.J. Three-dimensional Structure of *M. tuberculosis* Dihydrofolate Reductase Reveals Opportunities for the Design of Novel Tuberculosis Drugs. J. Mol. Biol. **2000**, 295, 307-323.
- Lowe, J.A. III, Annu. Rep. Med. Chem. **1982**, 17, 119.
- Maillard, J.Y. Bacterial target sites for biocide action. Journal of Applied Microbiology Symposium Supplement. **2002**, 99, 16s-27s.
- Mamalo, M.G., Vio L., Banfi, E., Predominato, M., Fabris, C., Asaro, F. Synthesis and antimycobacterial activity of some 2-pyridinecarboxyamidrazone derivatives. Farmaco **1992**, 47 (7), 1055-1066.
- Mamalo, M.G., Vio, L., Banfi, E., Predominato, M., Fabris, C., Asaro, F. Synthesis and antimycobacterial activity of some 4-pyridinecarboxyamidrazone derivatives. Farmaco. **1993**, 48 (4), 529-538.
- Mamalo, M.G., Vio, L., Banfi, E. Synthesis and antimycobacterial activity of some indole derivatives of pyridine-2-carboxamidrazone and quinoline-2-carboxamidrazone. Farmaco. **1996**, 51 (1), 65-70.
- Matsui, J., Miyoshi, Y., Matsui, R., Takeuchi, T. Rod-type affinity media for liquid-chromatography prepared by in- situ-molecular imprinting. Analytical Sciences. **1995**, 11, 1017-1019.
- Matsui, J., Nicholls, I.A., Karube, I., Mosbach, K. Carbon-carbon bond formation using substrate selective catalytic polymers prepared by molecular imprinting: An artificial class II aldolase. Journal Of Organic Chemistry. **1996**, 61, 5414-5417.
- Matsui, J., Higashi, M., Takeuchi, T. Molecularly imprinted polymer as 9-ethyladenine receptor having a porphyrin-based recognition center. Journal Of The American Chemical Society. **2000a**, 122, 5218-5219

- Matthews, D.A., Alden, R.A., Bolin, J.T., Freer, S.T., Hamlin, R., Xuong, N., Kraut, J., Poe, M., Williams, M., Hoogsteen, K. Dihydrofolate reductase: X-ray structure of the binary complex with methotrexate. *Science*, **1977**, 197, 452-455.
- Matthews, D.A., Bolin, J.T., Burrige, J.M., Filman, D.J., Volz, K.W., Kraut, J. Refined Crystal Structures of *Escherichia coli* and Chicken Liver Dihydrofolate Reductase containing Bound Trimethoprim. *J. of Biological Chem.* **1985**, 260, 381-391
- Mattioni, B.E., March, J. *Advanced* and Jurs, P.C. Predication of dihydrofolate reductase inhibition and selectivity using computational neural networks and linear discriminant analysis. *Journal of Molecular Graphics and Modeling*. 2003, 21, 391-419.
- Mayes, A.G., Andersson, L.I., Mosbach, K. Sugar binding polymers showing high anomeric and epimeric discrimination obtained by noncovalent molecular imprinting. *Analytical Biochemistry*. **1994**, 222, 483-488.
- Mayes, A.G., Mosbach, K. Molecularly imprinted polymer beads: Suspension polymerization using a liquid perfluorocarbon as the dispersing phase. *Analytical Chemistry*. **1996**, 68, 3769-3774.
- Meyer, S.C.C., Majumder, S.K., Cynamon, M.H., *In Vitro* Activities of PS-15, a New Dihydrofolate Reductase Inhibitor, and its Cyclic Metabolite against *Mycobacterium avium* Complex. *Antimicrobial Agents and Chemotherapy*. **1995**, 39, 8, 1862-1863.
- MMWR Weekly, December 23/ **2005**, 54(50); 1280-83
- Miyazaki, E., Miyazaki, M., Chen, J.M., Chaisson, R.E., Bishai, W.R. Moxifloxacin (BAY12-8039), a New Methoxyquinolone, Is Active in a Mouse Model of Tuberculosis. *Antimicrobial Agents and Chemotherapy*, **1999**, 43(1), 85-89
- Mohamed, S., Ibrahim, P., Sadikun, A. Susceptibility of *Mycobacterium tuberculosis* isoniazid and its derivatives, 1-isonicotinyl-2-nonanoyl Hydrazine: Investigation at cellular level Tuberculosis. **2004**, 84, 56-62.
- Morlock, G.P., Metchock, B., Sikes, D., Crawford, J.T., Cooksey, R.C. *ethA*, *inhA*, and *KatG* loci of ethionamide-resistant to clinical *Mycobacterium tuberculosis* isolates. *Antimicrobial Agents Chemother.* **2003**, 47, 3799-3805.
- Mosbach, Y., Yu, J., Andersch, L., Ye, L. Generation of new enzyme inhibitors using imprinted binding sites: the anti-idiotypic approach, a step toward the next generation of molecular imprinting. *J. Am. Chem. Soc.* **2001**, 123, 12420-12421.
- Motherwell, W.B., Bingham, M.J., Six, Y. Recent progress in the design and synthesis of artificial enzymes. *Tetrahedron*. **2001**, 57 4663-4686.

- Neilson, D.G., Roger, R., Heatlie, J.W.M., Newlands, L.R. The chemistry of amidrazones. *Chem. Rev.* **1970**, *70*, 151-170.
- Neu, H.C. *Science* **1992**, *257*, 1064.
- Nicholls, I.A., Ramström, O., Mosbach, K. Insights into the role of the hydrogen-bond and hydrophobic effect on recognition in molecularly imprinted polymer synthetic peptide receptor mimics. *Journal Of Chromatography A.* **1995a**, *691*, 349-353.
- Nilsson, K.G.I., Sakaguchi, K., Gemeiner, P., Mosbach, K. Molecular imprinting of acetylated carbohydrate-derivatives into methacrylic polymers. *Journal Of Chromatography A.* **1995**, *707*, 199-203.
- O'Brien, R.J., Geiter, L.J., Lyle, M.A. Rifabutin (ansamycin LM427) for the treatment of pulmonary *Mycobacterium avium* complex. *Am Rev Respir Dis* **1990**; *141*, 821-6.
- Opravil, M., Pechere, M., Lazzarin, A., Heald, S., Ruttimann, A., Iten, H., Furrer, D., Oertle, G., Praz, D.A., Vuitton, B., Luthy, H., Luthy, R. Dapson/pyrimethamine may prevent mycobacterial disease in immunosuppressed patients infected with the immunodeficiency virus. *Clin. Infect. Dis.* **1995**, *20*, 244-249.
- Pauling, L., A theory of the structure and process of formation of antibodies. *J. Am.Chem.Soc.*, **1940**, *62*, 2643-2657.
- Patric, G.L. *An Introduction to Medicinal Chemistry*, 3rd ed; Oxford University Press, **2005**.
- Pedersen J. C., *J. Am. Chem. Soc.*, **1967**, *89*, 2495-2496.
- Pedersen J. C., *J. Am. Chem. Soc.*, **1967**, *89*, 7017
- Perault, A.M., Pullman, B. Structure Electronique et Mode D'Action des Antimetabolites de L'Acide Folique, *Biochim, Biophys. Acta.* **1962**, *52*, 266-280.
- Piletsky, S.A., Piletska, E.V., Bossi, A., Karim, K., Lowe, P., Turner, A.P.F. Substitution of antibodies and receptors with molecularly imprinted polymers in enzyme-linked and fluorescent assays. *Biosensors & Bioelectronics.* **2001**, *16*, 701-707.
- Porkar, C., Gogtay, N., Gokhale, P., Kshirsagar, N.A., Ajay, S., Cooverji, N.D., Bruzzese, T. Phase 1 Pharmacokinetic study of a new 3-azinmethyl-Rifamycin (rifametane) as compared to rifampicin. *Chemotherapy.* **1999**, May-jun, *45* (3):147-5.
- Quaglia, M., Chenon, K., Hall, A.J., Lorenzi, E.De., Sellergren, B. Target analogue imprinted polymers with affinity for folic acid and related compounds. *J. Am. Chem. Soc.* **2001**, *123*(10), 2146-2154.
- Rachkov, A., McNiven, S., El'skaya, A., Y. K., Karube, I. Fluorescence detection of β -estradiol using a molecularly imprinted polymer. *Analytica Chimica Acta.* **2000**, *405*, 23-29.

- Rachkov, A., Minoura, N. Towards molecularly imprinted polymers selective to peptides and proteins. The epitope approach. *Biochimica Et Biophysica Acta-Protein Structure And Molecular Enzymology*. **2001**, 1544, 255-266.
- Ramström, O., Andersson, L., I. Mosbach, K. Recognition sites incorporating both pyridinyl and carboxy functionalities prepared by molecular imprinting. *Journal Of Organic Chemistry*. **1993**, 58, 7562-7564.
- Ramström, O., Ye, L., Mosbach, K. Artificial antibodies to corticosteroids prepared by molecular imprinting. *Chemistry & Biology*. **1996**, 3 471-477.
- Ramström, O., Yu, C., Mosbach, K. Chiral recognition in adrenergic receptor binding mimics prepared by molecular imprinting. *Journal Of Molecular Recognition*. **1996**, 9, 691-696.
- Ramstrom, O., Ye, L., Krook, M., Mosbach, K. *Anal. Commun.* **1998**, 35, 9.
- Rathbone, D.L., Su, D., Wang, Y., Billington, D.C. Molecular recognition by fluorescent imprinted polymers. *Tetrahedron Lett.* **2000**, 41, 123-126.
- Rathbone, D.L., Tims, K.J., Atkins, N., Cann, S.W., Billington, D.C. QSAR studies on a large set of antimycobacterial *N*¹-benzylideneheteroarylcarboxamidrazones. *J. Pharm. Pharmacol.* **2000**, 52 (Suppl), 97.
- Rathbone, D.L., Ge, Y. Selectivity of response in fluorescent polymers imprinted with *N*¹-benzylidene pyridine-2-carboxamidrazones. *Analytica Chimica Acta*, **2001**, 435, 129-136.
- Rathbone, D.L., Ali, A., Antonaki, P., Cheek, S. Towards a polymeric binding mimic for cytochrome CYP2D6. *Biosensors and Bioelectronics*. **2005**, 20, 2353-2363.
- Rathbone, D.L. Molecularly imprinted polymers in the drug discovery process. *Advanced Drug Delivery Reviews*. **2005**, 57, 1854-1874.
- Rathbone, D.L., Parker, K.J., Coleman, M.D., Lambert, P.A., Billington, D.C. Discovery of a potent phenolic *N*¹-benzylidene-pyridinecarboxamidrazones selective against Gram-positive bacteria. *Bioorganic & Medicinal Chemistry Lett.* **2006**, 16, 879-883.
- Rebek, R. "Molecular recognition with model systems." *Angew. Chem. Int. Ed. Engl.*, **1990**, 29, 245-255.
- Reddy, V.M., Nadadhur, G., Daneluzzi, D., O'Sullivan, J.F., Gangadharam, P.R.J. Antituberculosis activities of colfazimine and its new analogues B4154 And B4157. *Antimicrobial. Agents and Chemotherapy*. **1996**, 40 (3), 633-63.
- Remcho, V.T., Tan, Z.J. MIPs as chromatographic stationary phases for molecular recognition. *Analytical Chemistry*. **1999**, 71, A248-A255.

- Renau, T.E., Sanchez, J.P., Shapiro, M.A., Dever, J.A., Gracheck, S.J., Domagala, J.M. Effect of Lipophilicity at N-1 on Activity of louroquinolones against Mycobacteria. *J. Med. Chem.* **1995**, *38*, 2974-2977.
- Renau, T.E., Sanchez, J.P., Gage, J.W., Dever, J.A., Shapiro, M.A., Gracheck, S.T., Domagala, J.M. Structure-Activity Relationships of the Qinolone Antibacterials against Mycobacteria: Effect of structural Changes at N-1 and C-7. *J. Med. Chem.* **1996**, *39*, 729-735.
- Richardson, J.S. The anatomy and taxonomy of protein structure. *Adv. Protein Chem.* **1981**, *34*, 168-339.
- Robson, C., Meek, M.A., Grunwaldt, J. D., Lambert, P.A., Queener, S.F., Schmidt, D., Griffin, R.J. *J. Med. Chem.* **1997**; *40*, 3040.
- Saito, H., Tomioka, H., Sato, K., Emori, M., Yamane, T., Yamashita, K., Hosoe, K., Hidaka, T. *In-vitro* antimycobacterial activites of newly synthesided benzoxazinorifamycins. *Antimicrob. Agents Chemother.* **1991**, *35* (1), 542-547
- Sandbhor, U., Padhye, S., Billington, D., Rathbone, D.L., Franzblau, C.E., Powell, A.K., Metal complexes of carboxamidrazone analogs as antitubercular agents 1. Synthesis, X-ray crystal-structures, spectroscopic properties and antimycobacterial activity against *Mycobacterium tuberculosis* H₃₇Rv. *Journal of Inorganic Biochemistry.* **2002**, *90*, 127-136
- Sbardella, G., Mai, A., Artico, M., Setzu, M.G., Poni, G., Colla, P.L. New 6-nitroquinolones: synthesis and antimicrobial activities. *IL Farmaco.* **2004**, 463-471
- Sbardella, G., Mai, M.A., Loddo, R., Setzu, M.G., Colla, P.L. Synthesis and *in vitro* antimycobacterial activity of novel 3-(1H-Pyrrol-1-yl)- 2-oxazolidinone analogues of PNU-100480. *Bioorganic & Medicinal Chemistry letters.* **2004**, *14* 1537-1541.
- Schwalbe, C.H., Gallgher, C., Lowe, P.R., Rathbone, D.L., Billington, D.C., Tims, K.J. Comparison of structural features and antimycobacterial activity in isomeric pyridyl-carboxamidrazones. *J. Pharm. Pharmacol.* **1999**, *51* (Suppl), 262.
- Schwalbe, C.H., Rathbone, D.L., Tims, K.J., Billington, D.C., Sandbhor, U., Padhye, S. Effects of functional group deletion on structural features and antimycobacterial activity in pyridylcarboxamidrazones. *J. Pharm. Pharmacol.* **2000**, *52* (Suppl), 105.
- Scorpio, A., Zhang, Y. Mutations in *pncA*, a Gene Encoding Pyrazinamidase/ Nicotinamidase. Cause Resistance to the Antituberculosis Drug pyrazinamide in Tubercle Bacillus. *Natyre*, **1996**, *2*, 662-667.
- Sellergren, B., Ekberg, B., Mosbach, K. Molecular imprinting of amino-acid derivatives in macroporous polymers - demonstration of substrate-selectivity and enantio-selectivity by chromatographic resolution of racemic mixtures of amino-acid derivatives. *Journal Of Chromatography.* **1985**, *347*, 1-10.

Sellergren, B., Lepistö, M., Mosbach, K. Highly enantioselective and substrate-selective polymers obtained by molecular imprinting utilizing noncovalent interactions - NMR and chromatographic studies on the nature of recognition. *Journal Of The American Chemical Society*. **1988**, 110, 5853-5860.

Sellergren, B. Molecular imprinting by noncovalent interactions - tailor-made chiral stationary phases of high selectivity and sample load-capacity. *Chirality*. **1989**, 1, 63-68.

Sellergren, B., Andersson, L. Molecular recognition in macroporous polymers prepared by a substrate-analogue imprinting strategy. *Journal Of Organic Chemistry*. **1990**, 55, 3381

Sellergren, B., Shea, K. Influence of polymer morphology on the ability of imprinted network polymers to resolve enantiomers. *Journal Of Chromatography*. **1993**, 635, 31-49.

Sellergren, B. *Anal. Chem.* **1994**, 66, 1578.

Sellergren, B. Enantiomer separation using tailor-made phases prepared by molecular imprinting. *Pract. Approach Chiral Sep. Liq. Chromagogr.* 1994, 69-93.

Sellergren, B. Molecularly imprinted polymers man-made mimics of antibodies and their applications in analytical chemistry, published in **2003**., chapter 1, 1-10, A historical perspective of the development of molecular imprinting, Andersson S.Hakan, Nicholls A. Ian

Sellergren, B., Allender, C.J. Molecularly imprinted polymers: A bridge to advanced drug delivery. *Advanced Drug Delivery Reviews*. **2005**, 12, 1733-1741.

Shah, L.M., DeStefano, M.S., Cynamon, M.H. Enhanced *In Vitro* Activity of WR99210 in Combination with Dapsone against *Mycobacterium avium* Complex. *Antimicrobial Agents and Chemotherapy*. **1996**, 40, 11, 2644-2645.

Shah, L.M., Meyer, S.C.C., Cynamon, M.H. Enhanced *In Vitro* Activity of Pyrimethamine in Combination with Dapsone against *Mycobacterium avium* Complex. *Antimicrobial Agents and Chemotherapy*. **1996**, 40, 11, 2426-2427.

Sharma, S.K., Mohan, A. Co-infection of Human Immunodeficiency Virus (HIV) and Tuberculosis: Indian Perspective. *Indian Journal of Tuberculosis*. **2004**, 51(5): 161.

Shea, K.J., Dougherty, T.K. Molecular recognition on synthetic amorphous surfaces - the influence of functional-group positioning on the effectiveness of molecular recognition. *Journal of the American Chemical Society*. **1986**, 108, 1091-1093.

Shea, K.J., Spivak, D.A., Sellergren, B. Polymer complements to nucleotide bases - selective binding of adenine-derivatives to imprinted polymers. *Journal of the American Chemical Society*. **1993**, 115, 3368-3369.

- Shi, H.Q., Tsai, W.B., Garrison, M.D., Ferrari, S., Ratner, B.D. Template-imprinted nanostructured surfaces for protein recognition. *Nature*. **1999**, 398, 593-597.
- Shimizu, N., Nishigaki, S. Structure of 2,4-Diamino-5-(3,4,5-trimethoxybenzyl)pyrimidine-5,5-Diethylbarbituric Acid (1:1). *Acta Cryst.* **1982**, B38, 2309-2311.
- Sibrian-Vazquez, M., Spivak, D.A. Molecular imprinting made easy. *Journal of the American Chemical Society*. **2004**, 126(25), 7827-7833.
- Silva, D., Almeida, A.D., Souza, M.D., Couri, M.R.C. Biological Activity and Synthetic Methodologies for the preparation of Fluoroquinolones. A class of potent Antibacterial Agents. *Curr Med Chem*. **2003**, 10, 21-39.
- Silverman, R.B. *The organic Chemistry of Drug Design and Drug Action*, 2nd ed; Elsevier Academic Press, London, **2004**, pp.233-237.
- Singh, M.M., Chopra, K.K. MDR TB-Current issues, *Indian J. Tuberc.* **2004**, 51: 1-3.
- Smith, M.B., and March, J. *Advance Organic Chemistry, Reactions, Mechanisms and Structure*. **2001**, 5th ed. John Wiley & sons.
- Sorrell, T.N. *Organic Chemistry*. 2006, 2nd ed. The University of North Carolina at Chapel Hill.
- Souza, M.F.N. Promising Drugs Against Tuberculosis. *Recent Patents on Anti-Infective Drug Discovery*, **2006**, 1, 33-44
- Spivak, D.A., Shea, K. Investigation into the scope and limitations of molecular imprinting with DNA molecules. *J. Analytica Chimica Acta*. **2001**, 435, 65-74.
- Spivak, D.A., *et al*, Development of an asparatic acid-based cross-linking monomer for improved bioseparations. *Bioseparation*. **2001**, 10, (6), 331-336.
- Sreenivasan, K. Effect of the type of monomers of molecularly imprinted polymers on the interaction with steroids. *Journal Of Applied Polymer Science*. **1998**, 68, 1863-1866.
- Sriram, D., Yogeewari, P., Reddy, S.P. Synthesis of pyrazinamide Mannich bases and its Antitubercular properties. *Bioorganic Medicinal Chemistry Letters*. **2006**, 16, 2113-2116.
- Sriram, D., Aubry, A., Yogeewari, P., Fisher, M. Gatifloxacin derivatives: Synthesis, antimycobacterial activities, and inhibition of *Mycobacterium tuberculosis* DNA gyrase. *Bioorganic & Medicinal Chemistry Letters*. **2006**, 16: 2982-2985.
- Stevens, M.F., Phillip, K.S., Rathbone, D.L., O'Shea, D.M., Queener, S.F., Schwallbe, C.H., Lambert, P.A. Structural studies on Bioactive Compounds. 28.1 Selective Activity of Triazenyl-Substituted Pyrimethamine Derivatives against *Pneumocystis carinii* Dihydrofolate Reductase. *J. Med. Chem.* **1997**, 40, 1886-1893.

- Stover, C.K. Warrenner, P. VanDevanter, D.R. A small molecule nitroimidazopyran drug candidate for the treatment of tuberculosis. *Nature*. **2000**, 405, 962-966.
- Suedee, R., Srichana, T., Martin, G.P. Evaluation of matrices containing molecularly imprinted polymers in the enantioselective-controlled delivery of beta- blockers. *Journal Of Controlled Release*. **2000**, 66, 135-147.
- Takayma, K., Wang, C., Besra, G.S. Pathway to syntesis and Processing of Mycolic Acids in *Mycobacterium tuberculosis*. *Clin Microbiol Rev*. **2005**, 18(1); 81-101.
- Tanabe, K., Takeuchi, T., Matsui, J., Ikebukuro, K., Yano, K., karbue, I. Recognition of Barbiturates in molecularly Imprinted Copolymers using Multiple Hydrogen Bonding. *J. Chem. Soc. Chem. Comm*. **1995**, 2303-2304.
- Tecilla, P., Jubian, V., Hamilton, A.D. *Tetrahedron*, **1995**, 51, 435.
- Thomas, J.P., Baughn, C.O., Wilkinson, R.G., Shepherd, R.G. A new synthetic compound with antituberculous activity in mice: ethambutol (dextro-2,2'-(ethylenediimino)-di-butanol). *Am. Rev. Respir. Dis*. **1961**, 83, 291-93.
- Tims, K.J. Automated synthesis and evaluation of potential new anti-microbial agents. Thesis, Aston University, **2002**.
- Tomc, J.F., Minassian, B., Washo, T., Huczko, E., Bonner, D. *In Vitro* Antibacterial spectrum of a new broad-spectrum 8-methoxy fluoroquinolone, gatifloxacin. *Journal of Antimicrobial Chemotherpay*. **2000**, 45, 437-446.
- Turkewitsch, P., Wandelt, B., Darling, D.G., Powell, S.W. Fluorescent functional recognition sites through molecular imprinting. A polymer-based fluorescent chemonsensr for aqueous cAMP. *Anal. Chem*. **1998**, 70, 2025-2030.
- Valadas E., Antunes, F. Tuberculosis, a re-emergent disease. *European Journal of Radiology*, **2005**; 55: 154-157.
- Vazquez, M.S., Spivak, D.A. Molecular imprinting Made Easy. *Journal of the American Chemical Society*. **2004**, 126, 7827-7833.
- Vio, L., Mamalo, M.G., Ronsisvalle, G., Oliveri, S., Grego, A.M. Synthesis and antifungal activities of some amidrazone derivatives. *Farmaco* **1989**, 44 (9), 819-829.
- Viveiros, M., Leandro, C., Amaral, L. Mycobacterial efflux pumps and chemotherapeutic implications. *Int. J. Antimicrobial Agents*, **2003**, 22: 274-278.
- Vlatakis, G., Andersson, L.I., Müller, R., Mosbach, K. Drug assay using antibodymimics made by molecular imprinting. *Nature*. **1993**, 361, 645-647.

Volz, K.W., Matthew, D.A., Alden, R.A., Freer, S.T., Hansch, C., Kaufman, B.T., Kraut, J. J. Biol. Chem. **1982**, 257, 2528.

Walsh, C. Science **1993**, 261, 308.

Wang, W., Gao, S., Wang, B. Building fluorescent sensors by template polymerisation: The preparation of a fluorescent sensor for D- fructose. Organic letters. **1999**, 1, 1209-1212.

Whitcombe, M.J., Rodriguez, M.E., Villar, P., Vulfson, E.N. A new method for the introduction of recognition site functionality into polymers prepared by molecular imprinting - synthesis and characterization of polymeric receptors for cholesterol. Journal Of The American Chemical Society. **1995**, 117, 7105-7111.

Williams, D.A., Lemke, T.L. Foye's. Principles of Medicinal Chemistry 5th ed. **2002**, Lippincott Williams & Wilkins, pp 910.

Wilkinson, R.G., Shepherd, R.G., Thomas, J.P., Baughn, C. Stereospecificity in a new type of synthetic antituberculous agent. (Correspondence). J Am Chem Soc.1961; 83: 2212-3.

Wolucka, B.A., McNeil, M.R., de Hoffmann, E. Recognition of the Lipid Intermediate for Arabinogalactin/Arabinomannan Structure of Cell Wall of Mycobacterium: Biosynthesis and its Relation to the Mode of Action of Ethambutol in Mycobacteria. J. Biol. Chem. **1994**, 269, 23328-23335

Wulff, G., Gimpel, J. On polymers with enzyme-analogous structure 16. On the influence of the binding group flexibility on the ability for racemic-resolution. Makromolekulare Chemie-Macromolecular Chemistry And Physics. **1982**, 183, 2469-2477.

Wulff, G., Best, W., Akelah, A. Enzyme-analogue built polymers .17. Investigations on the racemic-resolution of amino-acids. Reactive Polymers. **1984**, 2, 167-174.

Wulff G. Minarik M. Enzyme-analog built polymers .20. Pronounced effect of temperature on racemic-resolution using template-imprinted polymeric sorbents. Journal Of High Resolution Chromatography & Chromatography Communications. **1986**, 9, 607-608.

Wulff, G., Poll, H.G., Minarik, M. Enzyme-analog built polymers .19. Racemic-resolution on polymers containing chiral cavities. Journal Of Liquid Chromatography. **1986**, 9, 385-405.

Wulff, G., Wolf, G. On the chemistry of binding-sites .6. On the suitability of various aldehydes and ketones as binding-sites for monoalcohols. Chemische Berichte-Recueil. **1986**, 119, 1876-1889.

Wulff, G. Molecular recognition in polymers prepared by imprinting with templates. Acs Symposium Series. **1986**, 308, 186-230.

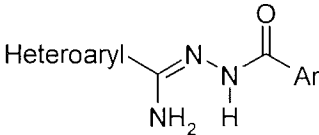
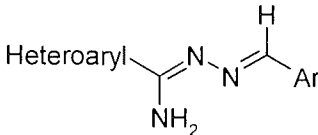
Wulff, G., Heide, B., Helfmeier, G. Molecular recognition through the exact placement of functional-groups on rigid matrices via a template approach. Journal Of The American Chemical Society. **1986**, 108, 1089-1091.

- Wulff, G., Vietmeier, J. Enzyme-analogue built polymers .25. Synthesis of macroporous copolymers from alpha-amino-acid based vinyl compounds. *Makromolekulare Chemie-Macromolecular Chemistry And Physics*. **1989**, 190, 1717-1726.
- Wulff, G., Sarhan, A. The use of polymers with enzyme-analogous structures for the resolution of racemates. *Angewandte Chemie-International Edition In English*. **1972**, 11, 341-341.
- Wulff, G., Haarer. Enzyme-analog built polymers .29. The preparation of defined chiral cavities for the racemic-resolution of free sugars. *J. Makromolekulare Chemie-Macromolecular Chemistry And Physics*. **1991**, 192, 1329-1338.
- Wulff, G. Molecular imprinting in cross-linked materials with the aid of molecular templates - a way towards artificial antibodies. *Angewandte Chemie-International Edition In English*. **1995** 34 1812-1832.
- Wulff, G., Knorr, K. Stoichiometric noncovalent interaction in molecular imprinting. *Bioseparation*. **2002**, 10, 257-276.
- Wulff, G., Gross, T., Schönfeld, R. Enzyme models based on molecularly imprinted polymers with strong esterase activity. *Angewandte Chemie-International Edition In English*. **1997**, 36, 1962-1964.
- Wulff, G. Molecular imprinting in polymers - New opportunities in separation and catalysis. *Abstracts Of Papers Of The American Chemical Society*. **1997**, 213, 96-IEC.
- Yavaniyama, P., Chitnumsub, S., Kamchonwongpaisan, J., Vanichtanankul, W., Sirawaraporn, P., Taylor, P., Walkinshaw, M.D., Yuthavong, Y. Insights into Antifolate Resistance from Maliral DHFR-TS Structures. *Nature Structural Biology*. **2003**, 10(5), 357-365.
- Ye, L., Ramström, O., Ansell, R.J., Mansson, M.O., Mosbach, K. Use of molecularly imprinted polymers in a biotransformation process. *Biotechnology And Bioengineering*. **1999**, 64, 650-655.
- Ye, L., Cormack, P.A.G., Mosbach, K. Molecularly imprinted monodisperse microspheres for competitive radioassay. *Analytical Communications*. **1999**, 36, 35-38.
- Yu, Y., Ye, L., Haupt, K., Mosbach, K. Formation of a Class of Enzyme Inhibitors (Drugs), Including a Chiral Compound, by Using Imprinted Polymers or Biomolecules as Molecular-Scale Reaction Vessels. *Angew. Chem. Int. Ed*. **2002**, 41 (23), 4460-4463.
- Zabicky, J. *The chemistry of amides*. 1970, Interscience publishers.
- Zhang, Y., Heym, B. Allen, B. Young, D., Cole, S. The catalase-peroxidase gene and isoniazid resistance of *Mycobacterium tuberculosis*. *Nature*, **1992**, 358 591-92.
- Zhang, Y., Wade, M.W., Scorpio, A., Zhang, H., Sun, Z. Mode of action of pyrazinamide: disruption of *Mycobacterium tuberculosis* membrane transport and energetics by pyrazinoic acid. *Journal of Antimicrobial Chemotherapy* **2003**, 52, 790-795.

Zurenko, G.E., *et al.*, *In vitro* activities of U-100592 and U-100766, novel oxazolidinone antibacterial agents. *Antimicrobial Agents and Chemotherapy*, **1996**, 40, 839-45.

Appendix 2

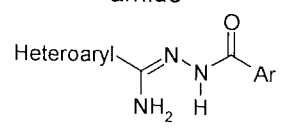
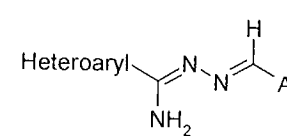
Antimicrobial activity of various pyridine-2-carboxamidrazone *N*¹-(benzoyl) amide and their corresponding imine; (the results for imine were provided by Dr. D.L. Rathbone), against *M. Fortitum* (*M. Fort.*), (+) indicates that, the compound is active at the single concentration of 32 $\mu\text{g mL}^{-1}$; (-) indicates that the compound is not active. X indicates that the compound was not made, xx indicates that the synthesis of the compound was attempted; and the crude material was tested against *M. fortitum*. The biological activity of the above carboxamidrazone amide was determined by the project students N. Ellahi (MPharm final year project student, Aston University, 2005 and F. Kusar (B.Sc Applied and Human Biology final year project student, Aston University, 2004). The biological activity results for an imine were obtained from the thesis (Tims. K, 2002).

Compound	<i>M. fortitum</i> at a single conc. of 32 $\mu\text{g mL}^{-1}$	<i>M. fort.</i> MIC ($\mu\text{g mL}^{-1}$) Carboxamidrazone amide 	<i>M. fort.</i> MIC ($\mu\text{g mL}^{-1}$) Corresponding imine 
2PYAc1	+	16-32	>32
2PYAc2	-	>32	>32
2PYAc3	+	4-8	N/A
2PYAc4	-	>32	N/A
2PYAc5	-	>32	>32
2PYAc6	-	>32	16-32
2PYAc7	-	>32	>32
2PYAc8	-	>32	16-32
2PYAc9	xx	>32	N/A
2PYAc10	xx	>32	>32
2PYAc11	-	>32	N/A
2PYAc12	xx	>32	N/A
2PYAc13	+	0.1-2	N/A
2PYAc14	-	>32	16-32
2PYAc15	+	8-16	16-32
2PYAc16	-	>32	N/A
2PYAc17	-	>32	N/A
2PYAc18	-	>32	N/A
2PYAc19	+	4-8	16-32
2PYAc20	+	8-16	8-16
2PYAc21	+	16-32	>32
2PYAc22	xx	>32	>128
2PYAc23	xx	>32	>128
2PYAc24	xx	>32	N/A
2PYAc25	-	>32	>32
2PYAnh1	-	>32	>32
2PYAnh2	-	>32	N/A
2PYCa1	+	16-32	4-8
2PYCa2	-	>32	N/A

2PYCa3	xx	N/A	>32
2PYCa4	+	16-32	16-32
2PYCa5	-	>32	>32
2PYCa6	-	>32	8-16
3PYCa5	-	>32	>32

Appendix 3

Antimicrobial activity of various pyridine-4-carboxamidrazone N^1 -(benzoyl)amide and the corresponding imine; (the results for imine were provided by Dr. D.L. Rathbone), against *M. Fortuitum* (*M. Fort.*), (+) indicates that, the compound is active at the single concentration of $32 \mu\text{g mL}^{-1}$, (-) indicates that the compound is not active X indicates that the compound was not made, xx indicates that the synthesis of the compound was attempted; and the crude material was tested against *M. fortuitum*. The biological activity of the above carboxamidrazone amide was determined by the project students Noman Ellahi and Farzana Kusar. The biological activity results for an imine were obtained from the thesis (Tims. K, 2002).

Compound	<i>M. Fort.</i> Gate test	<i>M. Fort.</i> MIC ($\mu\text{g mL}^{-1}$) carboxamidrazone amide 	<i>M. Fort.</i> MIC ($\mu\text{g mL}^{-1}$) Corresponding imine 
4PYAc1	+	16-32	>32
4PYAc2	+ *	16-32*	>32
4PYAc3	+	16-32	N/A
4PYAc4	-	>32	N/A
4PYAc5	-	>32	16-32
4PYAc6	-	>32	>32
4PYAc7	X		N/A
4PYAc8	-	>32	>32
4PYAc9	-	>32	N/A
4PYAc10	X	N/A	N/A
4PYAc11	X	N/A	N/A
4PYAc12	X	N/A	N/A
4PYAc13	-	>32	N/A
4PYAc14	+	16-32	>32
4PYAc15	+	16-32	>32
4PYAc16	-	>32	N/A
4PYAc17	x		N/A
4PYAc18	-	>32	N/A
4PYAc19	-	>32	>32
4PYAc20	x		8-16
4PYAc21	-	>32	N/A
4PYAc22	-	>32	>32
4PYAc23	-	>32	>32
4PYAc24	-	>32	N/A
4PYAc25	-	>32	8-16
4PYAnh1	X		N/A
4PYAnh2	-	>32	N/A
4PYCa1	-	>32	5-10
4PYCa2	xx	>32	N/A
4PYCa3	xx		>32

4PYCa4	-	>32	>32
4PYCa5	-	>32	>32
4PYCa6	-	>32	>32

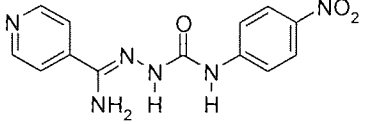
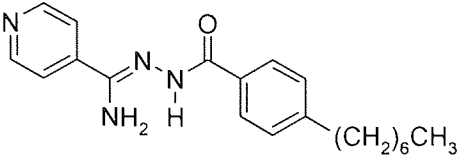
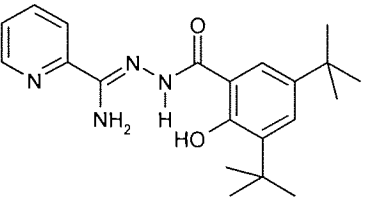
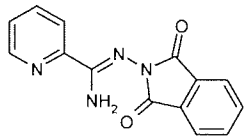
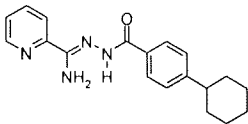
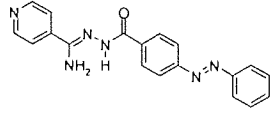
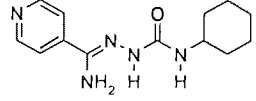
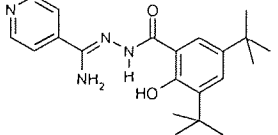
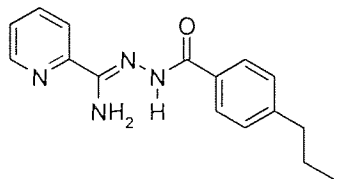
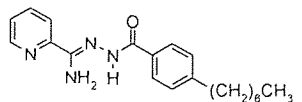
Appendix 4

Three Gram-positive and three Gram-negative organisms were exposed to various heteroarylacboxamidrazone amides. The results are compared with *M. fortuitum* and *M. tuberculosis* results. MIC (mg/mL) for microbacteria was determined by S. Chauhan (placement student, 2006), MIC ($\mu\text{g/mL}$) for *M. fortuitum* was determined by N. Ellahi (MPharm final year project student at Aston University, 2005) and % Inhibition for *M. tuberculosis* was determined by the TAACF. (-) indicates that compound was inactive.

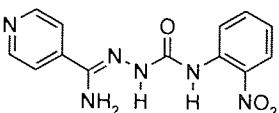
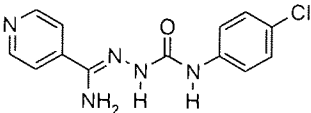
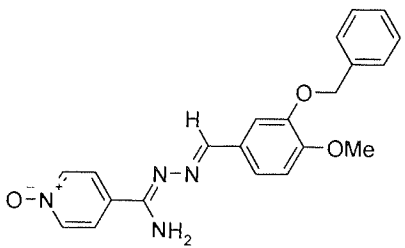
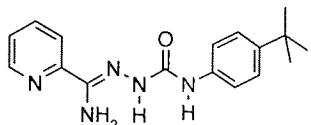
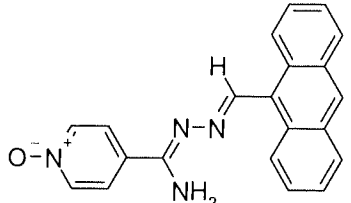
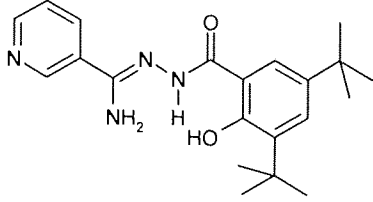
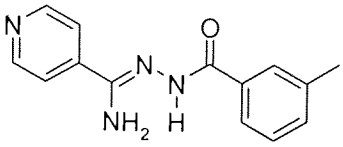
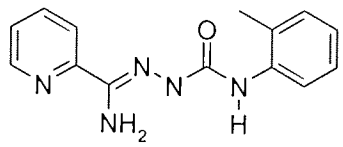
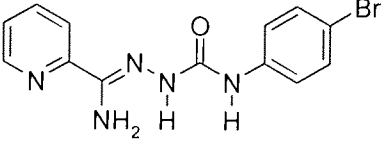
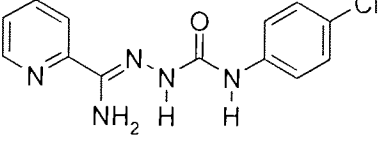
Compound	Microorganism							
	Gram +ve					Gram -ve		
	<i>M. tuber.</i> (%Inh)	<i>M. fort.</i> $\mu\text{g mL}^{-1}$)	<i>S. aureus</i>	<i>B. subtilis</i>	<i>Enterococcus faecalis</i>	<i>E. coli</i>	<i>P. aeruginosa</i>	<i>K. pneumoniae</i>
2PYCa5	100%	>32	64	>256	>256	>256	>256	>256
4PYCa5	94%	>32	>256	>256	16	>256	>256	>256
3PYCa5	64%	>32	>256	>256	>256	>256	>256	>256
2PYCa6	90%	>32	>256	>256	>256	>256	>256	>256
4PYCa6	53%	>32	>256	>256	>256	>256	>256	>256
2PYCa1	93%	16-32	>256	>256	>256	>256	>256	>256
4PYCa1	81%	>32	128	>256	>256	>256	>256	>256
2PYCa4	90%	16-32	>256	>256	>256	>256	>256	>256
4PYCa4	55%	>32	>256	>256	>256	>256	>256	>256
2PYCa2	97%	>256	>256	>256	>256	>256	>256	>256
2PYAnh1	99%	>32	>256	32	>256	>256	>256	>256
2PYAnh2	N/A	>32	>256	>256	>256	>256	>256	>256
4PYAnh2	47%	>32	>256	>256	>256	>256	>256	>256
2PYAc4	N/A	>32	>256	>256	>256	>256	>256	>256
2PYAc17	43%	>32	>256	>256	32	>256	>256	>256
2PYAc20	91%	8-16	>256	>256	>256	>256	>256	>256
2PYAc25	N/A	>32	256	>256	>256	>256	>256	>256
2PYAc11	N/A	>32	>256	>256	>256	>256	>256	>256
4PYAC4	52%	>32	>256	>256	>256	>256	>256	>256
4PYAC23	63%	>32	>256	>256	>256	>256	>256	>256

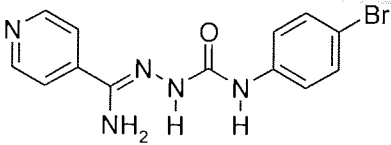
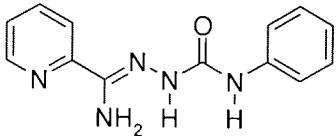
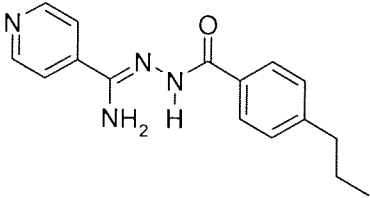
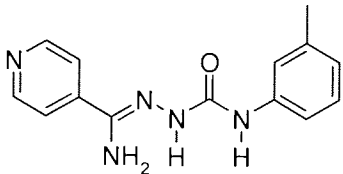
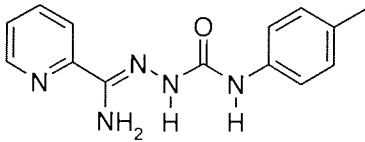
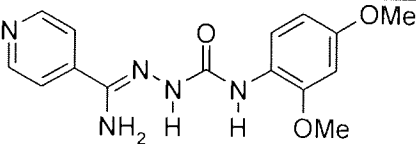
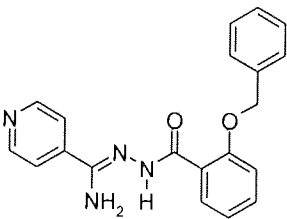
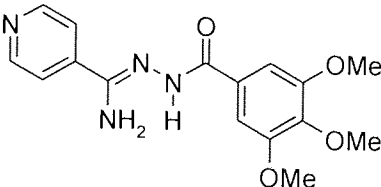
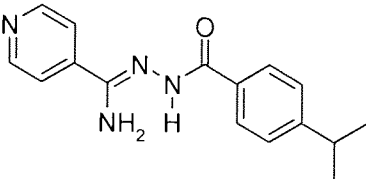
Appendix 5

Comparison of *M. fortuitum* MIC, with *M. tuberculosis* H37Rv (*M. tuber*) MIC and %Inhibition results

Code	Structure	MIC <i>M. fort</i> $\mu\text{g mL}^{-1}$.	MIC <i>M. tuber</i> $\mu\text{g mL}^{-1}$.	%Inh
4PYIs7		16-32	<6.25	100
4PYAc18		>32	<6.25	100
2PYCa5		>32	<6.25	100
2PYAnh 1		>32	<6.25	99
2PYCa2		>32	<6.25	97
4PYAc3		16-32	<6.25	95
4PYIs5		>32	<6.25	94
4PYCa5		>32	<6.25	94
2PYAc16		>32	<6.25	93
2PYAc18		>32	<6.25	93

2PYCa1		16-32	<6.25	93
2PYAc3		4-8	<6.25	92
2PYAc20		8-16	<6.25	91
2PYCa4		16-32	<6.25	90
2PYCa6		>32	<6.25	90
4PYau-NO		8-16	>6.25	88
4PYCa1		>32	>6.25	81
4PYat-NO		>32	>6.25	76

4PYIs16		>32	>6.25	73
4PYIs14		4-8	>6.25	69
4PYak-NO		>32	>6.25	67
2PYIs1		>32	>6.25	66
4PYai-NO		>32	>6.25	66
3PYCa5		>32	>6.25	64
4PYAc23		>32	>6.25	63
2PYIs15		>32	>6.25	62
2PYIs6		>32	>6.25	61
4PYIs14		4-8	>6.25	61

4PYIs		>32	>6.25	60
2PYIs2		>32	>6.25	58
4PYAc16		>32	>6.25	58
4PYIs9		>32	>6.25	56
2PYIs8		>32	>6.25	55
4PYIs10		8-16	>6.25	55
4PYCa4		>32	>6.25	55
4PYAC21		>32	>6.25	54
4PYCa6		>32	>6.25	53

4PYAc4		>32	>6.25	52
4PYIs1		>32	>6.25	51
4PYIs2		>32	>6.25	50
2PYAc16		>32	>6.25	49
4PYIs12		>32	>6.25	48
4PYAc5		>32	>6.25	48
4PYAnh2		>32	>6.25	47
4PYAc1		16-32	>6.25	46
2PYIs9		>32	>6.25	45
2PYIs5		>32	>6.25	44

4PYAc9		>32	>6.25	44
2PYIs10		>32	>6.25	43
2PYAc17		>32	>6.25	43
4PYAc13		>32	>6.25	43
4PYIs15		>32	>6.25	42
4PYAc8		>32	>6.25	39
2PYIs12		>32	>6.25	39
2PYIs3		>32	>6.25	38
2PYIs11		>32	>6.25	38
4PYAc15		16-32	>6.25	34

2PYIs16		>32	>6.25	31
4PYae-NO		>32	>6.25	30
2PYIs7		>32	>6.25	30
4PYIs11		>32	>6.25	29
2PYAc19		4-8	>6.25	23
4PYAc2		>32	>6.25	16
4PYAc14		16-32	>6.25	14
4PyAc16		>32	>6.25	11
2PYIs4		>32	>6.25	0

Appendix 6

Expanded panels of organisms exposed to pyridine-4-carboxamidrazones-4-N-oxide. The results are compared with *M. fortuitum* and *M. tuberculosis* results. MIC for microbacteria was determined by L. Wheedon (Microbiology research student, at Aston University, 2005) MIC for *M. fortuitum* was determined by F. Kusar (B.Sc. Applied and Human Biology final year student, at Aston University, 2004) and % Inhibition for *M. tuberculosis* was determined by the TAACF. (-) indicates that compound

Microorganism	4PYakN-O MIC (µg/ml)	4PYafN-O MIC (µg/ml)	4PYaeN-O MIC (µg/ml)	4PYagN-O MIC (µg/ml)	4PYauN-O MIC (µg/ml)	4PYaiN-O MIC (µg/ml)	4PYatN-O MIC (µg/ml)
GRAM POSITIVE							
<i>M. tuber.</i> (%Inh)	67	11	30	0	88	66	76
<i>M. fort.</i>	>32	16-32	>32	>32	8-16	>32	>32
W11 MRSA	-	-	-	-	128	-	-
<i>S. epidemidis</i> NCTC 11047	-	-	-	-	-	-	-
<i>E. faecium</i> NCTC 7171	32	32	32	32	128	128	-
<i>B. cereus</i>	32	32	16	16	128	-	-
<i>B. megaterium</i>	32	32	32	32	-	-	-
<i>B. subtilis</i> ATCC 6633	64	16	8	32	128	128	-
<i>S. aureus</i> NCTC 10788	32	-	-	-	-	-	-
<i>S. bovis</i> NCTC 11436	64	-	-	-	64	-	-
<i>E. faecalis</i> NCTC 5957	-	-	-	-	128	128	-
MRSA 96-7475	-	-	-	-	-	-	-
<i>S. aureus</i> NCTC 6571	-	-	-	-	-	-	-
<i>M. luteus</i>	16	-	-	32	128	-	-
<i>M. roseus</i>	32	16	32	32	128	64	64
GRAM NEGATIVE							
<i>M. catarrhalis</i>	16	64	-	32	64	-	128
<i>E. coli</i> ATCC 27325	-	-	-	-	-	-	-
<i>S. pullorum</i>	-	-	-	-	-	-	-
<i>P. aeruginosa</i> ATCC 15692	-	-	-	-	-	-	-
<i>Enterobacter cloacae</i> 1051E	-	-	-	-	-	-	-
<i>Citrobacter diversus</i> 2046E	-	-	-	-	-	-	-
<i>K. pneumoniae</i> 1082E	-	-	-	-	-	-	-
<i>P. mirabilis</i> NCTC 5887	-	-	-	-	-	-	-
<i>S. arizonae</i>	-	-	-	-	-	-	-
<i>S. banana</i>	-	-	-	-	-	-	-
<i>S. malawi</i>	-	-	-	-	-	-	-
<i>S. enteritidis</i>	-	-	-	-	-	-	-
<i>S. Cambridge</i>	-	-	-	-	-	-	-
<i>Serratia marcescens</i>	-	-	-	-	-	-	-
<i>Hafnia alvei</i>	-	-	-	-	-	-	-
<i>Citrobacter freundii</i>	-	-	-	-	-	-	-
<i>Shigella sonnei</i>	-	-	-	-	-	-	-

was inactive.

Appendix 7

Antimicrobial testing results versus *M. fortuitum* (*M.fort*) and *M. tuberculosis* (*M.tuber*) for various pyridine-2-carboxamidrazone urea and their corresponding imine. An MIC for imine was obtained from thesis (TIMS 2002) and an MIC for urea compounds was determined by project students N. Ellahi (MPharm final year project student, Aston University, 2005) and F. Kusar (B.Sc Applied and Human Biology final year project student, Aston University, 2004). Results against *M. tuberculosis* strain H₃₇Rv was provided by TAACF. (+) indicates that, the compound is active at the single concentration of 32 µg mL⁻¹, (-) indicates that the compound is not active

Compound	<i>M. Fort.</i> Gate test	<i>M. Fort.</i> MIC (µg mL ⁻¹)	<i>M. Fort.</i> MIC (µg mL ⁻¹) Corresponding imine	<i>M. Fort.</i> MIC (µg mL ⁻¹) Corresponding amide	<i>M. tuber.</i> % Inh
2PYIs1	-	>32	8-16	8-16	66
2PIs2	-	>32		16-32	58
2PYIs3	-	>32		>32	38
2PYIs4	-	>32	N/A	N/A	N/A
2PYIs6	-	>32		N/A	61
2PYIs7	-	>32		N/A	30
2PYIs8	-	>32		N/A	55
2PYIs9	-	>32		N/A	45
2PYIs10	-	>32		N/A	43
2PYIs11	-	>32		N/A	38
2PYIs12	-	>32		>32	39
2PYIs14	-	>32		N/A	61
2PYIs15	-	>32		N/A	62
2PYIs16	-	>32		N/A	31

Appendix 8

Antimicrobial testing results versus *M. fortuitum* (*M.fort*) and *M. tuberculosis* (*M.tuber*) for various pyridine-4-carboxamidrazone urea and their corresponding imine. An MIC for imine was obtained from thesis (TIMS 2002) and an MIC for urea compounds was determined by project students N. Ellahi (MPharm final year project student, Aston University, 2005) and F. Kusar (B.Sc Applied and Human Biology final year project student, Aston University, 2004).. Results against *M. tuberculosis* strain H₃₇Rv was provided by TAACF. (+) indicates that, the compound is active at the single concentration of 32 µg mL⁻¹, (-) indicates that the compound is not active

Compound	<i>M. Fort.</i> Activity	<i>M. Fort.</i> MIC (µg mL ⁻¹)	<i>M. Fort.</i> MIC (µg mL ⁻¹) Corresponding imine	<i>M. Fort.</i> MIC (µg mL ⁻¹) Corresponding amide	<i>M. tuber.</i> % Inh
4PYIs1	-	>32	8-16	N/A	51
4PIs2	-	>32	>32	16-32	50
4PYIs3	-	>32	16-32	>32	N/A
4PYIs4	-	>32	N/A	N/A	N/A
4PYIs5	-	>32	N/A	N/A	94
4PYIs6	-	>32	N/A	N/A	60
4PYIs7	+	16-32	>32	N/A	100
4PYIs8	+	8-16	16-32	N/A	N/A
4PYIs9	-	>32	>128	>32	56
4PYIs10	+	8-16	16-32	>32	55
4PYIs11	-	>32	>32	>32	29
4PYIs12	-	>32	>32	>32	48
4PYIs14	+	4-8	>32	N/A	69
4PYIs15	-	>32	>128	>32	42
4PYIs16	-	>32	N/A	N/A	73